



Universidad de Granada

Facultad de Farmacia

Departamento de Química Farmacéutica y Orgánica

**Design, synthesis and biological activity of *ortho*-substituted
benzene derivatives linked to purines: six-membered homochiral
heterocycles with estereospecific antiproliferative activity**

M^a EUGENIA GARCÍA RUBIÑO

PROGRAMA DE DOCTORADO EN QUÍMICA
TESIS DOCTORAL CON MENCIÓN INTERNACIONAL

Granada, diciembre de 2012

Editor: Editorial de la Universidad de Granada
Autor: María Eugenia García Rubiño
D.L.: GR 1011-2013
ISBN: 978-84-9028-513-8

La doctoranda María Eugenia García Rubiño y los directores de la tesis Joaquín María Campos Rosa, María del Carmen Núñez Carretero y Miguel Ángel Gallo Mezo garantizamos, al firmar esta tesis doctoral, que el trabajo ha sido realizado por el doctorando bajo la dirección de los directores de la tesis y hasta donde nuestro conocimiento alcanza, en la realización del trabajo, se han respetado los derechos de otros autores a ser citados, cuando se han utilizado sus resultados o publicaciones.

Granada, 5 de Noviembre de 2012

DIRECTORES

Fdo. Joaquín M^a Campos
Rosa
Catedrático de Química
Farmacéutica
Facultad de Farmacia.
Universidad de Granada.

Fdo. M^a del Carmen Núñez
Carretero
Prof. Titular de Química
Farmacéutica
Facultad de Farmacia.
Universidad de Granada.

Fdo. Miguel Ángel Gallo
Mezo
Catedrático de Química
Farmacéutica
Facultad de Farmacia.
Universidad de Granada.

DOCTORANDA

M^a Eugenia García Rubiño

El trabajo presentado en esta memoria ha sido realizado gracias a la concesión de una ayuda: ‘Ayuda Predoctoral para la Formación de Profesorado Universitario’ (AP 2007-02954) concedida por el Gobierno de España.

La estancia de cuatro meses en el ‘Dipartimento di Chimica e Tecnologia del Farmaco’ de la ‘Università degli Studi di Perugia’ (Italia) ha sido realizada gracias a la ayuda para “Estancias Breves de becarios del Programa Nacional de Formación de Profesorado Universitario” para la obtención de la Mención Internacional en el título de doctor concedida por el Ministerio de Educación.

La realización de este trabajo ha sido posible gracias a la financiación procedente del Ministerio de Ciencia e Innovación y del Instituto de Salud de Carlos III. (Ministerio de Salud Español). FIS PI0170227. FIS PI10/00592

*'Nuestra recompensa se encuentra en el esfuerzo,
constancia e ilusión y no en el resultado.
Un esfuerzo total es una victoria completa'.*

Mahatma Gandhi

AGRADECIMIENTOS

Son muchas las personas que han estado a mi lado durante estos años y que me han ayudado en esta etapa de mi vida. No es fácil llegar, se necesita constancia, lucha y mucha ilusión, pero sobre todo apoyo como el que he recibido durante este tiempo. Por eso me gustaría dar las gracias a las personas que han hecho posible la realización de este trabajo.

A ti Joaquín, por ser mi guía en esta tesis, por enseñarme el amor a la investigación, por tu ejemplo de profesionalidad y dedicación, por tu ánimo en los momentos bajos, por contribuir a mi empeño y por hacer más perfecto aquello en lo que creo. Sin tí no hubiese sido posible la realización de esta Memoria.

A ti Manme, (“mi Mary Puri”) por ser mi amiga antes que jefa, por tu cariño, por esa forma de ver la vida que transmites, por tus consejos, por pensar en mí y en lo que es bueno para mí, por todo lo que me has enseñado que va más allá de la ciencia y porque nunca olvidaré mi primer contacto en el laboratorio de tu mano.

A usted Don Miguel Angel, por su respeto, consejo y apoyo en los momentos más difíciles.

A usted Don Antonio, porque siempre recordaré sus clases y le doy las gracias por ser tan encantador y saber transmitir sus conocimientos con esa ilusión; porque gracias a ser como es, hoy sé lo que quiero hacer en mi vida profesional. Gracias por permitirme trabajar en este grupo de investigación.

A ti Antonio Entrena, por ser siempre tan cariñoso, porque siempre te has preocupado por saber como estaba y como me iba no solo en lo profesional sino también en lo personal.

A ti Encarna, porque siempre has tenido una sonrisa cada mañana, por ser un ejemplo de constancia y lucha.

A ti M^a José, por ser siempre tan optimista y simpática, por el buen ambiente que creas a tu lado y por esos buenos momentos compartidos dentro y fuera del laboratorio.

A mis amigos del laboratorio, porque nunca me ha faltado nadie con quien compartir los buenos y malos momentos y porque sin vosotros, hubiese sido más difícil llegar hasta aquí.

A ti Vero, porque siempre nos hemos entendido con mirarnos, porque sin hablar no los hemos dicho todo, por ser confidente y amiga, porque he aprendido muchas cosas de ti, por tu punto de vista siempre realista, por tu fortaleza. y porque siempre nos quedará el recuerdo de los “buenos ratos” que con un rayo de sol hemos sabido exprimir y compartir.

A ti Lucía, “mi Antoñita Trabuqueña”, porque nos hemos reído hasta no poder más y llorar. Por nuestro humor especial que pocas personas entienden...por todos los momentos inolvidables de premios guiners... por las estancias en Perugia que no coincidimos en persona pero que hemos vivido y compartido igualmente, por toda la energía, fuerza y positividad que transmites y esa ilusión por aprender cada día.

A ti Cayetana, porque aunque no hemos estado estos cinco años que ha durado mi tesis, no me ha hecho falta más tiempo para confiar en ti, para saber que eres un sol, por tu ternura e ingenuidad, por esos besos que me das y por no medir los te quiero. Yo a ti también gordita. Por esas sobremesas tan amenas que siempre echaré de menos.

A ti Angélica, por tu sencillez y humildad que tanto escasea hoy día, porque nunca olvidaré la libreta que me regalaste para que no siguiese con la mía que tanta “mala suerte” me estaba dando, pensando en que el rumbo de la química cambiaría. Al final resultaron los compuestos más activos aunque no se incluirán aquí. Por hacerme sentir especial por vivirlo todo tan intensamente.

A ti Esther Hernández, por ese empeño en poner fin a esta tesis con ese escarabajo azul, amuleto para conseguir obtener los ciclos y como no salían lo intentaste con hidrogenaciones industriales a pique de un replique de quedarnos sin laboratorio 😊. Porque en tu cara siempre dibujas una sonrisa.

A ti Esther García, porque siempre has sabido levantarte y has demostrado fortaleza. Por tu tenacidad y constancia, por esos días y fines de semana de columnas interminables compartidas. Por pedirle y rezarle tantas veces a Dios por mí. Porque siempre me has dicho que hay que luchar por los sueños. Esta etapa termina para mí y pronto lo harás tú también.

A ti Lourdes, lo más guapo del laboratorio, por tu bondad, ternura y ejemplo de constancia. Porque siempre te has alegrado por todo lo bueno que me ha pasado. Te mereces ser muy muy feliz y que te quieran como mínimo como demuestras siempre querer tú.

A ti Sonia, por los años que compartimos cuando estábamos en el mismo ala del laboratorio, por dejarme hacer columnas en vuestro sitio cuando aún no había campanas y usábamos salidas de aire para hacerlas y mi sitio estaba ocupado. Por aquellos momentos previos a mi boda que compartimos con la música del banquete... y porque siempre me he sentido muy reflejada en ti.

A ti Ana M^a, por esos abrazos matutinos en los que decíamos que eran tan reconforzantes como abrazar un árbol. Porque nunca dejaste de prestarme ayuda a pesar de que a veces la situación no fuese la más idónea, porque no olvidaré que me explicaste como usar el HPIC, fundamental para el desarrollo de esta tesis. Porque eres un referente de ilusión por lo que se hace y por tu dulzura.

A ti Santi, por ser un buen compañero con el que he compartido sitio en el laboratorio y risas. Por tu buen humor y sensibilidad.

A ti César, por demostrarme cada día que lo importante es trabajar con ilusión, por tu ayuda en los malos momentos y por ser tan buena persona.

A ti Olga, siempre silenciosa, por tu ayuda cuando siempre te he preguntado y necesitado. Por ese toque de elegancia a imitar imposible, por tu sensibilidad y porque de tí he aprendido a soñar en todos los ámbitos de la vida, incluso con la química. Por tu realismo en todos tus consejos.

A ti Ana, porque siempre has estado ahí, porque sé que se puede contar contigo, porque eres un referente en tantas cosas...por tu fortaleza y porque de ti he aprendido a que no hay que dejar de hacer ni de atender las obligaciones a pesar de que la situación sea adversa.

A Nawel, Mariam, Dori, Carlota, Fátima y Belén que con su colaboración y amistad han hecho que el trabajo en el laboratorio sea cada día más ameno y llevadero.

A todo el ala del Departamento de Orgánica, Juan, Paco, Jose Antonio, Pepe, Javi, Victoria, Rosario, Mavys por su ayuda en todo lo que he necesitado y en especial a Mónica y a Juanjo porque les agradezco el tiempo que me han dedicado sin nada a cambio.

A nuestro técnico de laboratorio Luis, porque su trabajo siempre ha facilitado el nuestro y a nuestro secretario Antonio por ser siempre tan agradable.

A todo el departamento de Inorgánica, Pepa, Almudena, Patel, Ricardo, Nono, las niñas Hannan, Alicia, Inma por todo su cariño y estar ahí siempre que lo he necesitado y en especial a Juan Niclós, por ser como un padre para mí en la Universidad. Todos ellos una gran familia y un departamento ejemplar.

A Duane y Juan Manuel García por su ayuda y paciencia con mis muestras.

A Juan Antonio Marchal, por la realización de los ensayos biológicos y todo su interés y disposición.

A todo el grupo de profesionales del Centro de Instrumentación Científica: por su diligencia y buen trato durante todos estos años.

En especial a la unidad de RMN, Alí y M^a Esther por su profesionalidad, buen trato y consejos de amigos que me han dado.

A la mejor unidad del CIC, la de Masas: A tí Jose Miguel, por ser tan alegre y simpático, a Juan Molís, por preocuparse en enseñarme con todo el cariño del mundo lo que he necesitado para el desarrollo de mi tesis, a Yolanda por su inestimable ayuda y amistad, a Samuel por todos las experiencias compartidas y los buenos ratos de casquera que hemos pasado juntos, a Rocío por ser tan cariñosa. No olvidaré los meses que estuve trabajando con vosotros durante el desarrollo de esta tesis, fueron los mejores en un lugar de trabajo, donde siempre hay buen ambiente y se regala una sonrisa. GRACIAS.

Al grupo de los Profesores Natalini y Pellicari, por enseñarme otros aspectos de la investigación, por su disposición y empeño en enseñarme, porque mi estancia con ellos me ha hecho ver que nunca se sabe lo suficiente y que cuanto más intentas aprender te das cuenta de que menos sabes. Porque hicisteis que mi estancia fuese inolvidable, Antimo, Maura, Roccaldò, Filomena, Sara, Federica, Emilia, Valentina, Melisa, Serena...os llevo en mi recuerdo.

A mis amigos, Inma, Lolo, Yolanda, Aurora, Luz, Juan Godoy, Fernando...por entender mis ausencias, por animarme a hacer lo que siempre he querido y por demostrarme en tantas ocasiones el significado de la amistad.

A Jorge, por ser mi amigo durante tantos años, porque siempre me has entendido en todo, por tus consejos, por alegrarte de mis logros, por sentir como tuyo todo lo que me afecta. Gracias por ser como eres.

A Luis, por ser una de las personas que más admiro, porque te has hecho a tí mismo y por todos los momentos inolvidables compartidos.

A mis sobrinas Alba y Julia, porque sin ellas saberlo me han ayudado a desconectar de la mejor manera que en esta vida se puede desconectar, con una sonrisa, jugando con ellas. Porque en muchos momentos, cuando las cosas eran difíciles, cuando estaba cansada e incluso perdida me habéis hecho recordar lo importante y la esencia de la vida.

A mis padres por ser el pilar fundamental de lo que soy, por su educación en todos los ámbitos de mi vida, por todo lo que me han inculcado, por su incondicional sacrificio y lucha, por quererme mucho y creer en mí. Por ser unos referentes en mi vida y estar siempre a mi lado.

A mis hermanos, porque me han ayudado en todo lo que emprendía, porque son un ejemplo de superación en mi vida, porque a pesar de la lejanía, no hubo un día que no estuvieran presentes en mis pensamientos. Gracias por quererme como soy.

Y sobre todo a la persona que más me ha marcado en mi vida, mi abuelita Dolores, gracias por quererme tanto, por enseñarme a ser fuerte y porque la sabiduría de los años hace que siempre tengas razón, “al final todo lo que se consigue con esfuerzo en esta vida es lo que merece la pena”.

En especial, esta tesis se la dedico a quien más la ha sufrido a mi lado, a tí Antonio, mi marido, por haberme apoyado en todo momento, en cada meta que me he propuesto, por tus consejos, tus valores, por la motivación constante que me has dado en todos estos años, por exigirme cuando sabías que podía dar más, por tu infinita paciencia, por no dejar que me desmoronase ante las adversidades, porque parte de este título es tuyo... por todo aquello que en esta vida nos queda por hacer juntos y sobre todo por tu amor y a nuestro pequeño/a que está por venir que es el mejor regalo que la vida nos pueda dar. TAM.

A todos lo que sin saberlo me hicieron redoblar esfuerzos, luchar por todo aquello en lo que creo y no renunciar nunca a mis sueños. A todos lo que escapan de mi mente pero que igualmente fueron indispensables y de gran ayuda en la realización de esta memoria.

INDEX

INTRODUCTION	1
1. CANCER	3
1.1. Cancer Epidemiology	3
1.2. Causal factors in cancer	6
1.3. Carcinogenesis	9
1.4. Cellular and molecular mechanisms altered in cancer cells	11
1.4.1. Cell cycle	11
1.4.2. Cell death	19
1.4.2.1. Apoptosis	20
1.4.2.1.1. eIF2	24
1.5. Tumor angiogenesis	27
1.5.1. Angiogenic growth factors	27
1.5.2. Inhibitors of angiogenesis	29
1.6. Metastasis	29
1.7. Core molecular signaling pathways involved in malignant cell behaviour.....	31
1.8. Cancer treatment	34
1.8.1. Cellular mechanisms as targets for antitumor therapy	36
1.8.2. Efforts to improve cancer treatment	37
1.9. Rational design	41
1.9.1. Preclinical development	42
1.9.1.1. In vitro preclinical development	42
1.9.1.2. In vivo assays for antitumor activity	44
2. STEREOCHEMISTRY	47
2.1. Introduction	47
2.2. Basic Concepts and Terminology.....	49
2.3. Classical Terminology	51
2.4. Stereochemical Descriptors	54
2.5. Using Descriptors to Compare Structures	56
2.6. Distinguishing Enantiomers	58
2.7. The Origin of Chirality in Nature	60

INDEX

3. BACKGROUND	63
3.1. Introduction.....	65
3.2. Benzo-Fused Seven-Membered Derivatives Linked To Pyrimidines	66
3.2.1. Antiproliferative Activities of Cyclic <i>O,N</i> -Acetals	67
3.2.2. Apoptosis Induction of Cyclic <i>O,N</i> -Acetals	68
3.2.3. Cell Cycle Distribution of Cyclic 5-FU <i>O,N</i> -Acetals	69
3.3. Modification of the Molecular Markers Caused by the Cyclic 5-FU <i>O,N</i> -Acetals..	70
3.3.1. Apoptosis Markers	71
3.4. Benzo-Fused Seven-Membered Derivatives Linked To Purines	72
3.4.1. Antiproliferative activities	72
3.5. The (1,2,3,5-tetrahydro-4,1-benzoxazepine-3-yl)moiety linked to pyrimidine and purine bases	74
3.5.1. Antiproliferative activities	75
3.6. Synthesis and anticancer activity of (<i>RS</i>)-9-(2,3-dihydro-1,4-benzoxathiin-3- ylmethyl)-9 <i>H</i> -purines	79
4. RESUMEN	83
4.1. Antecedentes	85
4.2. Bases sobre las que se sustenta esta tesis doctoral	89
4.3. Importancia de la quiralidad en los fármacos	89
4.4. Nuevas investigaciones	91
4.4.1. Síntesis y actividad anticancerosa de (<i>RS</i>)-9-(2,3-dihidro-1,4- benzoxaheteroin-2-ilmetil)-9 <i>H</i> -purinas.	91
4.4.2. Síntesis y actividad anticancerosa de (<i>R</i>)- y (<i>S</i>)-9-(2,3-dihidro-1,4- benzoxaheteroin-2-ilmetil)-9 <i>H</i> -purinas	92
4.4.3. Síntesis, caracterización química inequívoca y estudio de la reactividad de 2,3,4,5-tetrahidro-1,5-benzoxazepinas-3-ol	92
4.4.4. Alquilación estereoespecífica de adeninas sustituidas por medio de la reacción de Mitsunobu bajo condiciones asistidas por microondas	93
4.4.5. Compuestos selectivos frente a células madre cancerosas	94
5. AIMS	99

6. RESULTS	101
PAPER 1: Homochiral Drugs: A Demanding Tendency of the Pharmaceutical Industry	103
PAPER 2: Synthesis and anticancer activity of (<i>RS</i>)-9-(2,3-dihydro-1,4- benzoxaheteroin-2-ylmethyl)-9 <i>H</i> -purines	117
PAPER 3: Enantiospecific Synthesis of Heterocycles Linked to Purines: Different Apoptosis Modulation of Enantiomers in Breast Cancer Cells	127
PAPER 4: Stereospecific Alkylation of Substituted Adenines by the Mitsunobu Coupling Reaction under Microwave-Assisted Conditions	185
PAPER 5: Synthesis, unambiguous chemical characterization, and reactivity of 2,3,4,5-tetrahydro-1,5-benzoxazepines-3-ol	261
PAPER 6: Two tautomeric polymorphs of 2,6-dichloropurine	305
7. FUTURE PERSPECTIVES	311
8. CONCLUSIONES	317
9. REFERENCES	323

1. INTRODUCTION

1. CANCER

1.1. Cancer Epidemiology

The importance of cancer has increased over the last century as a result of the decline in deaths from infectious diseases and increasing life expectancy, since age is one of the major risk factors for this disease. Cancer is a leading cause of death worldwide according to the World Health Organization (WHO).

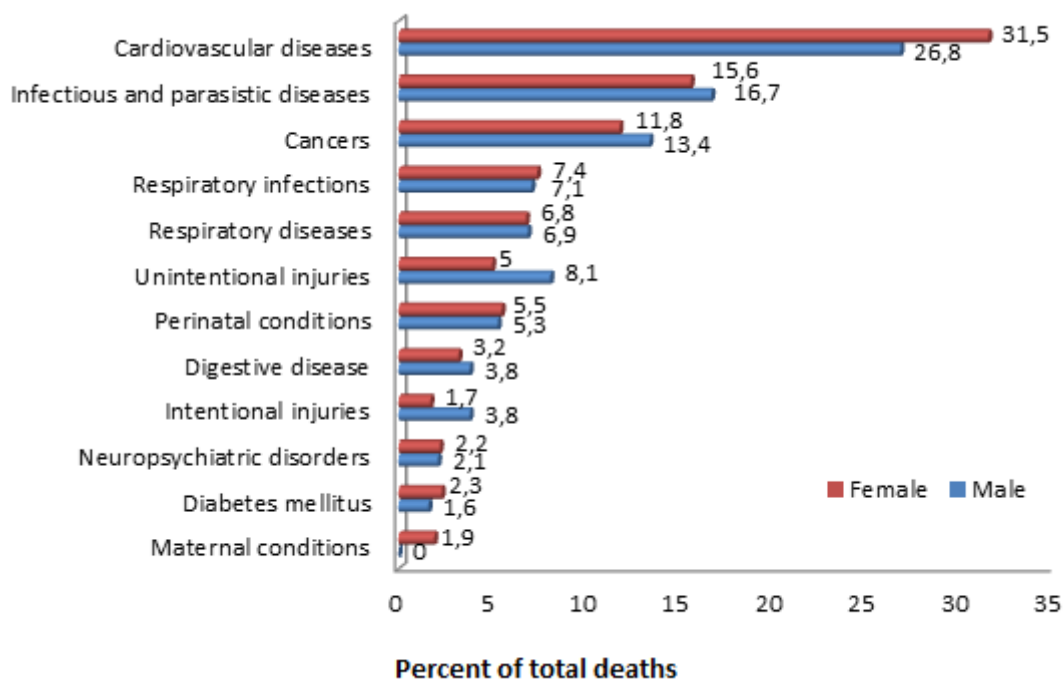


Figure 1.1. Distribution of global deaths bleeding cause groups. *Source: The Global Burden of Disease: 2004 update. World Health Organization, 2008.*¹

The International Agency of Research on Cancer (IARC) estimated that about 13.3 million people in the world developed cancer in 2008. Furthermore, it is estimated that about 7.6 million people died due to this disease (13% of global deaths). Approximately 72% of all deaths from cancer in 2008 occurred in countries of low and middle income.

The WHO expects that global annual deaths from cancer will continue increasing and will rise to 13.2 million in 2030 (Figure 1.2).

Cancer is the leading cause of death in developed countries and the second leading cause of death in developing countries. More than 10 million new cancer cases are reported each year. This fact represents a real concern and an important cost for a society, produces a major impact on the health system, a world market for the pharmaceutical industry and an intellectual challenge for the science.

As a whole, urbanization, aging and changing lifestyles are causing chronic and noncommunicable diseases (such as depression, diabetes, cardiovascular diseases and cancer) and traumatism to be a growing cause of morbidity and mortality.²⁻⁴

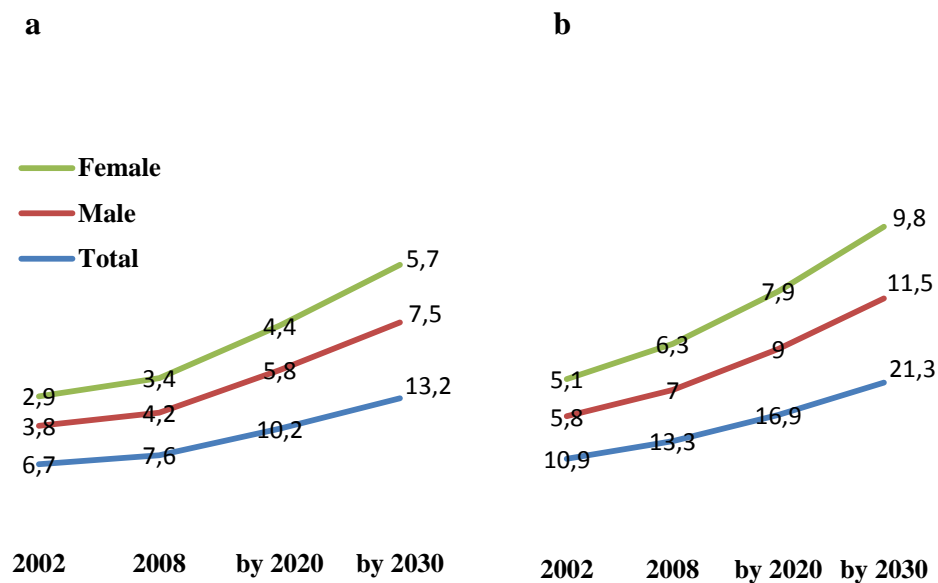


Figure 1.2. Predicted annual number of new cases in million (a) and percentage of cancer deaths (b). The predicted number of new cases of cancer is mostly due to a steadily increasing proportion of elderly people in the world. If current smoking levels and the adoption of unhealthy lifestyles persist, the increase will be even greater. *Source:* GLOBOCAN 2008. *Cancer Incidence and Mortality Worldwide.* IARC, 2010.⁵

The main types of cancer leading to overall annual mortality are: lung (1.4 million deaths), stomach (0.7 million deaths), liver (0.7 million deaths), colon (0.6 million deaths) and breast (0.5 million deaths) (Figure 1.3).

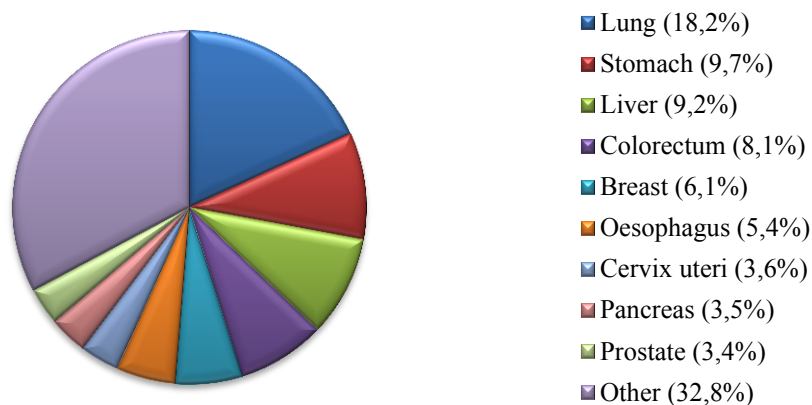


Figure 1.3. Estimated cases of cancer deaths. *Source:* Adapted from : *GLOBOCAN 2008. Cancer Incidence and Mortality Worldwide*. IARC, 2010.⁵

In 2008, there were an estimated 2.4 million new cases of cancer and 1.2 million death from cancer in the European Union. The most common cancers were colorectal cancer (13.7% of the total), breast cancer (13.6%), prostate cancer (13.2%) and lung cancer (11.8%). The most common causes of death from cancer were lung cancer (20.6% of the total), colorectal cancer (12.1%), breast cancer (7.3%) and prostate cancer (5.8%).⁶

In these 27 countries, the most common tumours in men were prostate and lung and in women the most frequent were breast and colorectal cancer in 2008 (Figure 1.4). Lung cancer was the most common cause of cancer death in men and the second leading cause in women, but in some countries like Denmark, Sweden, Netherlands, Poland and the United Kingdom, lung cancer already represents the leading cause of cancer death in the latter group. In Spain, cancer was responsible for the death of about 100,000 people in 2008, 38,000 of whom were under 70 years-old, being breast cancer in women and prostate cancer in men those with the highest incidence. However, Spain has the lowest rate of female cancer death of the continent and one of the lowest in the world.

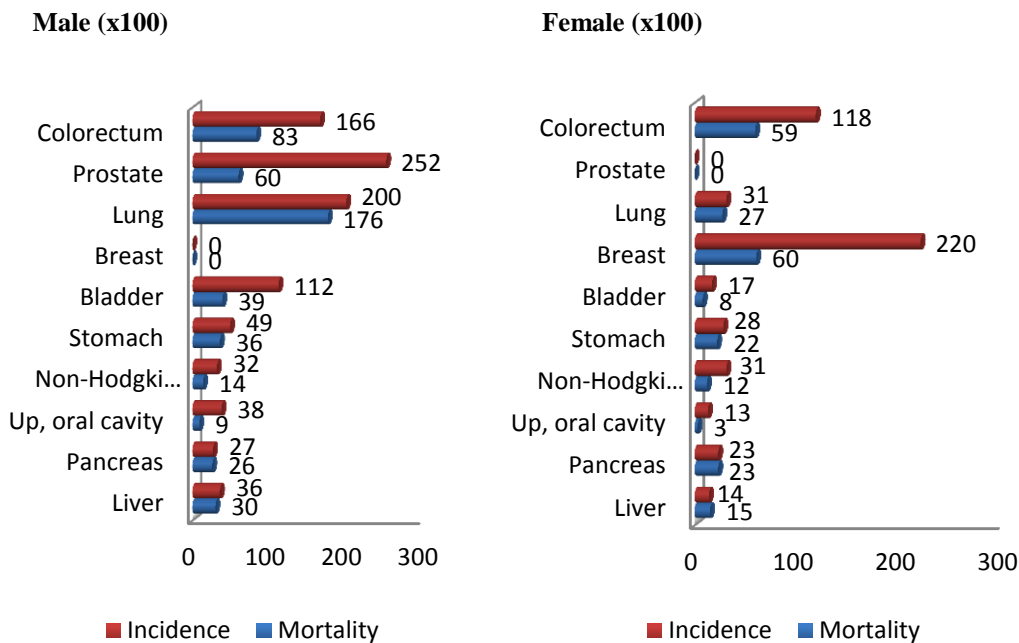


Figure 1.4. Incidence and mortality of some cancers in the European Union. *Source:* GLOBOCAN 2008. *Cancer Incidence and Mortality Worldwide.* IARC, 2010.⁵

The number of new cases of cancer increases, but mortality rates in diagnosed patients decrease due to increasingly early diagnosis and better treatment approaches. However, the absolute number of deaths rises slowly because of the increase in cancer incidence and the aging of the population.

1.2. Causal factors in cancer

Cancer is a generic term for a large group of diseases that can affect any part of the body. Other terms used are malignant tumours and neoplasms. One defining feature of cancer is the rapid creation of abnormal cells that grow beyond their usual boundaries, and which can then invade adjoining parts of the body and spread to other organs. This process is referred to as metastasis. Metastases are the major cause of death from cancer.

Cancer is mainly a genetic disease. There are many possible causes of genetic alterations that produce changes in specific genes, requiring that a cell accumulates generally a large number of genetic alterations to become cancerous. This accumulation of mutations is very rare in normal cells (1 to 3 times per 10^{14} cells).

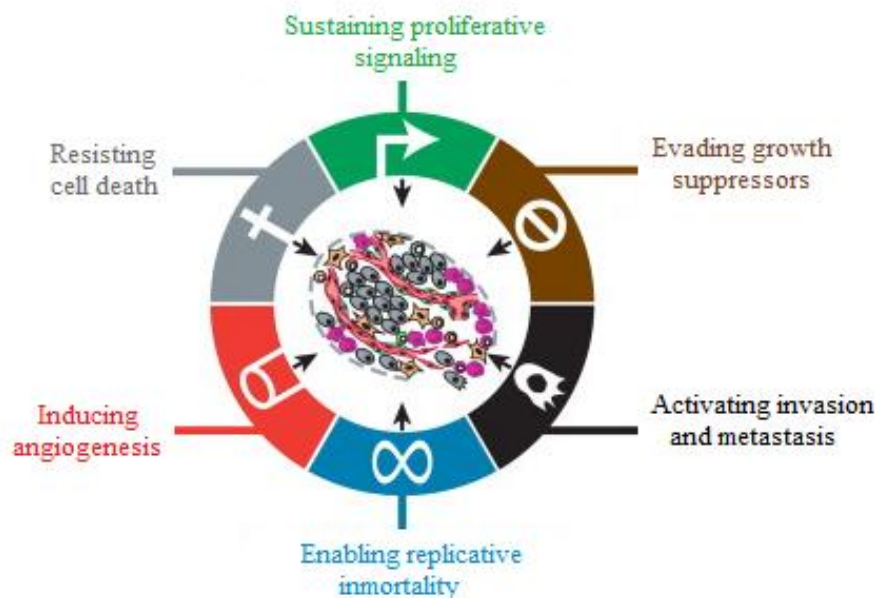


Figure 1.5. The six hallmarks of cancer cell. Most if not all cancers have acquired the same set of functional capabilities during their development, albeit through various mechanistic strategies. *Source:* Adapted from *Cell*, 2011. ²

Cancer arises from one single cell. The transformation from a normal cell into a tumour cell is a multi-stage process, typically a progression from a pre-cancerous lesion to malignant tumours.

These changes are the result of the interaction between a person's genetic factors and three categories of external agents, including:

- *physical carcinogens*, such as ultraviolet and ionizing radiation;
- *chemical carcinogens*, such as asbestos, components of tobacco smoke, aflatoxin (a food contaminant) and arsenic (a drinking water contaminant);
- *biological carcinogens*, such as infections from certain viruses, bacteria or parasites.

INTRODUCTION

Tobacco use (active and passive smokers), alcohol intake, low fruit and vegetable intake, and chronic infections from hepatitis B (HBV), hepatitis C virus (HCV) and some types of Human Papilloma Virus (HPV) are leading risk factors for cancer in low- and middle-income countries.

Cervical cancer, which is caused by HPV, is a leading cause of cancer death among women in low-income countries. In high-income countries, tobacco use, alcohol intake, and being overweight or obese are major risk factors for cancer (Figure 6).⁷

Ageing is another fundamental factor for the development of cancer. The incidence of cancer rises dramatically with age, most likely due to a buildup of risks for specific cancers that increase with age. The overall risk accumulation is combined with the tendency for cellular repair mechanisms to be less effective as a person grows older.

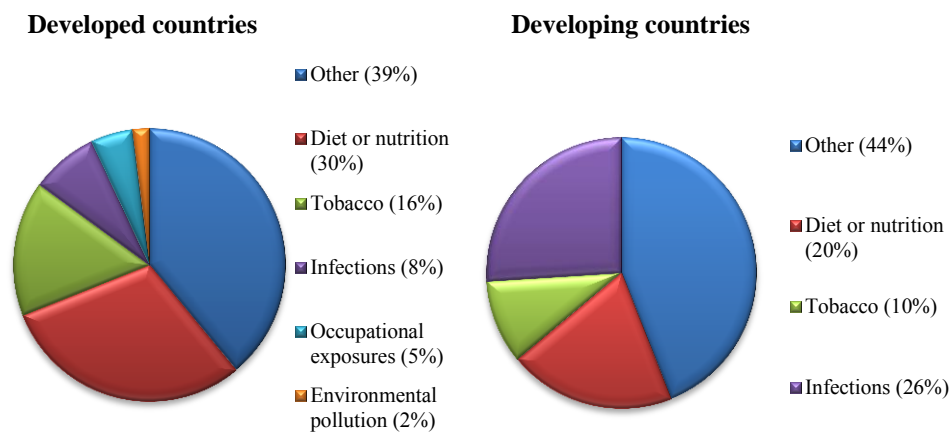


Figure 1.6. Proportion of cancer causes by major risk factor and level of economic development.
Source: Adapted from *The cancer atlas. American Cancer Society, 2016.*⁷

1.3. Carcinogenesis

Carcinogenesis is the molecular process by which cancer develops. It is a process that involves several steps: initiation, promotion, tumour progression and malignant conversion (Figure 1.7), in which the importance of cancer cell migration, proliferation and extracellular matrix degradation is well known.⁸

These stages may progress over many years. The first stage, **initiation**, involves a change in the genetic make up of a cell. This may occur randomly or when a carcinogen interacts with DNA causing damage. This initial damage rarely results in cancer because the cell has in place many mechanisms to repair damaged DNA. However, if repair does not occur and the damage to DNA is in the location of a gene that regulates cell growth and proliferation, DNA repair, or a function of the immune system, then the cell is more prone to becoming cancerous.

If the damage is not repaired, genetic defects and mutations may occur (initiation), which triggers a cell structurally modified or a cancer cell (promotion).

During **promotion**, the mutated cell is stimulated to grow and divide faster and becomes a population of cells. Eventually a benign tumour becomes evident. In human cancers, hormones, cigarette smoke, or bile acids are substances that are involved in promotion. This stage is usually reversible.

The **progression** phase is less well understood. During progression, there is further growth and expansion of the tumour cells over normal cells. The genetic material of the tumour is more fragile and prone to additional mutations. These mutations occur in genes that regulate growth and cell function such as oncogenes, tumour suppressor genes and DNA mismatch-repair genes. These changes contribute to tumour growth until conversion occurs, when the growing tumour becomes malignant even result in metastasis.

Although there are many different forms of cancer, the basic multistage process by which various tumours develop is similar for all cancers. This process is called

carcinogenesis and can be regarded as an accumulation of genetic and/or biochemical cell damage, which offers a variety of targets for chemopreventive agents to prevent or inhibit the slow progression from early genetic lesions to tumour development. Well established molecular mechanisms of chemoprevention include modulation of drug metabolism, antioxidation, radical scavenging, anti-inflammation, antitumour promotion and antiproliferative activity as well as induction of cell differentiation and apoptosis.

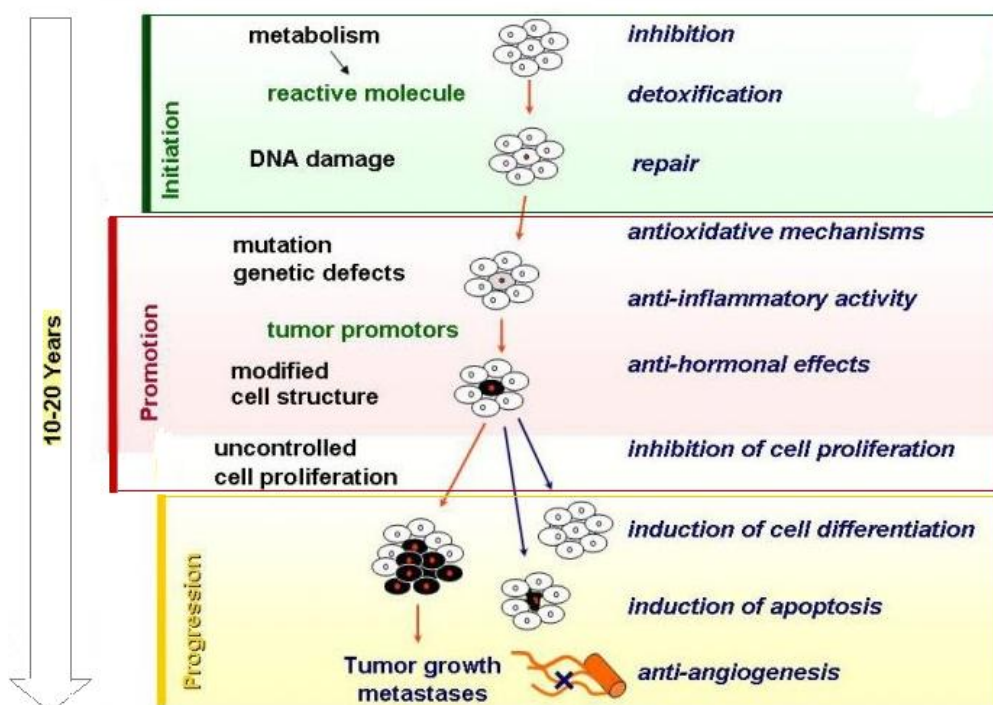


Figure 1.7. Scheme of multi-stage carcinogenesis and mechanisms of cancer chemoprevention. Source: Adapted from German Cancer Research Center.⁹

Knowledge of the cellular and molecular mechanisms is essential for the proper use of already known chemopreventive agents, but also for the development of new potential anticarcinogenic agents.

1.4. Cellular and molecular mechanisms altered in cancer cells

1.4.1. Cell cycle

Cancer is frequently considered to be a disease of the cell cycle. Cancer cells often show alterations in the signal transduction pathways that lead to proliferation in response to external signals. Cancer arises mainly from mutations in somatic cells. However, it is not the result of a single mutation, rather, it results from increasing genetic disarray accumulated over time. Tumourigenesis in humans is a multistep and age-dependent process. Uncontrolled cell proliferation is one of the main hallmarks of cancer, and tumour cells have acquired damage to genes that are involved in regulating the cell cycle. Cellular division is an ordered, tightly regulated process involving multiple checkpoints that assess extracellular growth signals, cell size and DNA integrity.

The cell cycle process in eukaryotic cells includes a series of events that occur between one division and the next one.

In multicellular organisms, as well as for reproduction, cell division is also necessary to allow the growth of the organism during development, and to replace damaged cells, or cells that have undergone senescence or apoptosis processes. Normally, in adult tissue, there is a delicate balance between cell death (programmed cell death or apoptosis) and proliferation (cell division) producing a steady state.

Disruption of this equilibrium by loss of cell cycle control may eventually lead to tumour development.

The basic cell cycle is divided into four phases. During two of these phases, cells execute the two basic events in cell division: generation of a single and faithful copy of its genetic material where DNA is synthesized (the synthetic or S phase) and partitioning of all the cellular components between two identical daughter cells (mitosis or M phase). The two other phases of the cycle include G₁ and G₂ phases represent the two 'gap' periods (G phase), during which cells prepare themselves for

the successful completion of the S and M phases, respectively. These are the quality control points of the cell cycle and are often referred to as checkpoints processes. At checkpoints, there are important mechanisms sensing damaged DNA before the cell enters the S phase (G_1 checkpoint) or the M phase (G_2 checkpoint).

G_1 phase (growth phase) the cell synthesizes RNA and proteins, phase during which the cell prepares for DNA synthesis.

The replication of DNA occurs in **S phase** (synthesis phase).

G_2 phase in which the DNA strands separate, and replication control mechanisms take over before the cell enters the mitosis (**M phase**) where the segregation of the chromosomes into daughter progeny occurs, which is divided into several stages. It includes the following phases: prophase, metaphase, anaphase, telophase, and it ends with cytokinesis, i.e. the physical division of cellular material.

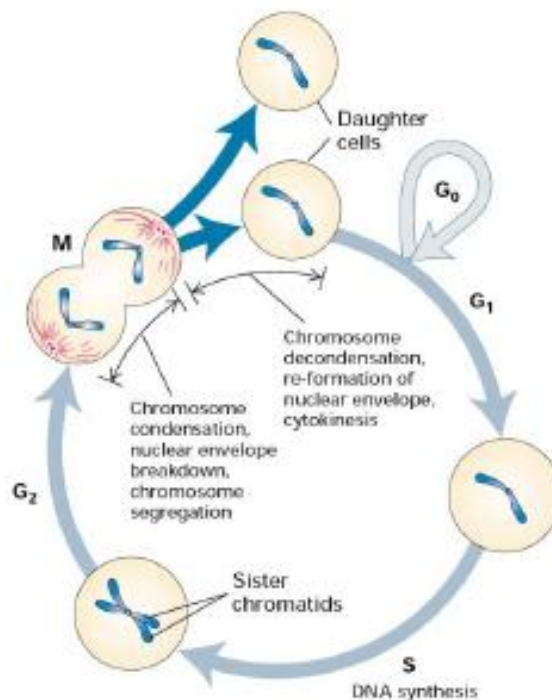


Figure 1.8. The eukaryotic cell cycle. Chromosomes are shown in condensed form emphasize the number of chromosomes at different cell-cycle stages. The nuclear envelope is not depicted. *Source: Molecular Cell Biology.*¹⁰

To keep within certain physiological limits the organization, structure and development of the organism, it is essential that cell proliferation be controlled and limited by a complex system of regulatory mechanisms. When cells cease proliferation, either due to specific antimitogenic signals or to the absence of proper mitogenic signalling, they exit the cycle and enter a non-dividing, quiescent state known as **G₀ phase** where the cells are in a state of duplicate rest, during which they perform the functions for which they were differentiated and specialized. Given this temporary rest or permanent state, external signals are required to stimulate the cell to start a new cell cycle and G₀ cells returning to the cell cycle enter into the S phase; this reentry is regulated, thereby providing control of cell proliferation. Exit from the cell cycle at G₁ is not occurring in every cell cycle.

To ensure proper progression through the cell cycle, cells have developed a series of checkpoints that prevent them from entering into a new phase until they have successfully completed the previous one. It is likely that newly divided or quiescent cells must also pass certain checkpoints before they can enter the cycle.

The cell cycle control systems consist in proteins, cyclins, and cyclin-dependent kinases, that regulate the entry of the cell into different stages of the cell cycle. These systems are also able to detect the behaviour of the cell during the cell cycle, thus delaying the entry into a particular phase when the cell is not ready yet.

Cyclins and their associated cyclin-dependent kinases (Cdks) are the central machinery that control cell cycle progression. Cdks that are required for cell cycle regulation consist of an active kinase subunit in complex with a regulatory subunit, or activator, commonly called cyclin. The cyclin-dependent kinases a group of serine/threonine kinases that form active heterodimeric complexes following binding to cyclins (Figure 1.9).¹¹ The Cdk/cyclin complex is subjected to several kinds of regulation, both positive and negative, for instance, by reversible protein phosphorylation. Phosphorylation at specific threonine residues by the Cdk activator kinase (CAK) and dephosphorylation at specific tyrosine residues by specific Cdk phosphatases render the Cdk active. At least nine different Cdks are known today, however, only some of them seem to be involved in cell cycle regulation.

INTRODUCTION

Each Cdk catalytic subunit can associate with different cyclins, and the associated cyclin determines which proteins are phosphorylated by the cyclin-Cdk complex. Several Cdks, mainly Cdk2, Cdk4, Cdk6 and possibly Cdk3, cooperate to drive cells through G₁ into S phase. Cdk4 and Cdk6 are thought to be involved in early G₁ whereas Cdk2 is required to complete G₁ and initiate S phase. Cdk4 and Cdk6 form active complexes with the D-type cyclins (cyclins D1, D2 and D3). Cdk2 is sequentially activated by the E-type cyclins (cyclin E1 and E2), during the G₁/S transition, and the A-type cyclins A1 and A2, during S phase.

An important mechanism for regulating Cdk activity involves the Cdk inhibitors, a diverse class of proteins that bind to and inactivate Cdks.^{12,13} These inhibitors are organized into two families based on structure and function: Waf or Cip/Kip Family; Waf1 (also known as p21 is one of the effectors of p53, a tumour suppressor that is important in the DNA-damage checkpoint, a crucial process for human cancer), Kip1 (p27) and Kip2 (p57) and the INK4 family (p16INK4a, p15INK4b, p18INK4c, p19INK4d).

Although the functions of Cdk inhibitors are complex, they are generally believed to regulate the cell cycle in response to growth-inhibitory signals, such as DNA damage, hypoxia and transforming growth factor (TGF).¹⁴ Alterations in any of these proteins, which lead to failure of cell cycle arrest, may thus serve as markers of a more malignant phenotype.¹⁵

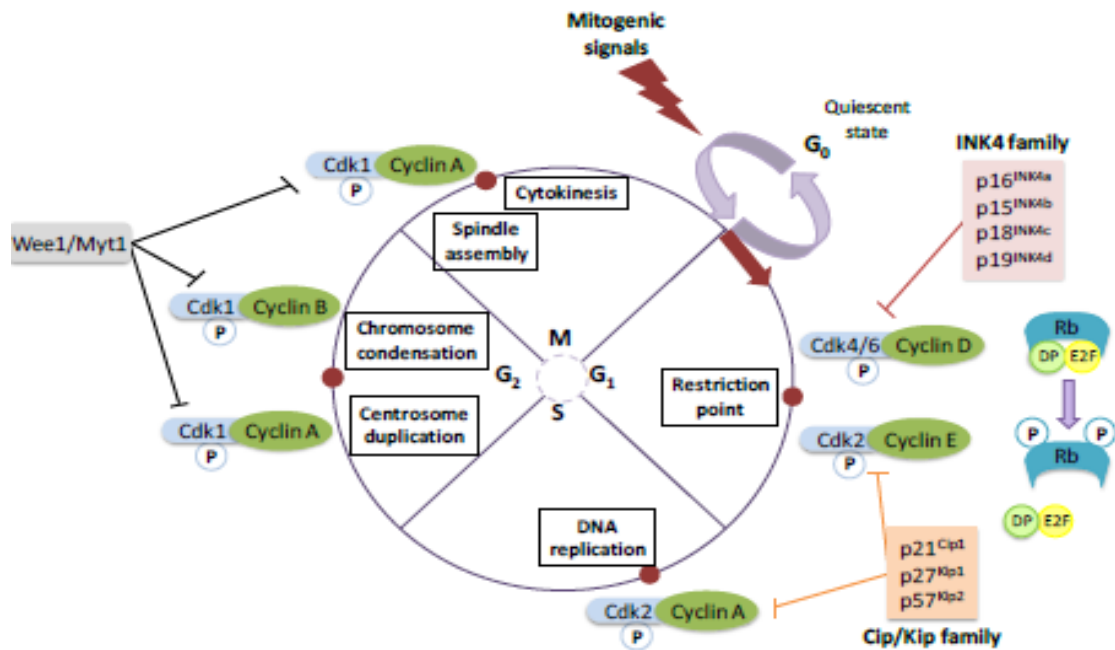


Figure 1.9. Cell cycle regulators and abnormalities in some human tumours. Alterations of cell cycle regulators in human tumours occur all along the different phases of the cell cycle. *Source:* Adapted from *Cell Adhesion & Migration*, 2010.¹⁶

In higher organisms, control of the cell cycle is achieved primarily by regulating the synthesis and activity of G₁-related Cdk complexes.¹⁰ Extracellular growth factors, called mitogens, induce the synthesis of G₁-related Cdk complexes. The activity of these and other Cdk complexes is regulated by phosphorylation at specific inhibitory and activating sites in the catalytic subunit. Once mitogens have acted for a sufficient period of time, the cell cycle continues through mitosis even when they are removed. The point in late G₁ where passage through the cell cycle becomes independent of mitogens is called the restriction point (Figure 1.10).^{17,18}

Failure of cell cycle arrest at the G₁-S transition can cause uncontrolled cellular proliferation. The product of the retinoblastoma susceptibility gene, the retinoblastoma protein (Rb), plays a central role in the G₁-S transition (Figure 1.10).

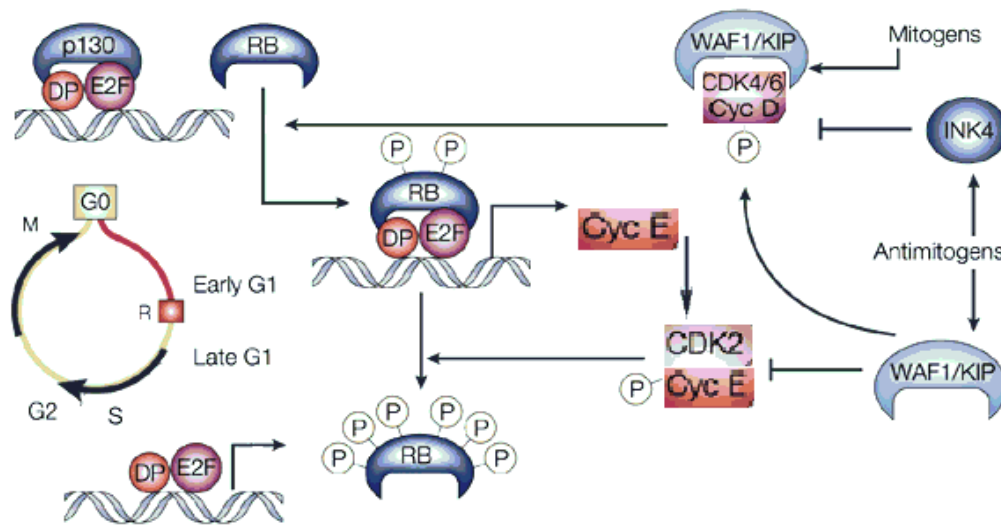


Figure 1.10. Regulation of G₁ phase and the G₁-S transition. R, restriction point. Adapted from *Nature Reviews Cancer*, 2001.¹⁹

In quiescent, G₀ cells, E2F-*DP* transcription factors are bound to p130, the principal pocket protein in these cells, which keeps them inactive.^{20,21} In G₁, however, Rb in its unphosphorylated state prevents progression from G₁ to S phase by binding the key transcription factor, E2F-*DP*.^{18,22} Mitogenic signalling results in cyclin D synthesis, formation of active cyclin D-Cdk4/6 complexes and initial phosphorylation of Rb. Partially phosphorylated Rb still binds to E2F-*DP*, but the transcription factor is still able to transcribe some genes, such as cyclin E, presumably due to impaired repression.^{23,24} Cyclin E binds to and activates Cdk2.¹² This then enables the cell to pass through the restriction point from which the cell proceeds through the remainder of the cycle.

It is generally accepted that Cdk2-dependent phosphorylation of Rb results in its complete inactivation, which allows induction of the E2F-responsive genes that are needed to drive cells through the G₁-S transition and to initiate DNA replication.^{23,25} Cyclin E-Cdk2 complex can also phosphorylate Rb, as well as other substrates, and is an important regulator of entry into the S phase of the cell cycle.¹² INK4 and WAF1/Kip proteins can inhibit Cdk4/6 or Cdk2 kinases, respectively, following specific antimitogenic signals.¹⁹ The Cdk4/6 complexes can also bind WAF1/Kip

inhibitors, while remaining active.^{26,27} This sequesters them from Cdk2, which facilitates its full activation.¹²

Progression through the S phase is principally regulated by the expression and kinase activity of the cyclin A-Cdk2 complex (see Figure 1.9).²⁸

The second major checkpoint in the cell cycle occurs at the transition from G₂ into M. Cyclin B1-Cdk1 is the classic M phase-promoting factor that drives entry into mitosis.²⁸ The association of cyclin B with the active form of Cdk1 initiates chromosome condensation, destruction of the nuclear membrane, and assembly of the mitotic spindle. Regulators of Cdk1 play a central role in the DNA damage-induced G₂ checkpoint, a cellular response to DNA damage that allows time for repair and prevents mitosis of damaged cells.¹¹

In cancer, there are fundamental alterations in the genetic control of cell division, resulting in an unrestrained cell proliferation.²⁸ In particular, genes that quite frequently undergo mutations are oncogenes and tumour suppressors. Damage is caused by mutations producing an oncogene with a dominant gain of function, and/or by mutations in tumour suppressor genes causing a recessive loss of function.

In normal cells, the products of proto-oncogenes act at different levels along the pathways that stimulate cell proliferation. Mutated versions of proto-oncogenes or oncogenes can promote tumour growth. Inactivation of tumour suppressor genes results in dysfunction of proteins that normally inhibit cell cycle progression.

Tumour suppressors are main effectors of the cell cycle clock; some of them are extrinsic factors in that they only act if the cell is damaged. The most important, in respect to cancer, are the well-known Rb protein and the transcription factor p53. Rb is a juvenile eye cancer that is caused by a mutation in the Rb gene, located on human chromosome 13. The main function of Rb is to connect the cell cycle clock to the transcriptional machinery (intrinsic mechanism). The Rb protein interacts with a protein called E2F, which is a nuclear transcription factor involved in cellular replication during the S phase. Interaction between Rb and E2F prevents E2F from functioning as a transcription factor. However, Rb is only able to bind E2F when it

is unphosphorylated. It will not interact with E2F in its hyperphosphorylated state. Rb mutants, which are constitutively phosphorylated and cannot bind E2F, provide uncontrolled cell division at the S-phase restriction site and cells may become tumourigenic. The “Rb pathway” is further discussed in view of the G₁-S transition phase below.

Another protein critical in regulating the cell cycle is the tumour suppressor protein p53, a DNA-binding protein regulating the expression of genes involved in cell cycle arrest. It senses DNA damage and tells the cell to either stop growing (until damage is repaired) or to kill itself by apoptosis (preventing unregulated cellular growth and formation of cancer), a typical extrinsic mechanism. p53 is the most frequently disrupted gene in human cancers. In fact, more than 50% of human cancers are associated with a p53 mutation, including cancers of the bladder, breast, cervix, colon, lung, liver, prostate, and skin. p53-related cancers are also very aggressive and have a high degree of lethality.

Cell cycle deregulation associated with cancer occurs through mutation of proteins important at different levels of the cell cycle. In cancer, mutations have been observed in genes encoding Cdks, cyclins, Cdk-activating enzymes, Cdk inhibitors, Cdk substrates, and checkpoint proteins.^{29,30}

The process of searching for new cancer drugs has undergone a major change: it has moved from a strategy of identifying drugs that kill tumour cells towards a more mechanistic strategy that seeks to act on molecular targets that underly cell transformation.³¹ The evidence that Cdks, their regulators and substrates are targets of genetic alteration in different types of human cancer has stimulated the search for chemical Cdk inhibitors.³² Different strategies for therapeutic intervention can modulate Cdk activity: targeting the major regulators of Cdk activity (indirect strategy) or inhibiting the catalytic activity of the Cdks (direct strategy). Approaches for the indirect strategy include overexpression of Cdk inhibitors, synthesis of peptides mimicking the effects of Cdk inhibitors, decrease of cyclin levels, modulation of the proteasomal machinery, modulation of the phosphorylated state of

Cdk and of the enzymes regulating it.^{30,33} Until now direct inhibition of Cdk kinase activity has been the most successful strategy for the development of potent cell cycle inhibitors. All inhibitors identified so far act by competitive inhibition of ATP (adenosine triphosphate) binding to Cdks. The potential for disruption of ATP binding to the small, defined ATP pocket of Cdks is much higher than disrupting a large protein–protein interface, such as a Cdk-cyclin binding surface.³¹

1.4.2. Cell death

Cells can be effectively eliminated following DNA damage by apoptosis, necrosis, mitotic catastrophe and autophagy,^{34,35} as well as by premature senescence, which irreversibly arrests cell division. Of these types of cell death, mitotic catastrophe and necrosis have traditionally been regarded as passive rather than programmed and genetically controlled. However recent studies have indicated that both necrosis³⁶ and mitotic catastrophe^{37,38} might sometimes be genetically regulated forms of death, following certain types of DNA damage.

Some of the characteristics of these different modes of cell death are summarized.³⁹

Apoptosis: cells visibly shrink and have condensed chromatin with nuclear margination and DNA fragmentation. Bebbing of cell membrane is often seen.

Necrosis: cells visibly swell and there is an early breakdown of the cell membrane. Cells have an atypical nuclear shape with vacuolization, non-condensed chromatin and disintegrated cellular organelles along with mitochondrial swelling. Typically not genetically determined.

Mitotic catastrophe: typically occurs after or during mitosis and is probably caused by missegregation of chromosomes and/or cell fusion. Cells often have micronuclei and it is common to see giant-cell formation or multinucleate cells. This can lead to apoptosis and is typically p53- independent.

Autophagy: this is a genetically regulated form of programmed cell death in which the cell digests itself. It is characterized by the formation of double-membrane vacuoles in the cytoplasm, which sequester organelles such as mitochondria and ribosomes. Autophagy is caspase- and p53-independent.

Senescence: senescent cells are metabolically active but non-dividing and show an increase in cell size. These cells express senescence-associated β -galactosidase and this process is generally p53-dependent.

1.4.2.1. Apoptosis

The term apoptosis is used to describe a series of events that lead to programmed cell death. In general, it is a physiological process that occurs during embryonic development, the development of central nervous system and in adult tissues with a high cell turnover. In addition, it plays an important role in the immune system. Therefore, it is an essential process for maintaining homeostasis in multicellular organisms.

Programmed cell death (apoptosis) is a natural process that removes unwanted cells such as those with potentially harmful mutations, aberrant substratum attachment, or alterations in cell cycle control. Deregulation of apoptosis can disrupt the delicate balance between cell proliferation and cell death and can lead to diseases such as autoimmune diseases or cancer.^{42,43} In many cancers, proapoptotic proteins have inactivating mutations, or the expression of antiapoptotic proteins is upregulated, leading to the unchecked growth of the tumour and the inability to respond to cellular stress, harmful mutations and DNA damage. In fact, the evasion of programmed cell death has been recognized as one of the essential alterations in cell physiology that dictate malignant growth and is a hallmark of most, and maybe all, types of cancer.¹

There are two fundamental pathways in apoptosis: the death receptor pathway and the mitochondrial pathway (Figure 1.11 shows a very simplified scheme of apoptosis). These pathways are intimately connected via a family of cysteine (Cys) proteases called caspases. There are two sets of caspases: initiator caspases and effector caspases. Initiator caspases (such as caspases 8, 9 and 10) transmit apoptotic signals and activate effector caspases (such as caspases 3, 6 and 7) that can then activate degradation enzymes that destroy the cell.

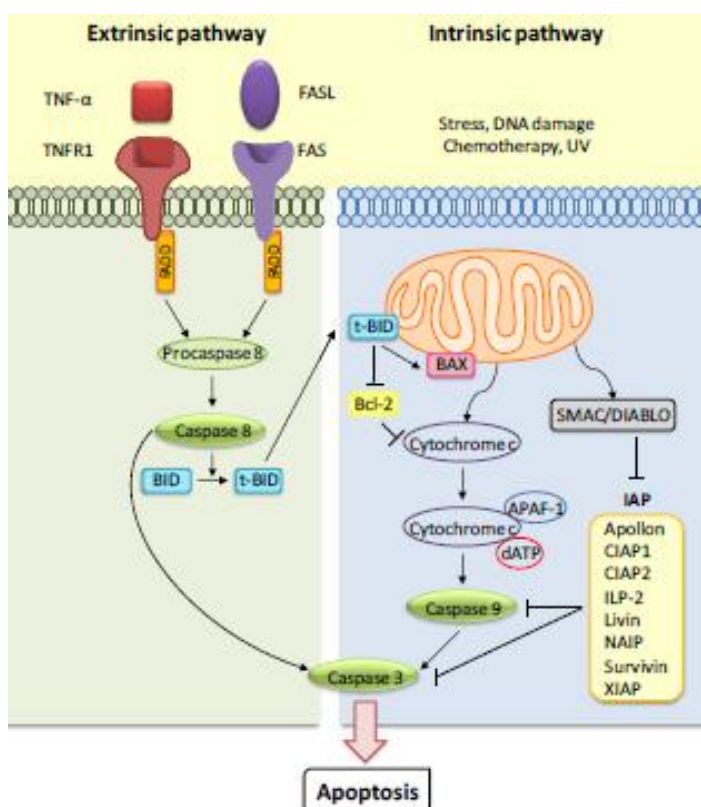


Figure 1.11. Source: Adapted from *Nature Reviews Cancer* 2005 .⁴⁴

The intrinsic pathway (Figure 1.11, right panel) involves the mitochondria. Upon receiving a death signal, cytochrome c is released from the intermembrane space of the mitochondria, which, together with dATP (2-deoxyadenosine-5-triphosphate) and apoptotic protease-activating factor 1 (APAF-1), activates caspase 9. Caspase 9 activates downstream caspases such as caspase 3, leading to apoptosis. Bcl-2 and Bcl-XL inhibit programmed cell death by preventing the release of cytochrome c, whereas pro-apoptotic Bcl-2 family members (such as BAK, BAX, BAD and BID) promote the release of cytochrome c.

The extrinsic cell death pathway (Figure 1.11, left panel) is mediated by death receptors. As an example, FAS ligand (FASL) interacts with the FAS receptor, leading to the interaction of the death domains of FAS with the death domain of the adaptor protein, FAS-associated death domain (FADD), which triggers the formation of activated caspase 8 and caspase 3 and causes the apoptotic response.

Cancers that possess alterations in proteins involved in cell death signalling are often resistant to chemotherapy and are more difficult to treat using chemotherapeutic agents than tumours lacking those alterations. Therefore, drugs designed to restore programmed cell death might be effective against many cancers.⁴⁵

Possible drug targets for modulating programmed cell death have been discovered from the work of many scientists in elucidating the protein components and regulators of the apoptosis signalling pathways. As previously mentioned, these pathways can be divided into two components: those that involve the mitochondria (intrinsic pathway) and those that signal through death receptors (extrinsic pathway) (Figure 1.11). In the death receptor pathway, ligands such as tumour-necrosis factor (TNF), FASL, or TNF-related apoptosis-inducing ligand (TRAIL) interact with their respective death receptors (TNF receptor 1 (TNFR1), FAS and death receptor 4 (DR4) or 5 (DR5), respectively).

These interactions ultimately lead to the recruitment of FADD and the activation of the protease caspase 8.⁴⁶ Caspase 8 cleaves and activates caspase 3 and other downstream caspases, which results in a proteolytic cascade that gives rise to the cell death phenotype characterized by DNA fragmentation, chromatin condensation, cell shrinkage and membrane blebbing. The intrinsic pathway involves the release of cytochrome c from the intermembrane space of the mitochondria. Cytochrome c interacts with APAF-1 and, together with dATP, they form a multimeric complex that recruits and activates caspase 9, leading to the activation of downstream caspases and the death response.⁴⁷

In addition to the proteins that are directly involved in cell death signalling, proteins that regulate programmed cell death could also represent potential cancer drug targets. For example, Bcl-2 family members⁴⁸ that are localized in the mitochondria can either prevent or cause the release of cytochrome c from the mitochondria to either inhibit or promote apoptosis. Another important protein family that regulates apoptosis is the inhibitor of apoptosis (IAP) proteins, which bind to and inhibit caspases and block apoptotic signalling.⁴⁶ IAPs are regulated by SMAC (second mitochondria-derived activator of caspases),⁴⁹ also known as DIABLO (direct IAP binding protein with low isoelectric point),⁵⁰ which is released from the mitochondria once the cell has received a death signal. SMAC binds to the IAPs and antagonizes their antiapoptotic activity.

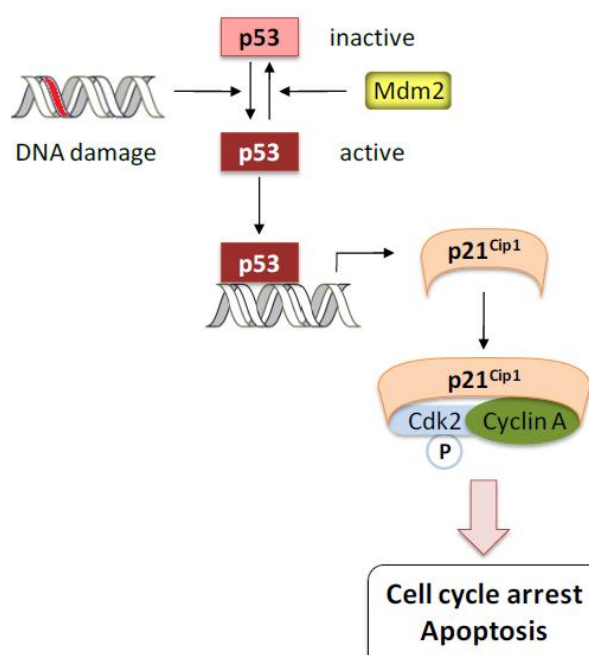


Figure 1.12. p53 gene activation process.

Murine double minute protein (Mdm2) and p53 are also important regulators of programmed cell death.⁵¹ Upon sensing DNA damage, p53 induces cell-cycle arrest and apoptosis (Figure 1.12). p53 is mutated and inactivated in half of all cancers analyzed, demonstrating the importance of disrupting the p53 pathway in cancer development. Inactivation of p53 can also occur by p53 binding to Mdm2, which leads to the degradation of p53 by the proteasome. Therefore, disruption of the

interaction between p53 and Mdm2 should stabilize p53 and enable its apoptotic function.⁵¹

1.4.2.1.1. eIF2

Eukaryotic initiation factor eIF2 originally was identified over 25 years ago as a protein that binds to GTP and to the initiator methionyl-tRNA_i eIF2 ternary complex (Met-tRNA_i) and mediates the association of Met-tRNA_i to the 40S ribosomal subunit.⁵²

eIF2 is a multimeric protein consisting of three dissimilar subunits termed α , β , and γ , in order of increasing molecular mass (Figure 1.13). cDNAs for each of the subunits have been cloned and sequenced from a variety of species, and the predicted amino acid sequences of the individual subunits show an exceptional level of conservation among species.

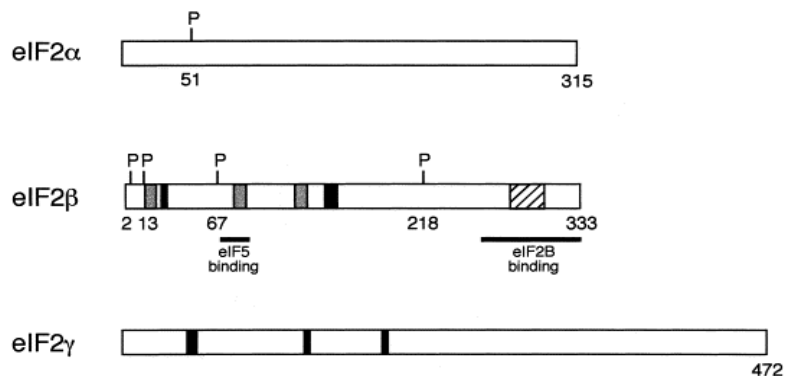


Figure 1.13. Domain structure of human eIF2 α -, β -, and γ -subunits. The number of amino acids in each eIF2 subunit is shown to the right and just below the open boxes representing the polypeptide chains. Known phosphorylation sites are represented by a 'P' above the boxes with the residue number shown below it. In eIF2 β , CK-II phosphorylates Ser2 and Ser67, PKC phosphorylates Ser13, and PKA phosphorylates Ser218.⁵³

The eIF2 α amino acid sequence is unremarkable with the exception of Ser51, which is a phosphate acceptor for protein kinases which are activated in response to cellular stresses. Physiological conditions which result in eIF2 alpha phosphorylation include

virus infection, heat shock, iron deficiency, nutrient deprivation, changes in intracellular calcium, accumulation of unfolded or denatured proteins and the induction of apoptosis.

The primary role of eIF2 in translation initiation (Figure 1.14), is to transfer Met-tRNA_i to the 40S ribosomal subunit.⁵² Following the association of mRNA with the 40S subunit and location of the subunit at the AUG start codon, eIF5 binds to eIF2 and stimulates the hydrolysis of eIF2-bound GTP. It has been proposed that either eIF5 or the β - or γ -subunits of eIF2 contains the GTPase activity responsible for GTP hydrolysis. However, eIF5 stimulates GTP hydrolysis only when eIF2 is bound to the 40S subunit as a ternary complex with GTP and Met-tRNA_i.⁵⁴

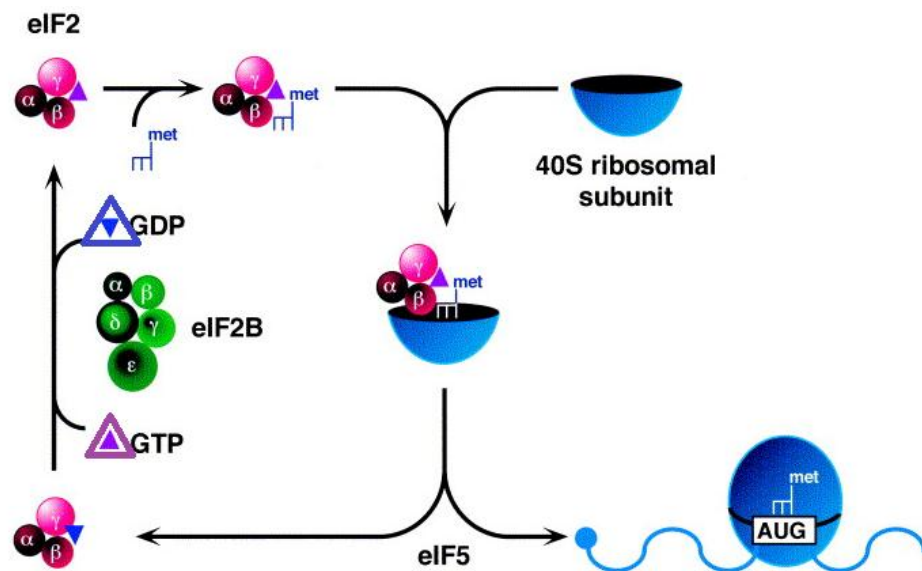


Figure 1.14. Scheme depicting the role of eIF2 in the initiation of mRNA translation.

Prior to binding Met-tRNA_i, the GDP bound to eIF2 must be exchanged for GTP, a reaction mediated by eIF2B.⁵⁵ Phosphorylation of eIF2 α on Ser51 converts eIF2 from a substrate into a competitive inhibitor of the guanine nucleotide exchange factor eIF2B and prevents the recycling of eIF2 between successive rounds of protein synthesis. Phosphorylation of eIF2 α in response to cellular stress reduces the exchange of eIF2-GDP to eIF2-GTP required to bind and deliver initiator to the translation machinery.⁵⁶

Therefore, it has always been assumed that one, or more, subunits of eIF2B bind to eIF2 α . However, in a recent study, the only detected interaction between eIF2 and eIF2B was the binding of eIF2 β to the δ - and ϵ -subunits of eIF2B,⁵⁷ suggesting that eIF2 α phosphorylation might cause a structural alteration in eIF2 β that results in a change in the affinity of eIF2B for eIF2. In addition, in yeast, point mutations in the α -, β -, and δ -subunits of eIF2B result in an apparent change in the affinity of the protein for phosphorylated eIF2. This result suggests that in vivo the α - and β -subunits of eIF2B may also be important in regulating interactions between eIF2 and eIF2B.

eIF2 α phosphorylation is a critical control point in the regulation of gene expression under conditions such as viral infection, apoptosis, and cell transformation.⁵⁸ Extensive phosphorylation of eucariotic initiation factor eIF2 alpha and strong inhibition of eIF2B activity can result in the downregulation of the overall rate of protein synthesis, inhibition of protein translation and it is a mode of inducing apoptosis (Figure 1.15). So, an increase in the phosphorylation of eIF2 alpha, can be responsible for the very early inhibition of protein synthesis, and it produces one of the earliest effect of apoptosis inducers.

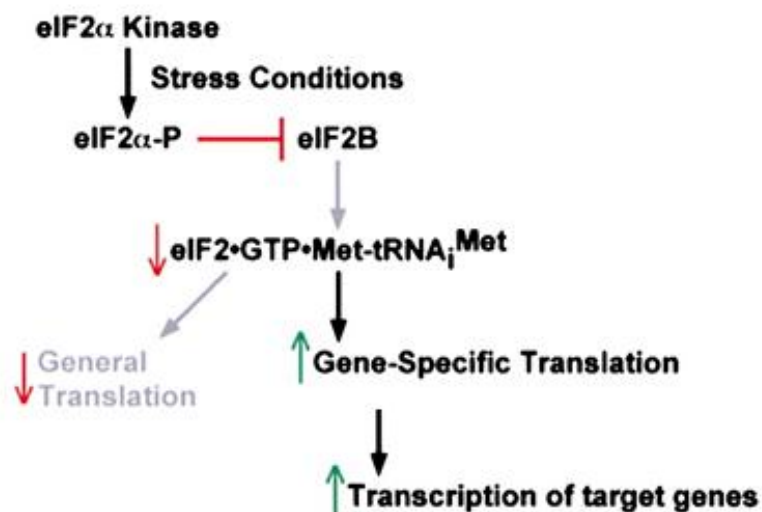


Figure 1.15. Phosphorylation of eIF2 α in response to cellular stress.

1.5. Tumour angiogenesis

Once malignant transformation has occurred, tumour cells, like all cells, require oxygen and nutrients for expansion. When tumours are small (<1 mm in diameter), they rely on diffusion to meet these needs. In order to grow larger, tumours must create a new blood supply to deliver nutrients and oxygen as well as to remove waste products. The transition from a prevascular, where the number of proliferating cells is counterbalanced by the number of apoptotic cells, to vascular stage is induced by a phenomenon called “angiogenic switch”, in which the tumour acquires a vascular phenotype, with formation of new capillaries, and begins the invasion of the surrounding tissue. This phenomenon depends on a positive balance between pro- and antiangiogenic factors⁵⁹ (Figure 1.16).

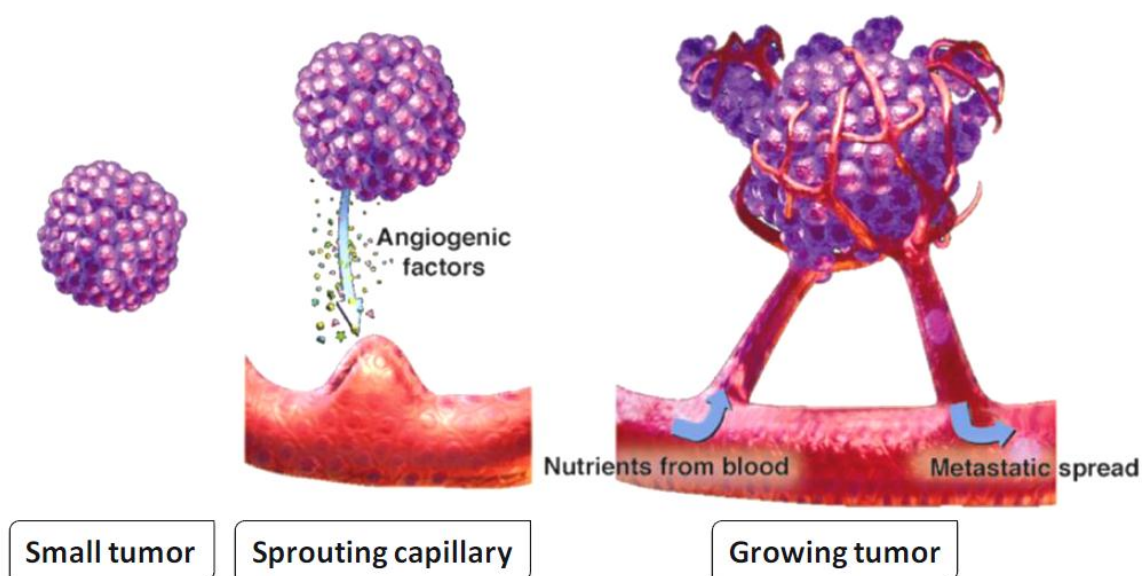


Figure 1.16. The angiogenic switch is necessary for tumour growth and metastasis. *Source: Horizons in Cancer Therapeutics: From Bench to Bedside. 2002.*⁵⁹

1.5.1. Angiogenic growth factors

Vascular endothelial cell growth factor (VEGF) is a potent growth factor for endothelial cells. Its expression is stimulated by tissue hypoxia, as well as several

different growth factors and cytokines. It binds to its receptors, VEGFR1 and VEGFR2, causing proliferation and migration of endothelial cells.⁶⁰

Platelet-derived growth factor (PDGF) is secreted from platelets and increases DNA synthesis, endothelial cell migration and tumour growth.⁶⁰ Basic fibroblast growth factor (bFGF) is released by proteolytic enzymes from the extracellular matrix, after which it increases the expression of other proteolytic molecules. It is proangiogenic and increases tumour growth.⁶⁰

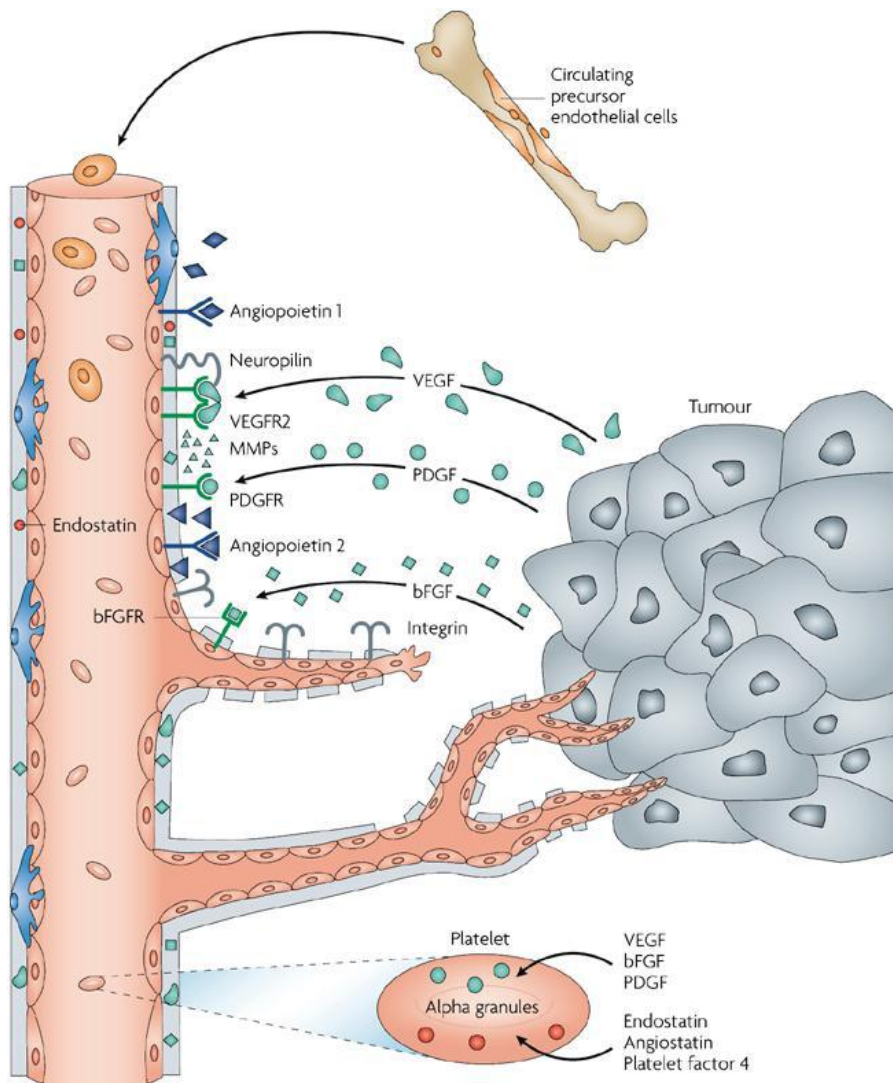


Figure 1.17. Growth factors involvement in tumour angiogenesis. bFGFR, fibroblast growth factor receptor; MMPs, matrix metalloproteinases; PDGFR, platelet-derived growth factor receptor.

Source: Adapted from *Nature Reviews Drug Discovery*, 2007.⁶¹

Although VEGF, PDGF and bFGF are the primary growth factors involved in the angiogenic process, several other growth factors also play a role in the development of tumoural blood supply. For instance, many cells types with proangiogenic properties can be mobilized from the bone marrow and can intravasate into sites of new blood-vessel formation.⁶² The main growth factors involvement in angiogenesis are schematically depicted in Figure 1.17.

1.5.2. Inhibitors of angiogenesis

Tumours may activate angiogenic inhibitors such as angiostatin and endostatin which control growth by suppressing endothelial cell proliferation and angiogenesis and by indirectly increasing apoptosis in tumour cells.

1.6. Metastasis

The final stage of tumour progression is metastasis. Neovascularization of the primary tumour induces that cancer cells come into contact with the bloodstream and are able to spread to other organs. Metastasis is a multi-stage process that requires cancer cells to escape from the primary tumour, survive in the circulation, seed at distant sites and grow. Each of these processes involves rate-limiting steps that are influenced by non-malignant cells of the tumour microenvironment. Many of these cells are derived from the bone marrow, particularly the myeloid lineage, and are recruited by cancer cells to enhance their survival, growth, invasion and dissemination.⁶³

A variety of stromal cells in the surrounding environment are recruited to tumours, and these not only enhance growth of the primary cancer but also facilitate its metastatic dissemination to distant organs.

Cancer cells in an aggressive primary mass are adept at exploiting that particular tissue microenvironment; however, once they leave these favourable surroundings, they must possess traits that will allow them to survive in new environments. In order for a metastasis to occur, the intravasated cancer cell must survive in the circulation, arrive at the target organ (seeding), extravasate into the parenchyma and show persistent growth⁶⁴ (Figure 18). Each of these stages is inefficient and some are rate limiting.^{64,65} For example, senescence or apoptosis of cancer cells at the stage of entry into the metastatic site prevents the spread of the majority of circulating cells.^{65,67} Seeding can occur to multiple organs, but metastatic tumours may grow in only one or a few.⁶⁸

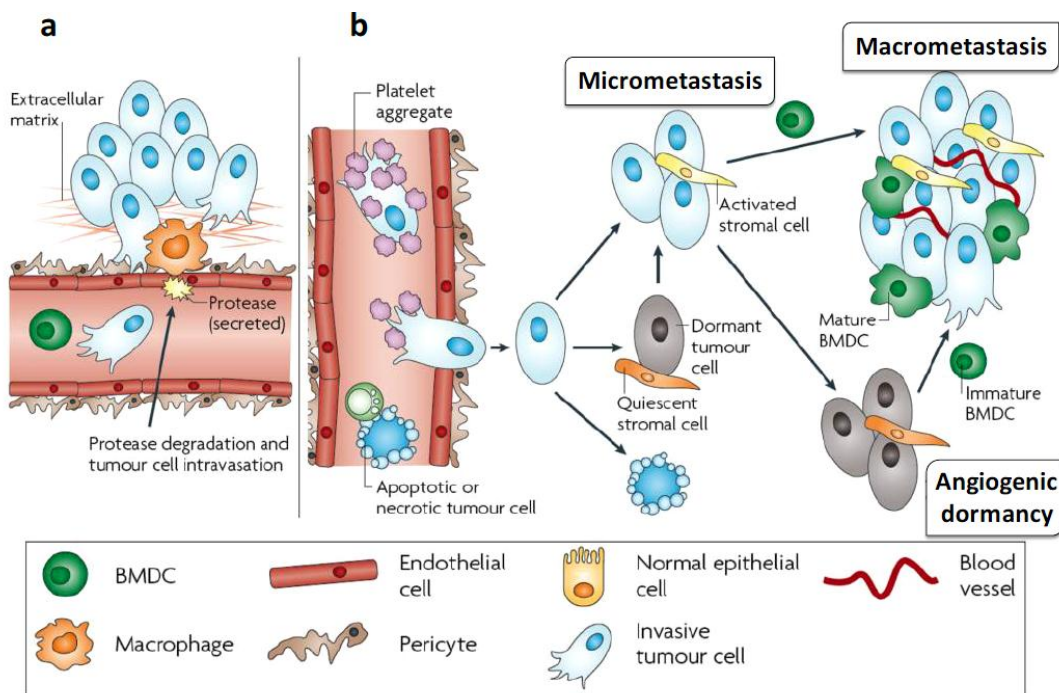


Figure 1.18. The invasive microenvironment. **a.** Cancer cell intravasation into the blood circulation preferentially occurs in close proximity to perivascular macrophages. Disruption of endothelial cell contacts and degradation of the vascular basement membrane is required for cancer cell intravasation, which is mediated by proteases supplied from the cancer cells, macrophages or both. **b.** Following cancer cell intravasation, a series of rate-limiting steps affect the ability of these cells to establish secondary tumours in the metastatic site. At each step, the tumour cells can meet several different fates (death, dormancy or survival), which can be modulated by microenvironmental factors, including shielding by platelet aggregates in the circulation, the activation of resident stromal cells, and the recruitment and differentiation of bone marrow-derived cells (BMDCs). *Source:* Adapted from *Nature Reviews Cancer*, 2009.⁶⁹

There is also increasing evidence that in some cases cancer cells can remain dormant for many years, and that seeding may occur several years before diagnosis of the primary tumour.⁷⁰⁻⁷⁴ In another phenomenon, termed angiogenic dormancy, there is a balance of proliferation and apoptosis that results in micrometastases that do not progress further.^{75,76} The microenvironment clearly suppresses the malignancy of these potentially metastatic cells,⁷⁴ and their re-activation to form a clinically relevant metastasis probably occurs through perturbations in the microenvironment.

1.7. Core molecular signalling pathways involved in malignant cell behaviour

Although cellular signalling processes are diverse and comprise multiple proteins that are interconnected in complex networks, several lines of evidence indicate that a limited set of mechanisms and major pathways are almost always affected, directly or indirectly, by oncogenic alterations.

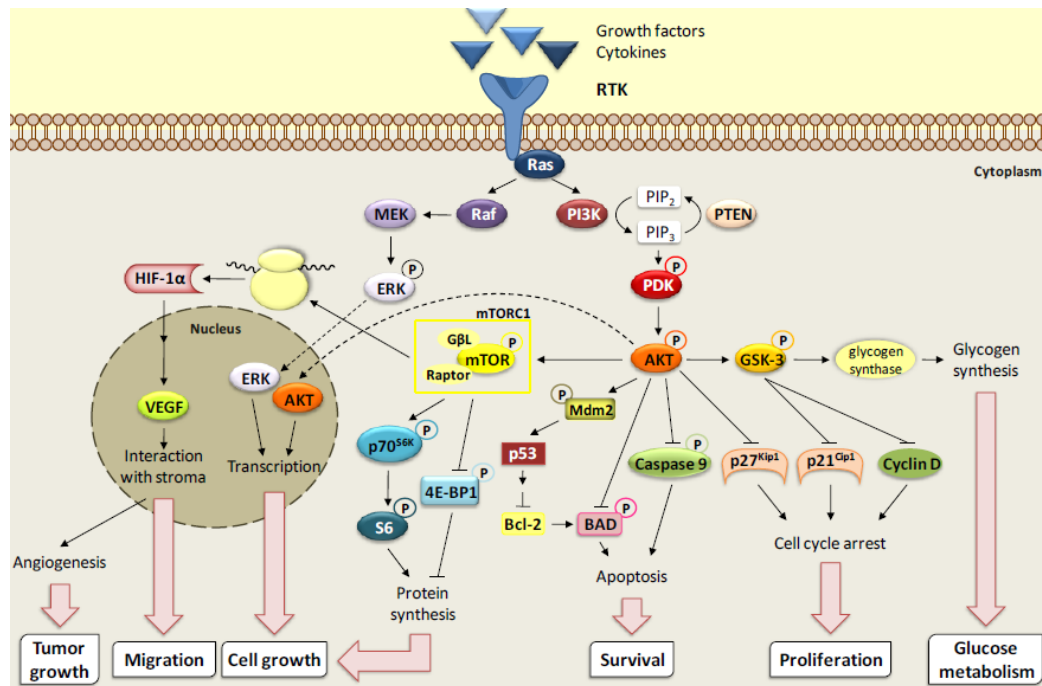


Figure 1.19. Schematic overview of cellular signalling through the PI3K/AKT pathway. Activation of receptor tyrosine kinases (RTK) by external growth factors initiates receptor

dimerization and subsequent events to activate intracellular pathways. AKT is activated downstream of PI3K and has multiple targets.

Consequently, the key components of these pathways are obvious target candidates for pharmacological treatment in cancer.⁷⁷

A simplified scheme of some of the major signalling pathways involved in cell growth and malignancy, some of which are drug targets, are shown in Figure 1.19.

One main road linking stimulation by external mitogens to cell proliferation, proceeds through receptor tyrosine kinases (RTKs), the signal-integrating proteins of the Ras family, and a protein kinase cascade that starts with the serine/threonine kinase Raf. This pathway leads to activation of the extracellular signal-regulated kinase (ERK), a dual specificity kinase (with isoforms ERK1 and ERK2) belonging to the mitogen-activated protein kinase (MAPK) family.⁷⁸ ERK signalling strength determines cell responses (Figure 1.20) and it controls a large variety of cell functions, including the expression of many genes, and is essential for cell proliferation, acting through transcription factors that trigger the cell cycle program.⁷⁹

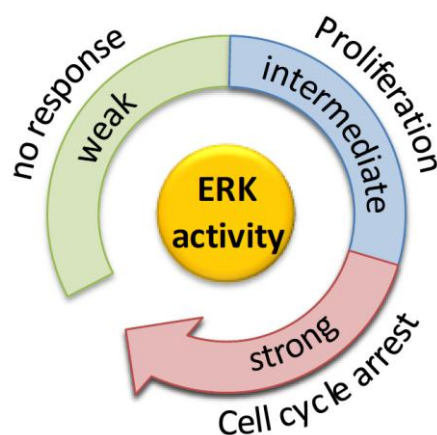


Figure 1.20. ERK signalling strength determines cell responses. Weak ERK signalling does not stimulate any cell responses. Intermediate cell responses lead to proliferation, whereas high levels of signalling stimulate cell cycle arrest and favor differentiation or senescence. *Source: Cancer Drug Design and Discovery.*⁸⁰

The pathway mediated by PI3K is another major signalling route frequently implicated in oncogenic alterations.^{81,82} PI3K is a lipid kinase that phosphorylates inositol lipids in the plasma membrane in 3-position, primarily converting phosphatidylinositol-4,5-bisphosphate (PIP2) to phosphatidylinositol-3,4,5-trisphosphate (PIP3), thereby creating points of attachment and activation for several signalling proteins. The serine/threonine protein kinase AKT (also termed protein kinase B, PKB) is a major downstream signalling component in this pathway. One of the downstream consequences of PI3K activation is stimulation of mTOR, a serine/threonine protein kinase which is a major coordinator of cell regulation and is a target for therapy.⁸³ There is also an inherent brake in the PI3K pathway, since the lipid phosphatase PTEN (phosphatase and tensin homologue) converts PIP3 back to PIP2 and thus reverses the effect of PI3K. PTEN is an important tumour suppressor,⁸⁴ reflecting the necessity of keeping the PI3K pathway under strict control. Signalling through PI3K and mTOR acts in concert with the ERK pathway in activation of the cell cycle, but, in addition, it has a particular role in downregulating apoptosis to sustain cellular viability.⁸⁵

Uncontrolled activity in these pathways, most often as a result of mutations, is commonly involved in oncogenesis. In some cases there are oncogenic mutations in RTKs⁸⁶⁻⁸⁸ (Table 1.1).

In the ERK pathway, the majority of cancer-associated alterations are activating mutations at the early steps, affecting Ras (K-Ras or N-Ras), Ras-regulating proteins such as neurofibromatosis-related protein (NF1), or Raf (usually B-Raf).⁸⁹⁻⁹¹ In the PI3K pathway, several oncogenic lesions are found, loss-of-function mutations or downregulation of PTEN being the most frequent.^{84, 92} Some of the dysregulated proteins in these pathways are targets for therapeutic strategies while others are currently not accessible to pharmacological approaches.⁹³

Table 1.1. Abnormalities in PI3K/AKT pathway in cancer. *Source:* Adapted from *The Journal of Urology*, 2009.⁹⁴ p55 γ , isoform of p85; p70S6K, 70 kDa S6 kinase; *PIK3CA*, gene encoding the p110 α PI3K subunit; PI3KCA, PI3K catalytic subunit, TCL1, T-cell leukemia 1; TSC1/2, tuberous sclerosis complex 1 and 2.

Molecule	Alteration	Frequency	Tumor Type(s)
Forkhead family	Translocations	>50%	Alveolar rhabdomyosarcoma, acute leukemia (low)
p55 γ	Deletion/mutation	Unknown	Lung
p70 ^{S6K}	Amplification	30%	Breast
p85	Activating mutations	Rare	Ovary, colon, glioma, lymphoma
	Fusion	Very rare	Lymphoma
PDK1	Mutation	Low	Colorectal
<i>PI3KCA</i>	Amplification	Up to 50%	Ovary, cervix, lung, breast cancer (BRCA-1 associated) (rare)
PI3KCA	Activating mutation	>25%	Breast
PTEN	Germline mutations	80% of Cowden's disease	High risk of breast, thyroid and endometrial carcinomas
	Somatic mutations	>50%	Glioma, melanoma, prostate, endometrial. Variable in sporadic breast cancers (2–30%)
B-Raf	Mutation	10-40%	Melanoma, thyroid, biliary tree, colon, ovary
H-Ras	Mutation	Low	Bladder, cervix, melanoma.
K-Ras	Mutation	10-50%	Pancreas, colon, biliary tree, lung, endometrial ovary
N-Ras	Mutation	Low	Melanoma, biliary tree
TCL-1	Rearrangement	Unclear	T-cell leukemia, chronic lymphocytic leukemia
TSC1/2	Mutation	>50%	Tuberous sclerosis

1.8. Cancer treatment

The current cancer treatment is multidisciplinary and rarely consists of a single strategy. Thus, it is common to employ at least two different treatments against cancer at the same time: surgery and chemotherapy, chemotherapy and radiotherapy... treatments against cancer are:

- **Surgery:** which is used in both pre-cancerous stages, eliminating lesions that may eventually become malignant (cutaneous carcinomas associated with burns, chronic skin ulcers ...) and treatment of cancer itself. In addition, surgery may be important in palliative care for particular patients in advanced stages.
- **Radiotherapy:** which is used in slightly more than 50% of patients with cancer, although it is applied with different intensities depending on the stage of the disease. Thus, it is used in small doses and low intensities in patients with advanced or metastatic stages (palliative radiotherapy) and at high doses and high intensities in early stages or after surgery (post-operative radiotherapy). Hypoxic cells are more resistant to X-, gamma- and beta- rays, so radiotherapy is usually administered in combination with chemotherapeutic agents that increase the sensitivity of these cells to radiation.
- **Chemotherapy:** nowadays between 20 and 30 valid chemotherapeutic agents are available for the treatment of cancer and many of them have side effects [neutropaenia, oral ulcers, diarrhea, pulmonary fibrosis (methotrexate), hair loss, nerve damage (cisplatin, taxanes, Vinca alkaloids), heart damage (anthracyclines), kidney damage...]. These compounds are usually administered jointly, in order to cover different mechanisms of cell death induction.
- **Anti-angiogenesis:** both chemotherapy and anti-angiogenesis use drugs that travel throughout the body to have their effects. But anti-angiogenesis drugs don't attack cancer cells directly. Instead, they target the blood vessels the cancer cells need to survive and grow.

By doing this, they may help prevent new tumours from growing and make large tumours shrink if their blood supply is cut off, with no toxicity to most healthy cells. These drugs may prove to be most useful when given with other forms of treatment.

1.8.1. Cellular mechanisms as targets for antitumour therapy

Table 1.2. Investigational therapeutic targets and agents in use for cancer treatment.

Pathway/ protein target	Oncogenic mechanism	Drug class	Molecular target(s)	Drugs in clinical trials	
PI3K/AKT pathway	Aberrant regulation of the cell cycle and, downregulation of apoptosis.	Tyrosine kinase inhibitors	PI3K	Wortmannin LY294002	BEZ235 BGT226 BKM120
			AKT	Perifosine (KRX-0401) VQD-002 (TCN-P)	MK2206 XL418
mTOR	Aberrant regulation of cell growth, proliferation, apoptosis, angiogenesis, nutrient uptake	Tyrosine kinase inhibitors	mTORC1	Rapamycin (Rapamune®) Temsirolimus (Torisel®) Everolimus (Afinitor®)	
MAPK pathway	Aberrant gene expression and cell proliferation	Tyrosine kinase inhibitors	Raf	Sorafenib (Nexavar®)	
			MEK	PD98059 U0126	CI-1040 (PD18435) PD0325901
RTKs	Tumor proliferation, angiogenesis	Tyrosine kinase inhibitors	EGFR, HER2, PDGFR, VEGFR, BCR- ABL, Kit	Cetuximab (Erbix®)	Lapatinib (Tykerb®)
				Trastuzumab (Herceptin®) Gefitinib (Iressa®) Erlotinib (Tarceva®) Sorafenib (Nexavar®)	Vandetanib (Vandetanib®) Imatinib (Gleevec®) Nilotinib (Tasigna®) Dasatinib (Sprycel®) Sunitinib (Sutent®)
Proangiogenic signaling	Angiogenesis	Antibody	VEGF	Bevacizumab (Avastin®)	
		Thioredoxin inhibitors	Trx-1	PX-12 Pleurotin (NSC-131233) Flavopiridol (Alvocidib®) R-roscovitine (Seliciclib®)	
Cell cycle	Aberrant regulation of the cell cycle and apoptosis. DNA damage	Small molecule	Cdk5		2-methoxyestradiol (Panzem®)
				Microtubule assembly dynamics	Paclitaxel (Taxol®) Docetaxel (Taxotere®) Eribulin mesylate (Halaven®) Cabazitaxel (Jevtana®)
Ubiquitin- proteasome pathway	Dysregulation of cell cycle proteins	Small- molecules	IκB	Bortezomib (Velcade™)	
Cell-mediated immunity, cytokines	Aberrant activation of prosurvival cytokines and cellular immune response	IMiDs	TNF-α, IL-6, IL- 8, and VEGF; T cells and NK cells	Lenalidomide (Revlimid®)	
Histone deacetylase 125	Dysregulated histone deacetylation in promoters of growth regulatory genes	HDACIs	HDAC	Vorinostat (Zolinza®) Romidepsin (Istodax®) Valproic acid Panobinostat (LBH589)	

EGFR, epidermal growth factor receptor; HDAC, histone deacetylase; HDACI, histone deacetylase inhibitor; HER2, human epidermal growth factor receptor 2; IL-6, interleukin-6; IL-8,

interleukin-8; IMiD, immuno-modulatory drug; I κ B, nuclear factor- κ B inhibitory protein; MEK, mitogen-activated protein kinase kinase; mTORC1, mammalian target of rapamycin complex 1; NK, natural killer; PARP, poly (ADP-ribose) polymerase; PDGFR, platelet-derived growth factor receptor; TNF- α , tumour necrosis factor-alpha; Trx-1, thioredoxin 1; VEGFR, vascular endothelial growth factor receptor.

Many cellular mechanisms are potential targets, but presently the majority of the signal inhibitors exert their effects by blocking the catalytic activity of the various protein kinases⁹⁵⁻⁹⁷ (Table 1.2).

Due to the crucial importance, ubiquity, and diversity of protein phosphorylation as a mechanism for regulation of cellular activities, the protein kinases that catalyze the specific transfer of phosphate to proteins from ATP are a major focus in the efforts to interfere therapeutically with signal transduction.⁹⁵ Virtually all signalling pathways involve protein phosphorylation. While both serine/threonine- and tyrosine-specific protein kinases are essential in cellular regulation, tyrosine phosphorylation is implicated particularly in signalling that stimulates proliferation and promotes malignant cell behaviour.⁹⁸ Many tyrosine kinases, but also some serine/threonine kinases, are affected by oncogenic mutations.⁹⁹ Since protein kinases are quite selective in their actions, they represent a wide spectrum of specific and exploitable targets for drugs.¹⁰⁰

1.8.2. Efforts to improve cancer treatment

The biggest impact on reducing the cancer burden to public health derives from screening programmes that detect cancer early, or even detect abnormal cells in the precancerous state.¹⁰¹ Experience has shown that cancer can be eradicated only if it is caught early. With the advent of genomic and proteomic arrays, it is likely that molecular markers will soon be available for early detection of many cancers. Proteomics profiles of serum that detect ovarian, breast, prostate, and head and neck cancers have been reported.¹⁰² It is important to find suitable markers for precancerous lesions and localized tumours and to develop inexpensive, robust

technologies that can be used in the clinical setting. Some of these new markers will also be effective targets for signal-transduction therapy.

Molecular targeting has a role in prevention of cancer, as well as in its treatment. Most of the current drugs cause side effects too harsh to warrant their administration for long periods of time or high doses. Better molecular drugs, with minimal side effects, will make their mark on reducing cancer progression, alongside with programmes to promote healthier nutrition and lifestyles.

For further progress in signal-targeted cancer therapy, it is crucially important to be able to individualize the treatment to a greater extent than that applied nowadays. As we learn more about the diversity of cancer biology and we are faced with an increasing repertoire of treatment options, it is necessary to have methods for selecting the patients that can benefit from a given therapeutic principle. Such methods, based on the knowledge of the molecular determinants of the specific cancer, are increasingly being used in diagnostic medical routine.¹⁰³ Further research focussing on translating basic insights into clinically useful predictive markers is essential.

Contrary to the earlier idea that signal-targeted drugs, particularly those inhibiting angiogenesis, are not likely to be affected by resistance development, the experience has clearly shown that resistance is a problem also with these agents, like any other antitumour drugs.

At the molecular level, primary or acquired resistance against signal inhibitors can involve mechanisms at different levels.^{104,105}

- Mutations affecting the target protein
- Pathway redundancy
- Activating alterations downstream of the target

Combination therapy is the best approach to avoid selection for cancer cells that are resistant to therapy. The approach of reducing tumour load by means of a targeted inhibitor combined with immunotherapies, to stimulate the immune response against the tumour, might succeed in controlling the disease for longer periods.¹⁰⁶ Nevertheless, a more thorough understanding of the complex interactions between signalling pathways is necessary before we will be able to predict the effects of inhibiting specific targets, individually or in combinations.¹⁰⁷ By assessing to what degree these drugs are fulfilling their promise, we can redirect strategies for combating cancer. The new drugs might allow us to ‘tame’ more advanced cancer into a controlled, quiescent state.

However, the major cause of death for cancer patients is metastasis.⁵ There is considerable evidence that metastases migrate to distant sites early, even before the primary tumour is diagnosed, but not all disseminated cancer cells develop into metastases.¹⁰⁸ In the future, it might be possible to determine the proliferative potential of disseminated cancer cells, and use this as a basis for choosing active treatment or surveillance.¹⁰⁹

In some cases, when patients stop taking a treatment they relapse. The re-emergent disease is not due to mutation, as it sometimes can be controlled by resuming treatment.^{110,111} The recurrence of the disease could be due to cancer stem cells (CSCs). CSCs refer to a subset of tumour cells that has the ability to self-renew and generate the diverse cells that comprise the tumour.¹¹²⁻¹¹⁴ These cells have been termed cancer stem cells to reflect their ‘stem-like’ properties and ability to continually sustain tumourigenesis.

CSCs share important properties with normal tissue stem cells, including self-renewal (by symmetric and asymmetric division) and differentiation capacity, albeit aberrant. Multilineage differentiation, however, is not a mandatory feature of a CSC. One implication of the CSC model is that cancers are hierarchically arranged with CSCs lying at the apex of the hierarchy¹¹² (Figure 21). The first evidence for the existence of CSCs came from acute myeloid leukemia,^{112,115,116} but cancer stem cells are not a peculiarity of leukemia as they have already been demonstrated for breast¹¹⁷ and brain tumours¹¹⁸⁻¹²³ and colorectal^{124,125} and pancreatic¹²⁶ carcinomas.

CSCs themselves undergo clonal evolution, as shown for leukemia stem cells.¹²⁷ Thus, a second, more dominant CSC may emerge if a mutation confers more aggressive self-renewal or growth properties. CSCs are distinct from the cell of origin. The cell of origin specifically refers to the cell type that receives the first oncogenic hit(s). Moreover, CSCs do not necessarily originate from the transformation of normal stem cells, but may arise from restricted progenitors or more differentiated cells that have acquired self-renewal capacity.

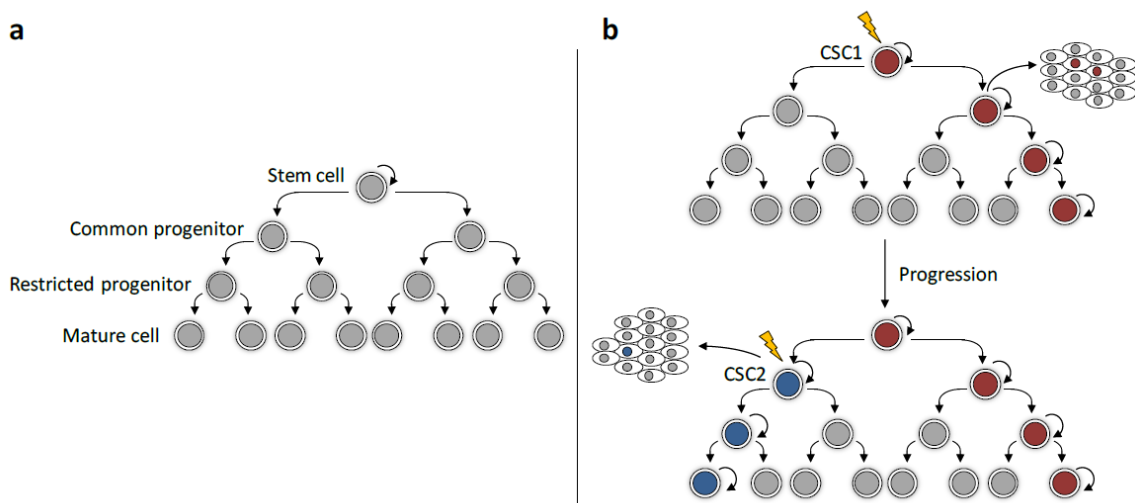


Figure 1.21. Models for tumour heterogeneity and propagation. **a.** A normal cellular hierarchy comprising stem cells (at the apex), which progressively generate common and more restricted progenitor cells, ultimately yielding all the mature cell types that constitute a particular tissue. **b.** In the cancer stem cell (CSC) model, only the CSC can generate a tumour, based on its self-renewal properties and enormous proliferative potential. Initially, tumour growth will be driven by a specific CSC (CSC1). With tumour progression, another distinct CSC (CSC2) may arise due to clonal evolution of CSC1. This may result from the acquisition of an additional mutation or epigenetic modification. This more aggressive CSC2 becomes dominant and drives tumour formation. *Source:* Adapted from *Nature Reviews Cancer*, 2008¹²⁸

From a clinical perspective, the CSC concept has significant implications, as these cells need to be eradicated in order to provide long-term disease-free survival. Cancer stem cells are refractory to treatment with most, if not all, cytotoxic drugs. They appear to be quiescent, enabling them to survive and cause relapses.¹²⁹ With novel drug cocktails, long-term treatment and careful surveillance, we should be

able to turn cancer into a ‘chronic’ disease that can be lived with (Figure 1.22). However, the discovery of molecular pathways specifically altered in CSCs is expected to identify novel therapeutic approaches to eliminate these cells. It is then possible that these new treatments may result in tumour eradication and cure of the patients.

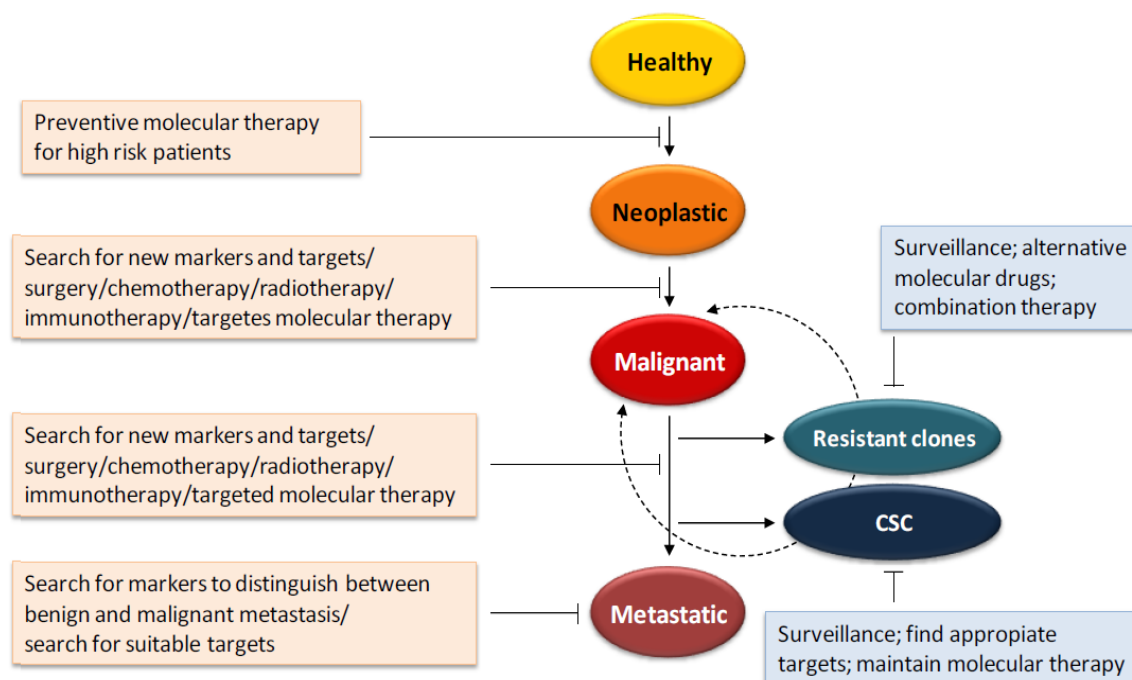


Figure 1.23. Targeted molecular therapy has roles to play in prevention and treatment of cancer. Long-term treatment and novel drug cocktails should nip cancer stem cells in the bud and prevent the emergence of resistant tumours. *Source:* Adapted from *Nature Reviews Cancer*, 2005.¹⁰⁶

1.9. Rational drug design and discovery

Resistance to chemotherapeutic agents has raised a new research line in the search for an effective anticancer therapy, an aim which is meant to be achieved by drugs of new synthesis and rational design. Medicinal chemistry is closely aligned to biochemistry, biology, and pharmacology, as selective target modulation combined with the desired cellular effect (for example, growth inhibition or induction of apoptosis) is sought using cell lines *in vitro*. This is followed by the demonstration of efficacy at non-toxic doses *in vivo*. Accordingly, the following scheme (Figure 23) has been proposed in order to develop new anticancer agents.

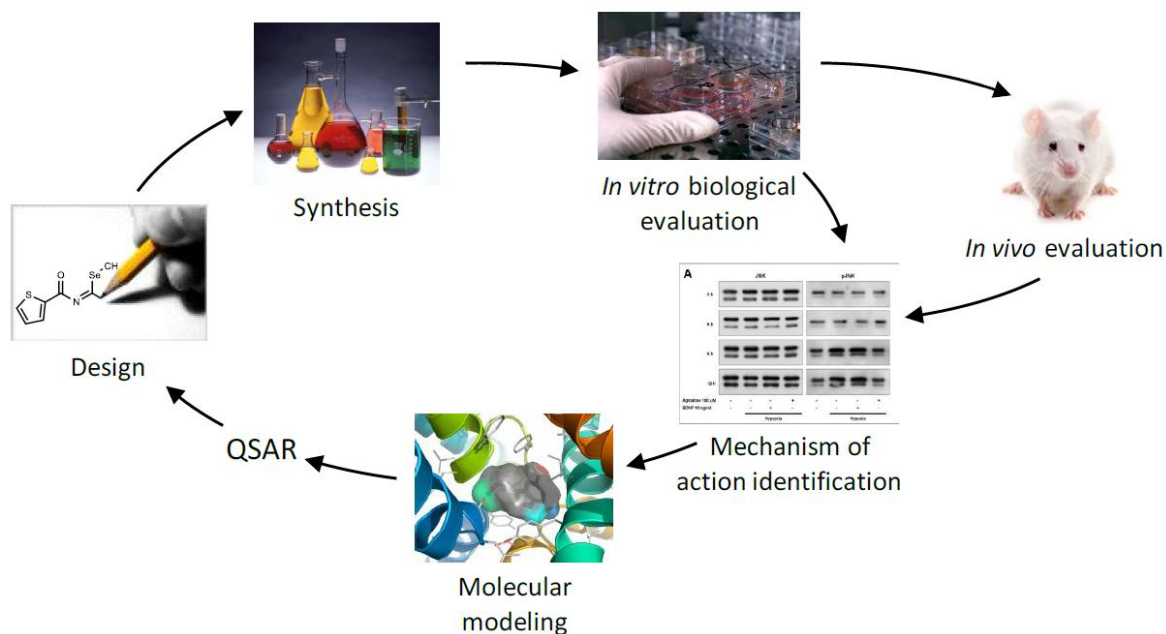


Figure 1.23. An integrated and non-linear way in drug discovery.

1.9.1. Preclinical development

1.9.1.1. In vitro preclinical development

A key property that all successful drug therapies possess is an adequate pharmacokinetic profile that allows the drug to produce an efficacious effect. In fact, a compound must possess three characteristics to be useful as a drug: efficacy, safety, and adequate absorption, distribution, metabolism, and elimination (ADME) properties. For these reasons, the determination and optimization of ADME properties is a critical activity that must be actively pursued in the drug discovery and development process. These are generally included in Lipinski's 'rules of 5,' derived from an analysis which showed that 90 percent of orally absorbed drugs had a molecular weight of less than 500 Da (daltons), lipophilicity ($\log P$, the partition coefficient between octanol and water) of less than 5, fewer than 5 hydrogen-bond donors, and less than 10 hydrogen-bond acceptors. In addition, molecules with less than 8 rotatable bonds and a lack of chemically reactive groups such as Michael acceptors are favored.^{130,131}

Studies aimed at elucidating the cellular pharmacological properties of potential drugs represent an essential component of the drug discovery cascade. Much useful information can be relatively quickly acquired primarily in order to rank compounds and promote only the most appropriate for *in vivo* studies. Biomarker modulation information is then combined with a phenotypic readout of anticancer activity (such as decreased proliferation, increased apoptosis, decreased migration, or invasion) (Figure 1.24). Generally these cell-based effects are sought at a concentration of low micromolar levels or below.

Cell lines, typically established human tumour cells, are selected for these studies on the basis of prior profiling for the target or pathway under study.

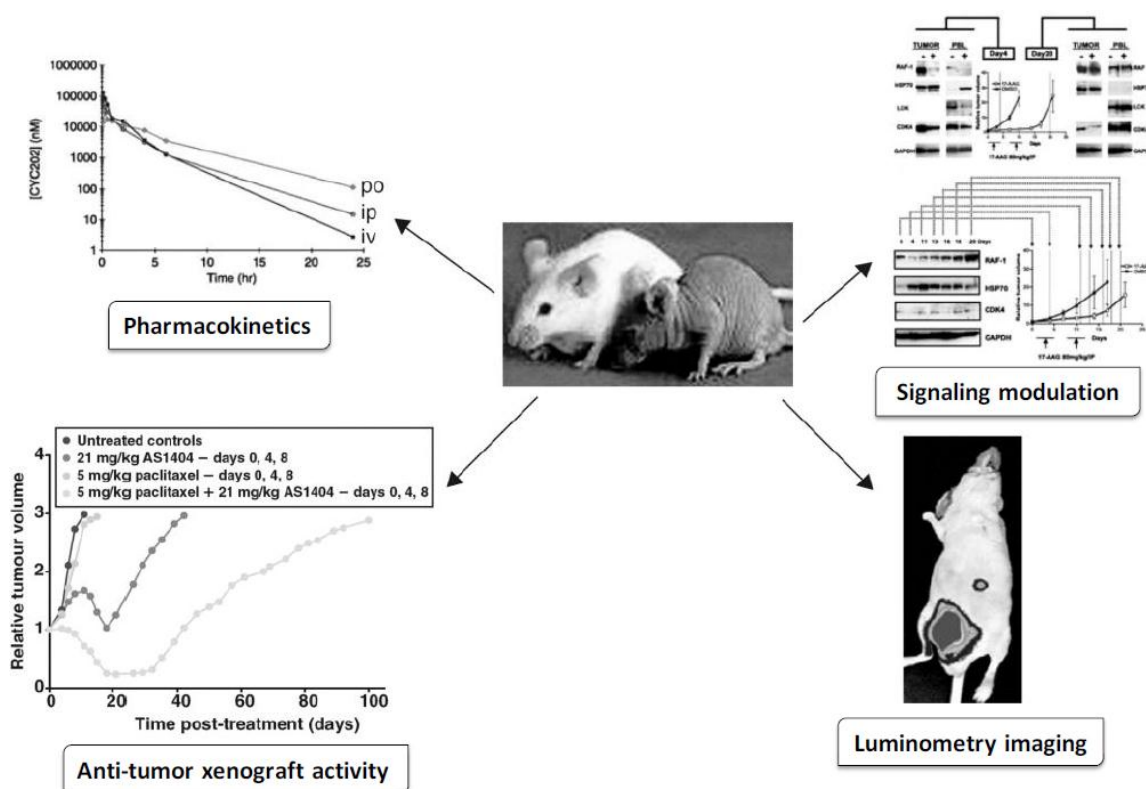


Figure 1.24. Some pharmacological information acquired from *in vivo* studies.

1.9.1.2. *In vivo* assays for antitumour activity

Around 90 percent of the *in vivo* studies are carried out in mice. Such studies can provide a significant amount of valuable information, such as agent tolerability, biomarker read outs, and efficacy determinations (Figure 1.25).

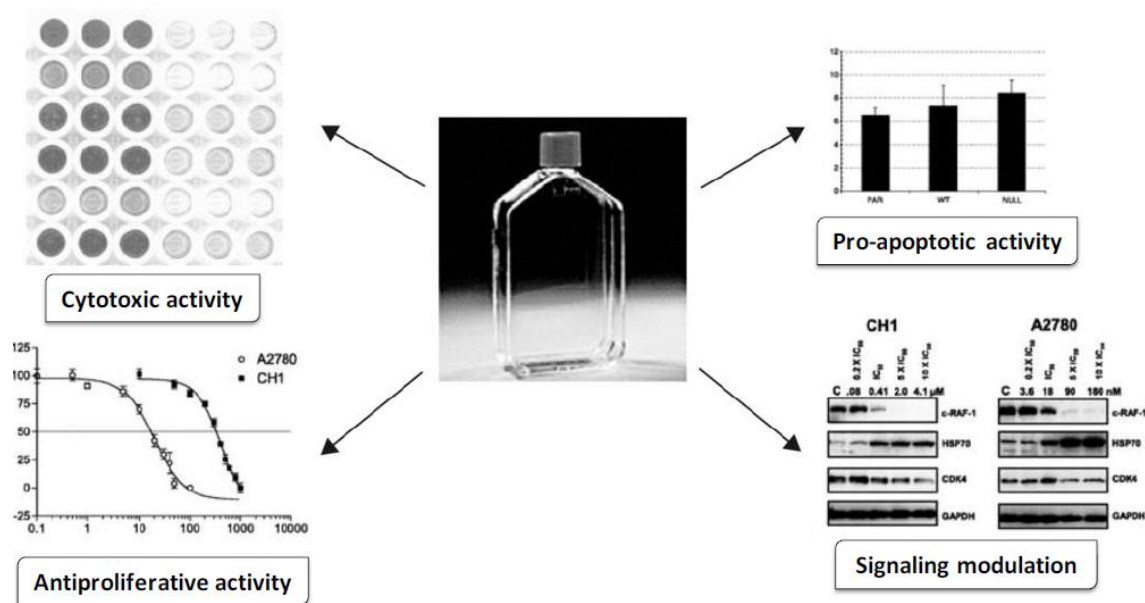


Figure 1.25. Some information acquired from *in vivo* studies of cancer drugs.

Which is the best model to use with respect to predicting Phase II/III clinical utility is not clear and is the subject of considerable current debate.¹³² Accordingly, over the last several decades, a great variety of preclinical *in vivo* tumour models has been established for performing these activities (Figure 1.26).

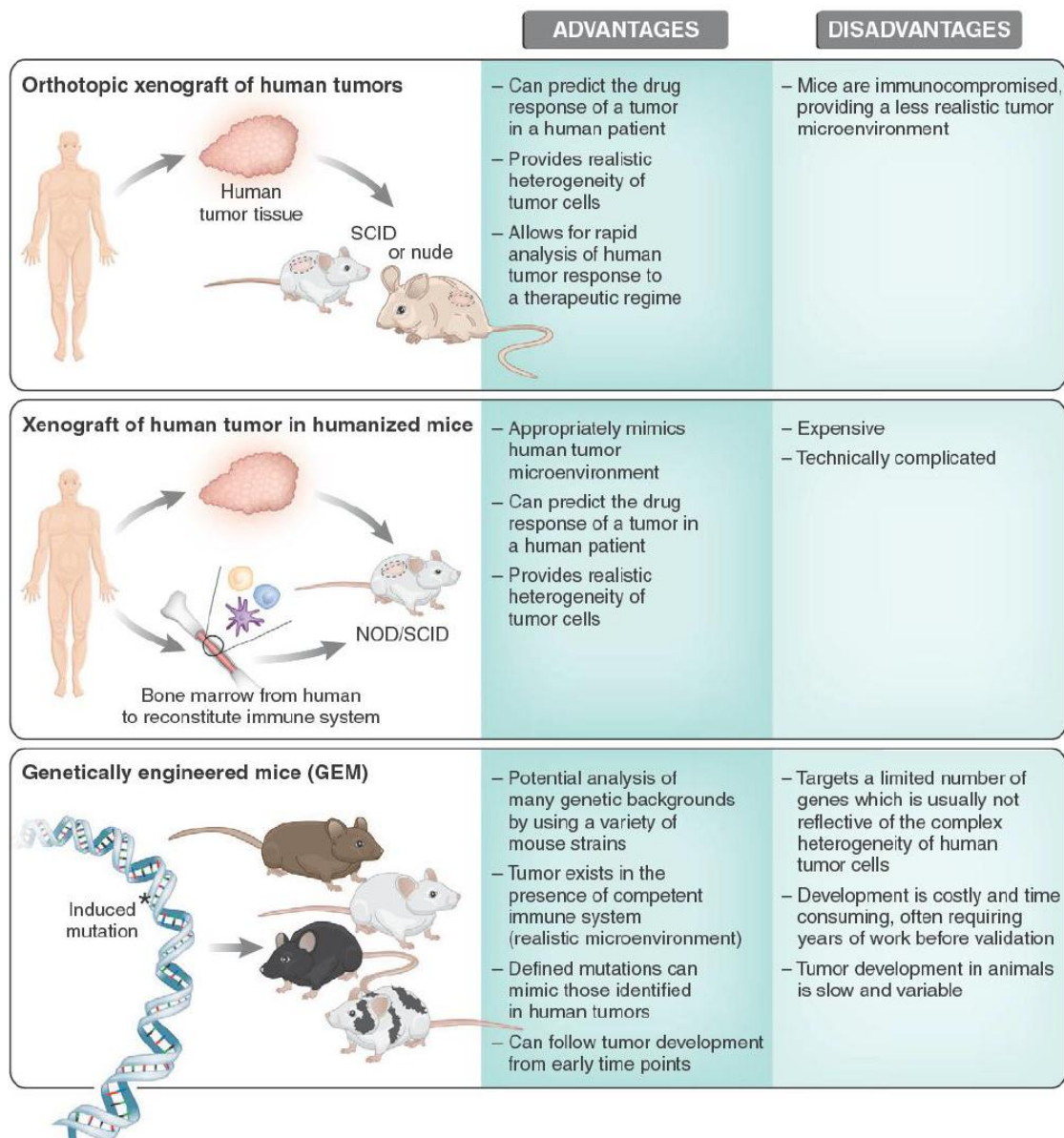


Figure 1.26. Types of murine model for studying human cancers.

The demonstration of antitumour efficacy in a preclinical, typically mouse-based, model of cancer, at a non-toxic dose (i.e. exhibiting a therapeutic index) is a key determinant both in selecting a molecule for further development from within a chemical series and in deciding whether to initiate the final, and relatively expensive, phase of preclinical development.

2. STEREOCHEMISTRY

2.1. Introduction

Stereochemistry is the study of the static and dynamic aspects of the three-dimensional shapes of molecules.

Nature is inherently chiral because the building blocks of life (amino acids, nucleotides, and sugars) are chiral and appear in nature in enantiomerically pure forms. Hence, any substances created by humankind to interact with or modify nature are interacting with a chiral environment. This is an important issue for bioorganic chemists, and a practical issue for pharmaceutical chemists. The Food and Drug Administration (FDA) now requires that drugs be produced in enantiomerically pure forms, or that rigorous tests be performed to ensure that both enantiomers are safe.

The study of stereochemistry can be used to probe reaction mechanisms, hence, understanding stereochemistry is necessary for most fields of chemistry. The study of chirality and symmetry has spanned the disciplines of chemistry, biology, and physics.

Early work by Arago (1811) and Biot (1812) demonstrated the effects of cut crystals on the plane of polarized light different crystals rotated light left or right. Biot later showed that natural organic products, such as oil of turpentine, sugar solutions, camphor and tartaric acid could produce similar rotation.

The existence of **optical isomerism** has been known since the first half of the 19th century. In 1815 Jean-Baptiste Biot discovered optical activity. In 1848 Louis Pasteur recrystallized the racemic sodium ammonium salt of tartaric acid and noted two different crystal forms; he picked out the differing crystal types by hand doing

so on the basis of the differing physical appearance of the salt crystals and with no more technical support than a pair of tweezers and a microscope, he separated them, and after redissolved them, found that they rotated polarized light differently (one to the left and the other to the right) for the first time in history a pair of non-superimposable mirror-image crystal forms. Pasteur recognized that two of the isomers polarized light differently and that this must be due to an asymmetric grouping of atoms in the optically active molecules. He noted that the cause of this phenomenon lay in the molecule structure and by extending these ideas he evolved the theory of the **asymmetrical carbon atom**. After acid treatment the isolated crystals of sodium ammonium tartrate liberated d- and l-tartaric acid. Subsequently, in 1857 Pasteur made the first observation of biological enantioselectivity, when he noted bacterial capacity to ferment only dextro-tartaric acid.

Following Kekule's recognition in 1858 that carbon has a valence of 4. Van't Hoff in 1874, recipient of the first Nobel Prize in Chemistry and Le Bel independently outlined the relationship between three-dimensional molecular structure and optical activity and the concept of the asymmetric carbon atom. They recognized that when four different groups are attached to a carbon atom, arrayed at the corners of a tetrahedron, the arrangements can be in two different form. In 1891, Fisher performed the unbelievable feat of identifying the 16 different spatial configurations of aldohexose ($C_6H_{12}O_6$), the most prominent member being D-glucose. He created eponymous Fisher projections to represent their three-dimensional structure and was awarded the second Nobel Prize in Chemistry.

The concept of **chirality** has been known in chemistry since the 1870's although it would be nearly a hundred years before chemists began using this term. Chirality is one of the words in the pharmaceutical language which comes from the Greek. The Greek used the word 'cheiros' to refer to handedness, i.e., being left-handed or right-handed, if an object is 'handed'. The term Chiral apparently was coined by Lord Kelvin in his Baltimore Lectures on Molecular Dynamics and the Wave Theory of Light in which he stated ..."I call any geometrical figure, or group of points, chiral, and say it has chirality, if its image in a plane mirror, ideally realized, cannot be brought to coincide with itself."

In extremely simple terms, chirality is a property of an object which is non-superimposable with its mirror image, it is "handedness," the existence of left/right opposition.

2.2. Basic Concepts and Terminology

There was considerable ambiguity and imprecision in the terminology of stereochemistry as it developed during the 20th century. In recent years, stereochemical terminology has clarified.

Stereoisomers are molecules that share identical molecular formula, atom-to-atom linkages, and bonding distances, solubility and stability but differ in their three-dimensional arrangement of the atoms in space; this is in contrast to **constitutional isomers**, which are molecules with the same molecular formula but different connectivity between the atoms. The constitution of a molecule is defined by the number and types of atoms and their connectivity, including bond multiplicity.

An historical distinction, but one that is not entirely clear cut, is that between configurational isomers and conformational isomers. **Conformational isomers** are interconvertible by rotations about single bonds and the conformation of a molecule concerns features related to rotations about single bonds. The term **configurational isomer** is generally used to encompass enantiomers and diastereomers as isomers, but **stereochemical isomers** is a better term. Mislow defines configuration as “the relative position or order of the arrangement of atoms in space which characterizes a particular stereoisomer”.

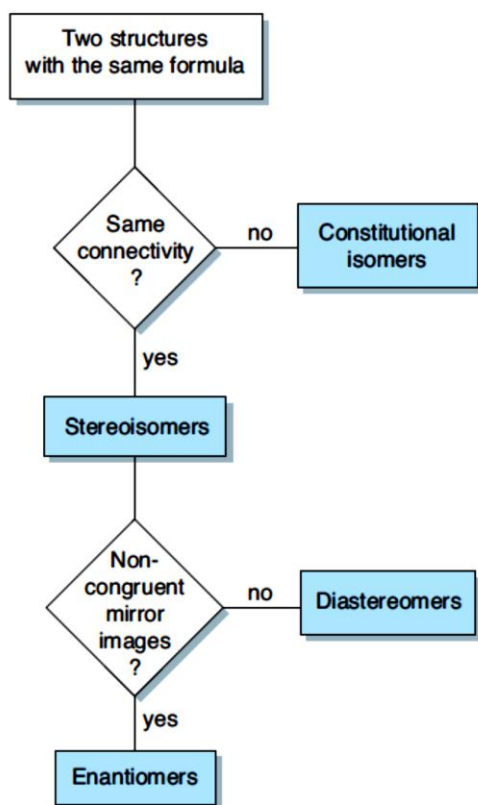


Figure 2.1. Different types of isomers.

When two stereoisomers are nonsuperposable mirror images of each other, they are known as **enantiomers**. Stereoisomers that are not enantiomers are known as **diastereomers**. Any object that is nonsuperposable (noncongruent) with its mirror image is chiral. If an object is not chiral that is, if its mirror image is congruent with the original, it is achiral. Thus, the energy content of a pair of enantiomers is essentially identical and therefore their physicochemical properties, e.g. lipid solubility, melting points etc., are also identical and the separation. Enantiomers have identical chemical and physical properties in a non-chiral environment except when they interact with chiral systems. However, in a chiral environment, e.g., the human body, also the properties of enantiomers differ. Both enantiomers will have the same boiling point, densities, and reaction rates as a chiral molecule. They do, however, generally possess differences in toxicity and biological activity. Enantiomers rotate the plane of polarized light in opposite directions and by equal amounts

2.3. Classical Terminology

There are a series of terms used in the context of stereochemistry that are ingrained in the literature confusion with respect to terminology arises with terms such as “**optically active**” and “**chiral centre**”. Optically active refers to the ability of a collection of molecules to rotate plane polarized light. In order for a sample to be optically active, it must have an excess of one enantiomer. Now comes the confusion. Optically active was generally used as a synonym for chiral in the earlier literature, and unfortunately this usage continues at times even today. There are many examples of chemical samples that contain chiral molecules, but the samples themselves are not optically active. A **racemic mixture**, a 50:50 mixture of enantiomers, with sign (\pm) or (d,l) does not exhibit optical activity, but every molecule in the sample is chiral. It is important to distinguish between a sample that is optically inactive because it contains a racemic mixture and a sample that is optically inactive because it contains achiral molecules.

Also, it is easy to imagine molecules, even when enantiomerically pure, that would not rotate plane polarized light to any measurable extent. The extent of rotation of plane polarized light depends upon differences in the refractive indices with respect to right and left circularly polarized light as it passes through the sample. Enantiomers that do not have dramatically different refractive indices would not result in measurable rotations. Examples would be a carbon with four different n-alkyl chains attached, with chain lengths of maybe 10, 11, 12, and 13 carbons; or one with four C10 chains, but terminating in $-\text{CH}_3$, $-\text{CH}_2\text{D}$, $-\text{CHD}_2$ and $-\text{CD}_3$. In each case the molecule is chiral, but any rotation of plane polarized light would be immeasurably small. Operationally, they are optically inactive. Finally, even an enantiomerically pure sample of a chiral molecule will show zero rotation at certain wavelengths of light since the rotation must pass through zero rotation as it changes from (+) to (-) rotation in the optical rotatory dispersion (ORD) curve, any chiral sample will be optically inactive at some wavelengths. Typically, light of one particular wavelength, the Na “D-line” emission, is used for conventional organic molecules. Thus, optical activity establishes that a sample is chiral, but a lack of optical activity does not prove a lack of chirality. “Optically active” is an ambiguous description.

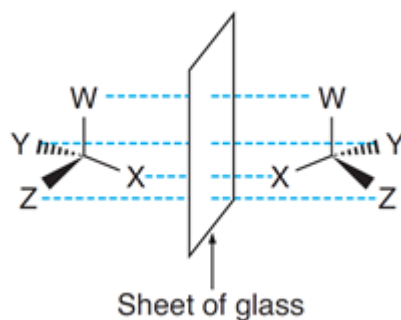


Figure 2.2. Two enantiomers are non superposable mirror images of each other

The prototype is the **chiral centre**, which is defined as an atom that has four different ligands attached. The particular case of a carbon with four different substituents has also been termed an **asymmetric carbon**, but the carbon is not the only atom that can act as an asymmetric centre. The central atom can also be another than carbon, e.g., sulfur, phosphorus or nitrogen. In addition, many molecules can exist in enantiomeric forms without having a “chiral centre”.

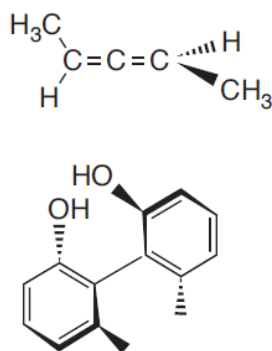


Figure 2.3. Chiral molecules without a “chiral centre”.

Stereogenic centre (or, equivalently, **stereocentre**). An atom, or a grouping of atoms, is considered to be a stereogenic centre if the interchange of two ligands attached to it can produce a new stereoisomer. Not all interchanges have to give a new stereoisomer, but if one does, then the centre is stereogenic. The centre therefore “generates” stereochemistry. A non-stereogenic centre is one in which exchange of any pair of ligands does not produce a stereoisomer. The term “stereogenic centre” is, in a sense, broader than the term “chiral centre”. It implies nothing about the molecule being chiral, only that stereoisomerism is possible.

Planar chirality and **axial chirality**. The justification for these terms is that such molecules do not have stereogenic centres, but rather stereogenic units. Admittedly, terms that address chirality without stereogenic centres could be useful. However, since a molecule that is truly planar (i.e., has a plane of symmetry) must be achiral, planar chirality is an odd use of the word “planar”. Developing precise, unambiguous definitions of these terms is a challenge that, in our view, has not yet been met. Currently, the best term is “stereogenic unit”.

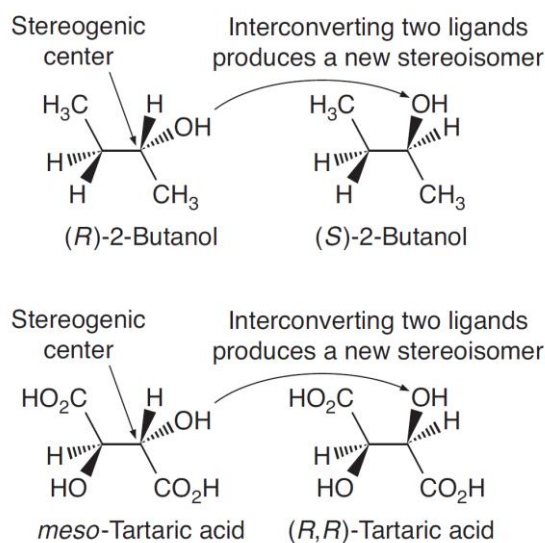


Figure 2.4. Illustration of the concept of the stereogenic centre in the context of carbon. Whether in a chiral molecule like 2-butanol or an achiral molecule like meso-tartaric acid, interconversion of two ligands at a stereocentre produces a new stereoisomer.

Tartaric acid has two stereogenic centres and exists as three possible stereoisomers. This is an exception to the norm. Typically, a molecule with n stereogenic, tetracoordinate carbons will have 2^n stereoisomers; 2^{n-1} diastereomers that each exist as a pair of enantiomers. For example, a structure with two stereogenic centres will exist as *RR*, *SS*, *RS*, and *SR* forms. In tartaric acid the *RS* and *SR* forms are identical, they are both the meso form because C2 and C3 have the same ligands. The 2^n rule quickly creates complexity in molecules with multiple stereogenic centres, where n = number of asymmetric atoms, chiral heteroatoms in the molecule.

2.4. Stereochemical Descriptors

All introductory organic chemistry texts provide a detailed presentation of the various rules for assigning descriptors to stereocentres.

Many of the descriptors for stereogenic units begin with assigning priorities to the attached ligands. Higher atomic number gets higher priority. If two atoms under comparison are isotopes, the one with higher mass is assigned the higher priority. Ties are settled by moving out from the stereocentre until a distinction is made. In other words, when two attached atoms are the same, one examines the next atoms in the group, only looking for a winner by examining individual atomic numbers (do not add atomic numbers of several atoms). Multiple bonds are treated as multiple ligands.

***R, S* System**

For tetracoordinate carbon and related structures we use the Cahn–Ingold–Prelog system.¹³³ In the nomenclature system, atoms or groups bonded to the chiral centre are prioritized first, based on the sequence rules. The rules can be simplified as follows: (1) An atom having a higher atomic number has priority over ones with a lower atomic number; for isotopic atoms, the isotope with a higher mass precedes the one with the lower mass. (2) If two or more of the atoms directly bonded to the asymmetric atom are identical, the atoms attached to them will be compared, according to the same rule. When two groups have different substituents, the substituent bearing the highest atomic number on each group must be compared first. The sequence decision for these groups will be made based on the sequence of the substituents, and the one containing prior substituents has a higher precedence. A similar rule is applicable in the case of groups with heteroatoms. (3) For multiple bonds, a doubly or triply bonded atom is duplicated or triplicated with the atom to which it is connected. This rule is also applicable to aromatic systems. Based on these sequence rules, configuration can be easily assigned to chiral molecules, which are classified into different types according to spatial orientation. This system based on decreasing atomic number (“substituents of the higher atomic number precede

those with lower ones”) for projection formulas that allows the absolute configuration assignments of *R* (for *rectus*, Latin for right or clockwise rotation) and *S* (for *sinister*, Latin for left or counterclockwise rotation). The highest priority group is given number 1, whereas the lowest priority group is given number 4. Sight down the bond from the stereocentre to the ligand of lowest priority behind. If moving from the highest (#1), to the second (#2), to the third (#3) priority ligand involves a clockwise direction, the centre is termed *R*; a counterclockwise direction implies *S*. The *R/S* system can also be used in cases where the molecule contains more than one chiral centre.

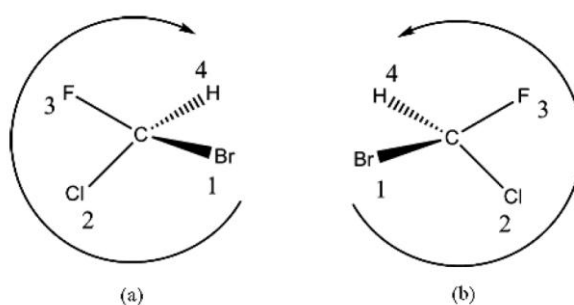


Figure 2.5. Tetrahedral chiral nomenclature: (a) (*R*)-bromochlorofluoromethane; (b) (*S*)-bromochlorofluoromethane.

E, Z System

For olefins and related structures we use the same priority rules, but we divide the double bond in half and compare the two sides. For each carbon of an olefin, assign one ligand high priority and one low priority according to the rules above. If the two high priority ligands lie on the same side of the double bond, the system is *Z* (*zusammen*); if they are on opposite sides, the system is *E* (*entgegen*). If an H atom is on each carbon of the double bond, however, we can also use the traditional “*cis*” and “*trans*” descriptors.

d and *l* System

The descriptors *d* (dextrorotatory) and *l* (levorotatory) represent an older system for distinguishing enantiomers. In a Fischer projection, the horizontal lines represent bonds coming out of the plane of the paper, while the vertical lines represent bonds projecting behind the plane of the paper. The isomer of glyceraldehyde that rotates

plane polarized light to the right was labelled d, while the isomer that rotates plane polarized light to the left was labelled l.

The d and l nomenclature system is fundamentally different than the *R/S* or *E/Z* systems. The d and l descriptors derive from only one stereogenic centre in the molecule and are used to name the entire molecule. The name of the sugar defines the stereochemistry of all the other stereogenic centres. Each sugar has a different arrangement of the stereogenic centres along the carbon backbone. In contrast, normally a separate *R/S* or *E/Z* descriptor is used to name each individual stereogenic unit in a molecule. The d/l nomenclature is now reserved primarily for sugars and amino acids. Thus, it is commonly stated that all natural amino acids are l, while natural sugars are d.

***erythro* and *threo* System**

Another set of terms that derive from the stereochemistry of saccharides are *erythro* and *threo*. The terms are the basis of a nomenclature system for compounds with two stereogenic centres and two groups in common. To determine the use of the *erythro* and *threo* descriptors, draw the compound in a Fischer projection with the distinguishing groups on the top and bottom. If the groups that are the same are both on the right or left side, the compound is called *erythro*; if they are on opposite sides, the compound is called *threo*.

2.5. Using Descriptors to Compare Structures

Compounds that have the same sense of chirality at their individual stereogenic centres are called homochiral. **Homochiral** molecules are not identical. As a chemical example, the amino acids L-alanine and L-leucine are homochiral. Those molecules with a differing sense of chirality at their stereogenic centres are called **heterochiral**. Homochiral has been used by some as a synonym for “enantiomerically pure”. This is another usage of a term that should be discouraged, as homochiral already had a clear and useful definition, and using the

same term to signify two completely different concepts can only lead to confusion. A better term for designating an **enantiomerically pure** sample is simply **enantiopure**.

When racemic drugs is examined, their activity can be divided into three main groups. The majority of racemic pharmaceuticals have one major bioactive enantiomer (**eutomer**), the other is inactive or less active (**distomer**) or toxic or can exert other desired or undesired pharmacological properties. The second category is intended to drugs where the two enantiomers are equally active and have the same pharmacodynamics. The last one is racemic drugs having only one eutomer, but the distomer could be transformed in body into its bioactive antipode by chiral inversion.

Epimers are two diastereoisomers having a different configuration at only one of the several stereogenic centres. Isomerization or enantiomerization is the conversion of one stereoisomeric form into another. When isomerization occurs by the change of configuration at a single chiral centre, the process is called epimerization, and when it leads to the formation of a racemate it is termed racemization.

A **stereoselective** reaction is one in which a single reactant can give two or more stereoisomeric products, and one or more of these products is preferred over the others, even if the preference is very small. In fact, the reactant may not even exist as stereoisomers, yet the reaction can be stereoselective. This term describe the stereochemical consequences of certain types of reactions. There can be degrees of stereoselectivity. All stereospecific reactions are stereoselective, but the converse is not true.

Stereospecific, a term describing the stereochemical consequences of certain types of reactions. A stereospecific reaction is one for which reactant A gives product B, and stereoisomeric reactant A' gives stereoisomeric product B', so one isomer leads to one product while another isomer leads to the opposite product. There can be degrees of stereospecificity. Stereospecific does not mean 100% stereoselective.

2.6. Distinguishing Enantiomers

Enantiomers are distinguishable if and only if they are placed in a chiral environment and all methods to separate or characterize enantiomers are based on this principle.

Figure 2.6 shows some chemical examples of this. If a racemic mixture of 2-aminobutane is allowed to react with an enantiomerically pure sample of mandelic acid, the two amides that are produced are diastereomers. The two diastereomers can be separated by any conventional method (such as crystallization or chromatography), and subsequent hydrolysis of a pure diastereomer gives enantiomerically pure 2-aminobutane. The interaction that creates diastereomers out of enantiomers need not be covalent. Weaker, non-covalent complexes are often discriminating enough to allow separation of enantiomers. The most classical way to separate enantiomeric amines is to form salts with a chiral acid and use crystallization to separate the diastereomeric salts. There are many variations on this theme, and this traditional approach is still very commonly used, especially for large scale, industrial applications.

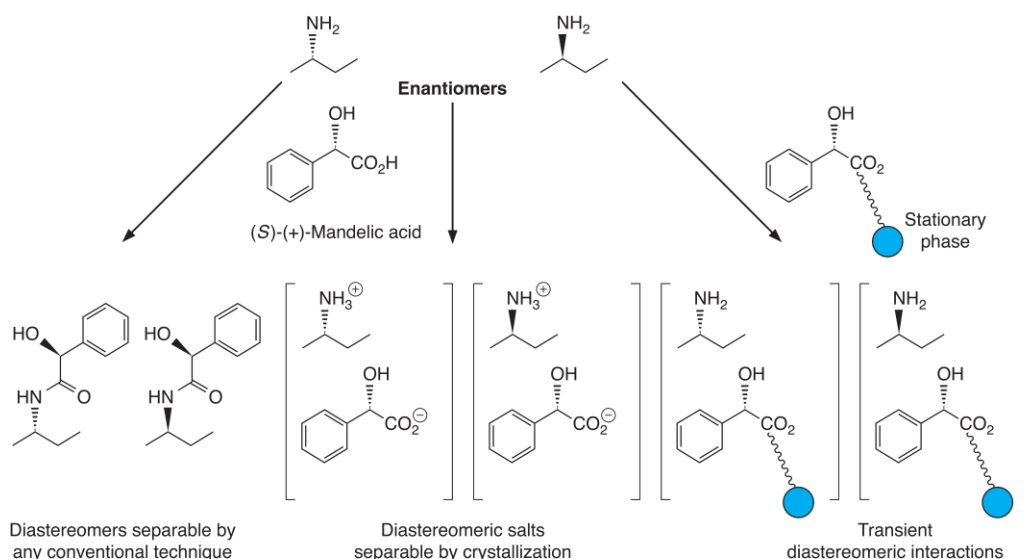


Figure 2.6. Hypothetical methods to separate a mixture of enantiomers.

For the smaller scales associated with the research laboratory, chiral chromatography is increasingly becoming the method of choice for analyzing and separating mixtures of enantiomers. We show in Figure 2.6 a hypothetical system in which the mandelic acid we have used in the previous examples is attached to a stationary phase. Now, transient, diastereomeric interactions between the 2-aminobutane and the stationary phase lead to different retention times and thus to separation of the enantiomers. Both gas chromatography and liquid chromatography are commonly used to separate enantiomers.

With a tool to discriminate enantiomers in hand, we can determine the **enantiomeric excess** (ee) of a sample. This commonly used metric is defined as $X_a - X_b$, where X_a and X_b represent the mole fraction of enantiomers a and b, respectively. Usually ee is expressed as a percentage, which is $100\% (X_a - X_b)$. Analogous terms such as **diastereomeric excess** (de) are also used. The traditional tools for evaluating ee are the chiroptical methods discussed below. However, methods such as high field NMR spectroscopy with chiral shift reagents, NMR spectroscopy of derivatives that are diastereomeric, and chromatography (HPLC and GC) with chiral stationary phases, are becoming ever more powerful and popular.

For example, the enantiomeric forms of 2-deutero-2-phenylethanol can be readily distinguished in the NMR using a complex known as Eu(dcm). Coordination of the alcohol to the Eu centre leads to diastereomers. The ^1H NMR spectrum shown to the side of the H on the stereogenic centre of 2-deutero-2-phenylethanol indicates that the two enantiomers (in a 50:50 ratio) are easily distinguished^{134,135} (Figure 2.7).

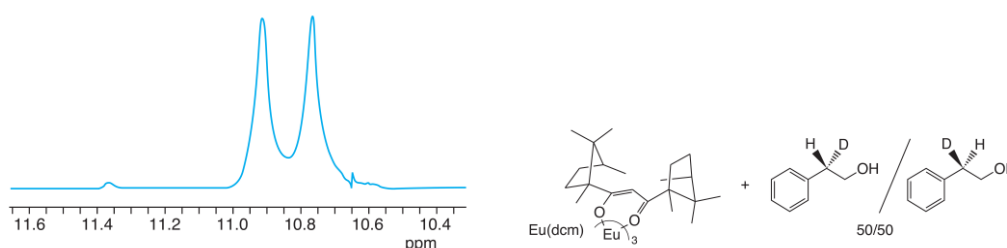


Figure 2.7. Chiral Shift Reagents

Advances with regard to structures of various sites of drug action and improvements in methods for synthesizing and analyzing stereochemically pure drugs has resulted in increased interest in marketing of individual pure enantiomers of chiral drugs. In the future, more stereochemically pure drug agents will become clinically available and pharmacists will be relied upon for their knowledge and expertise in this area.

2.7. The Origin of Chirality in Nature

The molecules of life are for the most part chiral, and in living systems they are almost always enantiomerically pure. In addition, groups of biomolecules are generally homochiral; all amino acids and sugars have the same sense of chirality. As already discussed, the chirality of the amino acids leads to chiral enzymes, which in turn produce chiral natural products. The enantiomers of a chiral drug may vary in their interactions with chiral environments such as enzymes, proteins, receptors, etc of the body. These variations may lead to differences in biological activities such as pharmacology, pharmacokinetics, metabolism, toxicity, immune response etc. Indeed, biological systems can recognize the two enantiomers as two different substances, and their interaction each other will therefore elicit different responses. But, why do enantiomers have different biological activities? The reason for chiral recognition by drug receptors is a three-point interaction of the drug with the receptor site proposed by Easson and Stedman.¹³⁶

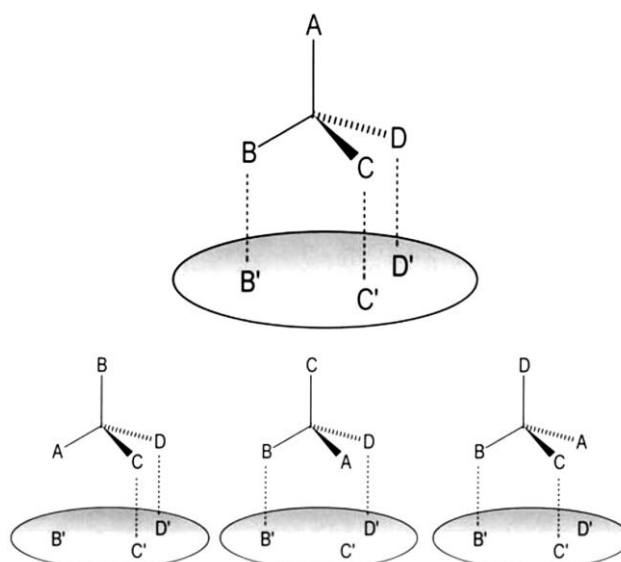


Figure 2.8. Easson–Stedman model of the drug–receptor interaction.¹³⁶ The more active stereoisomer (top) is involved with three simultaneous complementary bonding interactions with the receptor active site, B...B', C...C' and D...D'; its less active enantiomer (lower) may interact at two sites only irrespective of its orientation to the active site.

All the chiral compounds found in nature that are readily accessible to synthetic chemists for the construction of more complex molecules are referred to as the **chiral pool**; it is a procedure used to transform an old racemic drug into its single active enantiomer. This new enantiomeric drug developed by a pharmaceutical manufacturer will receive additional patent protection and a new generic name.

The body with its numerous homochiral compounds being amazingly chiral selector, will interact with each racemic drug differently and metabolize each enantiomer by a separate pathway to generate different pharmacological activity. Thus, one isomer may produce the desired therapeutic activities, while the other may be inactive or, in worst cases, produce undesired or toxic effects.

Development of pure enantiomers is currently more economically feasible. Improved methods of analyzing and preparing enantiomers have also developed. Our mechanistic understanding of the chiral structure of sites of drug action is continually evolving.

3. BACKGROUND

3.1. Introduction

In recent years, strategy in cancer therapy has been the use of high doses of toxic non-specific agents and to investigate a range of new agents that specifically target tumour-related molecules, in a variety of biological pathways. A basic knowledge of these pathways in the cancer cell is becoming fundamental for clinical practice since it can provide prognostic as well as predictive information for established therapies, and lead to the discovery of potential new targets. Two main therapeutic strategies may be followed to optimize cancer treatment: a better selection of patients who will benefit the most from a given hormonal or cytotoxic therapy, through the use of predictive markers determined by genomics and/or proteomics techniques and the development of new agents with innovative and tumor-specific mechanism of action.

Breast cancer is a common and often fatal disease. Excluding cancers of the skin, the breast is the most common cancer among women, accounting for nearly one out of every three cancers diagnosed in American women. Each year over 186,000 new cases and 46,000 deaths are reported in the United States alone.¹³⁷ Five main molecular pathways are of particular interest in terms of new drug development in breast cancer: the estrogen receptor pathway, the tyrosine signal transduction pathway, the angiogenesis pathway, the cell cycle regulation pathway and the apoptosis (programmed cell death) pathway. We will focus in this thesis on new cytotoxic, apoptotic and cell-cycle-regulator agents designed by us.

As part of their action on neoplastic cells, many anticancer drugs activate apoptosis that may be a primary mechanism of antineoplastic agents.¹³⁸ Although breast cancer is most often treated with conventional cytotoxic agents it has proved difficult to induce apoptosis in breast cancer cells using these drugs.¹³⁹ Improved clinical response may be obtained by identifying therapies that are particularly effective in activating apoptosis and determining how those therapies may be modified to effect maximum apoptosis induction. The cell cycle apparatus and

apoptosis have recently attracted the attention of researchers intent on developing new types of anticancer therapy.^{140,141} On the other hand, the MCF-7 human breast cancer cell line has been used as an excellent experimental model to improve the efficacy of different therapies before its use in patients.^{142,143}

In this thesis we will be concentrated on the evolution of the chemical structures and the biological properties whilst, in general, the chemical syntheses will be referred to through the corresponding original references.

3.2. Benzo-Fused Seven-Membered Derivatives Linked To Pyrimidines

Having previously reported the synthesis and anticancer activities of acyclic 5-fluorouracil (5-FU) *O,N*-acetalic compounds **1-2**,¹⁴⁴ cyclic *O,N*-acetalic compounds was synthesized with the objective of increasing the lipophilicity of the target molecules. In this way we have reported the synthesis and anticancer activities of compounds **3**,¹⁴⁵ **4-6**,¹⁴⁶ **7**,¹⁴⁷ **8-9**¹⁴⁶ and trans-**10**¹⁴⁸ (Figure 3.1). In all cases, the linkage between the 5-FU moiety and the membered ring was carried out through its *N*-1 atom.

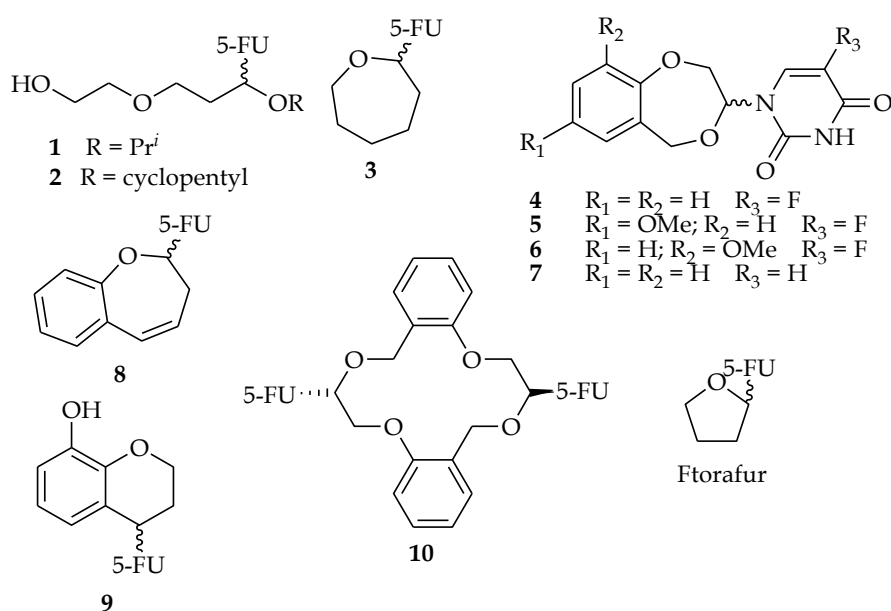


Figure 3.1. Several 5-FU derivatives showing interesting antitumour activities.

3.2.1. Antiproliferative Activities of Cyclic *O,N*-Acetals

The IC₅₀ values of the 5-FU cyclic *O,N*-acetals are shown in Table 3.1 (entries **4-6, 8-10**).

Table 3.1. Antiproliferative activities, cell cycle dysregulation, and apoptosis induction in the MCF-7 human breast cancer cell line after treatment for 24 and 48 h for the compounds.

Entry	Compound	clogP ^a	IC ₅₀ (μM) ^b	Cell Cycle (48 h) ^c			Apoptosis ^d	
				G ₀ /G ₁	G ₂ /M	S	24 h	48 h
1	Control			68.39	12.04	19.57	1.24	1.24
2	5-FU	-0.89 ^c	2.75	58.07	2.10	39.38	56.75	52.81
3	Ftorafur	-0.18 ^f	3 ± 0.11	45.62	0.00	54.38	52.20	58.06
4	3	0.86	23 ± 0.88	50.99	18.51	30.49	46.63	53.92
5	4	1.09	7 ± 0.61	74.41	15.77	9.82	8.45	12.17
6	5	1.16	4.5 ± 0.33	73.41	13.15	13.44	1.50	3.50
7	6	1.16	22 ± 0.93	71.76	10.08	18.16	40.08	46.73
8	7	0.87	5 ± 0.25	69.01	11.38	19.61	5.30	5.22
9	8	2.54	14 ± 1.02	86.14	1.60	12.26	57.33	51.37
10	9	0.70	69 ± 2.31	68.61	9.60	21.79	54.33	35.49
11	10	2.18	5.5 ± 0.58	82.48	5.13	12.40	14.37	19.05

a) Calculated by a fragmental system based on Rekker's method,¹⁴⁹ the CDR option of the PALLAS 2.0 programme (PALLAS FRAME MODULE, a) prediction tool of physicochemical parameters, is supplied by CompuDrug Chemistry Ltd, PO Box 23196, Rochester, NY 14696, USA). b) See ref.¹⁵⁰ c) Determined by flow cytometry: see ref.¹⁴⁶ d) Apoptosis was determined using an annexin V-based assay.¹⁵¹ The data indicate the percentage of cells undergoing apoptosis in each sample. All experiments were conducted in duplicate and gave similar results. The data are means ± SEM of three independent determinations. e) The experimental log *P* value is -0.83¹⁵² f) The experimental log *P* value, measured by the octanol-buffer partitioning technique at pH 7.4 is -0.36 ± 0.5.¹⁵³

The most active 5-FU-derived compounds are **4**, **5** and **10** (entries **5**, **6** and **11**). Compound **3** (entry **4**) shows low antiproliferative activity ($IC_{50} = 23 \pm 0.88 \mu\text{M}$). The lipophilicity in this structure has been increased by means of a fused benzene ring, and an unsaturation has been introduced to give **8**. An increase has been obtained in its antiproliferative activity ($IC_{50} = 14 \pm 1.02 \mu\text{M}$, entry **9**). On comparing structures **8** and **4**, it is worth emphasizing that the bioisosteric change of carbon for oxygen and the saturation of the double bond in compound **4** increases the antiproliferative activity twice ($IC_{50} = 7 \pm 0.61 \mu\text{M}$, entry **5**). The introduction of a methoxy group into the benzene ring of **4** provokes different influences on the antiproliferative activities. Thus, the C-7 substitution produces an increase of the antiproliferative activity (**5**, $IC_{50} = 4.5 \pm 0.33 \mu\text{M}$, entry **6**), whilst if C-9 is the substituted position it gives rise to a decrease in the antiproliferative activity (**6**, $IC_{50} = 22 \pm 0.93 \mu\text{M}$, entry **7**). The structural nature of **9** (entry **10**, Table 3.1) implies that this compound cannot be considered as a 5-FU prodrug and we suspected that the remaining compounds (entries **4-9** and **11**, Table 3.1) would not be 5-FU prodrugs. To start with and to confirm it we decided to change the 5-FU moiety of **4** for the naturally occurring pyrimidine base uracil to produce **7**, with the prospect of finding an antiproliferative agent endowed with a new mechanism of action.¹⁴⁷

3.2.2. Apoptosis Induction of Cyclic *O,N*-Acetals

Apoptosis has been studied in terms of cancer development and treatment with attempts made to identify its role in chemotherapeutic agent-induced cytotoxicity. Cytotoxic agents often induce only a fraction of the cells to become apoptotic. To fully exploit apoptosis as a mechanism of antineoplastic agent response, a larger proportion of cells need to be recruited into apoptosis. Paclitaxel (Taxol[®]), cyclophosphamide and cytosine arabinoside are the only commonly used cytotoxic agents shown to elicit apoptosis in breast cancer cells.^{154,155} Quantitation of apoptotic cells was done by monitoring the binding of fluorescein isothiocyanate (FITC)-labelledannexin V (a phosphatidylserine-binding protein) to cells in response to our title compounds as described.¹⁵¹ The apoptosis study shows that compounds **3**,

6, **8** and **9**, at their IC₅₀ concentrations, provoke early apoptosis in the cells treated for 24 and 48 h. It is worth pointing out that compound **6** (entry **7**) induces greater apoptosis at 48 h (46.73%) than at 24 h (40.08%) and so does compound **3** [48 h (53.92%) and 24 h (46.63%), entry **4**]. The compounds that show the most important apoptotic indexes at 24 h are **8** (57.33%, entry **9**) and **9** (54.33%, entry **10**), whereas at 48 h are **3** (53.92%, entry **4**) and **8** (51.37%, entry **9**). These compounds are more potent as apoptosis inducers against the MCF-7 human breast cancer cells than paclitaxel (Taxol[®]), which induced programmed cell death of up to 43% of the cell population.¹⁵⁶ Accordingly, the early apoptotic inductions and the low IC₅₀ values give rise to a significant antitumor activity.

3.2.3. Cell Cycle Distribution of Cyclic 5-FU *O,N*-Acetals

Cell cycle regulation has attracted a great deal of attention as a promising target for cancer research and treatment.^{157,158} The use of cell-cycle-specific treatments in cancer therapy has greatly benefited from the major advances that have been recently made in the identification of the molecular actors regulating the cell cycle and from the better understanding of the connections between cell cycle and apoptosis. As more and more “cell cycle drugs” are being discovered, their use as anticancer drugs is being extensively investigated.¹⁵⁸ To study the mechanisms of the antitumor and antiproliferative activities of the compounds, the effects on the cell cycle distribution were analyzed by flow cytometry. Control DMSO-treated cell cultures contained 68.39% G₀/G₁-phase cells, 12.04% G₂/M-phase cells and 19.57% S-phase cells. Cyclic *O,N*-acetals **4-10** (entries **5-11**) provoke a G₀/G₁-phase cell cycle arrest whereas Ftorafur [1-(2-tetrahydrofuran-5-yl)-5-fluorouracil], a known prodrug of 5-FU, induces a S-phase cell cycle arrest.

In fact, a correlation between treated cells with compounds **4-10** recruited in the G₀/G₁ phase when treated at their IC₅₀ concentrations, and their calculated lipophilicities by the CDR option of the PALLAS 2.0 programme:

$$\log (\% G_0/G_1) = 1.801 (\pm 0.009) + 0.055 (\pm 0.003) \text{ clog } P$$

$$n = 7, r^2 = 0.976, s = 0.006, F_{1,5} = 206.10, \alpha < 0.001$$

where n is the number of compounds, r^2 is correlation coefficient, s is the standard deviation, F is the F ratio between the variances of observed and calculated activities, and data within parentheses are standard errors of estimate. This equation means that the more lipophilic the compound is the more cells are recruited in the G_0/G_1 phase.

3.3. Modification of the Molecular Markers Caused by the Cyclic 5-FU *O,N*-Acetals

Due to the fact that the cyclic *O,N*-acetals accumulate the cells in the G_1 -phase the expression pattern of cyclin D1 was studied. This cyclin is one of the cyclin-dependent kinase (CDK) activator subunits, specifically to CDK4, being responsible of the progression of the cell through the G_1 -phase. Compounds **4** and **10** gave rise to a spectacular inhibition of cyclin D1 up to its total disappearance. This fact did not take place with 5-FU because the cyclin D1 level increased in relation to those of the parental MCF-7 cells. On one hand, this would explain why these compounds accumulate the cells in the G_1 -phase (on inhibiting cyclin D1 the cell cannot progress to the S phase) and on the other, they show a different mechanism of action from the one shown by 5-FU: in short, they are not prodrugs. 5-FU increases the cyclin D1 production so that cells pass in most cases toward the S phase where they are held back. It has been reported¹⁵⁹ that cyclin D1 works as an active “switch” in the progression of the cellular cycle and that elevated levels of cyclin D1 promote the entry of the cell into the S phase. Moreover, compound **10** increases the expression of proteins p21 or p27 even up to double of the control. These proteins belong to the family INK2 of the CDK inhibiting proteins that work by hindering the association and activation of cyclins with their complexes¹⁶⁰ and hence they halt cells in the G_1 and G_2/M phases.

Compounds also affect the *cdc2* activity that, regulated by their corresponding cyclins A or B, is essential for the entrance into mitosis during the cellular cycle.¹⁶¹ Compounds **4**, **10** and **5**, significantly decrease the *cdc2* activity. *cdc2* is needed

during the cellular cycle in the final phase of G₁, in the control point named “start” to be committed to the mitotic cycle. This is because at the end of G₂ (at the beginning of the mitosis)¹⁶² the inhibition of cdc2 by the *O,N*-acetals implies the halting of the cycle in G₁ and the non-entrance of the tumor cells in mitosis. The increase of the cdc2 expression caused by 5-FU is due to the fact that this higher activity is necessary for the cells to pass rapidly to the S phase, where cells are stopped by this fluoropyrimidine. Finally, compound **8** also significantly increases the cdc2 levels, which may be because its premature activation is one of the requirements for apoptosis¹⁶³ in fact this compound is the one that induces a higher proportion of programmed cellular death in the MCF-7 treated cells.

3.3.1. Apoptosis Markers

Since the synthesized compounds induce very important apoptosis, we have carried out studies of the expression of some of the genes that intervene in this phenomenon, among which p53 and the family bcl-2 are outstanding. The tumour suppressor gene p53 protects the integrity of the genome so that if the DNA of the cell is damaged by an agent, an overexpression of it is produced inducing the stopping in G₁ for the repair of the damage, or if this is not possible, enter in apoptosis.¹⁶⁴ On the other hand, the members of the family of proteins Bcl-2 work as regulators of apoptosis, Bcl-2 and Bcl-XL protecting against apoptosis. Bax, Bak and Bad induce such a phenomenon.¹⁶⁵

The treatment of the MCF-7 cells (wild-type p53) with these compounds provoked in general an increase in the protein expression of p53, mainly for 5-FU and **8**, and a marked decrease of the levels of bcl-2 for all of them. These data show that p53 activity is restored with the compounds, allowing the entrance of the tumour cells in apoptosis, which permits their elimination by this mechanism. In the same way bcl-2 inhibition facilitates the entrance of cells into the programmed cell death.

3.4. Benzo-Fused Seven-Membered Derivatives Linked To Purines

Later on, we substituted the pyrimidine bases for the purine one (with several substituents at its position 6), with the objective of increasing both the lipophilicity and the structural diversity of the target molecules (Figure 3.2). Their syntheses (using conventional heating and microwave irradiation) and biological activities have been recently published.¹⁶⁶

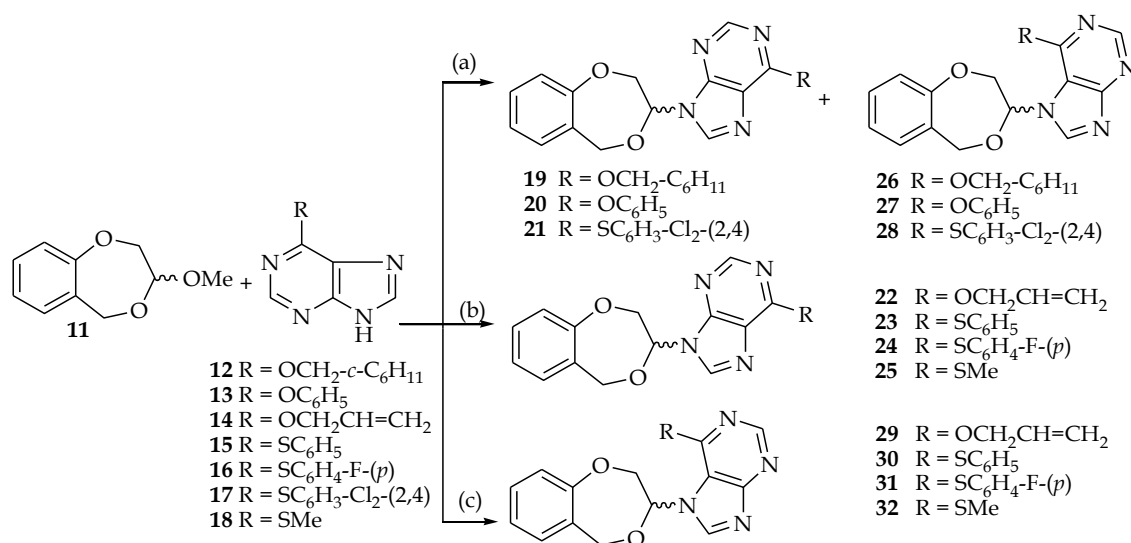


Figure 3.2. Reagents and conditions: Purine bases (12-18), TCS, HMDS, SnCl₄, anhydrous MeCN. Method (a), (b) or (c): 45 °C, 24-72 °C; (b) microwave, 130 °C, 5 min; (c) microwave, 100 °C, 5 min.

3.4.1. Antiproliferative activities

The antitumour potential of the target molecules is reported against the MCF-7 human breast cancer cell line including 5-FU as reference drug (Table 3.2).¹⁶⁶ The purine O,N-acetals 19-32 are more active than their corresponding purine bases 12-18. The differences in the antiproliferative effect of the N-7 and N-9 regioisomers are not significant with the exception of the allyloxy derivatives 22 and 29. The biological effect is dependent on the substituent present on position 6 of the purine

ring although a clear structure-activity relationship between the size of this moiety and the antiproliferative effect of the MCF-7 human breast cancer cell line is not observed. The most active compound (**22**), that presents an allyloxy group as substituent at position 6 of the purine ring, shows an $IC_{50} = 5.04 \pm 1.68 \mu\text{M}$ nearly equipotent as 5-FU. The following two more active compounds, **23** and **28**, present bulky substituents as the phenylthio and 2,4-dichlorophenylthio ones, respectively.

Table 3.2. Antiproliferative activities against the MCF-7 cell line for 5-FU¹⁶⁷ for the purine bases (**12-18**), and for the seven-membered alkylated purine derivatives (*N*-9 isomers: **19-25**; *N*-7 isomers: **26-32**).

Compound	IC ₅₀ (μM)	Compound	IC ₅₀ (μM)	Compound	IC ₅₀ (μM)
5-FU	4.32 ± 0.02	19	11.6 ± 0.93	27	21.1 ± 2.93
12	32.3 ± 1.42	20	24.7 ± 3.82	28	8.4 ± 0.91
13	28.4 ± 0.45	21	12.0 ± 0.59	29	20.9 ± 1.24
14	44.7 ± 0.74	22	5.04 ± 1.68	30	15.6 ± 3.74
15	31.0 ± 0.16	23	7.12 ± 0.46	31	14.1 ± 0.67
16	31.6 ± 0.54	24	11.2 ± 1.32	32	31.8 ± 5.46
17	21.4 ± 0.42	25	24.0 ± 1.95		
18	23.6 ± 4.11	26	13.4 ± 1.94		

To study the mechanisms of the antitumour and antiproliferative activities of the most active compounds (**22**, **23** and **28**), the effects on the cell cycle distribution were analyzed by flow cytometry (Table 3.3). DMSO-treated cell cultures contained a 58.62 ± 0.74 of the G₀/G₁-phase cells, a 33.82 ± 0.72 of the S-phase cells and a 7.55 ± 1.34 of the G₂/M-phase cells. In contrast, MCF-7 cells treated during 48 h with the IC₅₀ concentrations of **22**, **23** and **28** showed important differences in cell cycle progression compared with DMSO-treated control cells. The cell cycle regulatory activities can be divided into the following two groups: (a) with the compound **22** the breast cancer cells showed an accumulation in the S-phase, up to 37.00 ± 2.00 of the cells, mainly at the expense of the G₀/G₁-phase population that decreased to a percentage of 55.63 ± 1.57 of the cells; (b) compounds **23** and **28** accumulated the cancerous cells in the G₂/M-phase (11.08 ± 1.01 and 19.16 ± 0.56 , respectively) at the expense of the S-phase cells (26.82 ± 1.26 and 22.73 ± 0.37 , respectively).

In response to **23** (and **28**), the percentage of apoptotic cells increased, from 0.22 ± 0.31 in control cells to a maximum of 73.37 ± 0.12 (and 65.28 ± 1.92) apoptotic cells at a concentration equal to their IC_{50} against the MCF-7 cell line. This is a remarkable property because the demonstration of apoptosis in MCF-7 breast cancer cells by known apoptosis-inducing agents has proved to be difficult.

Table 3.3. Cell cycle distribution and apoptosis induction in the MCF-7 human breast cancer cell line after treatment for 48 h for the three most active compounds.

Compound	Cellcycle ^a			Apoptosis ^b
	G ₀ /G ₁	S	G ₂ /M	
Control	58.62 ± 0.74	33.82 ± 0.72	7.55 ± 1.34	0.22 ± 0.16
22	55.63 ± 1.57	37.00 ± 2.00	7.37 ± 0.43	44.47 ± 2.98
23	59.10 ± 1.28	26.82 ± 1.26	11.08 ± 0.01	73.37 ± 0.12
28	58.10 ± 0.19	22.73 ± 0.37	19.16 ± 0.56	65.28 ± 1.92

a) Determined by flow cytometry.¹⁶⁸ b) Apoptosis (48 h) was determined using an Annexin V-based assay.¹⁶⁸ The data indicate the percentage of cells undergoing apoptosis in each sample. All experiments were conducted in duplicate and gave similar results. The data are means \pm SEM of three independent determinations.

3.5. The (1,2,3,5-tetrahydro-4,1-benzoxazepine-3-yl) moiety linked to pyrimidine and -purine bases

The synthesis and the mechanistic aspects of bioisosteres containing a 4,1-benzoxazepine *N*-alkylated pyrimidine (**33-45**) or purine (**46-58**) (Figure 3.3) have been thoroughly discussed.^{169,170}

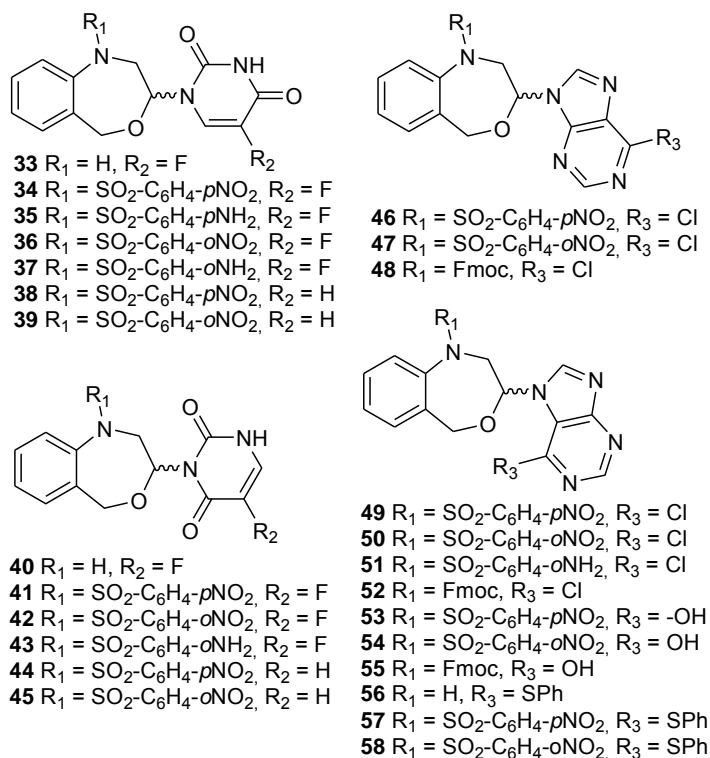


Figure 3.3. New benzoxazepine *O,N*-acetals containing pyrimidine and purine rings.

3.5.1. Antiproliferative activities

Table 3.4 show the antiproliferative activity (IC_{50} values) on MCF-7 human breast cancer cells found for the pyrimidine and purine derivatives **33-58**.¹³⁹ The most potent molecules were the purine derivatives. Compounds **48**, **50**, **52** and **57** presented IC_{50} values below 1 μ M. Between the pyrimidine derivatives **33-45**, those containing 5-fluorouracil ($R_2 = F$) showed improved activities than those derived of uracil ($R_2 = H$). Bonding of the pyrimidine ring through *N*-1 or *N*-3 affected the activity though only slightly, when $R_1 = H$, **33** versus **40**. The substitution on C-6 of the purine ring is essential for the activity. Bulky, lipophilic groups afforded the best values of IC_{50} [$R_3 = Cl$ (**46-52**), $-SPh$ (**57**, **58**)] while purinone compounds [$R_3 = OH$ (**53-55**)] were comparable to the pyrimidine analogues in terms of activity.¹⁷¹ Bonding of the purine ring through *N*-7 or *N*-9 affected the activity to a lesser extent, and the positive or negative character of this effect depended on the nature of R_1 (see **46/49** $R_1 = pNs$, **47/50** $R_1 = oNs$, **48/52** $R_1 = Fmoc$).

Both, pyrimidine and purine derivatives, were more potent when R₁ is not hydrogen. The lipophilic character of R₁ increased the activity and no limit of volume had been observed for the studied groups. The electron-withdrawing character of R₁ could help to increase the activity.¹⁷² Carbonyl derivatives were more potent than the sulfonyl ones.

Table 3.4. Antiproliferative activities against the MCF-7 cells for *N*-1- (**33-39**) and *N*-3- (**40-45**) pyrimidines and for *N*-9- (**46-48**) and *N*-7- purines (**49-58**).

Compds	IC ₅₀ (μM)	Compds	IC ₅₀ (μM)	Compds	IC ₅₀ (μM)	Compds	IC ₅₀ (μM)
33	>100	40	72.40 ± 11.3	47	2.10 ± 0.69	54	19.66 ± 5.27
34	19.33 ± 1.04	41	19.81 ± 0.08	48	0.67 ± 0.18	55	53.57 ± 13.1
35	14.37 ± 0.69	42	22.63 ± 0.11	49	1.22 ± 0.12	56	48.92 ± 9.89
36	19.70 ± 0.15	43	43.70 ± 0.09	50	0.92 ± 0.01	57	0.86 ± 0.12
37	54.82 ± 1.04	44	44.28 ± 4.65	51	9.14 ± 1.24	58	2.59 ± 0.57
38	39.78 ± 2.60	45	50.90 ± 3.87	52	0.84 ± 0.09		
39	45.17 ± 0.48	46	2.73 ± 0.17	53	>100		

When R₁ = benzenesulfonamido, it can be observed for pyrimidine and purine derivatives that the *ortho*-substitution on R₁ is preferred to *para*, in terms of potency, and the nitro group renders better results than the amino one. As an exception, compound **57** (R₁ = *p*Ns, R₃ = SPh), is more potent than **58** (R₁ = *o*Ns, R₃ = SPh). The new related acyclic *O,N*-acetals **59-69** (Figure 3.4) were obtained as minor products in the condensation reaction between the *O,O*-acetals and pyrimidine¹⁶⁹ or purine¹⁷⁰ bases. Their antiproliferative activities have also been studied on MCF-7 human breast cancer cells and the IC₅₀ values obtained are shown in Table 3.5. Acyclic purine *O,N*-acetals (**67-69**) show higher potency than the pyrimidine acyclic derivatives (**59-66**). The *N*-7- alkylated purine **68** presented an excellent value of IC₅₀. In contrast to the cyclic analogues, the presence of an *o*-NO₂ or *p*-NO₂ group does not modify the activity of the *N*-9-isomers (**67** and **69**).

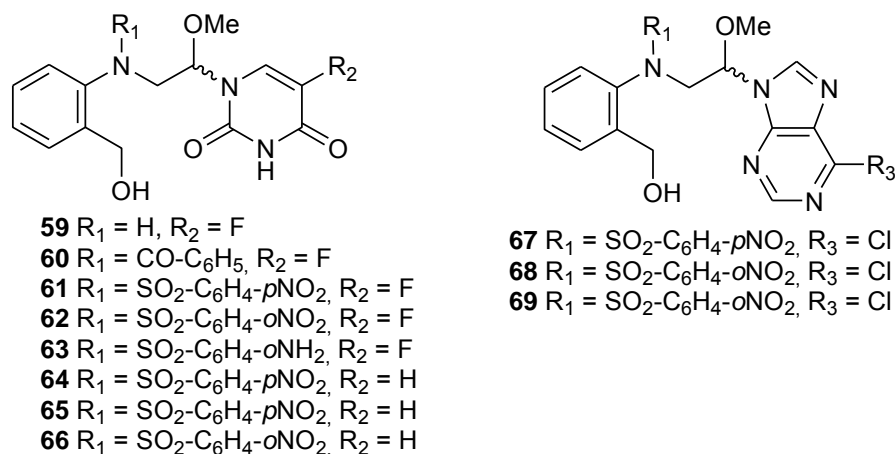


Figure 3.4. New acyclic *O,N*-acetals containing pyrimidine and purine moieties.

Compounds **48** and **57** were selected to identify the molecular key targets of its anti-cancer activity.¹⁷¹ Completion of the human genome sequence and the advent of DNA microarrays using cDNAs enhanced the detection and identification of hundreds of differentially expressed genes in response to anticancer drugs. In this way gene-expression patterns of treated human breast cancer cells in comparison with parental MCF-7 cells were obtained. For this purpose, the expression of about 22,000 different human genes was analyzed using the Agilent 60-mer oligo microarray platform and the Human 1A Oligo Microarray Kit (V2) (Agilent Technologies, CA, USA).

Table 3.5. Antiproliferative activities against the MCF-7 cell line for acyclic *N*-1- and *N*-3-pyrimidines (**59-66**) and *N*-9- and *N*-7 purines (**67-69**).

Compds	IC ₅₀ (μM)	Compds	IC ₅₀ (μM)
59	35.97 ± 0.40	65	55.22 ± 12.14
60	16.14 ± 0.77	66	64.81 ± 0.05
61	55.22 ± 12.14	67	18.70 ± 0.08
62	90.99 ± 6.06	68	3.25 ± 0.23
63	>100	69	11.30 ± 1.27
64	45.76 ± 2.45		

BACKGROUND

The up-regulated and the down-regulated genes include genes that encode for different metabolic pathways, cellular development process, signal molecules, response to stress, regulation of the cell cycle and apoptosis, etc. Analysis of the mRNAs, which are deregulated (up-regulated or down-regulated) at least 2-fold in treated cells, revealed the following results: 26 genes up-regulated and 59 genes down-regulated in **48**-MCF-7 treated cells; and 26 genes up-regulated and 17 genes down-regulated in **57**-treated human breast cancer cells. Each compound revealed a somewhat unique expression pattern together with the up-regulation of significant genes involved in different cellular functions and a significant down-regulation of genes for **48**. One of the more important results in the current study was the ability of **48** to modulate the expression of genes involved in apoptosis or its delay of mitosis. This effect can be explained by the accumulation of cells in the G₂/M checkpoint of cell cycle, particularly GP132, the receptor for an unknown ligand, which activates a G2 alpha protein.¹⁷¹ This is transcriptionally up-regulated by stress-inducing and cell-damaging agents and that is involved in caspase-mediated apoptosis.¹⁷³ Similarly, the ERN1 gene that belongs to the Ser/Thr protein kinase family is a potent unfolded-protein response transcriptional activator and acts by triggering growth arrest and apoptosis.¹⁷⁴ However, **57** induced the down-regulation of a gene involved in the metastatic progression of cancer such as RAC1, a Ras-like protein member of the Rho family of the GTPase key downstream target in Ras signaling.¹⁷⁵

The studies by microarray technology showed that the main molecular targets of some of these compounds (**48** and **57**) are pro-apoptotic genes with protein kinase activity such as GP132, ERN1 or RAC1, which prevent the metastatic progression.¹⁷¹

3.6. Synthesis and anticancer activity of (*RS*)-9-(2,3-dihydro-1,4-benzoxathiin-3-ylmethyl)-9*H*-purines

The 2,3-dihydro-1,4-benzodioxin ring system is present in a large number of structures of therapeutic agents possessing important biological activities.¹⁷⁶ Some of them are antagonists of α -adrenergic receptors, giving them antihypertensive properties.^{177,178} Others have affinities with serotonin receptors which are involved in nervous breakdown and schizophrenia.¹⁷⁹ Twelve years ago, 2,3-dihydro-1,4-benzodioxins were developed as inhibitors of 5-lipoxygenase, an enzyme involved in the oxygenation of arachidonic acid to the leukotriens; they are also useful for the treatment of inflammatory diseases such as asthma and arthritis.¹⁸⁰ The occurrence of the 2,3-dihydro-1,4-benzodioxin structure in various naturally abundant compounds has been also reported.¹⁸¹ Paradoxically, despite the considerable development of biologically active compounds with the 2,3-dihydro-1,4-benzodioxin moiety, the 2,3-dihydro-1,4-benzoxathiin skeleton has still remained inaccessible.

The importance of 5-FU as the first-choice drug in carcinomas of the gastrointestinal tract is well known despite its side-effects. With the aim of diminishing the toxicity and obtaining biologically active derivatives of 5-FU suitable for oral administration great effort has been made in the preparation of 5-FU prodrug derivatives. A review of the literature on the various prodrugs of 5-FU has been published.¹⁸²

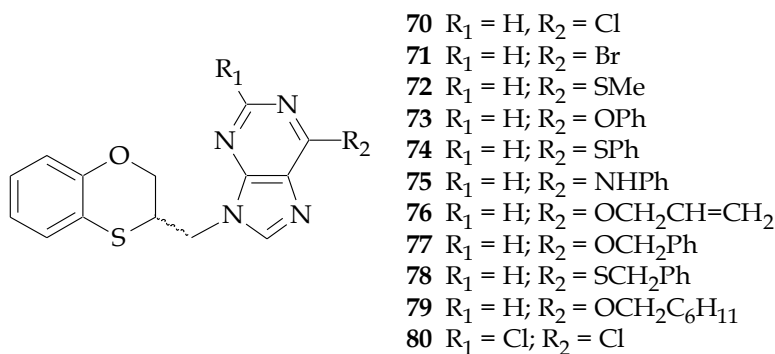


Figure 3.5. The 1,4-benzoxathiin system linked to several purines.

Various 5-FU prodrugs are active against certain malignant cell lines due to an inhibition of thymidilate synthase by the formation of 5-fluorodeoxyuridine monophosphate or by the incorporation of 5-fluorouridine triphosphate into RNA. During various synthetic studies on masked 5-FU derivatives, it has been found that the bond strength between the *N*-1 atom in the 5-FU ring and its *N*-1 substituent is an important factor influencing the antitumour activity and the toxicity of the compounds. The previous results indicated that the weaker the bond strength, the stronger are the antitumour activity and the toxicity of the masked compounds.¹⁸³ In the case of *N*-alkyl-5-FU derivatives, the strong *N*-15-FU-C_{exocyclic} bond conversely prevented these derivatives from being easily hydrolyzed in vivo and showed no antitumour activity against L1210 leukaemia.¹⁸⁴ When oxygen was introduced at the α -position to the alkyl group, the N-C bond became labile under hydrolytic conditions and the resulting derivatives showed antitumour activity.

As it has been demonstrated before, compounds **4-6**, **8-10** may be considered as drugs with their own entity and antitumour activity independent of that of 5-FU. If the previously described compounds are not prodrugs, it is not necessary to maintain the *O,N*-acetalic characteristic with the corresponding weakness of the *O,N*-acetalic bond. Therefore, molecules are being designed in which both structural entities (such as the benzoheterocyclic ring and the purine base) are linked by a heteroatom-C-C-base-N-atom bond. Very recently the design, synthesis and biological evaluation of a series of 2- and 6-disubstituted (*RS*)-9-(2,3-dihydro-1,4-benzoxathiin-3-ylmethyl)-9*H*-purine derivatives **70-80** were described [Figure 3.5, Table 3.6].¹⁸⁴

Table 3.6. Antiproliferative activities against the MCF-7 cell line for 5-FU¹⁸⁵ and the six-membered alkylated purine derivatives.

Compound	IC ₅₀ (μ M)	Compound	IC ₅₀ (μ M)	Compound	IC ₅₀ (μ M)
5-FU	4.32 \pm 0.02	73	20.5 \pm 1.11	77	23.2 \pm 1.26
70	10.6 \pm 0.66	74	10.5 \pm 1.06	78	16.7 \pm 3.03
71	6.18 \pm 1.70	75	11.2 \pm 2.73	79	17.4 \pm 1.60
72	20.5 \pm 1.81	76	17.5 \pm 0.25	80	8.97 \pm 0.83

Three of the most potent compounds (**70**, **71** and **80**) were subjected to cell cycle and apoptosis studies on the MCF-7 human breast cancer cell line (Table 3.7). The following two consequences can be stated: (a) in contrast to 5-FU, the six-membered compounds **70**, **71** and **80**, provoked a G₀/G₁-phase cell cycle arrest when the MCF-7 cells were treated during 48 h with the IC₅₀ of the compounds, mainly at the expense of the S-phase populations. The fact that at similar doses the novel derivatives exhibit different sequences of cell cycle perturbations in comparison with 5-FU indicates that these compounds act by different pathways.¹⁸⁶ In the case of **71** it is worth pointing out that, moreover, there is an increase in the G₂/M-phase of the cancerous cells; and (b) the apoptotic indices of the target compounds are very important, especially for **80** (58.29% for **70**, 63.05% for **71**, and 76.22% for **80**). Up to now and according to our knowledge, compound **80** is the most important apoptotic inducer against the MCF-7 human breast cancer cell line so far reported.

Table 3.7. Cell cycle distribution and apoptosis induction in the MCF-7 human breast cancer cell line after treatment for 48 h for the three most active compounds as antiproliferative agents.

Compound	Cellcycle ^a			Apoptosis ^b
	G ₀ /G ₁	S	G ₂ /M	
Control	58.62 ± 0.74	33.82 ± 0.72	7.55 ± 1.34	0.22 ± 0.16
5-FU ^c	58.07 ± 0.11	39.38 ± 0.98	2.10 ± 0.12	52.81 ± 1.05
70	69.71 ± 1.50	23.73 ± 1.65	6.56 ± 0.17	58.29 ± 0.75
71	62.85 ± 0.87	26.71 ± 1.25	10.43 ± 0.38	63.05 ± 0.26
80	70.30 ± 0.32	23.67 ± 2.40	6.06 ± 2.72	76.22 ± 2.02

a) Determined by flow cytometry.¹⁸⁶

b) Apoptosis was determined using an Annexin V-based assay.¹⁸⁶ The data indicate the percentage of cells undergoing apoptosis in each sample.

c) Data were taken from ref.¹⁸⁷ All experiments were conducted in duplicate and gave similar results. The data are means ± SEM of three independent determinations.

In short, breast cancer is the commonest malignancy in women and comprises 18% of all cancers in women. Normal breast development is controlled by a balance

between cell proliferation and apoptosis, and there is strong evidence that tumour growth is not just a result of uncontrolled proliferation but also of reduced apoptosis. The balance between proliferation and apoptosis is crucial in determining the overall growth or regression of the tumour in response to chemotherapy, radiotherapy and more recently, hormonal treatments. All of these approaches act in part by inducing apoptosis. Understanding these relationships could allow individually tailored treatments to maximize tumour regression and efficacy of treatment. It could also help to answer why some tumours fail to respond and thereby indicate new routes of drug development.

Starting from Ftorafur, a known 5-FU prodrug, which shows an 58% apoptosis induction in the MCF-7 human breast cancer cell line after treatment for 48 h, the seven-membered cyclohomologue 5-FU *O,N*-acetal **3** and the benzo-fused dihydrooxepine *O,N*-acetal **8** present apoptosis inductions higher than 50%. By using molecular modification strategies widely used in medicinal chemistry, lately compounds **23** and **28**, having in common the benzo-fused 2,3-dihydro-5*H*-1,4-dioxepin and a 6-substituted purine moieties, show 73% and 65% apoptosis inductions. Finally and following our Drug Anticancer Programme, the benzo-fused 1,4-oxathiane moiety linked to the *N*-9 atom of a 2,6-dichloropurine **80** was designed and synthesized. According to our knowledge this is the most important apoptotic inducer against the MCF-7 human breast cancer cell line so far reported. This compound is a more potent apoptosis inductor than the clinically-used drug paclitaxel (Taxol[®]), which induced programmed cell death up to 43% of cell population. Their mechanisms of action at molecular level are being studied at present.

4. RESUMEN

4.1. Antecedentes

Los *seco*-nucleósidos son nucleósidos no clásicos en los que el “azúcar” es lineal en lugar de cíclico. Entre ellos, los análogos isopropoxi **2a** y ciclopentoxi **2b** exhiben actividad antitumoral frente a la línea celular humana HEp de cáncer de laringe. La estructura más lipofílica resultó ser la más activa de todos los compuestos ensayados, siendo 4 veces más activo que el 5-fluorouracilo (5-FU, **1**). Ya que no se había llevado a cabo ningún tipo de estudio de relaciones estructura-actividad en *O,N*-acetales cíclicos de siete miembros de 5-FU, pensamos en dirigir nuestros esfuerzos hacia este interesante tipo estructural con el objetivo de la búsqueda de nuevos agentes antitumorales. Por una parte, con la idea de aumentar la lipofilia de **3**, propusimos una serie de *O,N*-acetales de siete miembros bioisósteros fusionados con un anillo de benceno tales como **4a-c** y **5**, derivados del alcohol o del aldehído salicílico.^{146,186,187} Por otra parte, la preparación del derivado de seis miembros tal como **6** podría recalcar la importancia de la actividad biológica de los *O,N*-acetales de 5-FU de siete miembros (Figura 1). En todos los casos la unión con el resto de 5-FU tiene lugar en la posición N-1' del anillo pirimidínico.

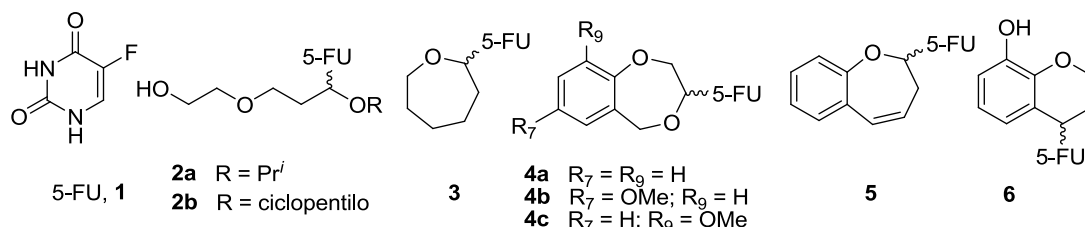


Figura 1.

Posteriormente, se preparó la estructura di-*O,N*-acetálica macrocíclica de 14 miembros que manifiesta una alta actividad biológica¹⁴⁸ (Figura 2).

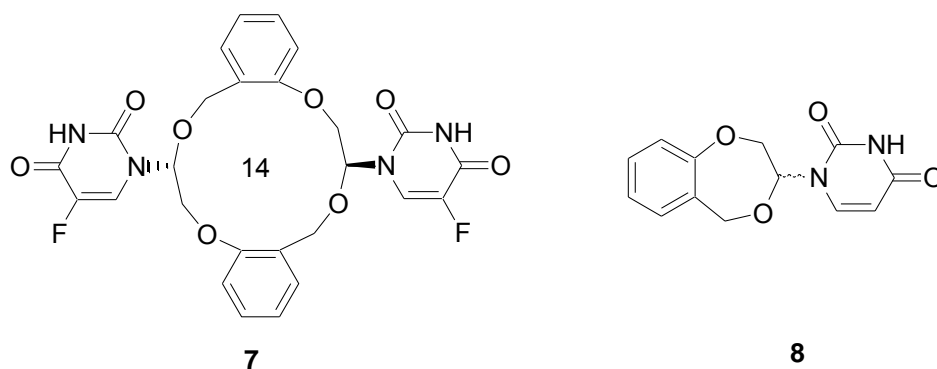


Figura 2.

El compuesto **6** presenta una actividad apoptótica notable y no puede ser profármaco del 5-FU, en consecuencia e intentando dar un giro más profundo a la investigación se preparó el compuesto **8**, que es análogo a **4a**, pero en el que la base citotóxica sintética 5-FU unida al anillo de siete miembros se sustituyó por la base natural uracilo. El hecho de que el compuesto (*RS*)-1-(2,3-dihidro-5*H*-1,4-benzodioxepin-3-il)uracilo **8** presente actividad antitumoral cuando en su estructura se encuentra presente una base natural, hace pensar que esta estructura es un fármaco “*per se*”. Sobre la base de las variaciones moleculares se llevaron a cabo sustituciones isostéricas sobre el prototipo **4a** y de esta forma se prepararon y ensayaron una serie de *O,N*-acetales con las estructuras de (*RS*)-1-(2,3-dihidro-5*H*-4,1-benzoxatiepín-3-il)-uracilo o -timina. Se encontró que los compuestos **9** y *trans*-**10** son inhibidores del crecimiento de la línea tumoral de cáncer de mama MCF-7¹⁸⁸ (Figura 3).

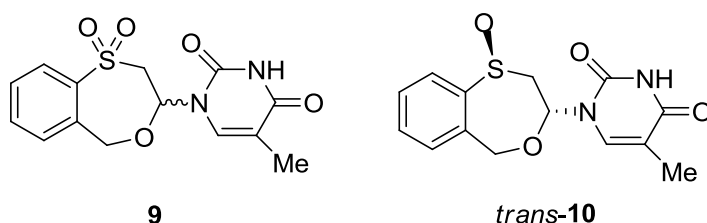


Figura 3.

Posteriormente y con objeto de completar un estudio SAR, se preparó y ensayó una serie de (*RS*)- 7- ó 9-(1,2,3,5-tetrahidro-4,1-benzoxazepina-3-il)-7*H*- ó 9*H*-purinas sustituidas en posición 6. Los estudios mediante la tecnología de microarrays muestran que los objetivos moleculares fundamentales de los

compuestos **11** y **12** son genes pro-apoptóticos con actividad quinasa tales como GP132, ERN1 o RAC1, que impiden la progresión metastática^{171,189} (Figura 4).

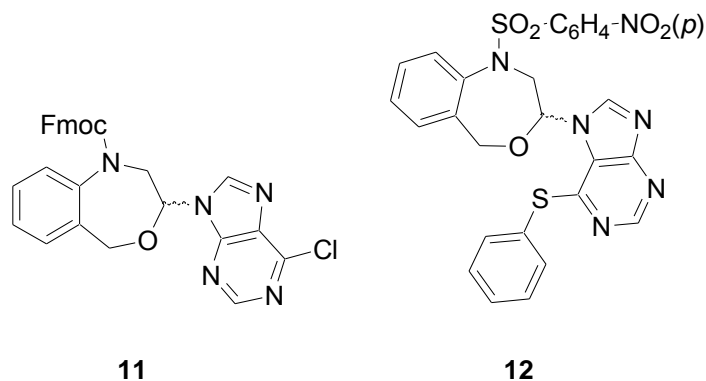


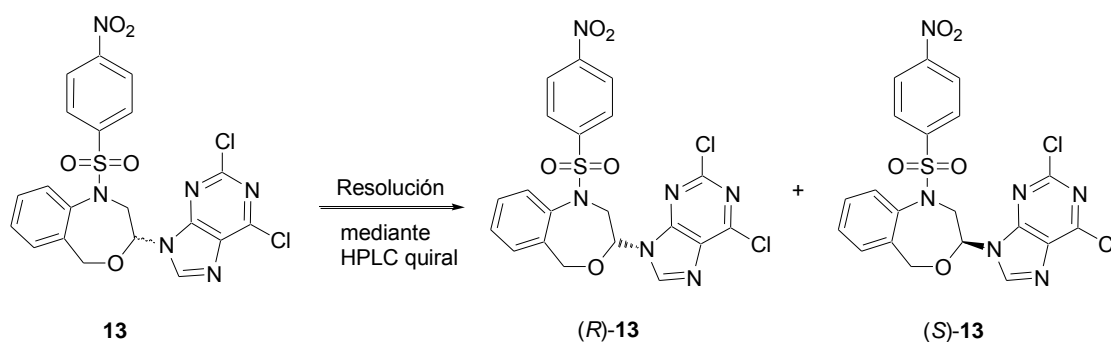
Figura 4.

Con el objeto de completar un estudio de relaciones-estructura actividad se llevó a cabo la síntesis asistida por microondas de dos series de 7- ó 9-(1,2,3,5-tetrahydro-4,1-benzoxazepino-3-il)-7*H* ó 9*H*-purinas sustituidas en 6. Para la mayoría de los compuestos los valores de CI_{50} de las actividades anti-proliferativas frente a las líneas cancerosas MCF-7 y MDA-MB-231 son inferiores a 1 μ M.¹⁹⁰

El conocimiento de las rutas moleculares que estimulan a los tumores ha conducido a las identificaciones tanto del EGFR como del factor de crecimiento vascular endotelial (VEGF) como componentes clave que están implicados en la regulación de la proliferación tumoral y de la angiogénesis, respectivamente. La inhibición doble de las rutas de señalización molecular, tales como la del receptor del factor de crecimiento epidérmico EGFR y la del factor del crecimiento vascular endotelial VEGF, puede solucionar el problema de la resistencia a fármacos (MDR) y fomentar la sinergia.¹⁹¹ Publicaciones científicas que se concentran en el período 2004-2012, afrontan la problemática de la inhibición doble de EGFR y de VEGF, lo que apoya el carácter innovador de esta aproximación terapéutica. Los fármacos utilizados son estructuras derivadas de 4-anilino-quinazolinas, tales como el gefitinib y erlotinib, y anticuerpos monoclonales como el trastuzumab, utilizados solos o en combinación con otros fármacos. Sin embargo, únicamente se han utilizado dos fármacos enantioméricamente puros: a) el (-)-gospol, que es un

polifenol derivado de la planta del algodón (género *Gossypium*, familia *Malvaceae*);¹⁹² y b) **AEE788**, producto sintético preparado por Novartis.¹⁹³

El derivado **AEE788** presenta la estructura básica de 7*H*-pirrolo[2,3-*d*]pirimidina, que puede considerarse un bioisómero de la unidad de quinazolina, presente en las moléculas lapatinib y gefitinib. En la patente¹⁹⁴ se presentan los dos enantiómeros de un nuevo prototipo tetracíclico, tal como el de 9-[1-(*p*-nitrobencénsulfonil)-1,2,3,5-tetrahidro-4,1-benzoxazepin-3-il]-2,6-dicloro-9*H*-purina (**13**),¹⁹⁵ con inhibición doble del EGFR y del VEGF, con producción de un elevado nivel de apoptosis en células tumorales y además, sin manifestación de toxicidad aguda y crónica. El compuesto **13** es muy selectivo frente a las líneas cancerosas de adenocarcinoma de mama MCF-7 y MDA-MB-231 (con índices terapéuticos de 5.1 y 11.0) en relación con la línea celular normal MCF-10A. La CI_{50} frente a la línea MDA-MB-231 es 166 ± 0.063 nM.¹⁹⁵



Esquema 1.

Últimamente, se obtuvo una serie de derivados de (*RS*)-9-(2,3-dihidro-1,4-benzoxatien-3-il)metil)-9*H*-purinas mediante la reacción de Mitsunobu que condujo a una contracción a un anillo de seis miembros a partir del (*RS*)-3,4-dihidro-2*H*-1,5-benzoxatien-3-ol *vía* un intermedio de episulfonio.¹⁹⁵ Merecen destacarse los índices apoptóticos de los compuestos más activos [**14** (63.05%) y **15** (76.22%), Figura 5].

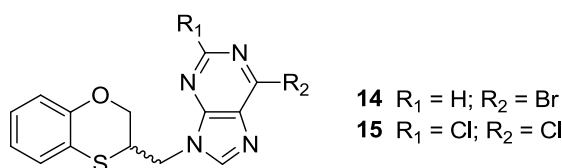


Figura 5.

De acuerdo con nuestros conocimientos, el derivado **15** es el inductor apoptótico más potente frente a la línea de cáncer de mama MCF-7, hasta este momento publicado.

4.2. Bases sobre las que se sustenta esta tesis doctoral

De acuerdo con los resultados obtenidos (sobre la línea MCF-7), son de destacar los siguientes aspectos que constituyen la hipótesis fundamental sobre la que se fundamentará esta tesis doctoral:

1. Las estructuras **4a,b,c-15** poseen actividad antiproliferativa frente a la línea tumoral MCF-7 de cáncer de mama humano.^{146,148,186,187}

2. Los derivados **8**, **9** y *trans*-**10** muestran interesantes actividades anticancerosas comportándose como agentes antiproliferativos cuando, en sus estructuras, están presentes las bases naturales uracilo y timina. Este hecho no tiene precedentes en la literatura científica y es un hallazgo de gran trascendencia.^{146,186,187}

3. Los compuestos **4a,b,c-8** producen una parada del ciclo celular en la fase G₀/G₁.^{146,186,187}

4. Los compuestos **4a,b,c-8** provocan una reducción de los niveles de la ciclina D1 y un aumento de p53. Estudios recientes han demostrado que la sobreexpresión de la ciclina D1 causa una proliferación celular descontrolada.¹⁹⁶

5. Los compuestos reseñados no manifiestan toxicidad cuando se inoculan por vía intravenosa en la cola de ratones, con un protocolo de dos inyecciones por semana con una dosis de 50 mg/kg en cada administración.

4.3. Importancia de la quiralidad en los fármacos

Aproximadamente el 80% de los compuestos activos que las compañías farmacéuticas tienen en proyecto lanzar al mercado son quirales y se estima que esta fracción se incrementará en un futuro muy próximo. Se está imponiendo el lanzamiento al mercado de sustancias activas enantioméricamente puras con la

normativa cada vez más restrictiva del organismo americano que regula a los alimentos y a los fármacos (US Food and Drug Administration, FDA). Las autoridades responsables del registro de nuevos compuestos activos exigen cada vez más la síntesis de un único enantiómero. Desde 1992 tanto la FDA americana como su análogo paralelo europeo (European Committee for Proprietary Medicinal Products) han establecido que hay que caracterizar de manera individual la acción fisiológica de cada enantiómero de todo producto farmacéutico con un centro estereogénico, y desde el año 1997 el programa “Un Único Isómero” ha permitido a las compañías farmacéuticas acortar los tiempos de registro con el llamado “cambio quiral”. Además de la disminución de las dosis y la mejora de la eficacia, las extensiones de las patentes han representado también la fuerza motriz para que las compañías farmacéuticas conviertan los compuestos activos racémicos en sus formas enantioméricamente puras.¹⁹⁷

Un reto importante de esta tesis es el del control estereoquímico en la síntesis de purinas alquiladas por heterociclos de seis miembros con un centro estereogénico y con actividad anticancerosa específica frente a genes apoptóticos.

Los siguientes datos son contundentes: las ventas en todo el mundo de fármacos quirales en forma de un único enantiómero han seguido creciendo un 13% anual hasta alcanzar los 133.000 millones de dólares en el año 2000, de acuerdo con los datos suministrados por la firma consultora Technology Catalysts International (EE UU). De acuerdo con la tendencia observada, en el año 2010, se alcanzaron los 250.000 millones de dólares. De acuerdo con la misma firma, el 40% de los fármacos vendidos a nivel mundial durante el 2000 fueron enantiómeros puros, mientras que en 1999, el porcentaje fue un tercio del anterior.

En resumen, la preparación de fármacos homoquirales representa un mercado potencial para la industria farmacéutica y un reto intelectual para la Ciencia, desde el punto de vista de metodología química y por la estereo-especificidad que suelen mostrar los fármacos en sus interacciones con las dianas biológicas.

4.4. Nuevas investigaciones

A continuación, se van a resumir brevemente las cuatro contribuciones más importantes de esta tesis doctoral:

4.4.1. Síntesis y actividad anticancerosa de *(RS)*-9-(2,3-dihidro-1,4-benzoxaheteroin-2-ilmetil)-9*H*-purinas

En este apartado se describe la síntesis y la actividad anticancerosa de dos series bioisostéricas [(*RS*)-9-(2,3-dihidro-1,4-benzoxatiin-2-ilmetil)purinas sustituidas **16-19** y (*RS*)-9-(2,3-dihidro-1,4-benzodioxin-2-ilmetil)purinas sustituidas **20-23**] (Figura 6).

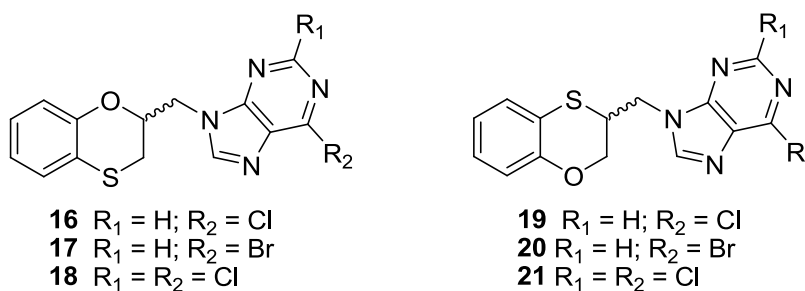


Figura 6.

Durante la preparación de **16-19**, se aíslan también productos de isomerización de la serie A. Formalmente, tiene lugar una migración 1,4-tio (desde el resto 2,3-dihidro-1,4-benzoxatiin-2-ilmetil para producir el esqueleto 2,3-dihidro-1,4-benzoxatiin-3-ilmetil) a través de dos participaciones de grupo vecino O-3 y S-3 (o S-4 más improbable) en el anillo de seis miembros. Los compuestos más activos son **18** y **17** (Figura 6) con $CI_{50} = 2.75 \pm 0.03$ y 4.87 ± 0.02 , respectivamente. El derivado **18** es 3.3 veces más activo como agente antiproliferativo frente a la línea celular de cáncer de mama humano MCF-7 que su correspondiente isómero **15**.¹⁹⁵ Por otra parte, la inducción de apoptosis tras tratamiento de 48 h con los compuestos **18** y **15** se encuentra en el mismo rango {con un porcentaje de células que sufren apoptosis del 70.08% (**18**) y del 76.22% (**15**)}. El compuesto **15** es el inductor apoptótico más potente publicado por nuestro grupo. La inducción de la parada del ciclo celular en la fase G₂/M y la de apoptosis por los tres compuestos más activos

está asociada con el aumento de fosforilación del factor eIF2 α en células cancerosas humanas de mama.

4.4.2. Síntesis y actividad anticancerosa de (*R*)- y (*S*)-9-(2,3-dihidro-1,4-benzoxaheteroin-2-ilmetil)-9*H*-purinas

Cuando se lleva a cabo la reacción de Mitsunobu entre las formas homoquirales (*R*)- y la (*S*)-3,4-dihidro-2*H*-1,5-benzoxatiepina-3-ol y varias purinas con irradiación en microondas, se reproduce la regioselectividad observada cuando se parte del alcohol secundario 3,4-dihidro-2*H*-1,5-benzoxatiepina-3-ol racémico y además, los productos de contracción de anillo se obtienen con excelentes enantioespecificidades, de la misma forma que se obtienen ... a partir del alcohol secundario...

4.4.3. Síntesis, caracterización química inequívoca y estudio de la reactividad de 2,3,4,5-tetrahidro-1,5-benzoxazepinas-3-ol

La Ciencia debe construirse sobre lo que otros investigadores han descubierto previamente, por lo que una investigación previa imprecisa, puede retrasar y entorpecer otros trabajos. Nuestra intención es la de ayudar a los investigadores que trabajan en el campo de los 1,4-diheterociclos de seis y de siete miembros, habiendo establecido de una manera clara y concluyente las diferencias espectroscópicas de estos dos sistemas bicíclicos. Creemos que la aclaración de la confusión estructural publicada en dos artículos y en una patente, podrá evitar la proliferación de los errores científicos y en consecuencia, evitará el efecto dominó negativo debido a la rapidez con que se divulga la información, incluida la científica, en nuestros días.¹⁹⁸

Los compuestos **22a-c** pueden servir como sintones para el desarrollo de nuevos prototipos biológicamente activos.

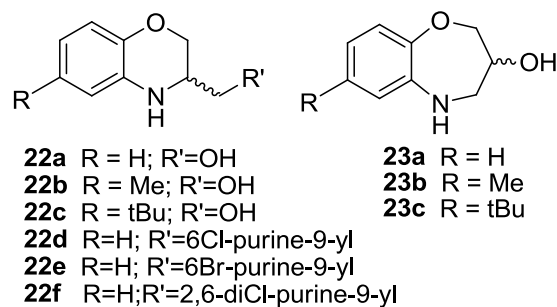
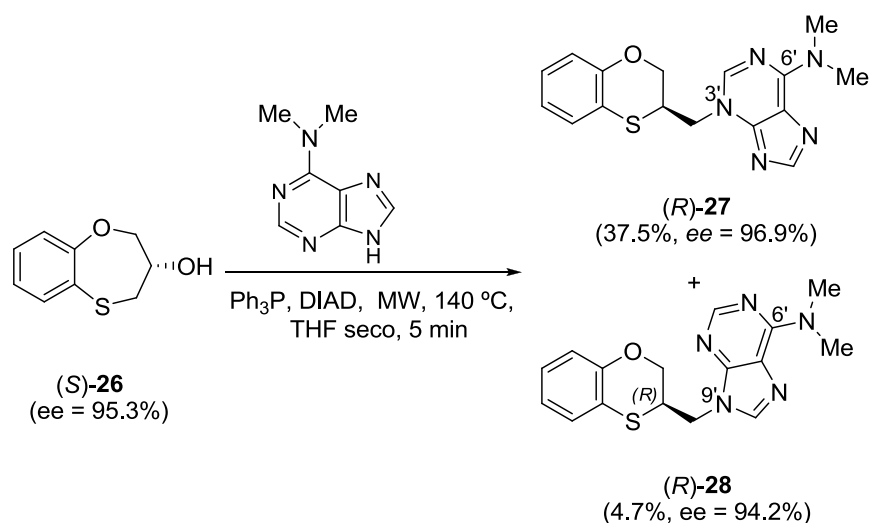


Figura 7.

Aunque los anillos de seis miembros son más estables que los correspondientes ciclo-homólogos superiores de siete miembros y en general, su formación se favorece cuando se dan ambas posibilidades estructurales, el uso de técnicas de resonancia magnética nuclear mono- y bi-dimensionales, ha aclarado de manera unívoca que lo que está publicado en la bibliografía científica (incluyendo una patente) como **22a-c**, en realidad es **23a-c** (Figura 7).

4.4.4. Alquilación estereoespecífica de adeninas sustituidas por medio de la reacción de Mitsunobu bajo condiciones asistidas por microondas

La purina es una estructura privilegiada. La importancia biológica y la incidencia de este heterociclo en la naturaleza convierten a este sistema bicíclico en un objetivo atractivo desde el punto de vista de modificación química.



Esquema 1.

Entre las purinas destaca la adenina frente a la amplia variedad de purinas, entre otras cosas, como componente fundamental tanto del ADN como del ARN. En este apartado se describe un novedoso y eficaz método sintético por reacción entre varias aminopurinas alquiladas [6-(*N,N*-dimetil)-, 2-cloro-6-(*N*-metil)-, y 6-(*N*-metil)-adeninas]] y los alcoholes secundarios aquiral y quiral 3,4-dihidro-2*H*-1,5-benzoxatíepin-3-ol por medio de la reacción de Mitsunobu bajo microondas. En este caso se confirma que el átomo de azufre del anillo de siete miembros ejerce un notable efecto de participación de grupo vecino en su reacción con varias aminopurinas, produciéndose una inversión S_N2 completa en el centro estereogénico, tras la correspondiente contracción del anillo. A título de ejemplo, el Esquema 1 muestra una de las reacciones estudiadas. La alquilación de las purinas da lugar, generalmente, a la formación de N-9' y de N-7' alquilpurinas, resultando ser generalmente el producto N-9' el producto mayoritario. Frente a los regioisómeros anteriores, los derivados N-3' de las purinas se conocen muy poco, especialmente cuando un resto quiral se encuentra unido al anillo de purina, y estas sub-estructuras pueden conducir a inhibidores específicos de objetivos biológicos conocidos y/o preparar el terreno hacia nuevos inhibidores o antagonistas de objetivos que todavía no se han descubierto.

4.4.5. Compuestos selectivos frente a células madre cancerosas

El hallazgo de células madre cancerosas podría conducir a un cambio radical en el diagnóstico y tratamiento de la enfermedad. Las investigaciones llevadas a cabo en ratones confirman la larga y controvertida hipótesis de que el desarrollo de los tumores está dirigido por estas células. Los tratamientos de cáncer disponibles actualmente, a menudo, logran reducir con éxito el tamaño de un tumor, pero muchos pacientes sufren una recaída y el tumor vuelve a crecer. Se piensa que esto ocurre porque las terapias no logran erradicar una pequeña proporción de células -las células madre- que son las encargadas de dirigir el desarrollo del tumor.

En pruebas con ratones, la salinomicina elimina las células madre del cáncer de mama de manera mucho más eficaz que algunos fármacos ya existentes y además, desacelera el crecimiento del tumor.¹⁹⁹ Disponemos de tres compuestos que, in vitro, presentan una actividad análoga al compuesto de referencia. Sin embargo, por razones de patentabilidad no se dará ningún tipo de información estructural de esta última familia de compuestos. En la síntesis de los compuestos objetivo, se hace necesario la protección de determinados grupos funcionales para evitar reacciones de transposición, que serán oportunamente publicadas, una vez que los compuestos estén protegidos intelectualmente.

5. AIMS

The main purpose of this thesis is the exploration of two series of racemic and homochiral benzannelated six-membered diheterocycles linked to purines as antitumour agents.

In general the strategy consists in the design and synthesis of the target compounds, and their study of *in vitro* biological evaluation against cancer cells. Some compounds will be selected, based on their *in vitro* biological data, to determine their mechanism of action and study further their *in vivo* activities.

Moreover, the following specific objectives are proposed in order to systematize and divide the main purpose of this thesis:

1. Design and synthesis of new compounds with antiproliferative activity.
2. Development of asymmetric synthesis for the preparation of enantiomerically pure compounds.
3. Analytical characterization of these compounds, such as the enantiomeric excesses (e.e) and absolute configurations of the homochiral compounds.
4. *In vitro* biological evaluation of all the synthesized derivatives: cellular viability and proliferation of the cancerous MCF-7 breast cancer cell line when treated with the target compounds.
5. Study for the most active compounds of their mechanisms of action which include:
 - Induction of apoptosis.
 - Alteration of cellular survival pathways.
 - Checking if the homochiral compounds synthesized in this thesis show a different apoptosis effect and if so, investigations of the different pathways.
6. Selection of the leader compounds for the *in vivo* studies: tumor growth, toxicity and mechanism of action in a xenograft model.

6. RESULTS

PAPER 1

Homochiral Drugs: A Demanding Tendency of the Pharmaceutical Industry

María C. Núñez, M. Eugenia García-Rubiño, Ana Conejo-García, Olga Cruz-López, María Kimatrai, Miguel A. Gallo, Antonio Espinosa and Joaquín M. Campos*

Departamento de Química Farmacéutica y Orgánica. Facultad de Farmacia, c/ Campus de Cartuja s/n, 18071 Granada, Spain

Abstract: The issue of drug chirality is now a major theme in the design and development of new drugs, underpinned by a new understanding of the role of molecular recognition in many pharmacologically relevant events. In general, three methods are utilized for the production of a chiral drug: the chiral pool, separation of racemates, and asymmetric synthesis. Although the use of chiral drugs predates modern medicine, only since the 1980's has there been a significant increase in the development of chiral pharmaceutical drugs. An important commercial reason is that as patents on racemic drugs expire, pharmaceutical companies have the opportunity to extend patent coverage through development of the chiral switch enantiomers with desired bioactivity.

Stimulated by the new policy statements issued by the regulatory agencies, the pharmaceutical industry has systematically begun to develop chiral drugs in enantiomerically enriched pure forms. This new trend has caused a tremendous change in the industrial small- and large-scale production to enantiomerically pure drugs, leading to the revisiting and updating of old technologies, and to the development of new methodologies of their large-scale preparation (as the use of stereoselective syntheses and biocatalyzed reactions).

The final decision whether a given chiral drug will be marketed in an enantiomerically pure form, or as a racemic mixture of both enantiomers, will be made weighing all the medical, financial and social proficiencies of one or other form. The kinetic, pharmacological and toxicological properties of individual enantiomers need to be characterized, independently of a final decision.

Keywords: Asymmetric synthesis, chiral pool, chiral switch, homochiral, racemates, separation of racemates.

INTRODUCTION

The importance of obtaining optically pure materials hardly requires restatement. The manufacture of chemical products applied either for the promotion of human health or to combat pests which otherwise adversely impact on human food supply is now increasingly concerned with enantiomeric purity. Large proportions of such products contain at least one chiral centre. The desirable reasons for producing optically pure materials include the following:

1. Biological activity often associated with only one enantiomer.
2. Enantiomers may exhibit different types of activity, both of which may be beneficial, or one may be beneficial and the other undesirable; the production of only one enantiomer allows the separation of the effects.
3. The unwanted isomer is at least "isomeric ballast" gratuitously applied to the environment.
4. Registration considerations: production of material as the required enantiomer is now a question of law in certain countries, the unwanted enantiomer being considered as an impurity.
5. When the switch from racemate to enantiomer is feasible, there is the opportunity to double the capacity of an industrial process.

6. The physical characteristics of enantiomers versus racemates may confer processing or formulation advantages [1].

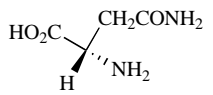
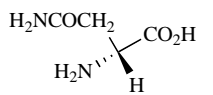
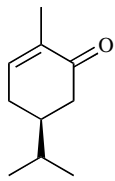
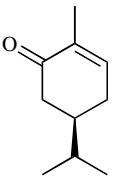
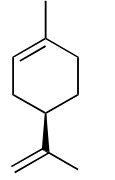
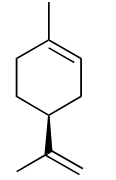
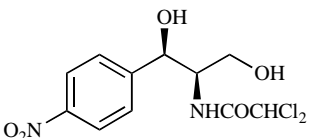
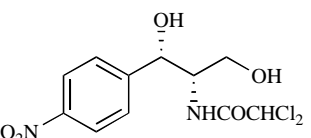
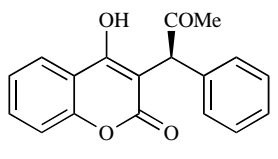
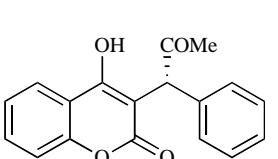
It has been recognized for a long time that the shape of a molecule has considerable influence on its physiological action. Examples of property differentiation within enantiomer pairs are numerous and often dramatic. A selection is given in Table 1.

The Thalidomide Tragedy

The thalidomide tragedy of 1961 in Europe is a landmark in drug regulation. The sedative-hypnotic drug thalidomide exhibited irreversible neurotoxicity and teratological (mutagenic) effects as a result of which babies were born deformed. The drug was prescribed to pregnant women to counter morning sickness. Thalidomide is a racemate – of a glutamic acid derivative – and in 1984, in the foreword of a book on X-ray crystallography [3], the following statement appeared: "The thalidomide tragedy would probably never have occurred if, instead of using the racemate, the (*R*)-isomer had been brought on to the market. It was shown that after *i.p.* administration only the (*S*)-(-)-enantiomer exerts an embryotoxic and teratogenic effect. The (*R*)-(+)-enantiomer is devoid of any of those effects under the same experimental conditions". This quote has been widely used subsequently, and was even alluded to in the citation for the 2001 Nobel Prize in Chemistry, which was awarded to Knowles, Noyori and Sharpless for the development of catalytic asymmetric synthesis, and has had a great impact on the development of new drugs [4].

*Address correspondence to this author at the Departamento de Química Farmacéutica y Orgánica, Facultad de Farmacia, c/ Campus de Cartuja s/n, 18071 Granada, Spain; Tel: +34 958243848; Fax: +34 958243845; E-mail: jmcampos@ugr.es

Table 1. Differences in the Properties of Enantiomers

 <p>(S) Bitter taste</p>	Asparagine	 <p>(R) Sweet taste</p>
 <p>(S) Caraway odor</p>	Carvone	 <p>(R) Spearmint odor</p>
 <p>(R) Orange odor</p>	Limonene	 <p>(S) Lemon odor</p>
 <p>(R,R) Antibacterial</p>	Chloramphenicol	 <p>(S,S) Inactive</p>
 <p>(S) 5-6 More potent hypoprothrombinaemic agent than (R)*</p>	Warfarin	 <p>(R) Less active</p>

*See ref. [2].

Regrettably, the proposal that the thalidomide tragedy could have been avoided if the single enantiomer had been used is misleading, for two reasons:

1. First, it is based on unreliable biological data: the studies purported to show that (*S*)-(-)-thalidomide, was in the mouse – a species that is generally regarded as unresponsive – and involved very high doses [5]. However, earlier work in the rabbit, the species that is most sensitive to thalidomide, clearly showed the equal teratogenic potency of its enantiomers [6].
2. Second, the chiral centre in thalidomide is unstable in protonated media and undergoes a rapid configurational inversion [7]. So, the individual enantiomers of thalidomide are both inverted rapidly to the racemic mixture, process that occurs faster *in vivo* than *in vitro* [8].

Therefore, even if there were differences in the toxicity of the enantiomers of thalidomide, their rapid racemization

in vivo would blunt them so that they could not be exploited. This case shows the importance of considering data in full and not leaping to conclusions, however tempting these may be [9].

The metabolic elimination of thalidomide is mainly driven by pH-dependent spontaneous hydrolysis in all body fluids with an apparent mean clearance of 10 L/h for the (*R*)-(+)- and 21 L/h for the (*S*)-(-)-enantiomer in adult subjects. Blood concentrations of the (*R*)-(+)-enantiomer are consequently higher than those of the (*S*)-(-)-enantiomer at pseudo-equilibrium. The metabolites in humans have been studied both from the incubation of thalidomide with human liver homogenates and *in vivo* in healthy volunteers. The *in vitro* studies demonstrated the hydrolysis products 5-hydroxythalidomide and 5'-hydroxythalidomide while *in vivo* only the 5'-hydroxy metabolite was found, in low concentrations, in plasma samples from eight healthy male volunteers who had received thalidomide orally. The hydrolysis of the thalidomide enantiomers by *in vitro* incubation was shown by Meyring *et al.* to be stereospecific [10a]. The chiral centre of the

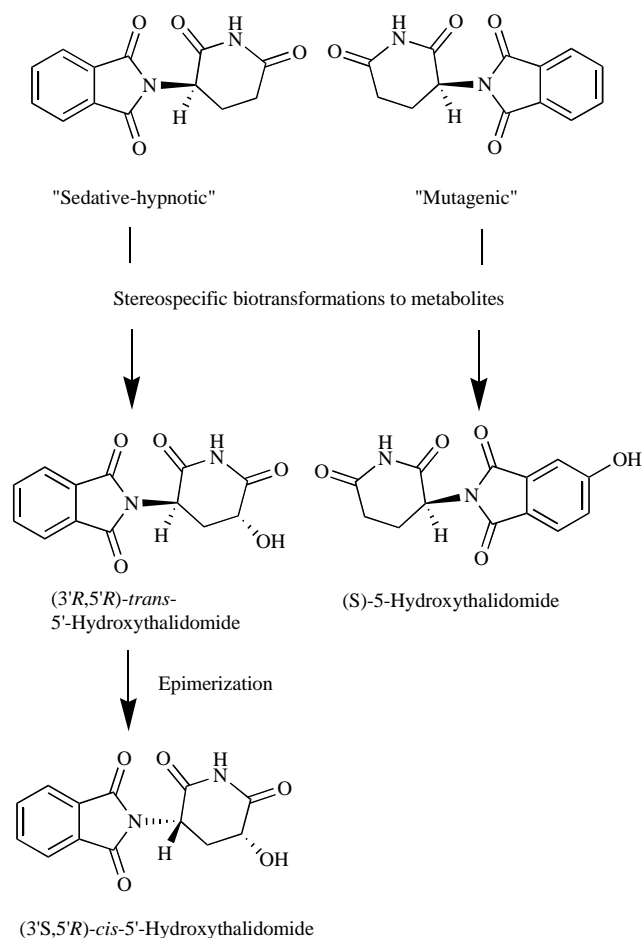


Fig. (1). Thalidomide and stereospecific biotransformation to its metabolites.

thalidomide enantiomers is unaffected by the stereoselective biotransformation process. (3'*R*,5'*R*)-*trans*-5'-Hydroxythalidomide is the main metabolite of (*R*)-(+)-thalidomide, which epimerizes spontaneously to give the more stable (3'*S*,5'*R*)-*cis* isomer. On the contrary, (*S*)-(-)-thalidomide is preferentially metabolized by hydroxylation in the phthalimide moiety, resulting in the formation of (*S*)-5-hydroxythalidomide [10] as shown in Fig. (1).

It seems that a multitude of its pharmacological activities could be due not only to the mother molecule but also to its numerous chiral and achiral metabolites. Because of this *in vivo* interconversion of thalidomide, it is difficult to determine exactly the pharmacological effect of each enantiomer.

Thalidomide has been a subject of numerous studies, although the former is tainted from its past history. In 1998 the U.S. FDA (Food and Drug Administration) approved thalidomide for use in treating leprosy symptoms and studies indicate some promising results for use in treating symptoms associated with AIDS, Behcet disease, lupus, Sjogren syndrome, rheumatoid arthritis, inflammatory bowel disease, macular degeneration, and some cancers [11].

Pharmacology

The body with its numerous homochiral compounds being amazingly chiral selective, will interact with each race-

mic drug differently and metabolize each enantiomer by a separate pathway to generate different pharmacological activities.

RACEMIC DRUGS WITH ONE MAJOR BIOACTIVE ENANTIOMER

In this group, there are a number of cardiovascular drugs, agents widely used for the treatment of hypertension, heart failure, arrhythmias, and other diseases. Among these are the β -adrenergic blocking agents, calcium channel antagonists and angiotensin-converting enzyme (ACE) inhibitors. The majority of racemic pharmaceuticals have one major bioactive enantiomer (called eutomer), the other is inactive or less active (called distomer) or toxic or can exert other desired or undesired pharmacological properties.

Levorotary-isomer of all β -blockers is more potent in blocking β -adrenoceptors than their dextrorotary-isomer, such as (*S*)-(-)-propranolol (Fig. (2)) is 100 times more active than its (*R*)-(+)-antipode [12,13]. A number of β -blockers are still marketed as racemic forms such as acebutolol, atenolol, alprenolol, betaxolol, carvedilol, metoprolol, labetalol, pindolol, etc., except timolol and penbutolol, which are used as single (*S*)-(-)-isomers (Fig. (2)).

Many calcium channel antagonists are used under racemic form such as verapamil, nifedipine, nimodipine, ni-

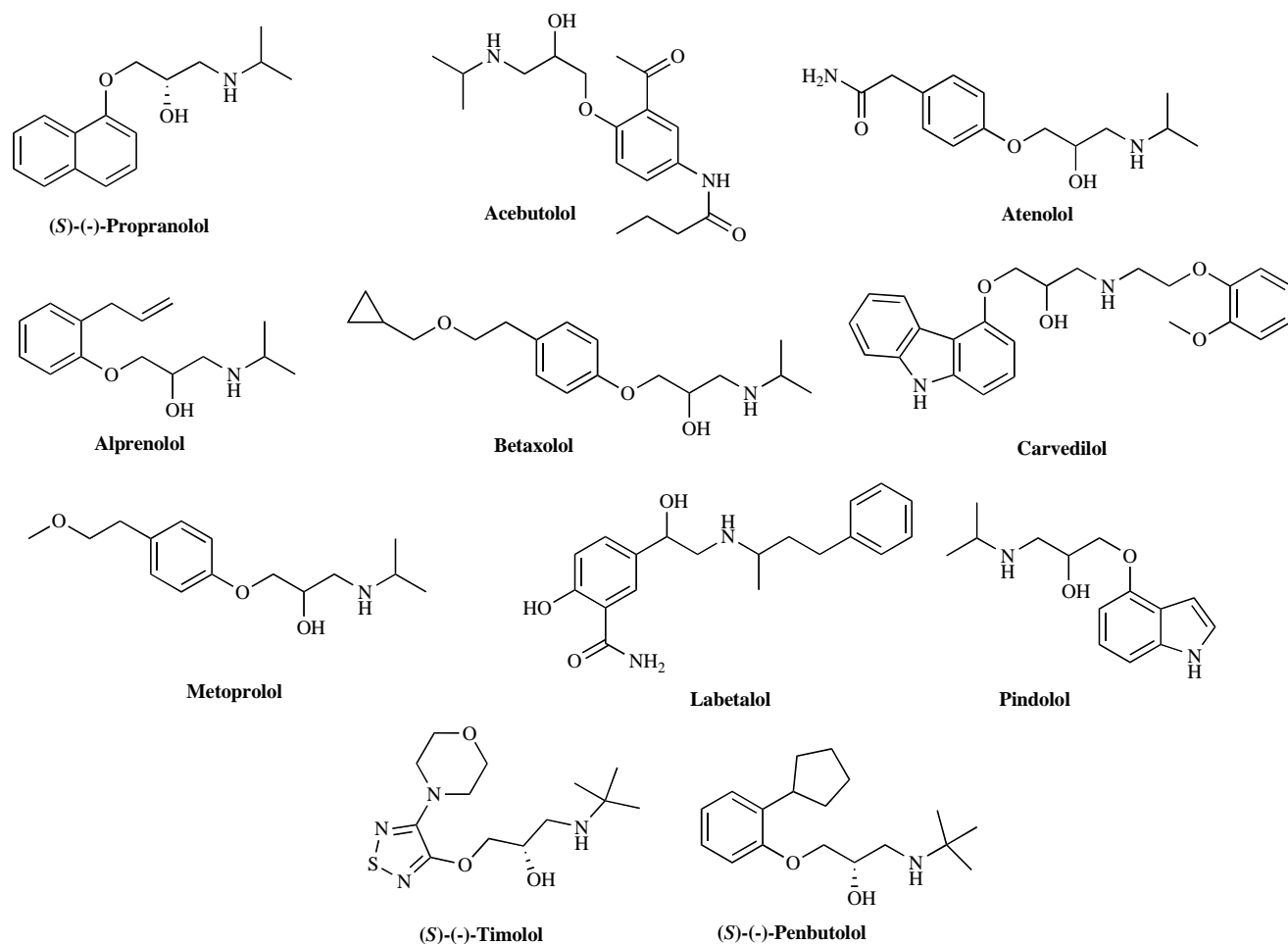


Fig. (2). Racemic drugs with one major bioactive enantiomer (β -blockers).

soldipine, felodipine, manidipin, except diltiazem (Fig. (3)) that is a single (*S,S*)-(+)-isomer. For example, the pharmacological potency of (*S*)-(-)-verapamil is 10-20 times greater than its (*R*)-(+)-antipode in terms of negative chronotropic effect on auricoventricular (AV) conduction and vasodilator in man and animals [14,15].

All ACE inhibitors, such as captopril, benazepril, enalapril, imidapril (Fig. (4)) are diastereoisomeric compounds and most of them are marketed as single isomers. Valsartan, an angiotensin II receptor antagonist, is used as its (*S*)-enantiomer and the activity of the (*R*)-enantiomer is clearly lower than the (*S*)-enantiomer (Fig. (4)) [16].

Albuterol (salbutamol) is the racemate of 4-[2-(*tert*-butylamino)-1-hydroxyethyl]-2-(hydroxymethyl)phenol and is the leading bronchodilator, an adrenoceptor agonist that can increase the bronchial airway diameter without increasing heart rate. The bronchodilator activity resides in (*R*)-(-)-albuterol [levalbuterol, Fig. (5)]. (*S*)-(+)-Albuterol, however, is not inert, as it indirectly antagonizes the benefits of (*R*)-(-)-albuterol and may have proinflammatory effects. There are pharmacokinetic differences between the enantiomers with (*S*)-(+)-albuterol being cleared more slowly. The (*S*)-(+)-enantiomer tends to accumulate in preference to the therapeutically effective (*R*)-(-)-enantiomer. The FDA approved a chiral switch drug, levalbuterol as a preservative-

free nebulizer solution. However, some clinical studies have reported that it is neither safer nor more effective than the same dose of racemic albuterol. In contrast, levalbuterol may cost as much as 5 times more than its racemate [17,18].

In neurology and psychiatry, many pharmaceuticals used are chiral compounds and most of them are marketed as racemates. For example, (*S*)-(-)-secobarbital is more potent as an anaesthetic agent than (*R*)-(+)-secobarbital (Fig. (5)), *i.e.* it causes a smoother more rapid anaesthetic effect [19,20]. Ketamine (Fig. (5)) is an intravenous anaesthetic. The (*R*)-(+)-isomer is more potent and less toxic than its (*S*)-(-)-antipode, but unfortunately, ketamine is still used as racemic drug [21,22]. (*S*)-(+)-Citalopram [Escitalopram] (Fig. (5)) is over 100-fold more potent as a selective serotonin reuptake inhibitor than the (*R*)-(-)-enantiomer in the treatment of depression [23].

Methadone, a central-acting analgesic with high affinity for μ -opioid receptors, has been used to treat opiate dependence and cancer pain. Methadone is a chiral synthetic compound used in therapy under a racemic mixture. In humans, (*R*)-(-)-methadone (Fig. (5)) is about 25-50 fold more potent as an analgesic than its (*S*)-(+)-antipode [23,24].

The list of racemic drugs with one eutomer is long in the fields of anticonvulsants, antibiotics, antihistamics, proton pump inhibitors [25-27]. Some of these racemates undergo

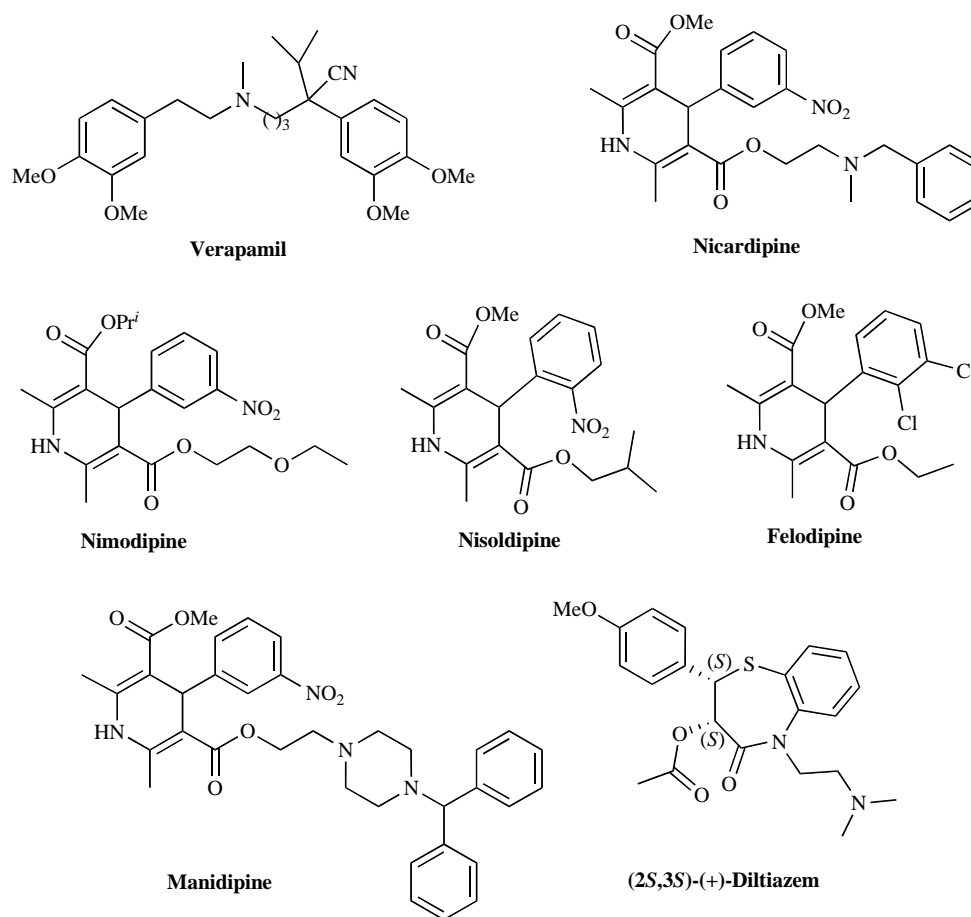


Fig. (3). Racemic drugs with one major bioactive enantiomer (calcium-channel antagonists).

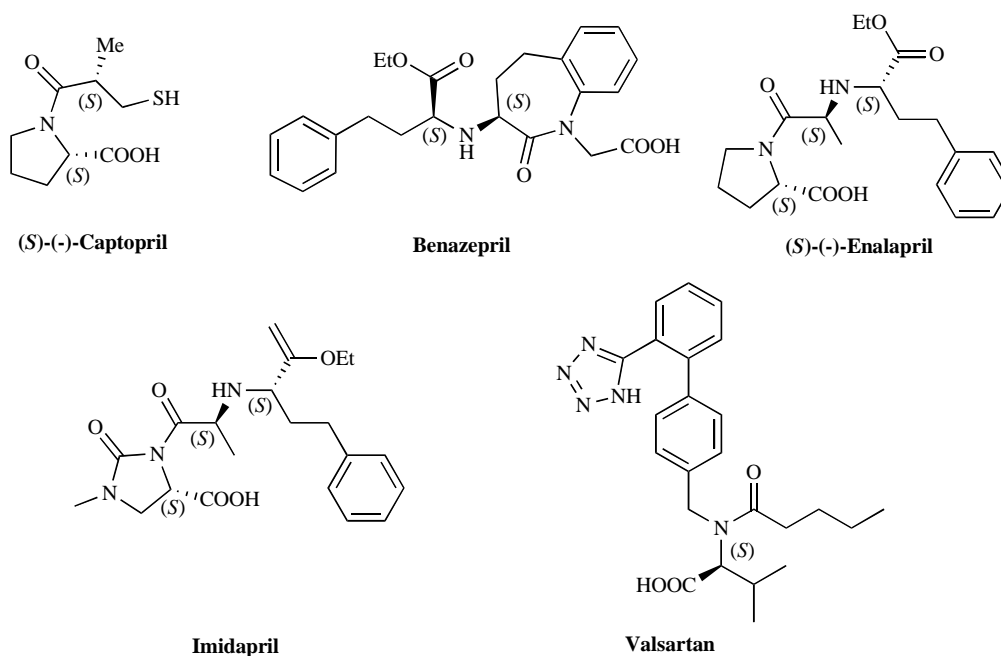


Fig. (4). Racemic drugs with one major bioactive enantiomer (ACE).

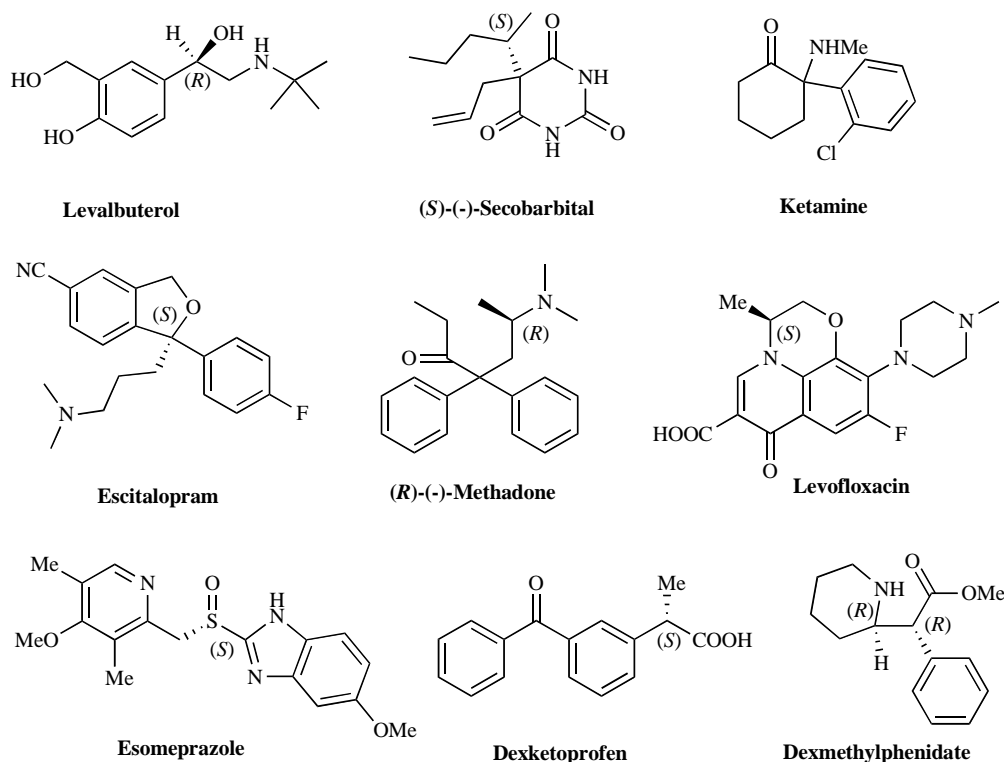


Fig. (5). Racemic drugs with one major bioactive enantiomer.

recently chiral switch to single enantiomer such as levofloxacin (from ofloxacin), levalbuterol (from albuterol), escitalopram (from citalopram), esomeprazole (from omeprazole), dexketoprofen (from ketoprofen), dexmethylphenidate (from methylphenidate).

RACEMIC DRUGS WITH EQUALLY BIOACTIVE ENANTIOMERS

There are few racemic drugs that could belong to this group such as cyclophosphamide (antineoplastic), flecainide (antiarrhythmic), and fluoxetine (antidepressant) [25] (Fig. (6)).

RACEMIC DRUGS WITH CHIRAL INVERSION

The most numerous group of non-steroidal anti-inflammatory drugs (NSAID) that are currently in use is the 2-arylpropionic acids or "profens". These are widely used for

the treatment of inflammatory diseases, such as rheumatoid arthritis, as both analgesics and antipyretics. However, the racemates are responsible for many adverse reactions reported each year. These adverse reactions affect a range of organs, including the gastrointestinal tract, kidney, bone marrow, the respiratory system and the liver. Unidirectional enzyme-mediated inversion was previously described only with profens, namely ibuprofen, ketoprofen, fenoprofen, benoxaprofen, (Fig. (7)). For example, the activities of the two enantiomers of ibuprofen and ketoprofen are essentially undistinguishable *in vivo*, owing to a unidirectional metabolic bioconversion of the (*R*)-enantiomers to the (*S*)-enantiomers. The combination of the stereospecificity of action, together with the configurational inversion reaction provided drug companies with a rationale for the use of the (*S*)-enantiomers of these drugs in therapy. The treatment with (*S*)-enantiomers reduces the total dose and also the toxicity associated with the (*R*)-enantiomer by removing the rate (and extent) of inversion as a source of variation in metabolism and pharmacological effects.

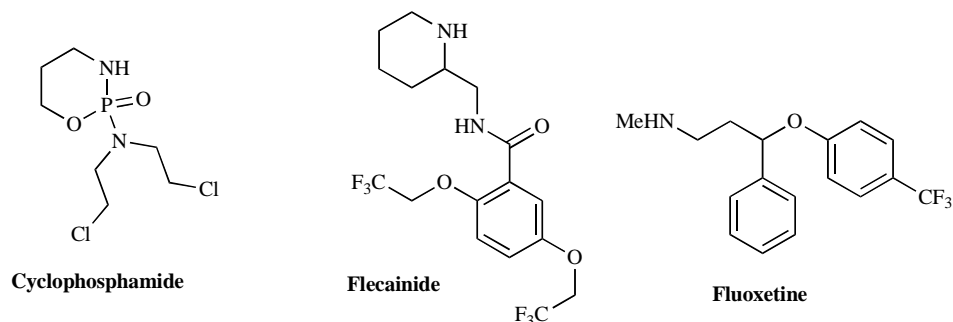


Fig. (6). Racemic drugs with equally bioactive enantiomers.

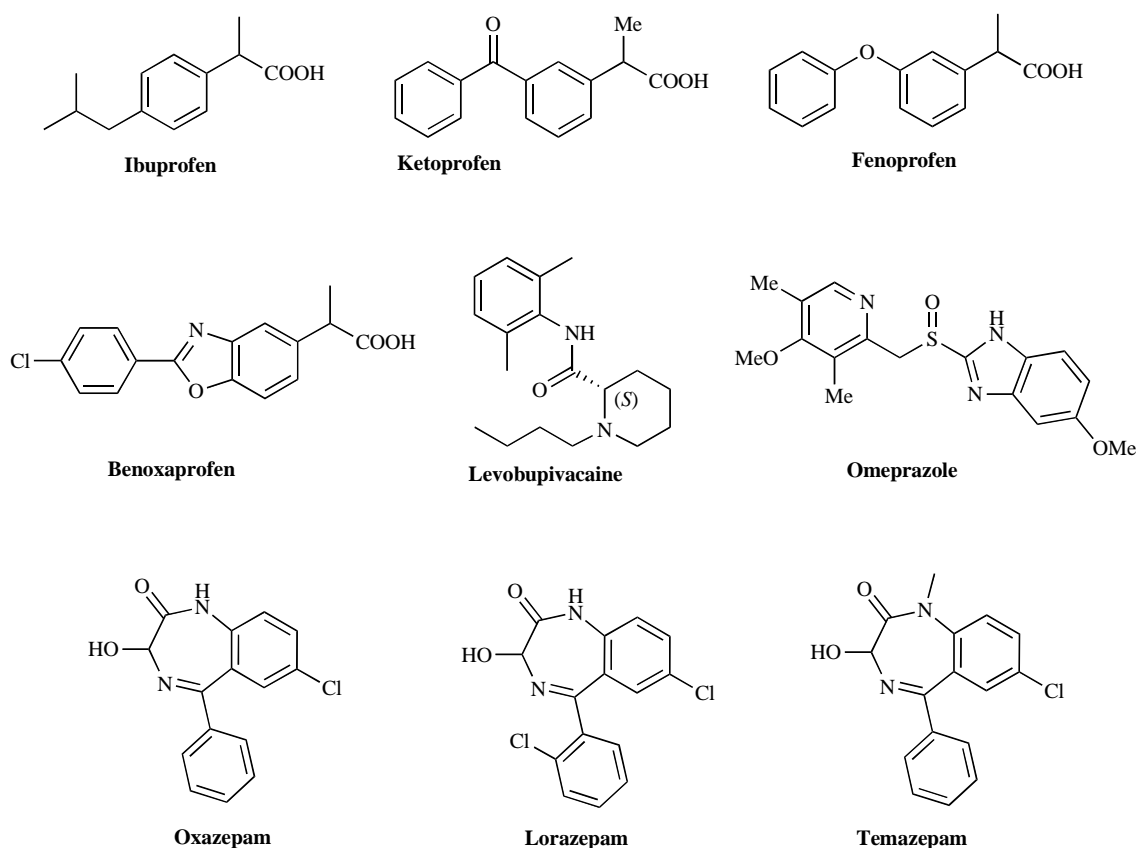


Fig. (7). Racemic drugs with chiral inversion.

The (*S*)-(+)-ketoprofen [dexketoprofen] (Fig. (5)) is several times more potent than the racemate. The presentation of dexketoprofen as the tromethamine salt provides three advantages: effective analgesia at lower doses, rapid onset, and reduced gastric irritation and improved tolerability (due to the novel salt form).

Similarly, racemic ibuprofen (Fig. (7)) undergoes rapid and substantial stereochemical inversion (about 50-60%), so that the metabolic exposure is principally due to (*S*)-(+)-ibuprofen [dexibuprofen], with the presence of little (*R*)-(-)-ibuprofen. The (*S*)-(+)-ibuprofen present is derived from both the 50% of the racemate in that form and the chiral inversion of the (*R*)-(-)-enantiomer. While racemic ibuprofen and (*S*)-(+)-ibuprofen are often viewed as being bioequivalent, the use of (*S*)-(+)-ibuprofen gives faster onset of action and reduces the variability in the stereochemical inversion as a source of variability in the pharmacological response [9].

Racemic bupivacaine is currently the most widely used long-acting local anaesthetic. Its uses include surgery and obstetrics; however, it has been associated with potentially fatal cardiotoxicity, particularly when given intravascularly by accident. (*S*)-(-)-Bupivacaine [levobupivacaine] (Fig. (7)) was introduced by Purdue Pharma LP under the tradename of Chirocaine® as a new long-acting local anaesthetic with a potentially reduced toxicity compared with bupivacaine. Numerous studies have compared levobupivacaine with bupivacaine and in most (but not all) studies there is evidence that levobupivacaine is less toxic [28]. Studies have also shown that, following i.v. administration, levobupiva-

caine produces significantly less effects on cardiovascular function than racemic bupivacaine does [29].

Omeprazole (Fig. (7)) presents one of the most interesting cases in drug development. Racemic omeprazole is a very potent inhibitor of gastric acid secretion, with a long-lasting duration of action. In clinical studies, it proved superior to previous treatments for gastroesophageal reflux disease and peptic ulcers. Omeprazole is a gastric anti-secretory proton pump inhibitor [30] marketed under the tradenames of Losec® and Prilosec® by AstraZeneca. Launched in 1988 by Astra AB (in 1999, Astra AB merged with Zeneca PLC to create AstraZeneca PLC), omeprazole was a blockbuster commercial success and became the world's best-selling drug with sales of US \$6.2 billion in 2000. The first patents on omeprazole expired in the European Union in 1999 and in the United States of America in 2001. Based partly on the fact that omeprazole exhibits polymorphic metabolism, *i.e.* a few individuals (3% among the Caucasian populations and 15-20% among Orientals) metabolize omeprazole slowly (slow metabolizers) compared to the rest of the population (rapid metabolizers), AstraZeneca developed the chiral switch drug esomeprazole [which is the (*S*)-(-)-enantiomer of omeprazole] (Fig. (5)) based on the premise that the therapeutic benefit would be achieved by less inter-individual variation (slow versus rapid metabolizers), and that average higher plasma levels would provide higher dose efficiency in patients [31].

Esomeprazole was introduced as the magnesium trihydrate salt first in Europe (in 2000) and later in the USA (in

2001) under the trade name of Nexium®. Reflux oesophagitis was healed with a 40 mg per day dose of esomeprazole magnesium in ~ 78% of patients after four weeks of treatment and in 93% of patients after eight weeks, compared with 65% and 87% of patients respectively, treated daily with 20 mg of omeprazole. The benefits of esomeprazole have been extensively studied [32].

From inception, omeprazole has been described and claimed in its patents as 5-methoxy-2-(4-methoxy-3,5-dimethylpyridin-2-ylmethanesulfinyl)-1*H*-benzimidazole.

But Jenkins *et al.* [33] confirmed that the synthetic methods of the prior art did not yield a single compound having the methoxy group in the 5-position on the benzimidazole ring as previously thought, nor did all of the methods of the prior art yield consistent results. In fact the presence of omeprazole as conventionally referred to as a bulk drug substance (in its solid state) was confirmed in the form of two pharmaceutically active compounds, having the methoxy group on the benzimidazole ring at the 6- and 5-positions.

3-Hydroxybenzodiazepines as oxazepam, lorazepam, temazepam (Fig. (7)) can racemize *in vitro* by aqueous solutions. For the first time some authors [34] have found the difference in (*R*)-(-)- and (*S*)-(+)-oxazepam concentrations in treated rabbit serum. They explained that the chiral inversion by tautomerization of oxazepam cannot occur *in vivo* because each enantiomer is transported by proteins (albumin) with different affinity. The binding affinities of the enantiomers to albumin may inhibit the attack of hydroxyl ions from water and thus retard the racemization *in vivo*. Therefore, (*R*)-(-)- and (*S*)-(+)-oxazepam concentrations are different in the serum of these treated rabbits. On the other hand, He *et al.* [35] have also demonstrated that the *in vitro* chiral inversion of these benzodiazepine enantiomers was temperature-dependent and was inhibited by lowering the temperature of the aqueous solutions to about 10 °C [35,36]. The (*S*)-(+)-oxazepam enantiomer is 100-200 fold more potent as a tranquilizer and sedative than (*R*)-(-)-oxazepam [36].

METHODS FOR OBTAINING OPTICALLY ACTIVE COMPOUNDS

This section is not concerned with detailed appraisal of the many and well known processes for obtaining pure enantiomers. Methodologies and principles of the techniques are described more fully in the corresponding references.

The Chiral Pool

The chiral pool customarily refers to relatively inexpensive, readily available optically active natural products, substances whose commercial availability generally falls in the range 10²-10⁵ tonnes per annum. The use of the chiral pool substances as building blocks includes aminoacids, hydroxyacids, terpenes, alkaloids and carbohydrates and derivatives [1].

Separation of Racemates

The separation of enantiomers by chromatography has advanced over the past few decades [37-42], notably with the development of supercritical fluid chromatography (SFC)

[38-42] and hybrid processes consisting of simulated moving bed (SMB) chromatography and crystallization [43,44]. However, the scale is often limited, and operational cost is high.

Racemic resolution by crystallization began in 1848 when Pasteur observed crystals of sodium ammonium tartarate that were mirror images with respect to each other. Until now, separation of enantiomers by crystallization can be classified into two main categories:

1. The use of a foreign chiral element to form diastereomers followed by fractional crystallization [45-49] or the formation of a diastereoselective host-guest inclusion complex [50]. The antituberculostatic drug ethambutol (Fig. (8)), and the cardiovascular drug diltiazem (Fig. (3)) are separated in this way. These methods of resolution are very widely used industrially.
2. The direct crystallization of one enantiomer from a racemic mixture, which includes the well-known "preferential crystallization" of pure enantiomers from conglomerate mixtures [45,51-53]. This unusual enantiomeric resolution is referred to as "preferential enrichment" [53-55], and the application of crystallization inhibitors to chiral separation in racemic compound-forming systems has been reported [56-58]. The anti-typhoid chloramphenicol (Fig. (8)) is separated in this way. This is widely used in the industry but hardly 20 per cent of racemates appear in this form of mechanical mixture or "conglomerates".

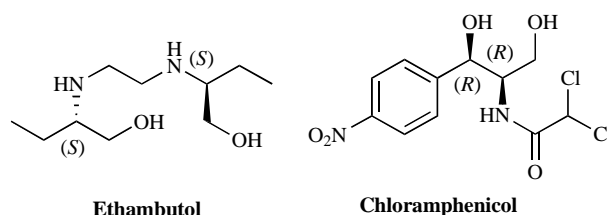


Fig. (8). Separation of racemates.

ASYMMETRIC SYNTHESIS

The field of asymmetric synthesis has enjoyed tremendous progress over the last few decades with the advent of asymmetric reactions and enantioselective catalysts [1,59]. There are two possibilities: (1) Non-enzymic methods, and (2) Enzymic methods.

Non-Enzymic Methods

The asymmetric hydrogenation, the Sharpless epoxidation amongst asymmetric oxidations, and cycloadditions are the most important non-enzymic processes [1].

Enzymic Methods

The potential of microorganisms and enzymes for the transformation of synthetic compounds with high chemo-, regio- and enantioselectivities has been demonstrated. Biocatalytic processes have been described for the synthesis of chiral intermediates for antiviral agents, antianxiety drugs,

anticancer drugs, antidiabetic drugs, and antiAlzheimer's drugs [60].

Biocatalysis takes advantage of the special properties such as high selectivity, mild conditions and the minimization of wastes. The advantages and drawbacks of biotransformations and the pros and cons in the use of isolated enzymes and whole cells have been reviewed [61]. Although biocatalysts still only account for a relatively small fraction of the total catalyst market, and an increasing number of companies are beginning to supplement their range of metal and chemical catalysts with biocatalysts. Consequently, researchers are trying to take advantage of new technologic developments to make biocatalysis a viable alternative to traditional synthetic options [62].

CONCLUSION

The intrinsically chiral and non-racemic nature of the living world often results in its different interactions with the enantiomers of a given substance. If this substance is a drug, it might well be that only one of the two isomers is capable of exerting the desired therapeutic effect. The other may be inert (but must still be metabolized by the organism), harmful (causing even dramatic biological damages), or responsible for difficult-to-predict (and possibly undesirable) side effects.

Well aware of this fact and stimulated by the new policy statements issued by the regulatory agencies, the pharmaceutical industry has, over the past decade or so, systematically begun to develop chiral drugs in enantiometrically enriched and possibly pure form. This new trend has caused a tremendous change in the industrial small- and large-scale production to enantiometrically pure drugs, leading to the revisiting and updating of old technologies (as the resolution of racemic mixtures), and to the development of new methodologies of their large-scale preparation (as the use of stereoselective syntheses and biocatalyzed reactions).

According to Agranat *et al.* [9] and contrary to popular belief, the thalidomide tragedies could not have been avoided by the use of single enantiomers, because both enantiomers have equal teratogenic potencies in the rabbit. In addition, the enantiomers rapidly racemize in the body, so even if they had differed in teratogenicity, the use of single enantiomers would have been precluded. The thalidomide tragedy increased awareness of stereochemistry in the action of drugs, and as a result the number of drugs administered as racemic compounds has steadily decreased. In 2001, more than 70% of the new chiral drugs approved were single enantiomers [9]. Approximately 1 in 4 therapeutic agents are marketed as racemic mixtures, the individual enantiomers of which frequently differ in both their pharmacodynamic and pharmacokinetic profiles. The use of racemates has become the subject of considerable discussion in recent years, and an area of concern for both the pharmaceutical industry and regulatory authorities. Pharmaceutical companies are required to justify each decision to manufacture a racemic drug in preference to its homochiral version. Moreover, the use of single enantiomers has a number of potential clinical advantages, including an improved therapeutic/pharmacological profile, a reduction in complex drug interactions, and simplified pharmacokinetics. In a number of instances stereochemical con-

siderations have contributed to an understanding of the pharmacological effects observed of a drug administered as a racemate. However, relatively little is known of the influence of patient factors (e.g. disease state, age, gender and genetics) on drug enantiomer disposition and action in man. Examples may also be cited where the use of a single enantiomer, nonracemic mixtures and racemates of currently used agents may offer clinical advantages. The issues associated with drug chirality are complex and depend upon the relative merits of the individual agent. In the future it is likely that a number of existing racemates will be re-marketed as single enantiomer products with potentially improved clinical profiles and possible novel therapeutic indications.

The research pharmaceutical industry is currently facing a number of increasingly complex challenges, such as the regulatory constraints, the dramatic increase in development costs with the boost of the crude oil and the generalized economic crisis, the development time periods and the protection of innovation, and human resources and organization. The development of innovative new drugs is a time-consuming, expensive and a risky process. Increasing the rate of innovation is a requirement to achieve much-needed advances in patient care, as well as to secure the future of the pharmaceutical industry. Currently, there is a perception in the external environment that the pharmaceutical R&D is no longer innovative, fails to bring out new drugs or, at best, produces a rising number of "me-too" drugs with no advantage over existing treatments. In addition, the cost to discover and develop new medicines (i.e. cost per launch) has risen dramatically in recent years.

The intellectual property status of single enantiomers from racemates may be unclear. Drug discoverers and patent attorneys must examine the examples of the past to establish an appropriate pathway towards the development and intellectual property protection of chiral drugs [63]. The final decision whether a given chiral drug will be marketed in an enantiomerically pure form, or as a racemic or non-racemic mixture of both enantiomers, will be made weighing all the medical, financial and social proficiencies of one or other form. The kinetic, pharmacological and toxicological properties of individual enantiomers need to be clearly characterized, independently of a final decision. Therefore, pure enantiomers of biologically active chiral compounds may be required at the very early stage of a drug development process. Enantioseparation may be the method of choice because in general it is both cheaper and more rapid to develop compared with an enantioselective synthesis.

ACKNOWLEDGEMENTS

The authors thank the Instituto de Salud Carlos III (Fondo de Investigación Sanitaria project no. PI070227), and the Consejería de Innovación, Ciencia y Empresa of the Junta de Andalucía (Excellence Research Project no. 00636) for financial support.

ABBREVIATIONS

ACE = Angiotensin-converting enzyme
AIDS = Acquired immune deficiency syndrome

AV	= Auricoventricular
FDA	= Food and Drug Administration
NSAID	= Non-steroidal anti-inflammatory drugs
R&D	= Research and development
SFC	= Supercritical fluid chromatography
SMB	= Simulated moving bed

REFERENCES

- [1] Collins, A.N.; Sheldrake, G.N.; Crosby, J. *Chirality in industry. The commercial manufacture and applications of optically active compounds*. John Wiley & Sons: New York, **1992**.
- [2] Testa, B.; Trager, W.F. Racemates versus enantiomers in drug development: dogmatism or pragmatism. *Chirality*, **1990**, *2*, 129-33.
- [3] Horn, A.S.; De Ranter, C.J. *X-Ray crystallography and drug action*. Clarendon: Oxford, **1984**.
- [4] Ahlberg, P. The Nobel Prize in Chemistry 2001 – presentation speech. *The Royal Swedish Academy of Science* [Online] 2001, (accessed Aug 26, **2002**).
- [5] Blaschke, G.; Kraft, H.P.; Fikentscher, K.; Köhler, F. Chromatographic separation of racemic thalidomide and teratogenic activity of its enantiomers. *Arzneimittelforschung*, **1979**, *29*, 1640-2.
- [6] Fabro, S.; Smith, R.L.; Williams, R.T. Toxicity and teratogenicity of optical isomers of thalidomide. *Nature*, **1967**, *215*, 296-7.
- [7] Reist, M.; Carrupt, P.A.; Francotte, E.; Testa, B. Chiral inversion and hydrolysis of thalidomide: mechanisms and catalysis by bases and serum albumin, and chiral stability of teratogenic metabolites. *Chem. Res. Toxicol.*, **1998**, *11*, 1521-8.
- [8] Eriksson, T.; Bjorkman, S.; Roth, B.; Fyge, A.; Höglund, P. Stereospecific determination, chiral inversion *in vitro* and pharmacokinetics in humans of the enantiomers of thalidomide. *Chirality*, **1995**, *7*, 44-52.
- [9] Agranat, I.; Caner, H.; Caldwell, J. Putting chirality to work: the strategy of chiral switches. *Nat. Rev. Drug Discov.*, **2002**, *10*, 753-68.
- [10] (a) Meyring, M.; Muhlbacher, J.; Messer, K.; Kastner-Pustet, N.; Bringmann, G.; Mannschreck, A.; Blaschke, G. *In vitro* biotransformation of (R)- and (S)-thalidomide: application of circular dichroism spectroscopy to the stereochemical characterization of the hydroxylated metabolites. *Anal. Chem.*, **2002**, *74*, 3726-35; (b) Eriksson, T.; Bjorkman, S.; Höglund, P. Clinical pharmacology of thalidomide. *Eur. J. Clin. Pharmacol.*, **2001**, *57*, 365-76; (c) Eriksson, T.; Bjorkman, S.; Roth, B.; Bjork, H.; Höglund, P. Hydroxylated metabolites of thalidomide: formation *in-vitro* and *in-vivo* in man. *J. Pharm. Pharmacol.*, **1998**, *5*, 1409-16.
- [11] (a) Gordon, J.N.; Goggin, P.M. Thalidomide and its derivatives: emerging from the wilderness. *Postgrad. Med. J.*, **2003**, *79*, 127-32. (b) Weeber, M.; Vos, R.; Klein, H.; de Jong-van den Berg, L.; Aronson, A.R.; Molema, G. Generating hypotheses by discovering implicit associations in the literature: A case report of a search for new potential therapeutic uses of thalidomide. *J. Am. Med. Inform. Assoc.*, **2003**, *10*, 252-9. (c) Weber, D.; Rankin, K.; Gavino, M.; Delasalle, K.; Alexanian, R. Thalidomide Alone or With Dexamethasone for Previously Untreated Multiple Myeloma. *J. Clin. Oncol.*, **2003**, *21*, 16-9. (d) Friedrich, M.J. Despite Checkered Past, Thalidomide and its Analogues Show Potential. *J. Natl. Cancer Inst.*, **2002**, *94*, 1270-2. (e) Lewis, R. The Return of Thalidomide. *Scientist*, **2001**, *15*, 1.
- [12] Stoschitzky, K.; Lindner, W.; Zernig, G. Racemic beta-blockers-fixed combinations of different drugs. *J. Clin. Basic Cardiol.*, **1998**, *1*, 15-9.
- [13] Barrett, A.; Cullum, C. The biological properties of the optical isomers of propranolol and their own cardiac arrhythmias. *Br. J. Pharmacol.*, **1968**, *34*, 43-55.
- [14] Echizen, H.; Manz, M.; Eichelbaum, M. Electrophysiologic effects on dextro- and levo- verapamil on sinus node and AV node function in humans. *J. Cardiovasc. Pharm.*, **1988**, *12*, 543-6.
- [15] Satoh, K.; Yanagisawa, T.; Taira, N. Coronary vasodilator and cardiac effects of optical isomers of verapamil in the dog. *J. Cardiovasc. Pharm.*, **1980**, *2*, 309-18.
- [16] Patocka, J.; Dvorak, A. Biomedical aspects of chiral molecules. *J. Appl. Med.*, **2004**, *2*, 95-100.
- [17] Nowak, R. Single-isomer levalbuterol: A review for the acute data. *Curr. Allergy Asthma Rep.*, **2003**, *3*, 172-8.
- [18] Asmus, M.J.; Hendeles, L. Levalbuterol nebulizer solution: Is it worth five times the cost of Albuterol? *Pharmacotherapy*, **2000**, *20*, 123-9.
- [19] Drayer, D.E. Pharmacodynamic and pharmacokinetic differences between drug enantiomers in human: an overview. *Clin. Pharmacol. Ther.*, **1986**, *40*, 125-33.
- [20] Ho, I.I.; Harris, R.A. Mechanism of action of barbiturates. *Annu. Rev. Pharmacol.*, **1988**, *37*, 1919-26.
- [21] Katzung, B.G. *Basic and clinical pharmacology*. Lange Medical Books/McGraw Hill : New York, **2004**.
- [22] Lee, E.J.D.; Williams, K.M. Chirality. Clinical pharmacokinetic and pharmacodynamic considerations. *Clin. Pharmacokinet.*, **1990**, *18*, 339-45.
- [23] Rentsch, K.M. The importance of stereoselective determination of drugs in the clinical laboratory. *J. Biochem. Bioph. Meth.*, **2002**, *54*, 1-9.
- [24] Pham-Huy, C.; Chikhi-Chorfi, N.; Galons, H.; Sadeg, N.; Laqueille, X.; Aymard, N.; Massicot, F.; Warnet, J.M.; Claude, J.R. Enantioselective high-performance liquid chromatography determination of methadone enantiomers and its major metabolite in human biologic fluids using a new derivatized cyclodextrin-bonded phase. *J. Chromatogr. B.*, **1997**, *700*, 155-63.
- [25] Davies, N.M.; Teng, X.V. Importance of chirality in drug therapy and pharmacy practice. Implication for psychiatry. *Adv. Pharm.*, **2003**, *1*, 242-52.
- [26] Marzo, A.; Heftman, E. Enantioselective analytical methods in pharmacokinetics with specific reference to genetic polymorphic metabolism. *J. Biochem. Bioph. Meth.*, **2002**, *54*, 57-70.
- [27] Jamali, F.; Mehver, R.; Pasutto, F.M. Enantioselective aspects of drug action and disposition: Therapeutic pitfalls. *J. Pharm. Sci. USA*, **1989**, *78*, 695-715.
- [28] (a) Gristwood, R.W. Cardiac and CNS toxicity of levobupivacaine: strength of evidence for advantage over bupivacaine. *Drugs Saf.*, **2002**, *25*, 153-63. (b) Gristwood, R.W.; Greaves, J.L. Levobupivacaine: a new safer long acting local anaesthetic agent. *Expert Opin. Inv. Drugs*, **1999**, *8*, 861-76.
- [29] Bardsley, H.; Gristwood, R.; Baker, H.; Watson, N.; Nimmo, W. A comparison of the cardiovascular effects of levobupivacaine and rac-bupivacaine following intravenous administration to healthy volunteers. *Br. J. Clin. Pharmacol.*, **1998**, *46*, 245-9.
- [30] Lindberg, P.; Brandstrom, A.; Wallmark, B.; Mattsson, H.; Rikner, L.; Hoffmann, K.J. Omeprazole: the first proton pump inhibitor. *Med. Res. Rev.*, **1990**, *10*, 1-60.
- [31] Lindberg, P.; Weidolf, L. Method for the treatment of gastric acid-related diseases and production of medication using the (-)-enantiomer of omeprazole. U.S. Patent 5877192, **1999**.
- [32] (a) Olbe, L.; Carlsson, E.; Lindberg, P. A proton-pump inhibitor expedition: the case histories of omeprazole and esomeprazole. *Nat. Rev. Drug Discov.*, **2003**, *2*, 132-9. (b) Kale-Pradhan, P.B.; Landry, H.K.; Sypula, W.T. Esomeprazole for acid peptic disorders. *Ann. Pharmacother.*, **2002**, *36*, 655-63. (c) Lindberg, P.; Keeling, D.; Frylund, J.; Andersson, T.; Lundborg, P.; Carlsson, E. Esomeprazole-enhanced bio-availability, specificity for the proton pump and inhibition of acid secretion. *Aliment. Pharmacol. Ther.*, **2003**, *17*, 481-8. (d) Chong, E.; Ensom, M.H. Pharmacogenetics of the proton pump inhibitors: a systematic review. *Pharmacotherapy*, **2003**, *23*, 460-71.
- [33] (a) Jenkins, D.J.; Sancilio, F.D.; Stowell, G.W.; Whittall, L.B.; Whittle, R.R. Alkoxy substituted benzimidazole compounds, pharmaceutical preparations containing the same, and methods of using the same, U.S. Patent 6,262,085, **2001**. (b) Jenkins, D.J.; Sancilio, F.D.; Stowell, G.W.; Whittall, L.B.; Whittle, R.R. Alkoxy substituted benzimidazole compounds, pharmaceutical preparations containing the same, and methods of using the same, U.S. Patent 6,369,087, **2002**.
- [34] Pham-Huy, C.; Villain-Pautet, G.; He, H.; Chikhi-Chorfi, N.; Galons, H.; Thevenin, M.; Claude, J.R.; Warnet, J.M. Separation of

- oxazepam, lorazepam and temazepam enantiomers by HPLC on a derivatized cyclodextrin-bonded phase: Application to the determination in plasma. *J. Biochem. Bioph. Meth.*, **2002**, *54*, 287-99.
- [35] He, H.; Liu, Y.; Sun, C.; Wang, X.; Pham-Huy, C. Effect of temperature on enantiomer separation of oxazepam and lorazepam by HPLC on a β -cyclodextrin derivatized bonded chiral stationary phase. *J. Chromatogr. Sc.*, **2004**, *42*, 62-6.
- [36] Mohler, H.; Richards, J.C. *The benzodiazepines. From molecular biology to clinical practice*. Raven Press: New York, **1983**.
- [37] Miller, L.; Orihuela, C.; Fronek, R.; Honda, D.; Dapremont, O. Chromatographic resolution of the enantiomers of a pharmaceutical intermediate from the milligram to the kilogram scale. *J. Chromatogr. A.*, **1999**, *849*, 309-17.
- [38] Williams, K.L.; Sander, L.C. Enantiomer separations on chiral stationary phases in supercritical fluid chromatography. *J. Chromatogr. A.*, **1997**, *785*, 149-58.
- [39] Liu, Y.; Lantz, A.W.; Armstrong, D.W. High efficiency liquid and super-subcritical fluid-based enantiomeric separations: An overview. *J. Liq. Chromatogr. Relat. Technol.*, **2004**, *27*, 1121-78.
- [40] Welch, C.J.; Leonard, W.R.; DaSilva, J.O.; Biba, M.; Albaneze-Walker, J.; Henderson, D.W.; Laing, B.; Mathre, D.J. Preparative chiral SFC as a green technology for rapid access to enantiopurity in pharmaceutical process research. *LC-GC Eur.*, **2005**, *18*, 264-6, 270, 272.
- [41] Zhang, Y.; Wu, D.; Wang-Iverson, D.B.; Tymiak, A.A. Enantioselective chromatography in drug discovery. *Drug Discov. Today.*, **2005**, *10*, 571-7.
- [42] Maftouh, M.; Granier-Loyaux, C.; Chavana, E.; Marini, J.; Pradines, A.; Heyden, Y.W.; Picard, C. Screening approach for chiral separation of pharmaceuticals. Part III. Supercritical fluid chromatography for analysis and purification in drug discovery. *J. Chromatogr. A.*, **2005**, *1088*, 67-81.
- [43] Amanullah, M.; Mazzotti, M. Optimization of a hybrid chromatography-crystallization process for the separation of Troeger's base enantiomers. *J. Chromatogr. A.*, **2006**, *1107*, 36-45.
- [44] Lorenz, H.; Polenske, D.; Seidel-Morgenstern, A. Application of preferential crystallization to resolve racemic compounds in a hybrid process. *Chirality*, **2006**, *18*, 828-40.
- [45] Jacques, J.; Collet, A.; Wilen, S.H. *Enantiomers, racemates and resolutions*. Wiley: New York, **1981**.
- [46] Kozma, D. DRC Handbook of optical resolutions via diastereomeric salt formation. CRC Press: Florida, **2002**.
- [47] Fogassy, E.; Nogradi, M.; Kozma, D.; Egri, G.; Pálovics, E.; Kiss, V. Optical resolution methods. *Org. Biomol. Chem.*, **2006**, *4*, 3011-30.
- [48] Kinbara, K. Design of resolving agents based on crystal engineering. *Synletters*, **2005**, *5*, 732-43.
- [49] Borghese, A.; Libert, V.; Zhang, T.; Alt, C.A. Efficient fast screening methodology for optical resolution agents: Solvent effects are used to affect the efficiency of the resolution process. *Org. Process. Res. Dev.*, **2004**, *8*, 532-4.
- [50] Toda, F. Isolation and optical resolution of materials utilizing inclusion crystallization. *Top Curr. Chem.*, **1987**, *140*, 43-69.
- [51] Eliel, E.; Wilen, S.H.; Mander, L.N. *Stereochemistry of organic compounds*. Wiley: New York, **1994**.
- [52] Kinbara, K.; Hashimoto, Y.; Sukegawa, M.; Nohira, H.; Saigo, K. Crystal structures of the salts of chiral primary amines with achiral carboxylic acids: Recognition of the commonly-occurring supramolecular assemblies of hydrogen-bond networks and their role in the formation of conglomerates. *J. Am. Chem. Soc.*, **1996**, *118*, 3441-9.
- [53] Sakai, K.; Hirayama, R.; Tamura, R. *Novel optical resolution technologies*. Springer-Verlag Berlin: Heidelberg, **2007**.
- [54] Ushio, T.; Tamura, R.; Takahashi, H.; Azuma, N.; Yamamoto, K. Unusual enantiomeric resolution phenomenon observed upon Recrystallization of a Racemic compound. *Angew. Chem. Int. Ed. Engl.*, **1996**, *35*, 2372-4.
- [55] Tamura, R.; Fujimoto, D.; Lepp, Z.; Misaki, K.; Miura, H.; Takahashi, H.; Ushio, T.; Nakai, T.; Hirotsu, K. Mechanism of preferential enrichment, an unusual enantiomeric resolution phenomenon caused by polymorphic transition during crystallization of mixed crystals composed of two enantiomers. *J. Am. Chem. Soc.*, **2002**, *124*, 13139-53.
- [56] Yokota, M.; Doki, N.; Shimizu, K. Chiral separation of a racemic compound induced by transformation of racemic crystal structures: DL-glutamic acid. *Cryst. Growth Des.*, **2006**, *6*, 1588-90.
- [57] Mughal, R.K.; Davey, R.J.; Blanden, N. Application of crystallization inhibitors to chiral separations. 1. Design of additives to discriminate between the racemic compound and the pure enantiomer of mandelic acid. *Cryst. Growth Des.*, **2007**, *7*, 218-24.
- [58] Mughal, R.K.; Davey, R.J.; Blagden, N. Application of crystallization inhibitors to chiral separations. 2. Enhancing the chiral purity of mandelic acid by crystallization. *Cryst. Growth Des.*, **2007**, *7*, 225-8.
- [59] Collins, A.N.; Sheldrake, G.N.; Crosby, J. *Chirality in industry II: Developments in the manufacture and applications of optically active compounds*. John Wiley & Sons: New York, **1997**.
- [60] Patel, R.N. *Biocatalysis and biotechnology for functional foods and industrial products*. CRC Press LLC: Boca Raton, Florida, **2007**.
- [61] Colonna, S.; Richelmi, C. Organic biotransformations. *Chimica e l'Industria*, **2004**, *86*, 58-62.
- [62] Eggert, T. *Industrial biotransformations*. Wiley-VCH Verlag GmbH & Co. KGaA: Weinheim, **2006**.
- [63] Miller, C.P.; Ullrich, J.W. A Consideration of the patentability of enantiomers in the pharmaceutical industry in the United States. *Chirality*, **2008**, *20*, 762-70.

Received: January 04, 2009

Revised: March 13, 2009

Accepted: March 15, 2009

PAPER 2



Original article

Synthesis and anticancer activity of (RS)-9-(2,3-dihydro-1,4-benzoxaheteroin-2-ylmethyl)-9H-purines

Ana Conejo-García^a, M. Eugenia García-Rubiño^a, Juan A. Marchal^b, M. Carmen Núñez^a, Alberto Ramírez^b, Sandro Cimino^a, M. Ángel García^{b,c}, Antonia Aránega^b, Miguel A. Gallo^a, Joaquín M. Campos^{a,*}

^a Departamento de Química Farmacéutica y Orgánica, Facultad de Farmacia, c/Campus de Cartuja s/n, 18071 Granada, Spain

^b Instituto de Biopatología y Medicina Regenerativa (IBIMER), Departamento de Anatomía y Embriología Humana, Facultad de Medicina, Avenida de Madrid s/n, 18071 Granada, Spain

^c Unidad de Investigación, Universitario Virgen de las Nieves, Avda. de las Fuerzas Armadas s/n, 18012 Granada, Spain

ARTICLE INFO

Article history:

Received 19 March 2011

Received in revised form

18 May 2011

Accepted 19 May 2011

Available online 26 May 2011

Keywords:

Apoptosis

1,4-Benzodioxin

1,4-Benzoxathiin

eIF2 α

Purine

Breast cancer cell line MCF-7

Neighboring-group participation

ABSTRACT

Herein are reported the synthesis and anticancer activity against the human breast cancer cell line MCF-7 of a series of substituted (RS)-9-(2,3-dihydro-1,4-benzoxathiin-2-ylmethyl)-9H-purine derivatives and (RS)-9-(2,3-dihydro-1,4-benzodioxin-2-ylmethyl)-9H-purine derivatives. When the Mitsunobu reaction was carried out between (RS)-2,3-dihydro-1,4-benzoxathiin-3-methanol and the heterocyclic bases 6-chloro-, 2,6-dichloro-, and 6-bromo-purines under microwave-assisted conditions, a formal 1,4-sulfur migration takes place through two consecutive oxiranium and episulfonium rings, giving rise to the corresponding (RS)-9-(2,3-dihydro-1,4-benzodioxin-3-ylmethyl)-9H-purine derivatives, previously reported by us. The most active compound (RS)-2,6-dichloro-9-(2,3-dihydro-1,4-benzoxathiin-2-ylmethyl)-9H-purine shows an $IC_{50} = 2.75 \pm 0.02 \mu M$. When the cancerous cells were treated with this compound, a significant increase of apoptotic cells ($70.08 \pm 0.33\%$) was obtained in relation to the control ones. The induction of the G₂/M cell cycle arrest and apoptosis by the three most active compounds is associated with increased phosphorylation of eIF2 α in human breast cancer cells.

© 2011 Elsevier Masson SAS. All rights reserved.

1. Introduction

Despite major breakthroughs in many areas of modern medicine over the past 100 years, the successful treatment of cancer remains a significant challenge at the start of the 21st century. Therefore, the development of new drugs against cancer continues to be the priority of the development of science and fundamental research.

As part of their action on neoplastic cells, many anticancer drugs activate apoptosis that may be a primary mechanism of antineoplastic agents [1]. Although breast cancer is most often treated with conventional cytotoxic agents, it has proved difficult to induce apoptosis in breast cancer cells using these drugs [2]. Improved

clinical response may be obtained by identifying therapies that are particularly effective in activating apoptosis and determining how those therapies may be modified to effect maximum apoptosis induction. The cell cycle and apoptosis have recently attracted the attention of researchers intent on developing new types of anti-cancer therapy [3,4]. The MCF-7 human breast cancer cell line has been used as an excellent experimental model to improve the efficacy of different therapies before its use in patients [5,6].

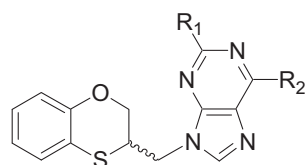
5-Fluorouracil (5-FU) was first introduced in cancer therapy in 1957, but even today it still remains an essential part of the treatment of a wide range of solid tumors. 5-FU has anti-tumor activity against epithelial malignancies arising in the gastrointestinal tract, breast, the head and neck, with single-agent response rates of only 10–30% [7]. Like the majority of the anticancer agents, 5-FU leads to several toxicities [7,8]. All these reasons explain the need for more effective and less toxic 5-FU derivatives. We have reported the evolution from 5-FU acyclonucleosides to benzo-fused six- and seven-membered rings linked to pyrimidine and purine bases [9].

Very recently, a series of 2- and 6-substituted (RS)-9-(2,3-dihydro-1,4-benzoxathiin-3-ylmethyl)-9H-purine derivatives

Abbreviations: MCF-7, Michigan Cancer Foundation; IC_{50} , concentration resulting in 50% inhibition; 5-FU, 5-fluorouracil; SEM, standard error of the mean; SRB, sulphorhodamine B; ECL, electrogenerated chemiluminescence; NALDI-TOF, high-resolution nano-assisted laser desorption/ionization; ESI-TOF, electrospray ionization.

* Corresponding author. Tel.: +34 958 243848; fax: +34 958 243845.

E-mail address: jmcampos@ugr.es (J.M. Campos).



- 1** R₁ = H, R₂ = Cl
2 R₁ = H; R₂ = Br
3 R₁ = R₂ = Cl
4 R₁ = H; R₂ = SMe
5 R₁ = H; R₂ = OPh
6 R₁ = H; R₂ = SPh
7 R₁ = H; R₂ = NHPH
8 R₁ = H; R₂ = OCH₂CH=CH₂
9 R₁ = H; R₂ = OCH₂Ph
10 R₁ = H; R₂ = SCH₂Ph
11 R₁ = H; R₂ = OCH₂C₆H₁₁

Fig. 1. Series of substituted (*RS*)-9-(2,3-dihydro-1,4-benzoxathiin-3-ylmethyl)-9H-purine derivatives **1–11** [10].

(**1–11**, Fig. 1) was obtained by applying a standard Mitsunobu protocol that led to a six-membered ring contraction from (*RS*)-3,4-dihydro-2*H*-1,5-benzoxathiepin-3-ol via an episulfonium intermediate [10]. The most active compounds were **2** and **3** with IC₅₀ = 6.18 ± 1.70 and 8.97 ± 0.83 μM, respectively. These results suggest that the presence of bulky substituents on position 6 of the purine ring reduces the anti-proliferative activity. Therefore, in this paper we propose the preparation and study of the anticancer activity of isomers of **1**, **2**, and **3** (with substituents on the purine moiety), in addition to the adenine natural fragment linked to the benzo-fused six-membered ring through a methylene linker. An approach that has guided the origin of novel drugs is bioisosterism, which we have carried out as suitable structural modifications of the seven-membered building block, such as the modification O-1/S [11,12].

The design, synthesis and biological evaluation of two series of substituted (*RS*)-9-(2,3-dihydro-1,4-benzoxathiin-2-ylmethyl)-9H-purines **12–15** (Series A), and (*RS*)-9-(2,3-dihydro-1,4-benzodioxin-2-ylmethyl)-9H-purines **16–19** (Series B, Fig. 2) are described. In series A, the methylene linker that connects the six-membered ring and the purine moiety has been changed from position 3 to 2 in relation to derivatives **1–11** (Fig. 1). Series B is the isosteric group in which sulfur is replaced by oxygen. We will explore the activity of these compounds in the inhibition of MCF-7 breast cancer cell growth to ascertain potential directions for synthetic lead-optimization studies.

Neighboring-group participation is a term which encompasses all intramolecular reactions and all reactions which involve non-electrostatic through-space interactions between groups within the same molecule [13]. Neighboring-group participation is well documented as far as the mechanism and scope of the reaction are concerned [14]. We have lately reviewed the application of the neighboring-group participation involving the oxygen atom of *O,O*- or *O,N*-acetals [15]. Herein we use this mechanism to explain the

isomerizations **12** → **1, 13** → **2** and **14** → **3**, that took place during the synthesis of the target molecules **12**, **13** and **14**, using the Mitsunobu protocol under microwave-assisted conditions.

2. Results and discussion

2.1. Chemistry

The starting material (*RS*)-2,3-dihydro-2*H*-1,4-benzoxathiin-2-methanol (**20**) was prepared as previously reported in Ref. [10] whilst (*RS*)-(2,3-dihydro-1,4-benzodioxin-2-yl)methanol (**21**) was synthesized by the reaction of catechol with epichlorohydrin in NaOH and water [16].

Final compounds **12–19** were synthesized by the Mitsunobu reaction in dry THF between **20** or **21** and the corresponding purines (6-chloropurine, 6-bromopurine, 2,6-dichloropurine and adenine) under microwave-assisted conditions (Scheme 1).

The quaternary signals $\sim \delta = 151$ ppm, which correspond to the C-4' carbon atom¹, is a proof of the *N*-9' regioisomers [10]. This chemical shift of C-4' in compounds **12–19** agrees with previous findings on related *N*-9' purine *O,N*-acetals [17,18].

It must be pointed out that when starting from **20** and using 6-chloro-, 6-bromo-, and 2,6-dichloro-purines, apart from the target compounds **12**, **13** and **14**, their corresponding previously reported isomers **1**, **2** and **3** [10] were also obtained as side-products. Therefore we committed ourselves to justifying the formation of such "abnormal" products through a neighboring-group mechanism.

The neighboring-group mechanism occurs with appropriate ring sizes. For example, it was previously observed that in the case of MeO(CH₂)_{*n*}OBs [Bs: brosylates or *p*-bromobenzene-sulfonates], neighboring-group participation occurred with *n* = 4 or 5 (corresponding to a five- or six-membered intermediates), but not with *n* = 2, 3, or 6 [19]. However, optimum ring size is not the same for all reactions. In general, the most rapid reactions occur when the ring size is three, five, or six, depending on the reaction type. The likelihood of four-membered ring neighboring-group participation is increased when there are alkyl groups α or β the neighboring group [20]. The OR group is more important as a neighboring group than the SR one [21]. Scheme 2 might explain the formation of **1**, **2** and **3**.

The starting triphenylphosphonium salt **22** through routes (a), (b), (c), and (e) gives rise to the target molecules **12–15** through intermediates **23** and/or **28**. Nevertheless, following the formation of the oxonium ion **23** and after the sulfur neighboring-group participation with the concomitant generation of the episulfonium ring **29** [route (g), Scheme 2], the nucleophilic attack of the purine anion to the less hindered α carbon atom of the thiiranium intermediate would give rise to molecules **1**, **2** and **3**. Accordingly, a formal 1,4-thio migration (from the 2,3-dihydro-1,4-benzoxathiin-2-ylmethyl to the 2,3-dihydro-1,4-benzoxathiin-3-ylmethyl moieties) can proceed through two consecutive O-3 and S-3² neighboring-group participations in a six-membered ring system. In the case of compound **15** (bearing the adenine moiety) there is no neighboring-group participation.

It has been demonstrated that a successful Mitsunobu displacement does not depend on the nucleophilicity of the incoming nucleophile but rather on the p*K*_a associated with the

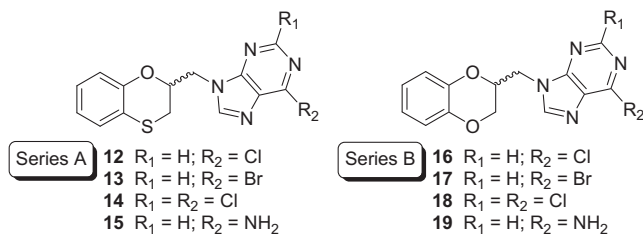
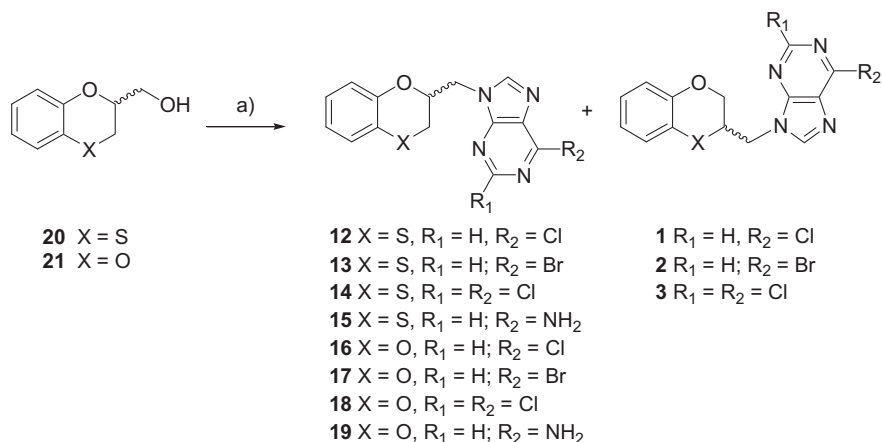


Fig. 2. Substituted (*RS*)-9-(2,3-dihydro-1,4-benzoxathiin-2-ylmethyl)-9H-purines **12–15** (series A) and (*RS*)-9-(2,3-dihydro-1,4-benzodioxin-2-ylmethyl)-9H-purines **16–19** (series B).

¹ For the numbering of the compounds, the atoms of the benzoxaheteroin ring are tagged with numbers without primes, while those of the purine bases are numbered with primes (').

² When describing nucleophilic participation it is frequently convenient to use the symbol *G-n*, where *G* is the participating group and *n* the size of the ring that is formed in the transition state.



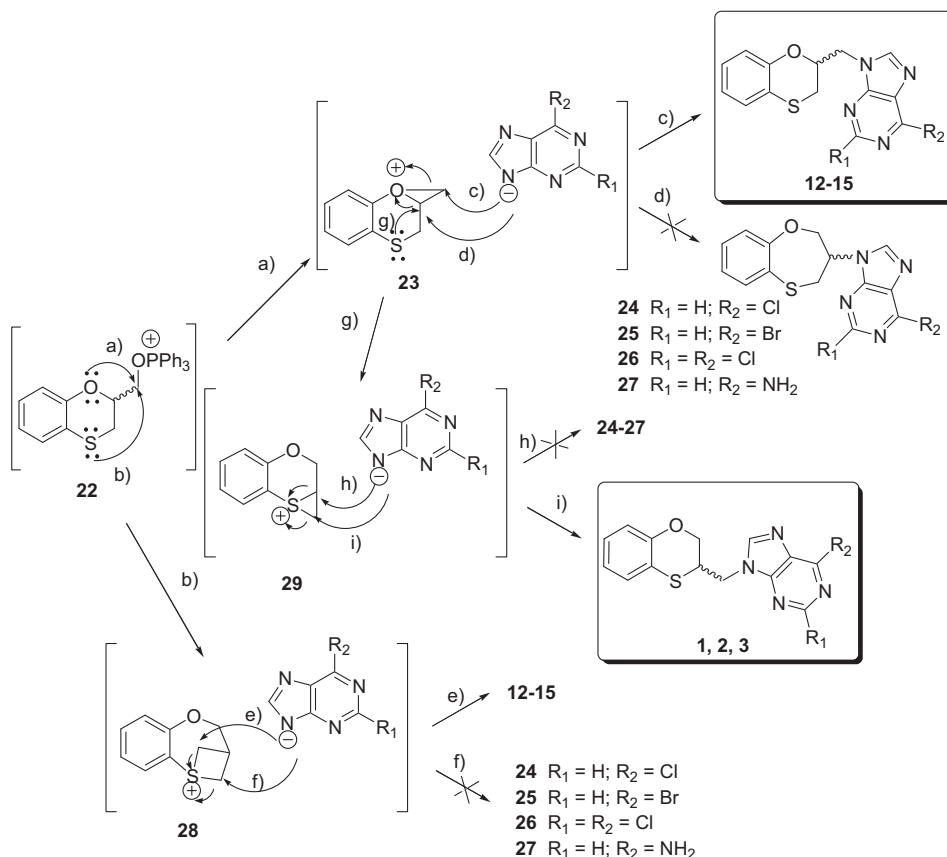
Scheme 1. Reagents and conditions: (a) Substituted purines, Ph₃P, DIAD, anhydrous THF, microwave irradiation, 140 °C, 5 min, or in the case of **17**, 160 °C, 15 min.

N–H bond [22]. Adenine is a poor nucleophile with a low solubility in the most common solvent, THF [23].

Although the *N*-9 alkylation of the purine ring takes place at two sites of the benzoxathiin moiety (through intermediates **23** and **29**, Scheme 2) to lead to a mixture of products, the overall yields of the target and “rearranged” compounds (**12** + **1**; **13** + **2**; and **14** + **3**) are good [88% = 78% (**12**) + 10% (**1**), 60% = 54% (**13**) + 6% (**2**), and 70% = 55% (**14**) + 15% (**3**)] in the ratios **12**:**1** = 7.8:1, **13**:**2** = 9.0:1, and **14**:**3** = 3.7:1. Starting from adenine, the target compound **15** is the only one obtained, although with only a modest yield (30%).

The effects of structures on reactivity need to be analyzed in order to rationalize all these experimental facts: (a) The

nucleophile, and (b) the electrophile. In relation to the nucleophile it must be pointed out that the yields for the non-rearranged purine derivatives having electron-withdrawing groups, such as 6'-Cl (**12**), 6'-Br (**13**), and 2',6'-diCl (**14**) are higher than that of the adenine derivative (**15**), bearing an electron-releasing group (6'-NH₂); (b) the two intermediates, such as the oxyranium **23** and the episulfonium **29** ions must be taken into account. Although in both cases the attack of the nucleophile takes place to the less hindered side of the three-membered ring [routes (c) and (i) on intermediates **23** and **29**, respectively], the higher electronegativity of the positively charged oxygen atom (in **23**) in relation to the positively charged sulfur (in **29**) would explain the greater yields of the target



Scheme 2. Proposed mechanism for the formation of **1**, **2** and **3** through neighboring-group participation.

derivatives **12–14** compared to the rearranged ones **1**, **2** and **3**. In the case of the adenine derivative (**15**), since the target compound is formed in a moderate yield (30%), the possible rearranged one is not detected under our experimental conditions. Finally, the attack of the bulky purine nucleophile against the more hindered position of intermediates **23** and **29** [routes (d) and (h), respectively (Scheme 2)] does not take place and not the slightest trace of the seven-membered rings **24–27** is detected.

2.2. Pharmacology

The anticarcinogenic potential of the target molecules is reported against the MCF-7 human breast cancer cell line (Table 1). In general, (*RS*)-9-(2,3-dihydro-1,4-benzoxathiin-2-ylmethyl)-9*H*-purines **12–15** (series A) show a better activity than their isosteres (*RS*)-9-(2,3-dihydro-1,4-benzodioxin-2-ylmethyl)-9*H*-purines **16–19** (series B). Compounds **12–14** bearing the purine moiety linked to the position 2 of the six-membered ring are more potent than compounds **1**, **2** and **3**, in which such a link is established at position 3. The anticancer activity depends on the substituent of the purine ring. The most active compound **14**, bearing two chlorine atoms at positions 2 and 6 of the purine ring, shows an $IC_{50} = 2.75 \pm 0.02 \mu\text{M}$. In general, compounds bearing electron-withdrawing substituents on the purine ring (**12–14** and **16–18**) present better activity than compounds substituted bearing an amino group (**15** and **19**).

In recent years, many studies have shown an association between cell cycle regulation and cancer in as much as the cell cycle inhibitors are being considered as a weapon for the management of cancer [24]. To study the mechanisms of the anti-tumor activity of the most active compounds (**12–14** and **17**), the effects on the cell cycle distribution were analyzed by flow cytometry (Table 2). DMSO-treated cell cultures contain a $62.79 \pm 1.30\%$ of the cells in the G_0/G_1 -phase, and a $19.29 \pm 2.98\%$ of the cells in the S-phase, a $13.26 \pm 2.98\%$ of the cells in the G_2/M -phase. In contrast, MCF-7 cells treated during 48 h with **12–14** and **17** show important differences in the cell cycle progression compared with DMSO-treated control cells. The following can be deduced from the analysis of the cell cycle distribution: compounds **12**, **13**, **14** and **17** accumulate the cancerous cells in the G_2/M -phase (23.35 ± 1.97 , 31.37 ± 1.45 , 43.89 ± 1.96 and 36.71 ± 7.40 , respectively) at the expense of the S-phase cells (13.77 ± 1.13 , 17.06 ± 0.75 , 10.83 ± 4.70 and 10.27 ± 6.24 , respectively) and of the G_0/G_1 -phase cells in the case of compounds **13**, **14** and **17** (51.56 ± 1.06 , 45.28 ± 2.73 and 53.02 ± 1.16 , respectively), except in the case of **12**, which induces a cell cycle arrest in the G_2/M -phase cells (23.35 ± 1.97) at the expense of the S-phase cells (13.77 ± 1.13).

Table 1

Anti-proliferative activities against the MCF-7 cell line for the (*RS*)-9-(2,3-dihydro-1,4-benzoxathiin-3-ylmethyl)-9*H*-purines (**1**, **2** and **3**), (*RS*)-9-(2,3-dihydro-1,4-benzoxathiin-2-ylmethyl)-9*H*-purines (**12–15**), and (*RS*)-9-(2,3-dihydro-1,4-benzodioxin-2-ylmethyl)-9*H*-purines (**16–19**).

Comp.	IC_{50} (μM)
1 [10]	10.6 ± 0.66
2 [10]	6.18 ± 1.70
3 [10]	8.97 ± 0.83
12	9.24 ± 0.01
13	4.87 ± 0.02
14	2.75 ± 0.03
15	>30
16	18.75 ± 0.02
17	7.64 ± 0.03
18	19.58 ± 0.02
19	>30

Table 2

Cell cycle distribution and apoptosis induction in the MCF-7 human breast cancer cell line after treatment for 48 h with the three most active compounds as anti-proliferative agents.

Compound	Cell cycle ^a			Apoptosis ^{b,c}
	G_0/G_1	S	G_2/M	
Control	62.79 ± 1.30	19.29 ± 1.68	13.26 ± 2.98	0.92 ± 1.29
12	62.87 ± 0.60	13.77 ± 1.13	23.35 ± 1.97	37.99 ± 8.56
13	51.56 ± 1.06	17.06 ± 0.75	31.37 ± 1.45	14.33 ± 1.23
14	45.28 ± 2.73	10.83 ± 4.70	43.89 ± 1.96	70.08 ± 0.33
17	53.02 ± 1.16	10.27 ± 6.24	36.71 ± 7.40	21.66 ± 0.30

^a Determined by flow cytometry [25].

^b Apoptosis was determined using an Annexin V-based assay [25]. The data indicate the percentage of cells undergoing apoptosis in each sample.

^c All experiments were conducted in duplicate and gave similar results. The data are means \pm SEM of three independent determinations.

The protein expression analysis by western blot showed that **12–14** have an important role in the activation and phosphorylation of the initiation factor eIF2 α . The initiation factor eIF2 α was phosphorylated in MCF-7 human breast cancer cell line after treatment with **12–14** (Fig. 3). It is well established that eIF2 α phosphorylation correlates with a translational block and consequently produces inhibition of protein synthesis [26]. These results are in concordance with the delay in the G_2/M cell cycle phase produced by compounds. Furthermore, a prolonged induction of eIF2 α finally triggers the cell cycle arrest and/or the apoptosis phenomena [27,28].

MCF-7 cells treated for 48 h with compounds **12–14** induced apoptosis, being **14** the compound that showed a significant increase of apoptotic cells in relation to the control culture with a percentage of 70.08 ± 0.33 (Table 2). Apoptosis is a major form of cell death characterized by changes in signaling pathways that lead to the recruitment and activation of caspases, a family of cysteine-containing, aspartate-specific proteases. Caspases exist as inactive proenzymes in cells, and are activated through their processing into two subunits in response to apoptotic stimulation. Activated caspases cleave a variety of important cellular proteins, other caspases, and Bcl-2 family members, leading to a commitment to cell death. Caspase-9 is involved in one of the relatively well characterized caspase cascades. It is triggered by cytochrome C release from the mitochondria, which promotes the activation of caspase-9 by forming a complex with Apaf-1 in the presence of dATP. Once activated, caspase-9 initiates a caspase cascade that finally induces

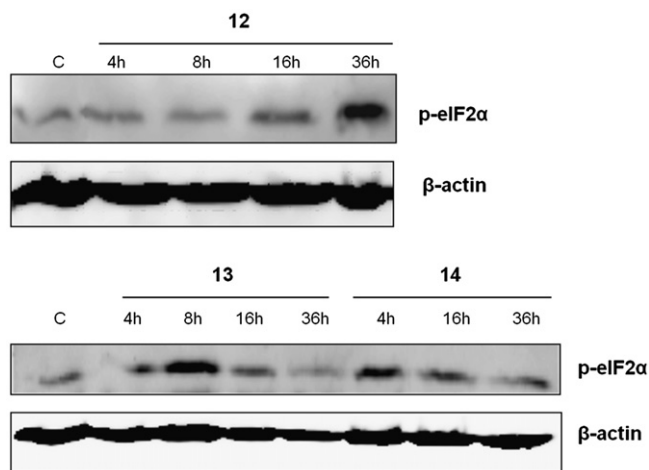


Fig. 3. Human breast cancer MCF-7 cells treated with **12–14** for 4, 8, 16 and 36 h. Total proteins were extracted for immunoblot analysis using anti-phospho-eIF2 α , and anti- β -actin antibodies.

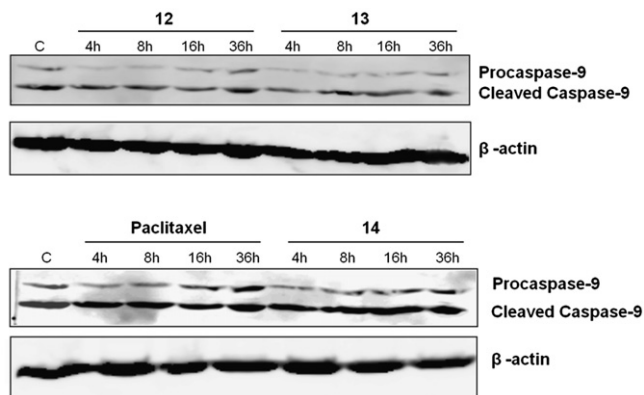


Fig. 4. Human breast cancer MCF-7 cells treated with **12–14** or paclitaxel for 4, 8, 16 and 36 h. Total proteins were extracted for immunoblot analysis using anti-caspase-9 and anti- β -actin antibodies.

cell death [29]. Western blot assays showed that compounds **12–14** induced activation of caspase-9 at late times (16 h and 36 h of treatment) similarly to paclitaxel used as control compound (Fig. 4). These data confirm that levels of apoptosis showed by annexin V assays are dependent of intrinsic pathway of cell death. p53 was not activated by the compounds which indicate that apoptosis was induced in a p53-independent manner (data not shown).

3. Conclusion

Two bioisosteric series [substituted (*RS*)-9-(2,3-dihydro-1,4-benzoxathiin-2-ylmethyl)purines **12–15**, and substituted (*RS*)-9-(2,3-dihydro-1,4-benzodioxin-2-ylmethyl)purines **16–19**] have been synthesized and screened for their anticancer activity against the MCF-7 cancer cell line. During the preparation of **12–14**, isomerization products have been isolated. A formal 1,4-thio migration (from the 2,3-dihydro-1,4-benzoxathiin-2-ylmethyl to the 2,3-dihydro-1,4-benzoxathiin-3-ylmethyl moieties) can proceed through two consecutive O-3 and S-3 neighboring-group participations in the six-membered ring system. Although it cannot be considered as a valuable synthetic tool for organic chemists, it may explain the complexity of the reaction products of the Mitsunobu reaction between (*RS*)-2,3-dihydro-1,4-benzoxathiin-3-methanol and the heterocyclic bases, 6-chloro- and 2,6-dichloro-purines under microwave-assisted conditions. The most active compounds are **14**, **13** and **17** with $IC_{50} = 2.75 \pm 0.03$, 4.87 ± 0.02 , and 7.64 ± 0.03 μ M, respectively. Compound **14** is 3.3-fold higher as anti-proliferative agent against the MCF-7 cell line than the previously reported bioisostere **3** [16]. Apoptosis induction in the MCF-7 human breast cancer cell line after treatment for 48 h with **14** and **3** are in the same range {percentage of cells undergoing apoptosis: 70.08% (for **14**) and 76.22% (for **3**) [15]}. Moreover our results demonstrate that compounds **12–14** have as molecular target the inhibition of translation by eIF2 α phosphorylation, and induction of cell apoptosis in a p53-independent manner.

4. Experimental protocols

4.1. Chemistry

Melting points were taken in open capillaries on an Electro-thermal melting point apparatus and are uncorrected. Analytical thin layer chromatography (TLC) was performed using Merck Kieselgel 60 F_{254} aluminum sheets, the spots being developed with UV light. All evaporation was carried out in vacuo with a Büchi rotary evaporator and the pressure controlled by a Vacuubrand CVC^{II} apparatus. For

flash chromatography, Merck silica gel 60 with a particle size of 0.040–0.063 mm (230–400 mesh ASTM) was used. Nuclear magnetic resonance spectra have been carried out at the Centro de Instrumentación Científica/Universidad de Granada, and recorded on a 400 MHz 1 H and 100 MHz 13 C NMR Varian NMR-System-TM 400 or 300 MHz 1 H and 75 MHz 13 C NMR Varian Inova-TM spectrometers at ambient temperature. Chemical shifts (δ) are quoted in parts per million (ppm) and are referenced to the residual solvent peak. Coupling values (J) are given in hertz (Hz). Spin multiplicities are given as s (singlet), d (doublet), dd (double doublet), t (triplet), dt (double triplet), m (multiplet). High-resolution Nano-Assisted Laser Desorption/Ionization (NALDI-TOF) or Electrospray Ionization (ESI-TOF) mass spectra were carried out on a Bruker Autoflex or a Waters LCT Premier Mass Spectrometer, respectively. Small scale microwave-assisted synthesis was carried out in an Initiator 2.0 single-mode microwave instrument producing controlled irradiation at 2.450 GHz (Biotage AB, Upsala). Reaction time refers to hold time at 140/160 °C, not to total irradiation time. The temperature was measured with an IR sensor on the outside of the reaction vessel. 6-Chloropurine, 6-bromopurine, 2,6-dichloropurine and adenine were purchased from Aldrich. Anhydrous solvents (DMF and THF) were purchased from VWR International Eurolab. Anhydrous conditions were performed under argon.

4.1.1. Synthesis of the starting materials

The starting materials (*RS*)-2,3-dihydro-1,4-benzoxathiin-2-methanol [10] and (*RS*)-2,3-dihydro-1,4-benzodioxin-2-methanol [16] were synthesized according to literature procedures.

4.1.2. General procedure for the microwave-assisted synthesis of compounds **12–19**

DIPAD (1.1 equiv) was slowly added to a suspension of the benzo-fused six-membered ring (**20** or **21**, 1 equiv), purine base (1 equiv) and triphenylphosphine (1.1 equiv) in dry THF (5 mL/mmol) in a microwave vial, cooled in an ice-bath. The vial was sealed and microwave irradiated at a set temperature of 140 °C for 5 min. In the case of **17**, the reaction was carried out at 160 °C within 15 min by microwave irradiation. Compounds **15** and **19** were purified by flash column chromatography on silica gel using a mixture of $CH_2Cl_2/MeOH$ (10/0.1 \rightarrow 10/0.5) as eluent, whilst **12–14** and **16–18** were purified using as eluent hexane/ethyl acetate (7/1 \rightarrow 1/1). The solvent was evaporated and the crude product was purified by flash column chromatography on silica gel using a mixture of hexane/EtOAc (7:1 \rightarrow 1/1) as eluent to afford **12–19**.

4.1.2.1. (*RS*)-6-chloro-9-(2,3-dihydro-1,4-benzoxathiin-2-ylmethyl)-9H-purine (12**) and (*RS*)-6-chloro-9-(2,3-dihydro-1,4-benzoxathiin-3-ylmethyl)-9H-purine (**1**).** Compound **12** was obtained from **20** as a white powder; (52.8 mg, 78%); mp: 146–148 °C; 1 H NMR (300 MHz, $CDCl_3$): δ = 8.73 (s, 1H), 8.21 (s, 1H), 7.04–6.96 (m, 2H), 6.88–6.83 (m, 1H), 6.77 (dd, J = 8.1 Hz, J = 1.42 Hz, 1H), 4.70–4.64 (m, 2H), 4.56 (dd, J = 14.8 Hz, J = 8.2 Hz, 1H), 3.15 (dd, J_{gem} = 13.2 Hz, J_2 = 2.1 Hz, 1H), 2.91 (dd, J_{gem} = 13.2 Hz, J_2 = 7.6, 1H); 13 C NMR (125 MHz, $CDCl_3$): δ = 152.09, 151.93 (C-4'), 151.29, 149.98, 145.96, 131.44, 127.46, 126.21, 122.33, 118.58, 116.74, 71.74, 47.13, 27.09; HRMS: m/z [M + H]⁺ calcd for $C_{14}H_{12}ClN_4OS$: 319.0420, found: 319.0421. Anal. $C_{14}H_{11}ClN_4OS$ (C, H, N, S). Moreover, compound **1** [10] was also obtained (6.8 mg, 10%).

4.1.2.2. (*RS*)-6-bromo-9-(2,3-dihydro-1,4-benzoxathiin-2-ylmethyl)-9H-purine (13**) and (*RS*)-6-bromo-9-(2,3-dihydro-1,4-benzoxathiin-3-ylmethyl)-9H-purine (**2**).** Compound **13** was obtained from **20** as an off-white powder (70.9 mg, 54%); mp: 63 °C melts, 118 °C foam, 150 °C liquefies; 1 H NMR (500 MHz, $CDCl_3$): δ = 8.76 (s, 1H, H-2'), 8.36 (s, 1H), 7.04–6.97 (m, 2H), 6.88–6.84 (m, 1H), 6.77 (dd,

$J = 7.26$ Hz, $J = 1.3$ Hz, 1H), 4.72–4.68 (m, 2H), 4.62–4.56 (m, 1H), 3.16 (dd, $J = 12.6$ Hz, $J = 1.41$ Hz, 1H), 2.92 (ddd, $J = 13.2$ Hz, $J = 7.7$ Hz, $J = 1.5$ Hz, 1H); ^{13}C NMR (125 MHz, CDCl_3): $\delta = 152.53$ and 152.44 (CH-2'), 151.99 (C-4'), 151.33, 150.16, 146.15 (CH-8'), 130.99, 127.69, 126.45, 122.58, 118.82, 116.93, 71.93, 47.53, 27.31; HRMS: m/z $[\text{M} + \text{H}]^+$ calcd for $\text{C}_{14}\text{H}_{12}\text{BrN}_4\text{O}_5$: 362.9915, found: 362.9914. Anal. $\text{C}_{14}\text{H}_{11}\text{BrN}_4\text{O}_5$ (C, H, N, S). Moreover, compound **2** [10] was also obtained (6.9 mg, 6%).

4.1.2.3. (RS)-2,6-dichloro-9-(2,3-dihydro-1,4-benzoxathiin-2-ylmethyl)-9H-purine (**14**) and (RS)-2,6-dichloro-9-(2,3-dihydro-1,4-benzoxathiin-3-ylmethyl)-9H-purine (**3**). Compound **14** was obtained from **20** as a white powder; (48.6 mg, 55%); mp: 78 °C melts, 130 °C foam, 143 °C liquefies; ^1H NMR (600 MHz, CDCl_3): $\delta = 8.18$ (s, 1H), 7.05–6.99 (m, 2H), 6.89–6.86 (m, 1H), 6.77 (dd, $J = 8.2$ Hz, $J = 1.0$ Hz, 1H), 4.69–4.63 (m, 2H), 4.51 (dd, $J = 14.7$ Hz, $J = 8.0$, 1H), 3.17 (dd, $J_{\text{gem}} = 13.2$ Hz, $J_2 = 2.1$ Hz, 1H), 2.93 (dd, $J_{\text{gem}} = 13.2$ Hz, $J_2 = 7.8$, 1H); ^{13}C NMR (150 MHz, CDCl_3): $\delta = 153.47, 153.43, 152.28$ (C-4'), 150.05, 146.85, 130.84, 127.74, 126.51, 122.68, 118.81, 116.98, 71.79, 47.44, 27.26. HRMS: m/z $[\text{M} + \text{H}]^+$ calcd for $\text{C}_{14}\text{H}_{11}\text{Cl}_2\text{N}_4\text{O}_5$: 353.0030, found: 353.0029. Anal. $\text{C}_{14}\text{H}_{10}\text{Cl}_2\text{N}_4\text{O}_5$ (C, H, N, S). Moreover, compound **3** [10] was also obtained (13.3 mg, 15%).

4.1.2.4. (RS)-6-amino-9-(2,3-dihydro-1,4-benzoxathiin-2-ylmethyl)-9H-purine (**15**). Compound **15** was obtained from **20** as a white powder; (31.1 mg, 30%); mp: 203–205 °C ^1H NMR (300 MHz, CDCl_3): $\delta = 8.34$ (s, 1H), 7.89 (s, 1H), 7.03–6.97 (m, 2H), 6.87–6.79 (m, 2H), 5.78 (s, 1H), 4.68–4.63 (m, 1H), 4.57 (dd, $J_{\text{gem}} = 14.50$ Hz, $J_2 = 3.61$ Hz, 1H), 4.47 (dd, $J_{\text{gem}} = 14.50$ Hz, $J_2 = 7.05$ Hz, 1H), 3.12 (dd, $J_{\text{gem}} = 13.18$ Hz, $J_2 = 2.1$ Hz, 1H), 2.89 (dd, $J_{\text{gem}} = 13.18$ Hz, $J_2 = 7.94$ Hz, 1H); ^{13}C NMR (75 MHz, CDCl_3): $\delta = 155.67, 152.36$ (C-4'), 150.48, 150.42, 141.61, 127.62, 126.25, 122.32, 119.54, 118.81, 117.11, 72.24, 46.83, 27.27. HRMS: m/z $[\text{M} + \text{H}]^+$ calcd for $\text{C}_{14}\text{H}_{14}\text{N}_5\text{O}_5$: 230.0919, found: 230.0919. Anal. $\text{C}_{14}\text{H}_{13}\text{N}_5\text{O}_5$ (C, H, N, S).

4.1.2.5. (RS)-6-chloro-9-(2,3-dihydro-1,4-benzodioxin-2-ylmethyl)-9H-purine (**16**). Compound **16** was obtained from **21** as a colorless oil; (50.7 mg, 56%); ^1H NMR (300 MHz, CDCl_3): $\delta = 8.74$ (s, 1H), 8.18 (s, 1H), 6.87–6.84 (m, 4H), 4.66–4.62 (m, 2H), 4.51 (dd, $J = 15.23$ Hz, $J = 8.51$ Hz, 1H), 4.36 (dd, $J_{\text{gem}} = 11.64$ Hz, $J_2 = 1.78$ Hz, 1H), 3.95 (dd, $J_{\text{gem}} = 11.64$ Hz, $J_2 = 5.37$ Hz, 1H); ^{13}C NMR (75 MHz, CDCl_3): $\delta = 152.35, 152.05$ (C-4'), 151.50, 146.17, 142.86, 141.75, 131.56, 122.53, 122.49, 117.67, 70.79, 65.04, 44.39. HRMS: m/z $[\text{M} + \text{H}]^+$ calcd for $\text{C}_{14}\text{H}_{12}\text{ClN}_4\text{O}_2$: 303.0649, found: 303.0651. Anal. $\text{C}_{14}\text{H}_{11}\text{ClN}_4\text{O}_2$ (C, H, N).

4.1.2.6. (RS)-6-bromo-9-(2,3-dihydro-1,4-benzodioxin-2-ylmethyl)-9H-purine (**17**). Compound **17** was obtained from **21** as a white powder. (35.3 mg, 34%); mp: 127–129 °C; ^1H NMR (300 MHz, CDCl_3): $\delta = 8.69$ (s, 1H, H-2'), 8.16 (s, 1H), 6.87–6.85 (m, 4H), 4.64–4.61 (m, 2H), 4.53–4.50 (m, 1H), 4.36 (dd, $J_{\text{gem}} = 11.60$ Hz, $J_2 = 4.0$ Hz, 1H), 3.95 (dd, $J_{\text{gem}} = 11.60$ Hz, $J_2 = 5.63$ Hz, 1H); ^{13}C NMR (75 MHz, CDCl_3): $\delta = 152.27, 150.85$ (C-4'), 146.01 (CH-8'), 143.69, 142.86, 141.75, 134.33, 122.56, 122.51, 117.70, 117.69, 70.78, 65.05, 44.37. HRMS: m/z $[\text{M} + \text{H}]^+$ calcd for $\text{C}_{14}\text{H}_{12}\text{BrN}_4\text{O}_2$: 347.0143, found: 347.0144. Anal. $\text{C}_{14}\text{H}_{11}\text{BrN}_4\text{O}_2$ (C, H, N).

4.1.2.7. (RS)-2,6-dichloro-9-(2,3-dihydro-1,4-benzodioxin-2-ylmethyl)-9H-purine (**18**). Compound **18** was obtained from **21** as a white powder; (25.6 mg, 25%); mp: 191–193 °C; ^1H NMR (300 MHz, CDCl_3): $\delta = 8.12$ (s, 1H), 6.88–6.84 (m, 4H), 4.62–4.59 (m, 2H), 4.46 (dd, $J = 15.19$ Hz, $J = 8.74$ Hz, 1H), 4.37 (dd, $J_{\text{gem}} = 11.60$ Hz, $J_2 = 2.30$ Hz, 1H), 4.00 (dd, $J_{\text{gem}} = 11.60$ Hz, $J_2 = 5.66$ Hz, 1H); ^{13}C NMR (75 MHz, CDCl_3): $\delta = 153.41$ (C-4'), 152.27, 146.78, 142.78, 141.43, 131.01, 122.64, 122.62, 117.76, 117.68,

70.63, 64.94, 44.46. HRMS: m/z $[\text{M} + \text{H}]^+$ calcd for $\text{C}_{14}\text{H}_{11}\text{Cl}_2\text{N}_4\text{O}_2$: 337.0259, found: 337.0259. Anal. $\text{C}_{14}\text{H}_{10}\text{Cl}_2\text{N}_4\text{O}_2$ (C, H, N).

4.1.2.8. (RS)-6-amino-9-(2,3-dihydro-1,4-benzodioxin-2-ylmethyl)-9H-purine (**19**). Compound **19** was obtained from **21** as a white powder; (26.3 mg, 28%); mp: 227–229 °C; ^1H NMR (300 MHz, CDCl_3): $\delta = 8.35$ (s, 1H), 7.85 (s, 1H), 6.87–6.85 (m, 4H), 5.66 (s), 4.62–4.58 (m, 1H), 4.53 (dd, $J_{\text{gem}} = 14.70$ Hz, $J_2 = 3.16$ Hz, 1H), 4.43 (dd, $J_{\text{gem}} = 14.70$ Hz, $J_2 = 7.2$ Hz, 1H), 4.34 (dd, $J_{\text{gem}} = 11.60$ Hz, $J_2 = 2.3$ Hz, 1H) 3.91 (dd, $J_{\text{gem}} = 11.60$ Hz, $J_2 = 6.10$ Hz, 1H); ^{13}C NMR (75 MHz, CDCl_3): $\delta = 155.39, 153.14, 150.18$ (C-4'), 142.76, 141.87, 141.32, 122.10, 122.02, 119.34, 117.44, 117.37, 70.89, 64.99, 43.62. HRMS: m/z $[\text{M} + \text{H}]^+$ calcd for $\text{C}_{14}\text{H}_{14}\text{N}_5\text{O}_2$: 284.1147, found: 284.1147. Anal. $\text{C}_{14}\text{H}_{13}\text{N}_5\text{O}_2$ (C, H, N).

4.2. Biology

4.2.1. Cell culture

MCF-7 cells were grown at 37 °C in an atmosphere containing 5% CO_2 , with Dubelcco's modified Eagle Medium (DMEM) (Gibco, Grand Island, NY, USA) supplemented with 10% heat-inactivated fetal bovine serum (FBS) (Gibco), 2% L-glutamine, 2.7% sodium bicarbonate, 1% HEPES buffer, 40 mg/L gentamicin and 500 mg/L ampicillin.

4.2.2. Drugs and drug treatments

The drugs were dissolved in DMSO or water and stored at –20 °C. For each experiment, the stock solutions were further diluted in medium to obtain the desired concentrations. The final solvent concentration in cell culture was $\leq 0.1\%$ v/v of DMSO, a concentration without effect on cell replication. Parallel cultures of cells in medium with DMSO were used as controls.

4.2.3. Cytotoxicity assays in vitro

The effect of anticancer drugs on cell viability was assessed using the sulforhodamine-B colorimetric assay [30]. Aliquots of MCF-7 cells suspension (1×10^3 cells/well) were seeded onto 24-well plates and incubated for 24 h. The cells were then treated with different concentrations of drugs in the culture medium. Three days later, the wells were aspirated, fresh medium and treatment were added, and cells were maintained for 3 additional days. Thereafter, cells were processed as described previously [30], using a Titertek Multiscan apparatus (Flow, Irvine, CA, USA) at 492 nm. We evaluated the linearity of the SRB assay with a cell number for each cell line before each cell growth experiment. The IC_{50} values were calculated from semilogarithmic dose-response curves by linear interpolation. All of the experiments were plated in triplicate wells and were carried out at least twice.

4.2.4. Cell cycle distribution analysis

The cells at 70% confluence were treated with either DMSO alone or with concentrations of compounds **12–14** and **17** determined by their IC_{50} values. FACS analysis was performed after 48 h of treatment as described in Ref. [25]. All experiments were performed in triplicate and yielded similar results.

4.2.5. Apoptosis detection by staining with annexin V-FITC and propidium iodide

The annexin V-FITC apoptosis detection kit I (Pharmingen, San Diego, CA, USA) was used to detect apoptosis by flow cytometry according to Marchal et al. [25]. Apoptosis induction in the MCF-7 human breast cancer cell line after treatment for 48 h was determined for compounds **12–14** and **17** at doses of their corresponding $3 \times \text{IC}_{50}$. All experiments were performed in triplicate and yielded similar results.

4.2.6. Western blot assays

Cells were plated on 6-well plates in their respective medium. After treatment during 4, 8, 16 and 36 h with **12**, **13** and **14** at their respective $3 \times IC_{50}$, medium was removed and the cells were lysed in Laemmli buffer (60 mM Tris–HCl (pH 6.8), 25% glycerol, 2% SDS, 14.4 mM 2-mercaptoethanol, and 0.1% bromophenol blue). The protein sample was subjected to electrophoresis, transferred onto nitrocellulose membranes (Bio-rad, 162-0115), and blocked in PBS containing 5% non-fat dry milk for 1 h at room temperature. Primary antibodies used included a polyclonal antibody to phospho-eIF2 α (Ser 51) (Invitrogen, 44-728,G), a polyclonal antibody to phospho-p53 (Ser 15) (Cell signaling, 92845), a monoclonal antibody to caspase-9 (Santa Cruz Biotechnology, Santa Cruz, CA, USA), and a monoclonal antibody to β -actin (Sigma, A2228) at 1:100 dilution. Secondary antibodies used included anti-rabbit IgG peroxidase conjugate (Sigma, A0545) and anti-mouse IgG peroxidase conjugate (Sigma, A9044). Bands were visualized using the ECL system (Amersham Pharmacia Biotech, UK).

4.2.7. Statistical analysis

The analysis of the data of the different assays was carried out by using the statistical programme Statgraphics plus for Windows v.5.1 (Statistical Graphics Corp, 2000). The statistically significant differences were considered with values of $p < 0.05$. The graphical representation of the obtained data was carried out by means of the software Microsoft Excel 2003 (Microsoft Corporation).

Acknowledgments

This study was supported by the Instituto de Salud Carlos III (Fondo de Investigación Sanitaria) through projects no. PI10/00592 and PI10/02295, and the Ministerio de Ciencia e Innovación through the project SAF-2010-18263.

Appendix. Supplementary material

Supplementary data associated with this article can be found, in the online version, at doi:10.1016/j.ejmech.2011.05.046.

References

- [1] J.A. Hickman, Apoptosis induced by anticancer drugs, *Cancer Metastasis Rev.* 11 (1992) 121–139.
- [2] S.A. Rasbridge, C.E. Gillet, A.M. Seymour, K. Patel, M.A. Richards, R. Rubens, R.R.R. Millis, The effects of chemotherapy on morphology, cellular proliferation, apoptosis and oncoprotein expression in primary breast carcinoma, *Brit. J. Cancer* 70 (1994) 335–341.
- [3] A.S. Lundberg, R.A. Weinberg, Control of the cell cycle and apoptosis, *Eur. J. Cancer* 35 (1999) 531–539.
- [4] L.F. Qin, I.O. Ng, Induction of apoptosis by cisplatin and its effect on cell cycle-related proteins and cell cycle changes in hepatoma cells, *Cancer Lett.* 175 (2002) 27–38.
- [5] S. Matsuo, S. Tanako, J. Yamashita, M. Ogawa, Synergistic cytotoxic effects of tumor necrosis factor, interferon- γ and tamoxifen on breast cancer cell lines, *Anticancer Res.* 12 (1992) 1575–1579.
- [6] A. Trouet, A. Passioukov, K.V. Derpooten, A.M. Fernández, J. Abarca-Quiñones, R. Baurain, T.J. Lobl, C. Ollila, V. Dubois, Extracellularly tumor-activated prodrugs for the selective chemotherapy of cancer: application to doxorubicin and preliminary in vitro and in vivo studies, *Cancer Res.* 61 (2001) 2843–2846.
- [7] M. Malet-Martino, P. Jolimaitre, R. Martino, The prodrugs of 5-fluorouracil, *Curr. Med. Chem.: Anti-Cancer Agents* 2 (2002) 267–310.
- [8] S. Chiara, M.T. Nobile, C. Barzacchi, O. Sanguineti, M. Vincenti, C. Di Somma, P. Meszaros, R. Rosso, Hand-foot syndrome induced by high-dose, short-term, continuous 5-fluorouracil infusion, *Eur. J. Cancer* 33 (1997) 967–969.
- [9] (a) M.C. Núñez, M. Díaz-Gavilán, A. Conejo-García, O. Cruz-López, M.A. Gallo, A. Espinosa, J.M. Campos, Design, synthesis and anticancer activity against the MCF-7 cell line of benzo-fused 1,4-dihetero seven- and six-membered tethered pyrimidines and purines, *Curr. Med. Chem.* 15 (2008) 2614–2631; (b) A. Conejo-García, M.C. Núñez, M.A. Gallo, A. Espinosa, J.M. Campos, From 5-fluorouracil acyclonucleosides to benzo-fused six- and seven-membered rings linked to pyrimidine and purine bases: the shift from differentiating anticancer agents to apoptotic inducers, *Expert Opin. Drug Discov.* 3 (2008) 1223–1235.
- [10] M. Díaz-Gavilán, A. Conejo-García, O. Cruz-López, M.C. Núñez, D. Choquesillo-Lazarte, J.M. González-Pérez, F. Rodríguez-Serrano, J.A. Marchal, A. Aránega, M.A. Gallo, A. Espinosa, J.M. Campos, Synthesis and anticancer activity of (R,S)-9-(2,3-dihydro-1,4-benzoxathiin-3-ylmethyl)-9H-purines, *ChemMedChem* 3 (2008) 127–135.
- [11] M.C. Núñez, A. Entrena, F. Rodríguez-Serrano, J.A. Marchal, A. Aránega, M.A. Gallo, A. Espinosa, J.M. Campos, Synthesis of novel 1-(2,3-dihydro-5H-4,1-benzoxathiepin-3-yl)-uracil and -thymine, and their corresponding S-oxidized derivatives, *Tetrahedron* 61 (2005) 10363–10369.
- [12] M.C. Núñez, F. Rodríguez-Serrano, J.A. Marchal, O. Caba, A. Aránega, M.A. Gallo, A. Espinosa, J.M. Campos, 6'-Chloro-7- or 9-(2,3-dihydro-5H-4,1-benzoxathiepin-3-yl)-7H- or 9H-purines and their corresponding sulfones as a new family of cytotoxic drugs, *Tetrahedron* 63 (2007) 183–190.
- [13] S. Winstein, R.E. Buckles, Role of neighboring groups in replacement reactions. I. Retention of configuration in the reaction of some dihalides and acetoxylalides with silver acetate, *J. Am. Chem. Soc.* 64 (1942) 2780–2786.
- [14] B. Capon, S.P. McManus, Neighboring Group Participation. Plenum, New York, 1976.
- [15] M. Kimatrai, O. Cruz-López, M.E. García-Rubiño, F. Morales, V. Gómez-Pérez, J.M. Campos, Neighbouring-group participation involving the oxygen atom of the O, O'- or O, N-acetal functional groups, *Curr. Org. Chem.* 14 (2010) 1461–1477.
- [16] M. Díaz-Gavilán, D. Choquesillo-Lazarte, J.M. Campos, (2,3-Dihydro-1,4-benzodioxin-2-yl)methanol, *Acta Cryst. E* E63 (6) (2007) o2940.
- [17] (a) E. Saniger, J.M. Campos, A. Entrena, J.A. Marchal, I. Suárez, A. Aránega, D. Choquesillo, J. Niclós, M.A. Gallo, A. Espinosa, Medium benzene-fused oxacycles with the 5-fluorouracil moiety: synthesis, antiproliferative activities and apoptosis induction in breast cancer cells, *Tetrahedron* 59 (2003) 5457–5467; (b) E. Saniger, J.M. Campos, A. Entrena, J.A. Marchal, H. Boulaiz, A. Aránega, M.A. Gallo, A. Espinosa, Neighbouring group participation as the key step in the reactivity of acyclic and cyclic salicyl-derived O,O-acetals with 5-fluorouracil. Antiproliferative activity, cell cycle dysregulation and apoptotic induction of new O,N-acetals against breast cancer cells, *Tetrahedron* 59 (2003) 8017–8026; (c) J.A. Marchal, M.C. Núñez, I. Suárez, M. Díaz-Gavilán, J.A. Gómez-Vidal, H. Boulaiz, F. Rodríguez-Serrano, A. Aránega, M.A. Gallo, A. Espinosa, J.M. Campos, A synthetic uracil derivative with antitumor activity through decreasing cyclin D1 and Cdk1, and increasing p21 and p27 in MCF-7 cells, *Breast Cancer Res. Treat.* 105 (2007) 237–246.
- [18] M.C. Núñez, M.G. Pavan, M. Díaz-Gavilán, F. Rodríguez-Serrano, J.A. Gómez-Vidal, J.A. Marchal, A. Aránega, M.A. Gallo, A. Espinosa, J.M. Campos, Synthesis and anticancer activity studies of novel 1-(2,3-dihydro-5H-1,4-benzodioxepin-3-yl)uracil and (6'-substituted)-7 or 9-(2,3-dihydro-5H-1,4-benzodioxepin-3-yl)-7H-or 9H-purines, *Tetrahedron* 62 (2006) 11724–11733.
- [19] E.L. Allred, S. Winstein, 6-Methoxyl participation and ion pairs in some solvolysis reactions, *J. Am. Chem. Soc.* 89 (1967) 4012–4017.
- [20] (a) E.L. Eliel, L. Clawson, D.E. Knox, Neighboring group participation by oxygen in the solvolysis of acyclic γ -alkoxy substituted *p*-toluenesulfonates, *J. Org. Chem.* 50 (1985) 2707–2711; (b) E.L. Eliel, D.E. Knox, Neighboring group participation by sulfur involving four-membered-ring intermediates (RS-4), *J. Am. Chem. Soc.* 107 (1985) 2946–2952.
- [21] M.B. Smith, J. March, March's Advanced Organic Chemistry. Reactions, Mechanisms, and Structure, Sixth Edition. John Wiley & Sons, Inc., Hoboken, New Jersey, 2007, p. 449.
- [22] I. Koppel, J. Koppel, F. Degerbeck, L. Grehn, U. Ragnarsson, Acidity of imido-dicarbonates and tosylcarbamates in dimethyl sulfoxide. Correlation with yields in the Mitsunobu reaction, *J. Org. Chem.* 56 (1991) 7172–7174.
- [23] K.C.K. Swamy, N.N.B. Kumar, E. Balaraman, K.V.P.P. Kumar, Mitsunobu and related reactions: advances and applications, *Chem. Rev.* 109 (2009) 2551–2651.
- [24] M. Hajdich, L. Havlieek, J. Vesely, R. Novotny, V. Mihal, M. Strnad, Synthetic cyclin-dependent kinase inhibitors: new generation of potent anti-cancer drugs, *Adv. Exp. Med. Biol.* 457 (1999) 341–353.
- [25] J.A. Marchal, H. Boulaiz, I. Suárez, E. Saniger, J. Campos, E. Carrillo, J. Prados, M.A. Gallo, A. Espinosa, A. Aránega, Growth inhibition, G1-arrest, and apoptosis in MCF-7 human breast cancer cells by novel highly lipophilic 5-fluorouracil derivatives, *Invest. New Drug* 22 (2004) 379–389.
- [26] M. Holcik, N. Sonenberg, Translational control in stress and apoptosis, *Nat. Rev. Mol. Cell Biol.* 6 (2005) 318–327.
- [27] J. Gil, J. Alcami, M. Esteban, Induction of apoptosis by double-stranded-RNA-dependent protein kinase (PKR) involves the alpha subunit of eukaryotic translation initiation factor 2 and NF-kappaB, *Mol. Cell Biol.* 19 (1999) 4653–4663.
- [28] Y. Dagon, S. Dovrat, S. Vilchik, D. Hacoheh, G. Shlomo, B. Sredni, S. Salzberg, U. Nir, Double-stranded RNA-dependent protein kinase, PKR, down-regulates CDC2/cyclin B1 and induces apoptosis in non-transformed but not in v-mos transformed cells, *Oncogene* 20 (2001) 8045–8056.
- [29] D.C. Altieri, Validating survivin as a cancer therapeutic target, *Nat. Rev. Cancer* 3 (2003) 46–54.
- [30] M. Villalobos, N. Olea, J.A. Brotons, M.F. Olea-Serrano, J.M. Ruiz de Almodovar, V. Pedraza, The E-Screen assay: a comparison of different MCF-7 cell stocks, *Env. Health Perspect.* 9 (1995) 844–849.

PAPER 3

Current Medicinal Chemistry (Submitted)

Enantiospecific Synthesis of Heterocycles Linked to Purines: Different Apoptosis Modulation of Enantiomers in Breast Cancer Cells

M. Eugenia García-Rubiño,¹ Ana Conejo-García,¹ María C. Núñez,¹ Esther Carrasco,²
María A. García,³ Duane Choquesillo-Lazarte,⁴ Juan M. García-Ruiz,⁴ Miguel A.
Gallo,¹ Juan A. Marchal,² Joaquín M. Campos^{1,*}

¹*Departamento de Química Farmacéutica y Orgánica, Facultad de Farmacia, c/
Campus de Cartuja, s/n, 18071 Granada (Spain)*

²*Instituto de Biopatología y Medicina Regenerativa (IBIMER), Departamento de
Anatomía y Embriología Humana, Facultad de Medicina, Avenida de Madrid s/n,
18071 Granada (Spain)*

³*Unidad de Investigación, Hospital Universitario Virgen de las Nieves, 18071 Granada
(Spain)*

⁴*Laboratorio de Estudios Cristalográficos, Instituto Andaluz de Ciencias de la Tierra
(UGR - CSIC), Avenida de las Palmeras N° 4, E-18100 Armilla, Granada (Spain)*

*Corresponding author: Tel.: +34 958 243850; fax: +34 958 243845; e-mail:
jmcampos@ugr.es

Short Running title: **Different Apoptosis Induction Caused by Enantiomers**

Abstract: Mitsunobu reaction was carried out between (*R*)- and (*S*)-3,4-dihydro-2*H*-1,5-benzoxathiepin-3-ol and purines under microwave irradiation. A contraction into a six-membered ring takes place with concomitant inversion at the stereocentre with excellent enantiomeric excesses giving rise to the homochiral 9-(2, 3-dihydro-1,4-benzoxathiin-3-ylmethyl)-9*H*-purines. Starting from both enantiomers of 2,3-dihydro-1,4-benzoxathiin-2-methanol, the 2- and 3-isomers of benzo-fused six-membered heterocycles linked to purines through a methylene group are obtained with excellent enantiospecificities. The antitumour activity of all enantiomers is reported against the MCF-7 human breast cancer. All homochiral compounds included in this study show a different apoptosis effect between the enantiomers of at least 30%. Different apoptosis percentages provided by enantiomers are scarcely reported in bibliography. An exception is D-(-)-lentiginosine, the non-natural enantiomer of an iminosugar indolizidine alkaloid, that acts as apoptosis inducer on different tumour cells in contrast to its natural enantiomer.

Key Words: Antitumour drugs, apoptosis, 1,4-benzoxathiin, breast cancer cell line MCF-7, eIF2 α , enantiospecific synthesis, neighbouring-group participation.

INTRODUCTION

Breast cancer is the most common malignancy amongst women in the United States, and the second leading cause of cancer-related death in women [1]. Standard treatments include cytotoxic non-specific chemotherapy and therapies targeted against the estrogen receptor (ER) or HER2. Despite the availability of effective ER- and HER2-targeted therapies [2,3], drug discovery efforts continue to seek additional agents that may prove to be effective in monotherapy or in combination with cytotoxic therapy or other targeted therapies. Our group reported the synthesis and biological activity against the MCF-7 cancer cell line of a series of substituted racemic 9-(2,3-dihydro-1,4-benzoxathiin-2 or 3-ylmethyl)-9*H*-purines **1-6** [4,5] [Fig. (1)].

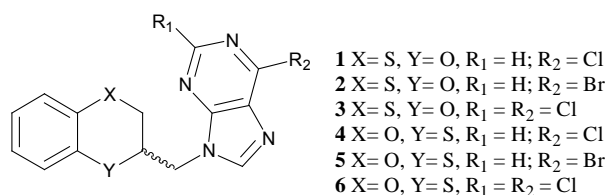


Fig. (1). Racemic compounds with antitumour activity against the breast cancer cell line MCF-7.

The issue of drug chirality is now a major theme in the design and development of new drugs, underpinned by a new understanding of the role of molecular recognition in many pharmacologically relevant events [6]. Racemic compounds **1-6** were selected because of their notable anticancer activity against the human breast cancer cell line MCF-7.

An interesting fringe benefit to studying the chemistry of the chiral glycidyl *m*-nitrobenzenesulfonyl and the chiral epichlorohydrin, was that it was possible to manipulate stereochemistry by judicious juxtaposition of the nucleophile and substrate. Nucleophilic displacement on the glycidyl *m*-nitrobenzenesulfonyl occurs by direct displacement of the carbon atom bearing the *m*-nitrobenzenesulfonyl group, the chiral centre not being affected. This is not true with epichlorohydrin, where the epoxide furnishes an alkoxide that effects a second displacement on the Cl-bearing carbon atom to re-produce again the three-membered ring, but with complete inversion of its stereochemistry. For the first time we report herein the enantiospecific synthesis of both enantiomers of **1-6** from 2-mercaptophenol and enantiomeric pure (*S*)-glycidyl *m*-nitrobenzenesulfonate **7** or (*S*)-epichlorohydrin **8** (see Schemes 1 and 2). Subsequent cyclization reaction produces the homochiral seven-membered secondary and six-membered primary alcohols, which after separation *via* flash chromatography undertakes the Mitsunobu reaction to yield the target compounds with excellent enantiomeric excesses (ee). Mitsunobu reaction normally takes place with inversion of the configuration of the substrate alcohol; nevertheless, the product of retention of configuration has been reported with a series of hindered alcohols [7]

MATERIALS AND METHODS

CHEMISTRY

Syntheses

Melting points were taken in open capillaries on an Electrothermal melting point apparatus and are uncorrected. Analytical thin layer chromatography was performed using Merck Kieselgel 60 F254 aluminum sheets, the spots being developed with UV light ($\lambda = 254$ nm). All evaporation was carried out *in vacuo* with a Büchi rotary evaporator and the pressure controlled by a Vacuubrand CVCII apparatus. For flash chromatography, Merck silica gel 60 with a particle size of 0.040-0.063 mm (230-400 mesh ASTM) was used. Nuclear magnetic resonance spectra have been carried out at the Centro de Instrumentación Científica/Universidad de Granada, and recorded on a 400MHz ^1H and 100MHz ^{13}C

NMR Varian NMR-System-TM400 or 300 MHz ^1H and 75MHz ^{13}C NMR Varian Inova-TM spectrometers at ambient temperature. Chemical shifts (δ) are quoted in parts per million (ppm) and are referenced to the residual solvent peak. Signals are designated as follows: s, singlet; d, doublet; dd, doublet of doublets; ddd, double doublet of doublets; dt, doublet of triplets; t, triplet; m, multiplet. The HMBC spectra were measured using a pulse sequence optimized for 10 Hz (inter-pulse delay for the evolution of long-range couplings: 50 ms) and a 5/3/4 gradient combination. In this way, direct responses (J couplings) were not completely removed. High-resolution Nano-Assisted Laser Desorption/Ionization (NALDI-TOF) or Electrospray Ionization (ESITOF) mass spectra were carried out on a Bruker Autoflex or a Waters LCT Premier Mass Spectrometer, respectively. Small scale microwave-assisted synthesis was carried out in an Initiator 2.0 single-mode microwave instrument producing controlled irradiation at 2.450 GHz (Biotage AB, Uppsala). Reaction time refers to hold time at 140°C, not to total irradiation time. The temperature was measured with an IR sensor outside the reaction vessel. Anhydrous THF was purchased from VWR International Eurolab. Anhydrous conditions were performed under argon. 6-Chloropurine, 6-bromopurine and 2,6-dichloropurine were purchased from Aldrich. Homochiral compounds **1-6** and intermediates (*R*)-**9**, (*R*)-**10**, (*S*)-**10**, (*R*)-**11** and (*S*)-**11** were synthesized according to our previously reported procedure [4,5], except that the (*RS*)-epichlorohydrin was changed for the (*S*)-epichlorohydrin **8** [(*S*)-**8**] and the intermediate (*S*)-**9** was synthesized from (*S*)-glycidyl-*m*-nitrobenzene sulfonate (*S*)-**7**. Analytical HPLC was carried out by using a HPLC WaterTM 2996 Photodiode Array Detector, WaterTM 600 Controller and WaterTM 600 Pump with a semipreparative column CHIRALPAK[®] IA. Optical rotations were measured for solutions in CH_2Cl_2 (1 dm tube) with a Jasco DIP-370 polarimeter.

(*R*)-3-[(2-Hydroxyphenyl)thio]-1,2-epoxypropane [(*R*)-9**]** [obtained from 2-mercaptophenol and (*S*)-**8**]: 98% yield, 99.9 ee, $[\alpha]_D^{25} = -46.6$ (c 1.0 in CH_2Cl_2); HPLC analysis: Chiralpak IA, hexane/2-propanol = 90/10, flow rate 1.0 mL/min, $\lambda = 250$ nm, t_R (*R*)-**9** = 12.436 min [Fig. (S25)].

(*R*)-3,4-Dihydro-2*H*-1,5-benzoxathiepin-3-ol [(*R*)-10**]** [obtained from (*R*)-**9**]: 45% yield, 99.9 ee, $[\alpha]_D^{25} +39.0$ (c 1.0 in CH_2Cl_2); HPLC analysis: Chiralpak IA, hexane/ CH_2Cl_2 = 65/35, flow rate 1.0 mL/min, $\lambda = 250$ nm, t_R (*R*)-**10** = 10.717 min [Fig. (S28)].

(S)-2,3-Dihydro-1,4-benzoxathiin-2-methanol [(S)-11] [obtained from (R)-9]: 20% yield, 95.84 ee, $[\alpha]_D^{25}$ -39.8 (*c* 1.0 in CH₂Cl₂); HPLC analysis: Chiralpak IA, hexane/CH₂Cl₂ = 65/35, flow rate 1.0 mL/min, λ = 250 nm, t_R (S)-11 = 14.899, t_R (R)-11 = 16.249 min [Fig. (S32)].

(S)-3-[(2-Hydroxyphenyl)thio]-1,2-epoxypropane [(S)-9] [obtained from 2-mercaptophenol and (S)-7]: NaH 60% (1.989 mmol, 80 mg) was added to a solution of 2-mercaptophenol (1.989 mmol, 0.2 mL) in anhydrous DMF (30 mL) cooled in an ice-water bath under argon atmosphere. The reaction mixture was stirred at room temperature for 30 min. A solution of (S)-glycidyl-*m*-nitrobenzene sulfonate (S)-7 (3.978 mmol, 1.025 g) in anhydrous DMF (20 mL) was added dropwise during 30 min to the above solution previously cooled to -30 °C. The reaction mixture was allowed to reach -5 °C progressively during one hour and 45 min. (10 min: -30 °C, 10 min: -25 °C, 10 min: -23 °C, 10 min: -21 °C, 20 min: -10 °C, 30 min: -7 °C, 15 min: -5 °C). The colour of the solution changed from brown-red to yellow. The pH was fixed to 4-5 with HCl (1N). The solvent was evaporated and water (30 mL) was added to the residue. The aqueous layer was extracted (CH₂Cl₂, 3 × 30 mL) and the organic phase dried (Na₂SO₄), filtered and the solvent removed under reduced pressure. The purification from the crude product by flash column chromatography on silica gel with a gradient elution (CH₂Cl₂/MeOH: 9.9:0.1 → 9:1) provided (S)-9 (294.5 mg, 96.6%) as a yellow oil. 99.9 ee, $[\alpha]_D^{25}$ = +43.5 (*c* 1.0; CH₂Cl₂); HPLC analysis: Chiralpak IA, hexane/2-propanol = 90/10, flow rate 1.0 mL/min, λ = 250 nm, retention time (t_R) (S)-9 = 11.346 min [Fig. (S26)].

(S)-3,4-Dihydro-2H-1,5-benzoxathiepin-3-ol [(S)-10] [obtained from (S)-9]: 45% yield, 95.3 ee, $[\alpha]_D^{25}$ -36.7 (*c* 1.0 in CH₂Cl₂); HPLC analysis: Chiralpak IA, hexane/CH₂Cl₂ = 65/35, flow rate 1.0 mL/min, λ = 250 nm, t_R (R)-10 = 10.896 min, t_R (S)-10 = 12.079 min [Fig. (S29)].

(R)-2,3-Dihydro-1,4-benzoxathiin-2-methanol [(R)-11] [obtained from (S)-9]: 20% yield, 98.54 ee, $[\alpha]_D^{25}$ +38.1 (*c* 1.0 in CH₂Cl₂); HPLC analysis: Chiralpak IA, hexane/CH₂Cl₂ = 65/35, flow rate 1.0 mL/min, λ = 250 nm, t_R (S)-11 = 14.682 min, t_R (R)-11 = 15.890 min [Fig. (S31)].

(S)-6-Chloro-9-(2,3-dihydro-1,4-benzoxathiin-2-ylmethyl)-9H-purine [(S)-1] [obtained from (S)-11]: 12% yield, 96.9 ee, $[\alpha]_D^{25}$ -23.2 (*c* 1.0 in CH₂Cl₂); HPLC analysis: Chiralpak IA, hexane/EtOH = 80/20, flow rate 1.0 mL/min, λ = 250 nm, t_R (R)-1 = 14.163 min, t_R (S)-1 = 18.574 min [Fig. (S3)].

(S)-6-Bromo-9-(2,3-dihydro-1,4-benzoxathiin-2-ylmethyl)-9H-purine [(S)-2] [obtained from (S)-11]: 32% yield, 92.3 ee, $[\alpha]_D^{25}$ -93.7 (*c* 1.0 in CH₂Cl₂); HPLC analysis: Chiralpak IA, hexane/EtOH = 80/20, flow rate 1.0 mL/min, λ = 250 nm, t_R (R)-2 = 18.622 min, t_R (S)-2 = 19.785 min [Fig. (S6)].

(S)-2,6-Dichloro-9-(2,3-dihydro-1,4-benzoxathiin-2-ylmethyl)-9H-purine [(S)-3] [obtained from (S)-11]: 20% yield, 97.6 ee, $[\alpha]_D^{25}$ -37.7 (*c* 1.0 in CH₂Cl₂); HPLC analysis: Chiralpak IA, hexane/2-propanol = 90/10, flow rate 1.0 mL/min, λ = 250 nm, t_R (S)-3 = 15.231 min, t_R (R)-3 = 17.392 min [Fig. (S9)].

(S)-6-Chloro-9-(2,3-dihydro-1,4-benzoxathiin-3-ylmethyl)-9H-purine [(S)-4] a) from (R)-10: 29% yield, 97.1 ee, $[\alpha]_D^{25}$ +26.9 (*c* 1.0 in CH₂Cl₂); HPLC analysis: Chiralpak IA, hexane/2-propanol = 90/10, flow rate 1.0 mL/min, λ = 250 nm, t_R (R)-4 = 19.176 min, t_R (S)-4 = 21.388 min [Fig. (S13)]; b) from (R)-11: 9% yield, 95.1 ee, $[\alpha]_D^{25}$ +26.4 (*c* 1.0 in CH₂Cl₂); HPLC analysis: Chiralpak IA, hexane/2-propanol = 90/10, flow rate 1.0 mL/min, λ = 250 nm, t_R (R)-4 = 19.167 min, t_R (S)-4 = 21.378 min [Fig. (S14)].

(S)-6-Bromo-9-(2,3-dihydro-1,4-benzoxathiin-3-ylmethyl)-9H-purine [(S)-5] a) from (R)-10: 47% yield, 90.6 ee, $[\alpha]_D^{25}$ +53.9 (*c* 1.0 in CH₂Cl₂); HPLC analysis: Chiralpak IA, hexane/2- EtOH = 90/10, flow rate 1.0 mL/min, λ = 250 nm, t_R (R)-5 = 19.018 min, t_R (S)-5 = 21.216 min [Fig. (S17)]; b) from (R)-11: 3% yield, 94.6 ee, $[\alpha]_D^{25}$ +56.4 (*c* 1.0 in CH₂Cl₂); HPLC analysis: Chiralpak IA, hexane/2-propanol = 90/10, flow rate 1.0 mL/min, λ = 250 nm, t_R (R)-5 = 19.008 min, t_R (S)-5 = 21.226 min [Fig. (S18)].

(S)-2,6-Dichloro-9-(2,3-dihydro-1,4-benzoxathiin-3-ylmethyl)-9H-purine [(S)-6] a) from (R)-10: 64% yield, 94.3 ee, $[\alpha]_D^{25}$ +64.7 (*c* 1.0 in CH₂Cl₂); HPLC analysis: Chiralpak IA, hexane/2-propanol = 90/10, flow rate 1.0 mL/min, λ = 250 nm, t_R (R)-6 = 14.353min, t_R (S)-6= 16.92 min [Fig. (S22)]; b) from (R)-11: 4% yield, 92.3 ee, $[\alpha]_D^{25}$ +63.2 (*c* 1.0 in CH₂Cl₂); HPLC analysis: Chiralpak IA, hexane/2-propanol = 90/10, flow rate 1.0 mL/min, λ = 250 nm, t_R (R)-6 = 14.355 min, t_R (S)-6= 16.922 min [Fig. (S23)].

(R)-6-Chloro-9-(2,3-dihydro-1,4-benzoxathiin-2-ylmethyl)-9H-purine [(R)-1] [obtained from (R)-11]: 34% yield, 94.1 ee, $[\alpha]_D^{25} +22.8$ (*c* 1.0 in CH₂Cl₂); HPLC analysis: Chiralpak IA, hexane/EtOH = 80/20, flow rate 1.0 mL/min, $\lambda = 250$ nm, t_R (R)-1 = 13.881 min, t_R (S)-1 = 18.751 min [Fig. (S2)].

(R)-6-Bromo-9-(2,3-dihydro-1,4-benzoxathiin-2-ylmethyl)-9H-purine [(R)-2] [obtained from (R)-11]: 54% yield, 94.3 ee, $[\alpha]_D^{25} +101.2$ (*c* 1.0 in CH₂Cl₂); HPLC analysis: Chiralpak IA, hexane/EtOH = 80/20, flow rate 1.0 mL/min, $\lambda = 250$ nm, t_R (R)-2 = 18.19 min, t_R (S)-2 = 19.804 min [Fig. (S5)].

(R)-2,6-Dichloro-9-(2,3-dihydro-1,4-benzoxathiin-2-ylmethyl)-9H-purine [(R)-3] [obtained from (R)-11]: 72% yield, 96.2 ee, $[\alpha]_D^{25} +38.2$ (*c* 1.0 in CH₂Cl₂); HPLC analysis: Chiralpak IA, hexane/2-propanol = 90/10, flow rate 1.0 mL/min, $\lambda = 250$ nm, t_R (S)-3 = 15.021 min, t_R (R)-3 = 17.032 min [Fig. (S8)].

(R)-6-Chloro-9-(2,3-dihydro-1,4-benzoxathiin-3-ylmethyl)-9H-purine [(R)-4] a) From (S)-10: 78% yield, 92.12 ee, $[\alpha]_D^{25} -24.9$ (*c* 1.0 in CH₂Cl₂); HPLC analysis: Chiralpak IA, hexane/2-propanol = 90/10, flow rate 1.0 mL/min, $\lambda = 250$ nm, t_R (R)-4 = 19.017 min, t_R (S)-14 = 21.754 min [Fig. (S11)]; b) from (S)-11: 4% yield, 91.3 ee, $[\alpha]_D^{25} -25.1$ (*c* 1.0 in CH₂Cl₂); HPLC analysis: Chiralpak IA, hexane/2-propanol = 90/10, flow rate 1.0 mL/min, $\lambda = 250$ nm, t_R (R)-4 = 19.019 min, t_R (S)-4 = 21.755 min [Fig. (S12)].

(R)-6-Bromo-9-(2,3-dihydro-1,4-benzoxathiin-3-ylmethyl)-9H-purine [(R)-5] a) from (S)-10: 53% yield, 94.4 ee, $[\alpha]_D^{25} -55.9$ (*c* 1.0 in CH₂Cl₂); HPLC analysis: Chiralpak IA, hexane/2-propanol = 90/10, flow rate 1.0 mL/min, $\lambda = 250$ nm, t_R (R)-5 = 20.075 min, t_R (S)-5 = 21.698 min [Fig. (S16)]; b) non isolated from (S)-11.

(R)-2,6-Dichloro-9-(2,3-dihydro-1,4-benzoxathiin-3-ylmethyl)-9H-purine [(R)-6] a) from (S)-10: 32% yield, 91.8 ee, $[\alpha]_D^{25} -62.5$ (*c* 1.0 in CH₂Cl₂); HPLC analysis: Chiralpak IA, hexane/2-propanol = 90/10, flow rate 1.0 mL/min, $\lambda = 250$ nm, t_R (R)-6 = 14.183 min, t_R (S)-6 = 17.006 min [Fig. (S20)]; b) from (S)-11: 2% yield, 92.2 ee, $[\alpha]_D^{25} -62.97$ (*c* 1.0 in CH₂Cl₂); HPLC analysis: Chiralpak IA, hexane/2-propanol = 90/10, flow rate 1.0 mL/min, $\lambda = 250$ nm, t_R (R)-6 = 14.184 min, t_R (S)-6 = 17.001 min [Fig. (S21)].

X-ray structure determinations.

Crystals of (*RS*)-**1**, (*RS*)-**6**, (*R*)-**6**, (*S*)-**10**, (*R*)-**11** were grown from acetone (*RS*)-**1** and CH₂Cl₂ (*RS*)-**6**, (*R*)-**6**, (*S*)-**10**, (*R*)-**11** saturated solutions under slow evaporation at room temperature. Measured crystals were prepared under inert conditions immersed in perfluoropolyether as protecting oil for manipulation. Suitable crystals were mounted on MiTeGen MicromountsTM and these samples were used for data collection. Data were collected with a Bruker X8 Proteum (*RS*)-**6**, (*R*)-**6**, (*S*)-**10**, (*R*)-**11** diffractometer whereas (*RS*)-**1** was collected at the ESRF synchrotron BM16 beamline (Grenoble, France). The data were processed with APEX2 [8]. The structures were solved by direct methods [9], which revealed the position of all non-hydrogen atoms. These atoms were refined on F² by a full-matrix least-squares procedure using anisotropic displacement parameters [9]. All hydrogen atoms were located in difference Fourier maps and included as fixed contributions riding on attached atoms with isotropic thermal displacement parameters 1.2 times those of the respective atom. In the structure of (*RS*)-**6** the 2,3-dihydro-1,4-benzoxathiin-3-ylmethyl moiety is disordered over two alternative positions in a ratio 0.68:0.32.

Crystal data for (*RS*)-**1**: data were obtained on BM16 Beamline at ESRF Synchrotron at 100 K ($\lambda=0.7378$), on a colourless block, monoclinic, space group P2₁/c, with $a = 11.0383(4)$ Å, $b = 17.4635(6)$ Å, $c = 6.9851(2)$ Å, $\beta = 90.3670(10)^\circ$, $V = 1346.47(8)$ Å³, $Z = 4$, $\rho_{\text{calcd}} = 1.573$ g/cm³, $\mu = 0.482$ mm⁻¹. 17581 reflections were measured, 2314 of which were independent. Refinement converged at final $wR_2 = 0.1149$, $R_1 = 0.0486$ and $S = 1.125$ (for 2181 reflections with $I > 2\sigma(I)$). CCDC 861612.

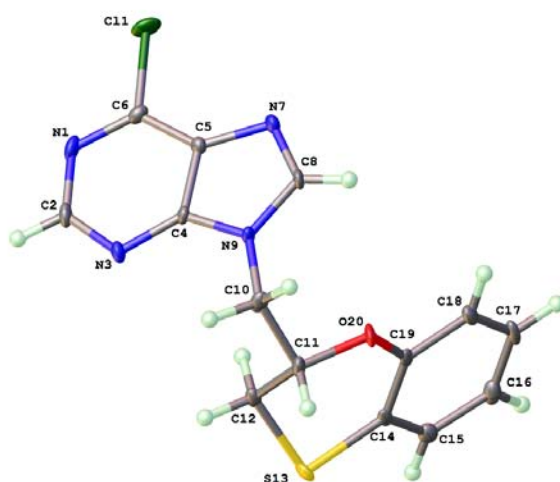


Fig. (2). The content of the asymmetric unit of (*RS*)-**1**, showing the atom-numbering schemes. Displacement ellipsoids are drawn at the 50% probability level.

Crystal data for (*RS*)-**6**: data were obtained on a Bruker X8 Proteum diffractometer at 296 K from CuK α ($\lambda=1.54178$), on a colourless block, monoclinic, space group $P2_1/n$, with $a = 10.2965(7)$ Å, $b = 13.2863(9)$ Å, $c = 11.8510(8)$ Å, $\beta = 112.725(3)^\circ$, $V = 1495.39(18)$ Å³, $Z = 4$, $\rho_{\text{calcd}} = 1.569$ g/cm³, $\mu = 5.273$ mm⁻¹. 18654 reflections were measured, 2596 of which were independent. Refinement converged at final $wR_2 = 0.1144$, $R_1 = 0.0463$ and $S = 1.077$ (for 2088 reflections with $I > 2\sigma(I)$). CCDC 861614.

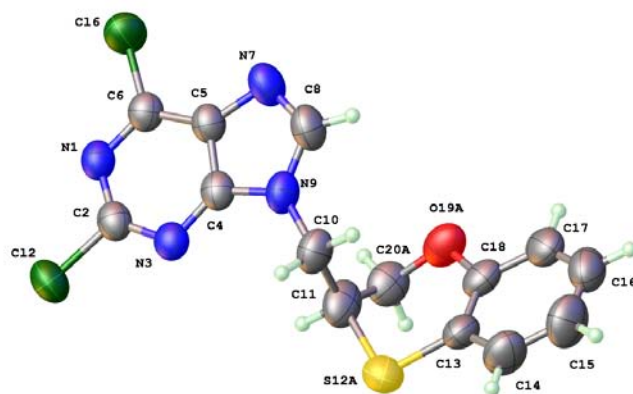


Fig. (3). The content of the asymmetric unit of (*RS*)-**6**, showing the atom-numbering schemes. Displacement ellipsoids are drawn at the 50% probability level. Only one of the disordered positions of the 2,3-dihydro-1,4-benzoxathiazin-3-ylmethyl moiety is represented.

Crystal data for (*R*)-**6**: data were obtained on a Bruker X8 Proteum diffractometer at 296 K from CuK α ($\lambda=1.54178$), on a colourless block, monoclinic, space group $P2_1$, with $a = 10.2531(7)$ Å, $b = 13.4210(9)$ Å, $c = 11.7963(8)$ Å, $\beta = 112.274(3)^\circ$, $V = 1502.13(18)$ Å³, $Z = 4$, $\rho_{\text{calcd}} = 1.562$ g/cm³, $\mu = 5.249$ mm⁻¹. 5188 reflections were measured, 5188 of which were independent. Refinement converged at final $wR_2 = 0.1391$, $R_1 = 0.0531$ and $S = 1.137$ (for 3836 reflections with $I > 2\sigma(I)$). CCDC 863309.

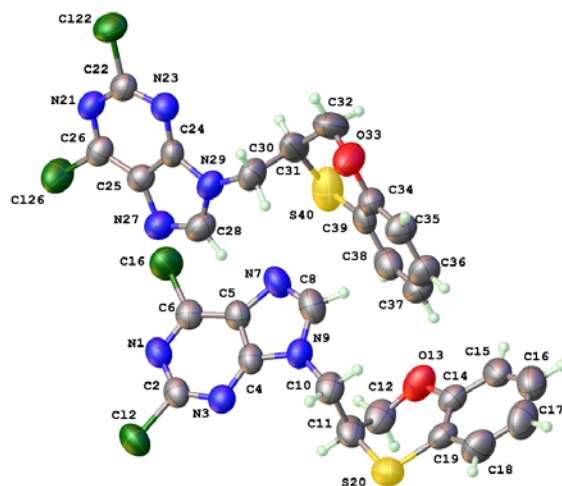


Fig. (4). The content of the asymmetric unit of (*R*)-**6**, showing the atom-numbering schemes. Displacement ellipsoids are drawn at the 50% probability level.

Crystal data for (*S*)-**10**: data were obtained on a Bruker X8 Proteum diffractometer at 296 K from CuK α ($\lambda=1.54178$), on a colourless block, monoclinic, space group $P2_1$, with $a = 12.494(6)$ Å, $b = 12.259(6)$ Å, $c = 12.615(6)$ Å, $\beta = 117.595(10)^\circ$, $V = 1712.5(14)$ Å 3 , $Z = 8$, $\rho_{\text{calcd}} = 1.414$ g/cm 3 , $\mu = 2.987$ mm $^{-1}$. 13043 reflections were measured, 5306 of which were independent. Refinement converged at final $wR_2 = 0.2060$, $R_1 = 0.0780$ and $S = 1.074$ (for 4696 reflections with $I > 2\sigma(I)$). CCDC 861615.

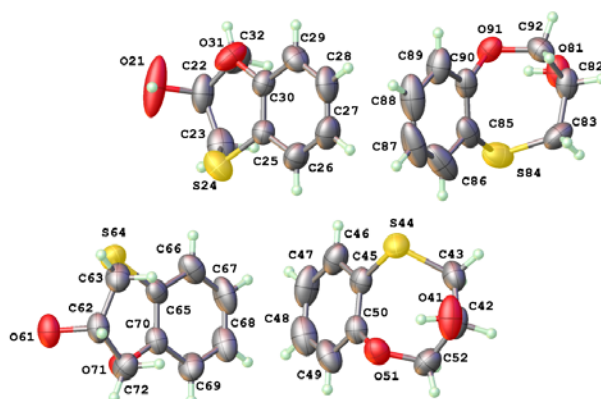


Fig. (5). The content of the asymmetric unit of (*S*)-**10**, showing the atom-numbering schemes. Displacement ellipsoids are drawn at the 50% probability level.

Crystal data for (*R*)-**11**: data were obtained on a Bruker X8 Proteum diffractometer at 296 K from CuK α ($\lambda=1.54178$), on a colourless block, tetragonal, space group P4₁, with $a = 10.3122(7)$ Å, $b = 10.3122(7)$ Å, $c = 8.3332(6)$ Å, $V = 886.16(11)$ Å³, $Z = 4$, $\rho_{\text{calcd}} = 1.366$ g/cm³, $\mu = 2.886$ mm⁻¹. 11543 reflections were measured, 1519 of which were independent. Refinement converged at final $wR_2 = 0.1304$, $R_1 = 0.0483$ and $S = 1.111$ (for 1510 reflections with $I > 2\sigma(I)$). CCDC 861613.

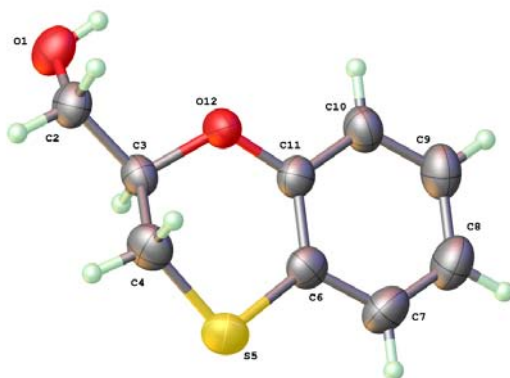


Fig. (6). The content of the asymmetric unit of (*R*)-**11**, showing the atom-numbering schemes. Displacement ellipsoids are drawn at the 50% probability level.

BIOLOGY

Cell culture

MCF-7 cells were grown at 37 °C in an atmosphere containing 5% CO₂, with Dubelcco's modified Eagle Medium (DMEM) (Gibco, Grand Island, NY, USA) supplemented with 10% heat-inactivated fetal bovine serum (FBS) (Gibco), 2% L-glutamine, 2.7% sodium bicarbonate, 1% HEPES buffer, 40 mg/L gentamicin and 500 mg/L ampicillin.

Drugs and drug treatments

Compounds **1-6** were dissolved in DMSO and stored at -20 °C. For each experiment, the stock solutions were further diluted in medium to obtain the desired concentrations. The final solvent concentration in cell culture was $\leq 0.1\%$ v/v of DMSO, a concentration without effect on cell replication. Parallel cultures of cells in medium with DMSO were used as controls.

Cytotoxicity assays *in vitro*

The effect of anticancer drugs on cell viability was assessed using the sulforhodamine-B colorimetric assay [10]. Aliquots of MCF-7 cells suspension (1×10^3 cells/well) were seeded onto 24-well plates and incubated for 24 h. The cells were then treated with different concentrations of drugs in the culture medium. Three days later, the wells were aspirated, fresh medium and treatment were added, and cells were maintained for 3 additional days. Thereafter, cells were processed as described previously [10] using a Titertek Multiscan apparatus (Flow, Irvine, CA, USA) at 492 nm. We evaluated the linearity of the SRB assay with a cell number for each cell line before each cell growth experiment. The IC_{50} values were calculated from semilogarithmic dose-response curves by linear interpolation. All of the experiments were plated in triplicate wells and were carried out at least twice.

Cell cycle distribution analysis

The cells at 70% confluence were treated with either DMSO alone or with concentrations of compounds **1-6** determined by their IC_{50} values. FACS analysis was performed after 48 h of treatment [11]. All experiments were performed in triplicate and yielded similar results.

Apoptosis detection by staining with annexin V-FITC and propidium iodide

The annexin V-FITC apoptosis detection kit I (Pharmlingen, San Diego, CA, USA) was used to detect apoptosis by flow cytometry [11]. Apoptosis induction in the MCF-7 human breast cancer cell line after treatment for 48 h was determined for compounds **1-6** at doses of their corresponding IC_{50} and $3 \times IC_{50}$. All experiments were performed in triplicate and yielded similar results.

Western blot assays

Cells were plated on 6-well plates in their respective medium. After treatment during 4, 8, 16 and 36 h with (*RS*)-**3**, (*R*)-**3**, (*S*)-**3**, (*S*)-**1**, (*R*)-**4**, (*S*)-**5** and (*S*)-**6** at their respective IC_{50} medium was removed and the cells were lysed in Laemmli buffer [60 mM TrisHCl (pH 6.8), 25% glycerol, 2% SDS, 14.4 mM 2-mercaptoethanol and 0.1% bromophenol blue]. The protein sample was subjected to electrophoresis, transferred onto nitrocellulose membranes (Bio-rad, 162-0115) and blocked in PBS containing 5% non-fat dry milk for 1 h at room temperature. Primary antibodies used included a polyclonal antibody to phospho-eIF2 α (Ser 51) (Invitrogen, 44-728,G), a polyclonal antibody to phospho-p53 (Ser 15) (Cell signaling,

92845), a monoclonal antibody to caspase-9 (Santa Cruz Biotechnology, Santa Cruz, CA, USA) and a monoclonal antibody to β -actin (Sigma, A2228) at 1:100 dilution. Secondary antibodies used included anti-rabbit IgG peroxidase conjugate (Sigma, A0545) and anti-mouse IgG peroxidase conjugate (Sigma, A9044). Bands were visualized using the ECL system (Amersham Pharmacia Biotech, UK).

Statistical analysis

The analysis of the data of the different assays was carried out by using the statistical programme Statgraphics plus for Windows v.5.1 (Statistical Graphics Corp, 2000). The statistically significant differences were considered with values of $p < 0.05$. The graphical representation of the obtained data was carried out by means of the software Microsoft Excel 2003 (Microsoft Corporation).

Caspases activity assay.

Caspase-2, -3 and -8 activity of treated cells was determined using an ApoAlert caspase assay plates (Clontech, CA, USA) containing fluorogenic substrates specific for the different caspases. The lysate of 2×10^5 cells were processed following the manufacturer's instructions. Fluorometric detection of caspase activities was read with a 380-nm excitation and 460-nm emission filters.

RESULTS AND DISCUSSION

The intrinsically chiral and non-racemic nature of the living world often results in its different interactions with the enantiomers of a given substance. If this substance is a drug, it might well be that only one of the two isomers is capable of exerting the desired therapeutic effect. The other may be inert, harmful or responsible for possibly undesirable side effects.

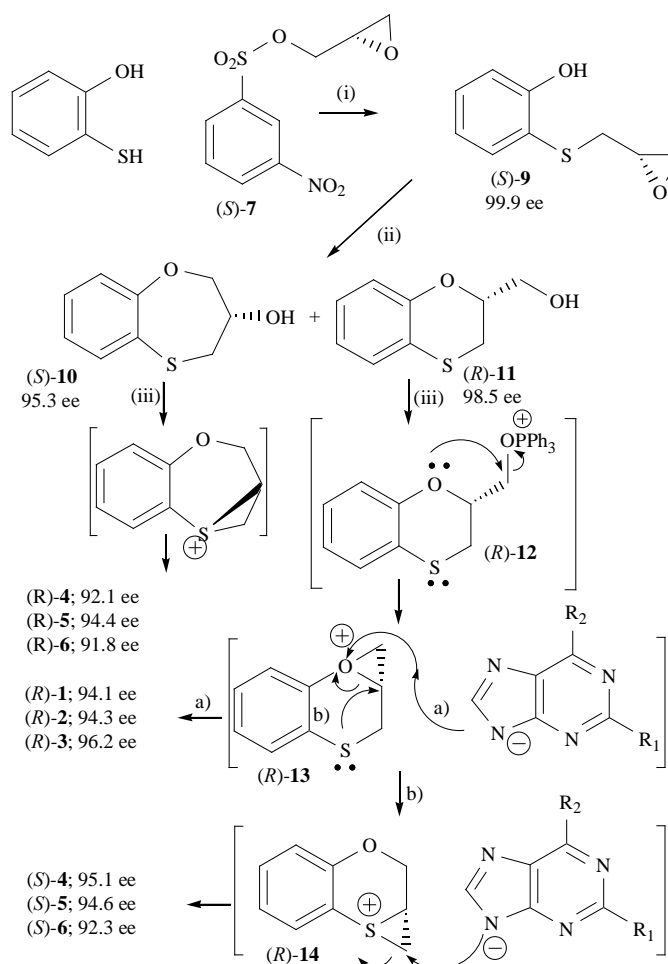
Three-carbon (C-3) epoxides bearing halide substituents are highly versatile synthetic building blocks because each carbon is functionalized and is a potential site of nucleophilic attack. Sharpless *et al.* described the preparation of a series of crystalline arenesulfonate derivatives of enantiomerically enriched glycidol and their application to the synthesis of homochiral α -adrenergic blocking agents [12]. Epichlorohydrin a readily available C-3 unit is widely employed in organic and polymer synthesis [13]. We thus decided to compare both (*S*)-glycidyl sulfonate (*S*)-**7** and (*S*)-epichlorohydrin (*S*)-**8** as reagents for the preparation of the enantiomeric compounds **1-6** (Schemes 1 and 2).

As expected, the attack by the (*S*)-glycidyl sulfonate (*S*)-**7** takes place with retention of configuration

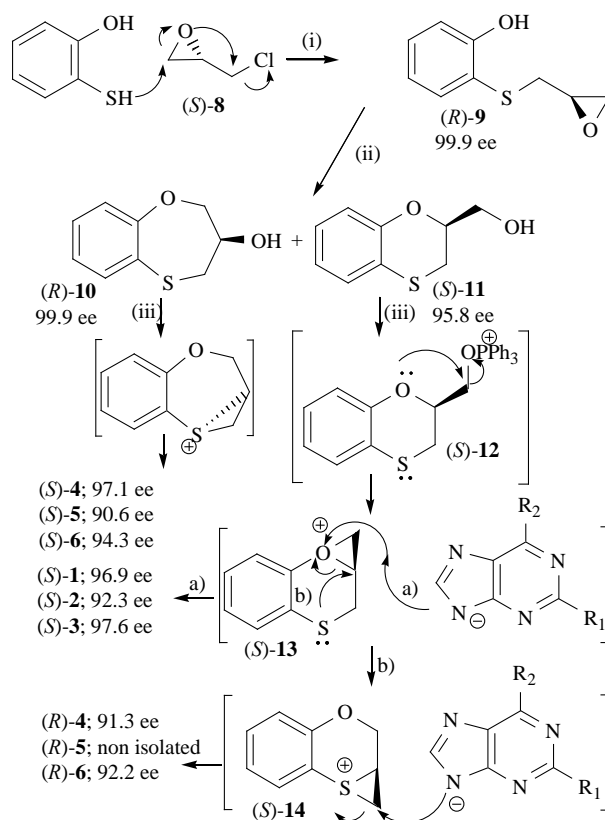
giving a single enantiomer of the epoxide (*S*)-**9** (Scheme 1). Interestingly, when (*S*)-epichlorohydrin (*S*)-**8** is used instead of (*S*)-**7** the inverted homochiral epoxide (*R*)-**9** is obtained with complete inversion of its configuration (Scheme 2). The preparation of the homochiral derivative **9** from (*S*)-epichlorohydrin **8** is easier than the one starting from (*S*)-glycidyl sulfonate (*S*)-**7**.

The cyclization step from both (*S*)-**9** and (*R*)-**9** occurs with configuration retention to produce the seven-membered derivative (*S*)- and (*R*)-**10** and the opposite configuration of the six membered ring (*R*)- and (*S*)-**11**. The absolute configuration of (*S*)-**10**, (*R*)-**10**, (*S*)-**11** and (*R*)-**11** has been determined by the X-ray crystal structure of (*S*)-**10** and (*R*)-**11** and by HPLC analysis of the four intermediates.

It must be pointed out that when starting from (*R*)- and (*S*)-**11**, apart from the target compounds (*R*)- and (*S*)-**1-3**, their corresponding regioisomers (*S*) and (*R*)-**4-6** with the opposite configuration is also obtained as side-products through a neighbouring-group mechanism (Scheme 1 and 2).



Scheme 1. Reagents and conditions: (i) NaH, DMF, from -30 °C to -5 °C, 95 min; (ii) NaOH, H₂O, 95 °C, 6 h; (iii) substituted purines, Ph₃P, DIAD, anhydrous THF, microwave irradiation, 140 °C, 5 min.



Scheme 2. Reagents and conditions: (i) Pyr, H₂O, rt, 24 h, (ii) NaOH, H₂O, 95 °C, 6h; (iii) substituted purines, Ph₃P, DIAD, anhydrous THF, microwave irradiation, 140 °C, 5 min.

Compounds (*R*)-**1-6** and (*S*)-**1-6** have been subjected to antiproliferative, apoptosis (Table 1) and cell cycle studies on the MCF-7 human breast cancer cell line.

Table 1. Antiproliferative effect and apoptosis induction for the target compounds **1-6**.

Comp.	IC ₅₀ (μM) ^a	Total apoptosis	Comp.	IC ₅₀ (μM) ^a	Total apoptosis
(<i>RS</i>)- 1 ⁵	9.24 ± 0.01	67.35 ± 0.90 ^b 10.3 ± 0.14 ^c	(<i>RS</i>)- 4 ⁴	10.6 ± 0.66	73.8 ± 0.42 ^b 22.55 ± 0.07 ^c
(<i>R</i>)- 1	4.73 ± 0.02	42.95 ± 0.63 ^b 9.7 ± 0.42 ^c	(<i>R</i>)- 4	15.2 ± 0.03	71.95 ± 0.21 ^b 20.25 ± 0.21 ^c
(<i>S</i>)- 1	11.4 ± 0.06	89.5 ± 0.70 ^b 19.05 ± 0.63 ^c	(<i>S</i>)- 4	3.30 ± 0.02	31.55 ± 1.40 ^b 13.95 ± 0.6 ^c
(<i>RS</i>)- 2 ⁵	4.87 ± 0.02	99.45 ± 0.07 ^b 38.45 ± 4.73 ^c	(<i>RS</i>)- 5 ⁴	6.18 ± 1.70	63.45 ± 1.50 ^b 30.6 ± 6.78 ^c

(<i>R</i>)- 2	4.45 ± 0.07	63.75 ± 6.0 ^b 15.95 ± 2.33 ^c	(<i>R</i>)- 5	6.17 ± 0.07	55.75 ± 12 ^b 26.55 ± 0.2 ^c
(<i>S</i>)- 2	3.33 ± 0.13	50.2 ± 1.13 ^b 25.15 ± 0.49 ^c	(<i>S</i>)- 5	6.32 ± 0.04	60.5 ± 9.0 ^b 41.8 ± 0.56 ^c
(<i>RS</i>)- 3 ⁵	2.75 ± 0.03	97.7 ± 0.56 ^b 29.35 ± 0.30 ^c	(<i>RS</i>)- 6 ⁴	8.97 ± 0.83	51.35 ± 0.21 ^b 15.75 ± 0.49 ^c
(<i>R</i>)- 3	3.33 ± 0.04	99.1 ± 0.65 ^b 76.95 ± 2.80 ^c	(<i>R</i>)- 6	10.3 ± 0.01	27.35 ± 0.07 ^b 6.25 ± 3.30 ^c
(<i>S</i>)- 3	1.85 ± 0.05	89.4 ± 1.50 ^b 33.15 ± 0.20 ^c	(<i>S</i>)- 6	6.93 ± 0.09	58.75 ± 2.75 ^b 60.35 ± 2.40 ^c

^aAll experiments were conducted in duplicate and gave similar results. The data are means ± SEM of three independent determinations. IC₅₀ was determined after 6 days of treatment. ^bCells were treated with the 3 × IC₅₀ values of compounds. ^cCells were treated with the IC₅₀ values of compounds. Apoptosis was detected after 48 h of treatment.

Compounds **1-4** and **6** show one major bioactive enantiomer against the MCF-7 human breast cancer whereas compound **5** has presented equally bioactive enantiomers. In all cases, the IC₅₀ values of the racemates (*RS*)-**1-6** are similar to the average IC₅₀ of the corresponding enantiomers (*R*)-**1-6** and (*S*)-**1-6**. Structure-activity relationship between the configuration of the enantiomers and the antiproliferative effect indicates that, in general, (*S*)-enantiomers are more active. Thus, (*S*)-**2**, (*S*)-**3**, (*S*)-**4** and (*S*)-**6** are more potent than their corresponding racemates while (*R*)-**1** is more active than (*RS*)-**1**.

Racemic and homochiral compounds **1**, **2** and **3**, with the purine moiety at position 2, are more active than their corresponding regioisomers **4**, **5** and **6**, with the purine moiety at position 3, except for (*S*)-**1**. The most active compound (*S*)-**3**, with 2,6-dichloropurine moiety at position 2, shows an IC₅₀ = 1.85 ± 0.05 μM being 2.5- fold times more potent than the clinically used drug 5-FU (IC₅₀ = 4.32 ± 0.02 μM) [14].

The cell cycle does not show significant differences among the compounds (data not shown). However, since the eukaryotic initiation factor 2 alpha (eIF2α) kinase is critical for mRNA translation, cell proliferation, and apoptosis [15], the protein activation of this factor has been analysed by western

blot. eIF2 α is significantly phosphorylated in MCF-7 cancer cells after treatment with (S)-3, (S)-5 and (R)-4 at 16 h and 36 h (Fig.7A).

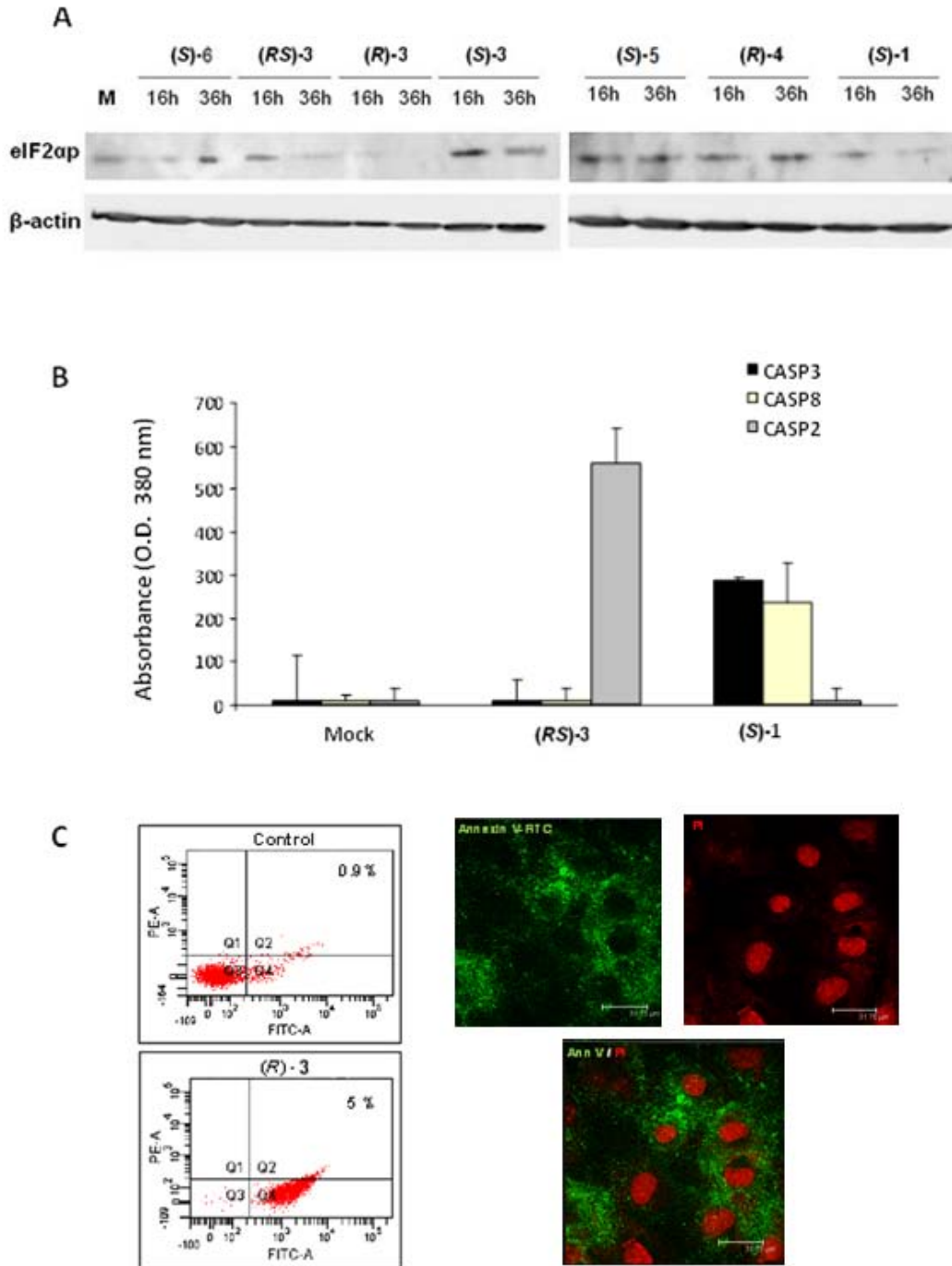


Fig. (7). Effects on the eIF2 α transcription factor and apoptotic activity in the MCF-7 human breast cancer cell line. (A) Modification of the expression of eIF2 α kinase analysed by western blot. (B) Fluorometric detection for caspase-3, caspase-2 and caspase-8. (C) Cytometry analysis and confocal microscopy for control cells treated with 0.5% DMSO and (R)-3.

Interestingly, (*S*)-**3** induces high eIF2 α phosphorylation in comparison with its racemate and its enantiomer, where no activation is shown (Figure 7A). These results support the highest antiproliferative activity displayed by (*S*)-**3** and suggest that no modifications in the cell cycle are due to the suppression of protein synthesis provoked by eIF2 α [16]. Furthermore, a prolonged induction of eIF2 α finally triggers the apoptosis phenomena [17,18].

Paclitaxel is the most important apoptotic anticancer agent for the treatment of breast cancer [19,20]. Homochiral compounds (*R*)-**3** and (*S*)-**6** are more potent as apoptosis inducers (77% and 60% at their IC₅₀, respectively) against the MCF-7 human breast cancer cells than paclitaxel which induces programmed cell death of up to 43% of the cell population [21].

Different apoptosis percentages provided by enantiomers are scarcely reported in bibliography. An exception is D-($-$)-lentiginosine, the nonnatural enantiomer of the iminosugar indolizidine alkaloid, that acts as an apoptosis inducer on different tumour cells in contrast to its natural enantiomer [22]. All homochiral compounds included in this study show a different apoptosis effect between the two enantiomers of at least 30%.

Apoptotic defects in cancer cells are the primary obstacle that limit the therapeutic efficacy of anticancer agents, and hence the development of novel agents targeting novel canonical and non-canonical programmed cell death pathways has become an imperative mission for clinical research [23]. Compounds **1-6** induce strong levels of cell death measured by cytotoxicity analysis and by phosphatidylserine externalization (Annexin V binding) (Table 1 and Figure 7C) even in the MCF- 7 breast cancer cells that have shown deficiency in the caspase-activation mechanisms [24]. Whereas compound (*S*)-**1** activates the canonical intrinsic caspase-8/caspase-3 apoptotic pathway, compound (*RS*)-**3** induces caspase-2 activation (Figure 7B). However, a strong apoptosis induction is also detected in the rest of the compounds analysed. The caspase-independent apoptosis in cells exposed to different drugs with diverse cellular effects has been previously described [23]. While caspase-2 activation could induce cell death through cytochrome *c*/mitochondria damage [25], noncaspase-mediated increase in phosphatidylserine externalization can occur in response to high intracellular Ca²⁺ levels, which alters scramblase and translocase [26,27]. Additionally, noncaspase proteases may activate and cleave the cytoskeleton proteins attached to phospholipids, including focal adhesion kinase and the actin-capping protein α -adducin [28]. These and other antitumour effects such as autophagy or senescence events could be involved in the caspase-dependent and caspase-independent cell death induced by the compounds

included in this study. This fact opens an important line of research that is yet to be explored.

CONCLUSION

In summary, we have reported here an efficient enantiospecific synthesis of 9-(2,3-dihydro-1,4-benzoxathiin-2 and 3-ylmethyl)-9*H*-purine derivatives and antitumour activity against the human breast cancer cell line MCF-7. The enantiomers of all the compounds included in this study show an important different apoptosis effect and may serve as prototypes for the development of more potent structures endowed with a so far unknown apoptotic mechanism of action. At present we are studying several targets in order to solve the mechanism of action at the molecular level of such benzannelated six-membered derivatives.

CONFLICTS OF INTEREST NOTIFICATION

There are no potential conflicts of interest to report

ACKNOWLEDGMENT

This study was supported by the Instituto de Salud Carlos III (Fondo de Investigación Sanitaria) through projects no. PI10/00592 and PI10/02295. The M.E. G.-R. FPU grant AP2007-02954 from the Ministerio de Ciencia e Innovación of Spain is greatly acknowledged. The project "Factoría de Cristalización" Consolider Ingenio-2010 (CSD2006-00015) provided X-ray structural facilities for this work.

SUPPORTIVE/SUPPLEMENTARY MATERIAL

Supplementary material is available on the publishers Web site along with the published article: Chromatograms of racemates and enantiomers of **1-6** and **9-11** are provided.

REFERENCES

- [1] Jemal, A.; Siegel, R.; Xu, J.; Ward, E. Cancer Statistics, 2010. *CA Cancer J. Clin.*, **2010**, *60*(5), 277-300.
- [2] Slamon, D.J.; Leyland-Jones, B.; Shak, S.; Fuchs, H.; Paton, V.; Bajamonde, A.; Fleming, T.; Eiermann, W.; Wolter, J.; Pegram, M.; Baselga J.; Norton, L. Use of chemotherapy plus a monoclonal antibody against HER2 for metastatic breast cancer that overexpresses HER2. *New Engl. J. Med.*, **2001**, *344*(11), 783-792.
- [3] Miller, K.; Wang, M.; Gralow, J.; Dickler, M.; Cobleigh, M.; Pérez, E.A.; Shenkier, T.; Cella, D.; Davidson, N.E. Paclitaxel plus bevacizumab versus paclitaxel alone for metastatic breast cancer. *New Engl. J. Med.*, **2007**, *357*(26), 2666-2676.
- [4] Díaz-Gavilán, M.; Conejo-García, A.; Cruz-López, O.; Núñez, M.C.; Choquesillo-Lazarte, D.; González-Pérez, J.M.; Rodríguez-Serrano, F.; Marchal, J.A.; Aránega, A.; Gallo, M.A.; Espinosa, A.; Campos, J.M. Synthesis and anticancer activity of (*R,S*)-9-(2,3-dihydro-1,4-benzoxathiin-3-ylmethyl)-9*H*-purines. *ChemMedChem*, **2008**, *3*(1), 127-135.
- [5] Conejo-García, A.; García-Rubiño, M.E.; Marchal, J.A.; Núñez, M.C.; Ramírez, A.; Cimino, S.; García, M.A.; Aránega, A.; Gallo, M. A.; Campos, J. M. Synthesis and anticancer activity of (*RS*)-9-(2,3-dihydro-1,4-benzoxaheteroin-2-ylmethyl)-9*H*-purines. *Eur. J. Med. Chem.*, **2011**, *46*(9), 3795-3801.
- [6] Núñez, M.C.; García-Rubiño, M.E.; Conejo-García, A.; Cruz-López, O.; Kimatrai, M.; Gallo, M.A.; Espinosa, A.; Campos, J.M. Homochiral drugs: a demanding tendency of the pharmaceutical industry. *Curr. Med. Chem.*, **2009**, *16*(16), 2064-2074.
- [7] (a) Hughes, A.B.; Sleebs, M.M. Total Synthesis of Bassiatin and Its Stereoisomers: Novel Divergent Behavior of Substrates in Mitsunobu Cyclizations. *J. Org. Chem.*, **2005**, *70*(8), 3079-3088; (b) Dinsmore, C.J.; Mercer, S.P. Carboxylation and Mitsunobu reaction of amines to give carbamates: Retention vs inversion of configuration is substituent-dependent. *Org. Lett.*, **2004**, *6*(17), 2885-2888; (c) Ahn, C.; DeShong, P. An Approach to the Stereoselective Synthesis of syn- and anti-1,3-Diol Derivatives. Retention of Configuration in the Mitsunobu Reaction. *J. Org. Chem.*, **2002**, *67*(6), 1754-1759.
- [8] Bruker, APEX2 Software, Bruker AXS Inc.V2009, Madison, Wilconsin, USA **2009**.
- [9] Sheldrick, G.M. A short history of SHELX. *ActaCryst.* **2008**, *A64*(1), 112-122.

- [10] Villalobos, M.; Olea, N.; Brotons, J.A.; Olea-Serrano, M.F.; Ruiz de Almodóvar, J.M.; Pedraza, V. The E-Screen assay: a comparison of different MCF-7 cell stocks. *Env. Health Perspect.*, **1995**, *103*(9), 844-850.
- [11] Marchal, J.A.; Boulaiz, H.; Suárez, I.; Saniger, E.; Campos, J.; Carrillo, E.; Prados, J.; Gallo, M.A.; Espinosa, A.; Aránega, A. Growth inhibition, G1-arrest, and apoptosis in MCF-7 human breast cancer cells by novel highly lipophilic 5- fluorouracil derivatives, *Invest. New Drug*, **2004**, *22*(4), 379-389.
- [12] Klunder, J.M.; Onami, T.; Sharpless, K.B. Arenesulfonate derivatives of homochiral glycidol: versatile chiral building blocks for organic synthesis. *J. Org. Chem.*, **1989**, *54*(6), 1295-1304.
- [13] *Encyclopedia of Reagents for Organic Synthesis*; L.A. Paquette, Ed.; Wiley: New York, **1995**; Vol. 4, pp. 2326.
- [14] Nuñez, M.C.; Rodríguez-Serrano, F.; Marchal, J.A.; Caba, O.; Aránega, A.; Gallo, M.A.; Espinosa, A.; Campos, J.M. 6'-Chloro-7- or 9-(2,3-dihydro-5H-4,1-benzoxathiepin-3-yl)-7H- or 9H-purines and their corresponding sulfones as a new family of cytotoxic drugs. *Tetrahedron*, **2007**, *63*(1), 183-190.
- [15] Baltzis, D.; Pluquet, O.; Papadakis, A.I.; Kazemi, S.; Qu, L.-K.; Koromilas, A.E. The eIF2 α Kinases PERK and PKR Activate Glycogen Synthase Kinase 3 to Promote the Proteasomal Degradation of p53. *J. Biol. Chem.*, **2007**, *282*(43), 31675-31687.
- [16] Holcik, M.; Sonenberg, N. Translational control in stress and apoptosis. *Nat. Rev. Mol. Cell Biol.*, **2005**, *6*(4), 318-327.
- [17] Gil, J.; Alcamí, J.; Esteban, M. Induction of apoptosis by double-stranded-RNA-dependent protein kinase (PKR) involves the α subunit of eukaryotic translation initiation factor 2 and NF- κ B. *Mol. Cell Biol.*, **1999**, *19*(7), 4653-4663.
- [18] Dagon, Y.; Dovrat, S.; Vilchik, S.; Hacoheh, D.; Shlomo, G.; Sredni, B.; Salzberg, S.; Nir, U. Double-stranded RNA-dependent protein kinase, PKR, down-regulates CDC2/cyclin B1 and induces apoptosis in non-transformed but not in v-mos transformed cells. *Oncogene*, **2001**, *20*(56), 8045-8056.
- [19] Horwitz, S.B.; Cohen, D.; Rao, S.; Ringel, I.; Shen, H.J.; Yang, C.P. Taxol: mechanisms of action and resistance. *J. Natl. Cancer Inst. Monogr.*, **1993**, *15*, 55-61.
- [20] Sangrajrang, S.; Fellous, A. Taxol resistance. *Chemotherapy*, **2000**, *46*(5), 327-334.
- [21] Saunders, D. E.; Lawrence, W.D.; Christensen, C.; Wappler, N.L.; Ruan, H.; Deppe, G. Paclitaxel-induced apoptosis in MCF-7 breast-cancer cells. *Int. J. Cancer*, **1997**, *70*(2), 214-220.

- [22] Macchi, B.; Minutolo, A.; Grelli, S.; Cardona, F.; Cordero, F.M.; Mastino, A.; Brandi, A. The novel proapoptotic activity of nonnatural enantiomer of Lentiginosine. *Glycobiology*, **2010**, *20*(5), 500-506.
- [23] Cummings, B.S.; Kinsey, G.R.; Bolchoz, L.J.; Schnellmann, R.G. Identification of caspase-independent apoptosis in epithelial and cancer cells. *J. Pharmacol. Exp. Ther.*, **2004**, *310*(1), 126-134.
- [24] Kagawa, S.; Gu, J.; Honda, T.; McDonnell, T.J.; Swisher, S.G.; Roth, J. A.; Fang, B. Deficiency of caspase-3 in MCF7 cells blocks Bax-mediated nuclear fragmentation but not cell death. *Clin. Cancer Res.*, **2001**, *7*(5), 1474-1480.
- [25] Robertson, J.D.; Enoksson, M.; Suomela, M.; Zhivotovsky, B.; Orrenius, S. Caspase-2 acts upstream of mitochondria to promote cytochrome c release during etoposide-induced apoptosis. *J. Biol. Chem.*, **2002**, *277*(33), 29803-29809.
- [26] Vanags, D.M.; Poern-Ares, M.I.; Coppola, S.; Burgess, D.H.; Orrenius, S. Protease involvement in fodrin cleavage and phosphatidylserine exposure in apoptosis. *J. Biol. Chem.*, **1996**, *271*(49), 31075-31085.
- [27] Kagan, V.E.; Fabisiak, J.P.; Shvedova, A.A.; Tyurina, Y.Y.; Tyurin, V.A.; Schor, N.F.; Kawai, K. Oxidative signaling pathway for externalization of plasma membrane phosphatidylserine during apoptosis. *FEBS Lett.*, **2000**, *477*(1,2), 1-7.
- [28] van de Water, B.; Nagelkerke, J.F.; Stevens, J.L. Dephosphorylation of focal adhesion kinase (FAK) and loss of focal contacts precede caspase-mediated cleavage of FAK during apoptosis in renal epithelial cells. *J. Biol. Chem.*, **1999**, *274*(19), 13328-13337.

Supplementary Material

Current Medicinal Chemistry

Enantiospecific Synthesis of Heterocycles Linked to Purines: Different Apoptosis Modulation of Enantiomers in Breast Cancer Cells

M. Eugenia García-Rubiño,¹ Ana Conejo-García,¹ María C. Núñez,¹ Esther Carrasco,²
María A. García,³ Duane Choquesillo-Lazarte,⁴ Juan M. García-Ruiz,⁴ Miguel A.
Gallo,¹ Juan A. Marchal,² Joaquín M. Campos^{1*}

¹*Departamento de Química Farmacéutica y Orgánica, Facultad de Farmacia, c/ Campus de Cartuja, s/n, 18071
Granada (Spain)*

²*Instituto de Biopatología y Medicina Regenerativa (IBIMER), Departamento de Anatomía y Embriología Humana,
Facultad de Medicina, Avenida de Madrid s/n, 18071 Granada (Spain)*

³*Unidad de Investigación, Hospital Universitario Virgen de las Nieves, 18071 Granada (Spain)*

⁴*Laboratorio de Estudios Cristalográficos, Instituto Andaluz de Ciencias de la Tierra (UGR - CSIC), Avenida de las
Palmeras N° 4, E-18100 Armilla, Granada (Spain)*

INDEX: HPLC Chromatograms

Figure S1: (RS)-1	3
Figure S2: (R)-1	4
Figure S3: (S)-1	5
Figure S4: (RS)-2	6
Figure S5: (R)-2	7
Figure S6: (S)-2	8
Figure S7: (RS)-3	9
Figure S8: (R)-3	10
Figure S9: (S)-3	11
Figure S10: (RS)-4	12
Figure S11: (R)-4	13
Figure S12: (R)-4	14
Figure S13: (S)-4	15
Figure S14: (S)-4	16
Figure S15: (RS)-5	17
Figure S16: (R)-5	18
Figure S17: (S)-5	19
Figure S18: (S)-5	20
Figure S19: (RS)-6	21
Figure S20: (R)-6	22
Figure S21: (R)-6	23
Figure S22: (S)-6	24
Figure S23: (S)-6	25
Figure S24: (RS)-9	26
Figure S25: (R)-9	27
Figure S26: (S)-9	28
Figure S27: (RS)-10	29
Figure S28: (R)-10	30
Figure S29: (S)-10	31
Figure S30: (RS)-11	32
Figure S31: (R)-11	33
Figure S32 : (S)-11	34

CHIRALPAK IA 250 x 4.6 mm
Flow rate: 1ml/min
room temperature
PDA 250.0 nm
n-hexane/Ethanol 80/20 v/v

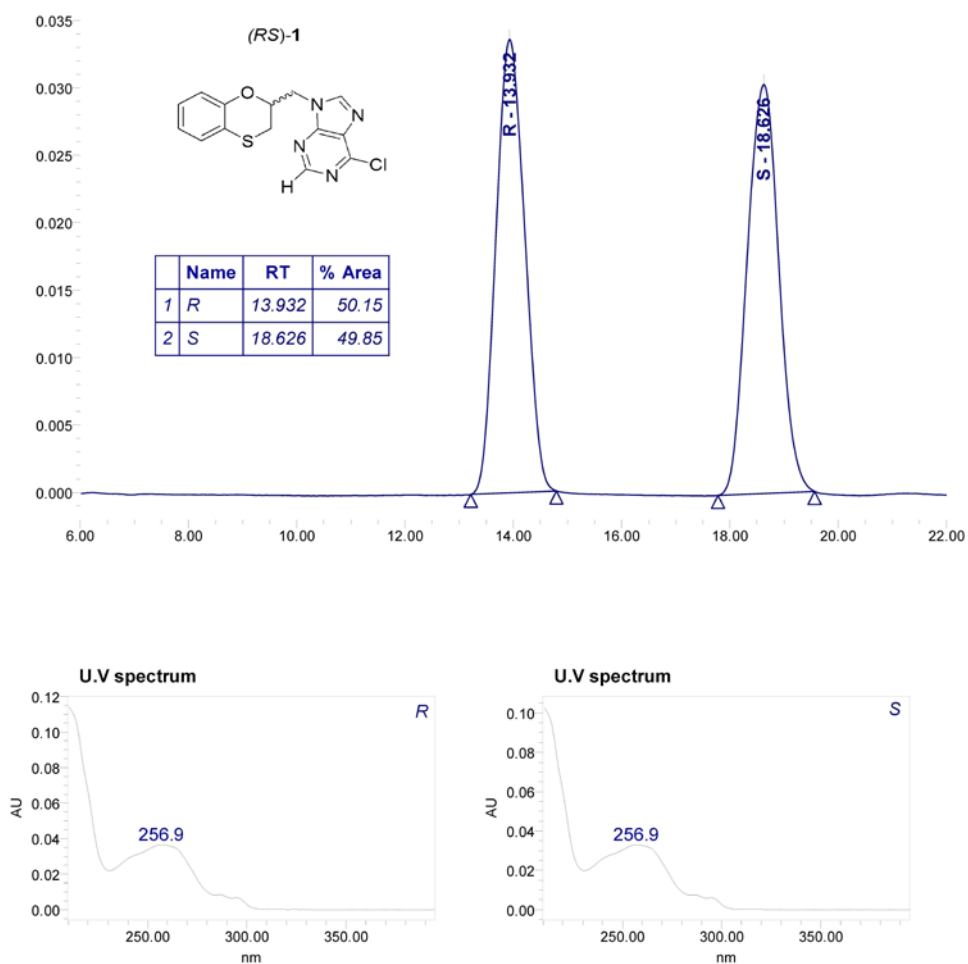


Figure S1

CHIRALPAK IA 250 x 4.6 mm
Flow rate: 1ml/min
room temperature
PDA 250.0 nm
n-hexane/ethanol 80/20 v/v

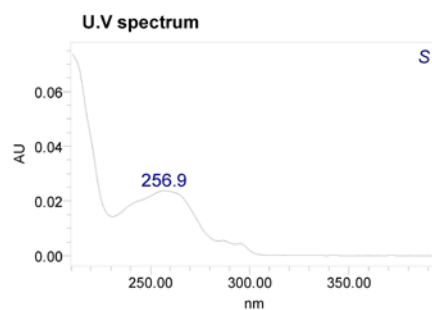
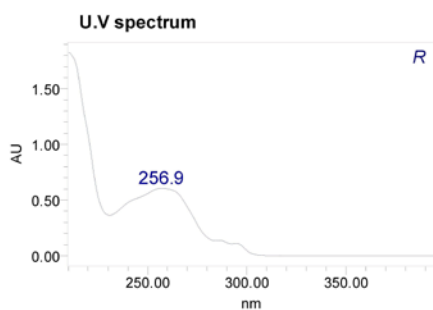
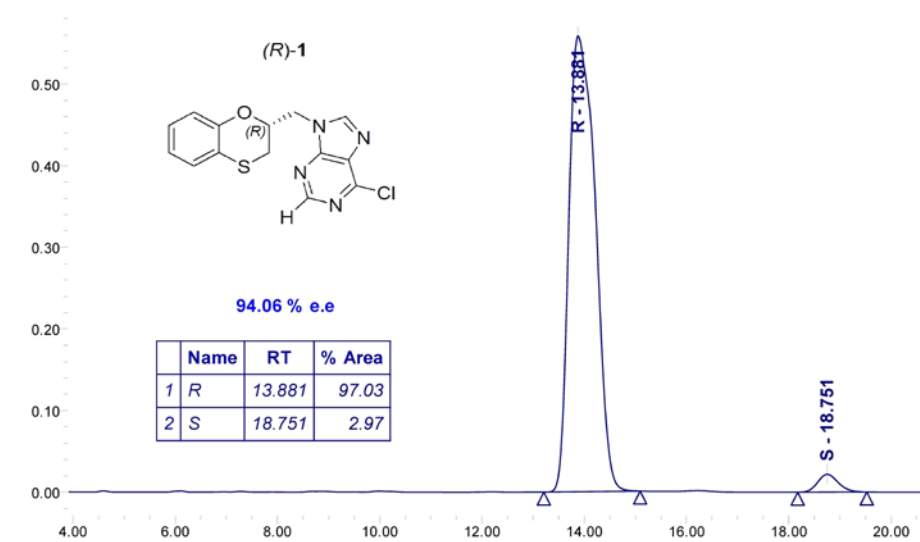


Figure S2

CHIRALPAK IA 250 x 4.6 mm
Flow rate: 1ml/min
room temperature
PDA 250.0 nm
n-hexane/ethanol 80/20 v/v

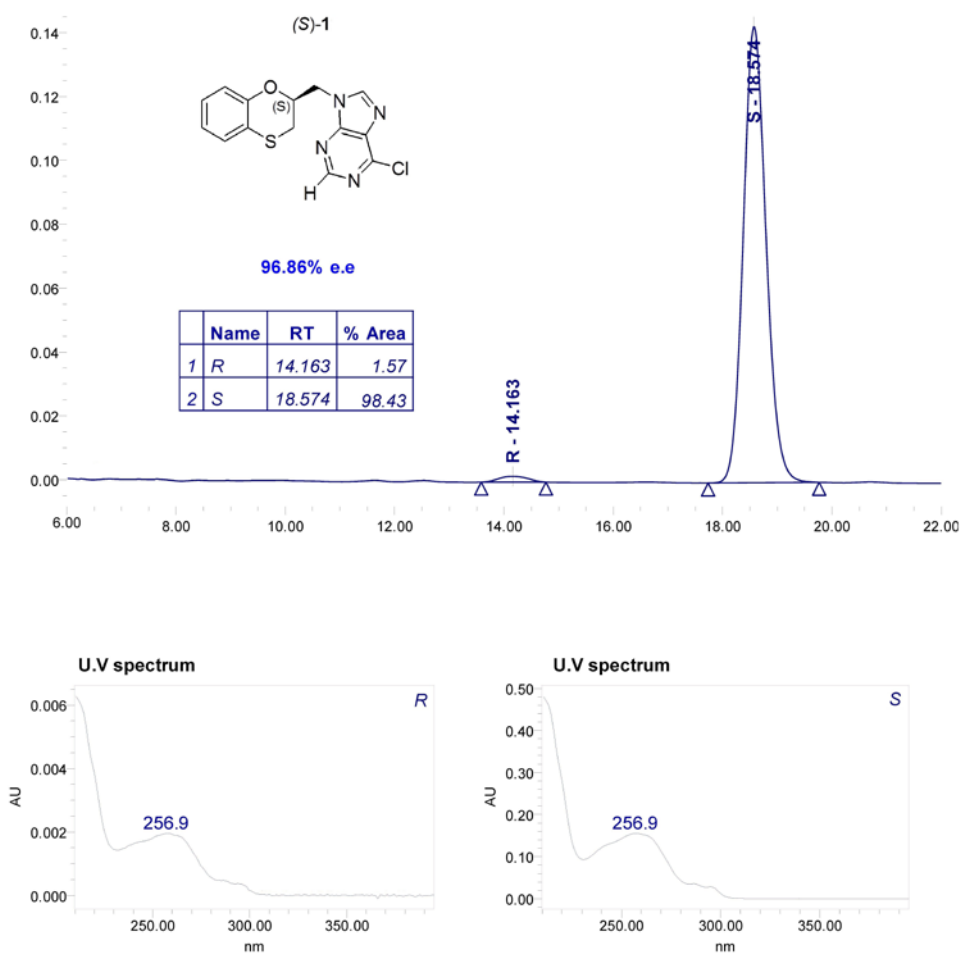


Figure S3

CHIRALPAK IA 250 x 4.6 mm
Flow rate: 1ml/min
room temperature
PDA 250.0 nm
n-hexane/ethanol 80/20 v/v

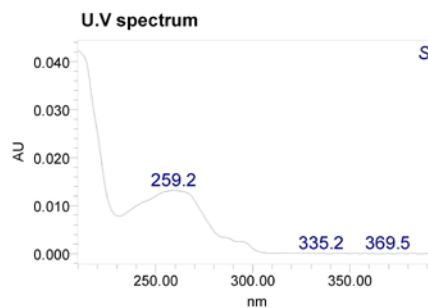
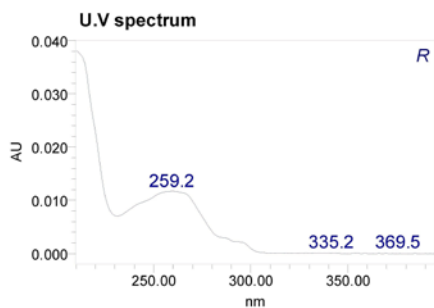
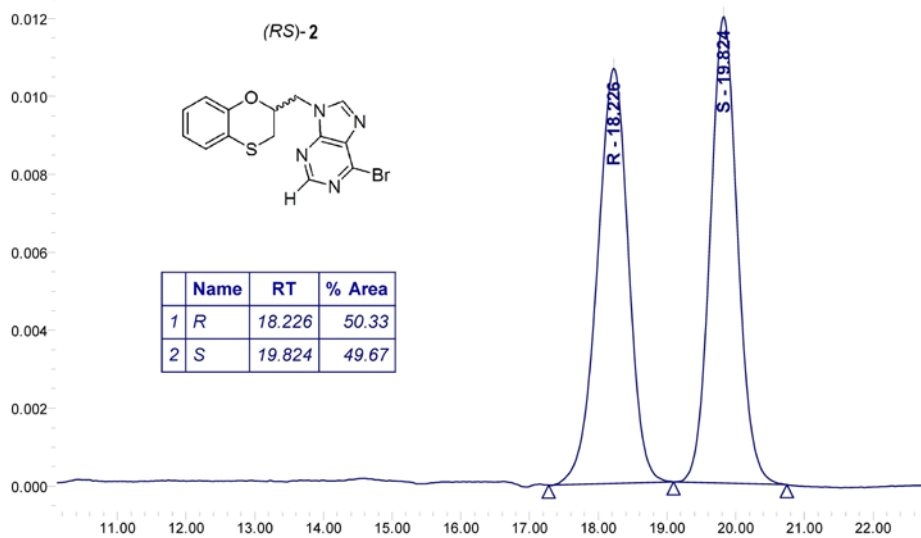


Figure S4

CHIRALPAK IA 250 x 4.6 mm
Flow rate: 1ml/min
room temperature
PDA 250.0 nm
n-hexane/ethanol 80/20 v/v

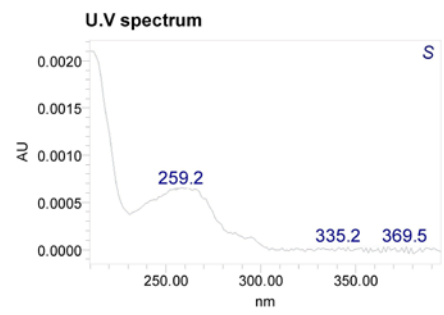
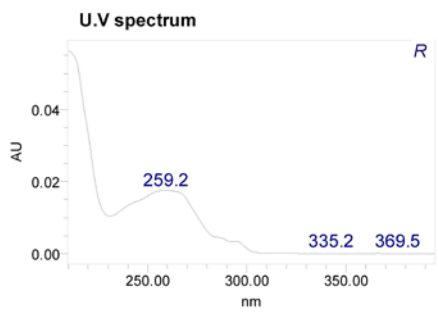
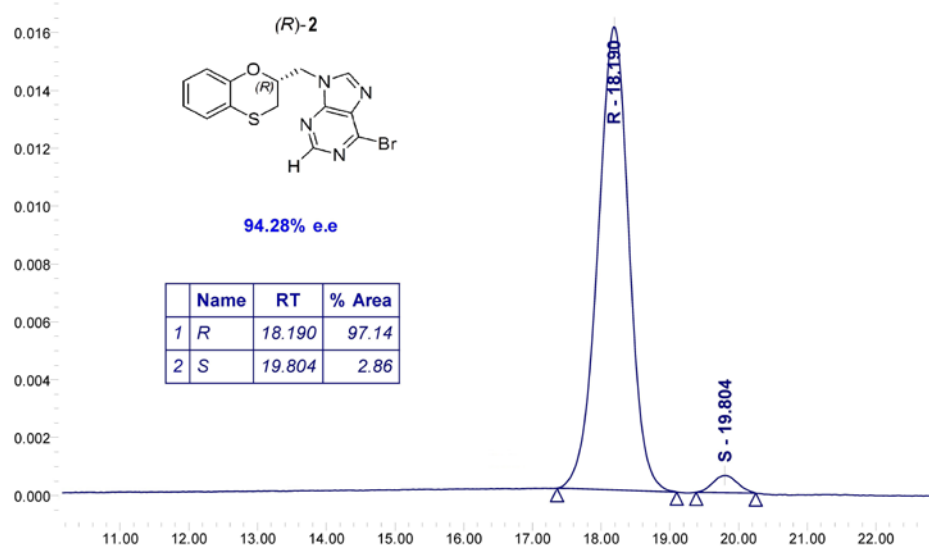


Figure S5

CHIRALPAK IA 250 x 4.6 mm
Flow rate: 1ml/min
room temperature
PDA 250.0 nm
n-hexane/ethanol 80/20 v/v

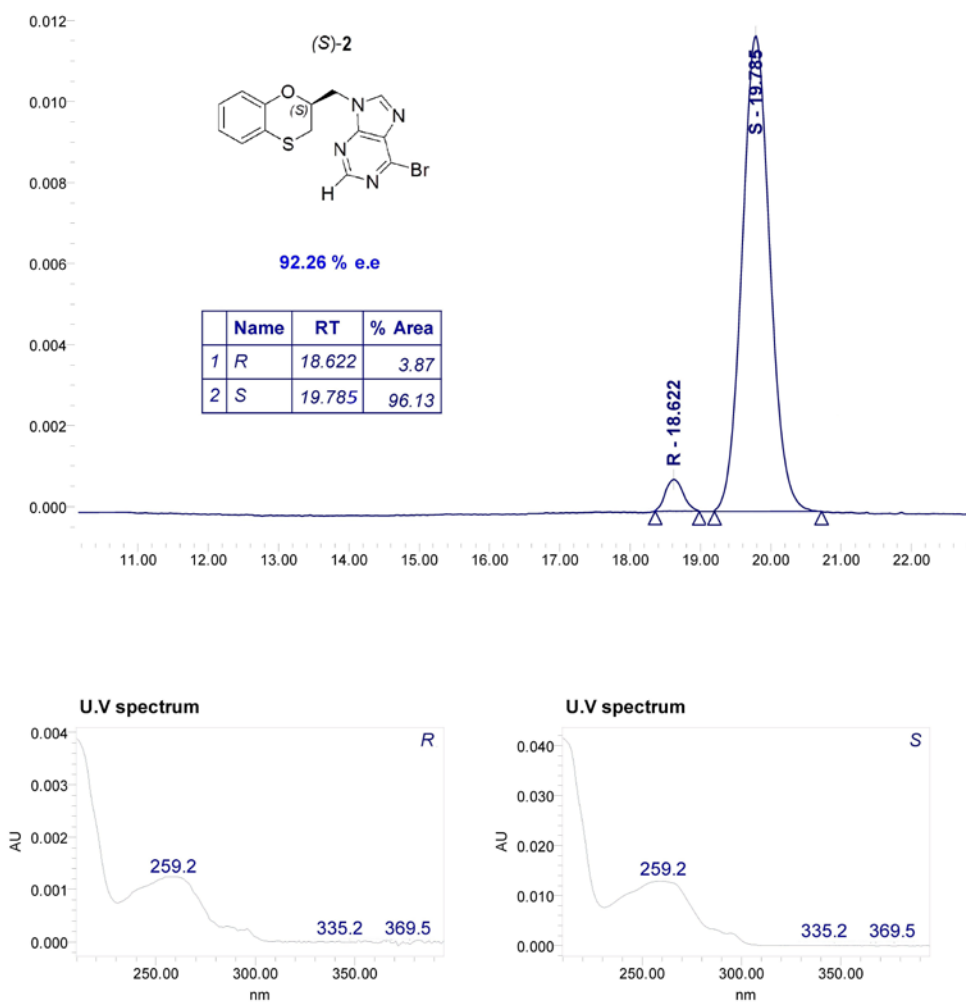


Figure S6

CHIRALPAK IA 250 x 4.6 mm
Flow rate: 1ml/min
room temperature
PDA 250.0 nm
n-hexane/2-propanol 90/10 v/v

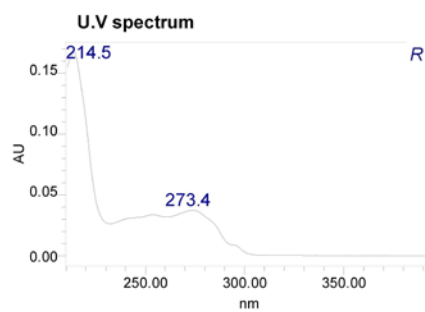
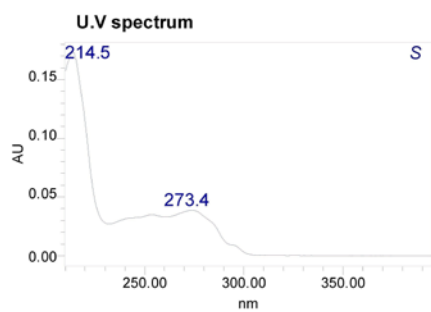
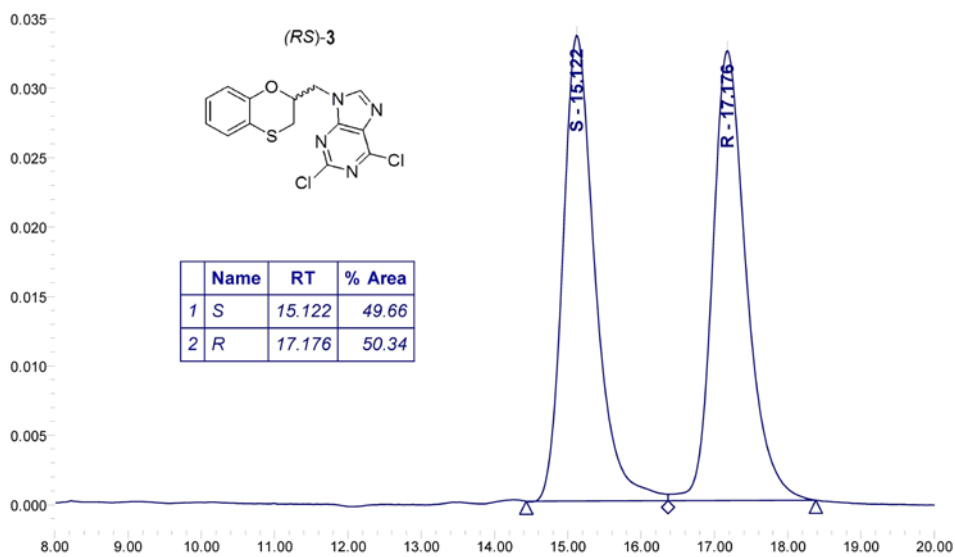


Figure S7

CHIRALPAK IA 250 x 4.6 mm
Flow rate: 1ml/min
room temperature
PDA 250.0 nm
n-hexane/2-propanol 90/10 v/v

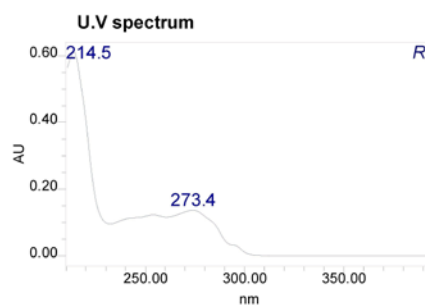
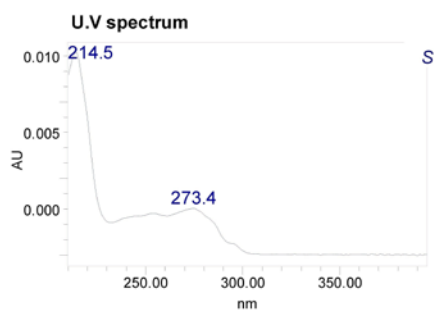
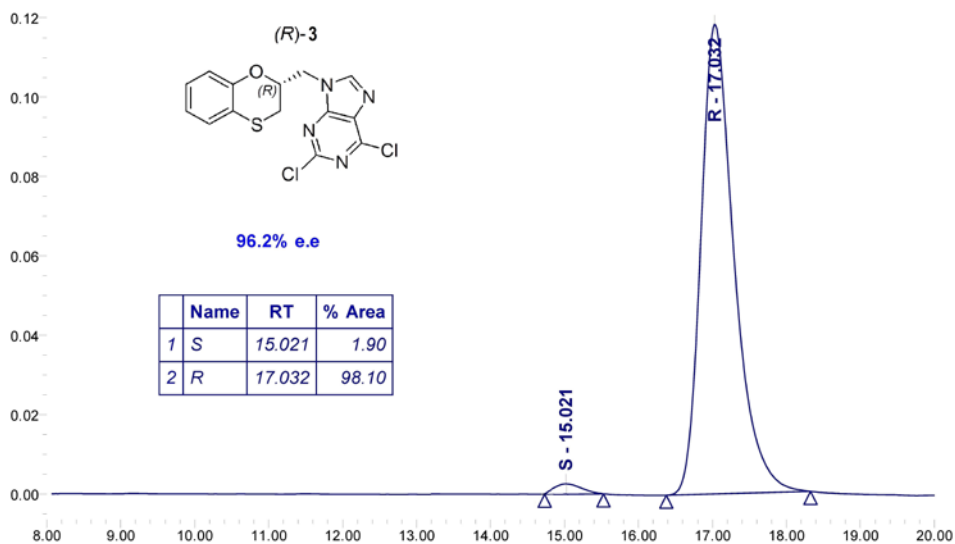


Figure S8

CHIRALPAK IA 250 x 4.6 mm
Flow rate: 1ml/min
room temperature
PDA 250.0 nm
n-hexane/2-propanol 90/10 v/v

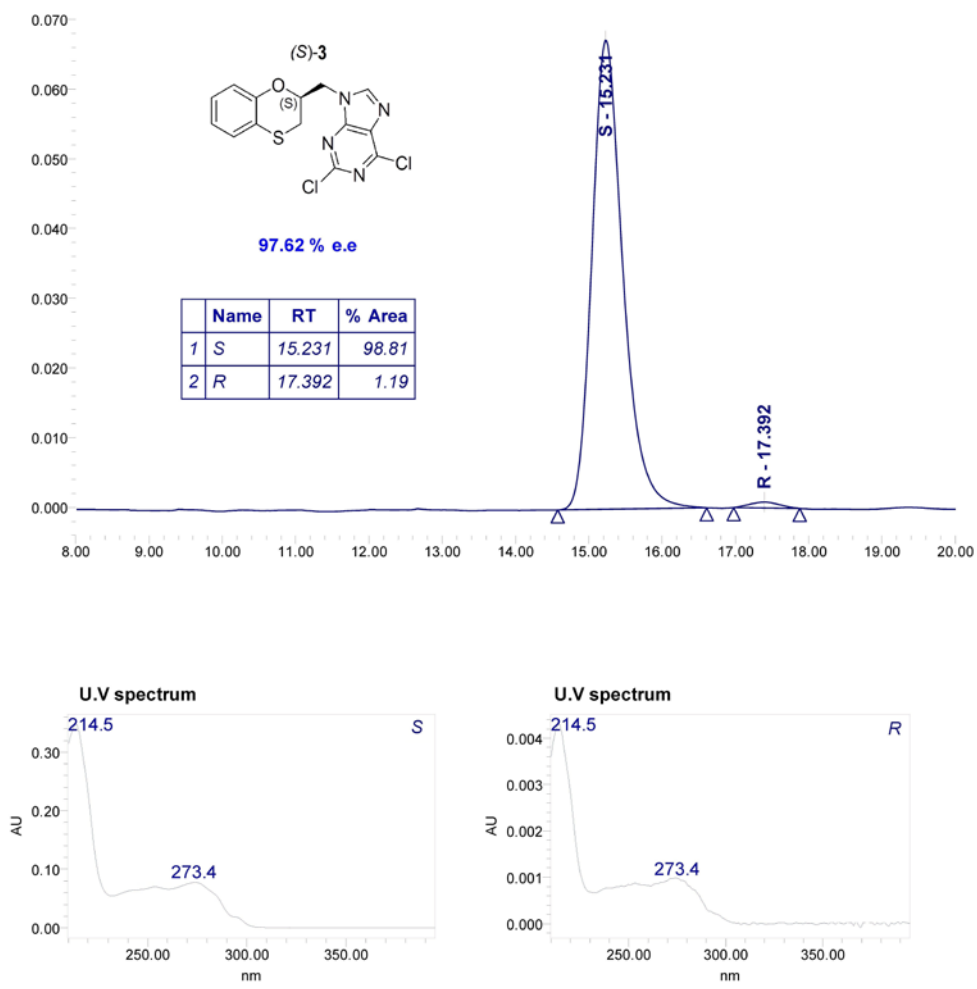


Figure S9

CHIRALPAK IA 250 x 4.6 mm
Flow rate: 1ml/min
room temperature
PDA 250.0 nm
n-hexane/2-propanol 90/10 v/v

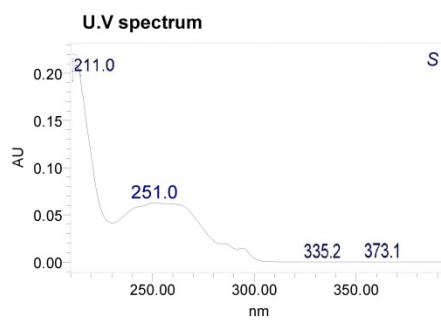
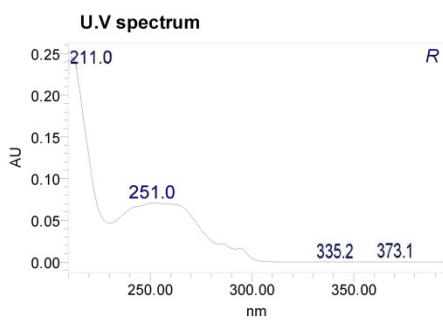
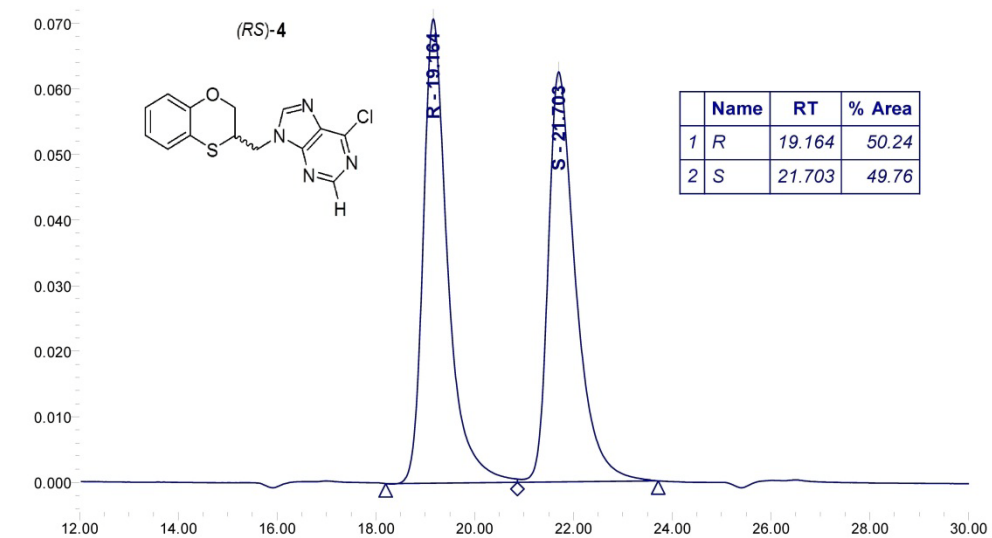


Figure S10

CHIRALPAK IA 250 x 4.6 mm
Flow rate: 1ml/min
room temperature
PDA 250.0 nm
n-hexane/2-propanol 90/10

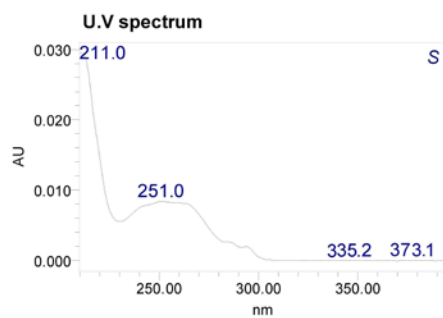
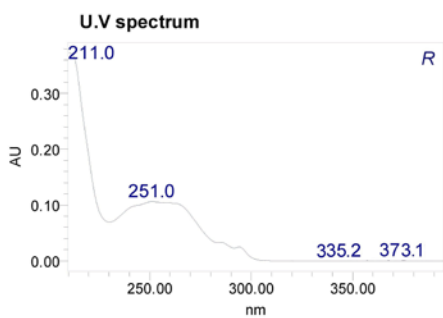
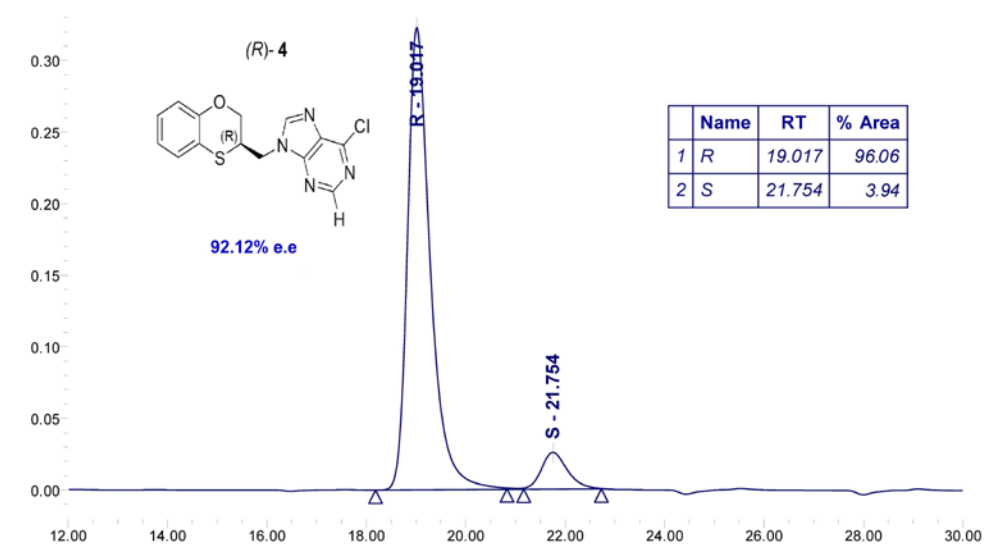


Figure S11

CHIRALPAK IA 250 x 4.6 mm
Flow rate: 1ml/min
room temperature
PDA 250.0 nm
n-hexane/2-propanol 90/10 v/v

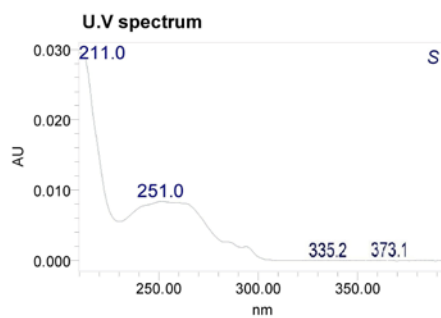
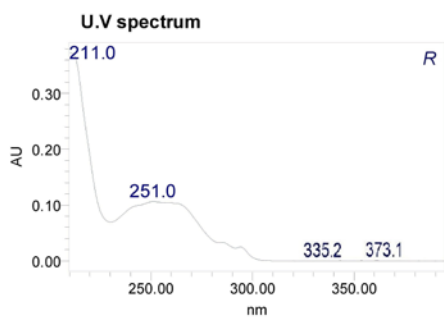
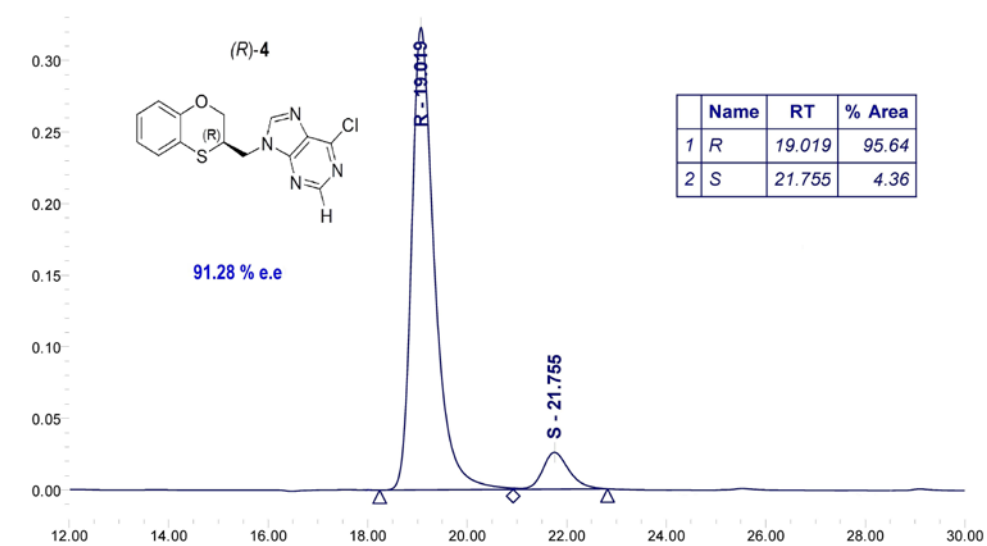


Figure S12

CHIRALPAK IA 250 x 4.6 mm
Flow rate: 1 ml/min
room temperature
PDA 250.0 nm
n-hexane/2-propanol 90/10 V/V

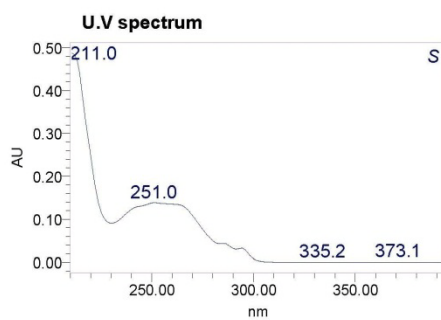
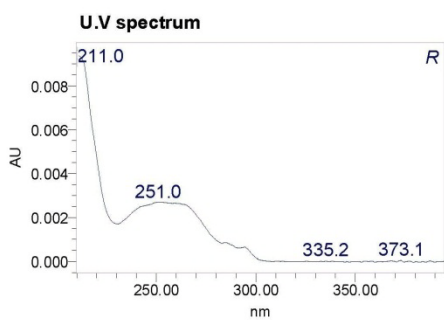
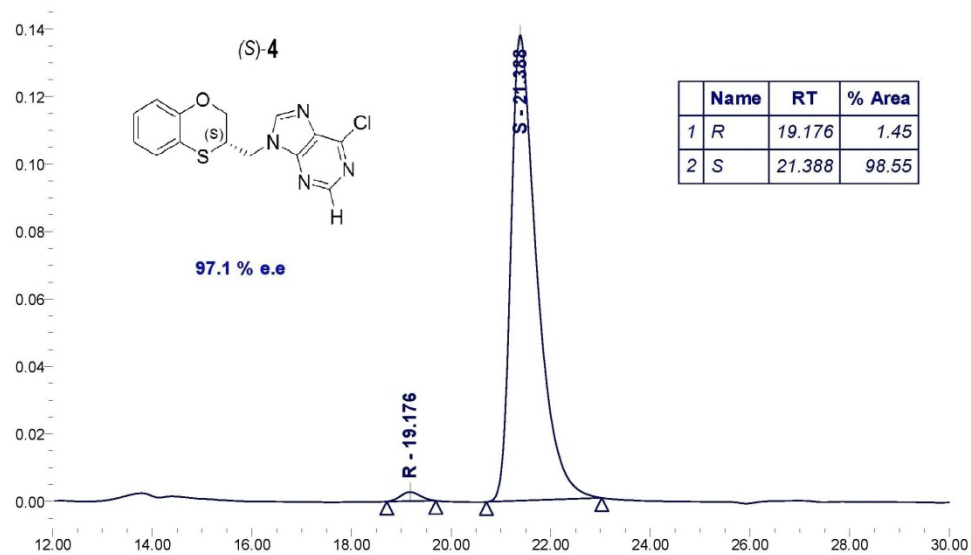


Figure S13

CHIRALPAK IA 250 x 4.6 mm
Flow rate: 1 ml/min
room temperature
PDA 250.0 nm
n-hexane/2-propanol 90/10 v/v

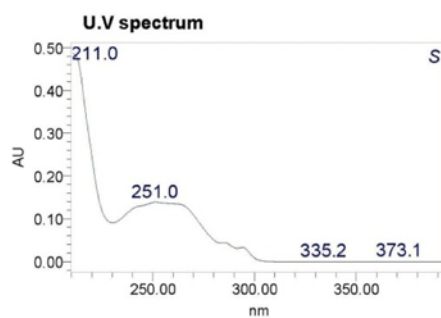
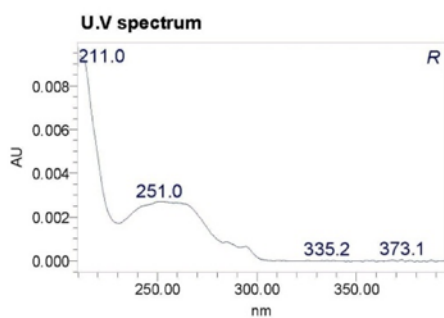
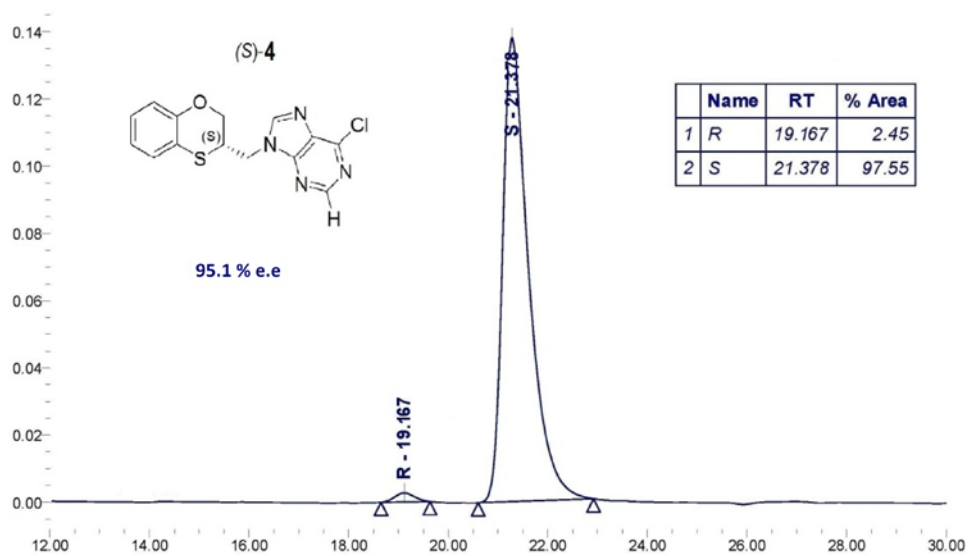


Figure S14

CHIRALPAK IA 250 x 4.6 mm
Flow rate: 1ml/min
room temperature
PDA 250.0 nm
n-hexane/2-ethanol 90/10 v/v

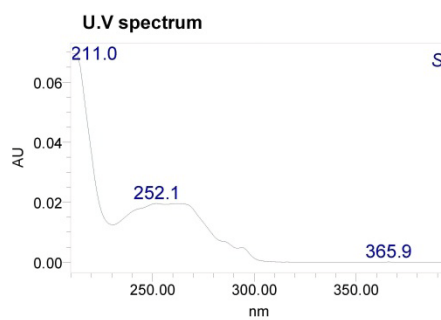
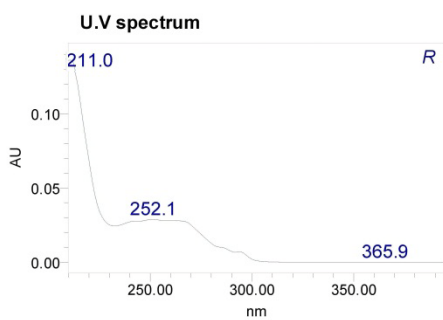
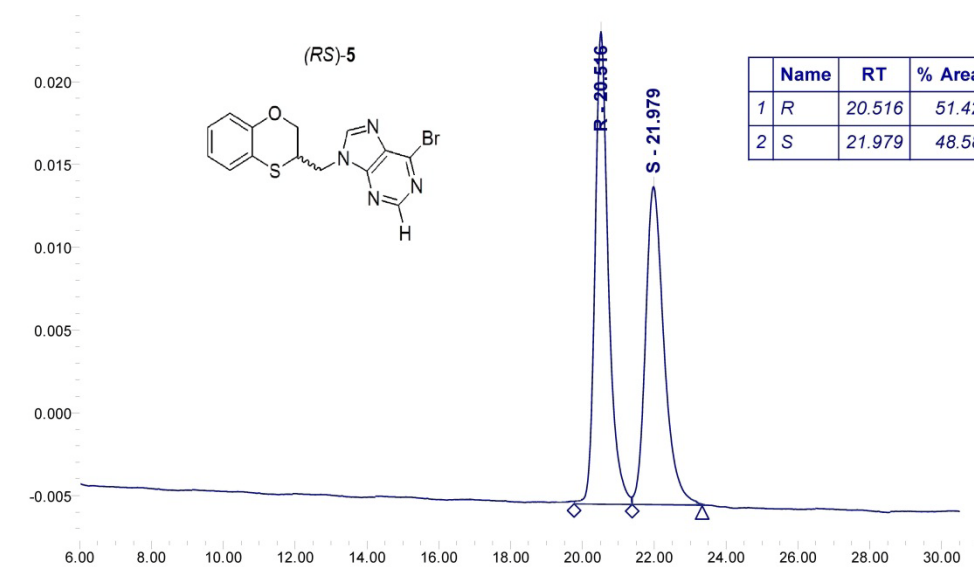


Figure S15

CHIRALPAK IA 250 x 4.6 mm
Flow rate: 1ml/min
room temperature
PDA 250.0 nm
n-hexane/2-ethanol 90/10 v/v

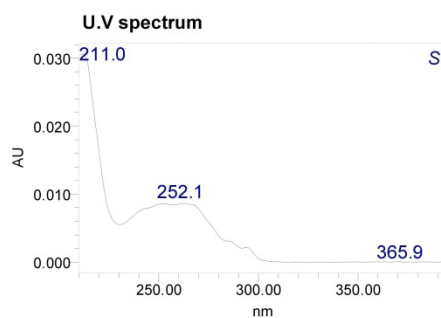
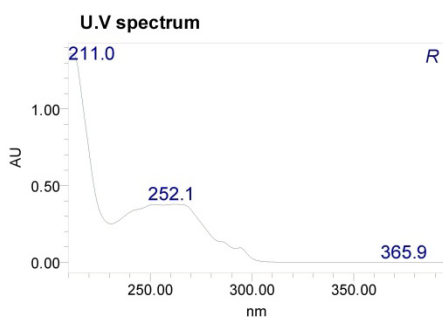
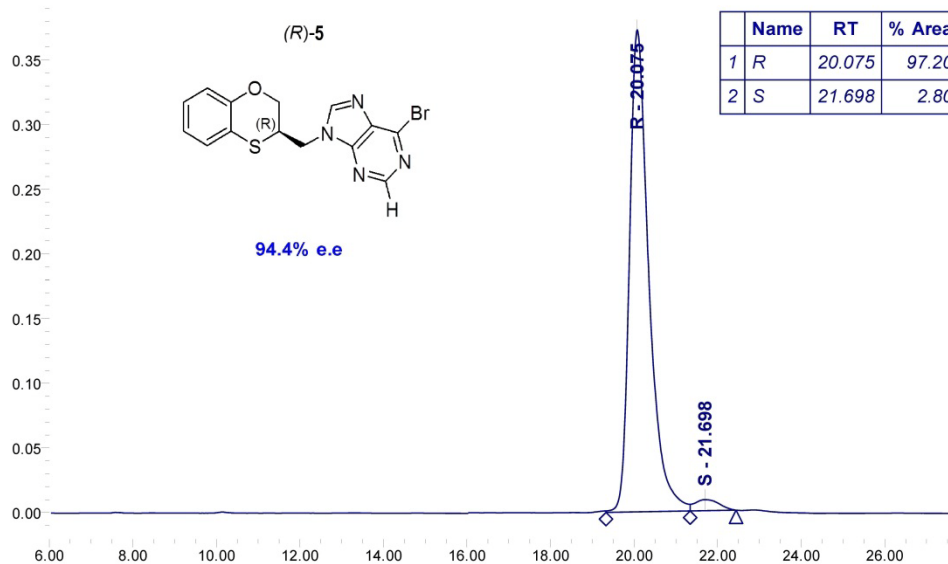


Figure S16

CHIRALPAK IA 250 x 4.6 mm
Flow rate: 1ml/min
room temperature
PDA 250.0 nm
n-hexane/2-ethanol 90/10 v/v

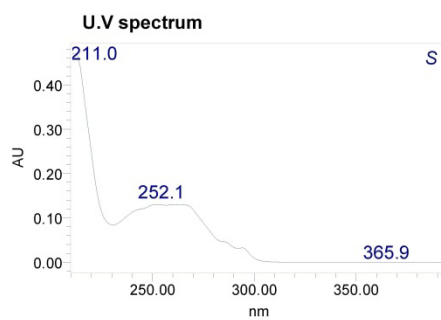
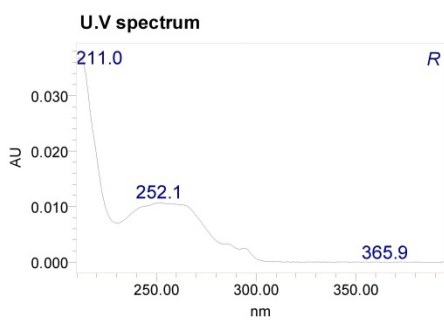
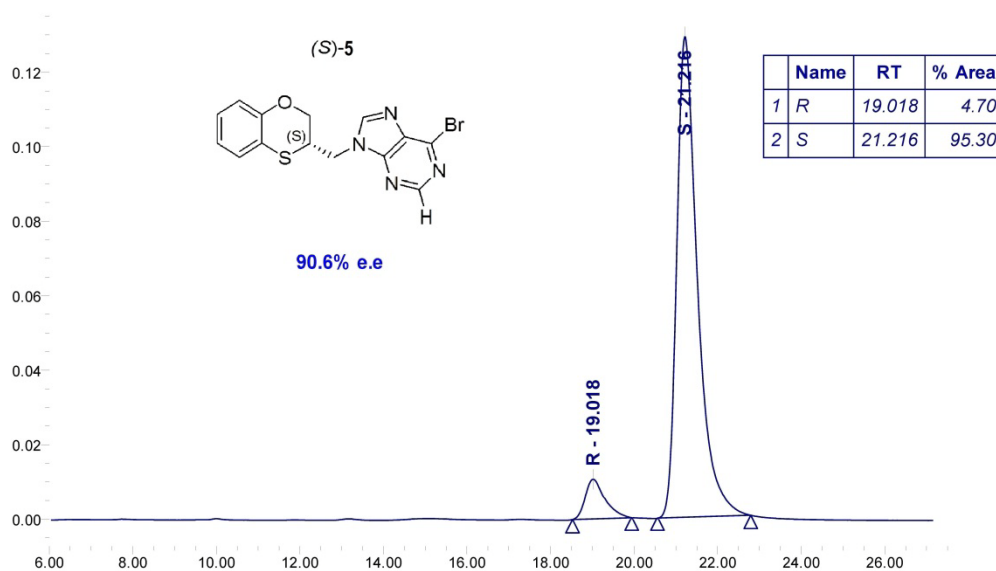


Figure S17

CHIRALPAK IA 250 x 4.6 mm
Flow rate: 1ml/min
room temperature
PDA 250.0 nm
n-hexane/2-ethanol 90/10 v/v

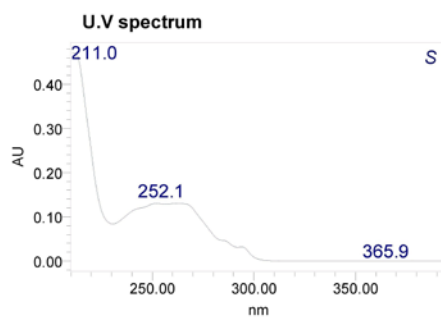
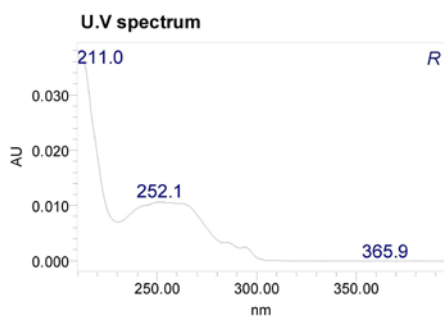
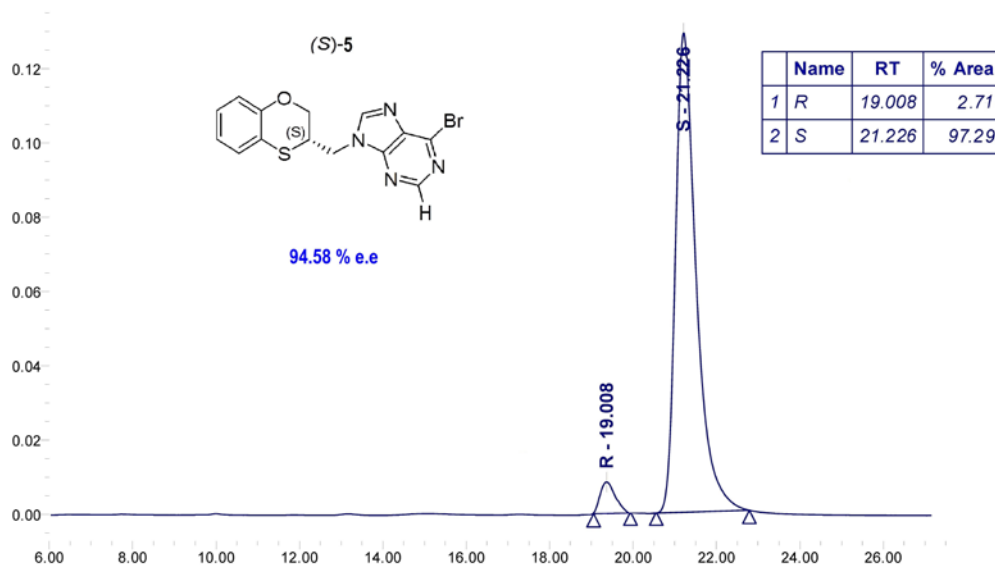


Figure S18

CHIRALPAK IA 250 x 4.6 mm
Flow rate: 1ml/min
room temperature
PDA 250.0 nm
n-hexane/2-propanol 90/10 v/v

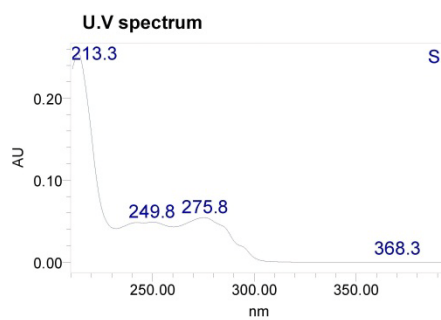
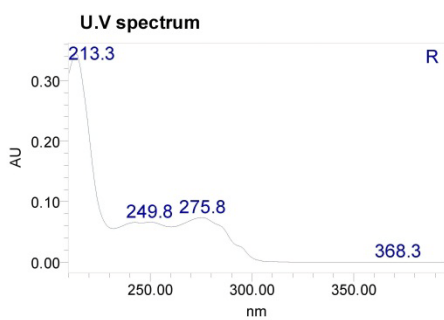
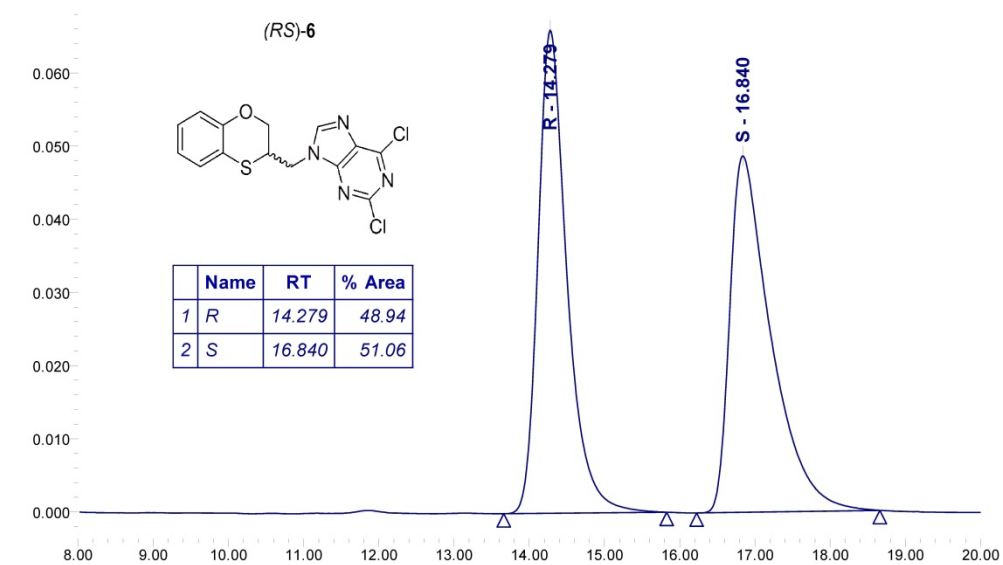


Figure S19

CHIRALPAK IA 250 x 4.6 mm
Flow rate: 1ml/min
room temperature
PDA 250.0 nm
n-hexane/2-propanol 90/10 v/v

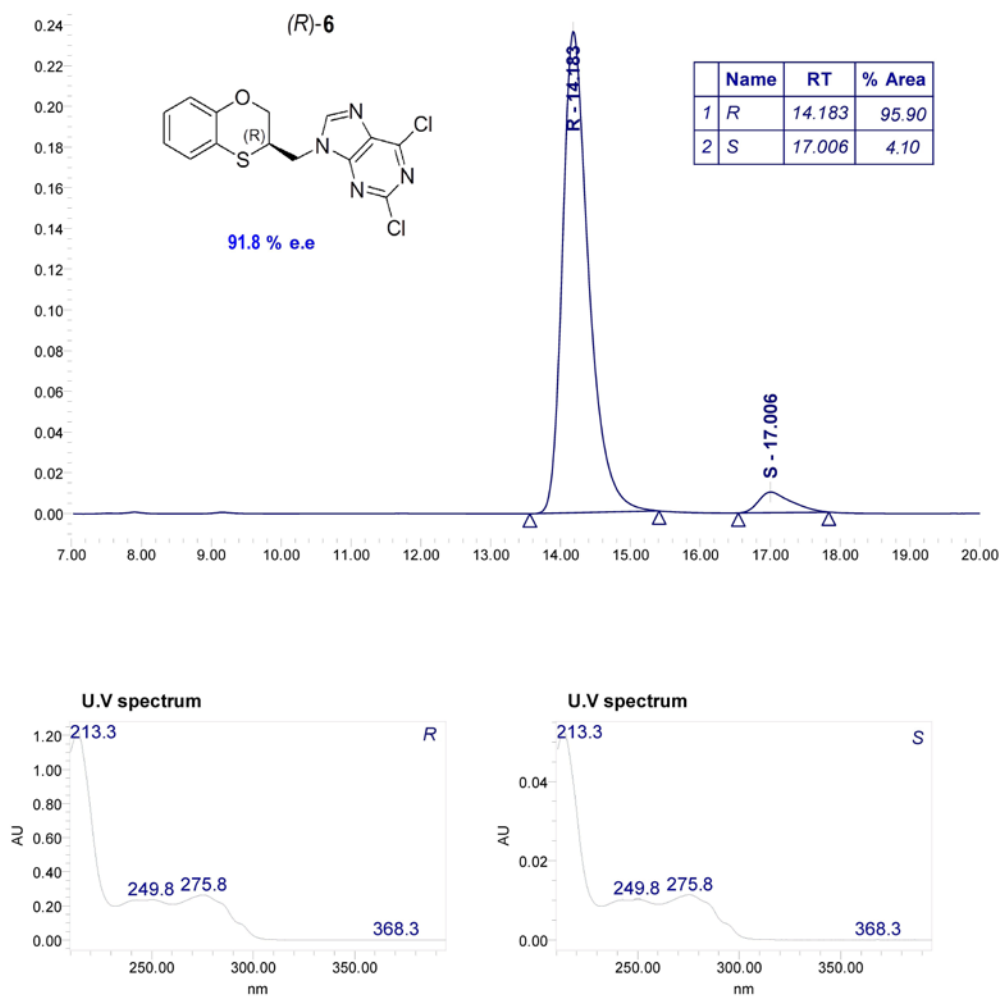


Figure S20

CHIRALPAK IA 250 x 4.6 mm
Flow rate: 1ml/min
room temperature
PDA 250.0 nm
n-hexane/2-propanol 90/10 v/v

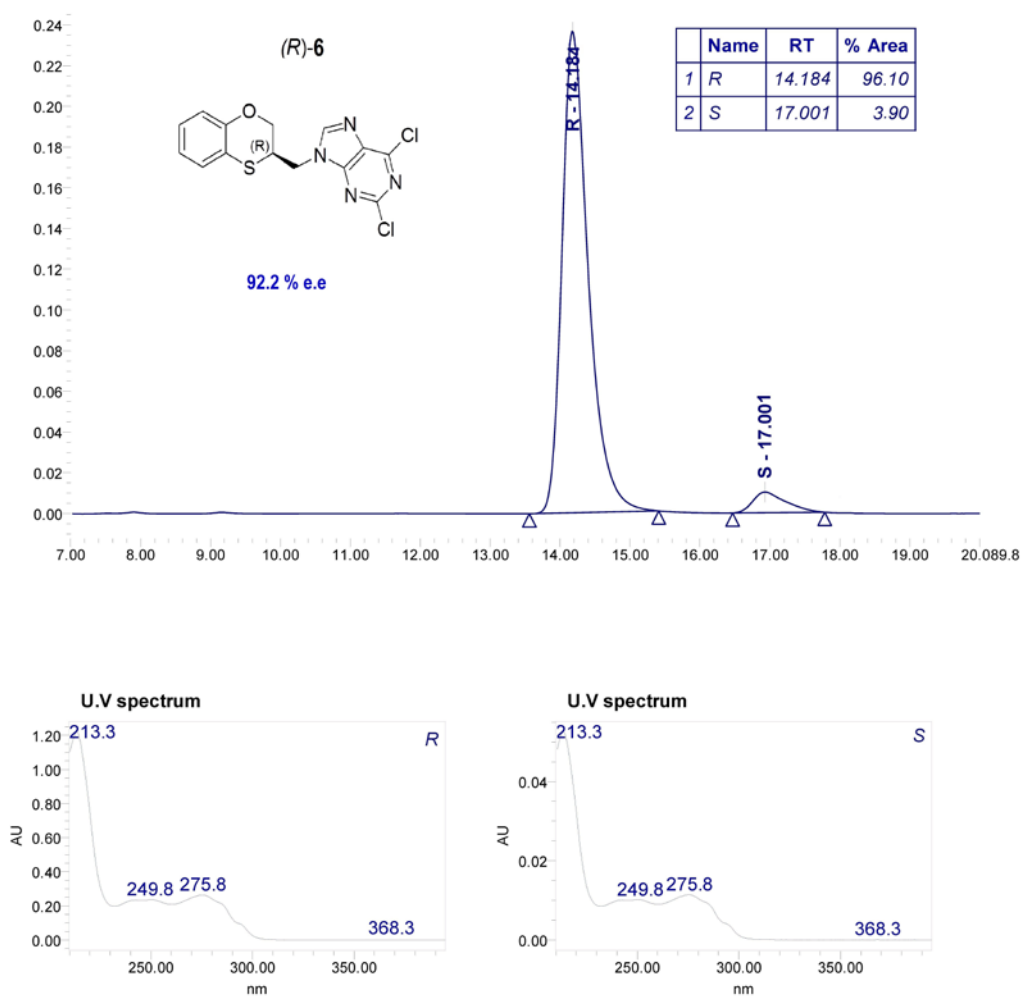


Figure S21

CHIRALPAK IA 250 x 4.6 mm
Flow rate: 1ml/min
room temperature
PDA 250.0 nm
n-hexane/2-propanol 90/10 v/v

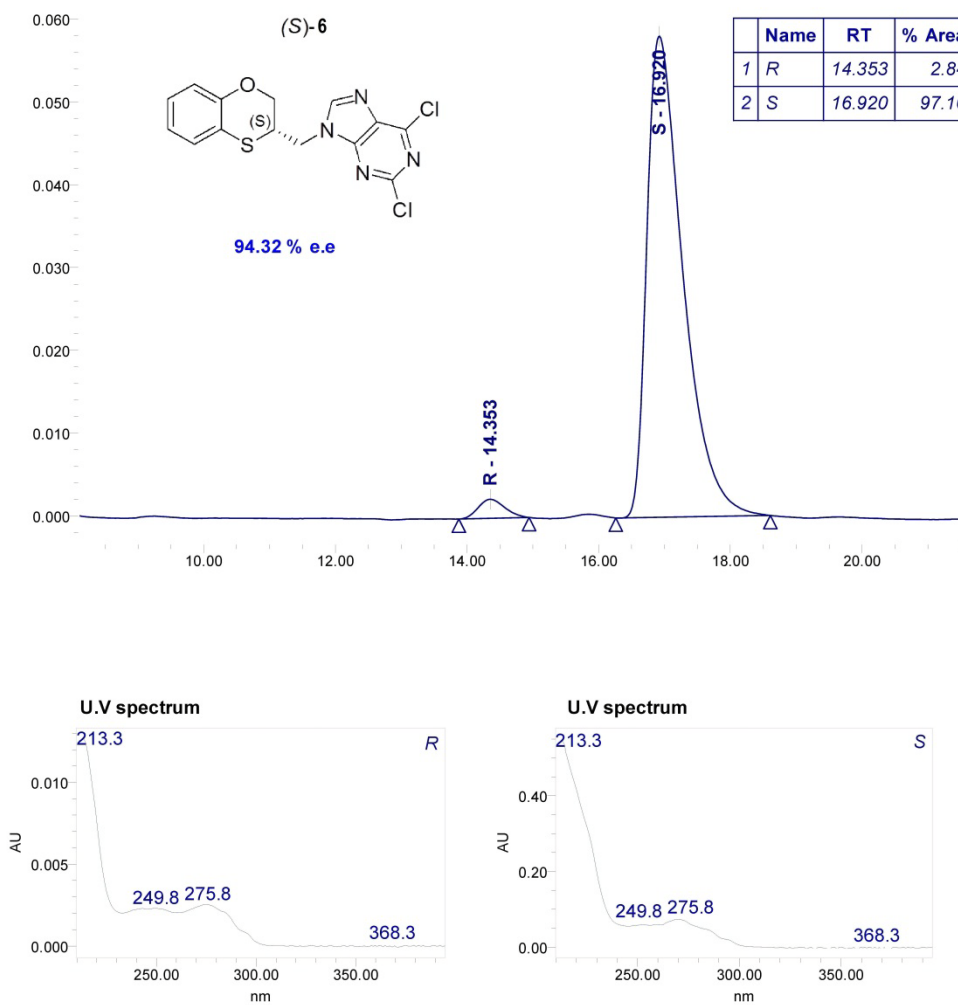


Figure S22

CHIRALPAK IA 250 x 4.6 mm
Flow rate: 1ml/min
room temperature
PDA 250.0 nm
n-hexane/2-propanol 90/10 v/v

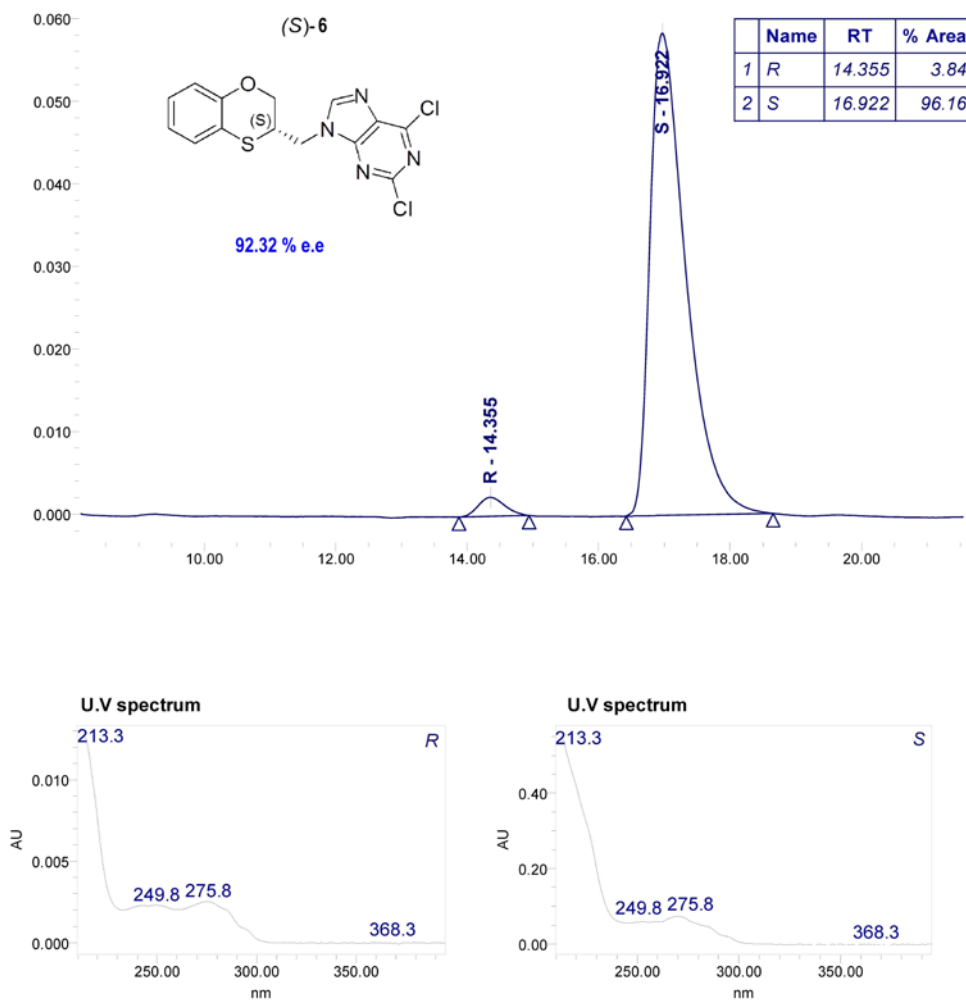


Figure S23

CHIRALPAK IA 250 x 4.6 mm
Flow rate: 1ml/min
room temperature
PDA 250.0 nm
n-hexane/2-propanol 90/10 v/v

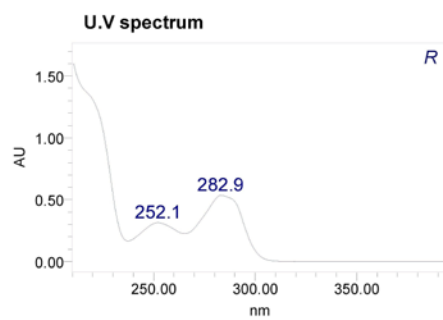
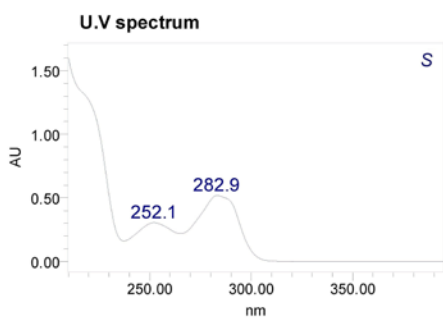
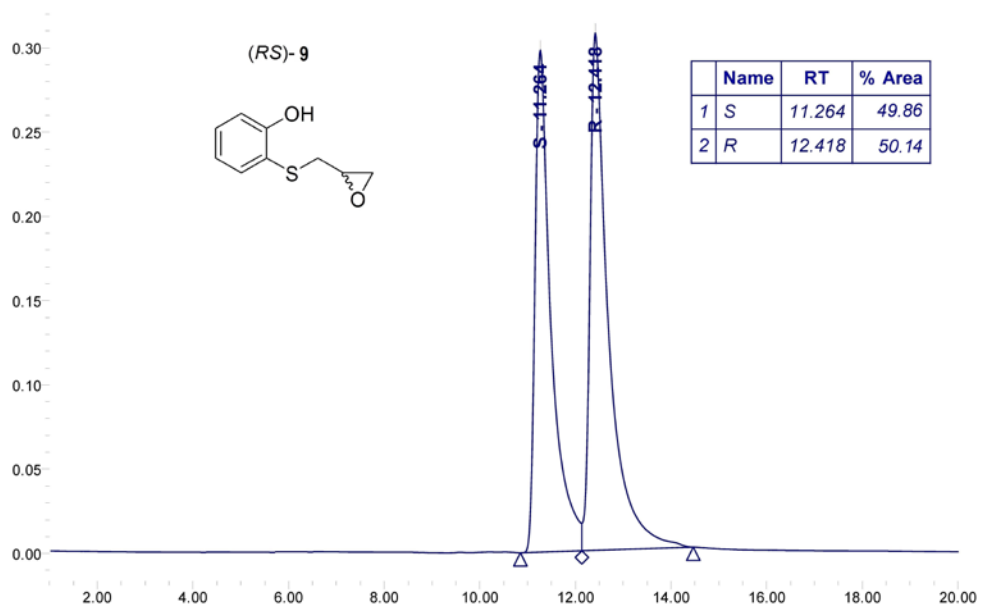


Figure S24

CHIRALPAK IA 250 x 4.6 mm
Flow rate: 1ml/min
room temperature
PDA 250.0 nm
n-hexane/2-propanol 90/10 v/v

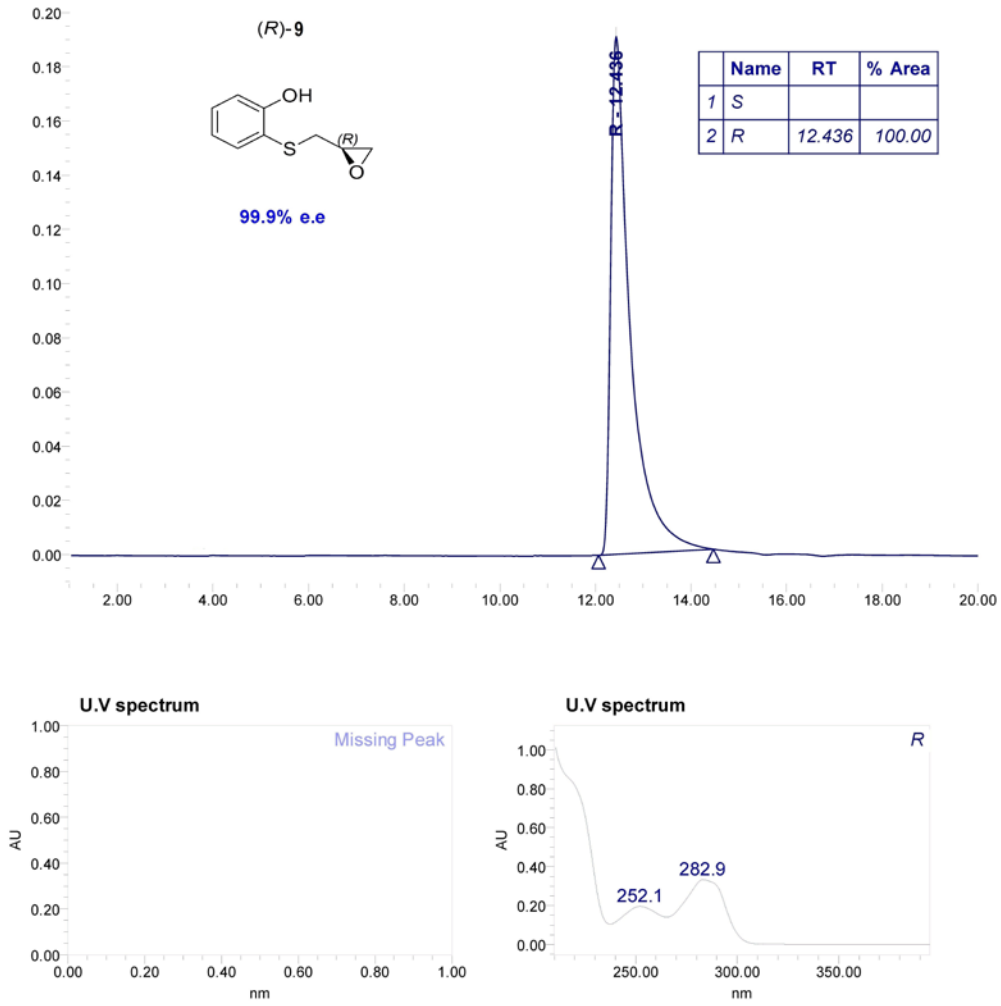


Figure S25

CHIRALPAK IA 250 x 4.6 mm
Flow rate: 1ml/min
room temperature
PDA 250.0 nm
n-hexane/2-propanol 90/10 v/v

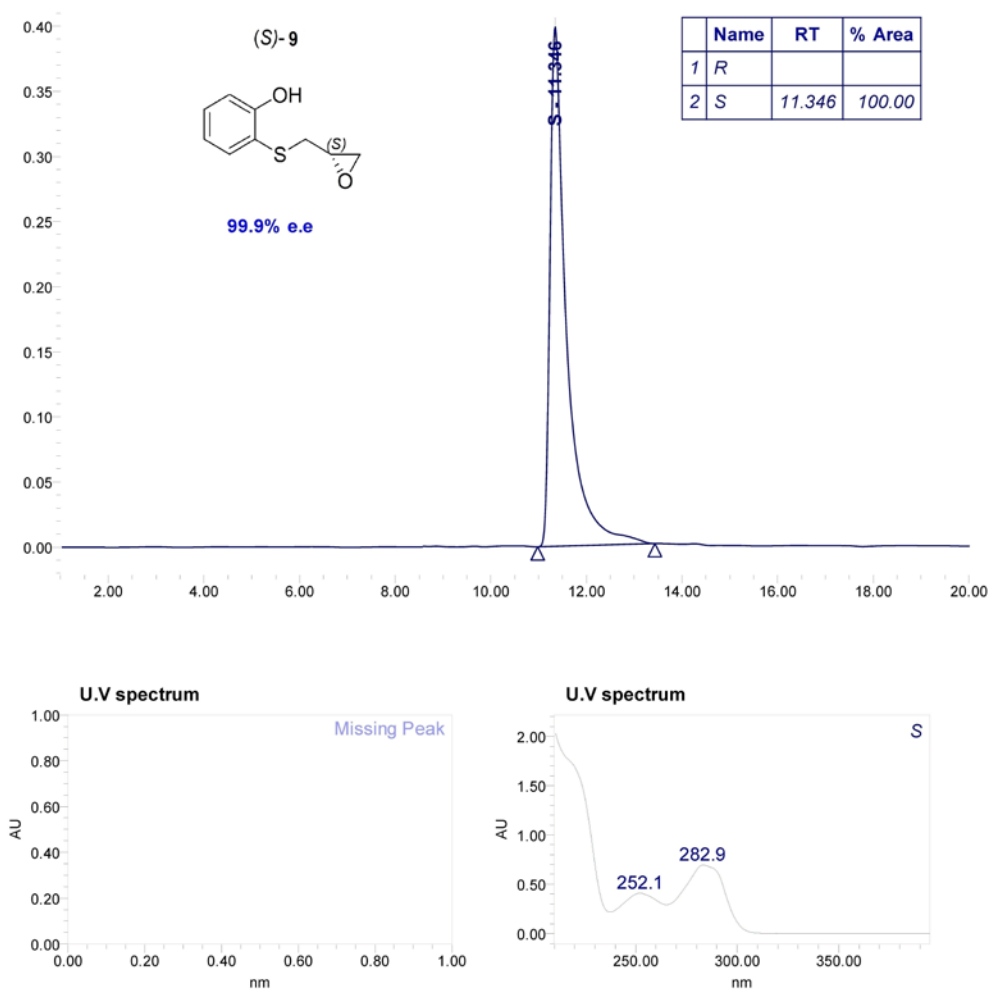


Figure S26

CHIRALPAK IA 250 x 4.6 mm
Flow rate: 1ml/min
room temperature
PDA 250.0 nm
n-hexane/dichloromethane 65/35 v/v

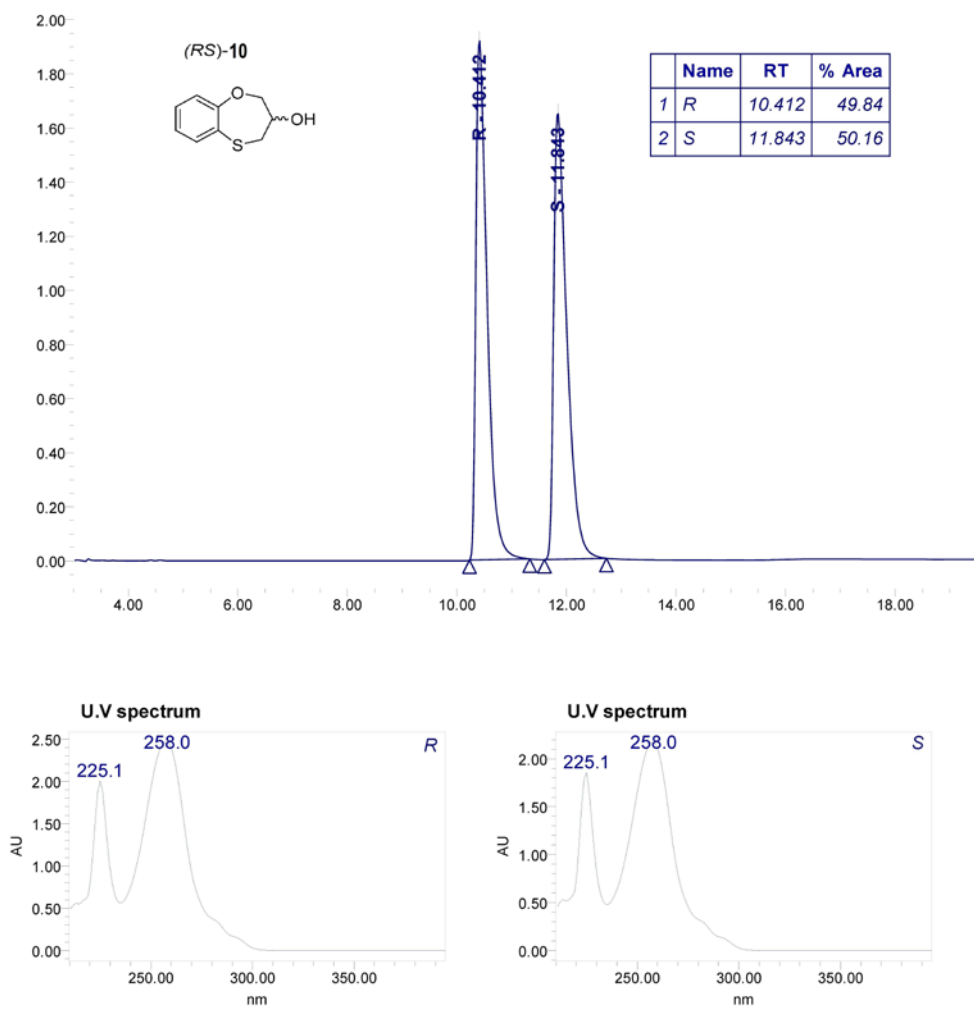


Figure S27

CHIRALPAK IA 250 x 4.6 mm
Flow rate: 1ml/min
room temperature
PDA 250.0 nm
n-hexane/dichloromethane 65/35 v/v

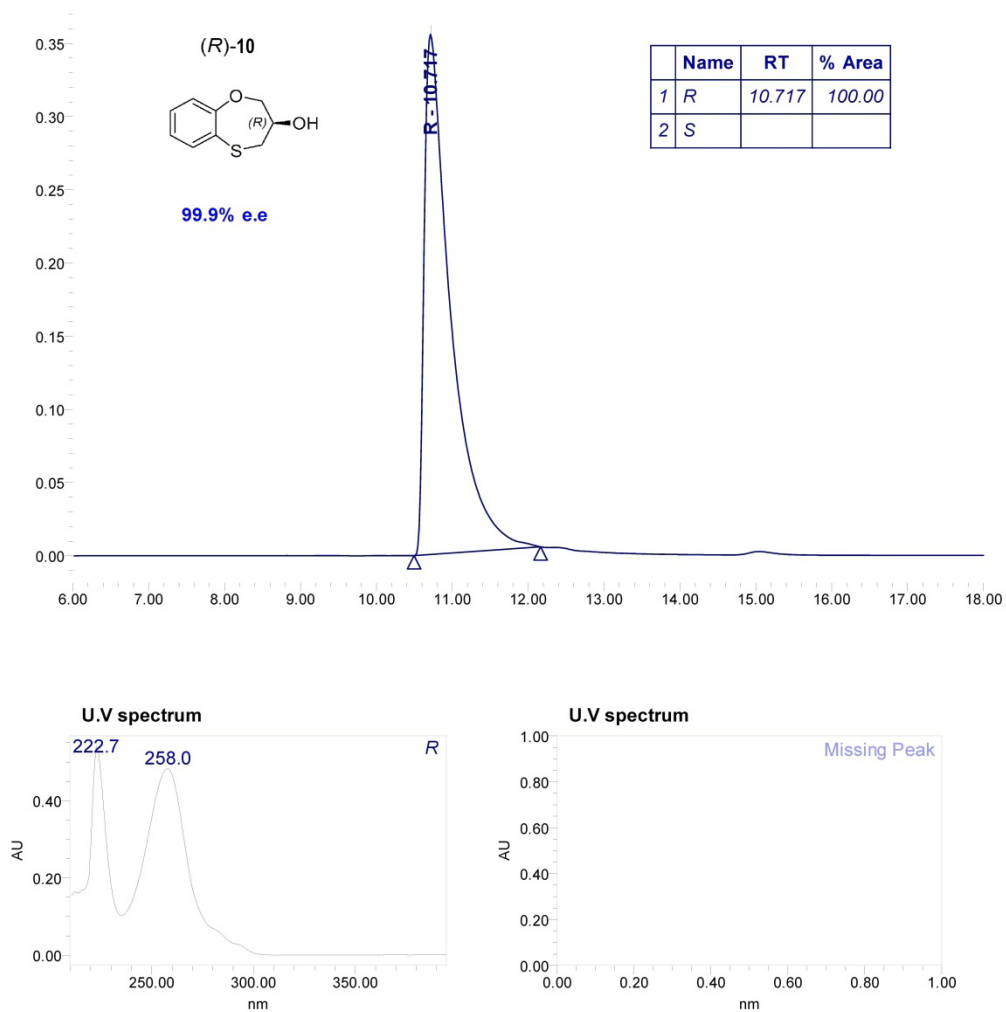


Figure S28

CHIRALPAK IA 250 x 4.6 mm
Flow rate: 1ml/min
room temperature
PDA 250.0 nm
n-hexane/dichloromethane 65/35 v/v

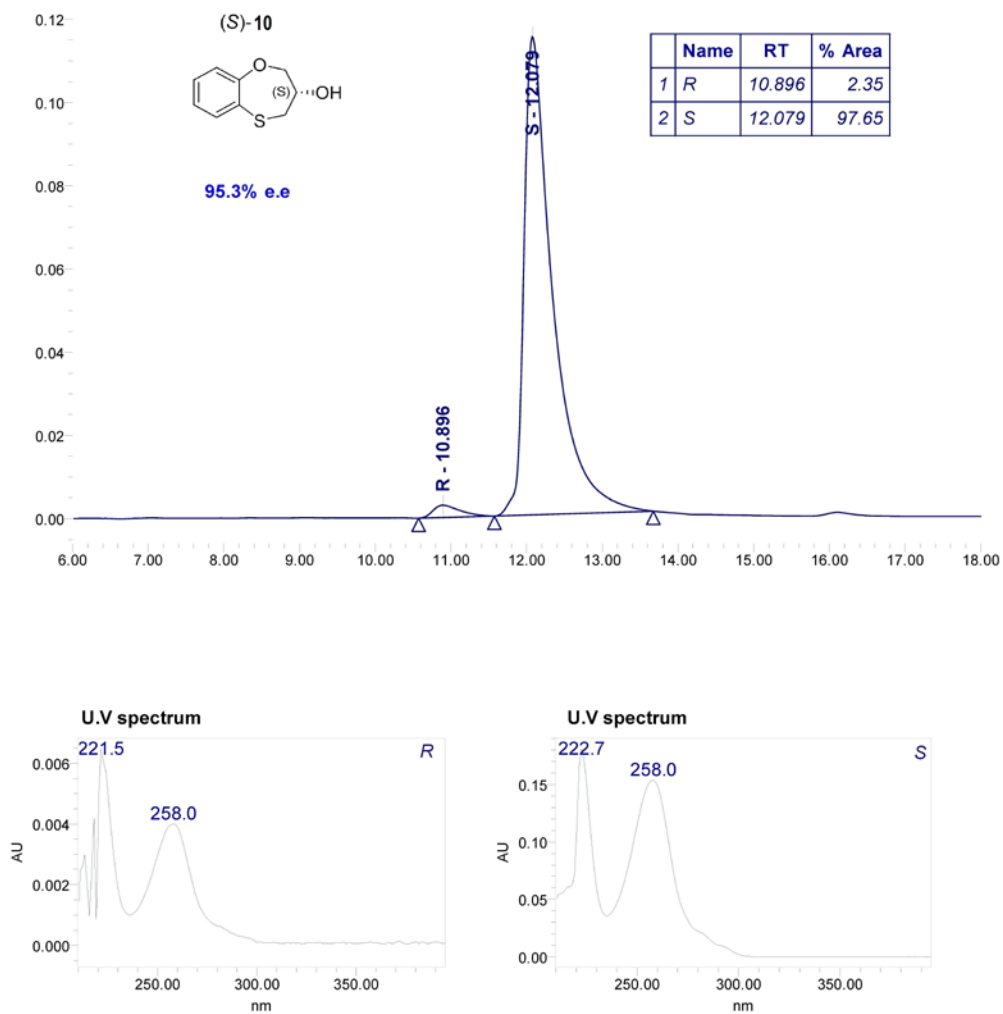


Figure S29

CHIRALPAK IA 250 x 4.6 mm
Flow rate: 1ml/min
room temperature
PDA 250.0 nm
n-hexane/dichloromethane 65/35 v/v

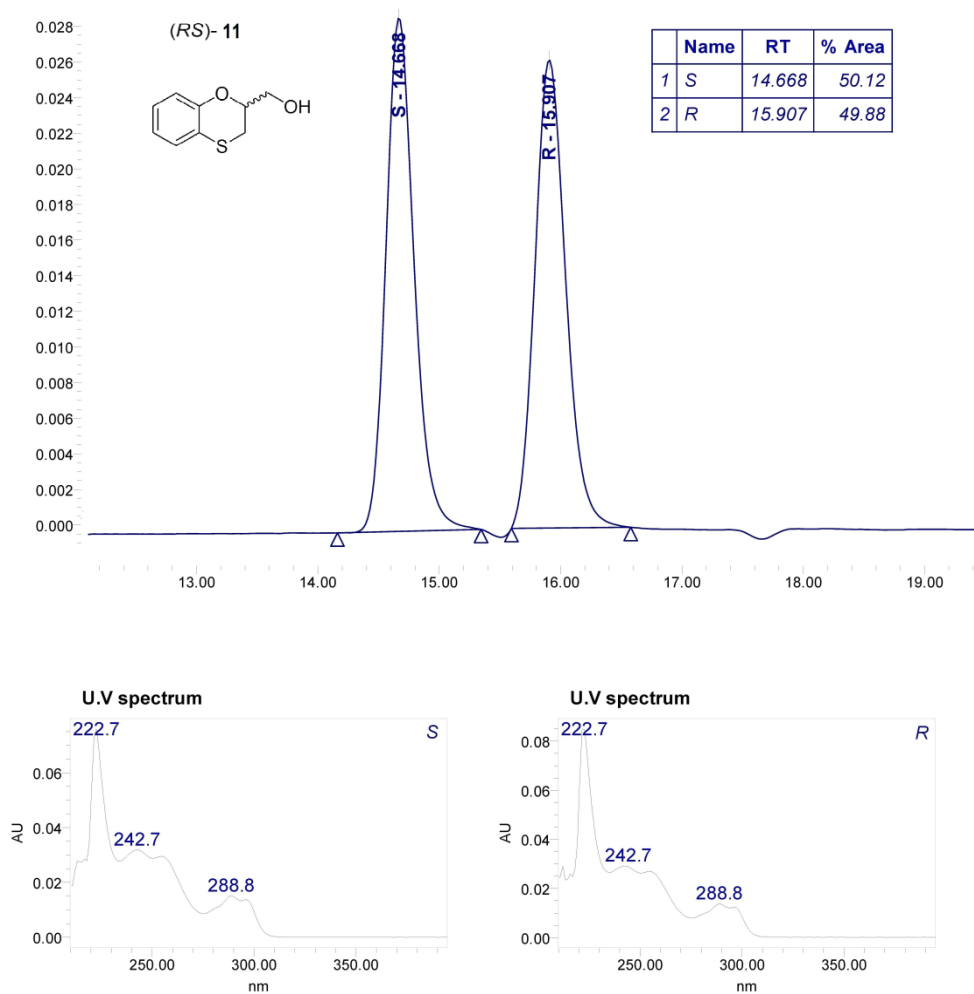


Figure S30

CHIRALPAK IA 250 x 4.6 mm
Flow rate: 1ml/min
room temperature
PDA 250.0 nm
n-hexane/dichloromethane 65/35 v/v

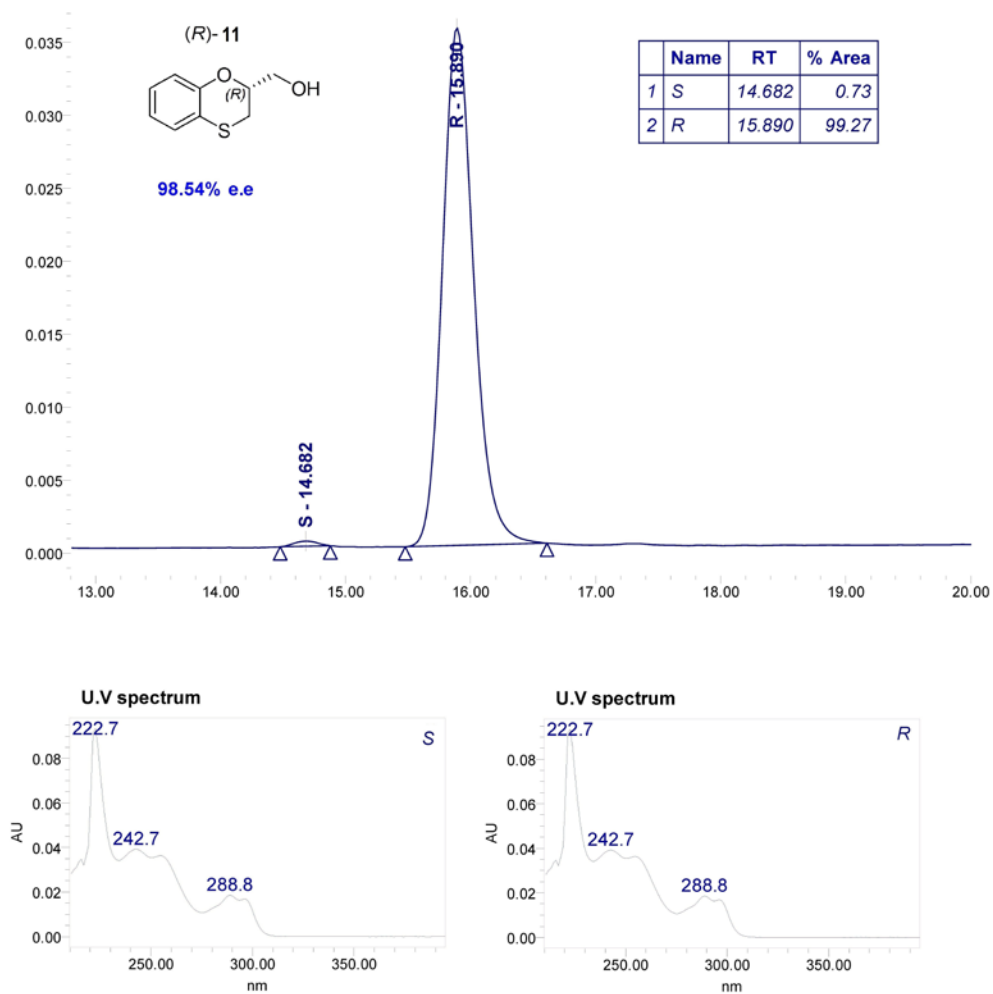


Figure S31

CHIRALPAK IA 250 x 4.6 mm
Flow rate: 1ml/min
room temperature
PDA 250.0 nm
n-hexane/dichloromethane 65/35 v/v

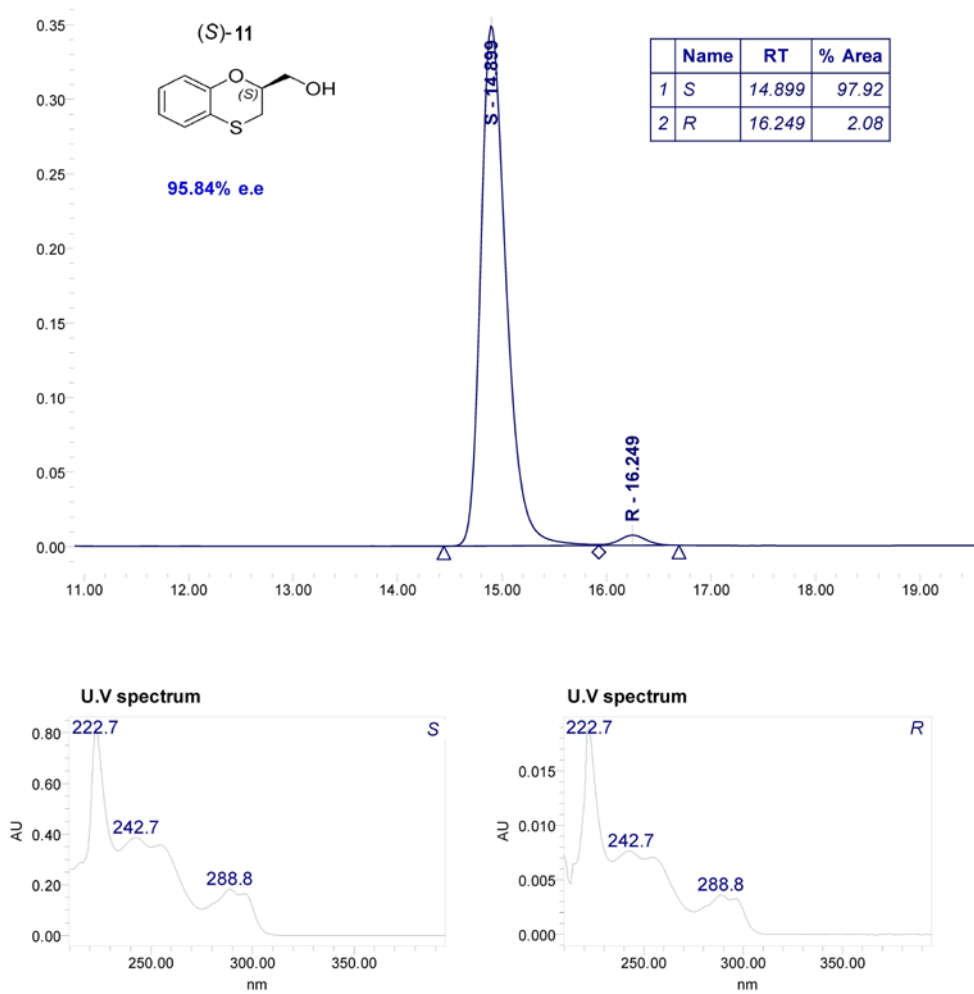


Figure S32

PAPER 4

.....Ewt t gpv'Qti cplk'U{ pvj guki'uwdo kwgf +

''

Stereospecific Alkylation of Substituted Adenines by the Mitsunobu Coupling Reaction under Microwave-Assisted Conditions

María E. García-Rubiño,^a María C. Núñez,^a Duane Choquesillo-Lazarte,^b Juan M. García-Ruiz,^b Yolanda Madrid,^c Miguel A. Gallo,^a Joaquín M. Campos^{a,*}

^a*Departamento de Química Farmacéutica y Orgánica, Facultad de Farmacia, c/ Campus de Cartuja s/n, 18071 Granada (Spain).*

^b*Laboratorio de Estudios Cristalográficos, IACT-CSIC, Factoría Española de Cristalización, Avenida de las Palmeras 4, 18100 Armilla (Granada, Spain).*

^c*Centro de Instrumentación Científica, Universidad de Granada, Edificio Mecenas. Campus Universitario de Fuente Nueva. 18071 Granada (Spain).*

Abstract: A novel and efficient synthetic method has been developed for the preparation of alkylated amino purines [6-(*N,N*-dimethyl)-, 2-chloro-6-(*N*-methyl)-, and 6-(*N*-methyl)-adenines] with achiral and chiral 3,4-dihydro-2*H*-1,5-benzoxathiepin-3-ol by the Mitsunobu reaction under microwave-assisted conditions. This reaction reveals a complete inversion of the carbon stereogenic centre of the secondary alcohol, after the ring contraction from the seven- to the six-membered ring, giving a homochiral alkylated purine. Fifty novel purine derivatives have been prepared. The alkylation sites have been determined by 2D NMR techniques and for three compounds have been confirmed by X-ray crystallography. The *N*'-9/*N*'-3 regioselectivity can be qualitatively justified mainly by the electronic effects of the substituents at positions 2' and 6' of the purine ring.

Keywords: 6-Aminoadenines, benzo-fused heterocycles, electronic effects, epichlorohydrin, microwave-assisted conditions, Mitsunobu reaction, stereospecific alkylation.

1. INTRODUCTION

In the search for new compounds of therapeutic interest, purine derivatives are very important for their possible interaction with many biological targets. We have reported the fast microwave-assisted synthesis of a series of (*RS*)-6-substituted-7 or 9-(2,3-dihydro-5*H*-1,4-benzodioxepin-3-yl)-7*H* or -9*H*-purines, with the advantage of the selective preparation of the *N*-3' or *N*-9' regioisomers [1, 2]. Following our interest in the topic, pyrimidines and purine alkylated products seem to be attractive structures in connection with antiproliferative studies [2, 3].

The essential biological functions of *N*-substituted adenine compounds have naturally led to extensive interest in the synthesis of a wide variety of alkylated purine systems as potential analogues or antagonists of naturally occurring adenine derivatives [4]. Direct alkylation of adenine, of its simple derivatives, and of its metal salts is the dominant synthetic route to *N*-substituted adenines, largely because of the convenience and simplicity of such reactions.

There are reports dealing with the alkylation reaction of adenine under the Mitsunobu conditions [5]. In a continuation of our studies on multident heterocyclic nucleophiles, we examined the alkylation of adenine using a variety of alkylating agents [6]. The wide variety of alkylation conditions involved in the literature reports makes it difficult to discern what influence the structural features of the alkylating agent has on the alkylation pattern (site or regioselectivity). To overcome this problem we have used a typical and standardized alkylation conditions to study the reaction of several substituted adenines [6-(*N,N*-dimethyl)-, 2-chloro-6-(*N*-methyl)-, and 6-(*N*-methyl)-adenines] with racemic 3,4-dihydro-2*H*-1,5-benzoxathiepin-3-ol, and its two enantiomers through the Mitsunobu reaction under microwave conditions. We have described a series of eleven 2- and 6-substituted (*RS*)-9'-(2,3-dihydro-1,4-benzoxathiin-3-ylmethyl)-9*H*-purine derivatives (**1-11**) (Figure 1), by applying a standard Mitsunobu protocol that led to a six-membered ring contraction from (*RS*)-3,4-dihydro-2*H*-1,5-benzoxathiepin-3-ol via an episulfonium intermediate [7].

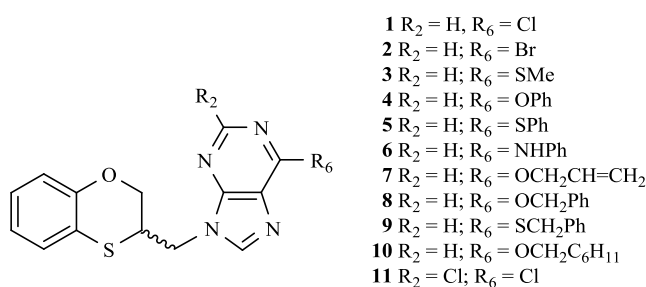


Figure 1. 2- And 6-substituted (*RS*)-9'-(2,3-dihydro-1,4-benzoxathiin-3-ylmethyl)-9'*H*-purine derivatives obtained by the Mitsunobu reaction.

We wish to report herein the reactivity of the racemic and enantiomers of 3,4-dihydro-2*H*-1,5-benzoxathiepin-3-ol (**12**) and several adenines, such as 6-(*N,N*-dimethyl)adenine, 2-chloro-6-(*N*-methyl)adenine, and 6-(*N*-methyl)adenine. The results will be interpreted in terms of multident nucleophile reactivity and S_N2 transition state structures for the alkylations. These concepts should allow more confident prediction of the effects that variations in structural features and conditions will have on the alkylation pattern of adenine derivatives during the varied syntheses of alkylated purines.

2. RESULTS AND DISCUSSION

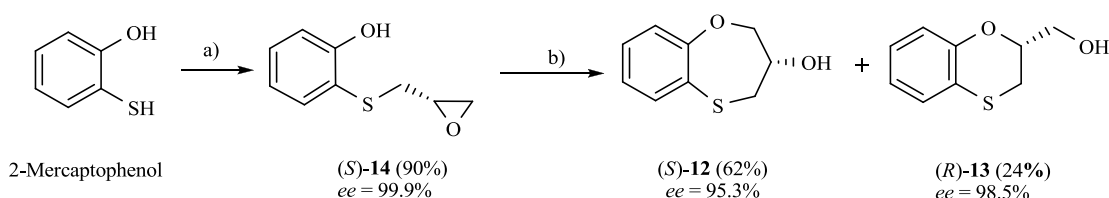
2.1. Synthesis of (*RS*)-, (*R*)- and (*S*)-3,4-Dihydro-2*H*-1,5-Benzoxathiepin-3-ol (**12**), and (*RS*)-, (*S*)- and (*R*)-2,3-Dihydro-1,4-Benzoxathiin-2-Methanol (**13**)

Three-carbon (C-3) epoxides bearing halide substituents are highly versatile synthetic building blocks because each carbon is functionalized and a potential site of nucleophilic attack. Epichlorohydrin, in particular, is a readily available C-3 unit that is widely employed in organic and polymer synthesis [8]. Compound (*RS*)-, (*R*)- and (*S*)-**14** were synthesized under microwave irradiation, 140 °C, 10 min, except that racemic epichlorohydrin was changed for their enantiomers. Both (*RS*)- and (*S*)-**14** were obtained with a 97% yield. Compound (*R*)-**14** was not isolated and the procedure for obtaining (*R*)-**12** and (*S*)-**13** was different (see Scheme 2). Nevertheless, the different experimental workup led to (*S*)-**12** and (*R*)-**13**, without isolating (*R*)-**14** (Scheme 2).

Microwave Temperature (°C)	Microwave Time	(<i>RS</i>)- 14 (% yield)	(<i>RS</i>)- 12 (% yield)	(<i>RS</i>)- 13 (% yield)
130	10 min	60		
130	30 min	86		
140	10 sec	50		
140	20 sec	75		
140	10 min	90		
150	10 min	45	16	
150	30 min		13	6

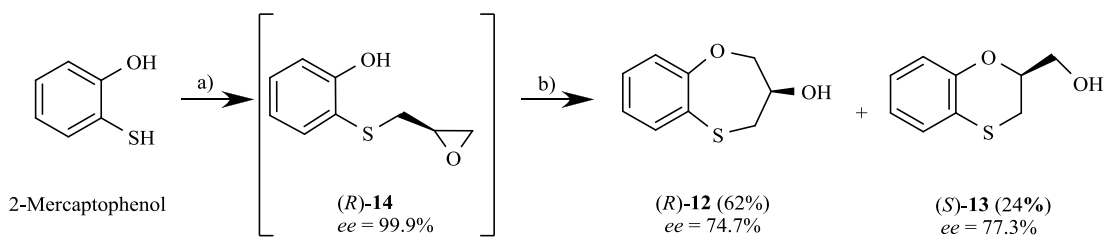
Table 1. Different reaction conditions between 2-mercaptophenol and epichlorohydrin in order to improve the yield for the preparation of (*RS*)-**14**., These experimental conditions are also used for the synthesis of the enantiomers (*R*)-**14** and (*S*)-**14**.

When 2-mercaptophenol is reacted with (*R*)-epichlorohydrin, (*S*)-**14** is obtained (90%) with an *ee* = 99.9% with *complete inversion* of the stereocentre of its oxirane moiety [9]. This implies a complete regioselective process as a consequence of the nucleophilic attack of the sulfanyl anion at the less hindered face of the oxirane moiety of (*R*)-epichlorohydrin, thus resulting in (*S*)-**14** with an excellent *ee*. After removing DMF *in vacuo* and purification by flash column chromatography of the reaction crude, heating (*S*)-**14** with NaOH in H₂O at 100 °C gives the cyclization products, (*S*)-**12** (62% yield, *ee* = 95.3%) and the six-membered primary alcohol (*R*)-**13** (24% yield, *ee* = 98.5%) (Scheme 1). The absolute configuration of these intermediates and of the final products of this manuscript has been established as previously [9].



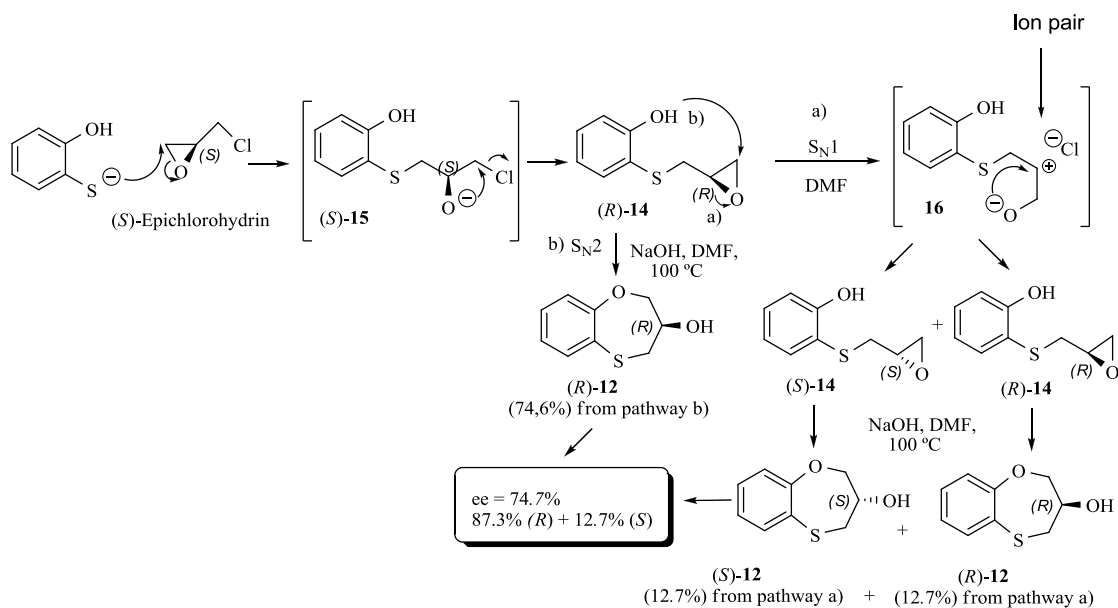
Scheme 1. Reagents and conditions: a) (*R*)-epichlorohydrin, pyridin, MW, 140 °C, 10 min, DMF; b) NaOH, H₂O, 100 °C, 24 hours.

Scheme 2 shows the different stereochemical behaviour when the experimental workup was modified using (*S*)-epichlorohydrin: although pathway a) is exactly the same as that shown in Scheme 1, compound (*R*)-**14** is not isolated and NaOH (1 equiv.) and more DMF is added (instead of water) and the resulting solution is heated at 100 °C for 24 hours. After removing DMF and subsequent flash chromatography, (*R*)-**12** (62%, *ee* = 74.7%) and (*S*)-**13** (24%, *ee* = 77.3%) are obtained.



Scheme 2. Reagents and conditions: a) (*S*)-epichlorohydrin, pyridin, MW, 140 °C, 10 min, DMF; b) without isolating (*R*)-**14**, NaOH, DMF, 100 °C, 24 hours.

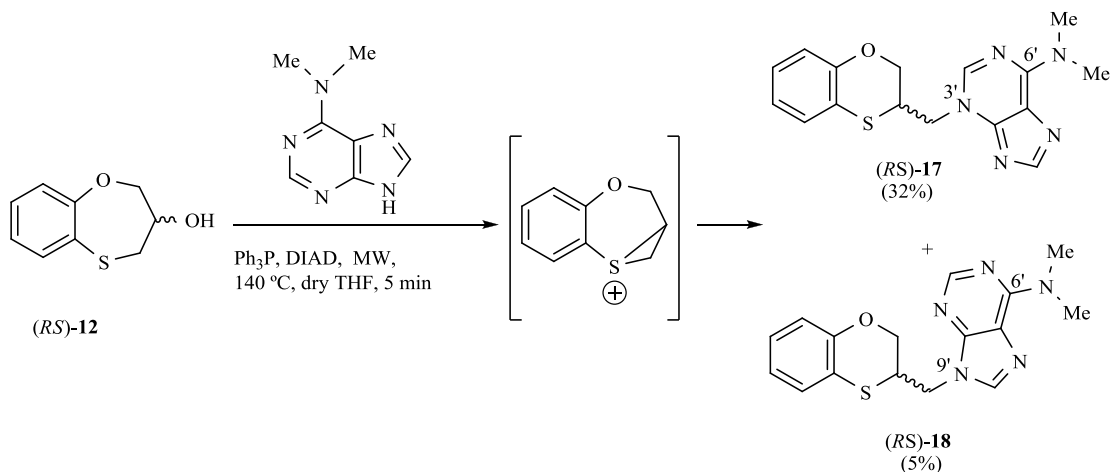
The interpretation for the formation of (*R*)-**12** [and for (*S*)-**13** would be very similar] with a marked erosion of its optical purity in relation to the method outlined in Scheme 2 could be rationalized in Scheme 3. The formation of (*R*)-**14** follows the same pattern for (*S*)-**14**. Nevertheless, HCl is present in the DMF solution and makes the solvent more polar (higher ionic strength) and generally increases S_N1 rates through the ion pair **16**, resulting in racemisation [10]. Accordingly, (*R*)-**14** follows two different pathways, *i.e.*, a preferential S_N2 process [presumably with an excellent ee, [see Scheme 1 with (*R*)-epichlorohydrin], and a S_N1 process with concomitant racemization. A non-solvating polar solvent such as DMF is necessary for the S_N1 mechanism to occur. Finally, cyclization of pure (*R*)-**14** [route a) of Scheme 3] and (*S*)-**14** with NaOH in DMF at 100 °C leads to (*R*)-**12** and (*S*)-**12**, respectively, the enantiomer (*R*)-**12** being produced mainly through pathway a) and to a lesser extent *via* pathway b), whilst (*S*)-**12** is formed only through pathway b) (Scheme 3).



Scheme 3. Tentative explanation for the formation of both (*R*)-**12** major and (*S*)-**12** minor compounds, starting from (*S*)-epichlorohydrin, without isolating (*S*)-**15**. Formations of the minor (*S*)-**13** compound is not included for simplicity, although the mechanism is similar.

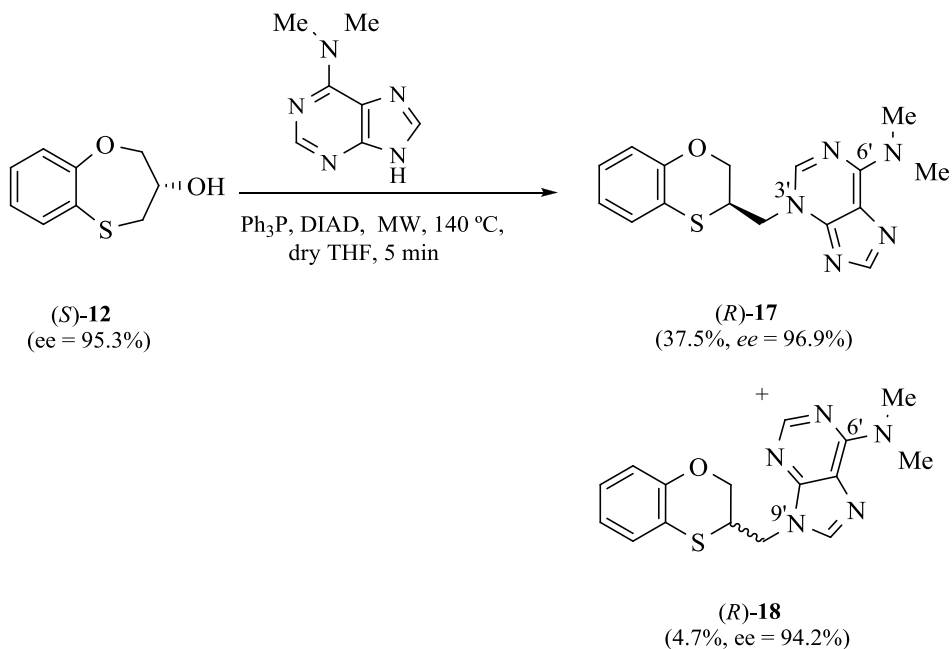
2.2. Reactivity between racemic and enantiomers of 4-dihydro-2H-1,5-benzoxathiepin-3-ol and 6-(*N,N*-dimethyl)adenine

Scheme 4 shows the reaction pattern between (*RS*)-**12** and 6-(*N,N*-dimethyl)adenine under microwave irradiation, the *N*-3' alkylated purine (*RS*)-**17** (32%) being the major compound, and the minor one the *N*-9' alkylated purine (*RS*)-**18** (5%).



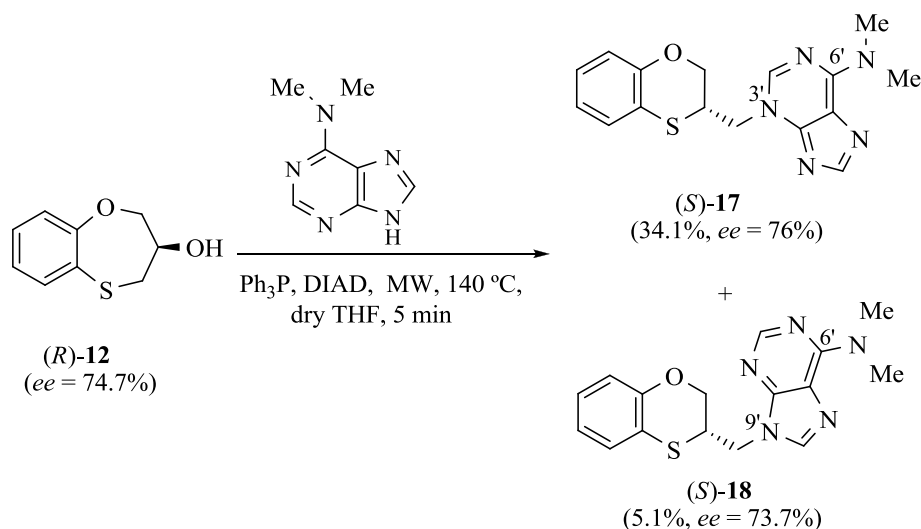
Scheme 4. Preparation of the (*RS*)-3'-alkylated-6'-(*N,N*-dimethyl)adenine (**17**) and (*RS*)-9'-alkylated-6'-(*N,N*-dimethyl)adenine (**18**).

On the other hand, when (*S*)-**12** (*ee* = 95.3%) is the starting reactant, the only product obtained is (*R*)-**17** (37.5%), with an excellent *ee* (*ee* = 96.9%) (Scheme 5):



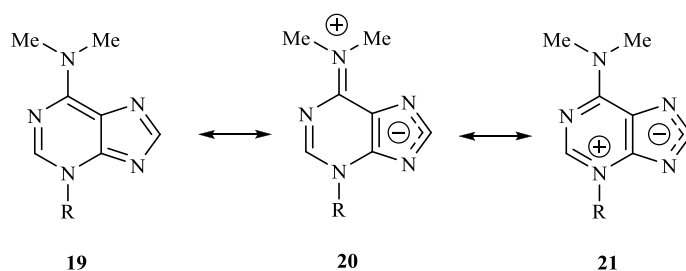
Scheme 5. Reactivity between (*S*)-**12** and 6-(*N,N*-dimethyl)adenine.

When (*R*)-**12** (*ee* = 74.7%) is the starting reactant, (*S*)-**17** (34.1%, *ee* = 74.7%) and (*S*)-**18** (5.1%, *ee* = 73.7%) are obtained (Scheme 6):



Scheme 6. Reactivity between (*R*)-**12** and 6-(*N,N*-dimethyl)adenine.

The structure of 3'-substituted-6'-(*N,N*-dimethyl)adenine is conditioned by the importance of the dipolar iminium form (**20**) to the possible resonance hybrid [**19** ↔ **20** ↔ **21**] (Scheme 7), as suggested by non-equivalent *N*-6'Me₂ signals in the ¹H NMR spectrum of (*RS*)-**18** and is substantiated by its X-ray analysis (Figure 3). This is consistent with the electron-releasing nature of the dimethylamino group: $\sigma_p = -0.83$ [11], -0.82 [12]. Although the electronic influence of the NMe₂ group on *N*-1' and *N*-3' of the purine nucleus is basically the same (its mesomeric electron-releasing effect is much more important than its inductive electron-withdrawing one), the lack of alkylation of 6-(*N,N*-dimethyl)adenine at its *N*-1' site could be attributed to the steric hindrance caused by the dimethylamino group. On the other hand, its steric influence also avoids the alkylation at the *N*-7' position of the adenine-derived compound.



Scheme 7. Resonance hybrid **20** can explain the alkylation at the *N*-3' atom of the purine moiety, as suggested by non-equivalent 6'-NMe₂ signals in the ¹H NMR spectrum of **17**.

The structure of (*RS*)-**17** has been determined by ¹H, ¹³C NMR, HMBC (Figure 2), HSQC and X-ray crystallography (Figures 1 and 2, Supporting Information). Heteronuclear Multiple Bond Correlation (HMBC) gives 2-bond and 3-bond information, *i.e.*, which of the ¹H are 2-bonds or 3-bonds away from a particular ¹³C. Heteronuclear Single Quantum Coherence (HSQC) and gives 1-bond information, *i.e.*, which ¹H is attached to which ¹³C. The combination of ¹H NMR and ¹H-¹³C HSQC spectra is very powerful, and will often allow complete assignment of all protons in a molecule. In the HMBC experiment to three bonds, the following two correlations are important: a) the first one between the

exocyclic methylene group and the quaternary carbon C-4' (common carbon atom that is correlated through three bonds to CH-2' and CH-8') of (*RS*)-**17**; and the second one: b) between the exocyclic methylene group and CH-2' (which is correlated to C-6') of the purine ring. This correlation proves unequivocally that the linkage between the six-membered moiety and the purine base takes place through N-3' in (*RS*)-**17** (Figure 2).

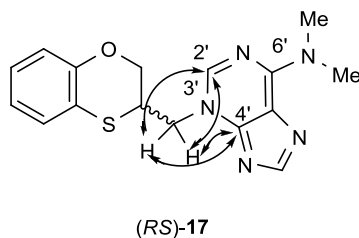


Figure 2. Representation of the HMBC interactions (with double-tipped arrows) that are observed between the exocyclic methylene group and the purine atoms.

Nevertheless, when the same reaction is carried out between (*RS*)-**12**, (*R*)-**12** (*S*)-**12**, and 6-(*N,N*-dimethyl)adenine, the 3-substitution on 6'-(*N,N*-dimethyl)adenine is still preferred, and is accompanied by the formation of the corresponding 9'-substituted-6'-(*N,N*-dimethyl)adenine (*S*)-**18**. Miyaki and Shimizu [13] found that, after chromatographic separation of the reaction products, the benzylation of 6-(*N,N*-dimethyl)adenine with PhCH₂OH in THF gave the *N*-3'- (36%) and *N*-9'-regioisomers (64%).

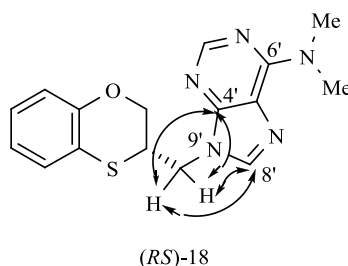


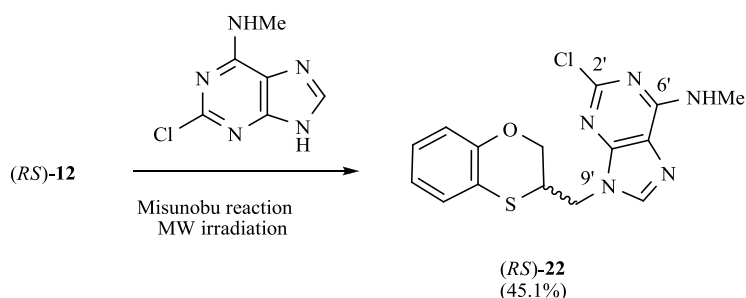
Figure 3. Representation of the HMBC interactions (with double-tipped arrows) that were observed between the exocyclic methylene group and the purine atoms

The structure of (*RS*)-**18**, (*R*)-**18** and (*S*)-**18**, has been determined by ¹H, ¹³C NMR, HMBC and HSQC (Figure 3). In the HMBC experiment to three bonds the following two correlations are important: a) the first one between the exocyclic methylene group and the quaternary carbon C-4' (common carbon atom that is correlated through three bonds to CH-2' and CH-8') of (*RS*)-**18**; and the second one: b) between the exocyclic methylene group and CH-8' (which is the CH group that is not correlated with C-6') of the purine ring. This correlation proves unequivocally that the linkage between the six-membered moiety and the purine base takes place through N-9' in (*RS*)-**18**, (*R*)-**18** and (*S*)-**18** (Figure 3).

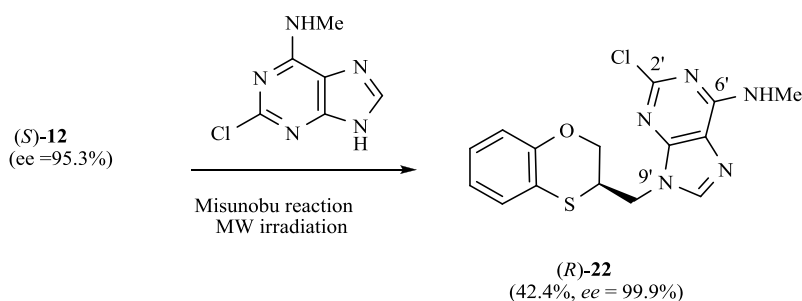
2.3. Reactivity between racemic and enantiomers of 4-dihydro-2*H*-1,5-benzoxathiepin-3-ol and 2-chloro-6-(*N*-methyl)adenine

The Mitsunobu coupling of allylic and benzylic alcohol with adenine and 6-chloro-2-aminopurine has been reported previously with good *N*-9' selectivity [14]. However, poor to modest yield (20-60%) and limited substrate scope were observed [15], which significantly limits the application of this method.

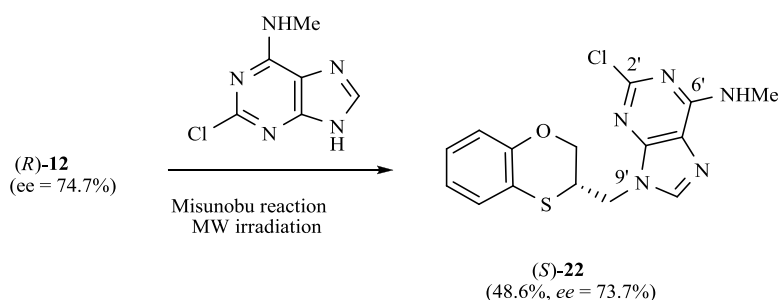
Currently, there is no detailed study regarding the Mitsunobu coupling between 6-chloro-2-aminopurine and a secondary alcohol through neighbouring-group participation.



Scheme 8. Preparation of $(RS)\text{-}N\text{-9'}$ -alkylated-2-chloro-6-(N -methyl)adenine $(RS)\text{-22}$.



Scheme 9. Preparation of $(R)\text{-}N\text{-9'}$ -alkylated-2-chloro-6-(N -methyl)adenine $(R)\text{-22}$.



Scheme 10. Preparation of $(S)\text{-}N\text{-9'}$ -alkylated-2-chloro-6-(N -methyl)adenine $(S)\text{-22}$.

The methylamino moiety is an electron-releasing group with a σ_p similar to that of the dimethylamino moiety $\{[\sigma_p(\text{MeHN}) = -0.76$ [12]; $\sigma_p(\text{Me}_2\text{N}) = -0.83$ [11], 0.82 [12] $\}$ and then favours the nucleophilicity of the $N\text{-3'}$ atom of purine. However the presence of an electron-withdrawing atom such as the chlorine one $\{\sigma_I(\text{Cl}) = 0.47$ [16] $\}$ neutralizes the effect of the methylamino group and consequently the alkylation site moves to the $N\text{-9'}$ atom of 2-chloro-6-(N -methyl)adenine, *i.e.*, going from **17** and **18** to **22**, there is a shift of π -electron-density from the six- to the five-membered ring of purine. On the other hand no exocyclic N -alkylation takes place due to its relatively weak nucleophilic character.

The structures of (*RS*)-**22**, (*R*)-**22** and (*S*)-**22** have been determined by ^1H , ^{13}C NMR, and HMBC. In the HMBC experiment to three bonds (Figure 6), the interaction between the exocyclic methylene group, and *CH*-8' and *C*-4' of the purine ring proves unequivocally that the linkage between the six-membered moiety and the purine base takes place through *N*-9' in (*RS*)-**22** (Figure 4).

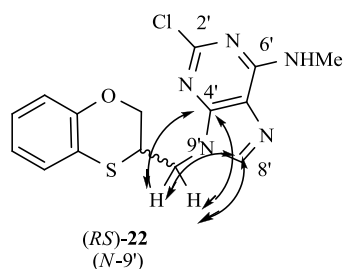
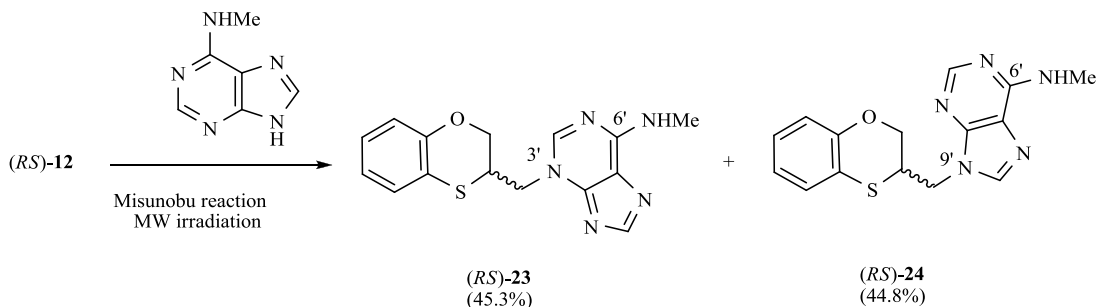


Figure 4. Representation of the HMBC interactions (with double-tipped arrows) that were observed between the exocyclic methylene group and the purine atoms of (*RS*)-**22**.

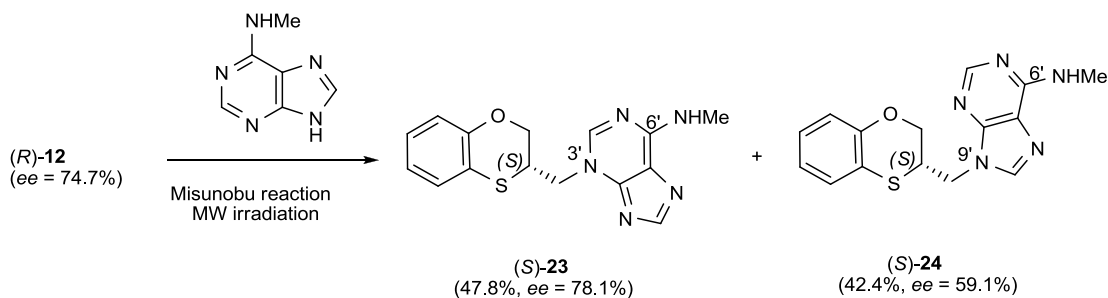
The stereochemistry of (*S*)-**22** shows the complete inversion of the stereogenic alcohol centre (Figure S26). This result is consistent with the $\text{S}_{\text{N}}2$ mechanism and strongly enhances the application of the reported method as a general approach for the stereospecific synthesis of alkylated purines.

2.4. Reactivity between Racemic and Enantiomers of 4-Dihydro-2*H*-1,5-Benzoxathiepin-3-ol and 6-(*N*-Methyl)Adenine

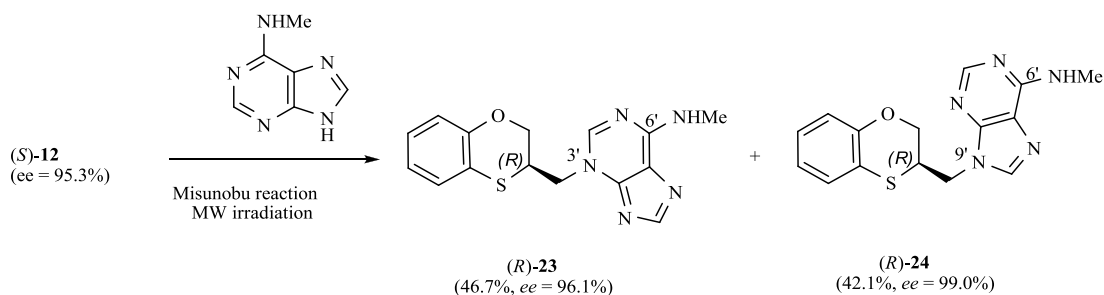
Reactions between (*RS*)-**12**, (*R*)-**12** or (*S*)-**12** and 6-(*N*-methyl)adenine produce the same regioisomers (*N*-9' and *N*-3') and the sum of the global yields of the final products are in the same range [90.1% from (*RS*)-**12**, 88.8% from (*S*)-**12** and 90.1% from (*R*)-**12**] (Schemes 12,13 and 14). Reactions between (*RS*)-**12** and 6-(*N*-methyl)adenine produce the regioisomers (*RS*)-**23** (*N*-3': 45.3%) and (*RS*)-**24** (*N*-9': 44.8%), (*S*)-**23** (*N*-3': 47.8%) and (*S*)-**24** (*N*-9': 42.4%), (*R*)-**23** (*N*-3': 46.7%) and (*R*)-**24** (*N*-9': 42.1%). This is consistent with the electron-releasing nature of the methylamino group: $\sigma_p = -0.76$ [12]. In the case of the NHMe group compared to the NMe_2 one, the lesser electron-releasing power of the former in relation to the latter explains the approximately equal amount of both *N*'-3 (**17**) and *N*'-9 (**18**) regioisomers in the reaction between **12** and 2-chloro-6-(*N*-methyl)adenine, whilst in the case of *N,N*-dimethyladenine the major product is the *N*-3' regioisomer **17**, being the ratio *N*-9'/*N*-3' $\approx 7/1$.



Scheme 11. Preparation of (*RS*)-*N*-3'-alkylated-6'-(*N*-methyl)adenine (**23**), (*RS*) *N*-9'-alkylated-6'-(*N*-methyl)adenine (**24**).



Scheme 12. Preparation of (*S*)-*N*-3'-alkylated-6'-(*N*-methyl)adenine (**23**), (*S*)-*N*-9'-alkylated-6'-(*N*-methyl)adenine (**24**).



Scheme 13. Preparation of (*R*)-*N*-3'-alkylated-6'-(*N*-dimethyl)adenine (**23**) and (*R*)-*N*-9'-alkylated-6'-(*N*-dimethyl)adenine (**24**).

In the HMBC experiment to three bonds, are the following two correlations is important: a) the first one between the exocyclic methylene group and the quaternary carbon C-4' (common carbon atom which is correlated to *CH*-2' and *CH*-8') of (*RS*)-**23**; and the second one: b) between the exocyclic methylene group and *CH*-2' (which is the group that is not correlated with C-6') of the purine ring. This correlation proves unequivocally that the linkage between the six-membered moiety and the purine base takes place through *N*-3' in (*RS*)-**23** (Figure 5).

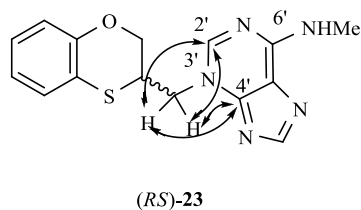


Figure 5. Representation of the HMBC interactions (with double-tipped arrows) that were observed between the exocyclic methylene group and the purine atoms.

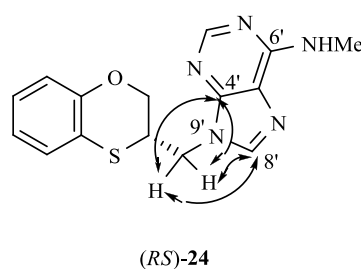


Figure 6. Representation of the HMBC interactions (with double-tipped arrows) that were observed between the exocyclic methylene group and the purine atoms

The structures of (*RS*)-**24**, (*R*)-**24** and (*S*)-**24**, have been determined by ^1H , ^{13}C NMR, HMBC and HSQC (Figure 10). In the HMBC experiment to three bonds the following two correlations are outstanding: a) the first one between the exocyclic methylene group and the quaternary carbon C-4' (common carbon atom that is correlated through three bonds to CH-2' and CH-8') of (*RS*)-**24**; and the second one: b) between the exocyclic methylene group and CH-8' (which is the CH group that is not correlated with C-6') of the purine ring. This correlation proves unequivocally that the linkage between the six-membered moiety and the purine base takes place through *N*-9' in (*RS*)-**24**, (*R*)-**24** and (*S*)-**24** (Figure 6).

Neither 2,6-diaminopurine nor 6,8-dichloro-2-(methylthio)purine, as possible purine bases in the Mitsunobu coupling, produced the desired coupling products with the secondary alcohols **12**. These results may be due to the poor solubility of the bases.

NMR data for adenine-derived compounds

The ^1H NMR (CDCl_3) CH-2' signal of adenines in *N*-9' isomer **18** is shifted upfield in relation to the corresponding signal of the *N*-3' isomer **17**, whereas the CH-8' signal of **18** is shifted downfield compared with the corresponding signal of *N*-3' (**17**). In summary, the signals of both proton atoms are interchanged in both regioisomers. Compounds **23** and **24** cannot be compared because the ^1H NMR spectra of both **23** and **24** were registered in different deuterated solvents (CDCl_3 and $\text{DMSO}-d_6$, respectively)

The chemical shift (CDCl_3) of the carbon atom for CH-2' group follows the same tendency in *N*-3' (**17** and **23**) and *N*-9' (**18** and **24**) isomers. These signals are shifted downfield in *N*-3' isomers (δ 141.9-145.1 ppm) compared with the corresponding signals in *N*-9' isomers (**18** and **24**, δ 152.8-152.4 ppm).

The chemical shift (CDCl_3) of the carbon atom for CH-8' are shifted upfield in *N*-9' (**18** and **24**) isomers (δ 152.7-148.2 ppm) compared with the corresponding signals in *N*-3' isomers (**17** and **23**, δ 139.5-140.7 ppm).

3. CONCLUSIONS

The purine motif is a privileged structure. Its biological relevance and the occurrence of the purine heterocycle in nature make it an attractive target for chemical modification. Adenine stands out against the ample variety of purines, among other things as a component of DNA and RNA. We have described herein a novel and efficient synthetic method between alkylated amino purines [6-(*N,N*-dimethyl)-, 2-chloro-6-(*N*-methyl)-, and 6-(*N*-methyl)-adenines] and the achiral and chiral secondary alcohol 3,4-dihydro-2*H*-1,5-benzoxathiepin-3-ol by the Mitsunobu reaction under microwave-assisted conditions. We have confirmed that the sulfur atom of the seven-membered heterocycle exerts a remarkable neighbouring group effect on its reaction with several amino-purines, producing a complete $\text{S}_{\text{N}}2$ inversion at the stereogenic centre after the corresponding ring-contraction. Alkylation of purines usually results in the formation of *N*-9' and *N*-7' alkylpurines, the *N*-9' regioisomer being normally the major product [3a-d]. Nevertheless, *N*-3' regioisomers of purines are scarcely reported, especially when a chiral moiety is linked to the purine ring, and these substructures could lead to specific inhibitors of known biological targets and pave the way to new inhibitors or antagonists of targets that have yet to be described. Several biological studies on the chiral and achiral molecules described here are underway and the corresponding results will be communicated in due course.

4. EXPERIMENTAL SECTION

Melting points were taken in open capillaries on an Electrothermal melting point apparatus and are uncorrected. Analytical thin layer chromatography was performed using Merck Kieselgel 60 F254 aluminum sheets, the spots being developed with UV light ($\lambda = 254$ nm). All evaporation was carried out *in vacuo* with a Büchi rotary evaporator and the pressure controlled by a Vacuubrand CVCII apparatus. For flash chromatography, Merck silica gel 60 with a particle size of 0.040-0.063 mm (230-400 mesh ASTM) was used. Nuclear magnetic resonance spectra have been carried out at the Centro de Instrumentación Científica (CIC) /Universidad de Granada (UGR), and recorded on a 400MHz ^1H and 100MHz ^{13}C NMR Varian NMR-System-TM400 or 300 MHz ^1H and 75MHz ^{13}C NMR Varian Inova-TM spectrometers at ambient temperature. Chemical shifts (δ) are quoted in parts per million (ppm) and are referenced to the residual solvent peak. Signals are designated as follows: s, singlet; b s, broad singlet; d, doublet; dd, doublet of doublets; ddd, double doublet of doublets; t, triplet; m, multiplet. The HMBC spectra were measured using a pulse sequence optimized for 10 Hz (inter-pulse delay for the evolution of long-range couplings: 50 ms) and a 5/3/4 gradient combination. In this way, direct responses (J couplings) were not completely removed. High-resolution Nano-Assisted Laser Desorption/Ionization (NALDI-TOF) or Electrospray Ionization (ESITOF) mass spectra were carried out on a Bruker Autoflex or a Waters LCT Premier Mass Spectrometer, respectively. Small scale microwave-assisted synthesis was carried out in an Initiator 2.0 single-mode microwave instrument producing controlled irradiation at 2.450 GHz (Biotage AB, Uppsala). Reaction time refers to hold time from 130 °C to 160 °C, not to total irradiation time. The temperature was measured with an IR sensor outside the reaction vessel. Anhydrous DMF was purchased from VWR International Eurolab. Anhydrous conditions were performed under argon. 6-(*N,N*-dimethyl)-, 2-chloro-6-(*N*-methyl)-, and 6-(*N*-methyl)-adenines were purchased from Aldrich. Analytical HPLC was carried out by using a HPLC WaterTM 2996 Photodiode Array Detector, WaterTM 600 Controller and WaterTM 600 Pump with a semipreparative column CHIRALPAK[®] IA. Optical rotations were measured for solutions in CH_2Cl_2 (1 dm tube) with a Jasco DIP-370 polarimeter.

Preparation of (S)-14.

A mixture of 2-mercaptophenol (0.2 g, 1.59 mmol) and 60% pyridin (0.13 g, 1.59 mmol) in anhydrous DMF (2.5 mL) under argon, was stirred at room temperature for 5 minutes, (*R*)-epichlorohydrin (0.17 g, 1.83 mmol) was added and the resulting mixture was irradiated at 140 °C for additional 10 minutes. The mixture was cooled, and the pH was fixed to 2-3 with HCl (1N). The DMF was removed *in vacuo*, and the residue was extracted ($\text{H}_2\text{O}/\text{CH}_2\text{Cl}_2$). Organic layers were combined and dried Na_2SO_4 . After filtration the solvent was removed *in vacuo* and the crude was purified by flash column chromatography using a 8/2 hexane/EtOAc mixture. (S)-14 (90%) was obtained as a brownish syrups [3f,7]

Preparation of (S)-12 and (R)-13.

Compounds (S)-12 and (R)-13 were synthesized according to our previously reported procedure [3f,7].

Preparation of (R)-12 and (S)-13.

The procedure was exactly the same as described for (S)-14, but compound (R)-14 was not isolated and NaOH (0.063 g, 1.59 mmol) and more DMF (10 mL) were added (instead of water) and the resulting solution was heated at 100 °C for 24 hours. After removing DMF and subsequent flash chromatography, (R)-12 (62%, *ee* = 74.7%) and (S)-13 (24%, *ee* = 77.3%) were obtained.

(R)-3,4-Dihydro-2H-1,5-benzoxathiepin-3-ol [(R)-12]: 45% yield, 74.7 ee, $[\alpha]_D^{25} +28.3$ (*c* 1.0 in CH_2Cl_2); HPLC analysis: Chiralpak IA, hexane/ CH_2Cl_2 = 65/35, flow rate 1.0 mL/min, $\lambda = 250$ nm, t_R (R)-10 = 9.854 min, t_R (S)-10 = 11.114 min [Fig. (S2)].

(S)-3,4-Dihydro-2H-1,5-benzoxathiepin-3-ol [(S)-12]: 45% yield, 95.3 ee, $[\alpha]_D^{25} -36.7$ (*c* 1.0 in CH_2Cl_2); HPLC analysis: Chiralpak IA, hexane/ CH_2Cl_2 = 65/35, flow rate 1.0 mL/min, $\lambda = 250$ nm, t_R (R)-12 = 10.896 min, t_R (S)-12 = 12.079 min [Fig. (S3)].

(R)-2,3-Dihydro-1,4-benzoxathiin-2-methanol [(R)-13]: 20% yield, 98.54 ee, $[\alpha]_D^{25} +38.1$ (*c* 1.0 in CH_2Cl_2); HPLC analysis: Chiralpak IA, hexane/ CH_2Cl_2 = 65/35, flow rate 1.0 mL/min, $\lambda = 250$ nm, t_R (S)-13 = 14.682 min, t_R (R)-13 = 15.890 min [Fig. (S5)].

(S)-2,3-Dihydro-1,4-benzoxathiin-2-methanol [(S)-13]: 20% yield, 77.3 ee, $[\alpha]_D^{25}$ -33.2 (*c* 1.0 in CH₂Cl₂); HPLC analysis: Chiralpak IA, hexane/CH₂Cl₂ = 65/35, flow rate 1.0 mL/min, λ = 250 nm, t_R (S)-13 = 14.899, t_R (R)-13 = 16.249 min [Fig. (S6)].

(S)-3-[(2-Hydroxyphenyl)thio]-1,2-epoxypropane [(S)-14]: 90% yield, 99.9 ee, $[\alpha]_D^{25}$ = -46.6 (*c* 1.0 in CH₂Cl₂); HPLC analysis: Chiralpak IA, hexane/2-propanol = 90/10, flow rate 1.0 mL/min, λ = 250 nm, t_R (R)-14 = 11.346 min [Fig. (S8)].

(RS)-6-*N,N*-Dimethyl-3-(2,3-dihydro-1,4-benzoxathiin-3-ylmethyl)-3*H*-purine [(RS)-17]: White solid; 39.2% yield, mp 152-154 °C. ¹H NMR (500 MHz, CDCl₃): δ 7.96 (s, 1H, H8'), 7.87 (s, 1H, H2') 7.03 (m, 2H, CH-aromatics), 6.89 (m, 2H, CH-aromatics), 4.65 (dd, J_{gem} = 13.7 Hz, J_2 = 6.9 Hz, 1H-exocyclic), 4.42 (dd, J_{gem} = 13.7 Hz, J_2 = 8.4 Hz, 1H-exocyclic), 4.37 (dd, J_{gem} = 12.0 Hz, J_2 = 2.9 Hz, 1H, CH-2), 4.27 (d, J_{gem} = 12.0 Hz, J_2 = 1.7 Hz, 1H, CH-2), 4.18 (m, 1H, CH-3), 3.92 (b s, 3H, CH₃), 3.35 (b s, 3H, CH₃). ¹³C NMR (125 MHz, CDCl₃): δ 153.85 (C-6'), 152.74 (1H, CH-8'), 151,27(C8a), 150.11 (C4'), 141.92 (CH-2'), 128.15, 126.38, 122.74, 118.91 (CH-aromatics), 122.02 (C5'), 115.92 (C4a), 66.14 (CH₂-2), 51.77 (CH₂-exocyclic), 39.95 (CH₃), 38.23 (CH₃), 36.99 (CH-3). HR LSIMS calcd. for C₁₆H₁₇N₅OS [M+H]⁺ 328.1232, found 328.1238.

(R)-6-*N,N*-Dimethyl-3-(2,3-dihydro-1,4-benzoxathiin-3-ylmethyl)-3*H*-purine [(R)-17]: 37.5% yield, 96.88 ee, $[\alpha]_D^{25}$ -135.49 (*c* 1.0 in CH₂Cl₂); HPLC analysis: Chiralpak IA, hexane/EtOH = 80/20, flow rate 1.0 mL/min, λ = 250 nm, t_R (R)-17 = 17.84 min, t_R (S)-17 = 23.430 min. [Fig. (S10)].

(S)-6-*N,N*-Dimethyl-3-(2,3-dihydro-1,4-benzoxathiin-3-ylmethyl)-3*H*-purine [(S)-17]: 36.1% yield, 76 ee, $[\alpha]_D^{25}$ +104.74 (*c* 1.0 in CH₂Cl₂); HPLC analysis: Chiralpak IA, hexane/EtOH = 80/20, flow rate 1.0 mL/min, λ = 250 nm, t_R (R)-17 = 18.242 min, t_R (S)-17 = 23.055 min. [Fig. (S11)].

(RS)-6-*N,N*-Dimethyl-9-(2,3-dihydro-1,4-benzoxathiin-3-ylmethyl)-9*H*-purine [(RS)-18]: White solid; 4.7% yield, mp 170-180 °C. ¹H NMR (500 MHz, CDCl₃): δ 8.33 (s, 1H, H2') 7.71 (s, 1H, H8') 7.02 (m, 2H, CH-aromatics), 6.89 (m, 2H, CH-aromatics), 4.50 (dd, J_{gem} = 14.2 Hz, J_2 = 7.7 Hz, 1H-exocyclic), 4.41 (dd, J_{gem} = 14.2 Hz, J_2 = 7.7 Hz, 1H-exocyclic), 4.25 (m, 2H, CH₂-2), 3.89 (m, 1H, CH-3), 3.52 (b s, 6H, N(CH₃)₂). ¹³C NMR (126 MHz, CDCl₃): δ 155.25 (C6'), 152.84 (CH-2'), 151,45(C8a), 150.65 (C4'), 139.15 (CH-8'), 127.96, 126.17, 122.63, 118.82 (CH-aromatics), 120.54 (C5'), 116.25 (C4a), 65.91 (CH₂-2), 45.76 (CH₂-exocyclic), 37.72 (CH-3), 29.93 (CH₃). HR LSIMS calcd. for C₁₆H₁₇N₅OS [M+H]⁺ 328.1232 found 328.1233.

(R)-6-*N,N*-Dimethyl-9-(2,3-dihydro-1,4-benzoxathiin-3-ylmethyl)-9*H*-purine [(R)-18]: 4.7% yield, 94.2 ee, $[\alpha]_D^{25}$ +67.1 (*c* 0.34 in MeOH); HPLC analysis: Chiralpak IA, hexane/EtOH = 80/20, flow rate 1.0 mL/min, λ = 250 nm, t_R (R)-18 = 20.053 min, t_R (S)-18 = 25.755 min. [Fig. (S13)].

(S)-6-*N,N*-Dimethyl-9-(2,3-dihydro-1,4-benzoxathiin-3-ylmethyl)-9*H*-purine [(S)-18]: 5.1% yield, 73.7 ee, $[\alpha]_D^{25}$ -53.3 (*c* 0.34 in MeOH); HPLC analysis: Chiralpak IA, hexane/EtOH = 80/20, flow rate 1.0 mL/min, λ = 250 nm, t_R (R)-18 = 20.050 min, t_R (S)-18 = 25.764 min. [Fig. (S14)].

General procedure for the microwave-assisted synthesis of homochiral compounds 17, 18, 22, 23 and 24: DIPAD (2 equiv) was slowly added to a suspension of the benzo-fused six-membered ring 12 (1 equiv), the purine base (1 equiv) and triphenylphosphine (1.1 equiv) in dry THF (5ml/mmol) in a microwave vial, cooled in an ice-bath. The vial was sealed and microwave irradiated at a temperature of 140 °C for 10 minutes. Compounds 17, 18, 22, 23 and 24 were purified by flash column chromatography on silica gel using a mixture of hexane/EtOAc (5/1 → 0/1) and then CH₂Cl₂/MeOH (10/0.1 → 7/3). The solvent was evaporated *in vacuo* and the products were obtained pure.

(RS)-2-Chloro,6-*N*-methyl-9-(2,3-dihydro-1,4-benzoxathiin-3-ylmethyl)-9*H*-purine [(RS)-22]: white solid; 45.1% yield, mp 117-119°C. ¹H NMR (500 MHz, CDCl₃): δ 7.73 (s, 1H, H-8'), 7.02 (m, 2H, CH-aromatics), 6.88 (m, 2H, CH-aromatics), 4.47 (dd, J_{gem} = 14.2 Hz, J_2 = 7.5 Hz, 1H, CH₂ exocyclic), 4.37 (dd, J_{gem} = 14.2 Hz, J_2 = 8.0 Hz, 1H, CH₂ exocyclic), 4.25 (m, 2H-CH₂-2), 4.23 (ddd, J_1 = 12.0 Hz, J_2 = 3.0 Hz J_3 = 1.9 Hz, 1H, CH-3), 3.82 (m, 1H, CH-3), 3.11 (m, 3H, CH₃). ¹³CNMR (126 MHz, CDCl₃): δ 155.86 (C-6'), 151,19 (C-8a), 149.63 (C-4'), 140.45 (CH-8'), 127.84, 126.20, 122.64, 118.74 (CH-aromatics), 118.21 (C5'), 115.72 (C4a), 65.70 (CH₂-2), 45.79 (CH₂-exocyclic), 37.53 (CH-3), 27.75 (CH₃). HR LSIMS calcd. for C₁₆H₁₄N₅ClOS [M+H]⁺ 348.0686 found 348.0687.

(R)-2-Chloro,6-N-methyl-9-(2,3-dihydro-1,4-benzoxathiin-3-ylmethyl)-9H-purine [(R)-22]: 42.4% yield, 99.9 ee, $[\alpha]_D^{25} +33.59$ (*c* 0.65 in DMSO); HPLC analysis: Chiralpak IA, hexane/EtOH = 80/20, flow rate 1.0 mL/min, $\lambda = 250$ nm, $t_R(R)-22 = 13.353$ min. [Fig. (S16)].

(S)-2-Chloro,6-N-methyl-9-(2,3-dihydro-1,4-benzoxathiin-3-ylmethyl)-9H-purine [(S)-22]: 48.6% yield, 73.68 ee, $[\alpha]_D^{25} -22.8$ (*c* 0.65 in DMSO); HPLC analysis: Chiralpak IA, hexane/EtOH = 80/20, flow rate 1.0 mL/min, $\lambda = 250$ nm, $t_R(R)-22 = 13.352$ min, $t_R(S)-22 = 14.560$ min. [Fig. (S17)].

(RS)-6-N-Methyl-3-(2,3-dihydro-1,4-benzoxathiin-3-ylmethyl)-3H-purine [(RS)-23]: white solid; mp 199-201 °C, 45.3% yield, $^1\text{H NMR}$ (500 MHz, CDCl_3) δ 8.07 (s, 1H, H2'), 8.00 (s, 1H, H8'), 7.04 (m, 2H), 6.90 (m, 2H), 4.72 (dd, $J = 13.8, 6.7$ Hz, 1H, CH_2 -exocyclic), 4.49 (dd, $J = 13.7, 8.5$ Hz, 1H, CH_2 -exocyclic), 4.40 (dd, $J = 12.1, 2.8$ Hz, 1H, CH_2 -2), 4.31 (dd, $J = 12.1, 1.5$ Hz, 1H, CH_2 -2), 4.08 (m, 1H-3), 3.24 (m, 3H, CH_3). $^{13}\text{C NMR}$ (126 MHz, CDCl_3): δ 153.86 (C-6'), 151.20 (C8a), 148.24 (CH-8'), 147.47 (C4'), 145.14 (CH-2'), 128.10, 126.59, 122.91, 118.96 (CH-aromatics), 117.19 (C-5'), 115.12 (C4a), 65.90 (CH_2 -2), 51.81 (CH_2 -exocyclic), 37.11 (CH-3), 28.32 (CH_3). HR (LSIMS) calcd. for $\text{C}_{15}\text{H}_{16}\text{N}_5\text{OS}$ $[\text{M}+\text{H}]^+$ 314.1076, found 314.1076.

(R)-6-N-Methyl-3-(2,3-dihydro-1,4-benzoxathiin-3-ylmethyl)-3H-purine [(R)-23]: 96.14 ee, $[\alpha]_D^{25} -61.81$ (*c* 1.0 in MeOH); HPLC analysis: Chiralpak IA, hexane/EtOH = 80/20, flow rate 1.0 mL/min, $\lambda = 250$ nm, $t_R(R)-23 = 14.343$ min, $t_R(S)-23 = 17.190$ min. [Fig. (S19)].

(S)-6-N-Methyl-3-(2,3-dihydro-1,4-benzoxathiin-3-ylmethyl)-3H-purine [(S)-23]: 47.8% yield, 78.14 ee, $[\alpha]_D^{25} +59.43$ (*c* 1.0 in MeOH); HPLC analysis: Chiralpak IA, hexane/EtOH = 80/20, flow rate 1.0 mL/min, $\lambda = 250$ nm, $t_R(R)-23 = 15.004$ min, $t_R(S)-23 = 17.299$ min. [Fig. (S20)].

(RS)-6-N-Methyl-9-(2,3-dihydro-1,4-benzoxathiin-3-ylmethyl)-9H-purine [(RS)-24]: white solid; mp 168-170 °C, 42.1% yield, $^1\text{H NMR}$ (600 MHz, $\text{DMSO}-d_6$): δ 8.23 (s, 1H, H-2'), 8.13 (s, 1H, H-8'), 7.06 (m, 2H), 6.90 (m, 2H), 4.56 (dd, $J_{\text{gem}} = 14.1$ Hz, $J_2 = 6.7$ Hz, 1H, CH_2 -exocyclic), 4.40 (dd, $J_{\text{gem}} = 14.1$ Hz, $J_2 = 8.2$ Hz, 1H, CH_2 -exocyclic), 4.28 (m, 2H, CH_2 -2), 4.12 (m, 1H, H-3), 2.95 (s, 3H, CH_3). $^{13}\text{C NMR}$ (151 MHz, $\text{DMSO } d_6$): δ 154.85 (C-6') 152.48 (CH-2'), 151.07 (C8a), 148.55 (C-4'), 140.77 (CH-8'), 127.29, 125.65, 122.10, 118.26 (CH-aromatics), 118.99 (C-4'), 116.45 (C4a), 65.95 (CH_2 -2), 44.65 (CH_2 -exocyclic), 37.82(CH-3), 26.96 (CH_3). HR (LSIMS) calcd. for $\text{C}_{15}\text{H}_{16}\text{N}_5\text{OS}$ $[\text{M}+\text{H}]^+$ 314.1076, found 314.1077.

(R)-6-N-Methyl-9-(2,3-dihydro-1,4-benzoxathiin-3-ylmethyl)-9H-purine [(R)-24]: 99.02 ee, $[\alpha]_D^{25} -65.83$ (*c* 1.0 in MeOH); HPLC analysis: Chiralpak IA, hexane/EtOH = 80/20, flow rate 1.0 mL/min, $\lambda = 250$ nm, $t_R(R)-24 = 26.679$ min, $t_R(S)-24 = 29.495$ min. [Fig. (S22)].

(S)-6-N-Methyl-9-(2,3-dihydro-1,4-benzoxathiin-3-ylmethyl)-9H-purine [(S)-24]: 42.4% yield, 59.1 ee, $[\alpha]_D^{25} +38.3$ (*c* 1.0 in MeOH); HPLC analysis: Chiralpak IA, hexane/EtOH = 80/20, flow rate 1.0 mL/min, $\lambda = 250$ nm, $t_R(R)-24 = 26.576$ min, $t_R(S)-24 = 28.695$ min. [Fig. (S23)].

CONFLICTS OF INTEREST NOTIFICATION

There are no potential conflicts of interest to report

ACKNOWLEDGMENTS

This study was supported by the Instituto de Salud Carlos III (Fondo de Investigación Sanitaria) through the project no. PI10/00592. The M.E. G.-R. FPU grant AP2007-02954 from the Ministerio de Ciencia e Innovación of Spain is greatly acknowledged. The project "Factoría de Cristalización" Consolider Ingenio-2010 (CSD2006-00015) provided X-ray structural facilities for this work.

SUPPORTIVE/SUPPLEMENTARY MATERIAL

Supplementary material is available on the publishers Web site along with the published article: Chromatograms and RMN studies of enantiomers of **12** and **13**, and racemates and enantiomers of **17** and **22-24** are provided. Crystal Structure of (*RS*)-**17**: CCDC 864711, (*R*)-**22**: CCDC 864709, (*RS*)-**24**: CCDC 864710.

REFERENCES

- [1] For the numbering of the compounds, the atoms of the benzodihetero six-membered rings are tagged with numbers without primes, while those of the purine bases are numbered with primes (').
- [2] Conejo-García, A.; Núñez, M.C.; Marchal, J.A.; Rodríguez-Serrano, F.; Aránega, A.; Gallo, M.A.; Espinosa, A.; Campos, J.M. Regioespecific Microwave-Assisted Synthesis and Cytotoxic Activity against Human Breast Cancer Cells of (*RS*)-6-Substituted-7- or 9-(2,3-Dihydro-5*H*-1,4-Benzodioxepin-3-yl)-7*H*- or -9*H*-Purines. *Eur. J. Med. Chem.*, **2008**, *43*, 1742-1748.
- [3] a) Díaz-Gavilán, M.; Gómez-Vidal, J.A.; Rodríguez-Serrano, F.; Marchal, J.A.; Caba, O.; Aránega, A.; Gallo, M.A.; Espinosa, A.; Campos, J.A. Anticancer Activity of (1,2,3,5-Tetrahydro-4,1-Benzoxazepine-3-yl)-Pyrimidines and -Purines against the MCF-7 Cell Line: Preliminary cDNA Microarray Studies. *Bioorg. Med. Chem. Lett.*, **2008**, *18*, 1457-1460; b) Núñez, M.C.; Díaz-Gavilán, M.; Conejo-García, A.; Cruz-López, O.; Gallo, M.A.; Espinosa, A.; Campos, J.M. Design, Synthesis and Anticancer Activity against the MCF-7 Cell Line of Benzo-Fused 1,4-Dihetero Seven- and Six-Membered Tethered Pyrimidines and Purines. *Curr. Med. Chem.*, **2008**, *15*, 2614-2631; c) Marchal, J.A.; Núñez, M.C.; Aránega, A.; Gallo, M.A.; Espinosa, A.; Campos, J.M. Acyclonucleosides, Modified *Seco*-Nucleosides, and Salicyl- or Catechol-Derived Acyclic 5-Fluorouracil *O,N*-Acetals: Antiproliferative Activities, Cellular Differentiation and Apoptosis. *Curr. Med. Chem.*, **2009**, *16*, 1166-1183; d) López-Cara, L.C.; Conejo-García, A.; Marchal, J.A.; Macchione, G.; Cruz-López, O.; Boulaiz, H.; García, M.A.; Rodríguez-Serrano, F.; Ramírez, A.; Cativiela, C.; Jiménez, A.I.; García-Ruiz, J.M.; Choquesillo-Lasarte, D.; Aránega, A.; Campos, J.M. New (*RS*)-Benzoxazepin-Purines with Antitumor Activity: The Chiral Switch from (*RS*)-2,6-Dichloro-9-[1-(*p*-Nitrobenzenesulfonyl)-1,2,3,5-Tetrahydro-4,1-Benzoxazepin-3-yl]-9*H*-Purine. *Eur. J. Med. Chem.*, **2011**, *46*, 249-258; e) Caba, O.; Díaz-Gavilán, M.; Rodríguez-Serrano, F.; Boulaiz, H.; Aránega, A.; Gallo, M.A.; Marchal, J.A.; Campos, J.M. Anticancer Activity and cDNA Microarray Studies of (*RS*)-1,2,3,5-Tetrahydro-4,1-Benzoxazepine-3-yl]-6-Chloro-9*H*-Purines, and Acyclic (*RS*)-*O,N*-Acetalic 6-Chloro-7*H*-Purines. *Eur. J. Med. Chem.*, **2011**, *46*, 3802-3809; f) Conejo-García, A.; García-Rubiño, M.E.; Marchal, J.A.; Núñez, M.C.; Ramírez, A.; Cimino, S.; García, M.A.; Aránega, A.; Gallo, M.A.; Campos, J.M. Synthesis and Anticancer Activity of (*RS*)-9-(2,3-Dihydro-1,4-Benzoxa-heteroin-2-ylmethyl)-9*H*-Purines. *Eur. J. Med. Chem.*, **2011**, *46*, 3795-3801; g) Caba, O.; Rodríguez-Serrano, F.; Díaz-Gavilán, M.; Conejo-García, A.; Álvarez, P.; Ortiz, R.; Martínez-Amat, A.; Campos, J.M.; Gallo, M.A.; Marchal, J.A.; Aránega, A. The Selective Cytotoxic Activity in Breast Cancer Cells by an Anthranilic Alcohol-Derived Acyclic 5-Fluorouracil *O,N*-Acetal is Mediated by Endoplasmic Reticulum Stress-induced Apoptosis. *Eur. J. Med. Chem.*, **2012**, *50*, 376-382.
- [4] Michelson, A.M. *The Chemistry of Nucleosides and Nucleotides*. Academic Press: London, **1963**.
- [5] a) Reynolds, J.; Kassiou, M. Recent Advances in the Mitsunobu Reaction: Modifications and Applications to Biologically Active Molecules. *Curr. Org. Chem.*, **2009**, *13*, 1610-1632; b) Li, W.; Yin, X.; Schneller, S.W. 5'-Fluoro-5'-deoxyaristeromycin. *Bioorg. & Med. Chem. Lett.*, **2008**, *18*, 220-222; c) Kumamoto, H.; Takahashi, N.; Shimamura, T.; Tanaka, H.; Nakamura, K.T.; Hamasaki, T.; Baba, M.; Abe, H.; Yano, M.; Kato, N. Synthesis of (±)-9-[*c*-4, *t*-5-bis(hydroxymethyl)cyclopent-2-en-r-1-yl]-9*H*-adenine (BCA) derivatives branched at the 4'

position based on intramolecular SH2' cyclization. *Tetrahedron*, **2008**, *64*, 1494-1505; d) Li, H.; Yoo, J.C.; Hong, J.H. Novel Synthesis and Anti-HIV Activity of 4'-Branched Exomethylene Carbocyclic Nucleosides Using a Ring-Closing Metathesis of Triene. *Nucleosides, Nucleotides & Nucleic Acids*, **2008**, *27*, 1238-1249.

- [6] a) Gómez, J.A.; Campos, J.; Marchal, J.A.; Trujillo, M.A.; Melguizo, C.; Prados, J.; Gallo, M.A.; Aránega, A.; Espinosa, A. Chemical Modifications on the Acyclic Moiety of [3-(2-Hydroxyethoxy)-1-Alkoxy]PropylNucleobases. 2. Differentiation and Growth Inhibition in Rhabdomyosarcoma Cells after Exposure to a Novel 5-Fluorouracil Acyclonucleoside. *Tetrahedron*, **1997**, *53*, 7319-7334; b) Núñez, M.C.; Pavani, M.G.; Díaz-Gavilán, M.; Rodríguez-Serrano, F.; Gómez-Vidal, J.A.; Marchal, J.A.; Aránega, A.; Gallo, M.A.; Espinosa, A.; Campos, J.M. Synthesis and Anticancer Activity Studies of Novel 1-(2,3-Dihydro-5H-1,4-Benzodioxepin-3-yl)Uracil and (6'-Substituted)-7 or 9-(2,3-Dihydro-5H-1,4-Benzodioxepin-3-yl)-7H-or 9H-purines. *Tetrahedron* **2006**, *62*, 11724-11733.
- [7] Díaz-Gavilán, M.; Conejo-García, A.; Cruz-López, O.; Núñez, M.C.; Choquesillo-Lazarte, D.; González-Pérez, J.M.; Rodríguez-Serrano, F.; Marchal, J.A.; Aránega, A.; Gallo, M.A.; Espinosa, A.; Campos, J.M. Synthesis and Anticancer Activity of (*RS*)-9-(2,3-Dihydro-1,4-Benzoxathiin-3-ylmethyl)-9H-Purines. *ChemMedChem*, **2008**, *3*, 127-135.
- [8] Huber, J.E. In *Encyclopedia of Reagents for Organic Synthesis*, Vol. 4; L.A. Paquette, Ed.; Wiley: New York, **1995**; p 2326.
- [9] García-Rubiño, M.E.; Conejo-García, A.; Núñez, M.C.; Carrasco, E.; García, M.A.; Choquesillo-Lazarte, D.; García-Ruiz, J.M.; Gallo, M.A.; Marchal, J.A.; Campos, J.M. Enantiospecific Synthesis of Heterocycles Linked to Purines: Different Apoptosis Modulation of Enantiomers in Breast Cancer Cells. *Curr. Med. Chem.*, accepted.
- [10] Smith, Michael B.; March, J. *March's Advanced Organic Chemistry*, 6th ed.; John Wiley & Sons, Inc: New Jersey, **2007**, pp 436-440.
- [11] McDaniel, D.H.; Brown, H.C. An Extended Table of Hammett Substituent Constants Based on the Ionization of Substituted Benzoic Acids. *J. Org. Chem.*, **1958**, *23*, 420-427.
- [12] Zakrzewska, A.; Gawinecki, R.; Kolehmainen, E.; Osmialowski, B. ¹³C-NMR Based Evaluation of the Electronic and Steric Interactions in Aromatic Amines. *Int. J. Mol. Sci.*, **2005**, *6*, 52-62.
- [13] Miyaki, M.; Shimizu, B. N.far. N alkyl and glycosyl migration of purines and pyrimidines. III. N.far. N alkyl and glycosyl migration of purine derivatives. *Chem. Pharm. Bull.*, **1970**, *18*, 1446-1456.
- [14] a) Kitade, Y.; Ando, T.; Yamaguchi, T.; Hori, A.; Nakanishi, M.; Ueno, Y. 4'-Fluorinated carbocyclic nucleosides: Synthesis and inhibitory activity against S-adenosyl-L-homocysteine hydrolase. *Bioorg. Med. Chem.*, **2006**, *14*, 5578-5583; b) Yang, M.; Schneller, S.W.; Korba, B.B. 5'-Homoneplanocin A Inhibits Hepatitis B and Hepatitis C. *J. Med. Chem.*, **2005**, *48*, 5043-5046; c) Yin, X.; Li, W.; Schneller, S.W. An efficient Mitsunobu coupling to adenine-derived carbocyclic nucleosides. *Tetrahedron Lett.*, **2006**, *47*, 9187-9189.
- [15] a) Yang, M.; Ye, W.; Schneller, S.W. Preparation of Carbocyclic S-Adenosylazamethionine Accompanied by a Practical Synthesis of (-)-Aristeromycin. *J. Org. Chem.*, **2004**, *69*, 3993-3996; b) Dyatkina, N.B.; Theil, F.; Von Janta-Lipinski, M. Stereocontrolled synthesis of the four stereoisomeric diphosphorylphosphonates of carbocyclic 2',3'-dideoxy-2',3'-didehydro-5'-noradenosine. *Tetrahedron*, **1995**, *51*, 761-772; c) Iyer, M.S.; Palomo, M.; Schilling, K.M.; Xie, Y.; Formanskii, L.; Zembower, D.E. Efficient reversed-phase purification of a hydrophobic

reaction product following Mitsunobu-mediated glycosylation. *J. Chromatogr. A*, **2002**, *944*, 263–267.

- [16] Taft Jr., R.W.; Lewis, I.C. Evaluation of Resonance Effects on Reactivity by Application of the Linear Inductive Energy Relationship. V. Concerning a σ_R Scale of Resonance Effects. *J. Am. Chem. Soc.*, **1959**, *81*, 5343-5352.

Supplementary Material

Current Organic Synthesis

Stereospecific Alkylation of Substituted Adenines by the Mitsunobu Coupling Reaction under Microwave- Assisted Conditions

María E. García-Rubiño,^a María C. Núñez,^a Duane Choquesillo-Lazarte,^b Juan M.
García-Ruiz,^b Yolanda Madrid,^c Miguel A. Gallo,^a Joaquín M. Campos,^{a*}

^a*Departamento de Química Farmacéutica y Orgánica, Facultad de Farmacia, c/ Campus de Cartuja, s/n, 18071
Granada (Spain)*

^b*Laboratorio de Estudios Cristalográficos, Instituto Andaluz de Ciencias de la Tierra (UGR - CSIC), Avenida de las
Palmeras N° 4, E-18100 Armilla, Granada (Spain)*

^c*Centro de Instrumentación Científica, Universidad de Granada, Edificio Mecenas. Campus Universitario de Fuente
Nueva. 18071 Granada (Spain).*

INDEX	Page
Figure S1: (<i>RS</i>)- 12	4
Figure S2: (<i>R</i>)- 12	5
Figure S3: (<i>S</i>)- 12	6
Figure S4: (<i>RS</i>)- 13	7
Figure S5: (<i>R</i>)- 13	8
Figure S6: (<i>S</i>)- 13	9
Figure S7: (<i>RS</i>)- 14	10
Figure S8: (<i>S</i>)- 14	11
Figure S9: (<i>RS</i>)- 17	12
Figure S10: (<i>R</i>)- 17	13
Figure S11: (<i>S</i>)- 17	14
Figure S12: (<i>RS</i>)- 18	15
Figure S13: (<i>R</i>)- 18	16
Figure S14: (<i>S</i>)- 18	17
Figure S15: (<i>RS</i>)- 22	18
Figure S16: (<i>R</i>)- 22	19
Figure S17: (<i>S</i>)- 22	20
Figure S18: (<i>RS</i>)- 23	21
Figure S19: (<i>R</i>)- 23	22
Figure S20: (<i>S</i>)- 23	23
Figure S21: (<i>RS</i>)- 24	24
Figure S22: (<i>R</i>)- 24	25
Figure S23: (<i>S</i>)- 24	26
¹ H NMR spectrum of 17 :.....	27
¹³ C NMR spectrum of 17 :.....	28
DEPT spectrum of 17 :.....	29
HSQC spectrum of 17 :.....	30
HMBC spectrum of 17 :.....	31
¹ H NMR spectrum of 18 :.....	32
¹³ C NMR spectrum of 18 :.....	33

DEPT spectrum of 18 :	34
HSQC spectrum of 18 :	35
HMBC spectrum of 18 :	36
¹ H NMR spectrum of 22 :.....	37
¹³ C NMR spectrum of 22 :	38
DEPT spectrum of 22 :	39
HSQC spectrum of 22 :	40
HMBC spectrum of 22 :	41
¹ H NMR spectrum of 23 :.....	42
¹³ C NMR spectrum of 23 :	43
DEPT spectrum of 23 :	44
HSQC spectrum of 23 :	45
HMBC spectrum of 23 :	46
¹ H NMR spectrum of 24 :.....	47
¹³ C NMR spectrum of 24 :	48
DEPT spectrum of 24 :	49
HSQC spectrum of 24 :	50
HMBC spectrum of 24 :	51
Figure S24: Crystal Structure (<i>RS</i>)- 17	52
Figure S25: Crystal Structure (<i>RS</i>)- 17	53
Figure S26: Crystal Structure (<i>R</i>)- 22	54
Figure S27: Crystal Structure (<i>R</i>)- 22	54
Figure S28: Crystal Structure (<i>RS</i>)- 24	55
Figure S29: Crystal Structure (<i>RS</i>)- 24	56

CHIRALPAK IA 250 x 4.6 mm
Flow rate: 1ml/min
room temperature
PDA 250.0 nm
n-hexane/dichloromethane 65/35 v/v

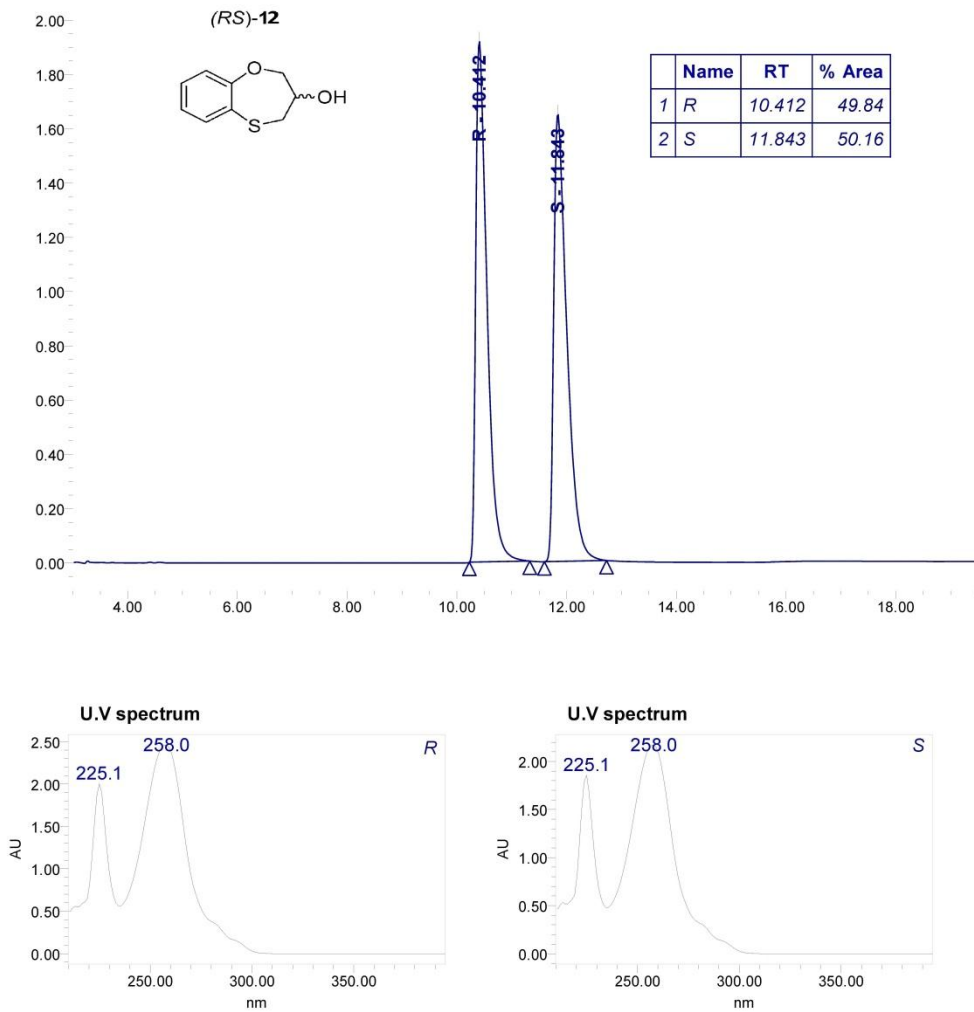


Figure S1

CHIRALPAK IA 250 x 4.6 mm
Flow rate: 1ml/min
room temperature
PDA 250.0 nm
n-hexane/dichloromethane 65/35 v/v

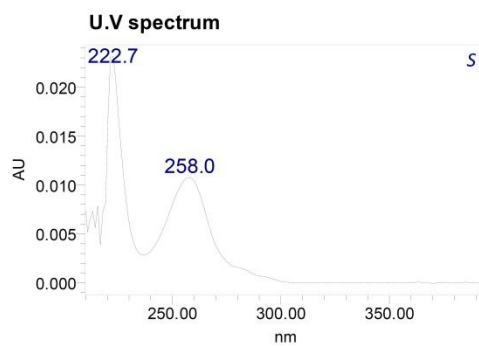
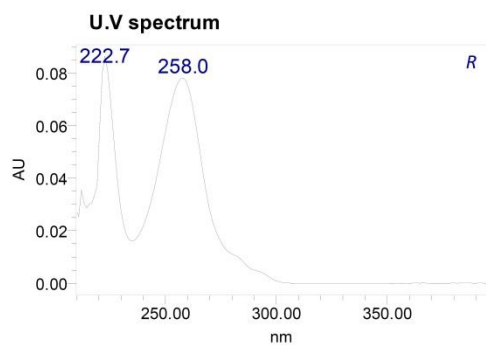
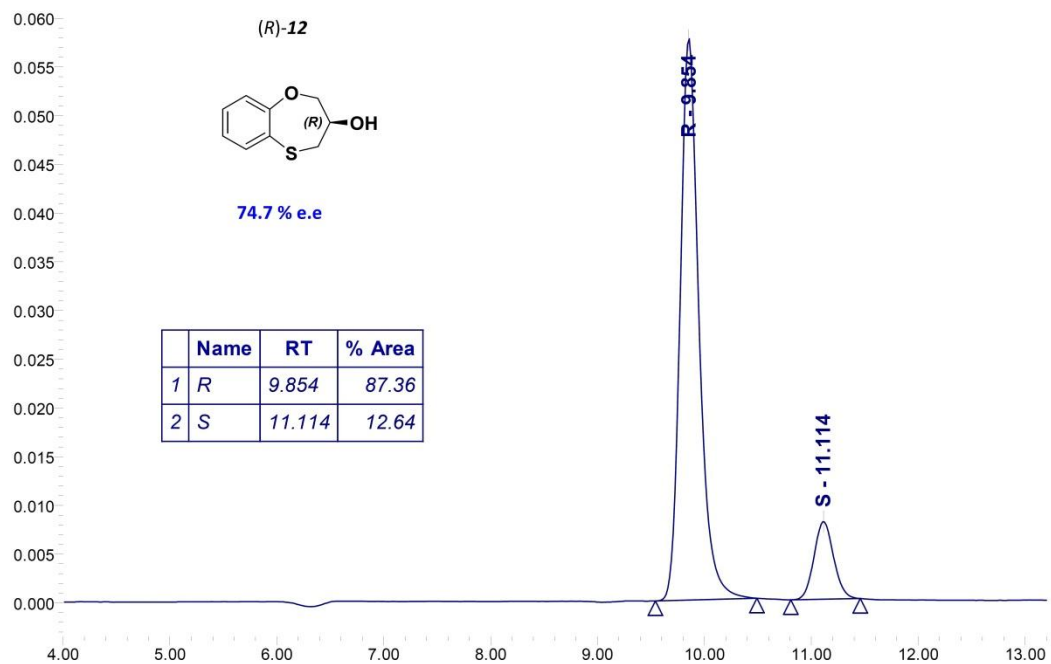


Figure S2

CHIRALPAK IA 250 x 4.6 mm
Flow rate: 1ml/min
room temperature
PDA 250.0 nm
n-hexane/dichloromethane 65/35 v/v

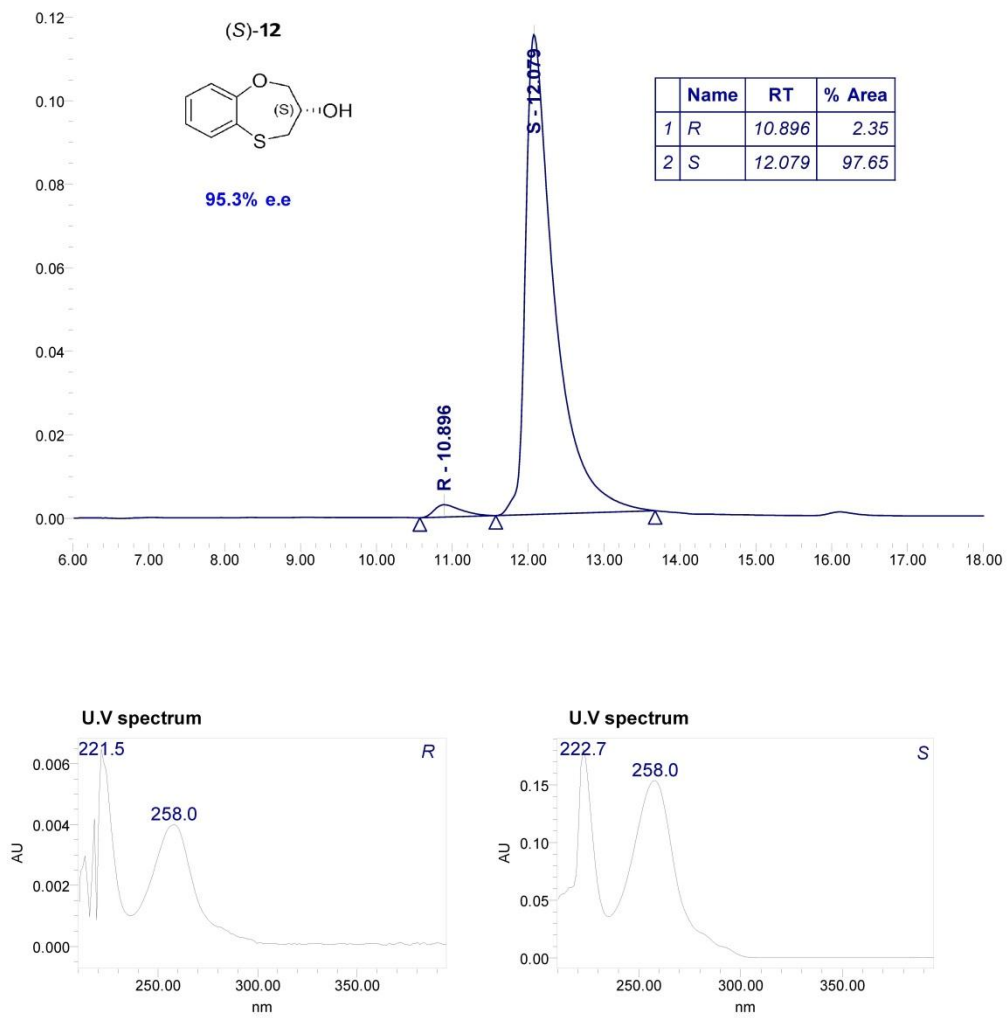


Figure S3

CHIRALPAK IA 250 x 4.6 mm
Flow rate: 1ml/min
room temperature
PDA 250.0 nm
n-hexane/dichloromethane 65/35 v/v

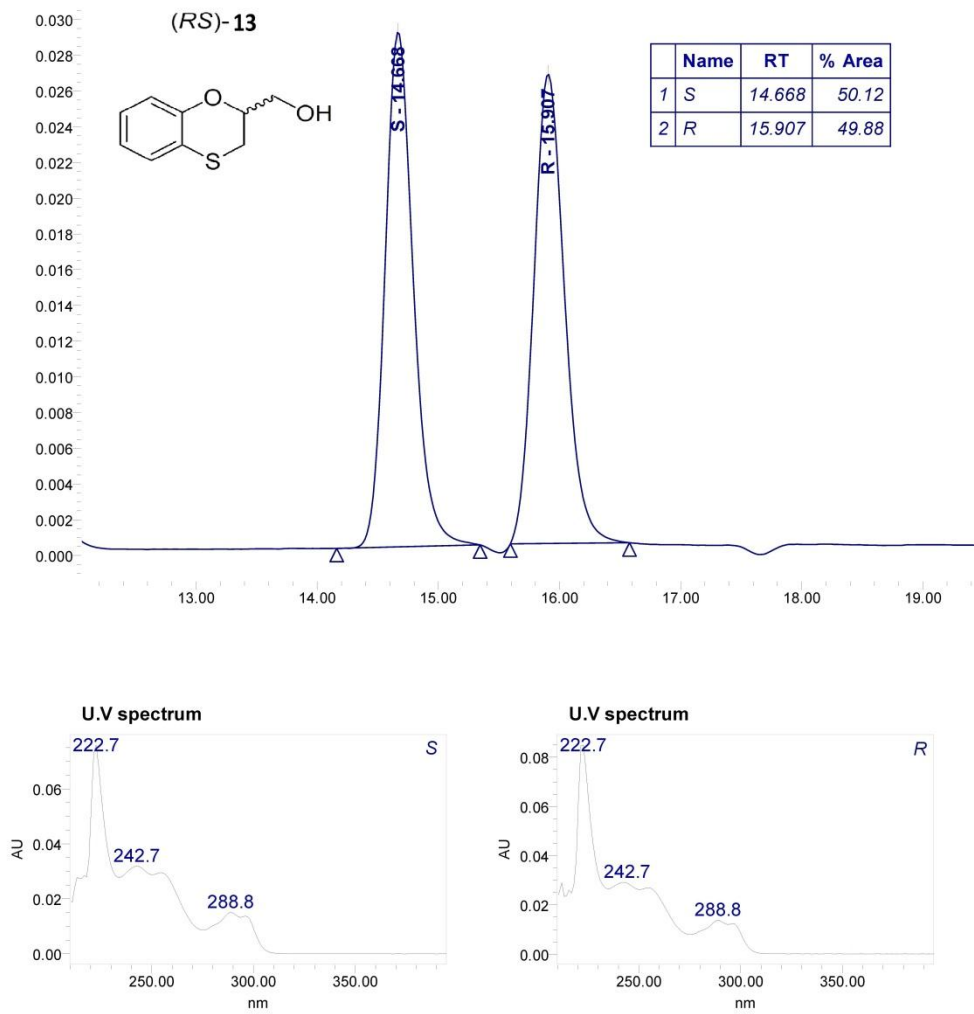


Figure S4

CHIRALPAK IA 250 x 4.6 mm
Flow rate: 1ml/min
room temperature
PDA 250.0 nm
n-hexane/dichloromethane 65/35 v/v

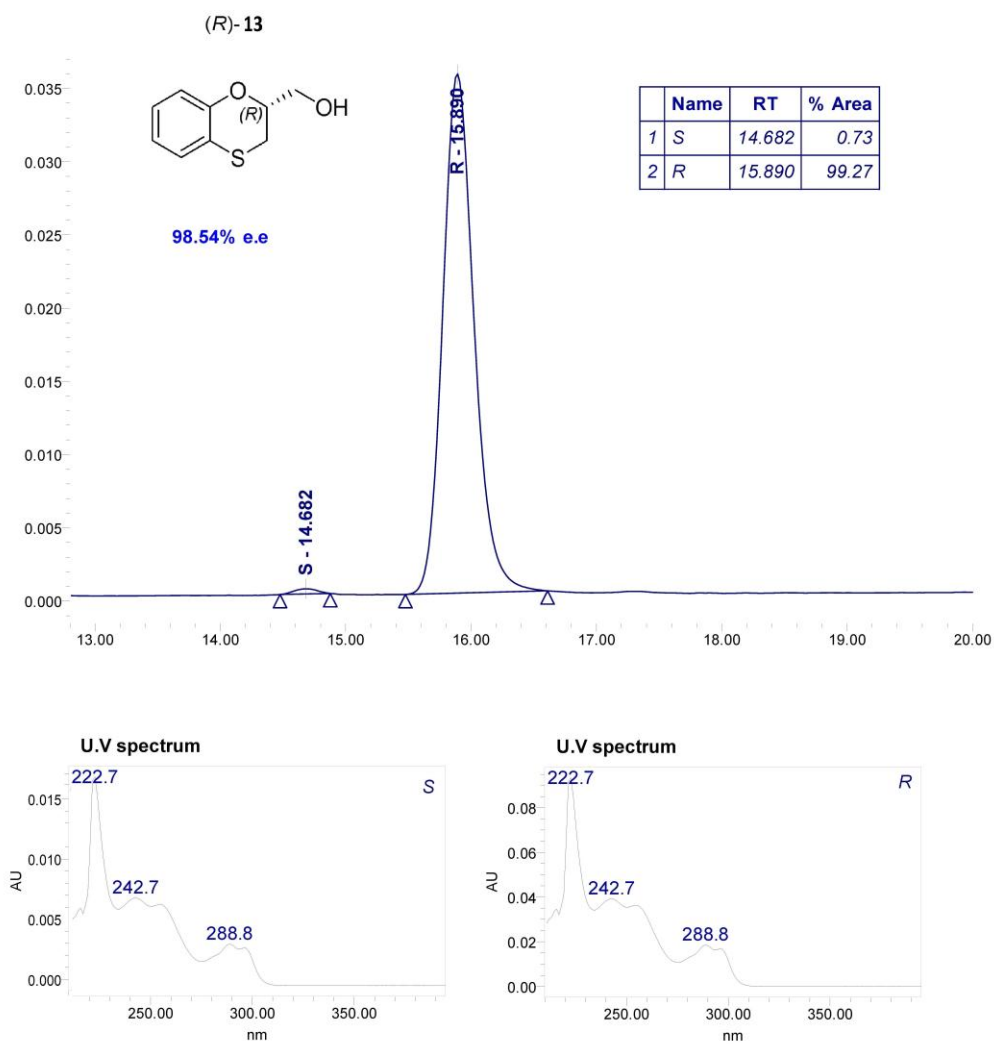


Figure S5

CHIRALPAK IA 250 x 4.6 mm
Flow rate: 1ml/min
room temperature
PDA 250.0 nm
n-hexane/dichloromethane 65/35 v/v

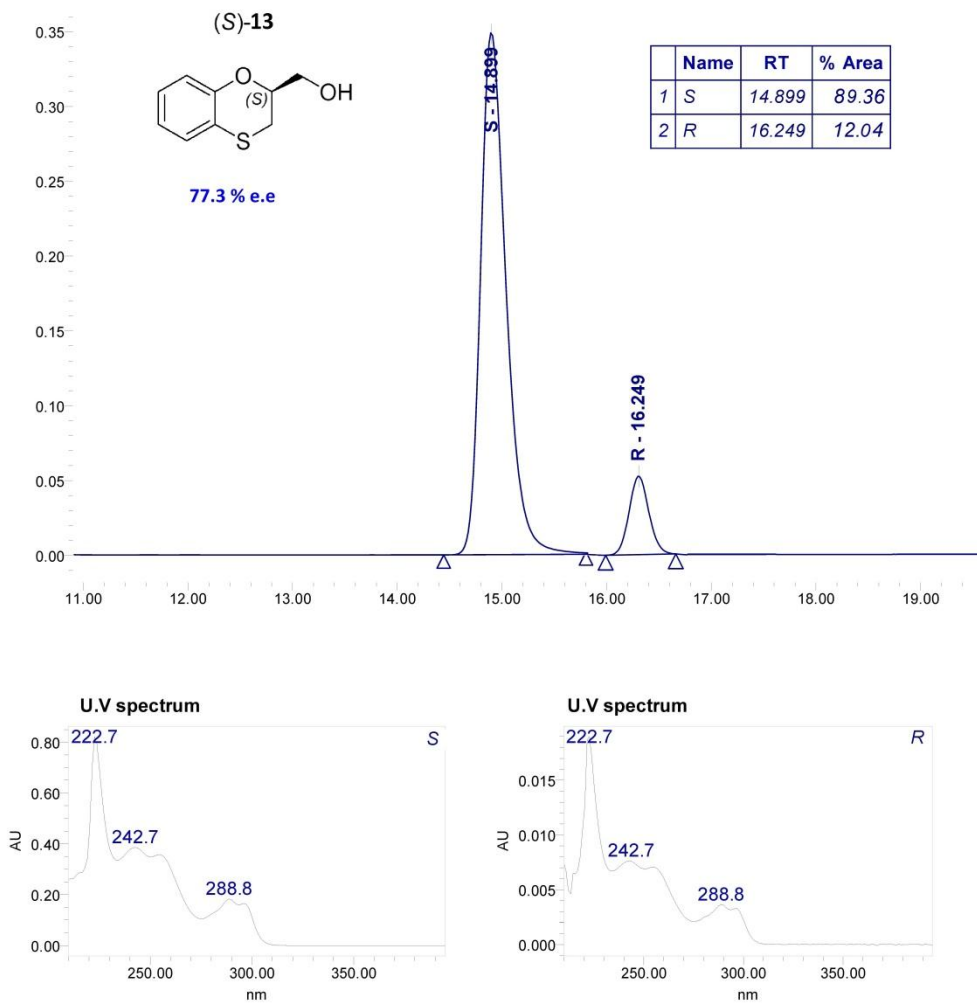


Figure S6

CHIRALPAK IA 250 x 4.6 mm
Flow rate: 1ml/min
room temperature
PDA 250.0 nm
n-hexane/2-propanol 90/10 v/v

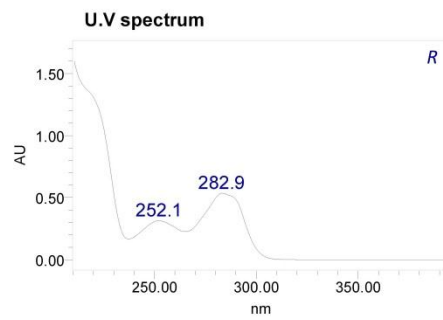
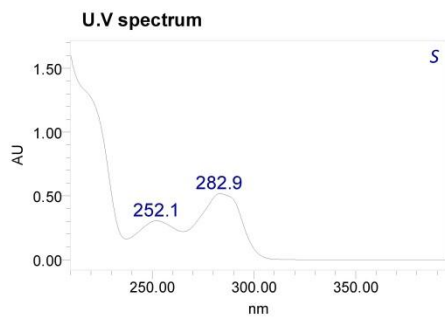
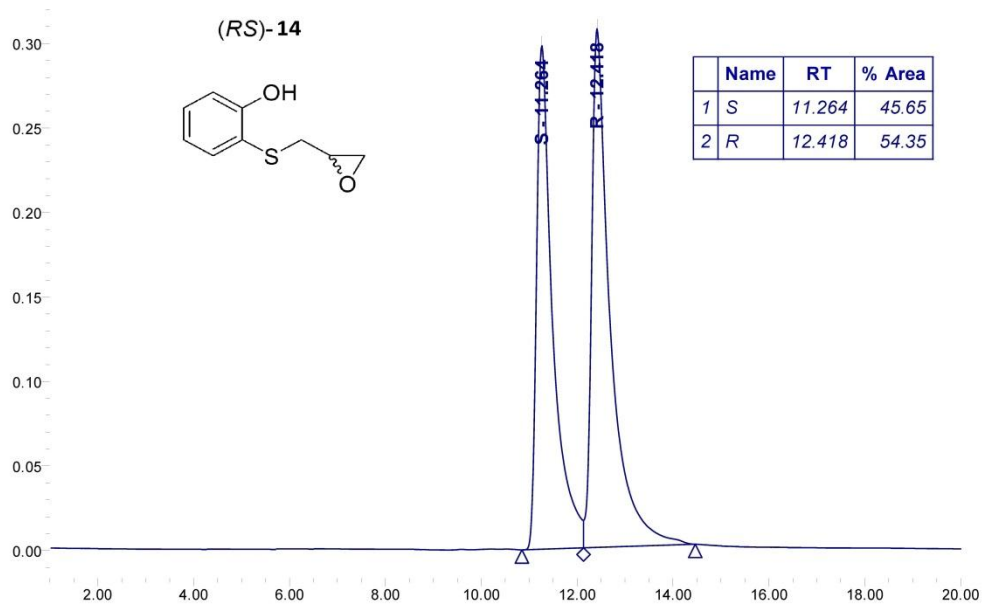


Figure S7

CHIRALPAK IA 250 x 4.6 mm
Flow rate: 1ml/min
room temperature
PDA 250.0 nm
n-hexane/2-propanol 90/10 v/v

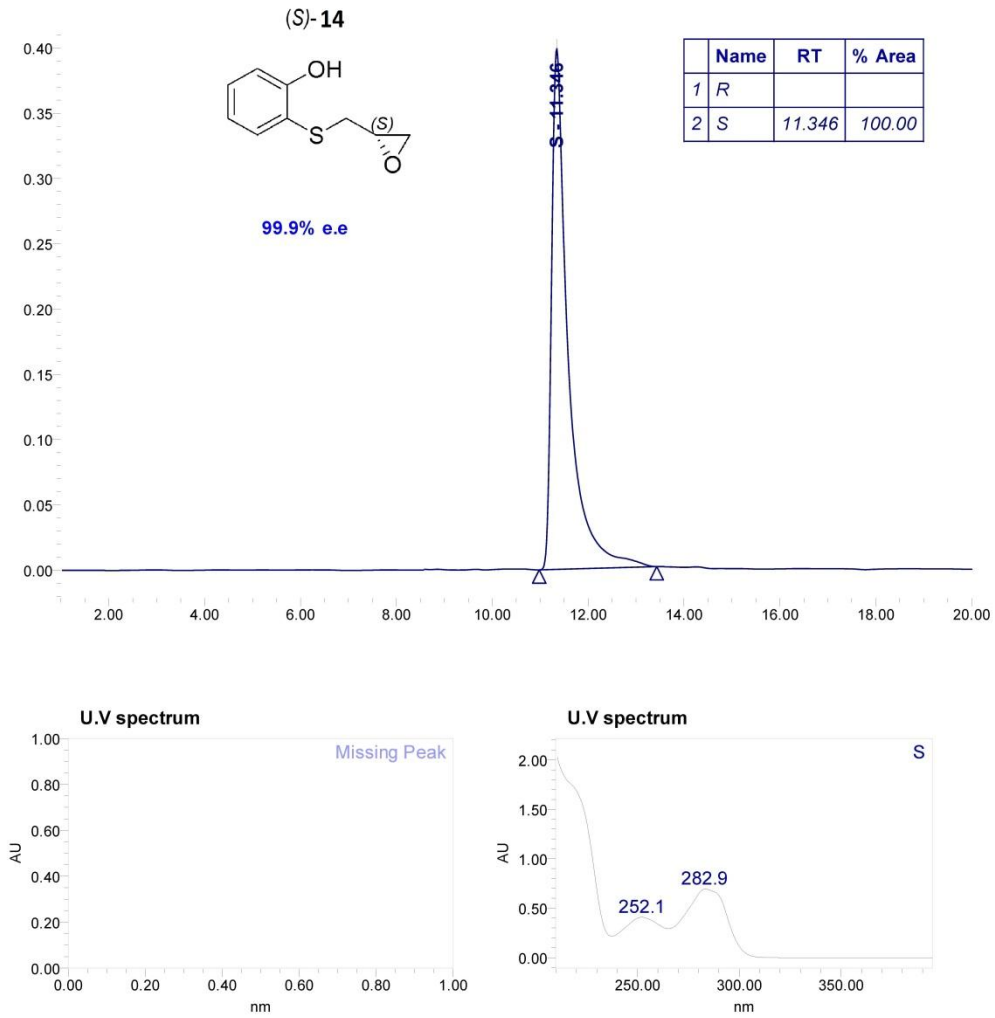


Figure S8

CHIRALPAK IA 250 x 4.6 mm
Flow rate: 1ml/min
room temperature
PDA 250.0 nm
n-hexane/ethanol 80/20 v/v

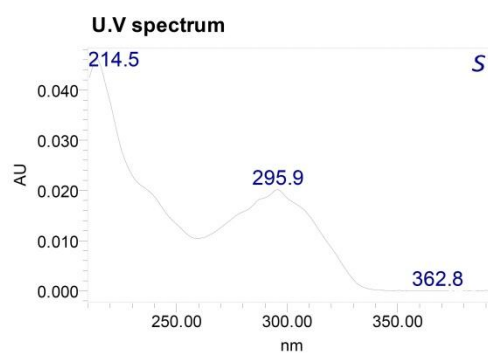
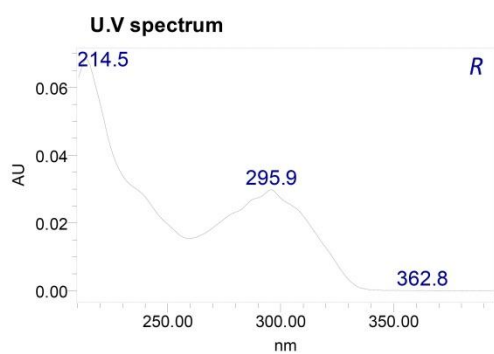
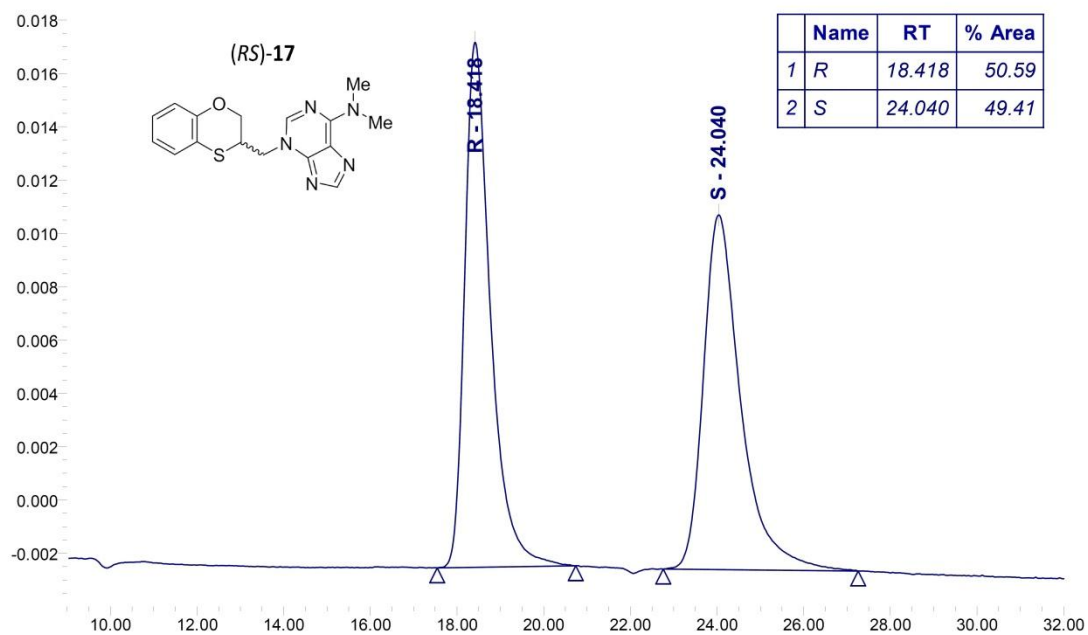


Figure S9

CHIRALPAK IA 250 x 4.6 mm
Flow rate: 1ml/min
room temperature
PDA 250.0 nm
n-hexane/ethanol 80/20 v/v

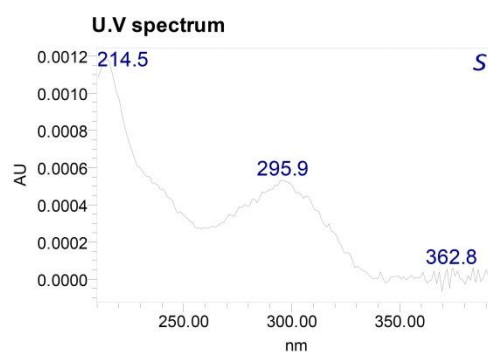
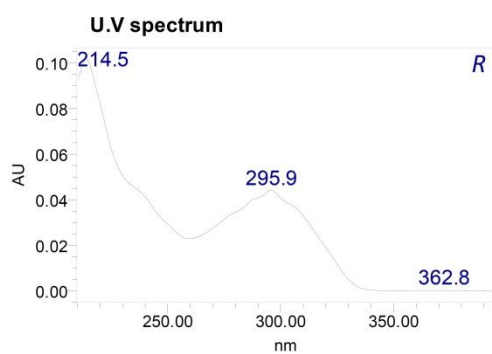
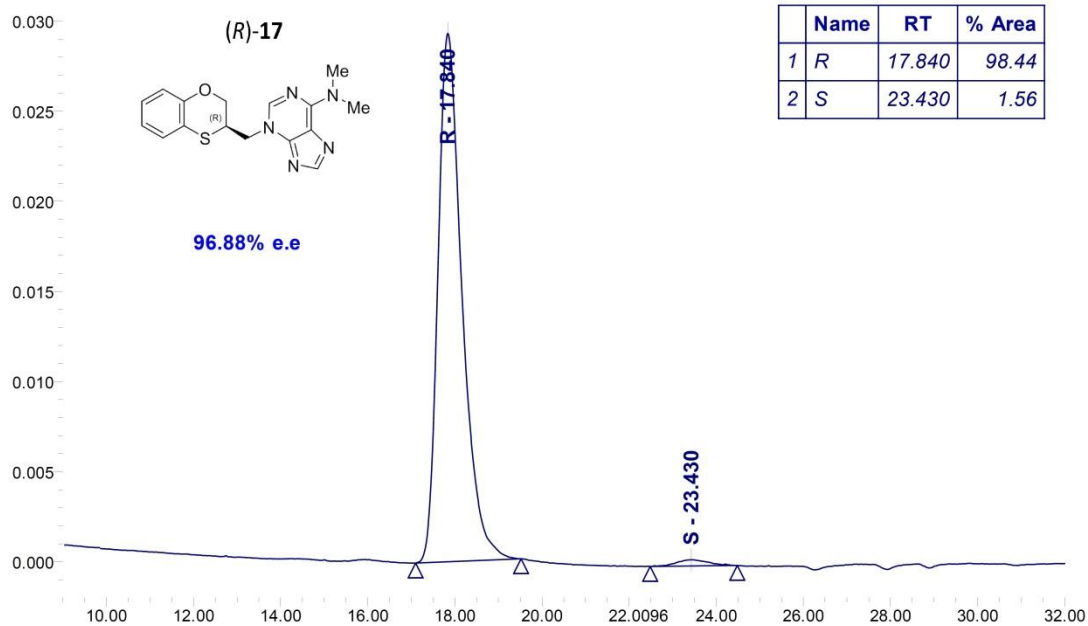


Figure S10

CHIRALPAK IA 250 x 4.6 mm
Flow rate: 1ml/min
room temperature
PDA 250.0 nm
n-hexane/ethanol 80/20 v/v

	Name	RT	% Area
1	R	18.242	12.00
2	S	23.055	88.00

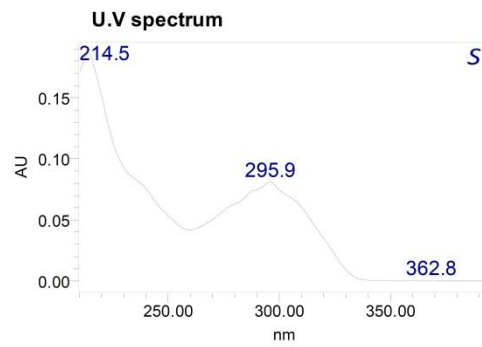
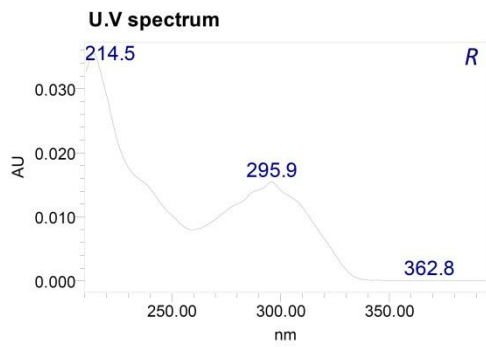
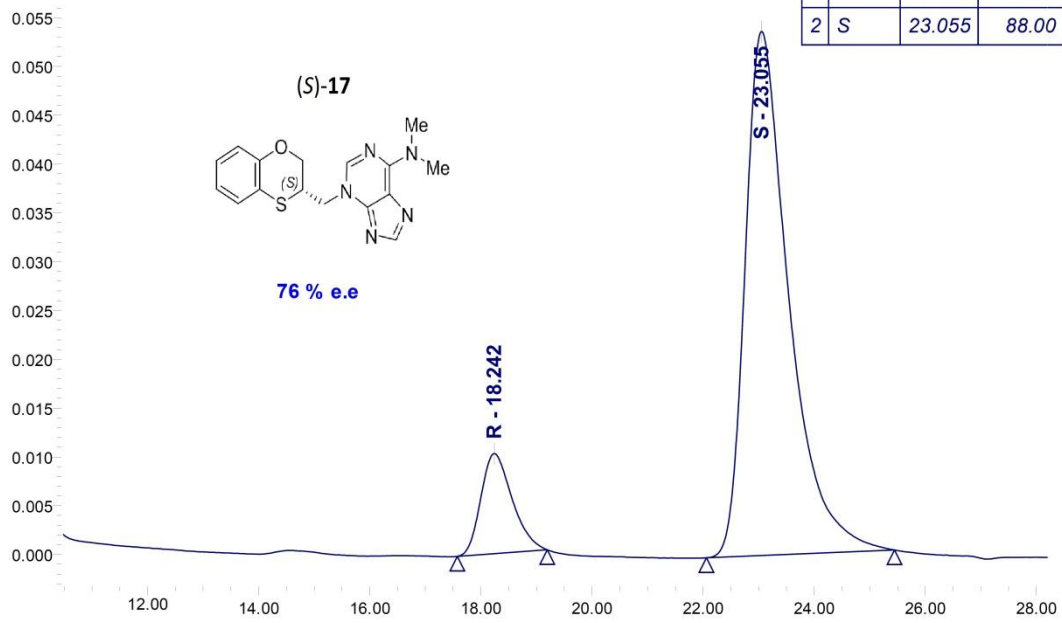


Figure S11

CHIRALPAK IA 250 x 4.6 mm
Flow rate: 1ml/min
room temperature
PDA 250.0 nm
n-hexane/ethanol 80/20 v/v

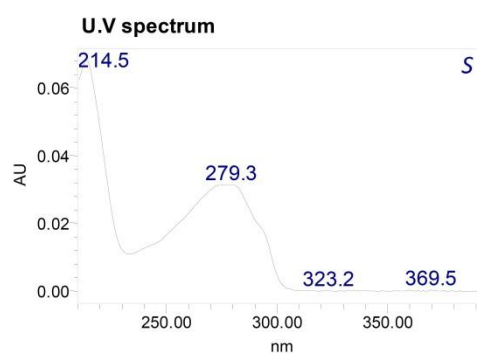
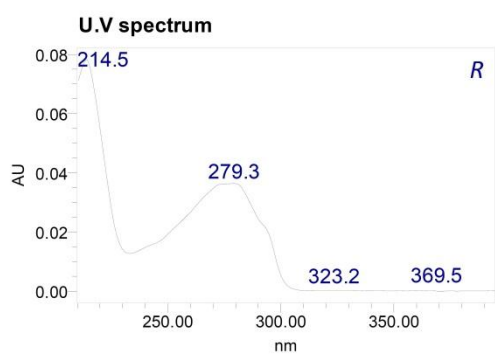
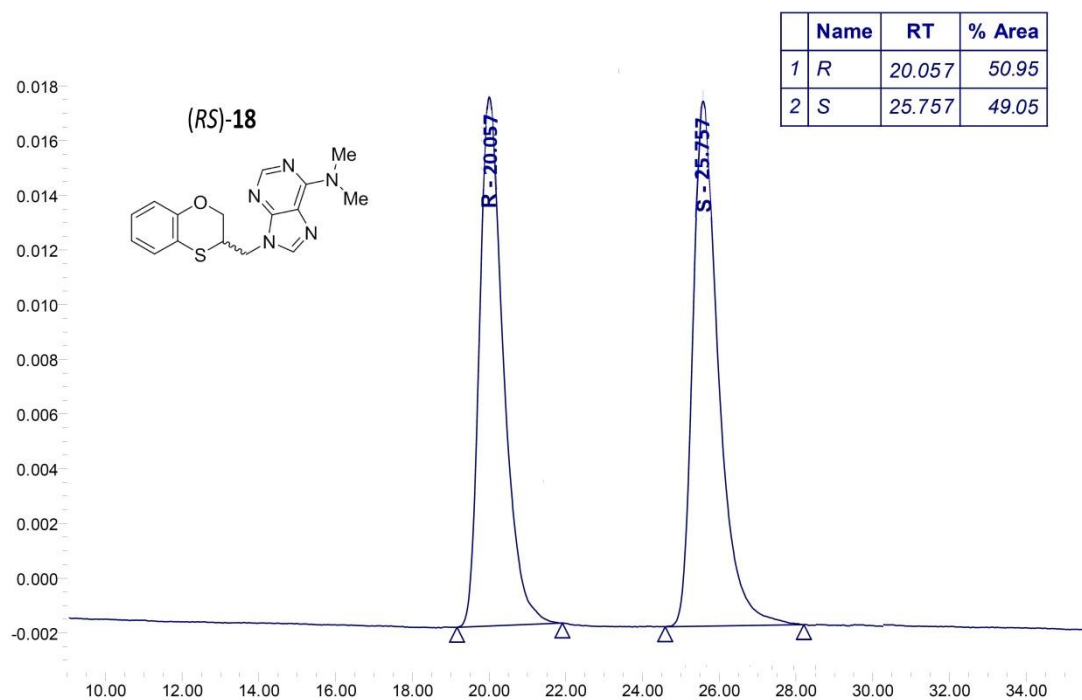


Figure S12

CHIRALPAK IA 250 x 4.6 mm
Flow rate: 1ml/min
room temperature
PDA 250.0 nm
n-hexane/ethanol 80/20 v/v

	Name	RT	% Area
1	R	20.053	97.10
2	S	25.755	2.90

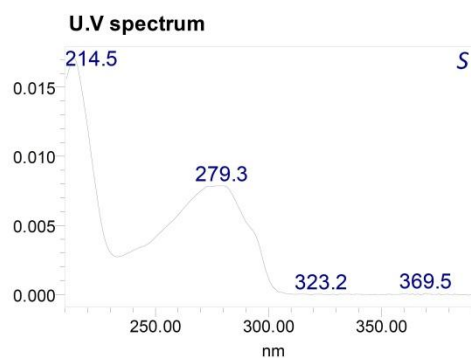
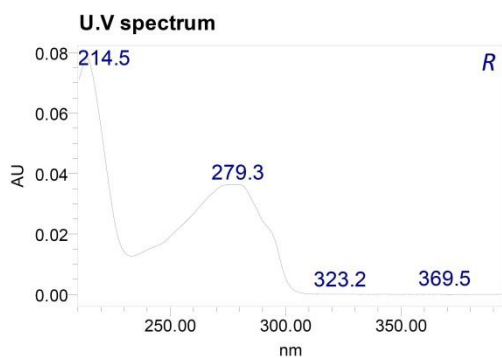
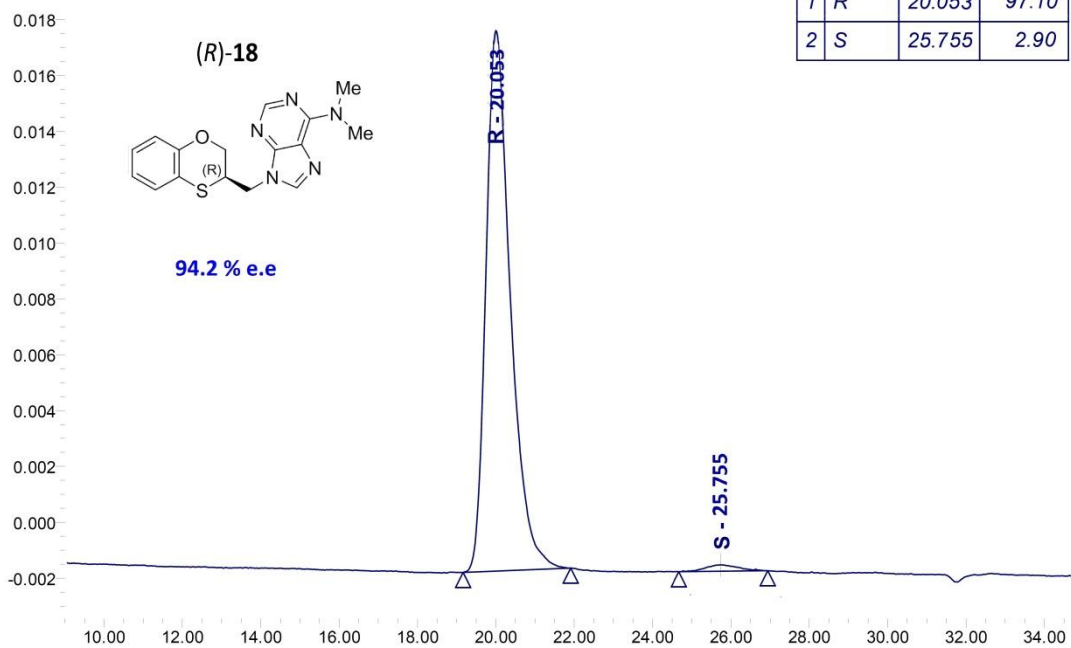


Figure S13

CHIRALPAK IA 250 x 4.6 mm
Flow rate: 1ml/min
room temperature
PDA 250.0 nm
n-hexane/ethanol 80/20 v/v

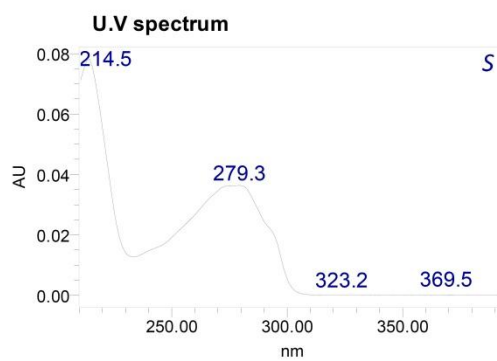
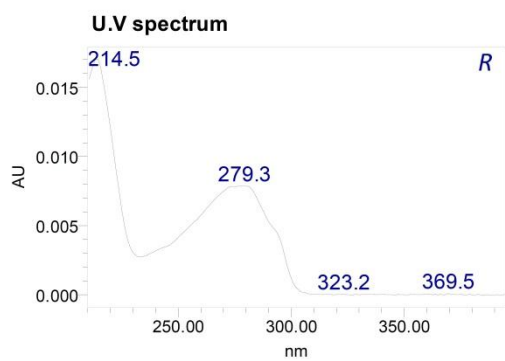
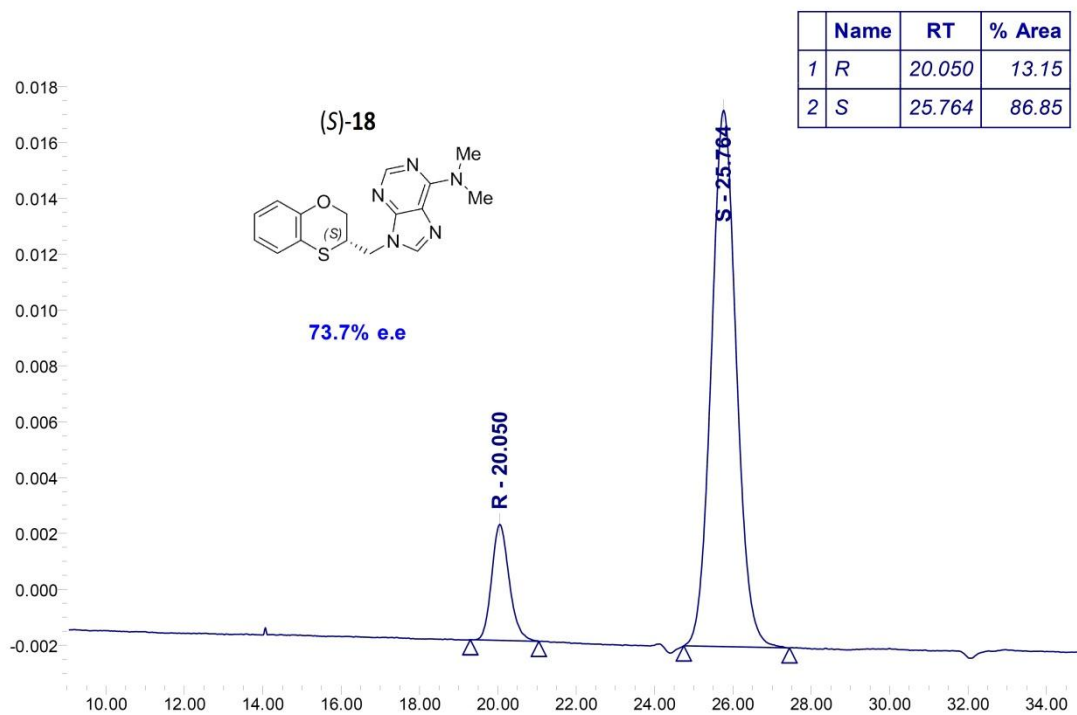


Figure S14

CHIRALPAK IA 250 x 4.6 mm
Flow rate: 1ml/min
room temperature
PDA 250.0 nm
n-hexane/ethanol 80/20 v/v

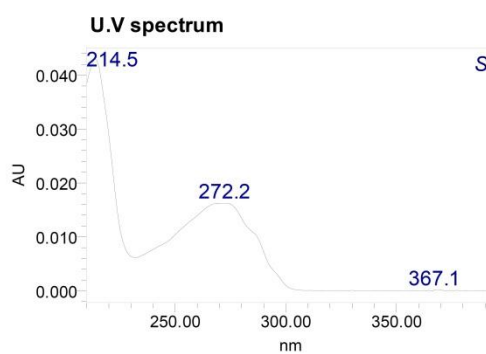
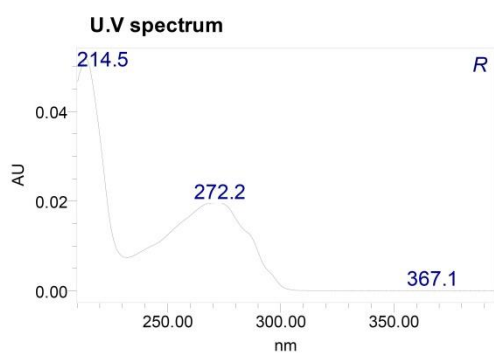
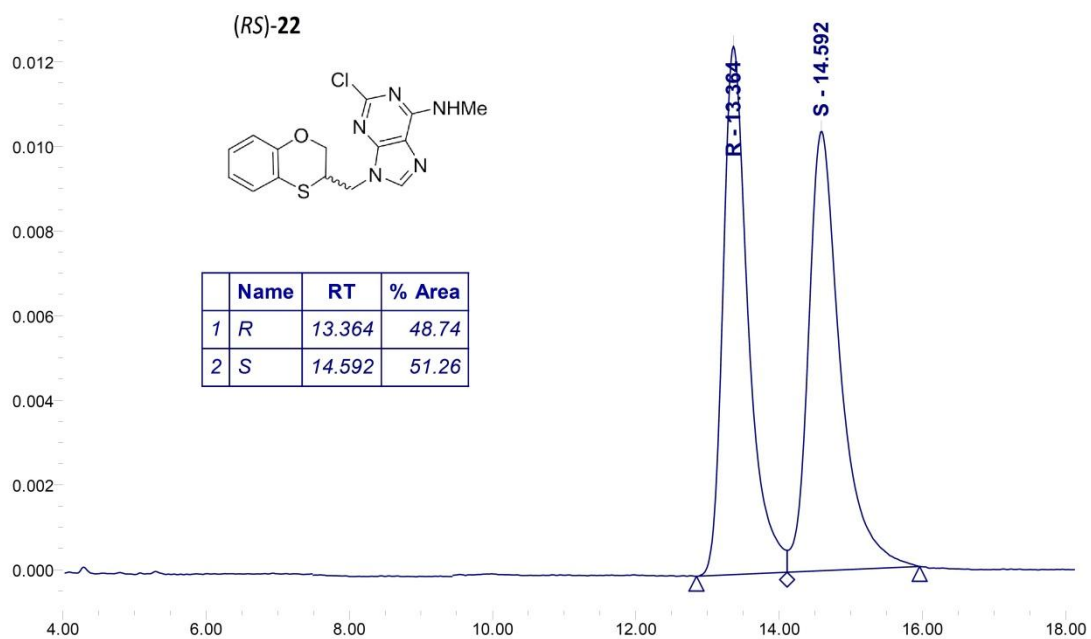


Figure S15

CHIRALPAK IA 250 x 4.6 mm
Flow rate: 1ml/min
room temperature
PDA 250.0 nm
n-hexane/ethanol 80/20 v/v

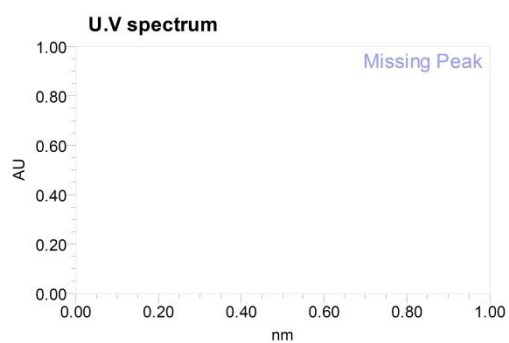
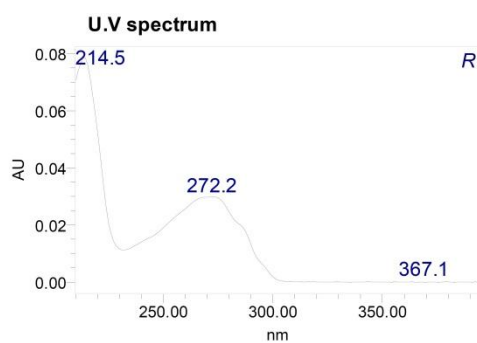
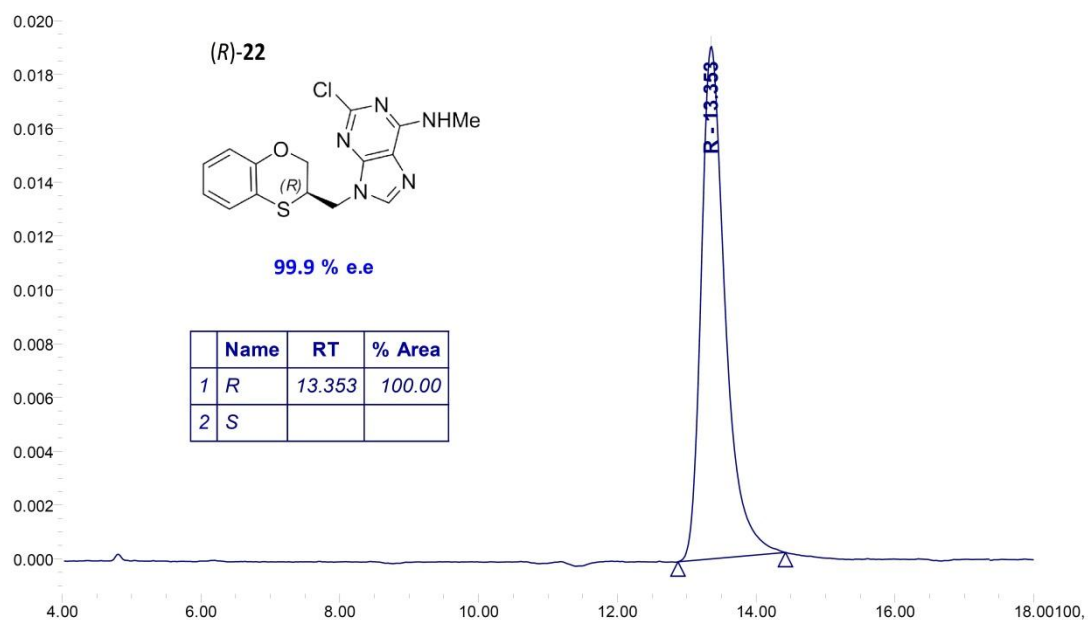


Figure S16

CHIRALPAK IA 250 x 4.6 mm
Flow rate: 1ml/min
room temperature
PDA 250.0 nm
n-hexane/ethanol 80/20 v/v

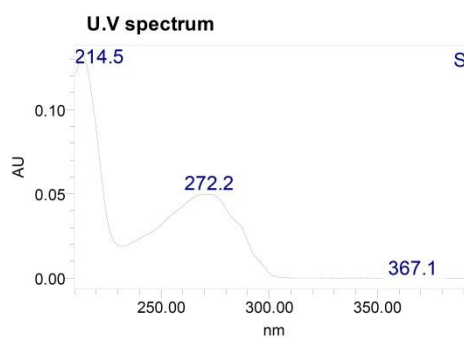
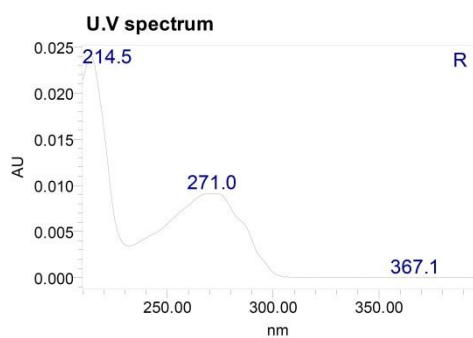
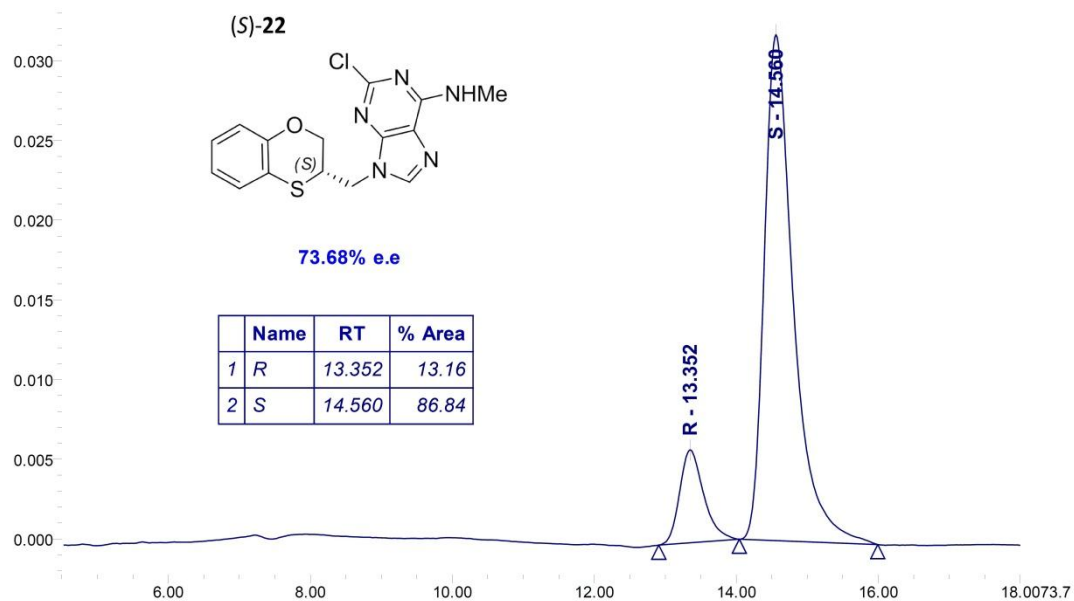


Figure S17

CHIRALPAK IA 250 x 4.6 mm
Flow rate: 1ml/min
room temperature
PDA 250.0 nm
n-hexane/ethanol 80/20 v/v

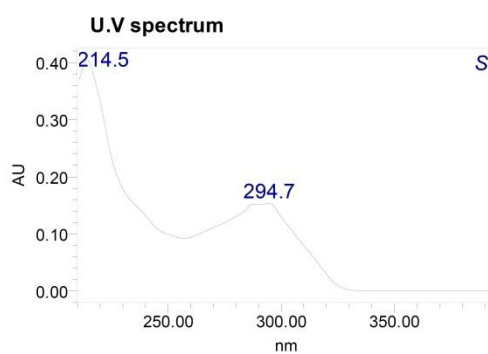
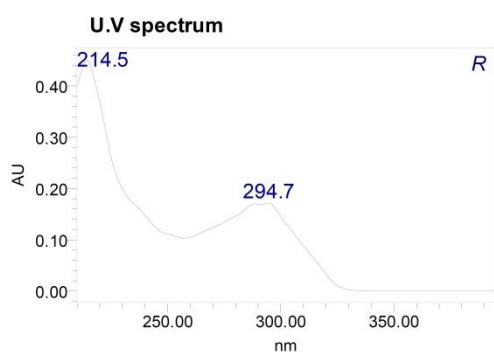
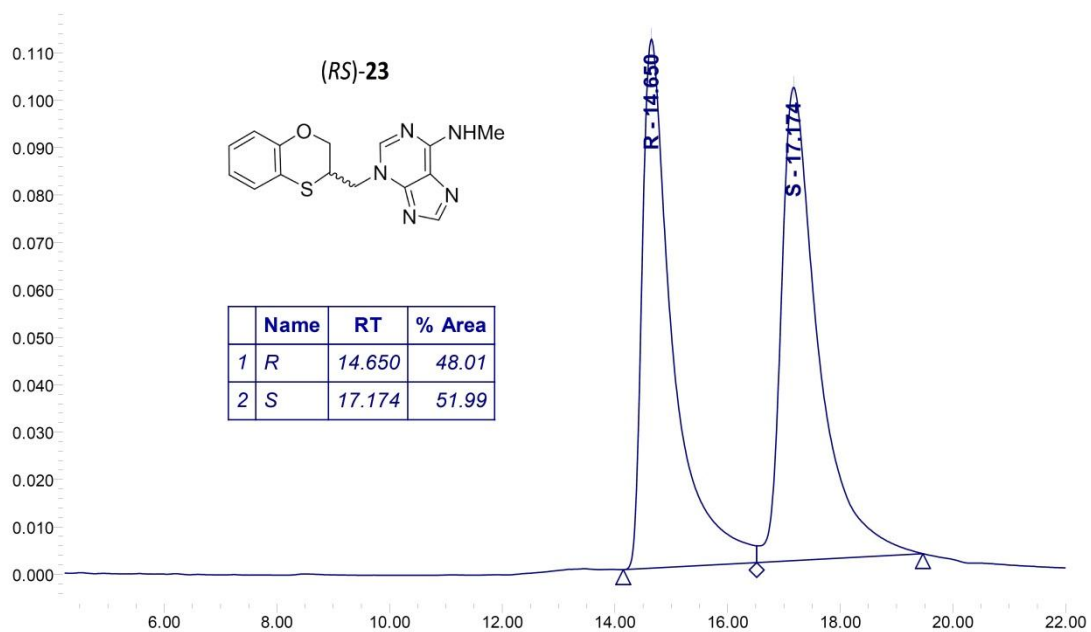


Figure S18

CHIRALPAK IA 250 x 4.6 mm
Flow rate: 1ml/min
room temperature
PDA 250.0 nm
n-hexane/ethanol 80/20 v/v

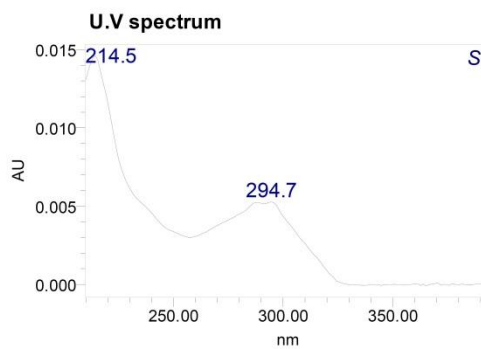
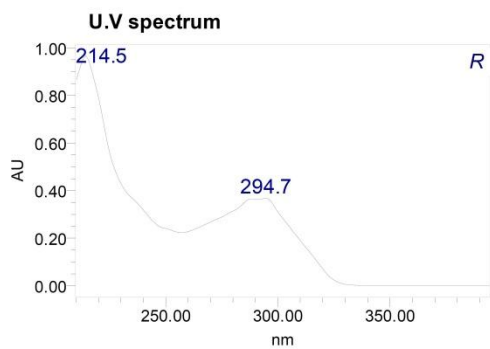
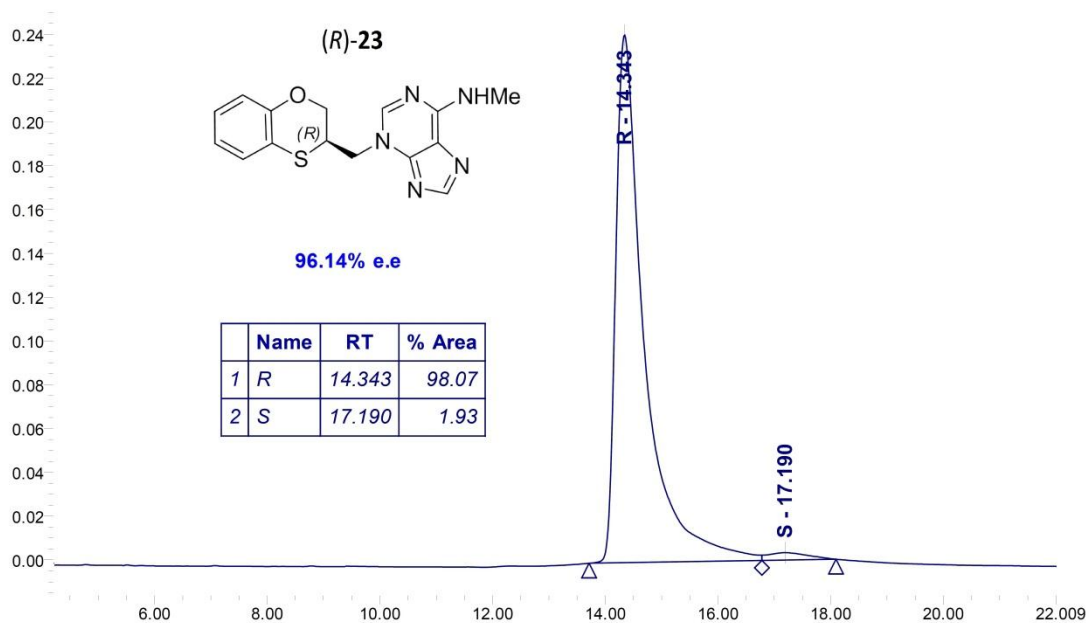


Figure S19

CHIRALPAK IA 250 x 4.6 mm
Flow rate: 1ml/min
room temperature
PDA 250.0 nm
n-hexane/ethanol 80/20 v/v

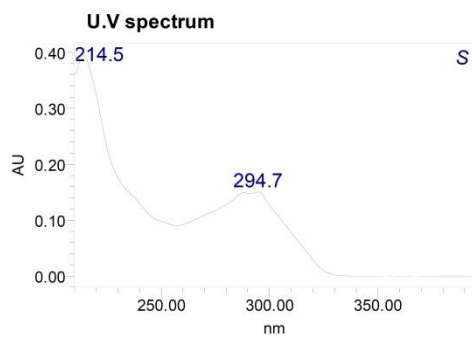
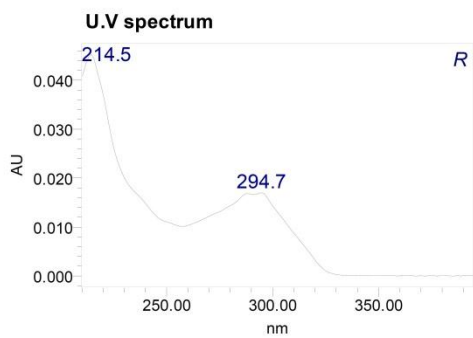
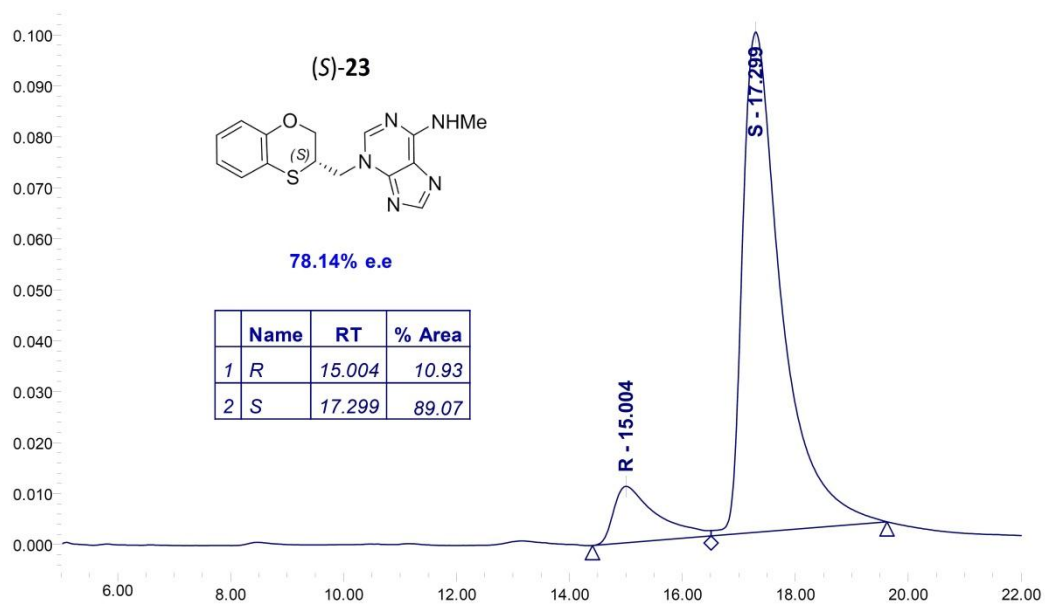


Figure S20

CHIRALPAK IA 250 x 4.6 mm
Flow rate: 1ml/min
room temperature
PDA 250.0 nm
n-hexane/ethanol 80/20 v/v

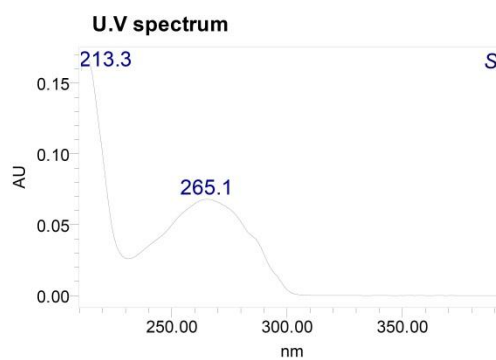
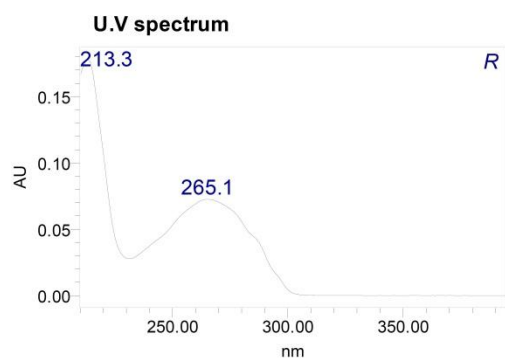
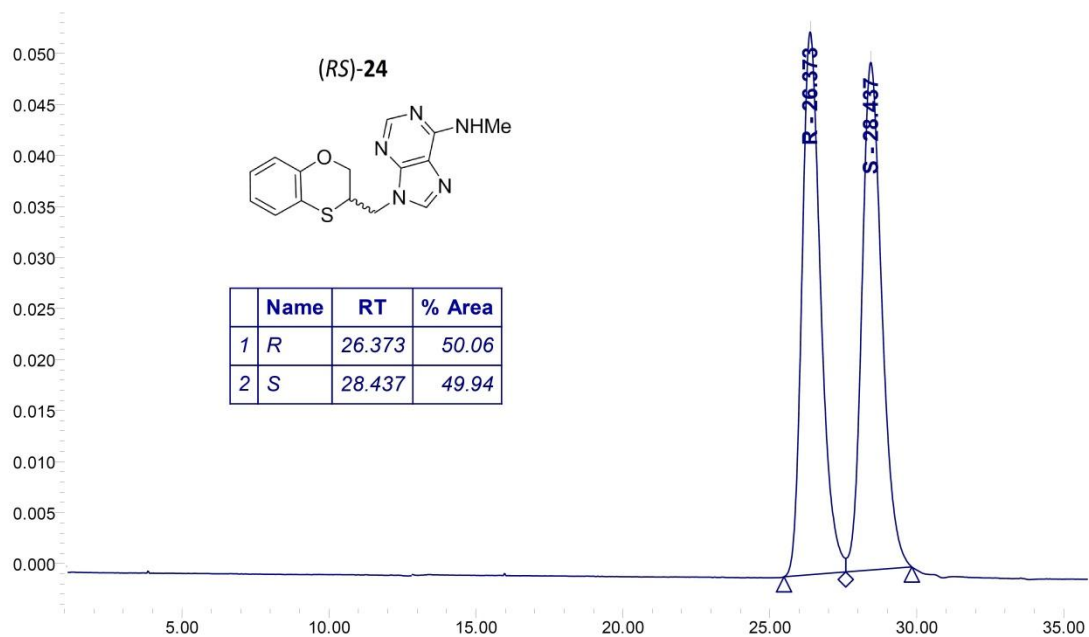


Figure S21

CHIRALPAK IA 250 x 4.6 mm
Flow rate: 1ml/min
room temperature
PDA 250.0 nm
n-hexane/ethanol 80/20 v/v

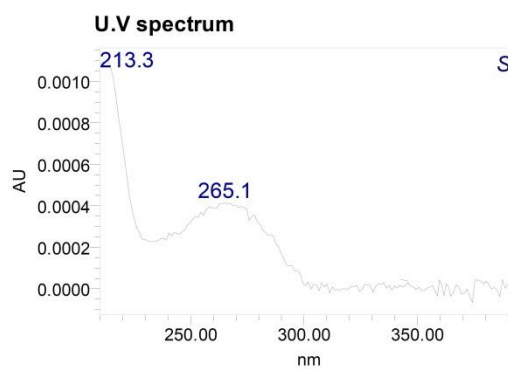
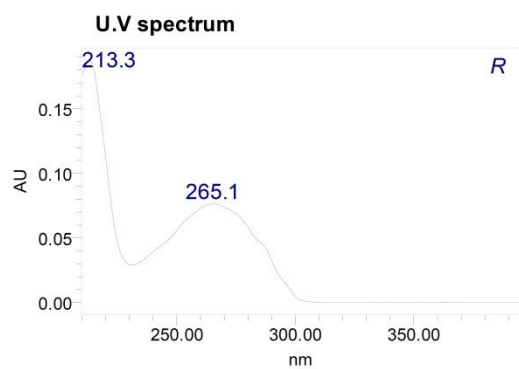
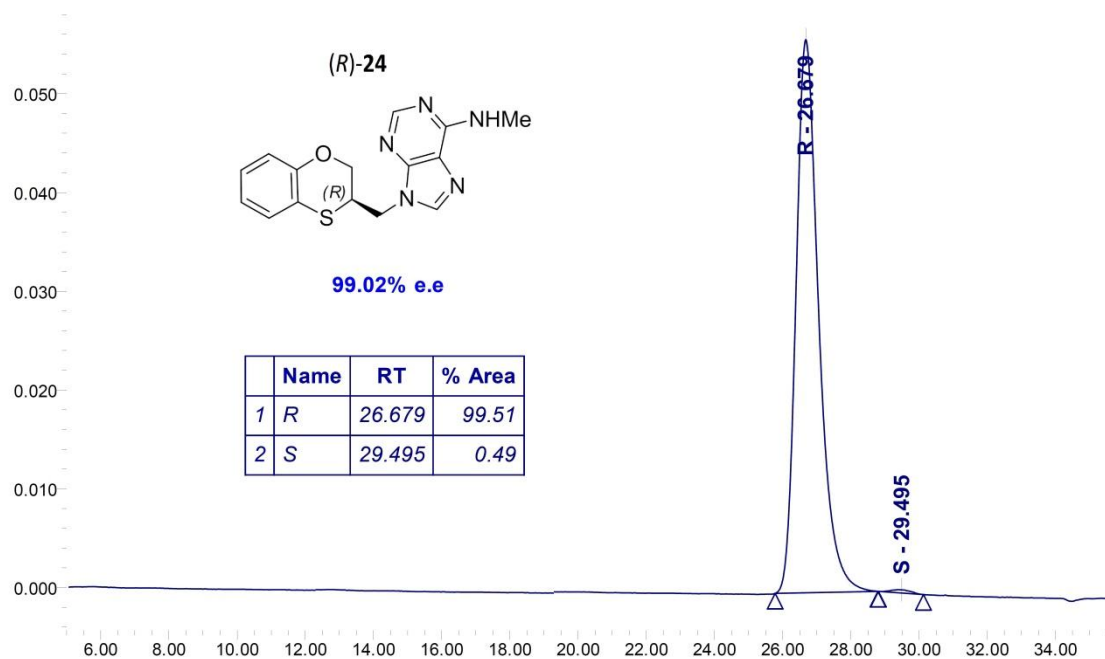


Figure S22

CHIRALPAK IA 250 x 4.6 mm
Flow rate: 1ml/min
room temperature
PDA 250.0 nm
n-hexane/ethanol 80/20 v/v

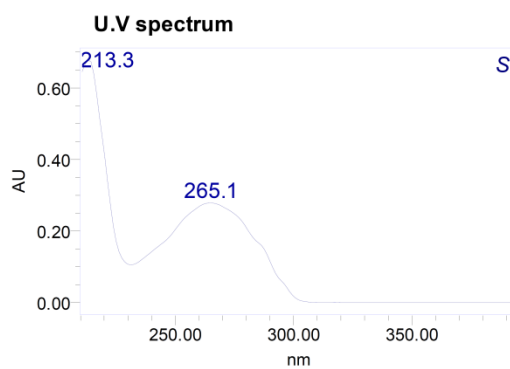
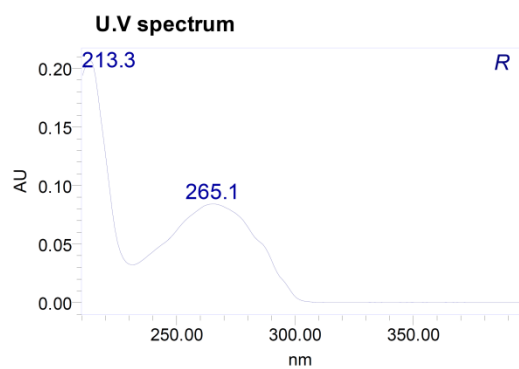
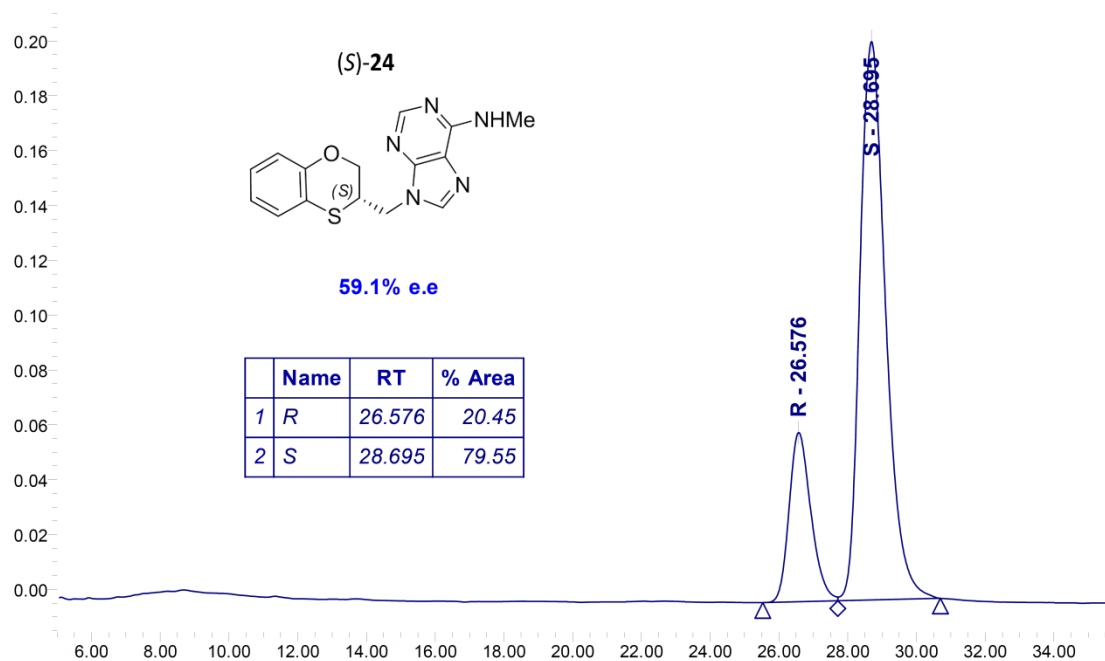
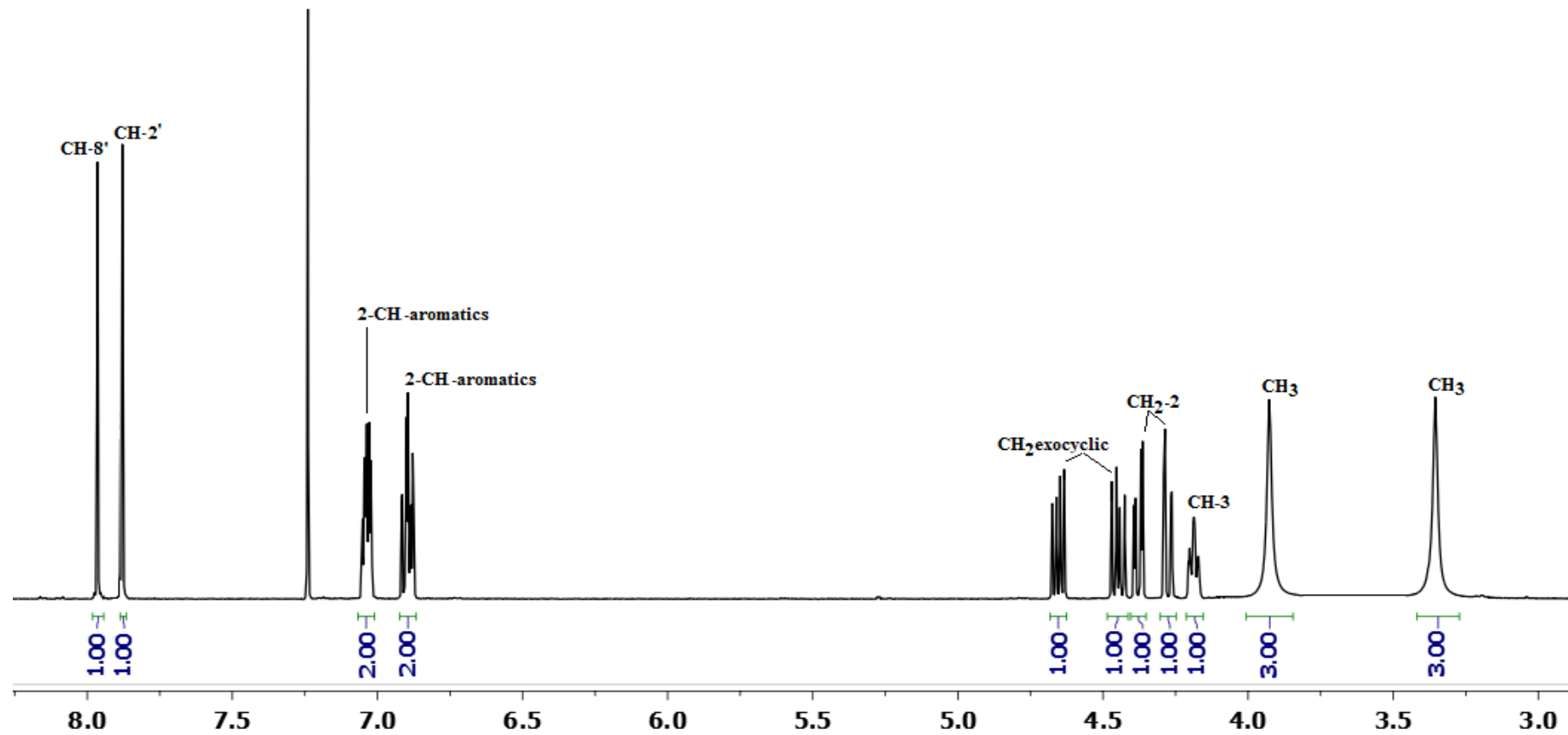
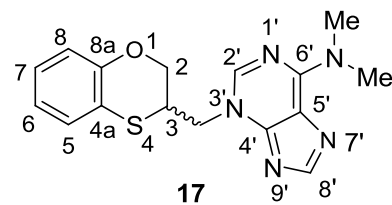


Figure S23

500 MHz, CDCl₃

500 MHz, CDCl₃

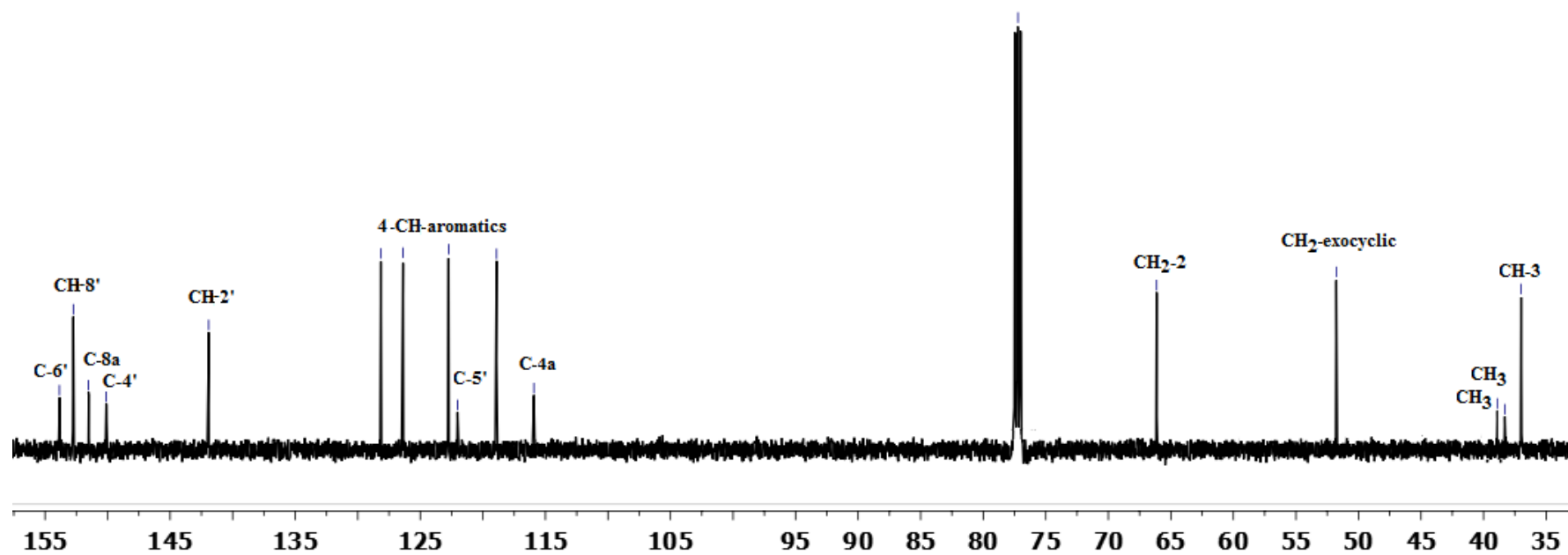
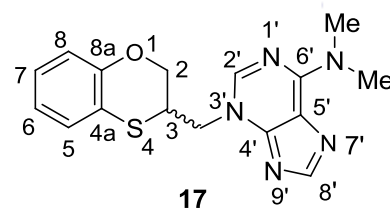
153.85
152.74
151.27
150.11
— 141.92

128.15
126.38
122.74
122.02
118.91
115.92

— 66.14

— 51.77

39.95
38.23
— 36.99



500 MHz, CDCl₃

— 152.74

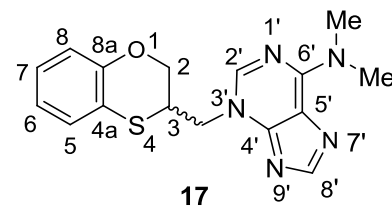
— 141.92

— 128.15

— 126.38

— 122.74

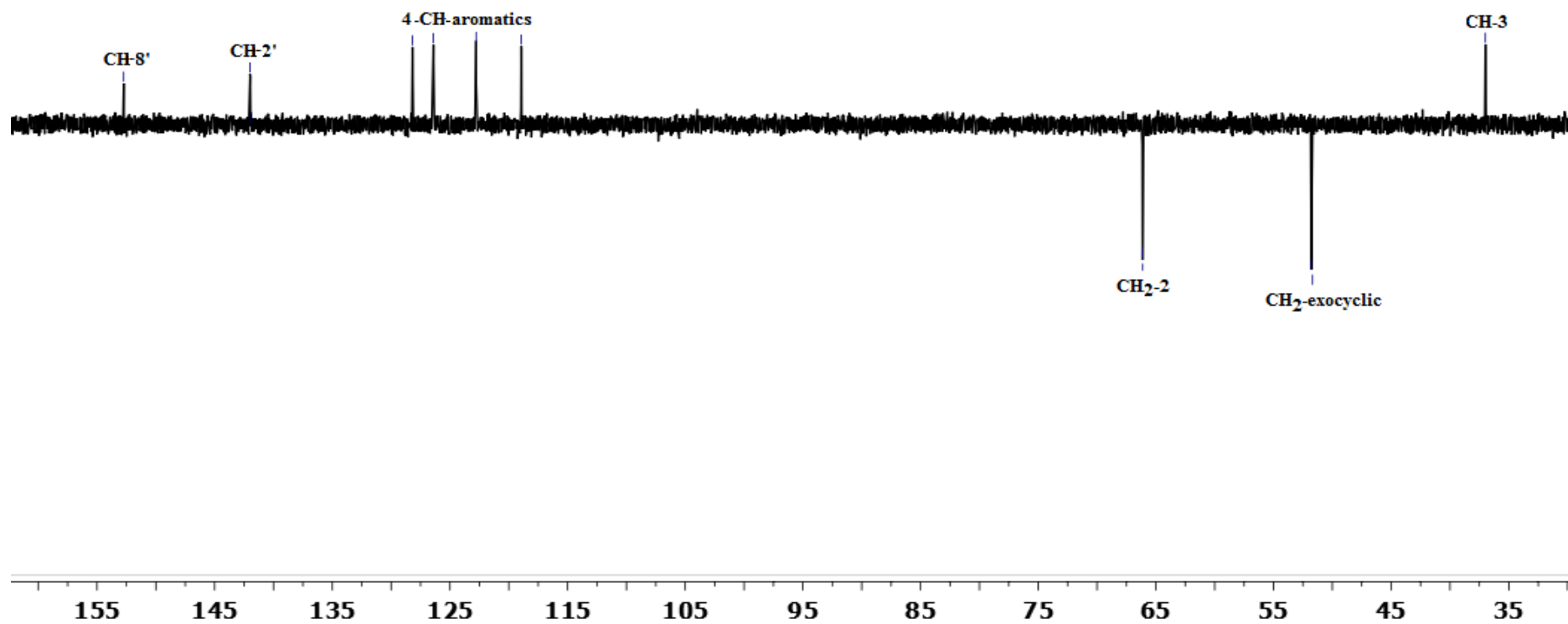
— 118.91

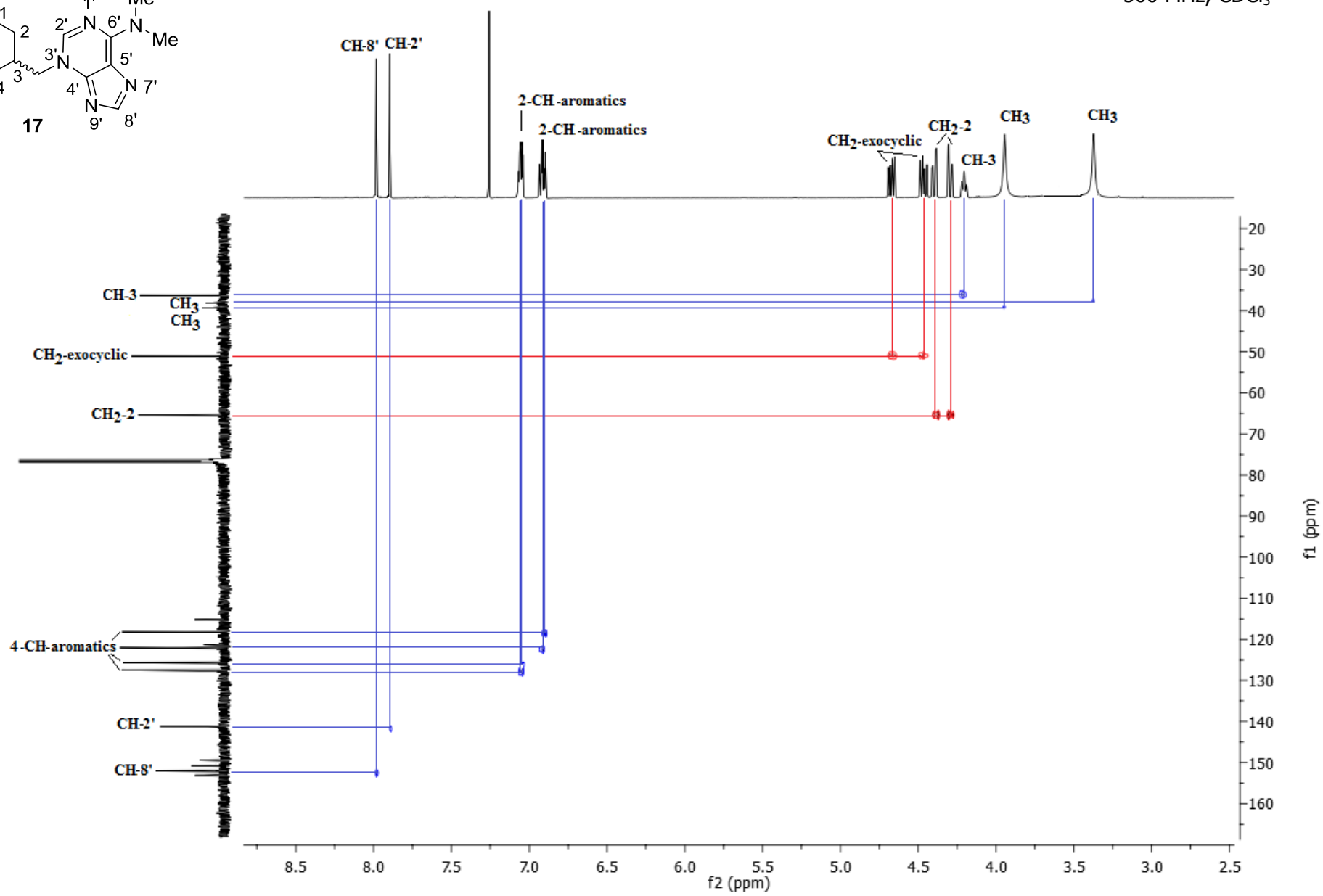
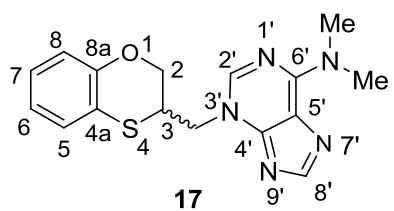


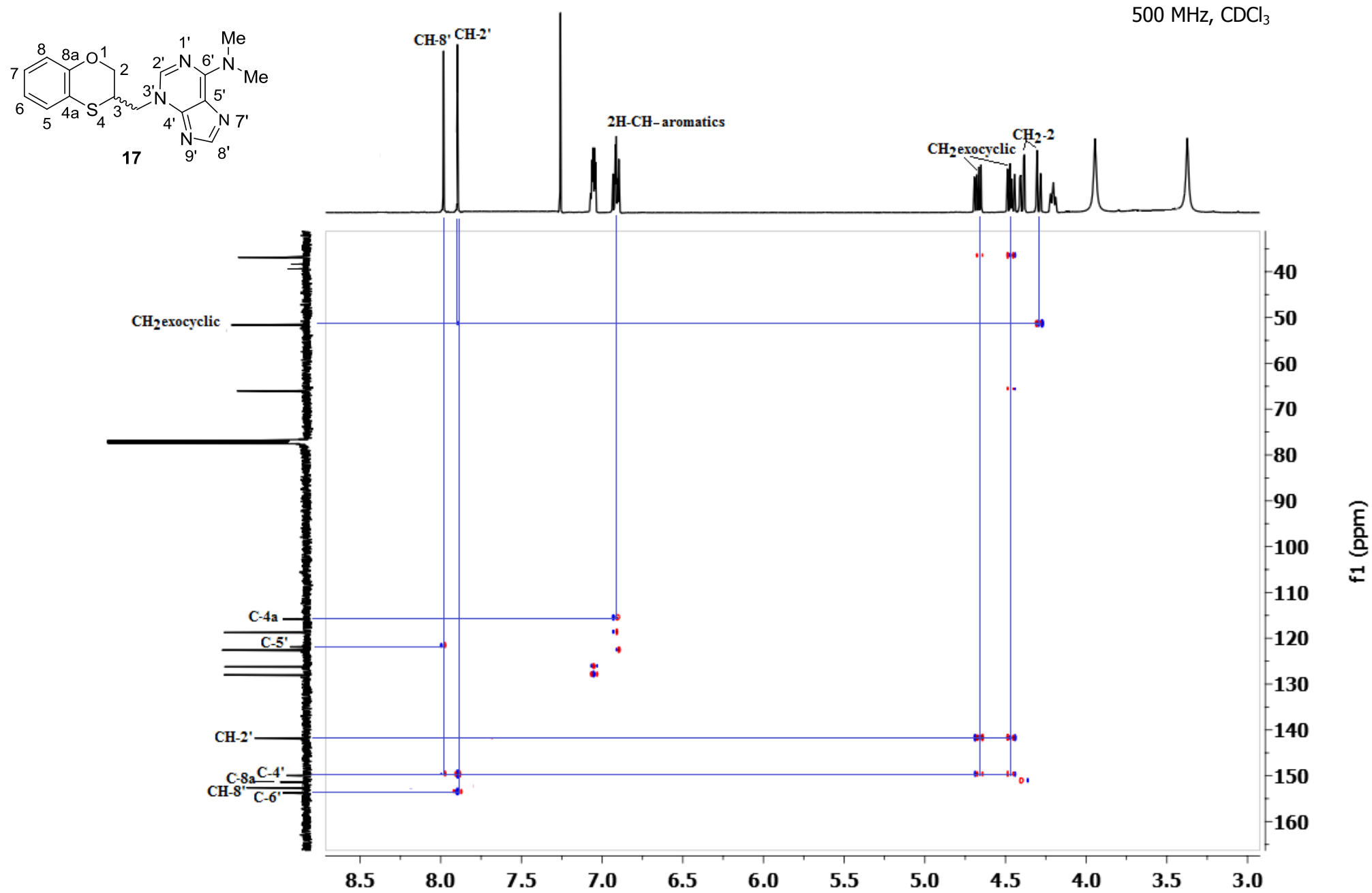
— 66.14

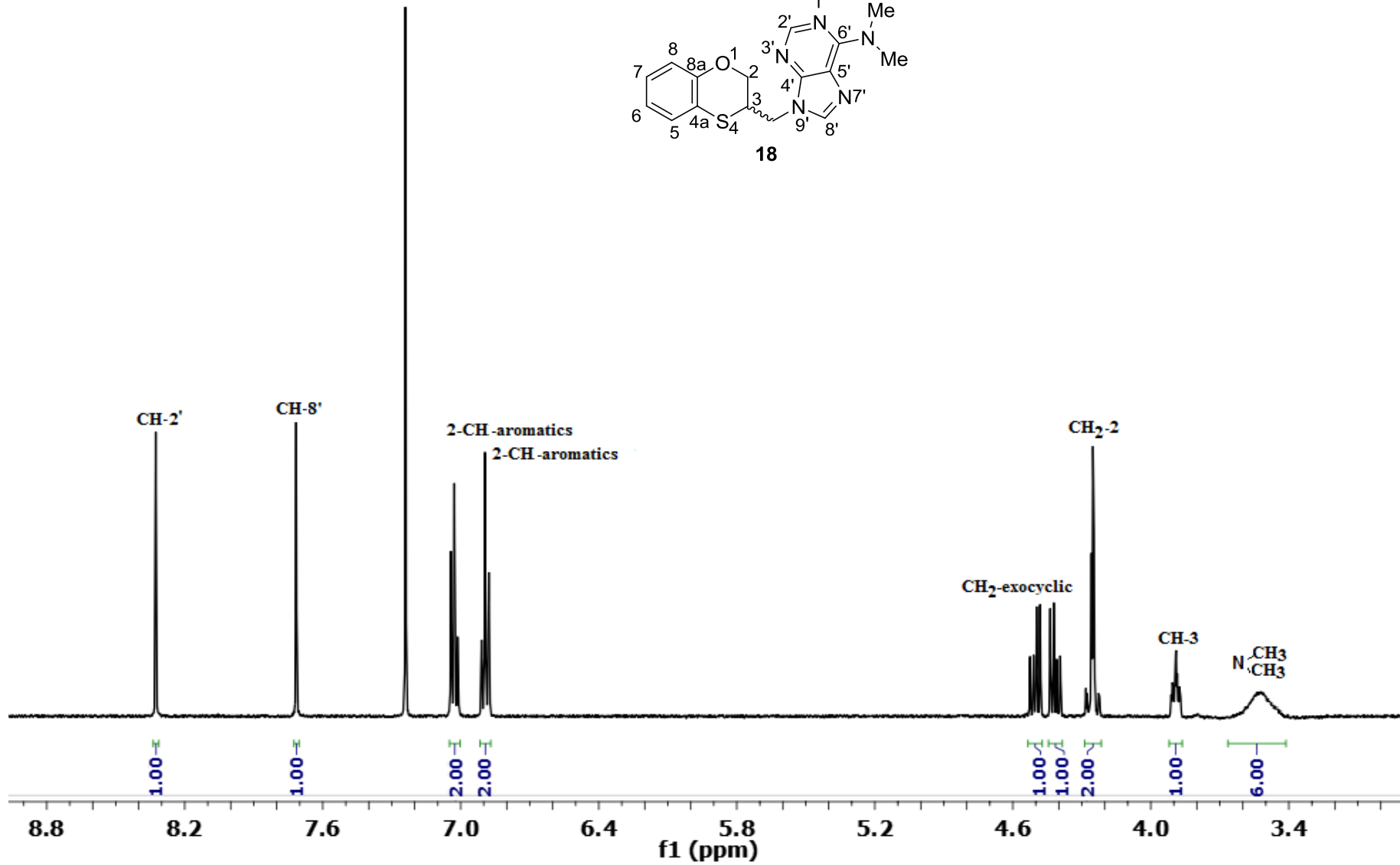
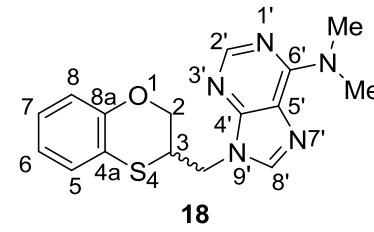
— 51.77

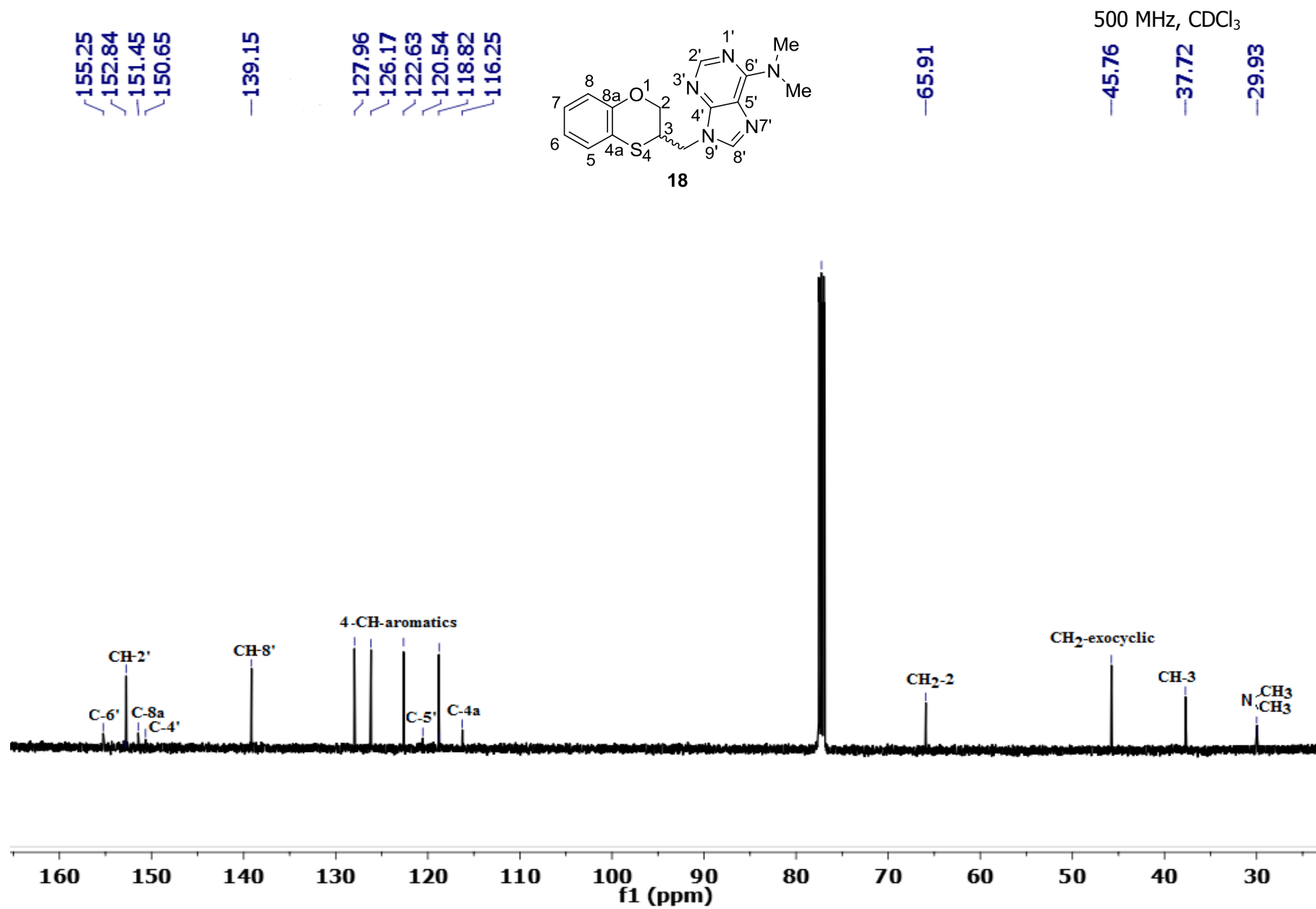
— 36.99



500 MHz, CDCl₃







500 MHz, CDCl₃

—152.84

—139.15

~127.96

~126.17

~122.63

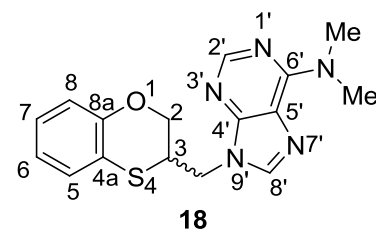
~118.82

—65.91

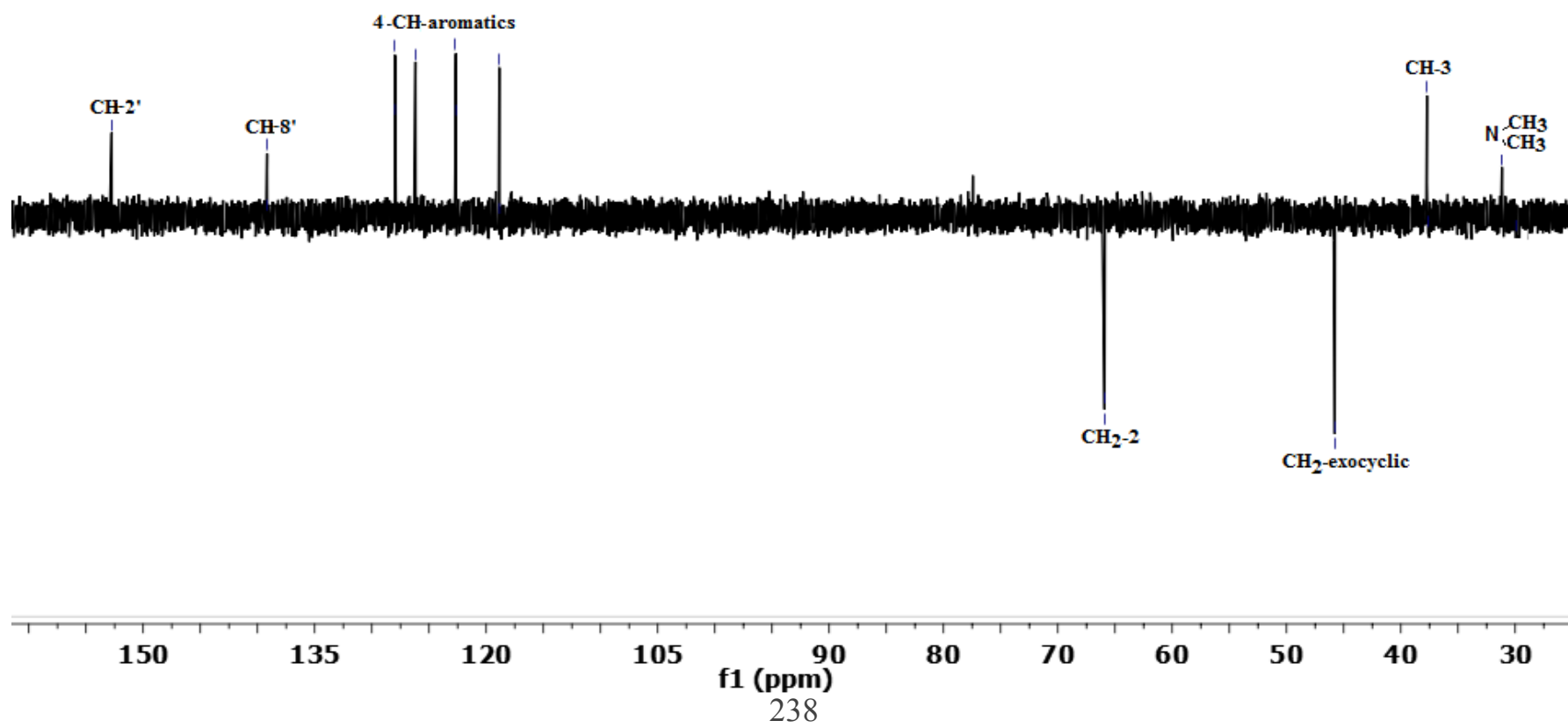
—45.76

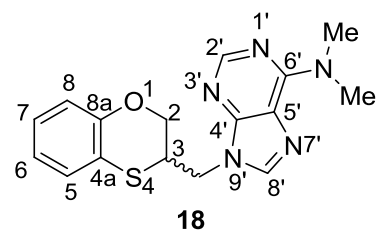
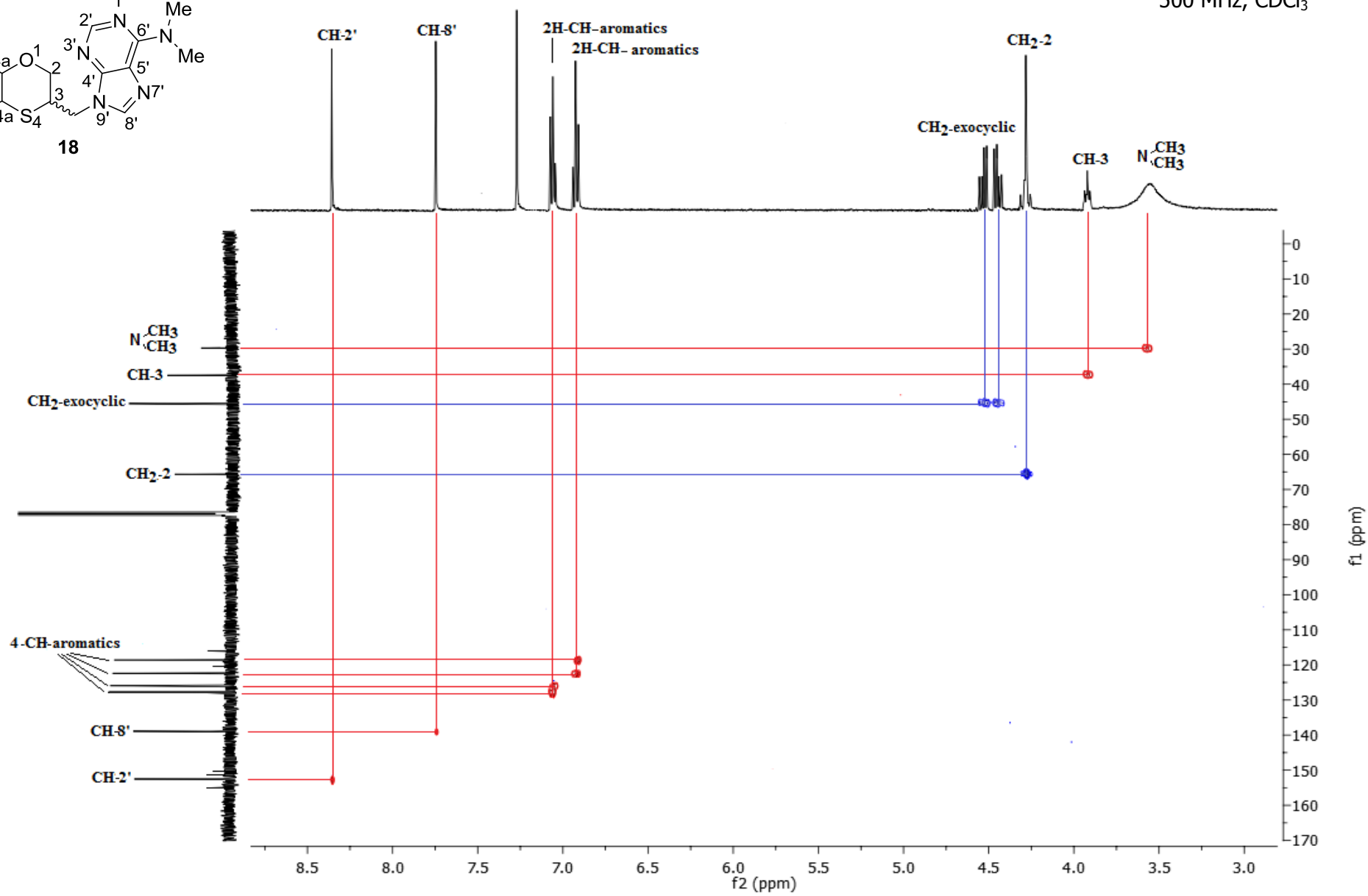
—37.72

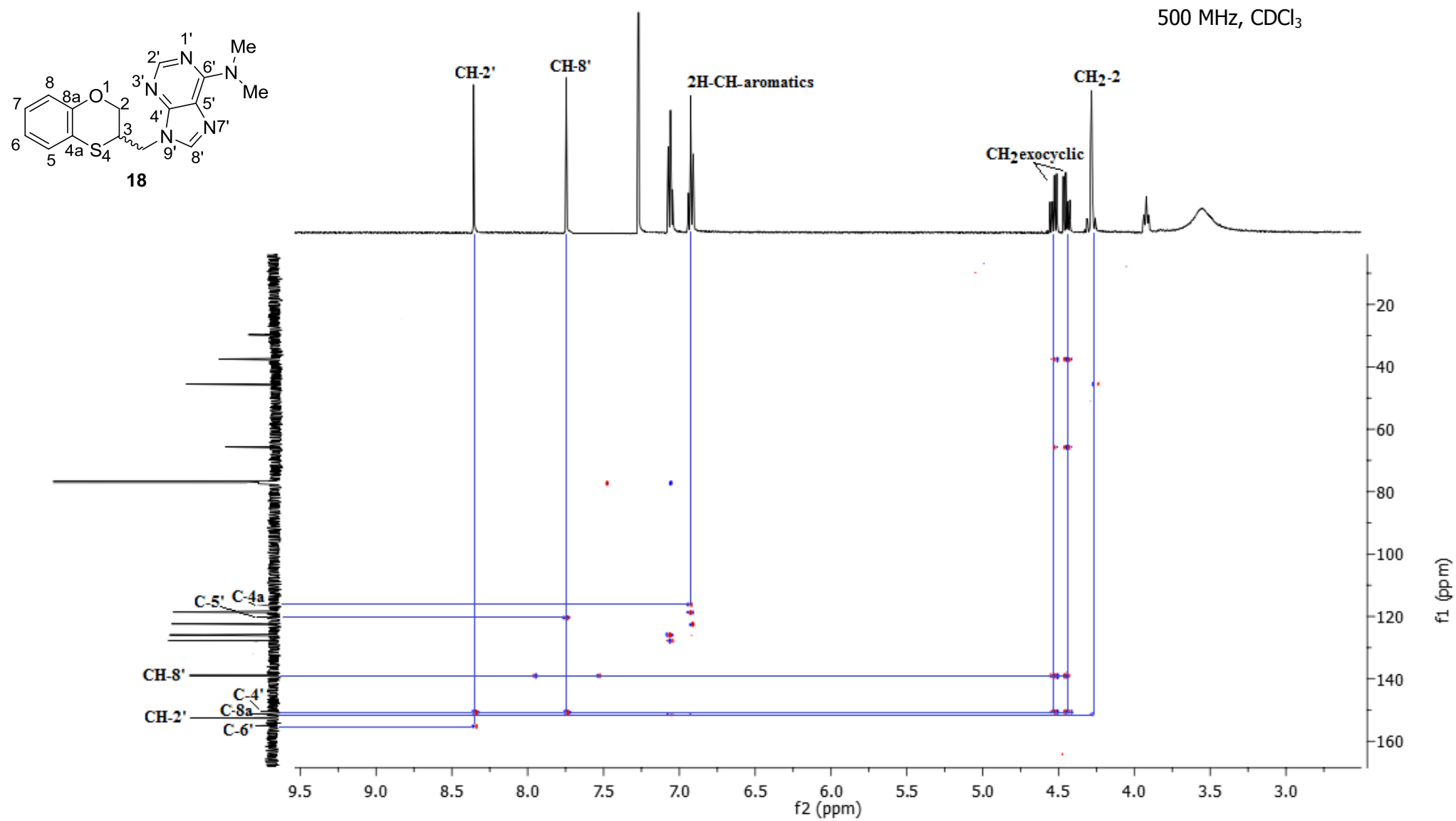
—29.93

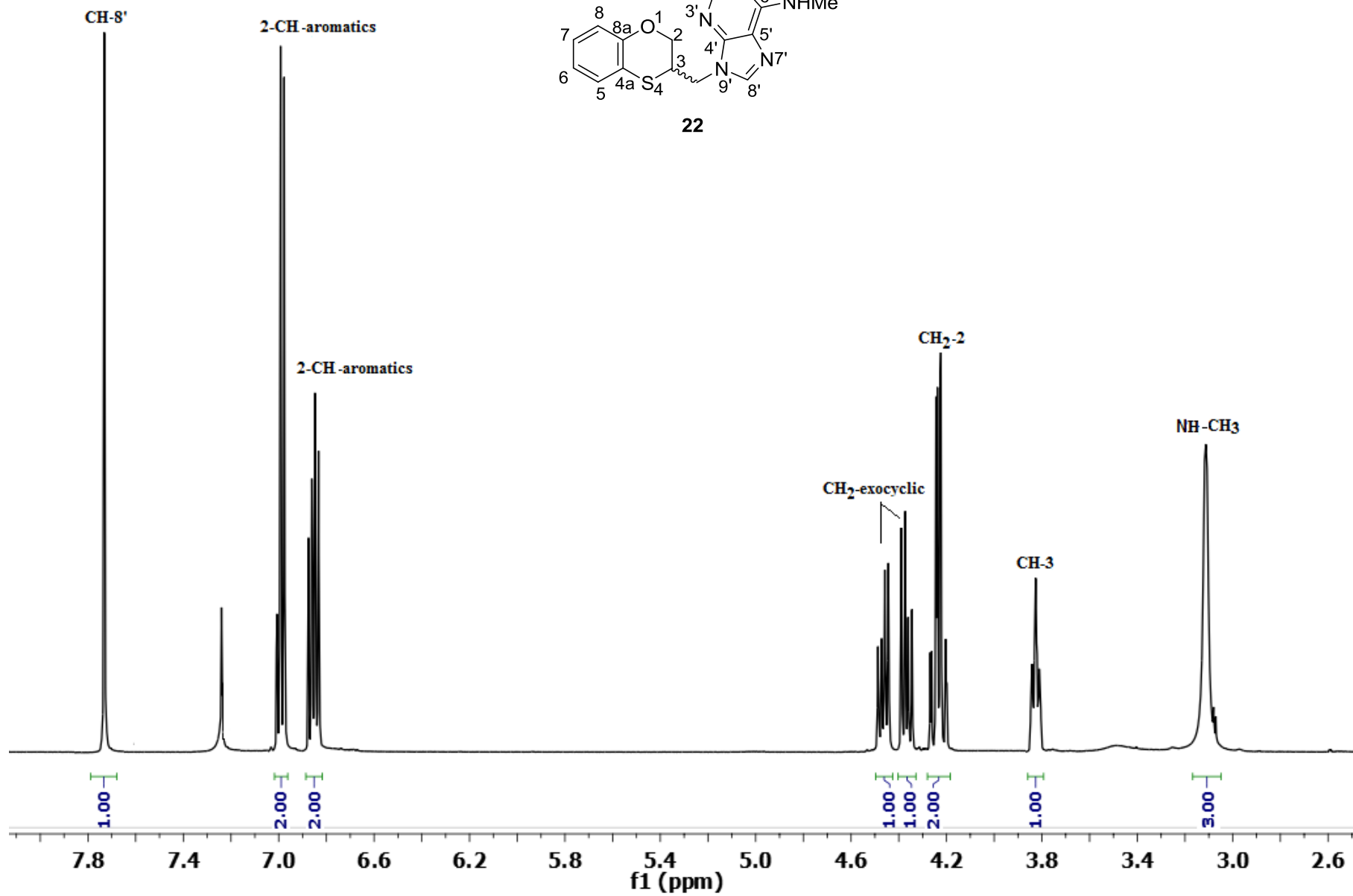
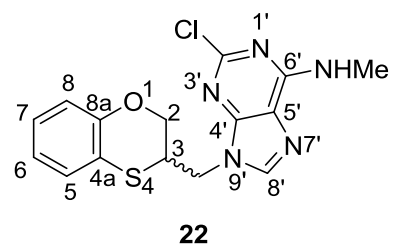


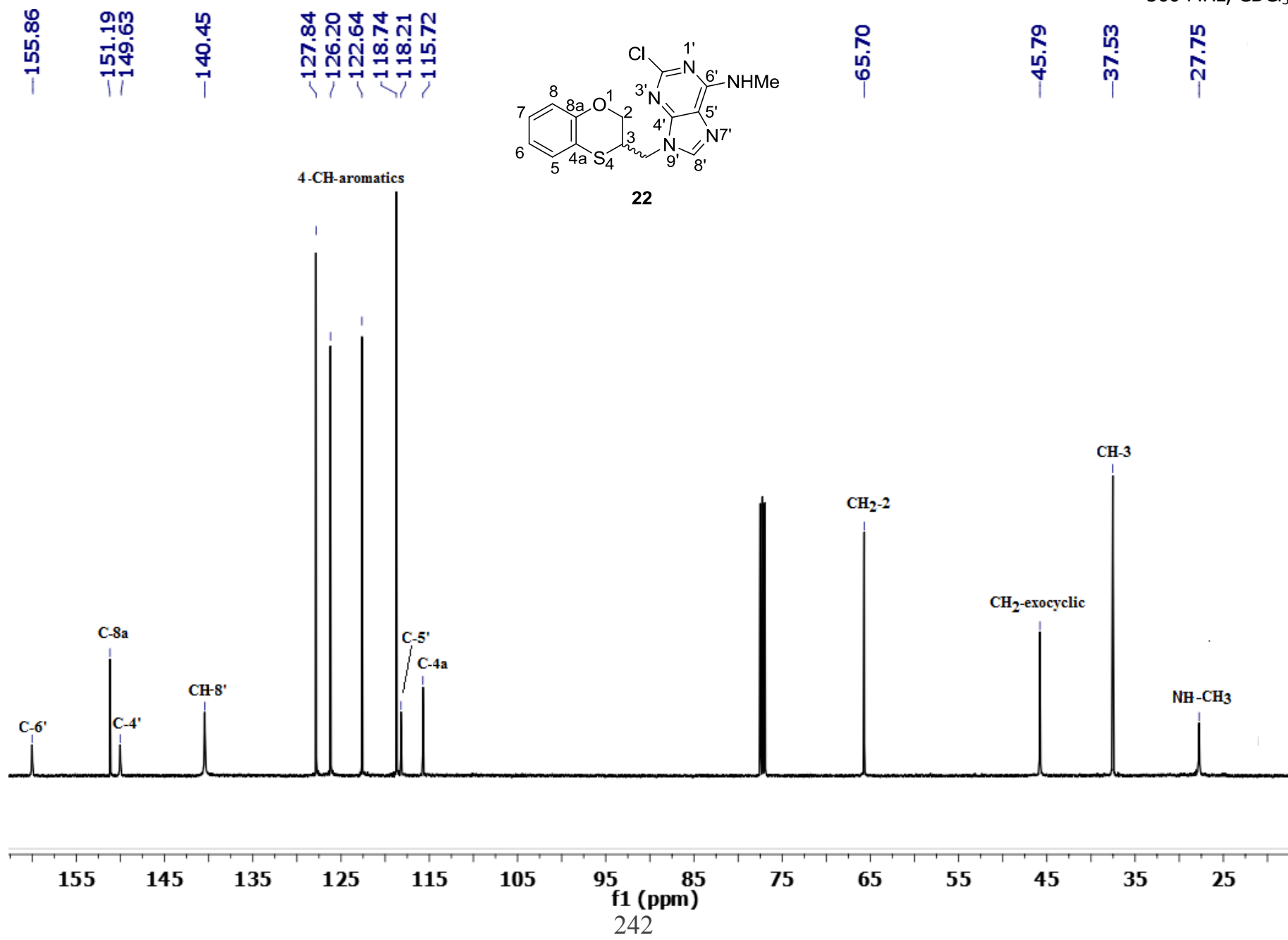
18

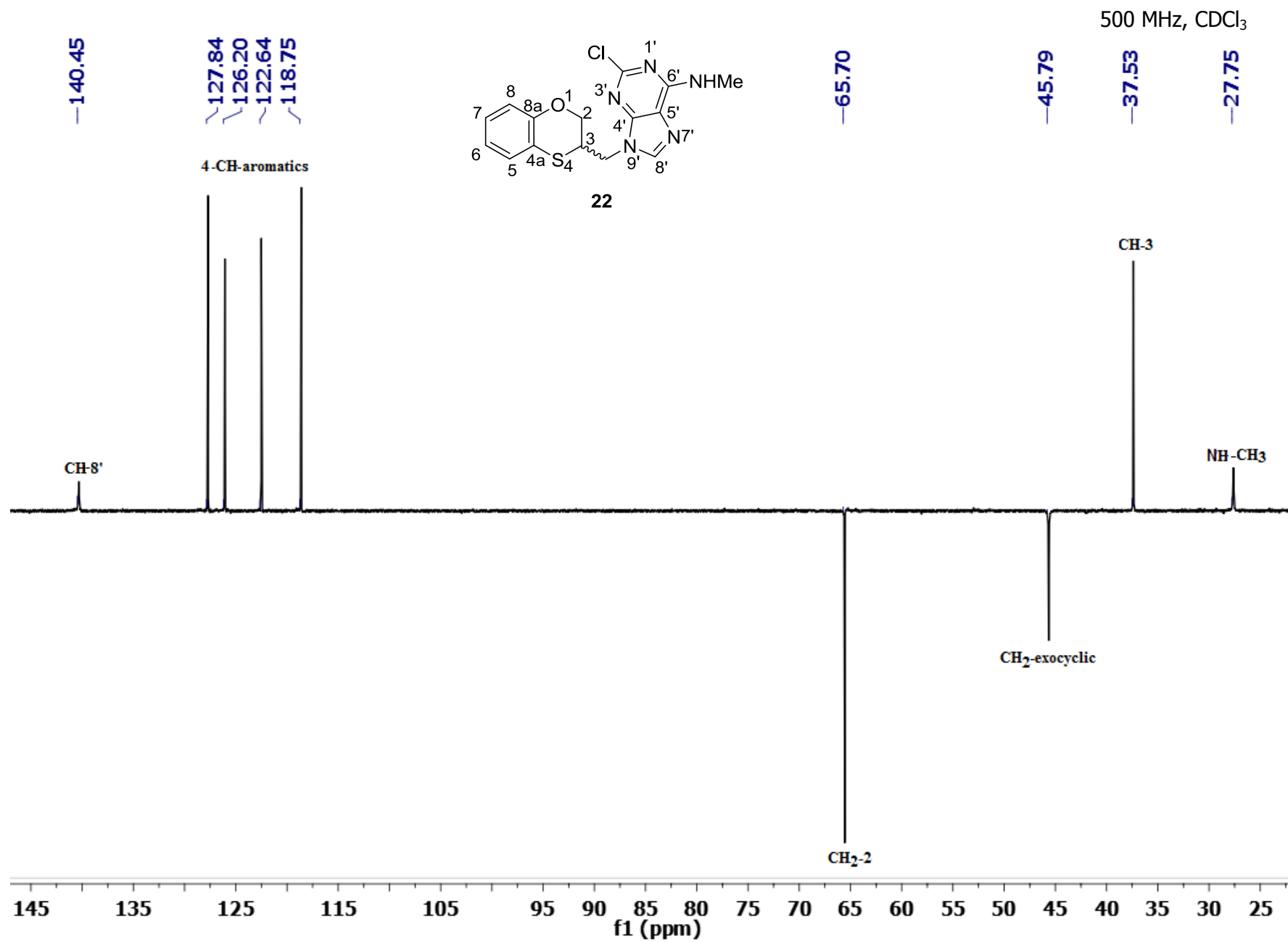


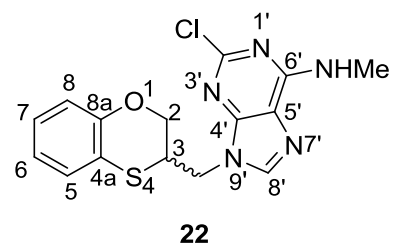
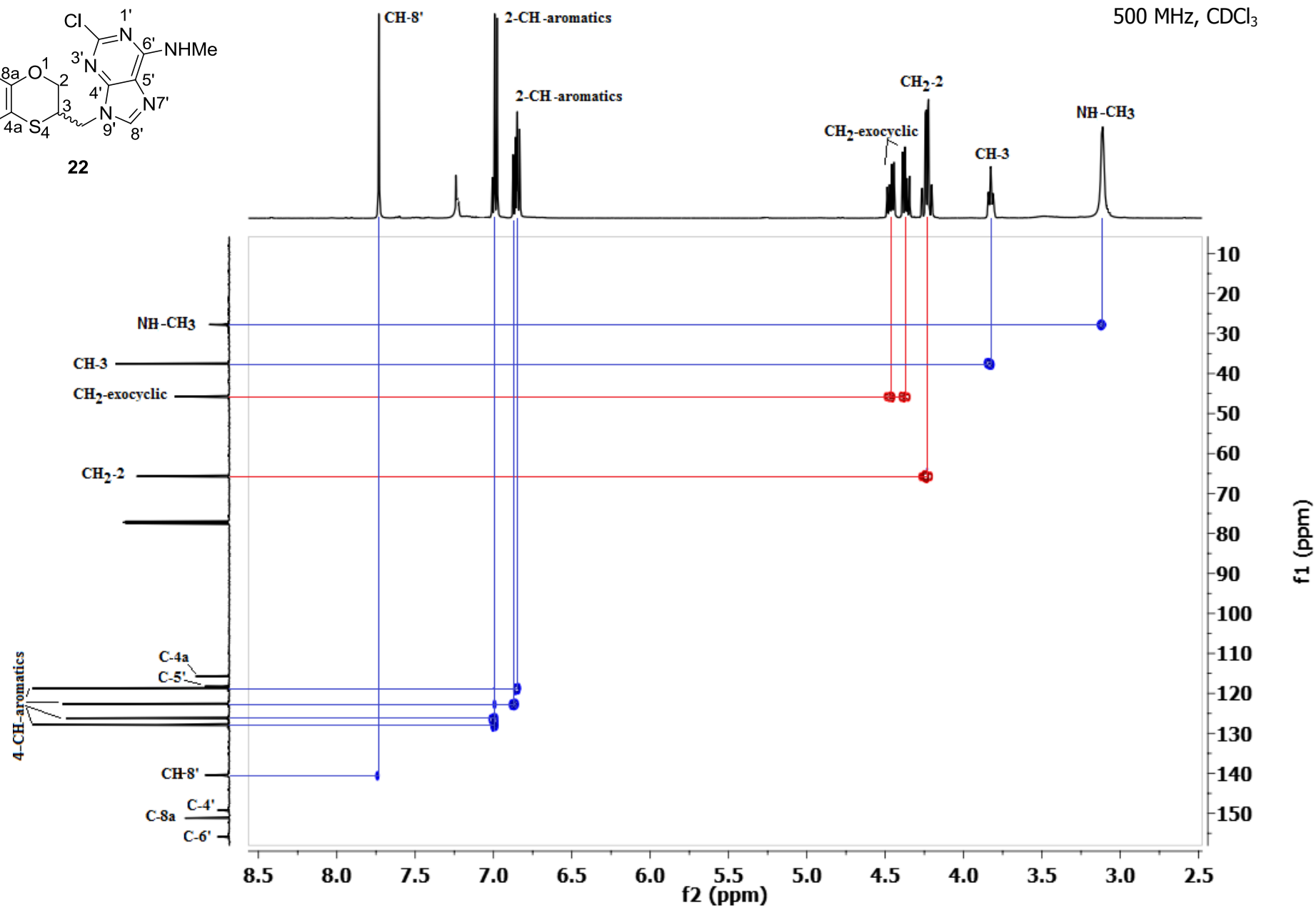
500 MHz, CDCl₃

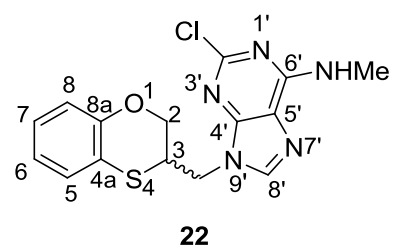
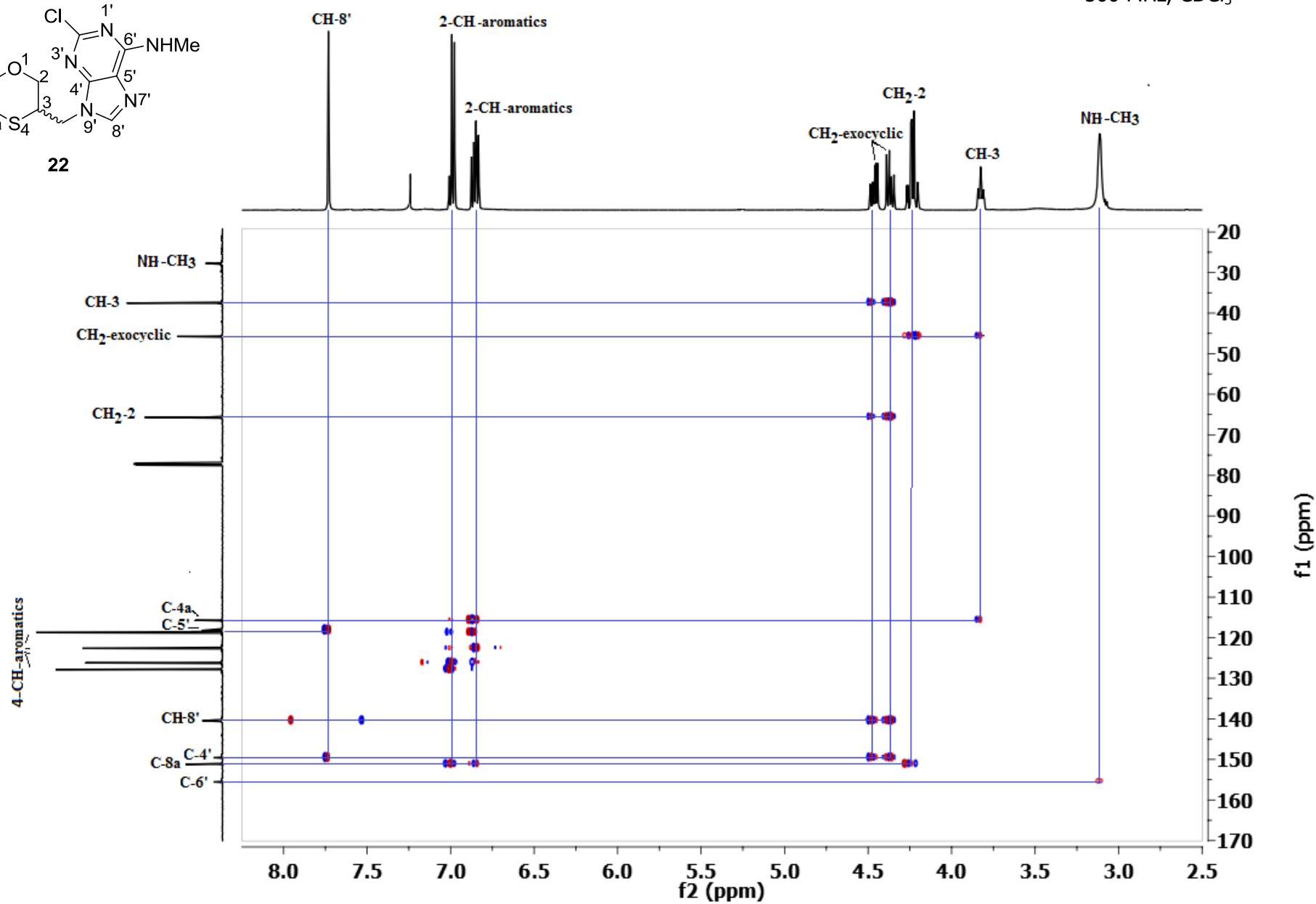


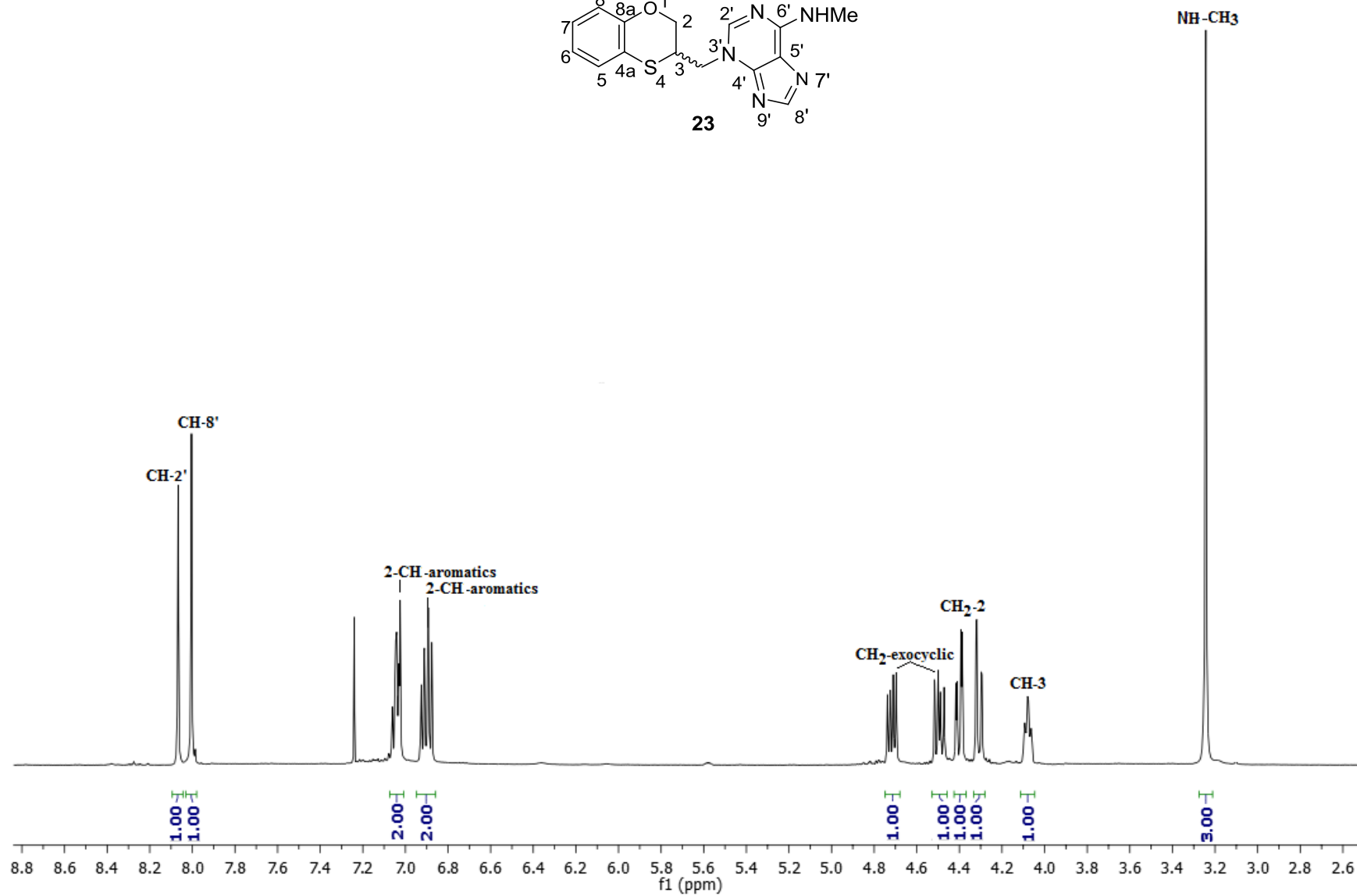
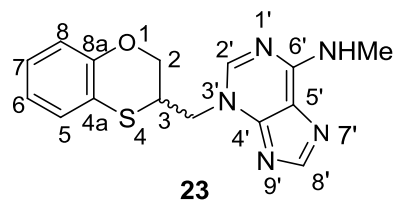
500 MHz, CDCl₃

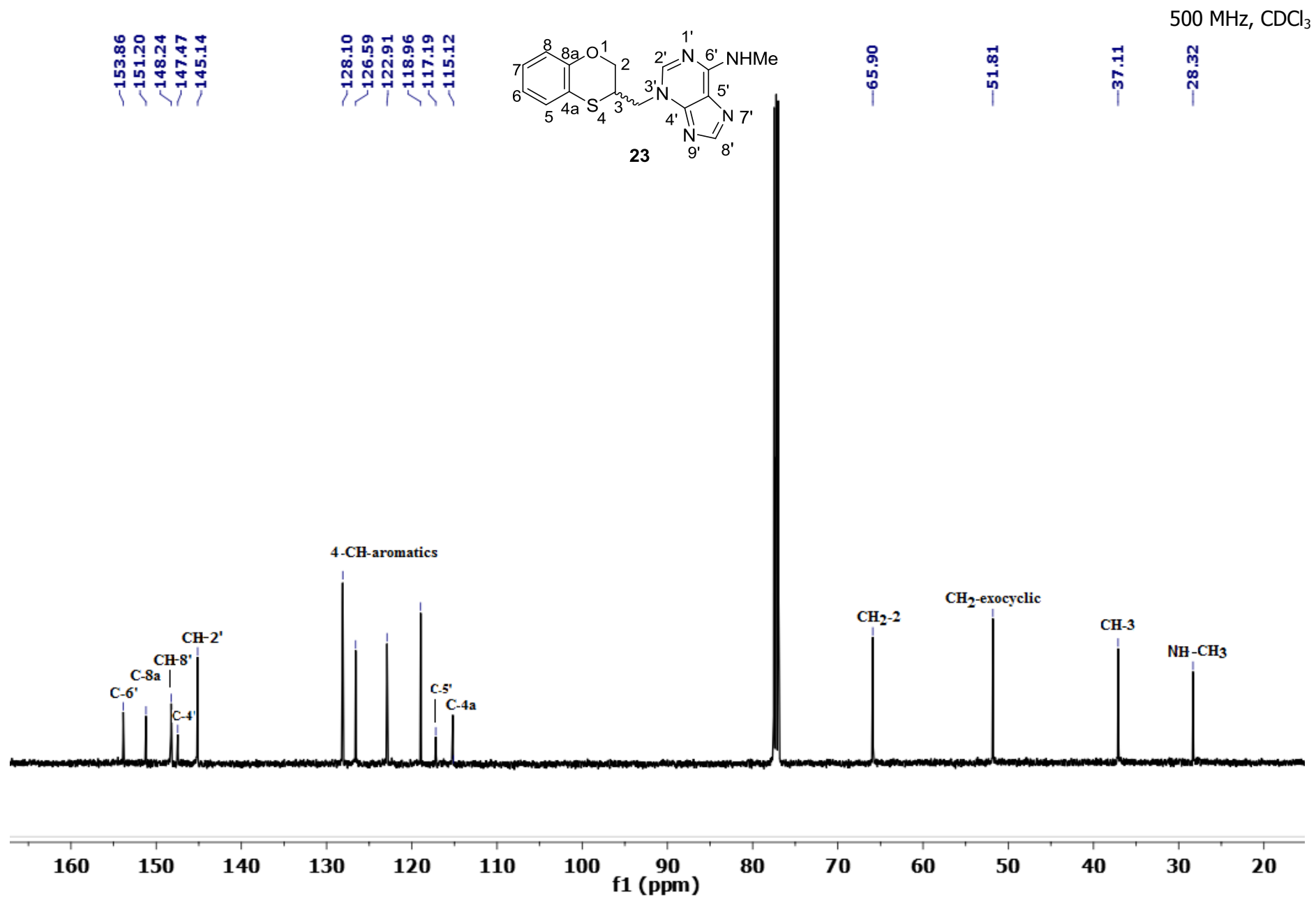
500 MHz, CDCl₃

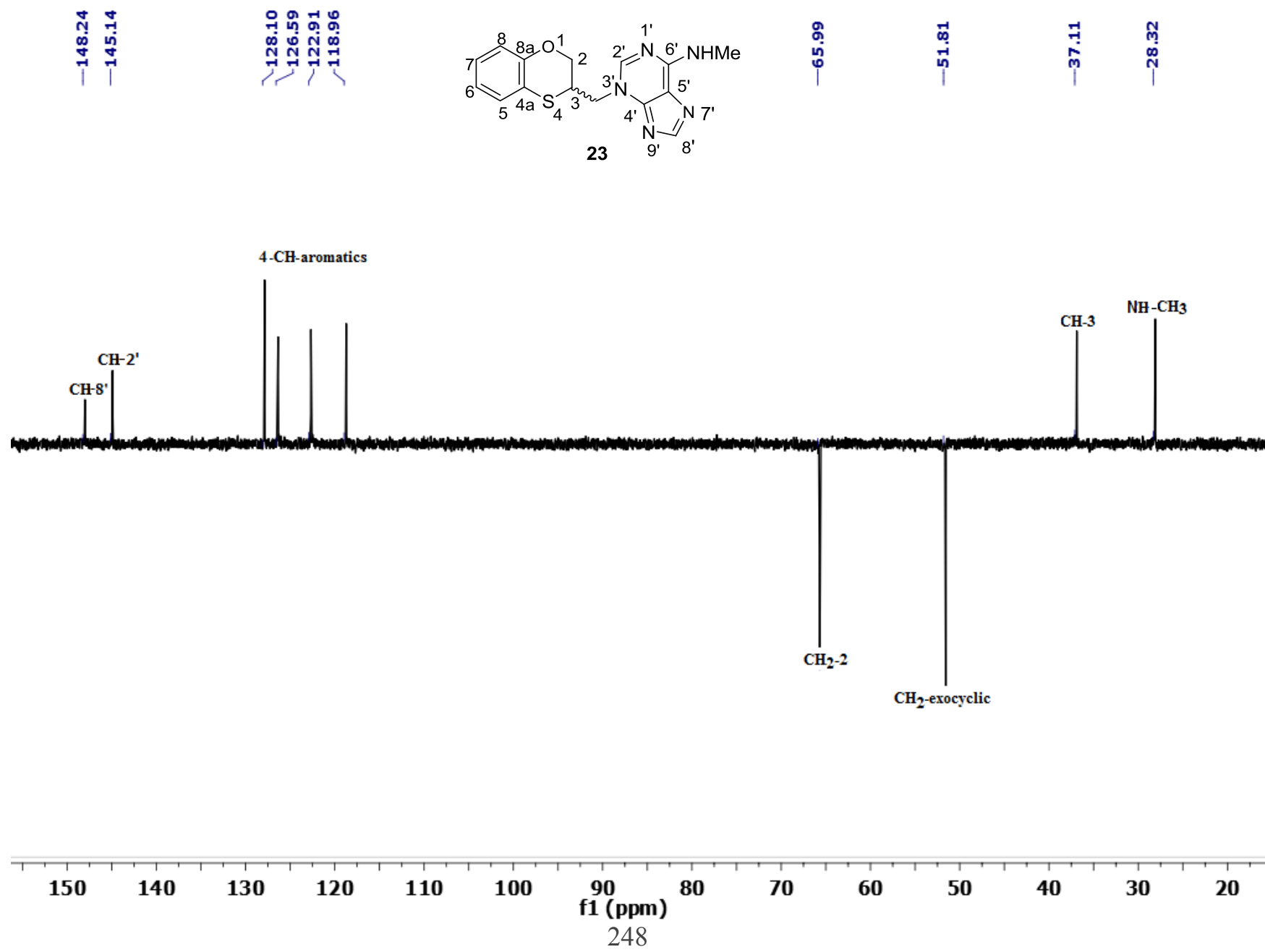


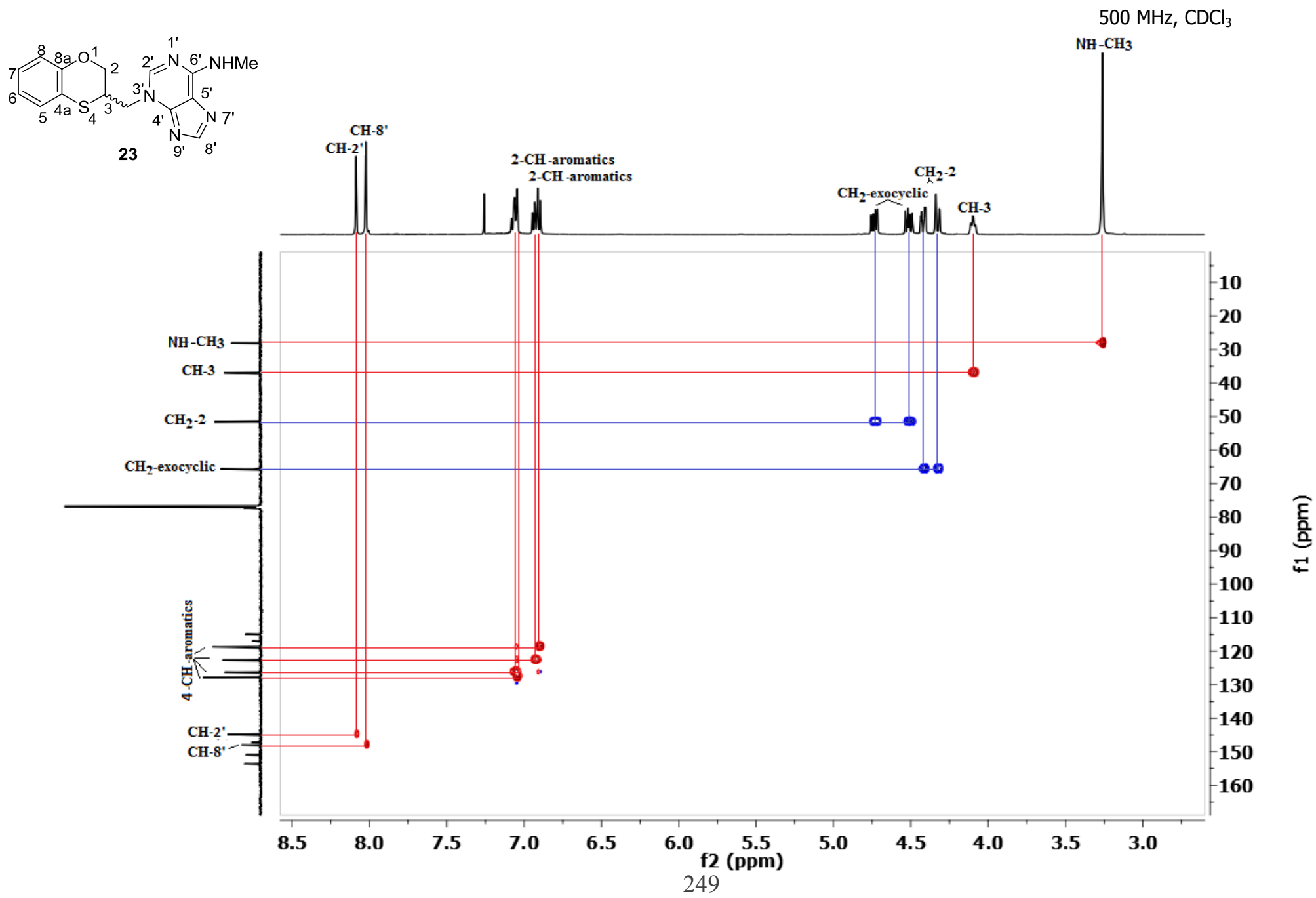
500 MHz, CDCl₃

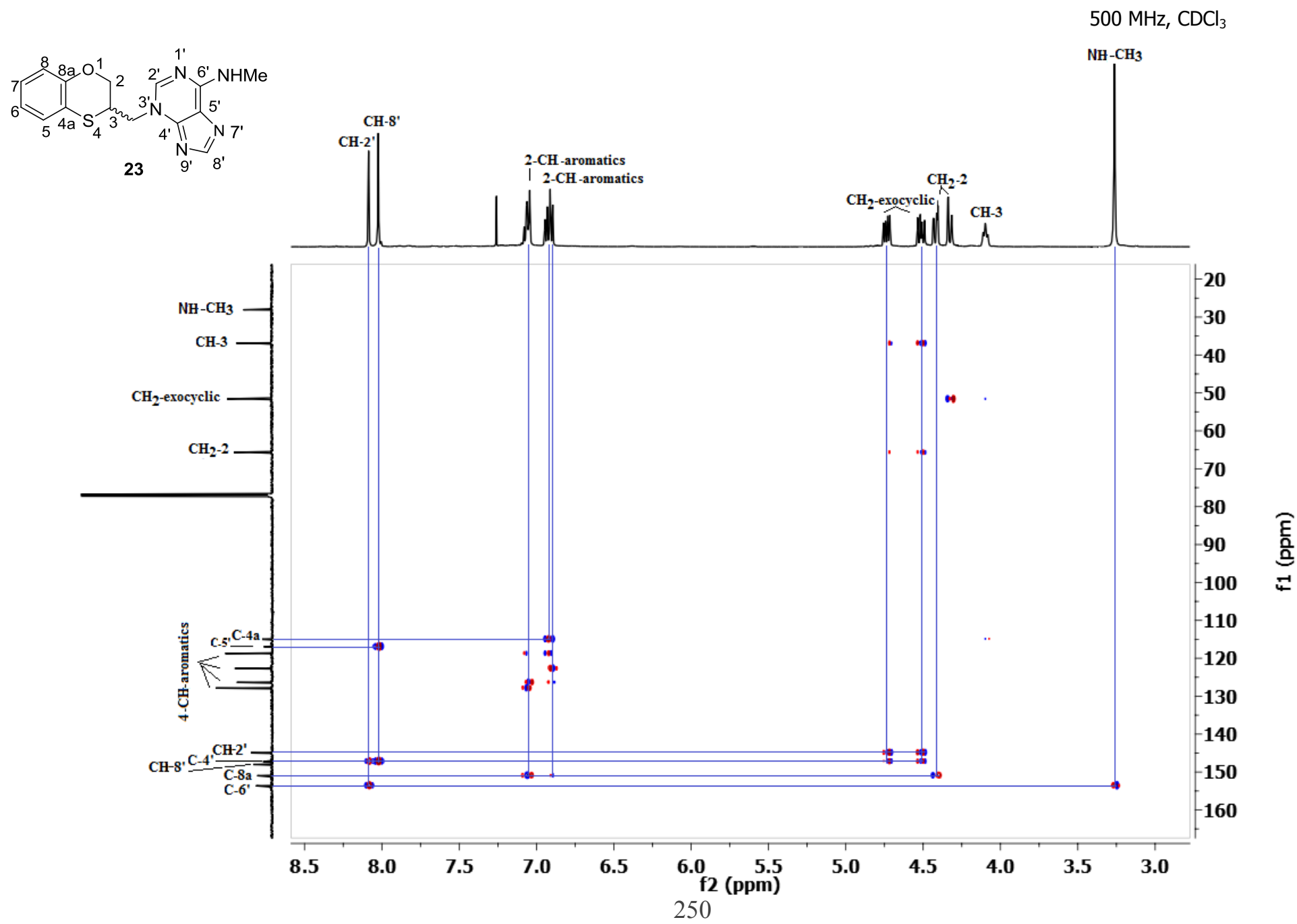
500 MHz, CDCl₃

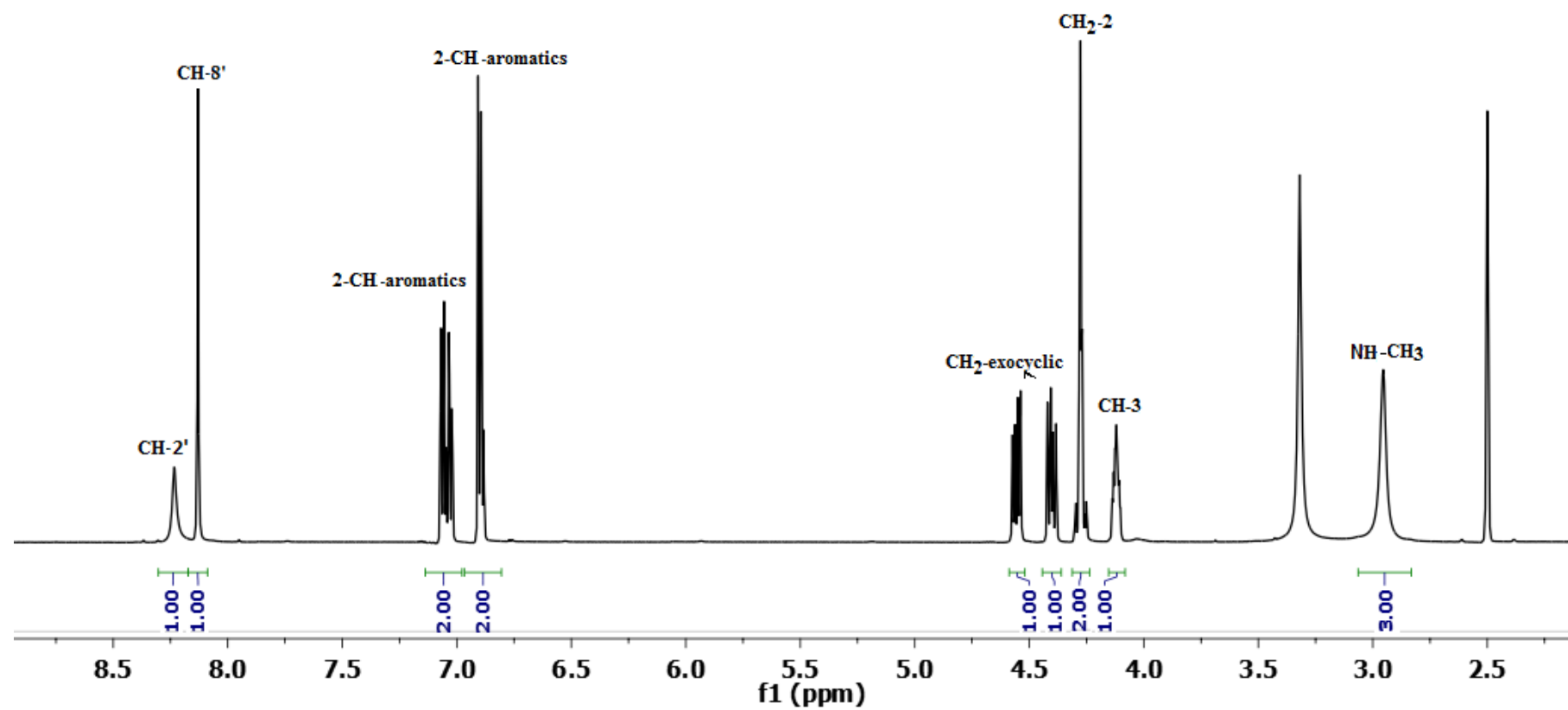
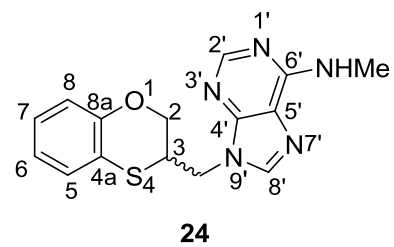
500 MHz, CDCl₃

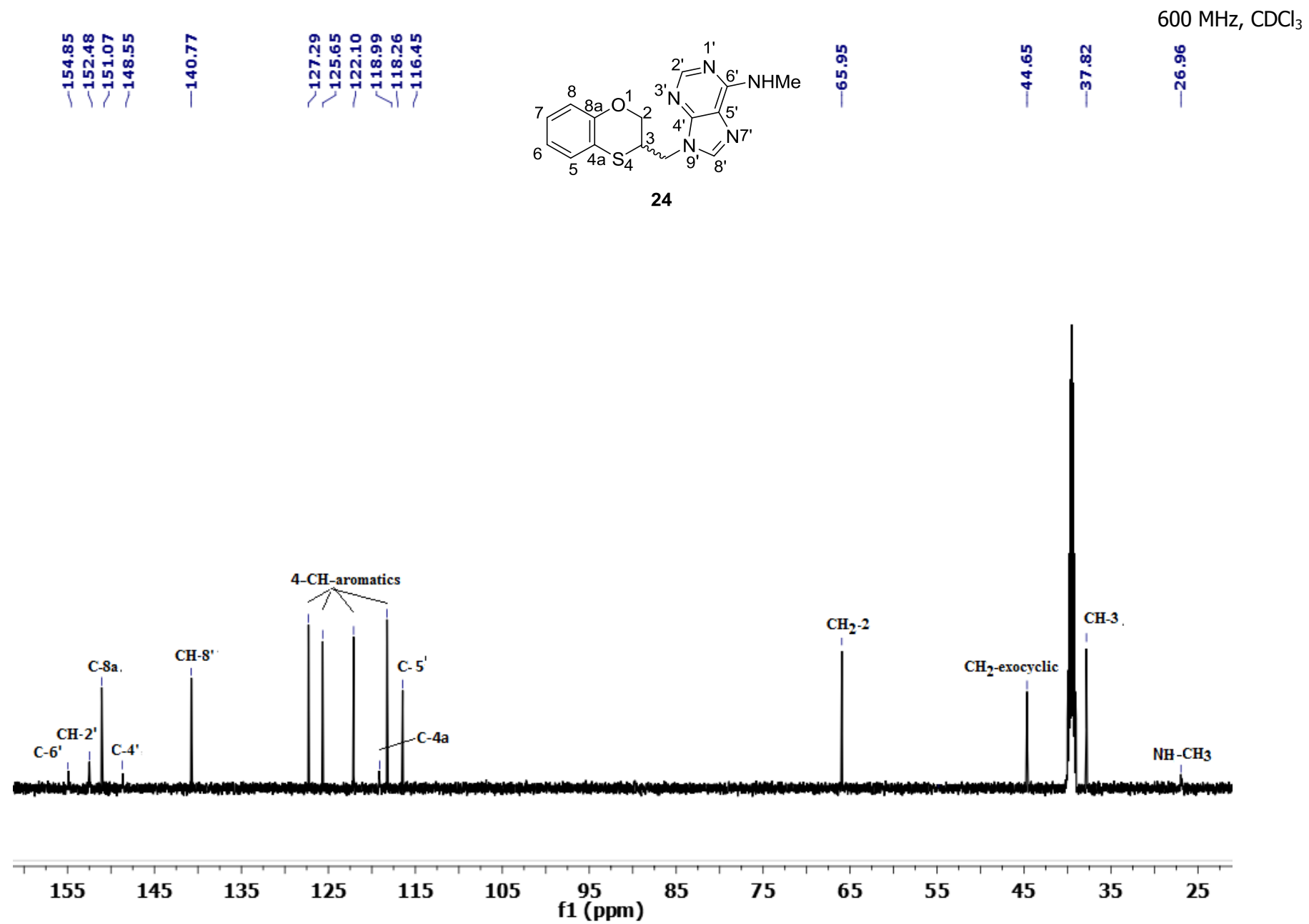


500 MHz, CDCl₃

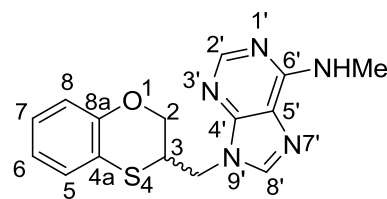




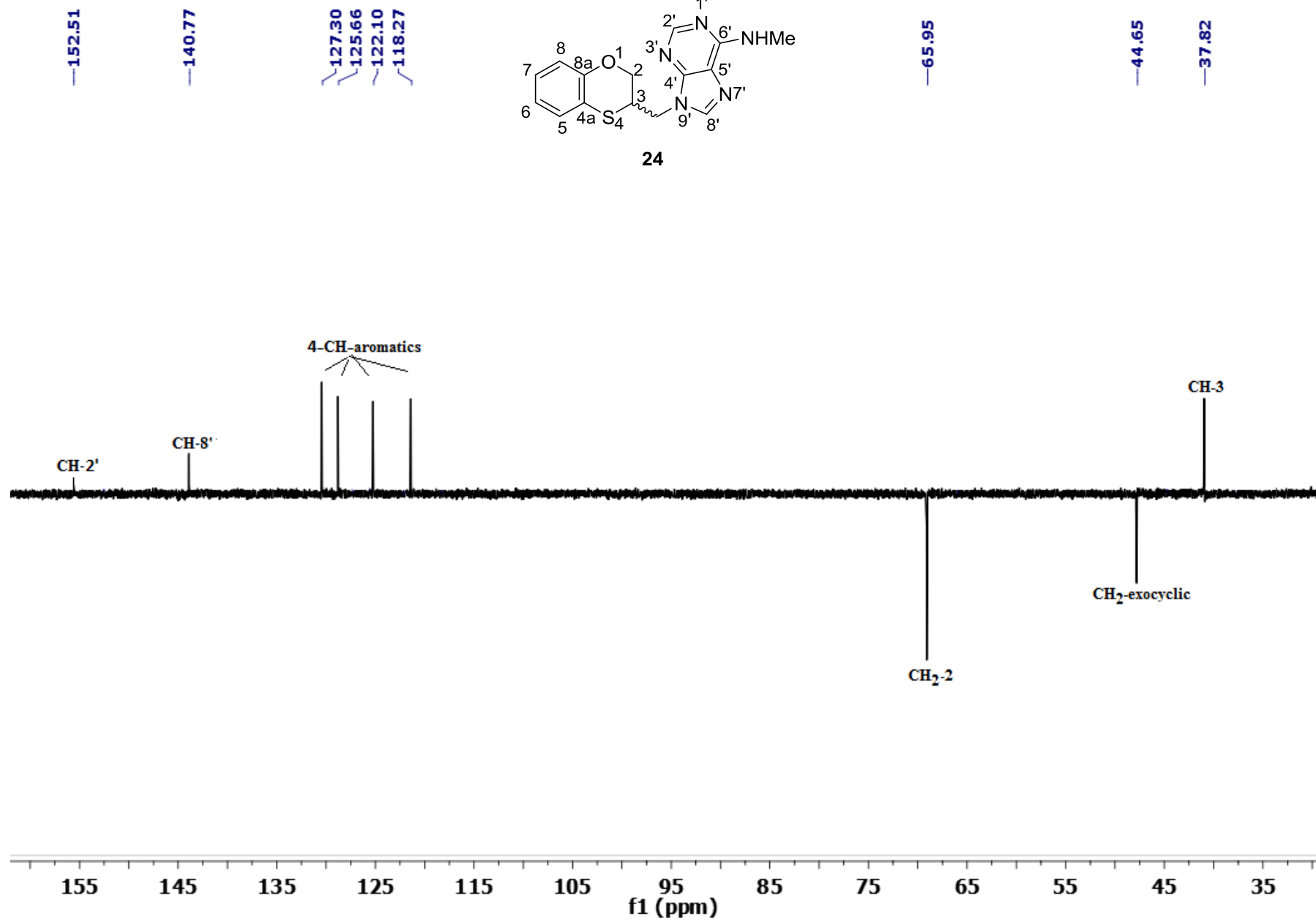




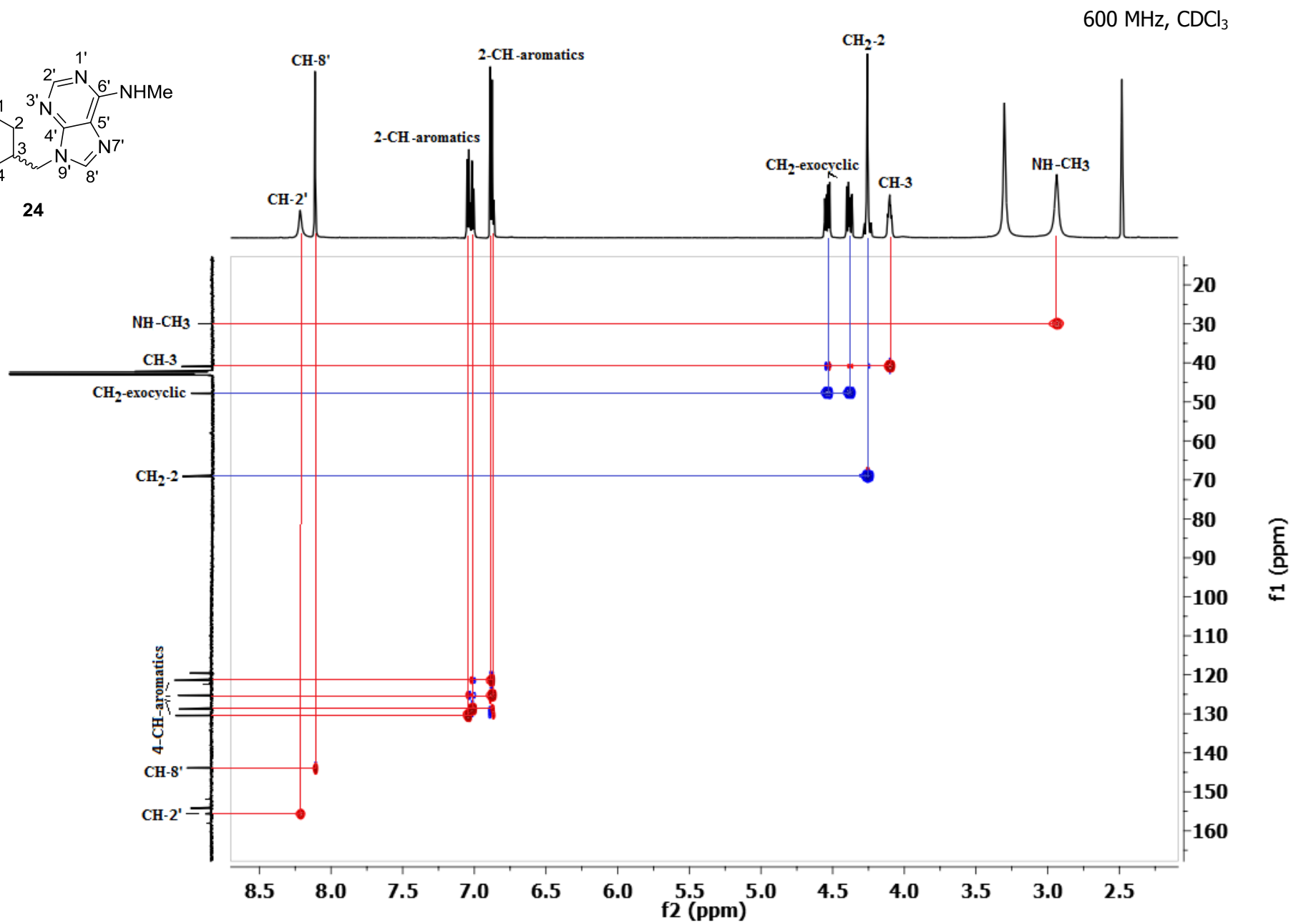
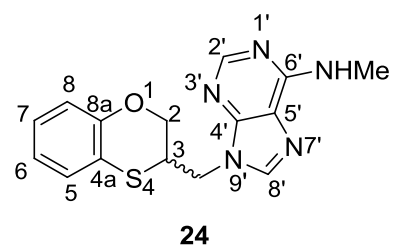
49

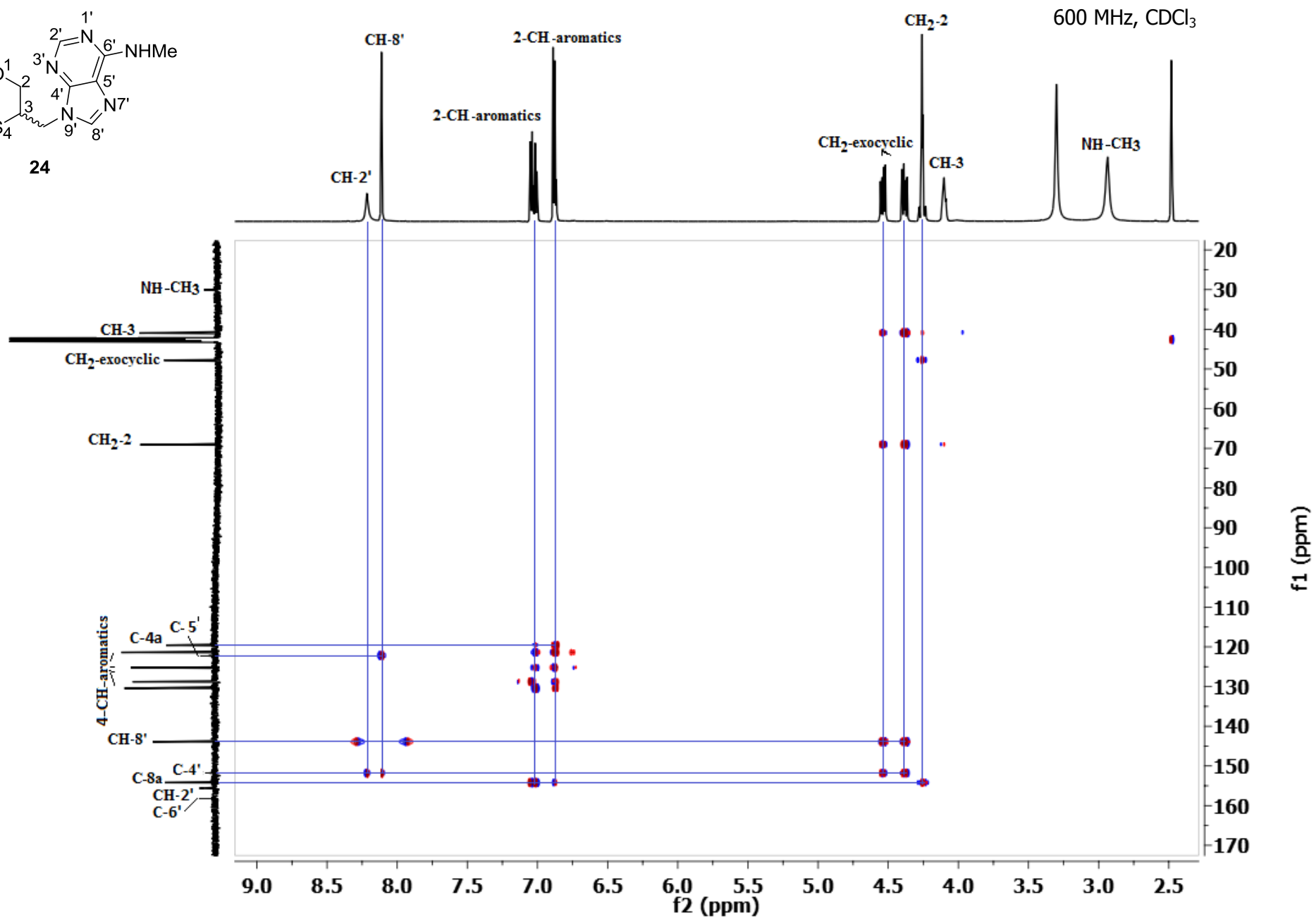
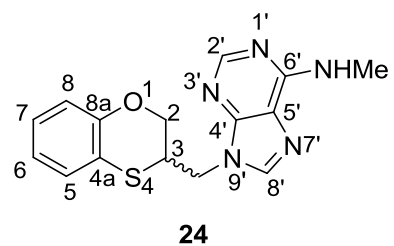
600 MHz, CDCl₃

24



253





Structure of (*RS*)-17

Figures S24 and S25 display the X-ray diffraction of (*RS*)-17. The crystal packing in (*RS*)-17 reveals that pairs of molecules form a dimeric structure by two symmetry-related $\text{C-H}\cdots\pi$ interactions involving the C10-H10A and the five-membered ring of the purine moiety of (*RS*)-17 ($\text{C-H}\cdots$ centroid distance: 2.90 \AA and $\text{C-H}\cdots$ centroid angle: 151.0°). In addition, there are additional $\text{C-H}\cdots\pi$ interactions connecting dimers involving the C22-H22B bond and the six-membered aromatic ring of the 2,3-dihydro-1,4-benzoxathiin moiety ($\text{C-H}\cdots$ centroid distance: 2.64 \AA and $\text{C-H}\cdots$ centroid angle: 166.0°). Therefore these $\text{C-H}\cdots\pi$ interactions build infinite chains. The cooperative effect of non-classical H-bond interactions ($\text{C22-H22A}\cdots\text{N1}$, 3.459 \AA and 149.0°) generates the 3D supramolecular architecture in the crystal.

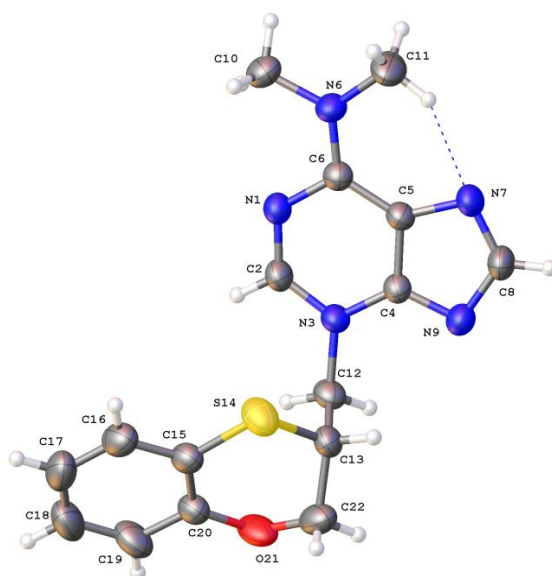


Figure S24. Molecular structure of (*RS*)-17. Hydrogen atoms are drawn as spheres of arbitrary radius. Ellipsoids of the non-hydrogen atoms are drawn at the 50% probability level.

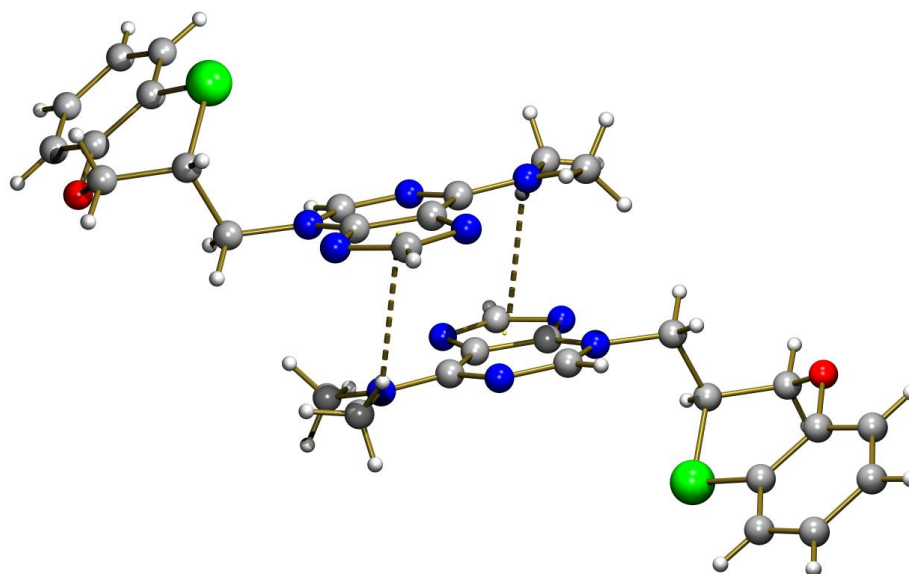


Figure S25. Detail of the dimeric structure of (*RS*)-**17** built by base pairing through --C-H \cdots π interactions.

Structure of (*R*)-**22**

Figures S26 and S27 show the X-ray structure of (*R*)-**22**. The crystal of (*R*)-**22** builds ribbons running along the *a* axis by intermolecular H-bonding interactions between adjacent (*R*)-**22** molecules by $\text{--N-H}\cdots\text{O}$ (2,3-dihydro-1,4-benzoxathiin moiety) interactions (2.985(5)Å, 139.64°). These ribbons are stabilized by $\text{--C-H}\cdots\pi$, involving the --C21-H21A bond and the six membered aromatic ring of the 2,3-dihydro-1,4-benzoxathiin moiety (C-H \cdots centroid distance: 2.62 Å and C-H \cdots centroid angle: 168.0°) and non-classical $\text{--C-H}\cdots\text{N}$ hydrogen interactions (C8-H8 \cdots N7, 3.311(6) Å, 153°). These ribbons are associated by $\text{--C-H}\cdots\text{Cl}$ interactions (3.559 Å, 125.11°) to build the 3D network.

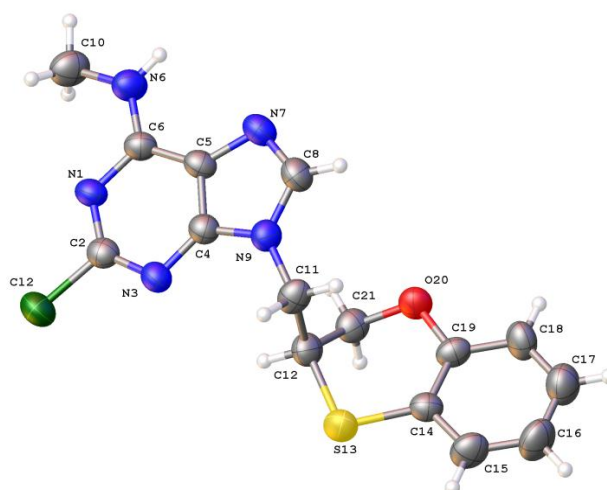


Figure S26. Molecular structure of (*R*)-**22**. Hydrogen atoms are drawn as spheres of arbitrary radius. Ellipsoids of the non-hydrogen atoms are drawn at the 50% probability level.

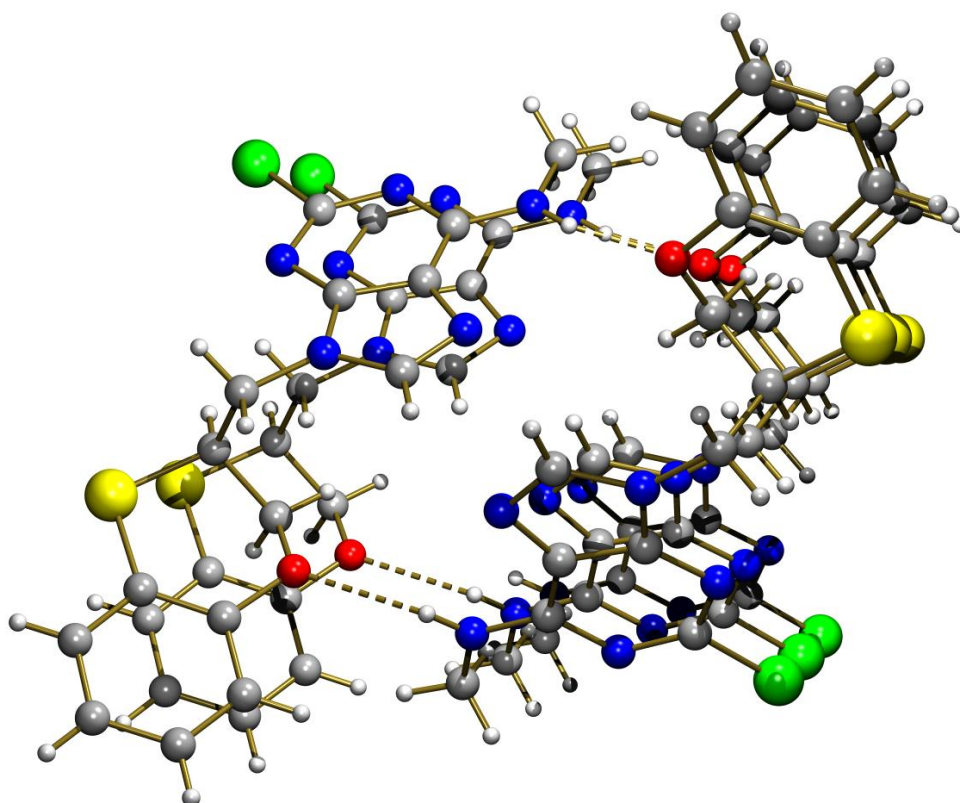


Figure S27. Fragment of a ribbon built by base pairing through $\text{-N-H}\cdots\text{O}$ interactions

X-ray structure of (*RS*)-**24**

Figures S28 and S29 display the X-ray diffraction of (*RS*)-**24**. In the crystal of (*RS*)-**24**, pairs of adjacent (*RS*)-**24** molecules are H-bonded by intermolecular symmetric interactions $\text{-N-H}\cdots\text{N}(\text{imidazole})$ (3.07 Å, 149.0°). π,π -stacking interactions are observed between five- and six-membered rings (purine moiety) of anti-parallel neighbouring (*RS*)-**24** molecules (centroid-centroid distances: 3.786 and 3.527 Å) connecting pairs and generating a ribbon structure running along the *a* axis. Ribbons are associated by $\text{C-H}\cdots\pi$ interactions (C-H \cdots six-membered aromatic ring of the 2,3-dihydro-1,4-benzoxathiin moiety: C-H \cdots centroid distance: 2.74 and 2.67 Å and C-H \cdots centroid angle: 161.0 and 173°) giving rise to two-dimensional frameworks parallel to the *ab* plane. Finally, additional C-H $\cdots\pi$ interactions involving the -C47-H47 bond and the six membered aromatic ring of the purine moiety (C-H \cdots centroid distance: 2.74 Å and C-H \cdots centroid angle: 173.0°) cooperate to reach the 3D structure.

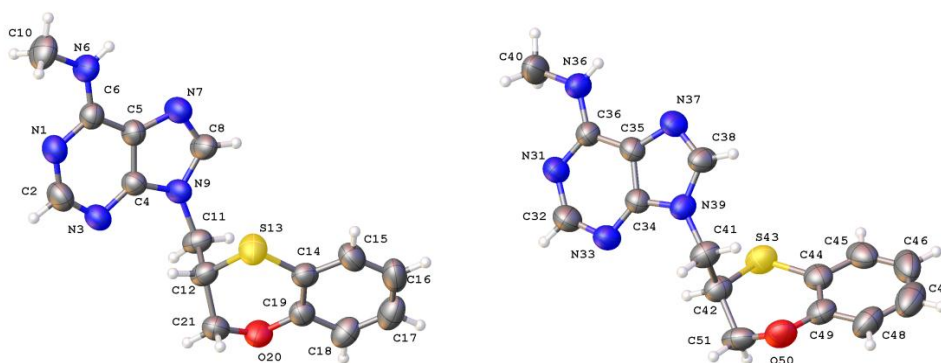


Figure S28. Molecular structure of (*RS*)-**24**. Hydrogen atoms are drawn as spheres of arbitrary radius. Ellipsoids of the non-hydrogen atoms are drawn at the 50% probability level.

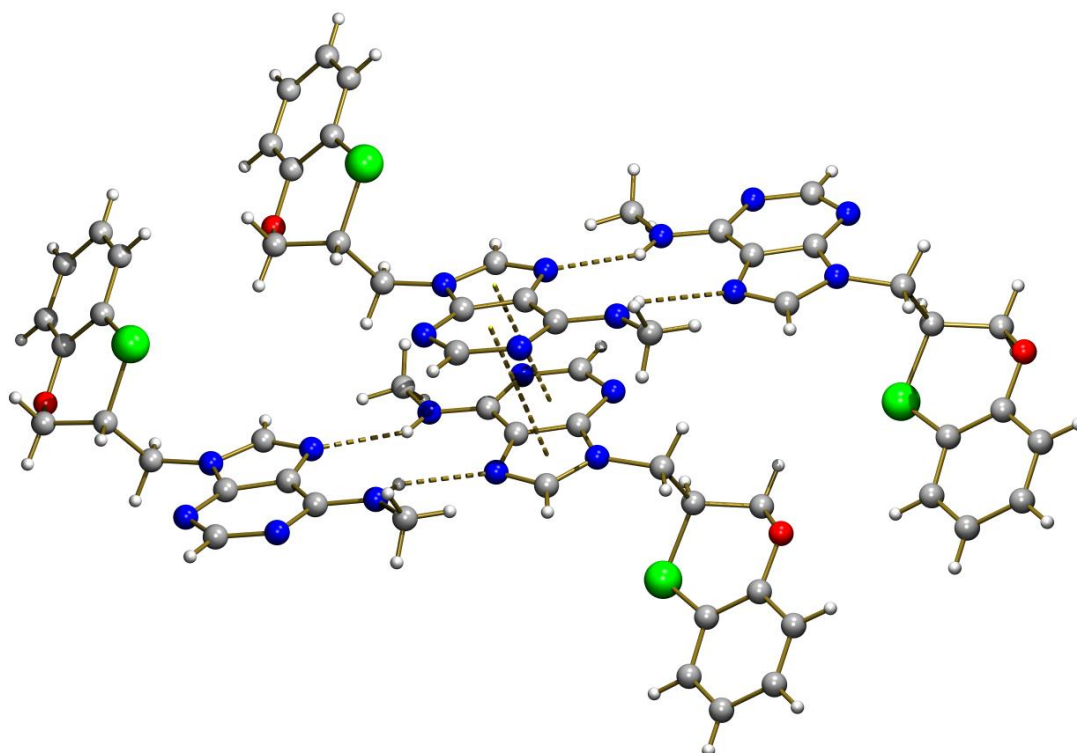


Figure S29. Fragment of a ribbon structure built by base pairing through symmetric N–H···N interactions and π,π -stacking interactions involving aromatic rings of the purine moiety of *(RS)*-**24**.

REFERENCES

- [1] BRUKER, APEX2 Software, Bruker AXS Inc, Madison, Wisconsin, USA, **2010**.
- [2] Sheldrick, G.M. A short history of SHELX. *Acta Cryst.*, **2008**, *A64*, 112–122.

PAPER 5

Cite this: DOI: 10.1039/c2ra21706f

www.rsc.org/advances

COMMUNICATION

Synthesis, unambiguous chemical characterization, and reactivity of 2,3,4,5-tetrahydro-1,5-benzoxazepines-3-ol†

M. Eugenia García-Rubiño, María C. Núñez, Miguel A. Gallo and Joaquín M. Campos*

Received 6th August 2012, Accepted 19th October 2012

DOI: 10.1039/c2ra21706f

The previous structures of several 3,4-dihydro-2*H*-3-hydroxymethyl-1,4-benzoxazines were erroneous (*Bioorg. Med. Chem. Lett.* 2006, 16, 2862; *Synlett* 2009, 3283 and Chinese Patent 2006-10043245). The results presented here are both detailed NMR experiments and synthetic aspects on this subject. We redress some points for the preparation of intermediates of the target molecules.

Introduction

The 2,3-dihydro-1,4-benzodioxin ring **1a** (Fig. 1) constitutes an important skeletal fragment in medicinal chemistry.¹ We have recently reviewed the chemistry of 2,3-dihydro-1,4 benzodioxins and bioisosteres as structural motifs for biologically active compounds.² We used the bioisosteres 3,4-dihydro-2*H*-1,5-benzoxathiepine-3-ol **2** and 2,3-dihydro-1,4-benzoxathiine-2-methanol **3** (Fig. 1) as intermediates to obtain a series of substituted-9-(2,3-dihydro-1,4-benzoxathiine-3- and -2-ylmethyl) purine derivatives with notable anti-proliferative activities.^{3,4} Benzoxazepines are a well-known pharmacophore in medicinal chemistry showing promising activity against various diseases such as antipsychotic, central nervous system activity along with anti-cancer profile against breast cancer cells.^{5,6}

Nitrogen-containing compounds are important chemical entities, many of which show unique bioactivity. 3,4-Dihydro-2*H*-1,4-benzoxazines have been used as a substructure of several biologically interesting agents between them.^{7–12}

Following a bioisosteric replacement as a useful strategy for the structural modification of compounds **1b**,¹³ **2** and **3**, we wish to report herein the synthesis and the correct chemical characterization of compounds **4a–f** and **5a–c**. We will discuss the misunderstanding in the scientific bibliography between the six-membered structures **4a–f** and the seven-membered ones **5a–c**, and the flaws encountered by us in the synthetic protocols that lead to both intermediates **4a** and **5a** and target molecules. Finally, we describe the Mitsunobu reaction³ of **5a** with several substituted purines to obtain **4d–f** (Fig. 2).

Departamento de Química Farmacéutica y Orgánica, Facultad de Farmacia, el Campus de Cartuja s/n, 18071 Granada, Spain.

E-mail: jmcampos@ugr.es; Fax: +34 958 243845; Tel: +34 958 243850

† Electronic supplementary information (ESI) available: Copies of the ¹H, ¹³C NMR, and DEPT spectra of **4a,d–f**, **5a**, **6**, **7**, and **8**, HSQC and HMBC charts for **4a,d–f** and **5a** are provided. See DOI: 10.1039/c2ra21706f

Results and discussion

After a search in literature we found two manuscripts dealing with the synthesis of 3,4-dihydro-2*H*-3-hydroxymethyl-1,4-benzoxazine (**4a**): (a) from **6** in the presence of Hantzsch 1,4-dihydropyridine (HEH) and Pd/C as catalyst¹⁴ (84%); (b) through a tandem reduction-oxirane opening of 1,2-epoxy-3-(*o*-nitrophenoxy)propane (**6**), in the presence of iron powder and acetic acid at reflux,¹⁵ or using Fe or Zn powder as reducing agent, and acetic acid or ammonium chloride as the acidic medium at the reflux temperature of H₂O/EtOH.¹⁶ According to them,^{14–16} the nitro group was reduced, leading to the attack of the amino group on the epoxide moiety in a 6-*exo-tet* fashion, according to the Baldwin rules.¹⁷

The preparation of **6** was published by Xu *et al.*¹⁸ Although they claim that **6** was obtained as a light yellow solid in a 35% yield after recrystallization (EtOH), we did not reproduce their results on repeating their experimental conditions and **7** (82%) was obtained instead as a yellow syrup (Scheme 1). Finally, **7** was subjected to an epoxide-forming process by using sodium hydride (1 equiv.) in anhydrous THF under an inert atmosphere (Scheme 1) and a very pure compound **6** (73%) was obtained as a light yellow solid. The synthetic procedure reported¹⁹ to **6** is different than that stated previously.

As we were surprised by the fact that Xu *et al.*¹⁸ only used 4 fold-less equivalents of the base in relation to *o*-nitrophenol, we decided to equalize both equivalents (1 equiv. of both *o*-nitrophenol and NaOH, but keep 5 equiv. of epichlorohydrin), and to increase the reaction time to 36 h, maintaining the reaction temperature at 85 °C (Scheme 1). The expected compound **6** was obtained in a fairly good yield (64%), together with a low yield (28%) of the propylene chlorohydrin **7**.

In order to speed up the process of formation of **6**, we used microwave irradiation and we obtained **7** (25%) and **6** (64%). When epichlorohydrin and *o*-nitrophenol were reacted in equimolecular quantities under MW irradiation at 95 °C for 40 min, the product of

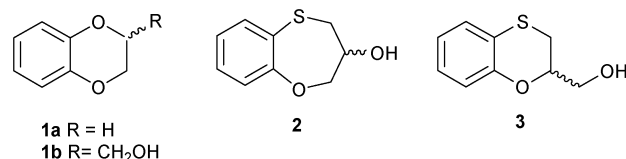


Fig. 1 Structures of benzo-fused six- and seven-membered derivatives.

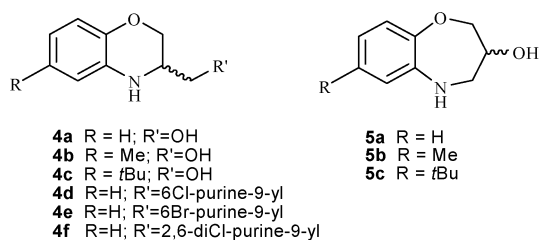


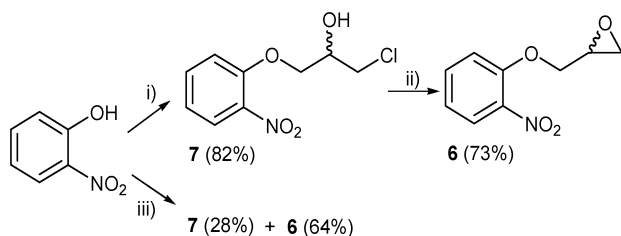
Fig. 2 Molecules discussed in this manuscript.

the reaction was the commercially available 1,3-bis(*o*-nitrophenoxy)-2-propanol (**8**, 83%).

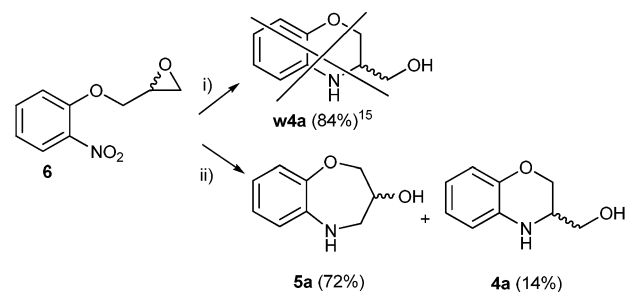
Nevertheless, the two following facts drew our attention after the cyclization reaction from epoxide **6**: (a) two compounds were obtained, whilst the exclusive formation of **w4a**¹⁵ was published (See Scheme 2 to understand this terminology) in 84% yield; and (b) the ¹H NMR spectrum of the mixture shows the presence of two isomers, as demonstrated by the presence of several sets of signals, each one composed of two splitting patterns.

The major isomer was identified as 2,3,4,5-tetrahydro-1,5-benzoxazine-3-ol (**5a**, 72%) and the minor one was 3,4-dihydro-2*H*-3-hydroxymethyl-1,4-benzoxazine (**4a**, 14%) (the ratio between **5a/4a** is 5 : 1). We then decided to carry out a shorter synthesis of **4a** and **5a** in a one-pot process. Starting from *o*-aminophenol (1 equiv.) and epichlorohydrin (1 equiv.), heating under MW-assisted conditions (160 °C, 30 min) produced a mixture of **4a** (34%) and **5a** (55%). Our complete ¹H and ¹³C assignment is based on ¹H signal integrals, multiplicity patterns, a DEPT(135) experiment, and HSQC/HMBC correlations. As the assignment is a routine task, only those points which are crucial to the unambiguous assignment of the previously incorrect structure are emphasized.

The separation of **4a** and **5a** was carried out by HPLC [a mixture of H₂O/MeCN (90/10) as eluent], semi-preparative column Nova-Pak C-18, 60 Å, 6 μm, 17.8 mm × 300 mm, retention time (*t*_R) of **4a**: 6.96 min, and *t*_R of **5a**: 7.27 min. The ¹H and ¹³C NMR spectra (500 MHz, CDCl₃), showed an important mistake, which is one of the key problems for the incorrect structure assignment of **w4a**.¹⁴⁻¹⁶ Zhao, Miao *et al.*¹⁵ literally state the following: *The structure of w4a*¹⁴ was confirmed by ¹H NMR and ¹³C NMR data, which showed the presence of two CH₂-O signals at δ 75.2 and δ 68.4 ppm, and a CH-N signal at δ 52.2 ppm (assigned to C-3), confirming the formation of only one regioisomer. The one-pot synthesis provides a novel and facile method of preparing the 2,3-dihydro-3-hydroxymethyl-1,4-benzoxazine derivatives.



Scheme 1 Reactivity of *o*-nitrophenol: (i) Conditions previously reported:¹⁸ epichlorohydrin (5 equiv.), NaOH (0.25 equiv.), deionized H₂O, 85 °C, 2 h; (ii) NaH (1 equiv.), anhydrous THF, rt, instantaneous reaction; (iii) epichlorohydrin (5 equiv.), NaOH (1 equiv.), deionized H₂O, 85 °C, 36 h.



Scheme 2 Regioselective reaction of the seven-membered ring **5a**: i) according to reference 15 ii) Pd/C, EtOH, reflux, 12 h, inert atmosphere. The identification tag **w4a**¹⁵ denotes the wrong **4a** with its bibliographic reference as superscript: it means “the incorrect structure **4a**, described in the corresponding ref. 14, 15 or 16 but that is actually **5a**”.

In the hetero-methylene zone of the ¹³C NMR spectrum we found the three signals at δ 75.3, 68.5 and 52.3 ppm, similar to those reported.¹⁵ In order to confirm these data and according to the DEPT(135) experiment we found that the signals at δ 75.3 and δ 52.3 ppm are negative peaks, and therefore can be assigned to CH₂-O and CH₂-N signals, whereas the signal at δ 68.5 ppm is positive and can be assigned to the CH-O moiety. Accordingly, the presence of one CH₂-O, one CH₂-N, and one CH-O group is compatible with **5a**. Three years later Liu and Zhou *et al.*¹⁴ committed the same mistake with the incorrect structure **w4a**¹⁴ based on the same spectroscopic data already reported.¹⁵ Following a similar reasoning for **4a**, we found two negative CH₂-O signals at δ 66.1 ppm and δ 63.0 ppm, and one positive (CH-N) at δ 51.4 ppm. This structure was also confirmed with HSQC and HMBC experiments to unambiguously establish the structures **4a** and **5a** (Fig. 3).

In the HMBC experiment to three bonds, the interaction between the hydrogen atoms of the *geminal* H-2 and H-2' with the quaternary C-8a of the benzene ring should be observed in **4a**, whilst interactions between H-2 [δ 4.25 (ddd)] and H-2' [δ 3.86 (dd)], and H-4 [δ 3.36 (ddd)] and H-4' [δ 3.17 (dd)], with the quaternary C-9a (δ 150.7 ppm) and C-5a (δ 142.0 ppm) respectively, are unequivocal proofs for the structure of **5a** (Fig. 3).

Both NMR data and the structure of the alcohol obtained fit in with **5a** but not with the reported results published.¹⁴⁻¹⁶ To reinforce our conclusions even more, we made a deep bibliographic search and found a patent, written in Japanese, in which the synthesis and ¹H NMR data of **4a** were correctly reported.²⁰

Having found controversial results between our research and that published,¹⁴⁻¹⁶ we decided to carry out the reduction of **6** under the

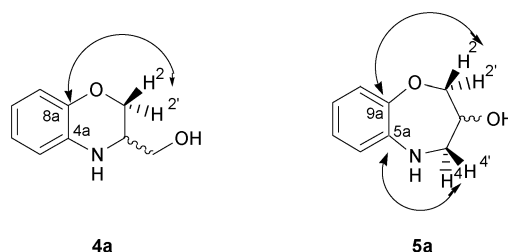


Fig. 3 Representation of the HMBC interactions observed in the six- and seven-membered rings (**4a** and **5a**).

Table 1 Comparison of the chemical shifts (δ), multiplicity patterns and coupling constants (J , Hz) of the ^1H NMR spectra for compounds **4a**, **5a** and **w4a,b,c**

Compd	R	H-2	H-2'	H-3	H-4	H-4'
5a	H	4.25 (ddd) $J = 12.3, 3.8, 1.4$	3.86 (dd) $J = 12.3, 2.0$	3.93 (m)	3.36 (ddd) $J = 12.9, 4.9, 1.4$	3.17 (dd) $J = 12.9, 2.4$
4a	H	4.18 (dd) $J = 10.8, 2.9$	4.06 (dd) $J = 10.8, 5.9$	3.55 (m)	3.72 (dd) $J = 10.7, 4.9$	3.64 (dd) $J = 10.7, 7.1$
w4a	H	4.26 (dd) $J = 12.8, 3.8$	3.88 (dd) $J = 12.8, 2.0$	3.91–3.97 (m)	3.36 (dd) $J = 12.9, 4.8$	3.19 (dd) $J = 12.9, 2.4$
w4b	7-Me	4.25 (dd) $J = 12.3, 2.7$	3.80 (dd) $J = 12.3, 1.5$	3.89–3.95 (m)	3.37 (dd) $J = 12.8, 3.9$	3.14 (dd) $J = 12.8, 1.9$
w4c	7- <i>t</i> Bu	4.25 (dd) $J = 12.3, 3.7$	3.84 (dd) $J = 12.3, 1.9$	3.89–3.97 (m)	3.39 (dd) $J = 12.8, 4.7$	3.18 (dd) $J = 12.8, 2.2$

conditions previously reported (Fe/HOAc, EtOH/H₂O at reflux).¹⁵ This procedure provides **5a** and not **4a** as stated, which we confirmed after an in-depth NMR study and the unambiguous demonstration of the **5a** structure, in spite of the fact that it was published as **w4a**.^{14–16} Compounds **w4b,c** were prepared according to a reported procedure,¹⁵ and we found that these compounds were actually **5b,c** based on DEPT(135) data: **5b** and **5c** show peaks at δ 52.10 and at δ 52.13 ppm (N–CH₂), respectively and negative peaks at δ 75.12 ppm and at δ 75.18 ppm (O–CH₂) while the positive peaks at δ 68.30 ppm (O–CH) for both **5b** and **5c** are unambiguously assigned to the methine carbons. Table 1 shows the correct chemical shifts, multiplicity patterns and coupling constants (J) in Hz of compounds **5a–c** and **4a**.¹⁵

In spite of the fact that Liu and Zhou¹⁴ reported the incorrect structure of **w4a**, the formation of six- and/or seven-membered alcohols starting from di- or three-substituted epoxides is accurate. In these cases 2D NMR data correctly supported the target structures and the aromatic splitting patterns comply with our above-mentioned rules.

Conclusively and to emphasize the reactivity of the seven-membered secondary alcohol **5a**, its reaction with several purines under the microwave-mediated Mitsunobu conditions was studied (Scheme 3).

The product of the three reactions are the six-membered compounds **4d–f** (3,4-dihydro-2*H*-3-hydroxymethyl-1,4-benzoxazines

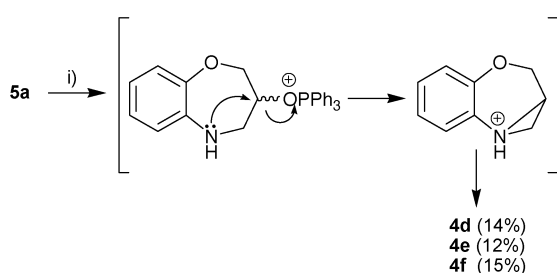
linked to the *N*-9' purine atom through a methylene linker), demonstrated by the 2D NMR data. The ring contraction can be explained through an aziridinium ion, as previously published in a similar reaction *via* an episulfonium intermediate.³ The anticancer activity and study of the mechanism of action of **4d–f** are underway.

In summary, 2,3,4,5-tetrahydro-1,5-benzoxazepines-3-ol **5a–c** have not been reported yet because they were mistaken as being the 3,4-dihydro-2*H*-3-hydroxymethyl-1,4-benzoxazines **4a–c**.¹⁴ We have also improved the method of synthesis of **4a** and **5a**, in a one-step and one-pot reaction from *o*-aminophenol and epichlorohydrin under microwave irradiation. Compounds **5a–c** may serve as synthons for the development of new biologically active prototypes. Although six-membered rings are more stable than their seven-membered counterparts, and in general favored when there are both possibilities of formation, the use of the DEPT, HSQC and HMBC techniques would have made clear the correct assignment of the target scaffold.

We wish to help people working on benzo-fused six- and seven-membered diheterocycles to facilitate their research after having made clear and unambiguous the differences between these two scaffolds. Clarification of the confusion reported in previous works will prevent the proliferation of scientific mistakes and consequently avoid a negative domino effect due to the rapid divulgation of information nowadays.

Experimental section

Melting points were taken in open capillaries on an electrothermal melting point apparatus and are uncorrected. Analytical thin layer chromatography was performed using Merck Kieselgel 60 F254 aluminum sheets, the spots being developed with UV light ($\lambda = 254$ nm). Evaporations were carried out *in vacuo* with a Büchi rotary evaporator and the pressure was controlled by a Vacuubrand CVCII apparatus. For flash chromatography, Merck silica gel 60 with a particle size of 0.040–0.063 mm (230–400 mesh ASTM) was used. Nuclear magnetic resonance spectra have been carried out at the Centro de Instrumentación Científica/Universidad de Granada, and recorded on a 500 MHz ^1H and 125 MHz ^{13}C NMR DEPT, HMBC and HSQC NMR Varian NMR-System-TM400 (compounds



Scheme 3 Reagents and conditions: substituted purines, Ph₃P, DIAD, anhydrous THF, microwave irradiation, 140 °C, 5 min.

4d-f,5a) or 400 MHz ^1H and 100 MHz ^{13}C NMR and DEPT NMR Varian Inova-TM spectrometers (compounds **6-8**) at ambient temperature. Chemical shifts (δ) are quoted in parts per million (ppm) and are referenced to the residual solvent peak. Signals are designated as follows: s, singlet; d, doublet; dd, doublet of doublets; ddd, double doublet of doublets; dt, doublet of triplets; t, triplet; m, multiplet. The HMBC spectra were measured using a pulse sequence optimized for 10 Hz (inter-pulse delay for the evolution of long-range couplings: 50 ms) and a 5/3/4 gradient combination. In this way, direct responses (J couplings) were not completely removed. High-resolution nano-assisted laser desorption/ionization (NALDI-TOF) or electrospray ionization (ESITOF) mass spectra were carried out on a Bruker Autoflex or a Waters LCT Premier Mass Spectrometer, respectively. Small scale microwave-assisted synthesis was carried out in an Initiator 2.0 single-mode microwave instrument producing controlled irradiation at 2.450 GHz (Biotage AB, Uppsala). Reaction time refers to hold time at 140 °C, not to total irradiation time. The temperature was measured with an IR sensor outside the reaction vessel. Anhydrous THF was purchased from VWR International Eurolab. Anhydrous conditions were performed under argon. 6-Chloropurine, 6-bromopurine and 2,6-dichloropurine were purchased from Aldrich. Compounds **4d-f** were synthesized according to our previously reported procedure.³ An HPLC apparatus and a fluorescence detector were used for separation of **4a** and **5a** (semi-preparative column C-18, 60 Å, 6 μm , 17.8 mm \times 300 mm).

1,2-Epoxy-(*o*-nitrophenoxy)propane (**6**) and 1-(*o*-nitrophenoxy)-3-chloro-2-propanol (**7**)

Method a): preparation of **6 and **7**.** The general procedure below was previously reported,¹⁸ but our experimental results were different (see Scheme 1): Xu *et al.*¹⁸ described the formation of **6** in a 35% yield as a yellow solid, but we obtained **7** (82%) as a yellowish syrup. ^1H NMR (400 MHz, CDCl_3) δ 7.71 (d, $J = 8.1$ Hz, 1H), 7.43 (t, $J = 7.9$, 1H), 7.01 (d, $J = 8.4$ Hz, 1H), 6.93 (t, $J = 7.7$ Hz, 1H), 4.17 (m, 3H), 3.69 (m, 2H), 3.60 (d, $J = 5.6$ Hz, 1H). ^{13}C NMR (100 MHz, CDCl_3) δ 151.7, 139.1, 134.6, 125.6, 120.9, 114.8, 69.9, 69.3, 45.3. HR TOF MS ES+, calculated for $\text{C}_9\text{H}_{11}\text{ClNO}_4$ 232.0377, found $\text{C}_9\text{H}_{11}\text{ClNO}_4$ 232.0377. Anal. Calcd for $\text{C}_9\text{H}_{10}\text{ClNO}_4$: C, 46.67; H, 4.35; N, 6.05. Found: C, 46.89; H, 4.33; N, 5.89. HR TOF MS ES+.

Method b): preparation of **6 and **7**.** Following the general procedure,¹⁸ but increasing from 0.25 equiv. to 1 equiv. of NaOH, **6** (64%) and **7** (28%) were obtained (see Scheme 1) as a yellowish solid (mp 81.5–82 °C, lit.⁴² 79 °C) and a yellowish syrup, respectively. Compound **6**: ^1H NMR (400 MHz, CDCl_3) δ 7.84 (dd, $J = 8.1$, 1.3 Hz, 1H), 7.57 (dt, $J = 8.2$, 1.2 Hz, 1H), 7.19 (d, $J = 8.5$ Hz, 1H), 7.09 (t, $J = 7.9$ Hz, 1H), 4.51 (dd, $J = 11.3$, 2.1 Hz, 1H), 4.11 (dd, $J = 11.3$, 5.6 Hz, 1H), 3.42 (m, 1H), 2.91 (m, 2H). ^{13}C NMR (100 MHz, CDCl_3) δ 151.4, 139.5, 134.1, 125.1, 120.6, 114.8, 69.6, 49.5, 43.9. HR TOF MS ES+, calcd for $\text{C}_9\text{H}_9\text{NO}_4\text{Na}$ ($\text{M} + \text{Na}$)⁺ 218.0429, found 218.0427. Anal. Calcd for $\text{C}_9\text{H}_9\text{NO}_4$: C, 55.39; H, 4.65; N, 7.18. Found: C, 55.23; H, 4.29; N, 7.00.

1,2-Epoxy-(*o*-nitrophenoxy)propane (**6**) from 1-(*o*-nitrophenoxy)-3-chloro-2-propanol (**7**)

To a solution of **7** (2.175 g, 9.3 mmol) in anhydrous THF (30 mL) under argon, 60% NaH (0.373 g, 9.3 mmol) was added dropwise at

room temperature. The reaction changed instantaneously from a yellow to a cloudy orange color. 2N HCl was added at pH = 6–7, the mixture was extracted (H_2O and CH_2Cl_2), the organic layers decanted, dried (Na_2SO_4) and filtered to give **6** (1.33 g, 73%, Scheme 1).

1,2-Epoxy-(*o*-nitrophenoxy)propane (**6**), 1-(*o*-nitrophenoxy)-3-chloro-2-propanol (**7**) and 1,3-bis(*o*-nitrophenoxy)-2-propanol (**8**) under microwave irradiation

Epichlorohydrin was added to a solution of *o*-nitrophenol and aqueous NaOH. The reaction was irradiated in a microwave oven at 95 °C for 40 min. The mixture was cooled and poured into ice water, and the aqueous layer was extracted with CH_2Cl_2 . Organic layers were combined and dried (Na_2SO_4). After filtration, the solvent was removed *in vacuo* and the crude was purified by gradient-elution flash column chromatography using hexane/EtOAc (9/1 \rightarrow 8/2 \rightarrow 0/10) mixtures.

Method a): preparation of **6 and **7**.** After using 1 equiv. of *o*-nitrophenol, 2 equiv. of epichlorohydrin, and 1.25 equiv. of NaOH in 7 mL of H_2O and following the general method, **6** (64%) and **7** (25%) were obtained.

Method b): preparation of **8**

Same conditions as method a), except that 2.5 equiv. of NaOH were used and following the general method, **8** (83%) was obtained as a yellowish syrup. ^1H NMR (400 MHz, CDCl_3) δ 7.82 (d, $J = 8.1$ Hz, 1H), 7.50 (t, $J = 7.5$ Hz, 1H), 7.07 (d, $J = 8.3$ Hz, 1H), 7.00 (t, $J = 7.7$, 1H), 4.14 (m, 3H), 3.79 (m, 2H). ^{13}C NMR (100 MHz, CDCl_3) δ 152.3, 139.6, 134.9, 126.1, 121.1, 115.0, 71.3, 70.0. HR TOF MS ES+, calcd for $\text{C}_{15}\text{H}_{14}\text{N}_2\text{O}_7\text{Na}$ ($\text{M} + \text{Na}$)⁺ 357.0699, found 357.0694. Anal. Calcd for $\text{C}_{15}\text{H}_{14}\text{N}_2\text{O}_7$: C, 53.89; H, 4.22; N, 8.38. Found: C, 53.97; H, 4.12; N, 8.61.

2,3,4,5-Tetrahydro-1,5-benzoxazepine-3-ol (**5a**) and 3,4-dihydro-2H-3-hydroxymethyl-1,4-benzoxazine (**4a**)

Method a) (starting from **6).** Following exactly the procedure formerly described,¹⁵ **4a** (14%) and **5a** (72%) were obtained as brownish syrups in both cases, and not **w4a**,¹⁵ as stated.¹⁵ Both compounds were separated by HPLC [a mixture of $\text{H}_2\text{O}/\text{MeCN}$ (100/0 \rightarrow 0/100) as eluent]. Compound **4a**: ^1H NMR (500 MHz, CDCl_3) δ 6.76 (m, 2H), 6.63 (m, 2H), 4.18 (dd, $J = 10.8$, 2.9 Hz, 1H), 4.06 (dd, $J = 10.8$, 5.9 Hz, 1H), 3.72 (dd, $J = 10.7$, 4.9 Hz, 1H), 3.64 (dd, $J = 10.7$, 7.1 Hz, 1H), 3.55 (m, 1H). ^{13}C NMR (125 MHz, CDCl_3) δ : 144.1, 132.9, 121.9, 119.3, 116.9, 116.1, 66.1, 63.0, 51.4. HR TOF MS ES+, calcd for $\text{C}_9\text{H}_{12}\text{NO}_2$ ($\text{M} + \text{H}$)⁺ 166.0868, found 166.0866. Anal. Calcd for $\text{C}_9\text{H}_{11}\text{NO}_2$: C, 65.44; H, 6.71; N, 8.48. Found: C, 65.30; H, 6.85; N, 8.49. Compound **5a**: ^1H NMR (500 MHz, CDCl_3) δ 6.99 (dd, $J = 7.8$, 1.5 Hz, 1H), 6.89 (dt, $J = 7.5$, 1.5 Hz, 1H), 6.82 (dt, $J = 7.6$, 1.7 Hz, 1H), 6.75 (dd, 1H), 4.25 (ddd, $J = 12.3$, 3.8, 1.4 Hz, 1H), 3.93 (m, 1H), 3.86 (dd, $J = 12.3$, 2.0 Hz, 1H), 3.36 (ddd, $J = 12.9$, 4.9, 1.4 Hz, 1H), 3.17 (dd, $J = 12.9$, 2.4 Hz, 1H). ^{13}C NMR (125 MHz, CDCl_3) δ 150.7, 142.0, 124.1, 122.2, 122.1, 120.0, 75.4, 68.6, 52.4. HR TOF MS ES+, calcd for $\text{C}_9\text{H}_{12}\text{NO}_2$ ($\text{M} + \text{H}$)⁺ 166.0868, found 166.0868. Anal. Calcd for $\text{C}_9\text{H}_{11}\text{NO}_2$: C, 65.44; H, 6.71; N, 8.48. Found: C, 65.42; H, 6.54; N, 8.69.

Method b) (starting from *o*-aminophenol). A mixture of *o*-aminophenol (0.2 g, 1.83 mmol), 60% NaH (0.07 g, 1.83 mmol) and anhydrous DMF (6 mL) was stirred at room temperature for 10 min, and irradiated in a microwave oven at 160 °C for 20 min. Epichlorohydrin (0.17 g, 1.83 mmol) was added and the resulting mixture was irradiated at 160 °C for an additional 10 min. The mixture was cooled, the DMF was removed *in vacuo*, and the residue was extracted (H₂O/CH₂Cl₂). Organic layers were combined and dried (Na₂SO₄). After filtration, the solvent was removed *in vacuo* and the crude was purified by flash column chromatography using an hexane/EtOAc (8/2) mixture. Both compounds, **4a** (34%) and **5a** (55%) were separated by HPLC [a mixture of H₂O/MeCN (90/10) as eluent], semi-preparative column Nova-Pak C-18, 60 Å, 6 µm, 17.8 mm × 300 mm, retention time (*t_R*) of **4a**: 6.96 min, and *t_R* of **5a**: 7.27 min.

6-Chloro-9-(2,3-dihydro-1,4-benzoxazine-3-ylmethyl)-9H-purine (4d)

Yellowish solid (14%), (mp 77–78 °C), ¹H NMR (500 MHz, CDCl₃) δ 8.74 (s, 1H), 8.06 (s, 1H), 6.82 (m, 2H), 6.70 (td, *J* = 7.8, 1.5 Hz, 1H), 6.58 (dd, *J* = 7.8, 1.5 Hz, 1H), 4.49 (dd, *J* = 14.1, 5.2 Hz, 1H), 4.36 (dd, *J* = 14.1, 8.2 Hz, 1H), 4.13 (ddd, *J* = 25.6, 11.1, 2.7 Hz, 2H), 4.03 (m, 1H), 3.96 (s, 1H). ¹³C NMR (125 MHz, CDCl₃) δ 152.36, 152.20, 151.64, 146.29, 143.52, 132.08, 131.15, 122.78, 119.80, 117.55, 116.33, 65.44, 49.46, 46.53. HR TOF MS ES⁺, calcd for C₁₄H₁₃ClN₅O (M + H)⁺ 302.0808, found 302.0808. Anal. Calcd for C₁₄H₁₂ClN₅O: C, 55.73; H, 4.01; N, 23.21. Found: C, 55.70; H, 4.05; N, 23.50.

6-Bromo-9-(2,3-dihydro-1,4-benzoxazine-3-ylmethyl)-9H-purine (4e)

Yellowish solid (12%), (mp 72–73 °C), ¹H NMR (500 MHz, CDCl₃) δ 8.70 (s, 1H), 8.07 (s, 1H), 6.82 (m, 2H), 6.71 (td, *J* = 7.8, 1.5 Hz, 1H), 6.58 (dd, *J* = 7.8, 1.5 Hz, 1H), 4.49 (dd, *J* = 14.1, 5.2 Hz, 1H), 4.35 (dd, *J* = 14.1, 8.3 Hz, 1H), 4.13 (ddd, *J* = 26.6, 11.1, 2.7 Hz, 2H), 4.02 (m, 1H), 3.90 (s, 1H). ¹³C NMR (125 MHz, CDCl₃) δ 152.21, 150.84, 150.71, 146.05, 143.69, 134.60, 131.00, 122.69, 119.75, 117.48, 116.27, 65.33, 49.37, 46.46. HR TOF MS ES⁺, calcd for C₁₄H₁₃BrN₅O (M + H)⁺ 346.0303, found 346.0305. Anal. Calcd for C₁₄H₁₂BrN₅O: C, 48.57; H, 3.49; N, 20.23. Found: C, 48.61; H, 3.55; N, 20.00.

2,6-Dichloro-9-(2,3-dihydro-1,4-benzoxazine-3-ylmethyl)-9H-purine (4f)

White solid (15%), (mp 89–90 °C), ¹H NMR (500 MHz, CDCl₃) δ 8.03 (s, 1H), 6.82 (m, 2H), 6.71 (td, *J* = 7.7, 1.5 Hz, 1H), 6.59 (dd, *J* = 7.8, 1.5 Hz, 1H), 4.46 (dd, *J* = 14.1, 5.2 Hz, 1H), 4.32 (dd, *J* = 14.1, 8.3 Hz, 1H), 4.17 (dd, *J* = 11.2, 2.5 Hz, 1H), 4.08 (dd, *J* = 11.2, 2.6 Hz, 1H), 4.00 (s, 1H), 3.88 (s, 1H). ¹³C NMR (125 MHz, CDCl₃)

δ 153.44, 153.33, 152.26, 146.91, 143.41, 131.13, 130.78, 122.77, 119.87, 117.53, 116.39, 65.20, 49.25, 46.45. HR TOF MS ES⁺, calcd for C₁₄H₁₂Cl₂N₅O (M + H)⁺ 336.0419, found 336.0419. Anal. Calcd for C₁₄H₁₁Cl₂N₅O: C, 50.02; H, 3.30; N, 20.83. Found: C, 49.90; H, 3.35; N, 20.91.

Acknowledgements

This study was supported by the Instituto de Salud Carlos III (FIS) through project no. PI10/00592. The M.E.-G.R. FPU grant AP2007-02954 is greatly acknowledged.

References

- G. Guillaumet, A. R. Katritzky, C. W. Rees and E. F. V. Scriven. Editors (1st ed.), *Comprehensive Heterocyclic Chemistry II*, Pergamon, Oxford, 1996, 447.
- O. Cruz-López, M. C. Núñez, A. Conejo-García, M. Kimatrai and J. M. Campos, *Curr. Org. Chem.*, 2011, **15**, 869.
- M. Díaz-Gavilán, A. Conejo-García, O. Cruz-López, M. C. Núñez, D. Choquesillo-Lazarte, J. M. González-Pérez, F. Rodríguez-Serrano, J. A. Marchal, A. Aránega, M. A. Gallo, A. Espinosa and J. M. Campos, *ChemMedChem*, 2008, **3**, 127.
- A. Conejo-García, M. E. García-Rubiño, J. A. Marchal, M. C. Núñez, A. Ramírez, S. Cimino, M. A. García, A. Aránega, M. A. Gallo and J. M. Campos, *Eur. J. Med. Chem.*, 2011, **46**, 3795.
- Y. Liao, B. J. Venhuis, N. Rodenhuis, W. Timmerman, H. Wikstrom, E. Meire, G. D. Bartoszyk, H. Botcher, C. A. Seyfried and S. Sundell, *J. Med. Chem.*, 1999, **42**, 2235.
- M. Díaz-Gavilán, J. A. Gómez-Vidal, F. Rodríguez-Serrano, J. A. Marchal, O. Caba, A. Aránega, M. A. Gallo, A. Espinosa and J. M. Campos, *Bioorg. Med. Chem. Lett.*, 2008, **18**, 1457.
- M. Iwahashi, E. Takahashi, M. Tanaka, Y. Matsunaga, Y. Okada, R. Matsumoto, F. Nambu, H. Nakai and M. Toda, *Bioorg. Med. Chem.*, 2011, **19**, 5361.
- A. N. Matralis, M. G. Katselou, A. Nikitakis and A. P. Kourounakis, *J. Med. Chem.*, 2011, **54**, 5583.
- N. Siddiqui, R. Ali, M. S. Alam and W. J. Ahsan, *Chem. Pharm. Res.*, 2010, **2**, 309.
- M. Akhter, S. Habibullah, S. M. Hasan, M. M. Alam, N. Akhter and M. Shaquiquzzaman, *Med. Chem. Res.*, 2011, **20**, 1147.
- L. Wang, H. Ankati, S. K. Akubathini, M. Balderamos, Ch. A. Storey, A. V. Patel, V. Price, D. Kretschmar, E. R. Biehl and S. R. D'Mello, *J. Neurosci. Res.*, 2010, **88**, 1970.
- E. N. Koini, P. Papazafiri, A. Vassilopoulos, M. Koufaki, Z. Horvath, I. Koncz, L. Virag, G. J. Papp, A. Varro and Th. Calogeropoulou, *J. Med. Chem.*, 2009, **52**, 2328.
- M. Díaz-Gavilán, D. Choquesillo-Lazarte and J. M. Campos, *Acta Crystallogr., Sect. E: Struct. Rep. Online*, 2007, **63**, o2940.
- Q.-y. Meng, Q. Liu, J. Li, R.-G. Xing, X.-X. Shen and B. Zhou, *Synlett*, 2009, 3283.
- P.-F. Jiao, B.-X. Zhao, W.-W. Wang, Q.-X. He, M.-Sh. Wan, D.-S. Shin and J.-Y. Miao, *Bioorg. Med. Chem. Lett.*, 2006, **16**, 2862.
- B. Zhao, S. Zhang and P. Jiao, CN 1847232 A, Appl. No. CN 2006-10043245, March 21st, 2006.
- J. E. Baldwin, *J. Chem. Soc., Chem. Commun.*, 1976, 734.
- Y. Xu, J.-H. Xu, J. Pan, L. Zhao and S.-L. Zhang, *J. Mol. Catal. B: Enzym.*, 2004, **27**, 155.
- B. M. Khadilkar and P. M. Bendale, *Synth. Commun.*, 1997, **27**, 2051.
- K. Hamamura, T. Oda, M. Kusaka and N. Kanzaki, WO 2005019188 A1 20050303, 2005; Appl. No. WO 2004-JP12322, August 20th, 2004.

RSC.Advances: Supplementary information

Synthesis, unambiguous chemical characterization, and reactivity of 2,3,4,5-tetrahydro-1,5-benzoxazepines-3-ol

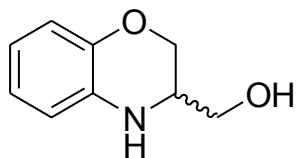
M. Eugenia García-Rubiño, María C. Núñez, Miguel A. Gallo, Joaquín M. Campos*

Departamento de Química Farmacéutica y Orgánica, Facultad de Farmacia, c/ Campus de Cartuja s/n 18071 Granada, Spain. Fax: +34 958 243845; Tel: +34-958-243850; E-mail: jmcampos@ugr.es

Table of Contents

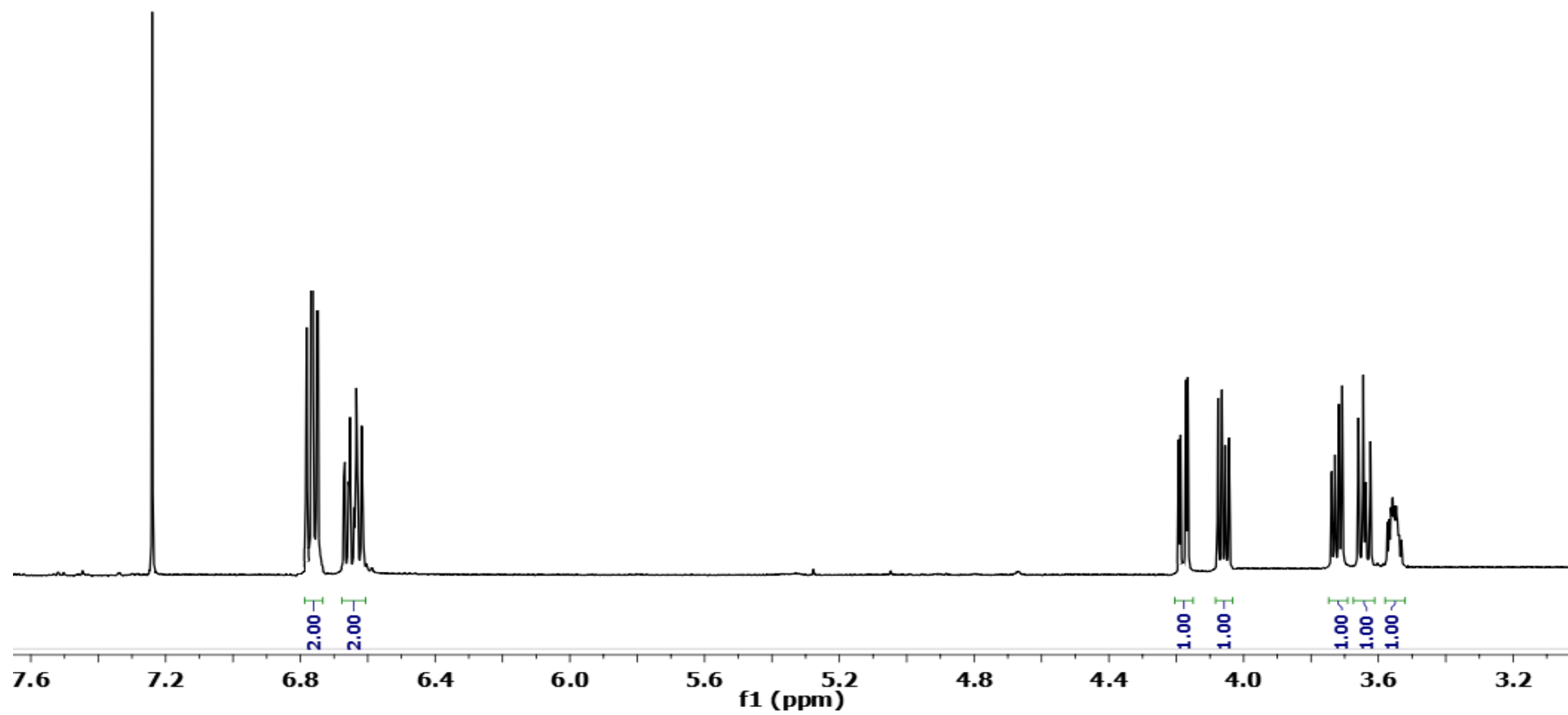
¹ H NMR spectrum of 4a	S2
¹³ C NMR spectrum of 4a	S3
DEPT spectrum of 4a	S4
HSQC spectrum of 4a	S5
HMBC spectrum of 4a	S6
¹ H NMR spectrum of 4d	S7
¹³ C NMR spectrum of 4d	S8
DEPT spectrum of 4d	S9
HSQC spectrum of 4d	S10
HMBC spectrum of 4d	S11
¹ H NMR spectrum of 4e	S12
¹³ C NMR spectrum of 4e	S13
DEPT spectrum of 4e	S14
HSQC spectrum of 4e	S15
HMBC spectrum of 4e	S16
¹ H NMR spectrum of 4f	S17
¹³ C NMR spectrum of 4f	S18
DEPT spectrum of 4f	S19
HSQC spectrum of 4f	S20
HMBC spectrum of 4f	S21
¹ H NMR spectrum of 5a	S22
¹³ C NMR spectrum of 5a	S23
DEPT spectrum of 5a	S24
HSQC spectrum of 5a	S25
HMBC spectrum of 5a	S26
¹ H NMR spectrum of 6	S27
¹³ C NMR spectrum of 6	S28
DEPT spectrum of 6	S29
¹ H NMR spectrum of 7	S30
¹³ C NMR spectrum of 7	S31
DEPT spectrum of 7	S32
¹ H NMR spectrum of 8	S33
¹³ C NMR spectrum of 8	S34
DEPT spectrum of 8	S35

S2



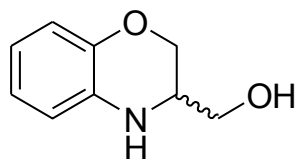
4a

500 MHz, CDCl₃

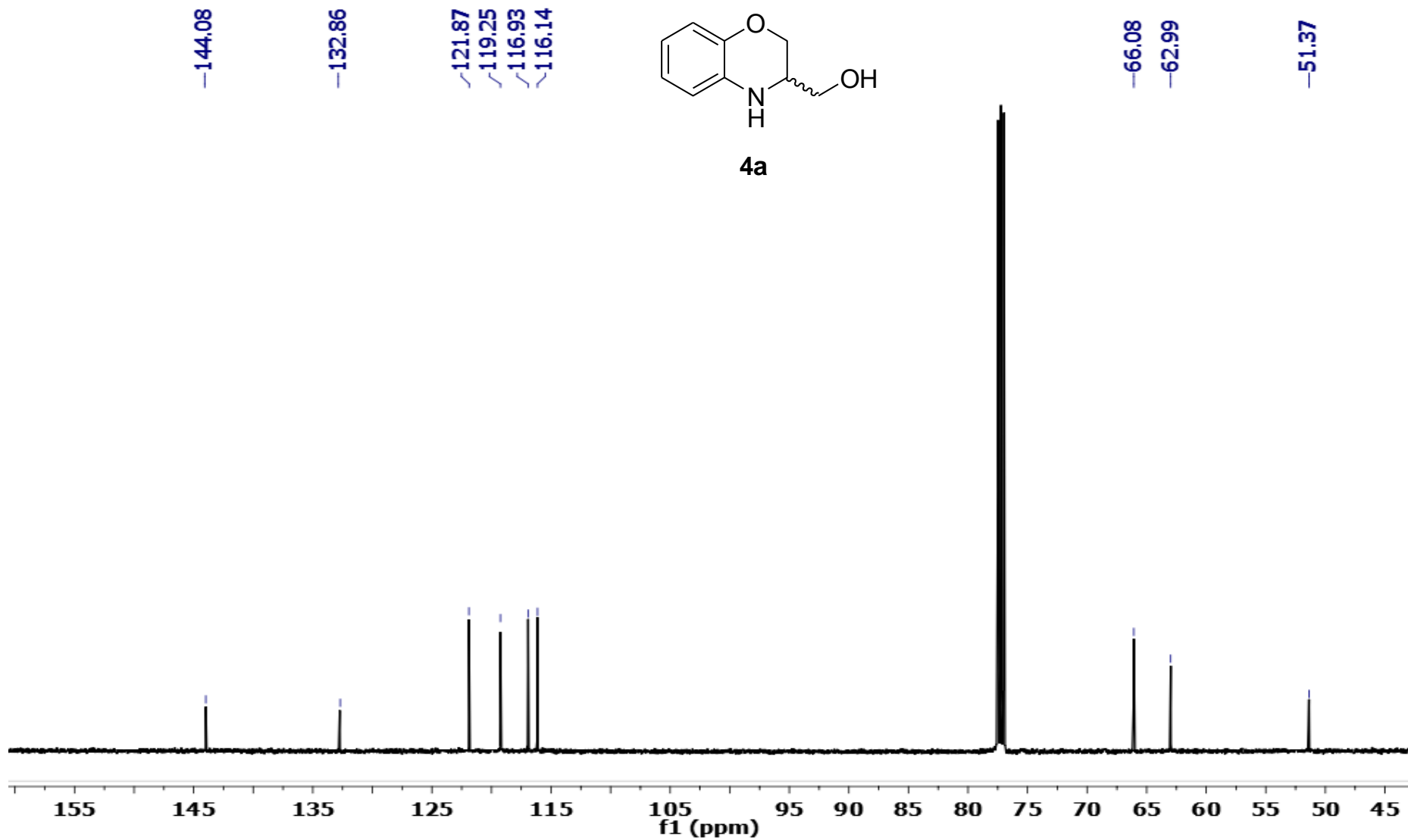


S 3

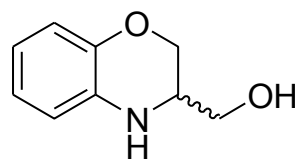
500 MHz, CDCl₃



4a



S 4



4a

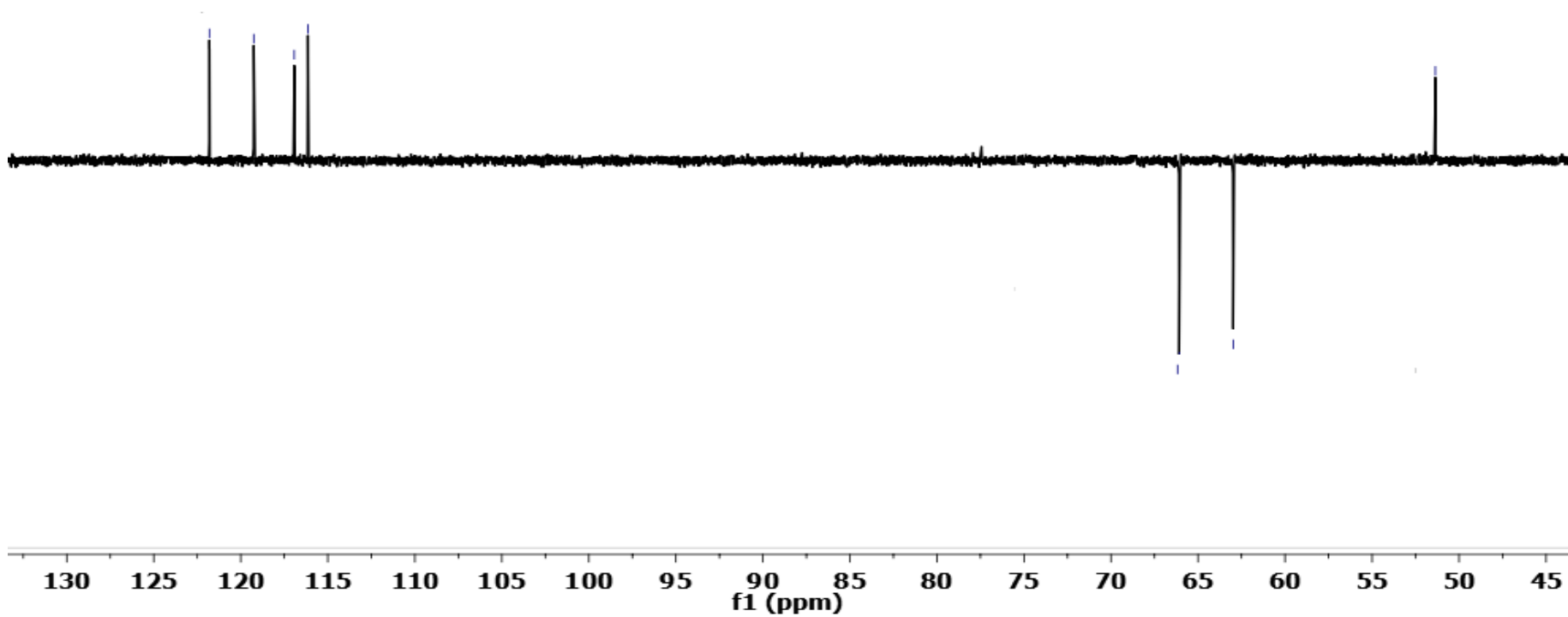
500 MHz, CDCl₃

121.87
119.25
116.93
116.14

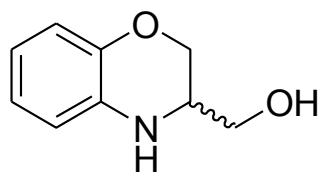
66.08

62.99

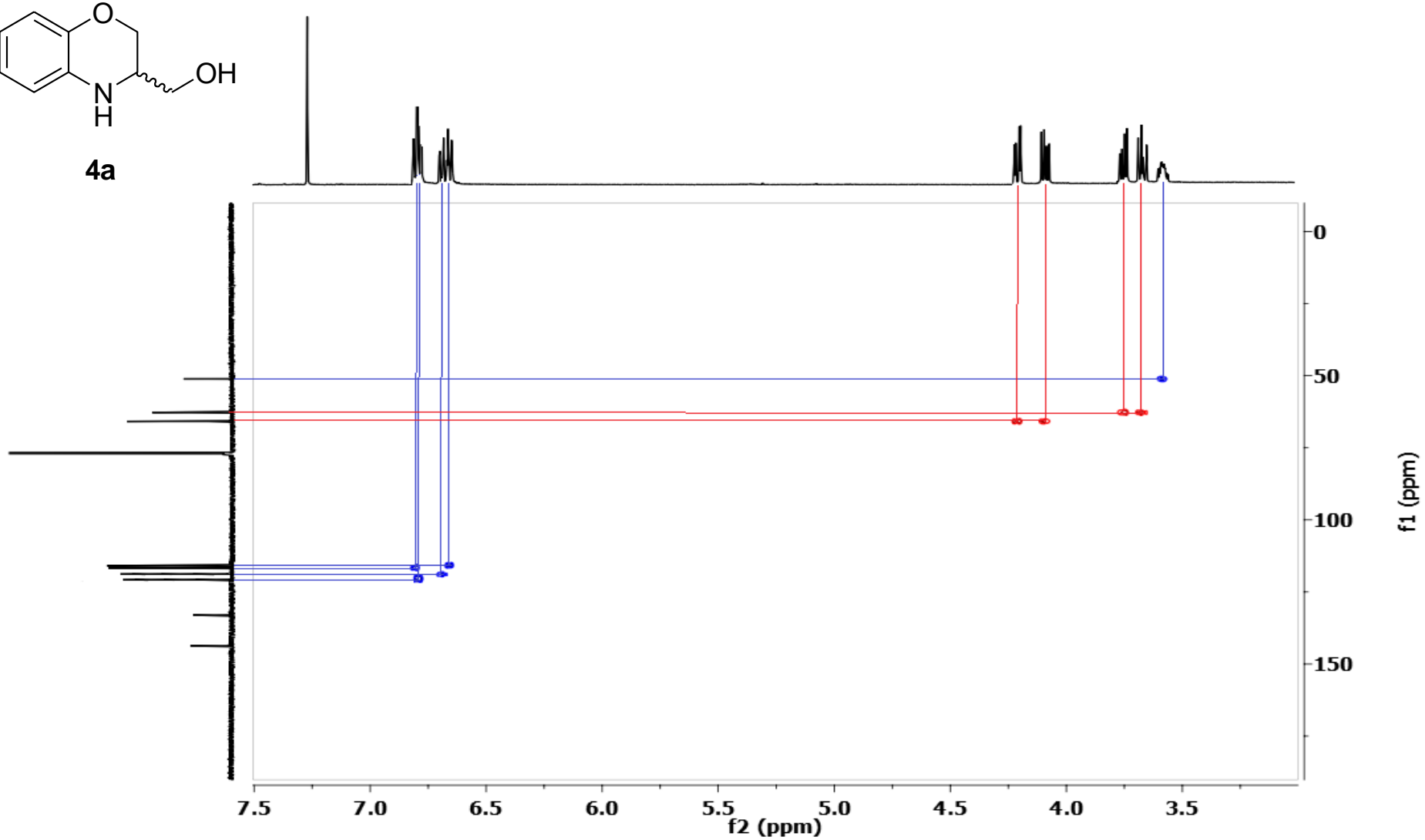
51.37



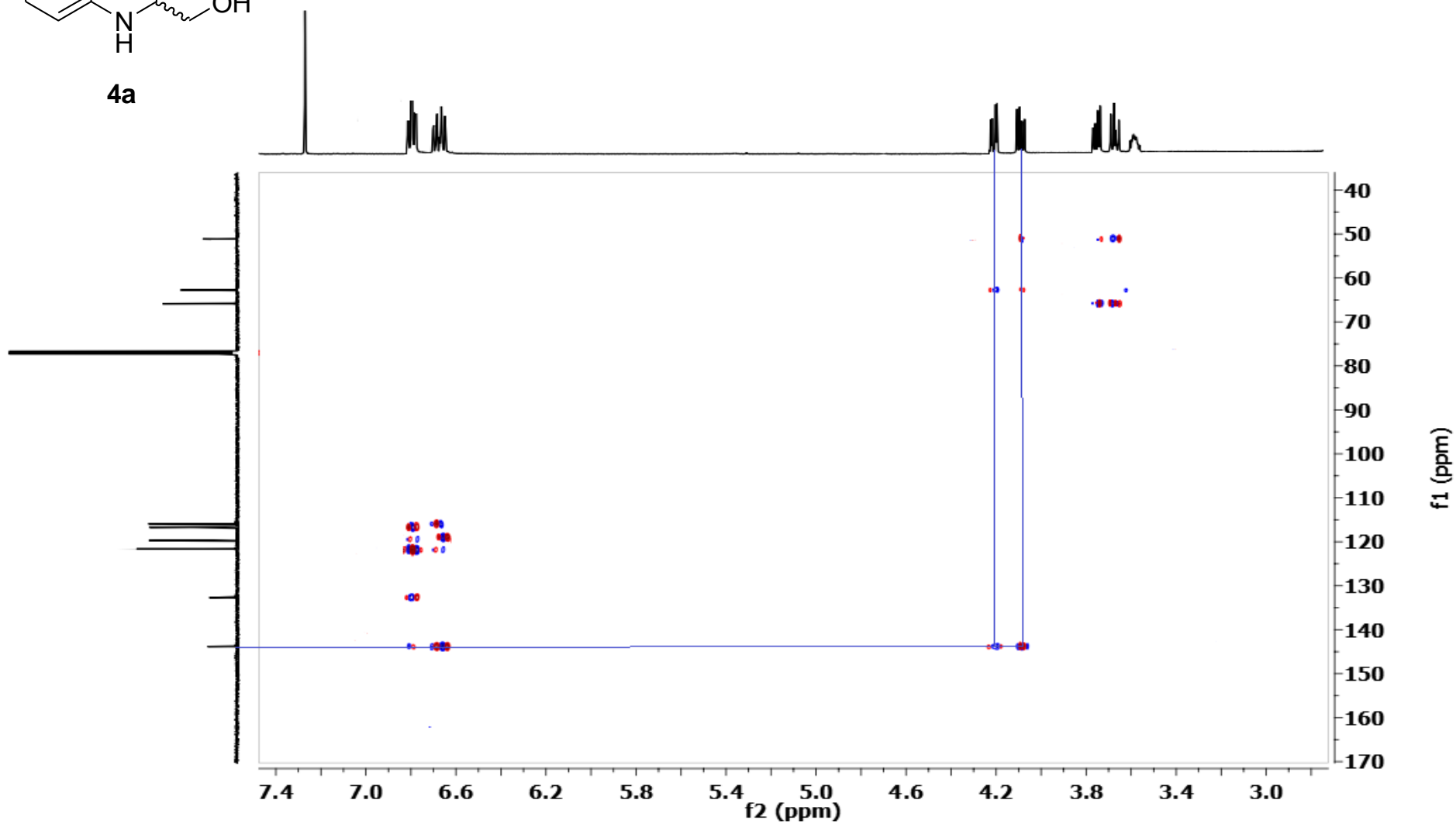
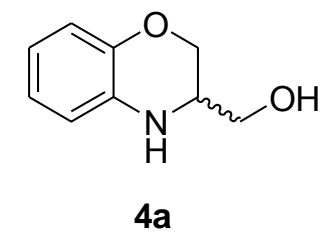
500 MHz, CDCl₃



4a

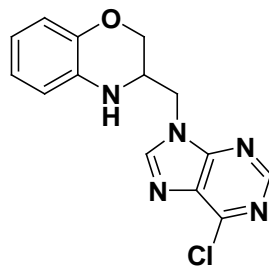


500 MHz, CDCl₃

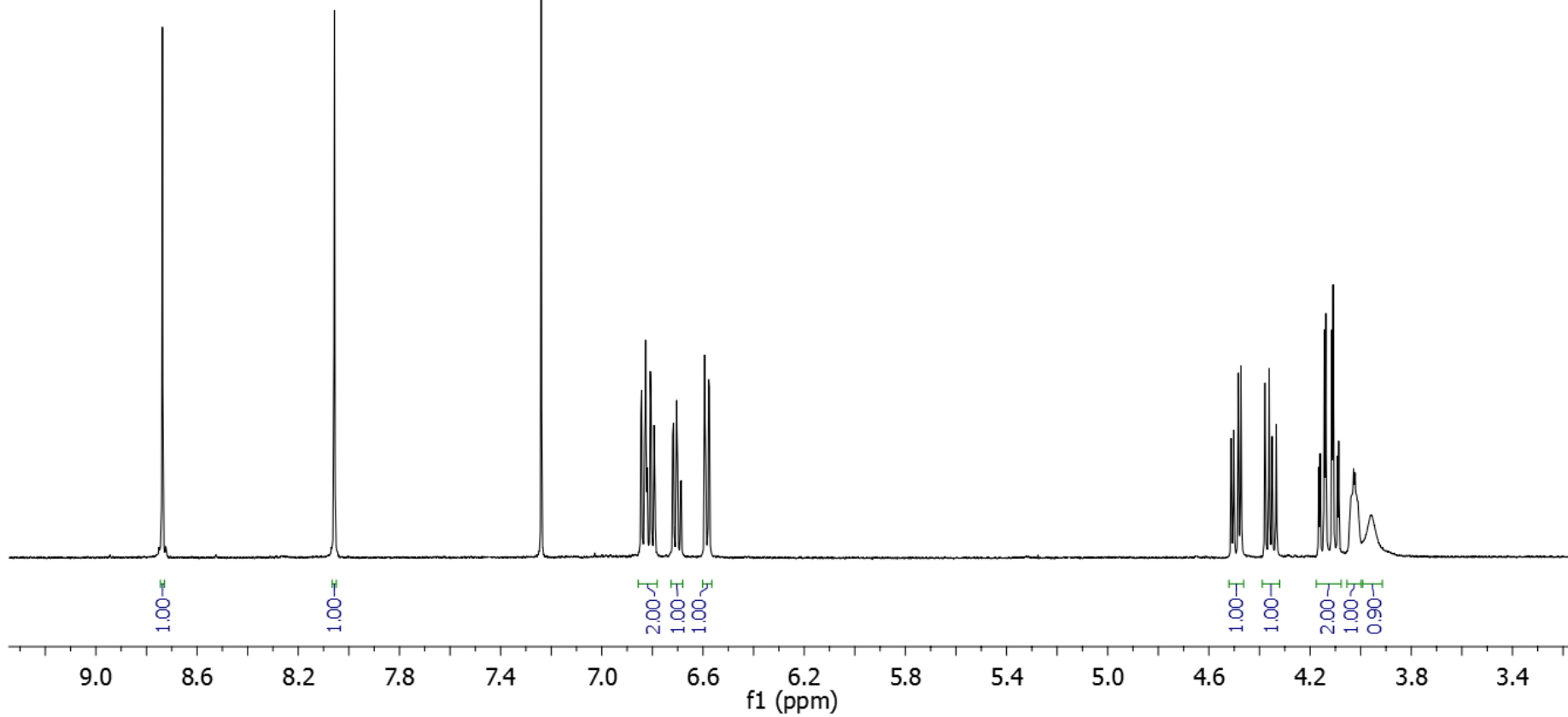


S 7

500 MHz, CDCl₃

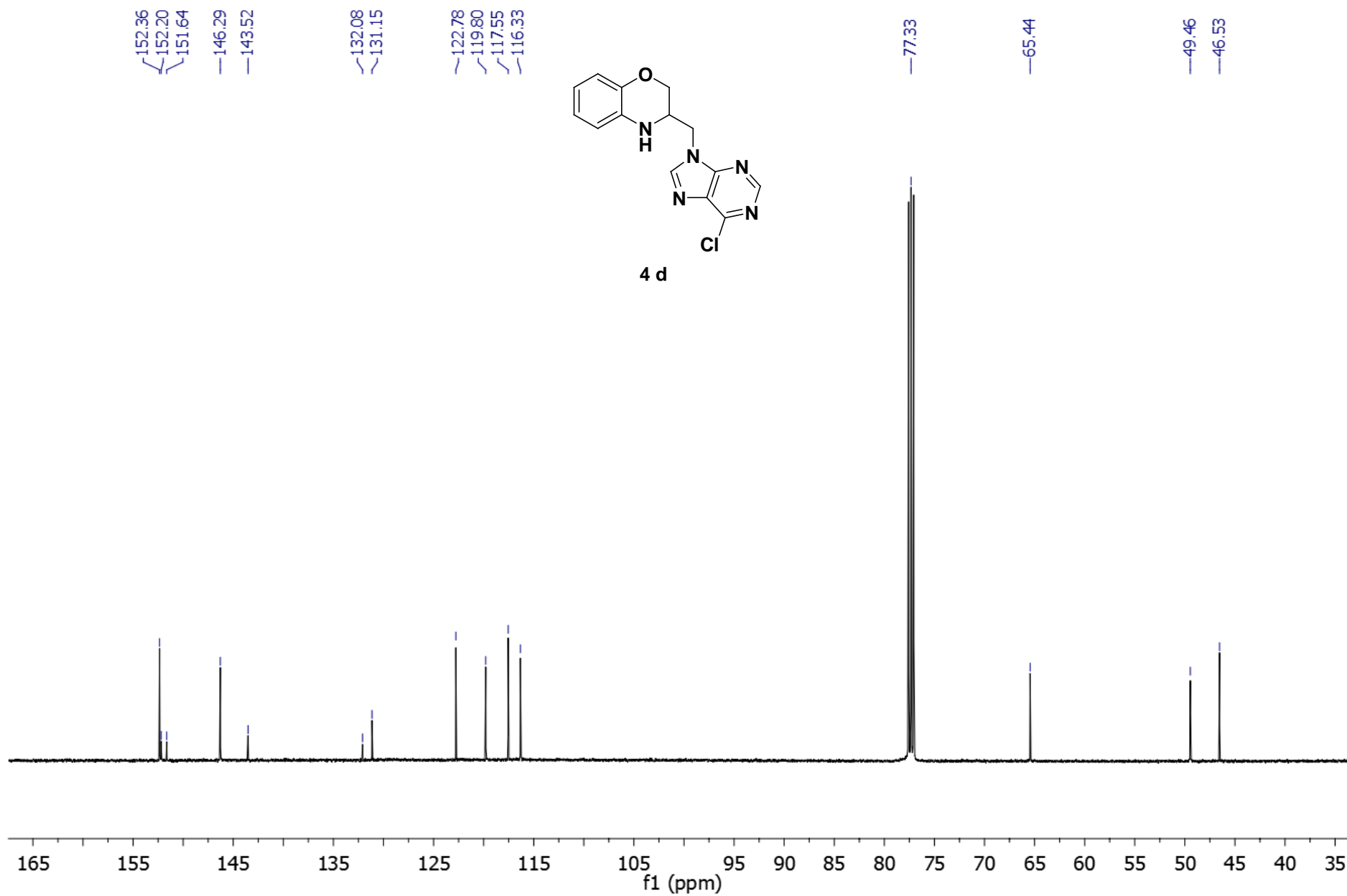


4 d



S 8

500 MHz, CDCl₃



S 9

500 MHz, CDCl₃

—152.36

—146.29

—122.78

—119.80

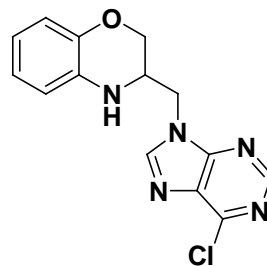
—117.55

—116.33

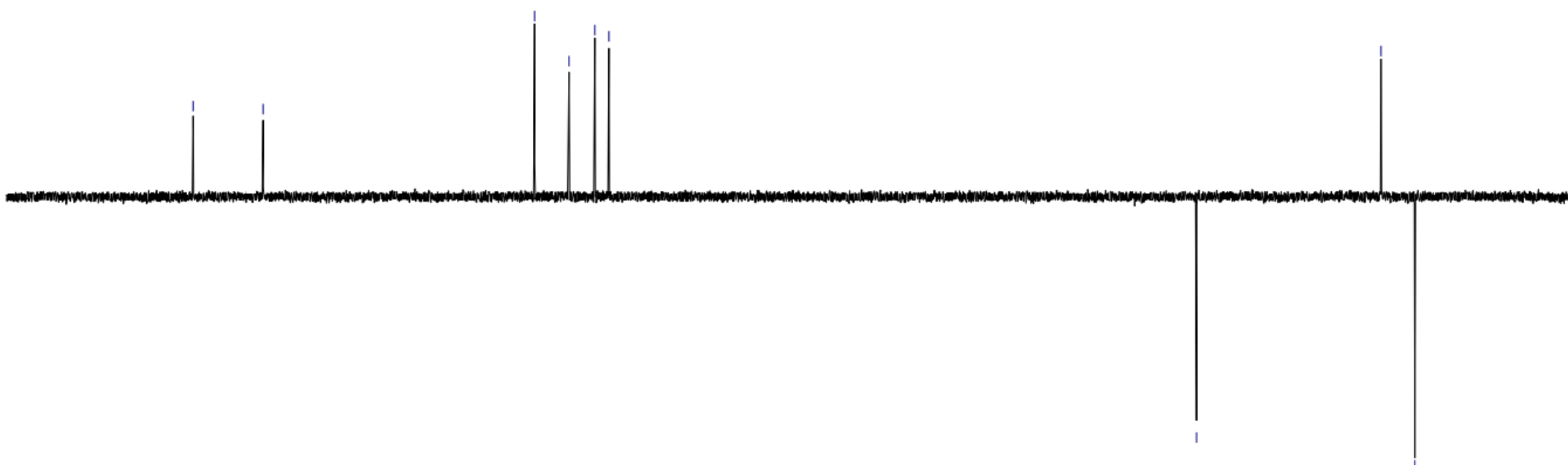
—65.44

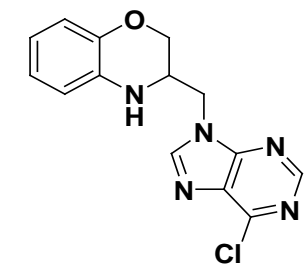
—49.46

—46.53

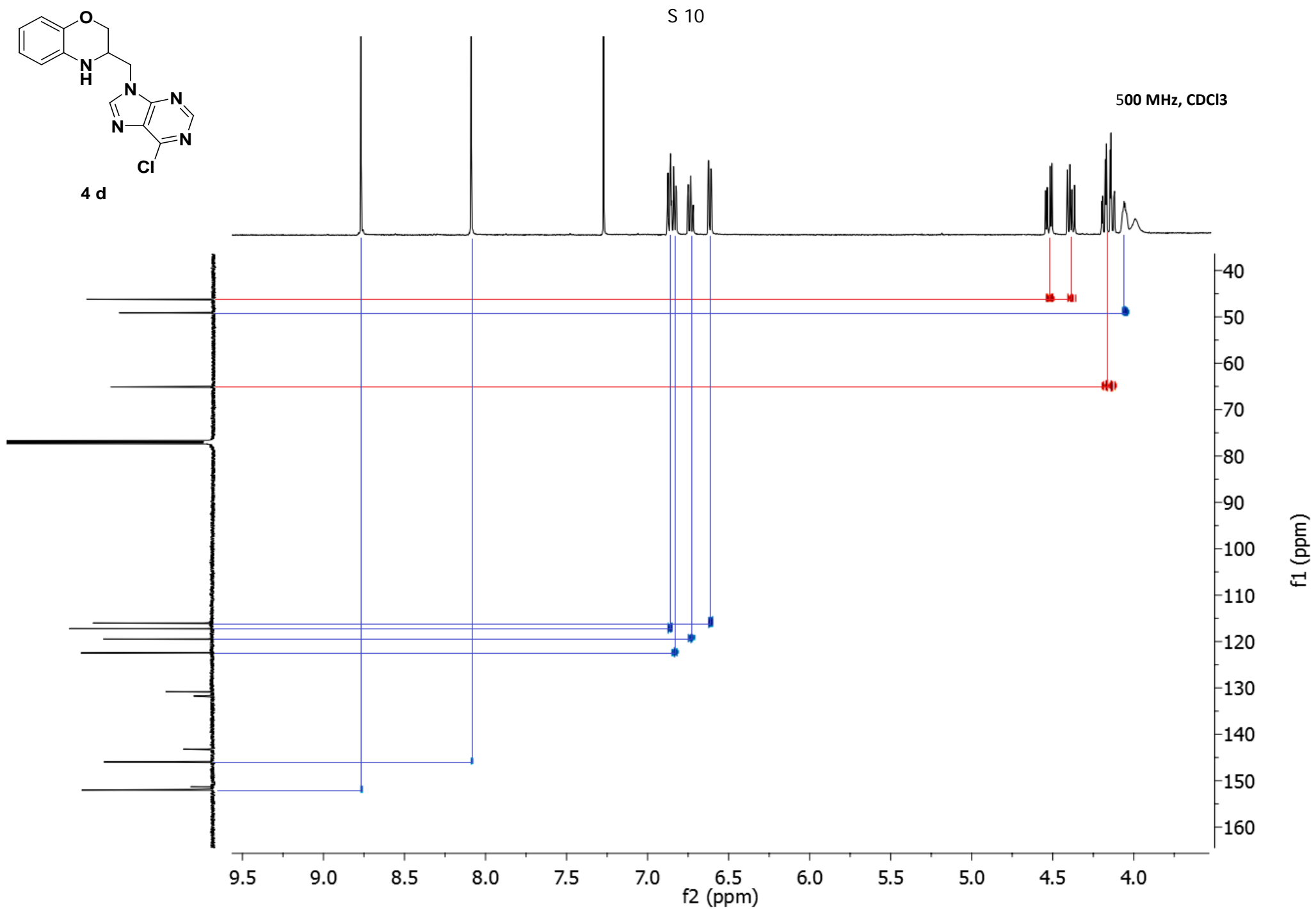


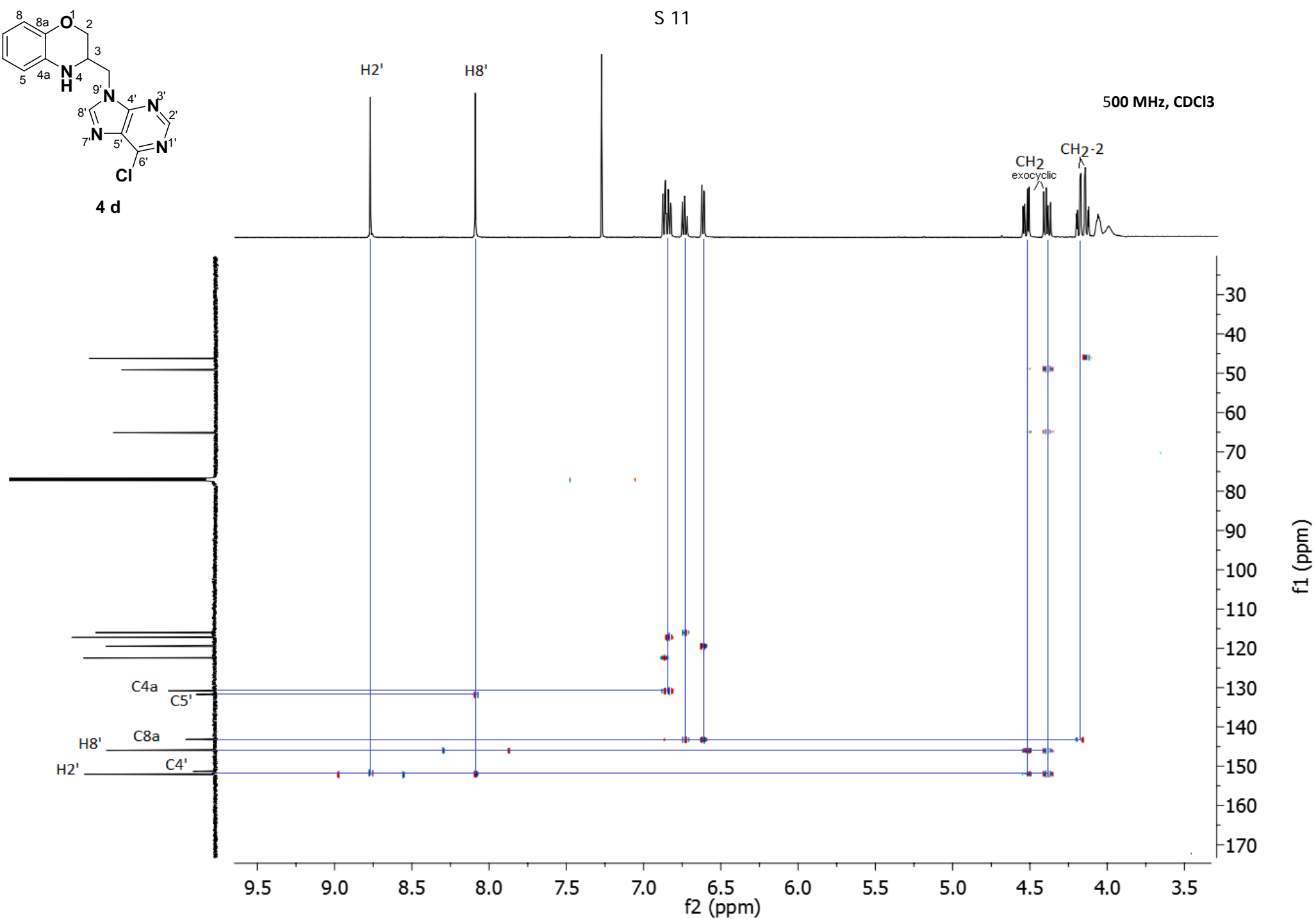
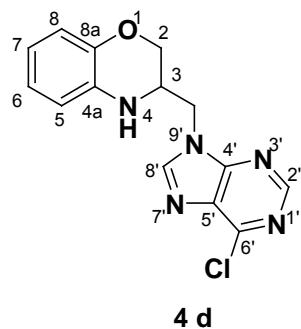
4 d





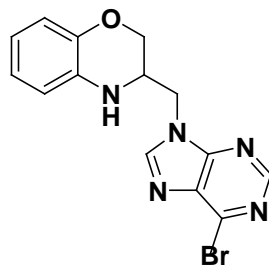
4 d



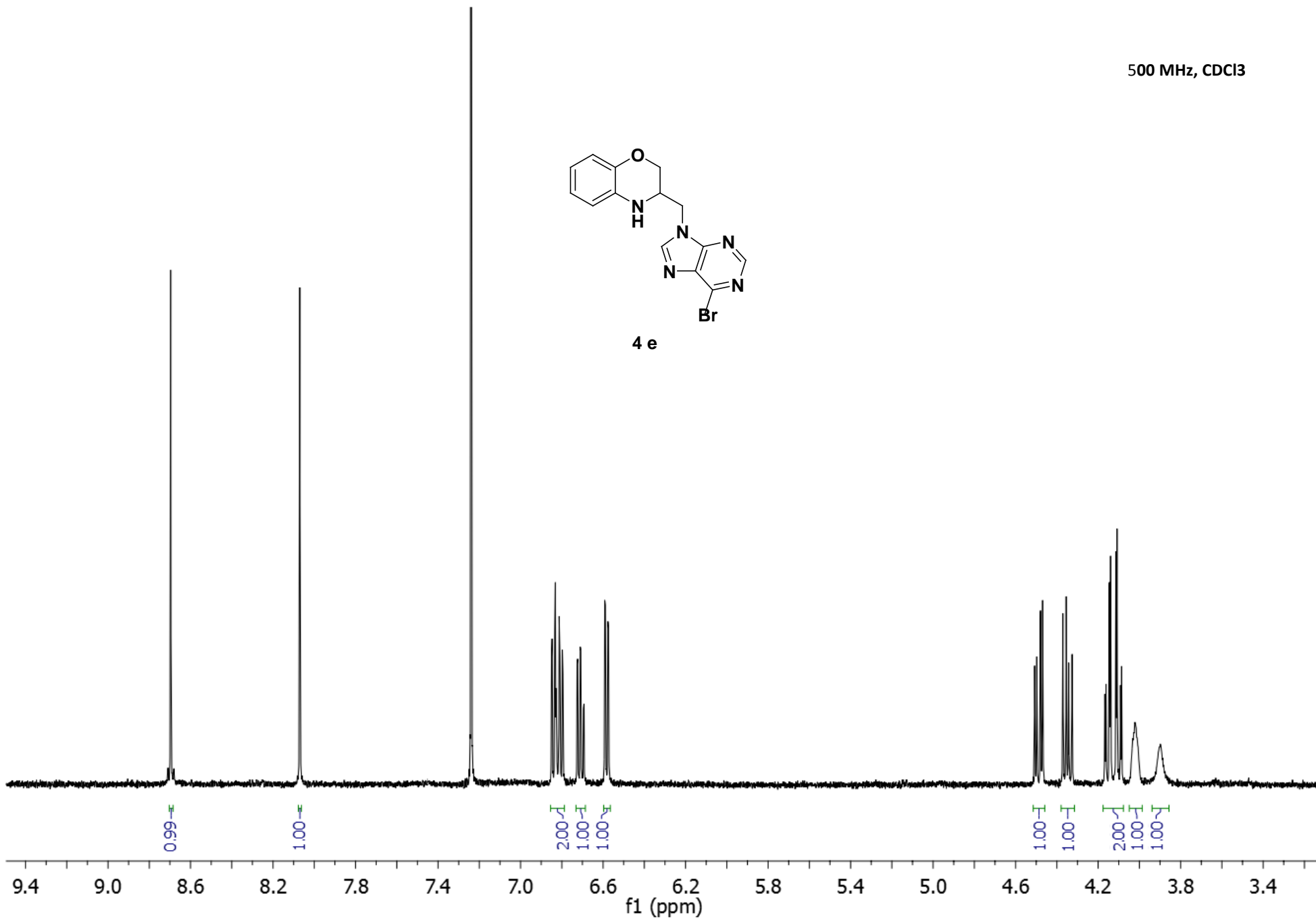


S 12

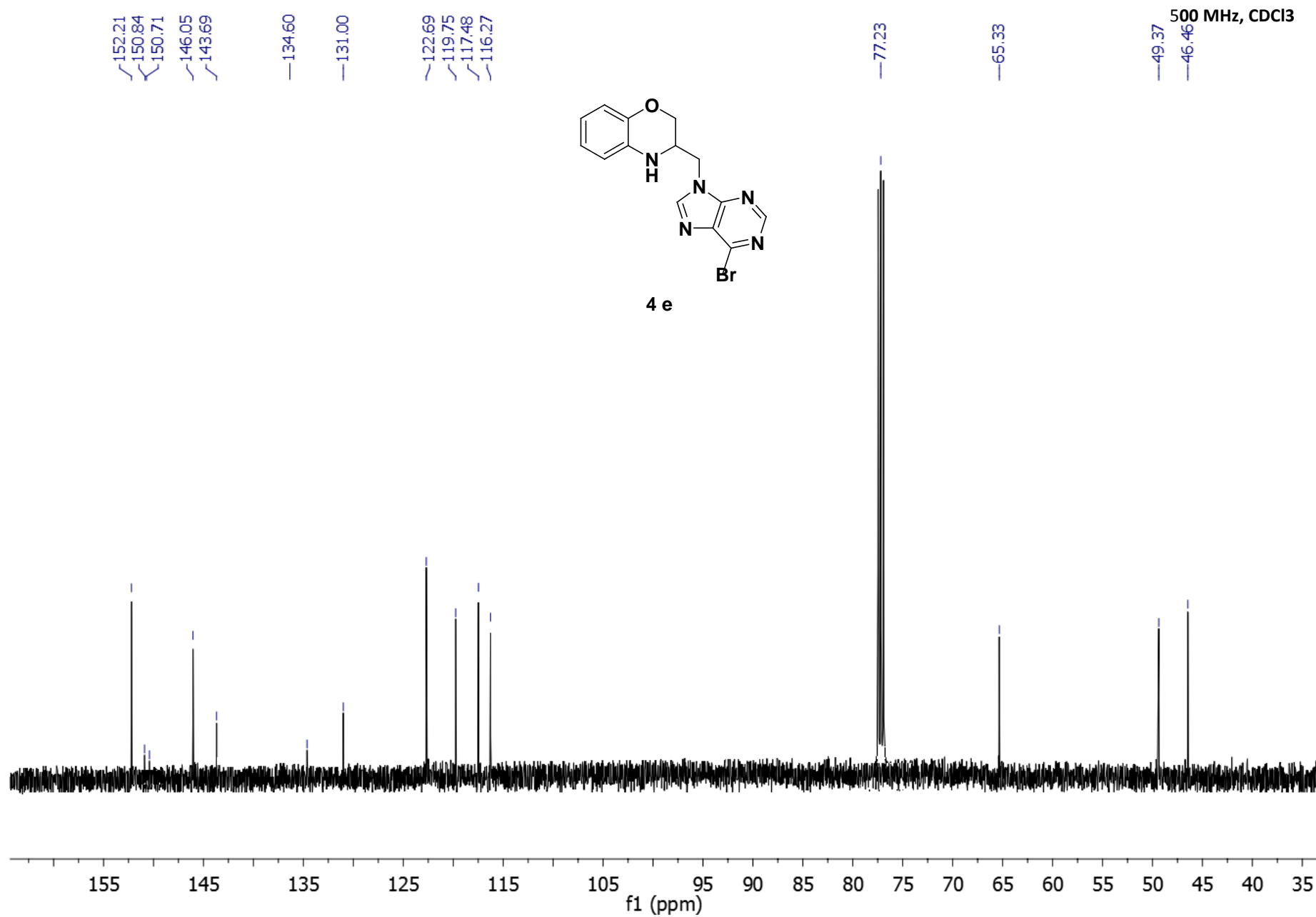
500 MHz, CDCl₃



4 e



S 13



S 14

500 MHz, CDCl₃

—152.21

—146.05

—122.69

—119.75

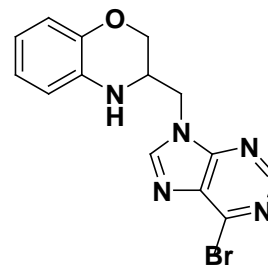
—117.48

—116.27

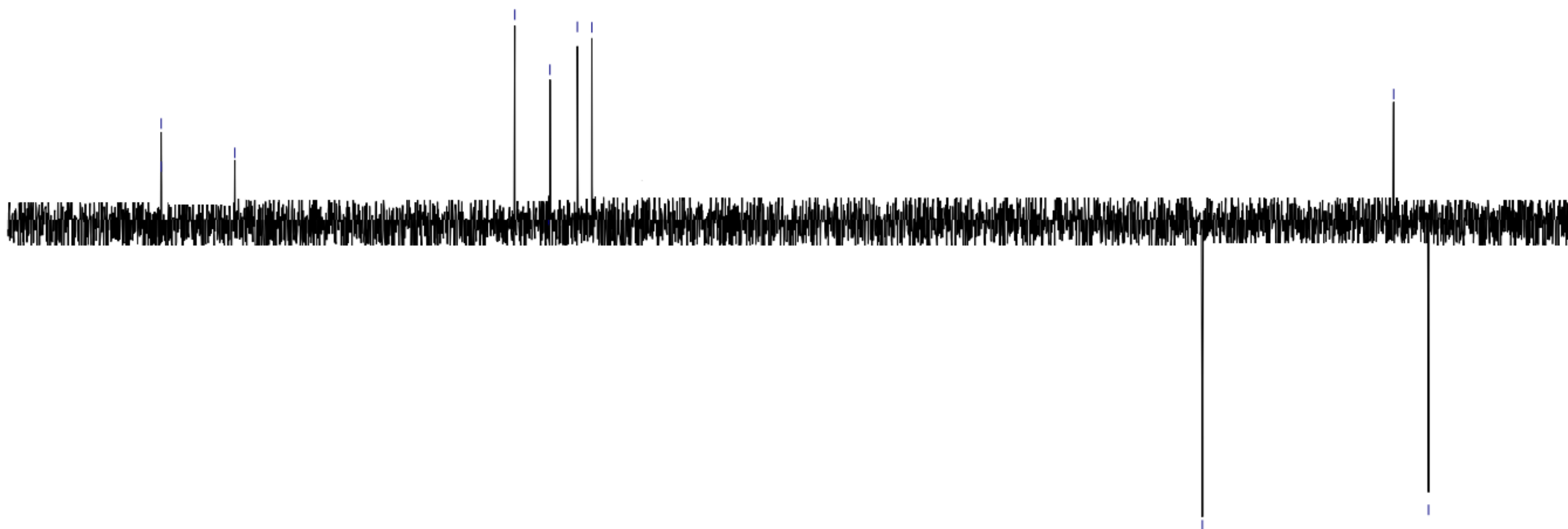
—65.33

—49.37

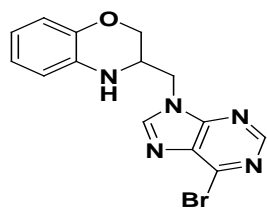
—46.46



4 e

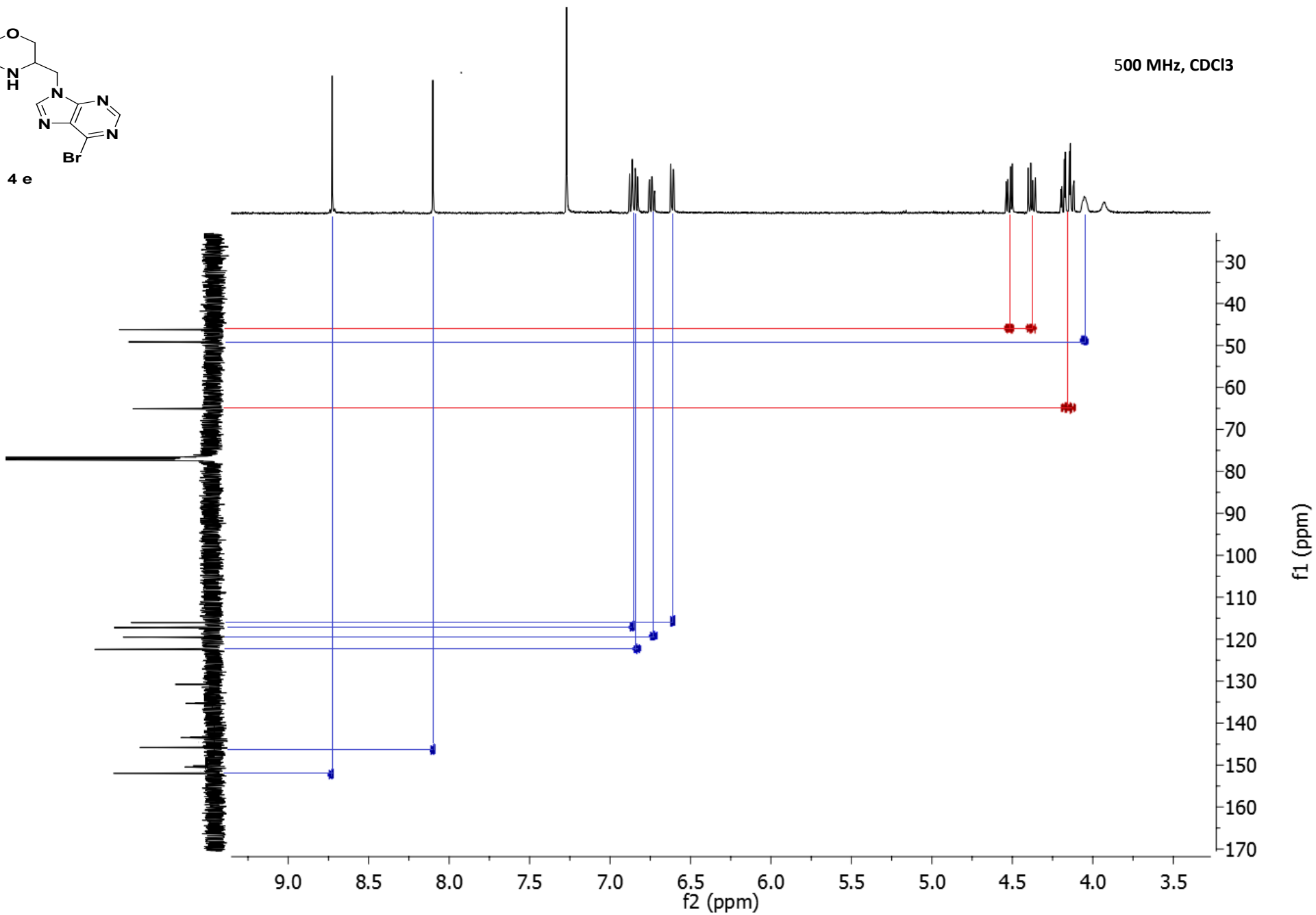


S 15

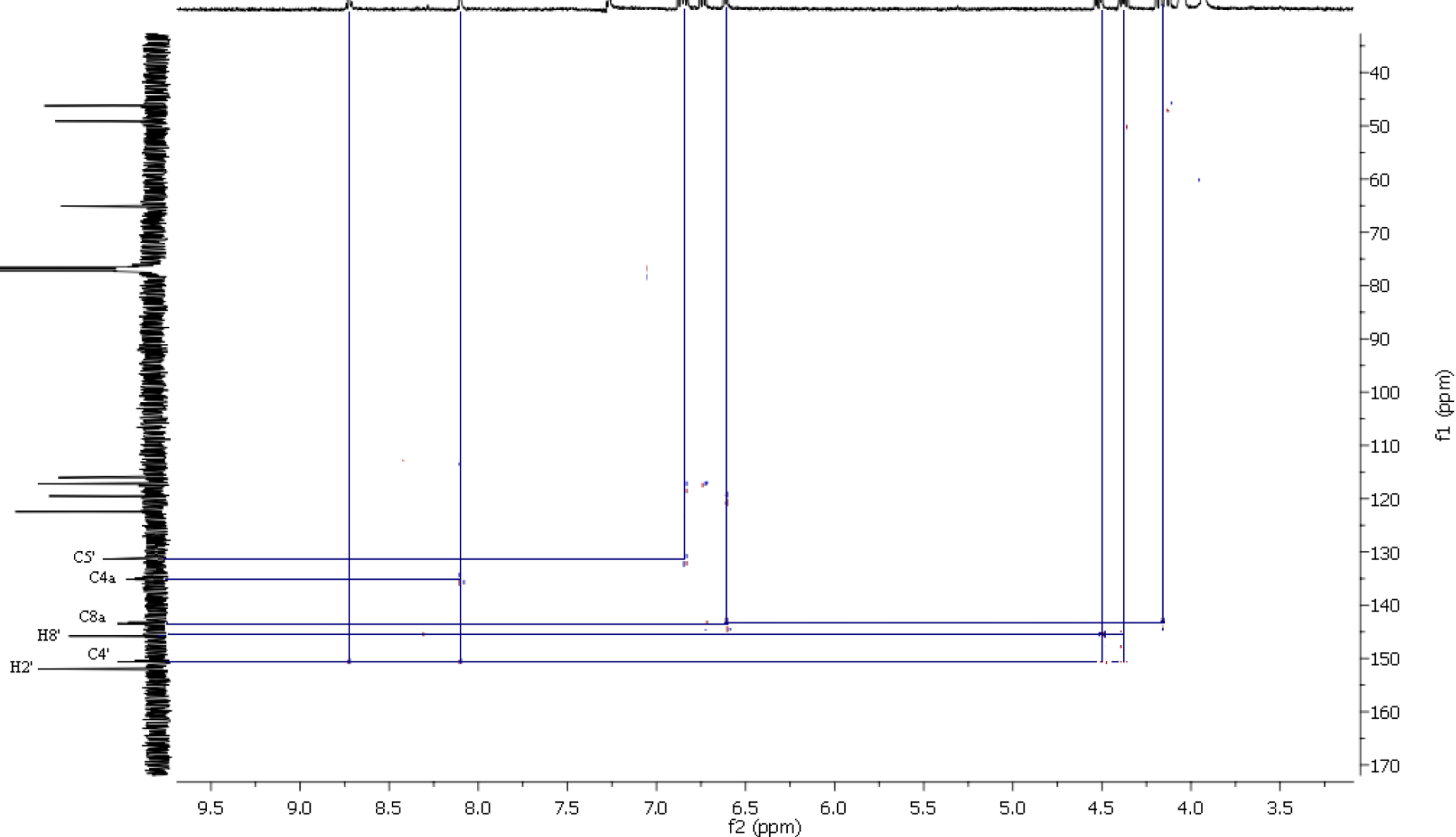
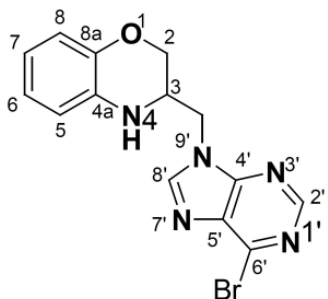


4 e

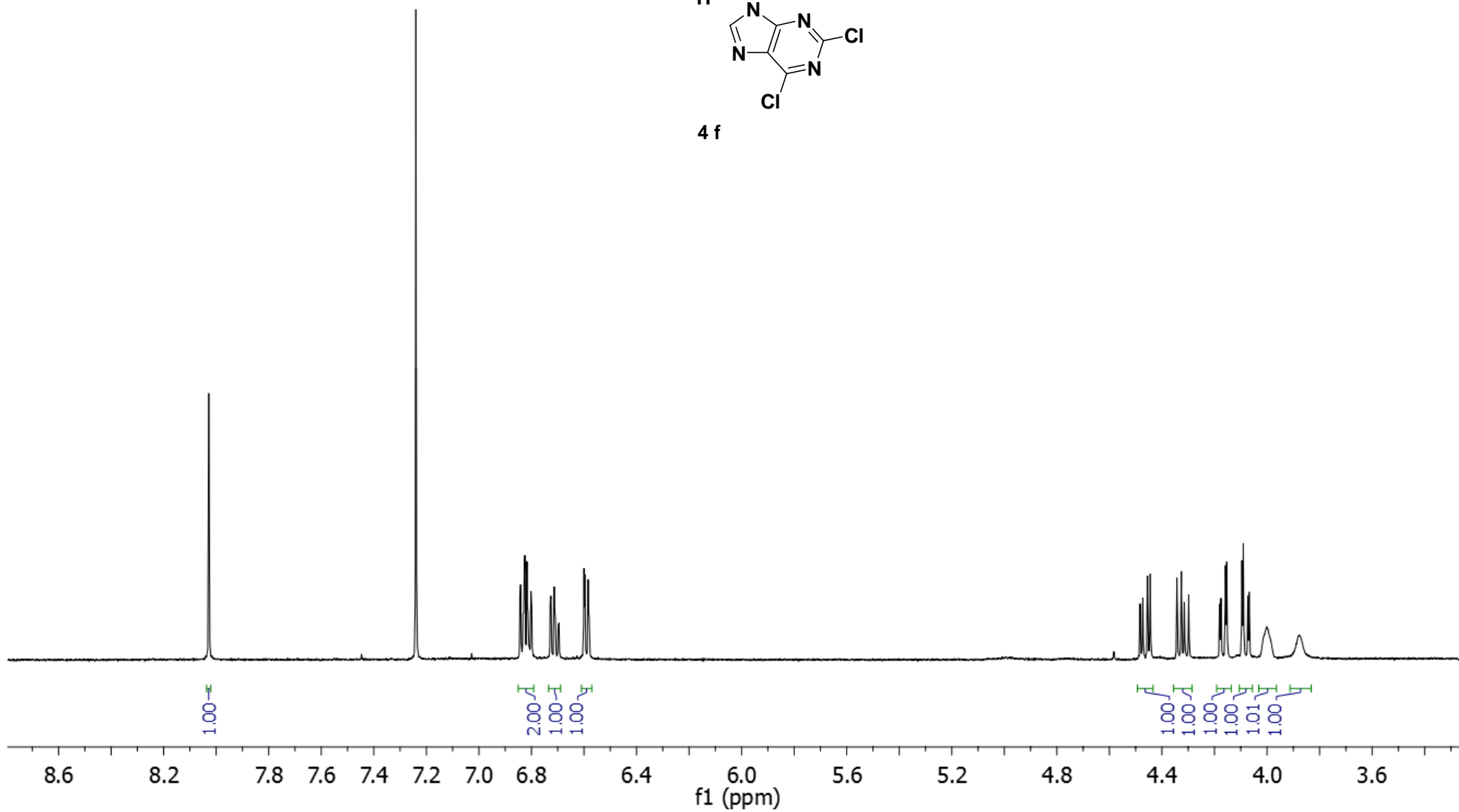
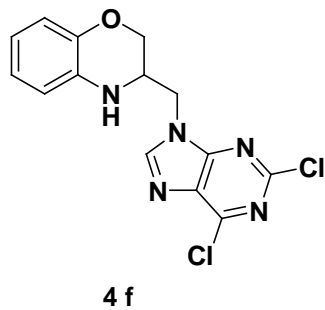
500 MHz, CDCl₃



500 MHz, CDCl₃

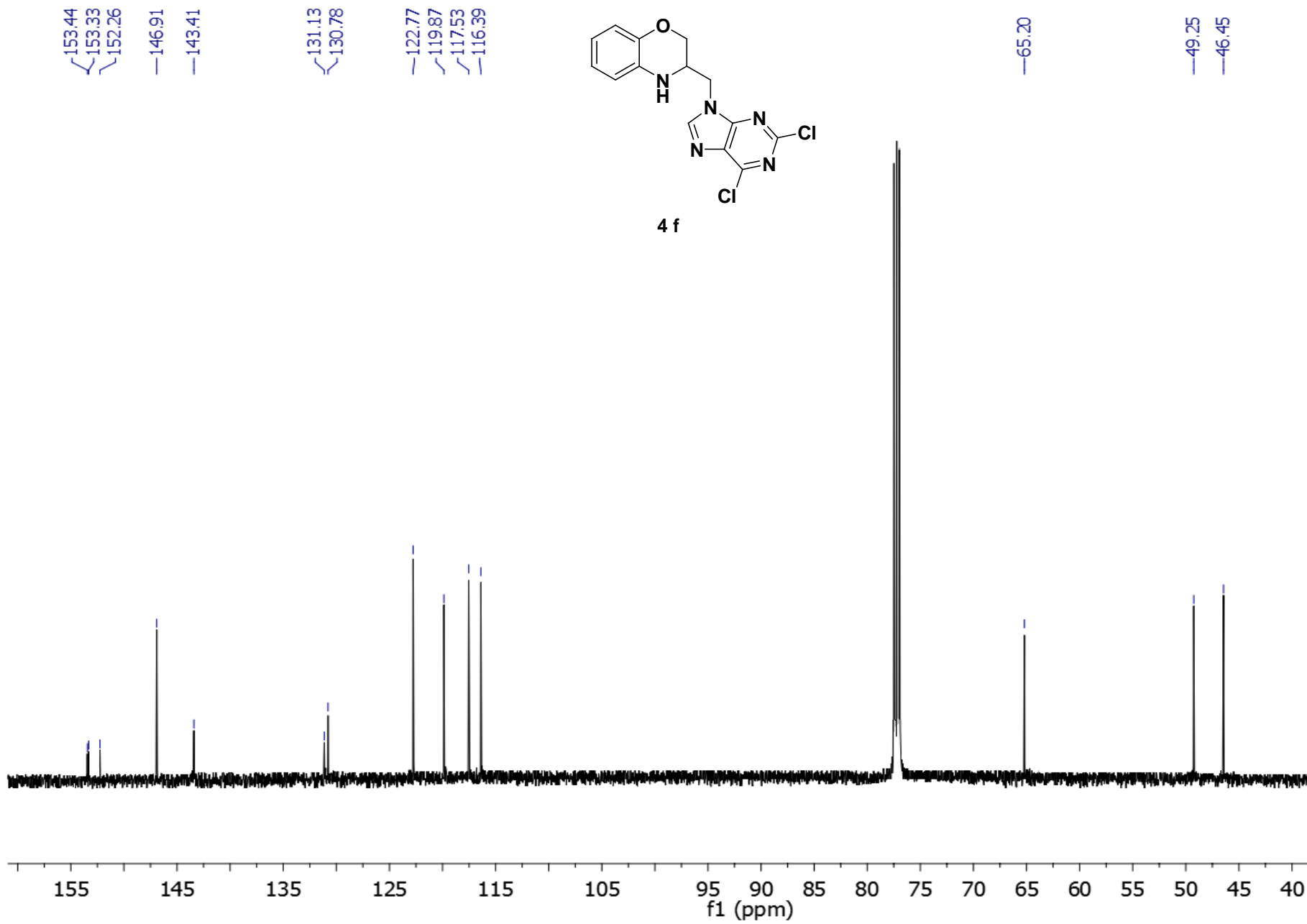
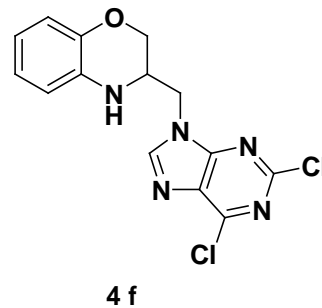


500 MHz, CDCl₃



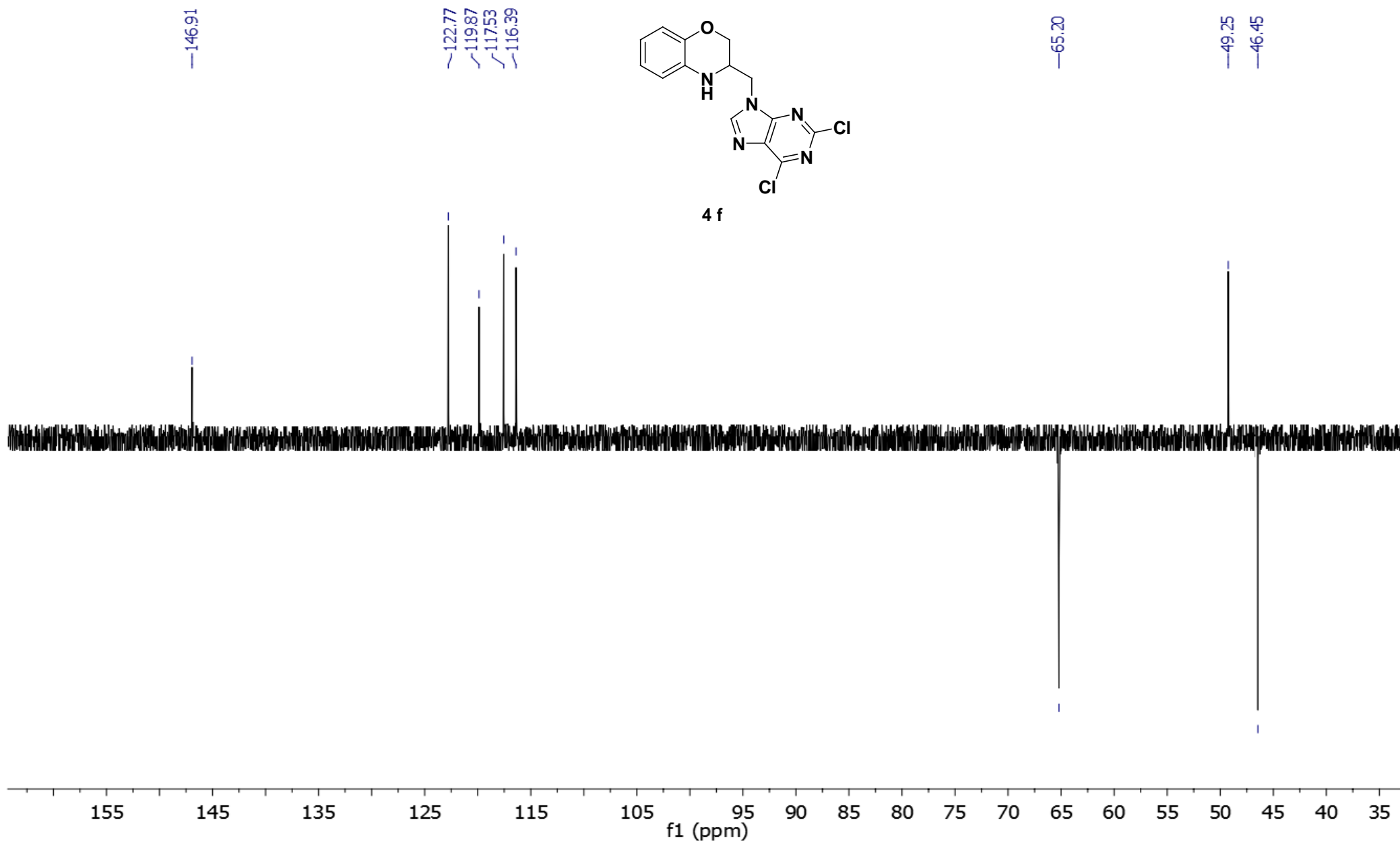
S 18

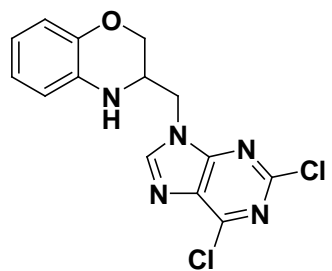
500 MHz, CDCl₃



S 19

500 MHz, CDCl₃

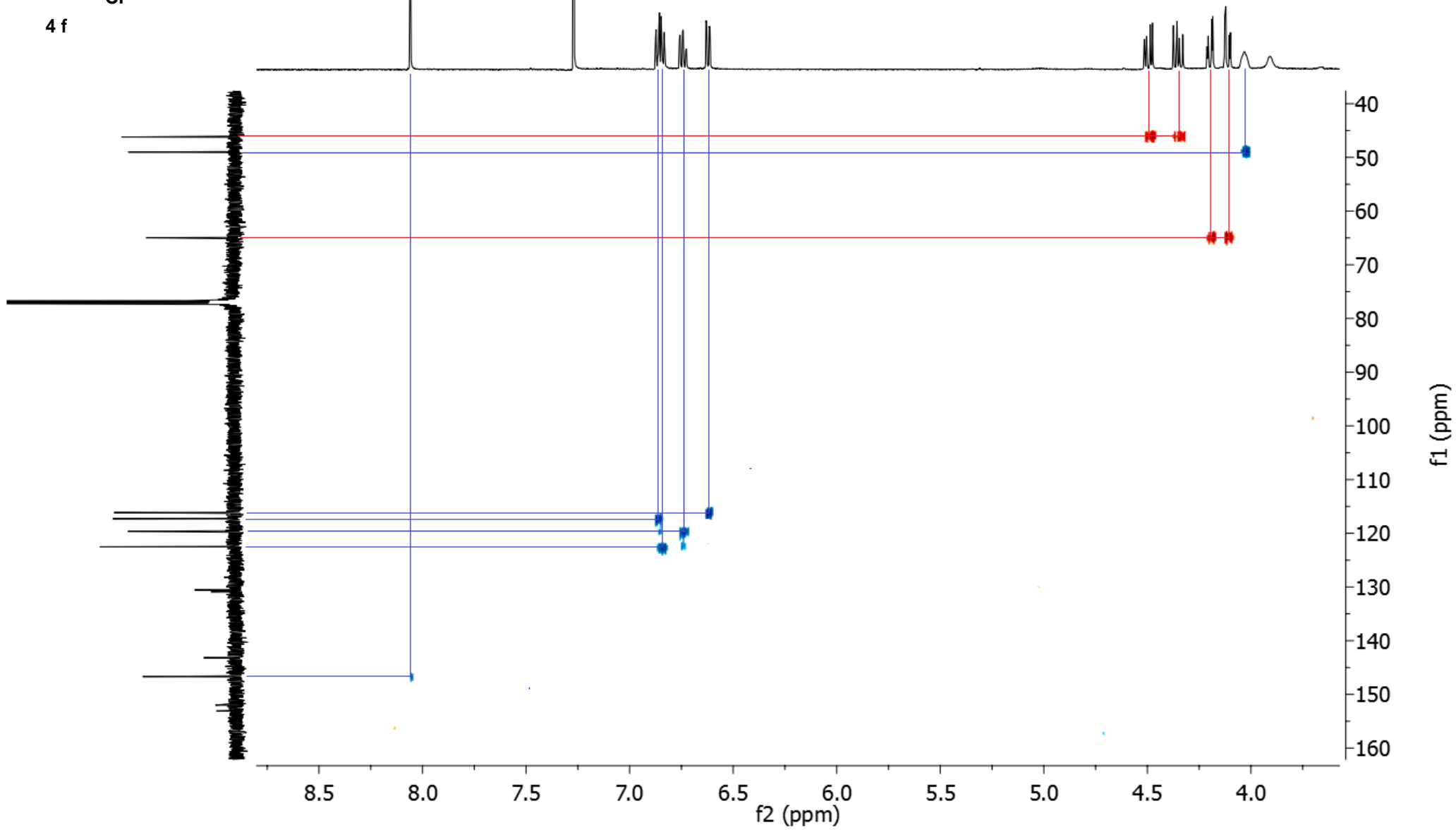


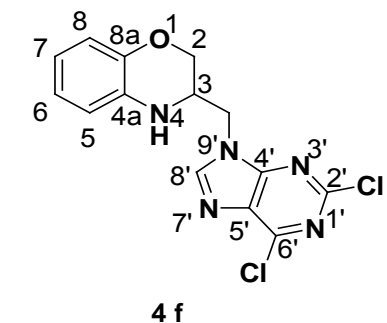


4 f

S 20

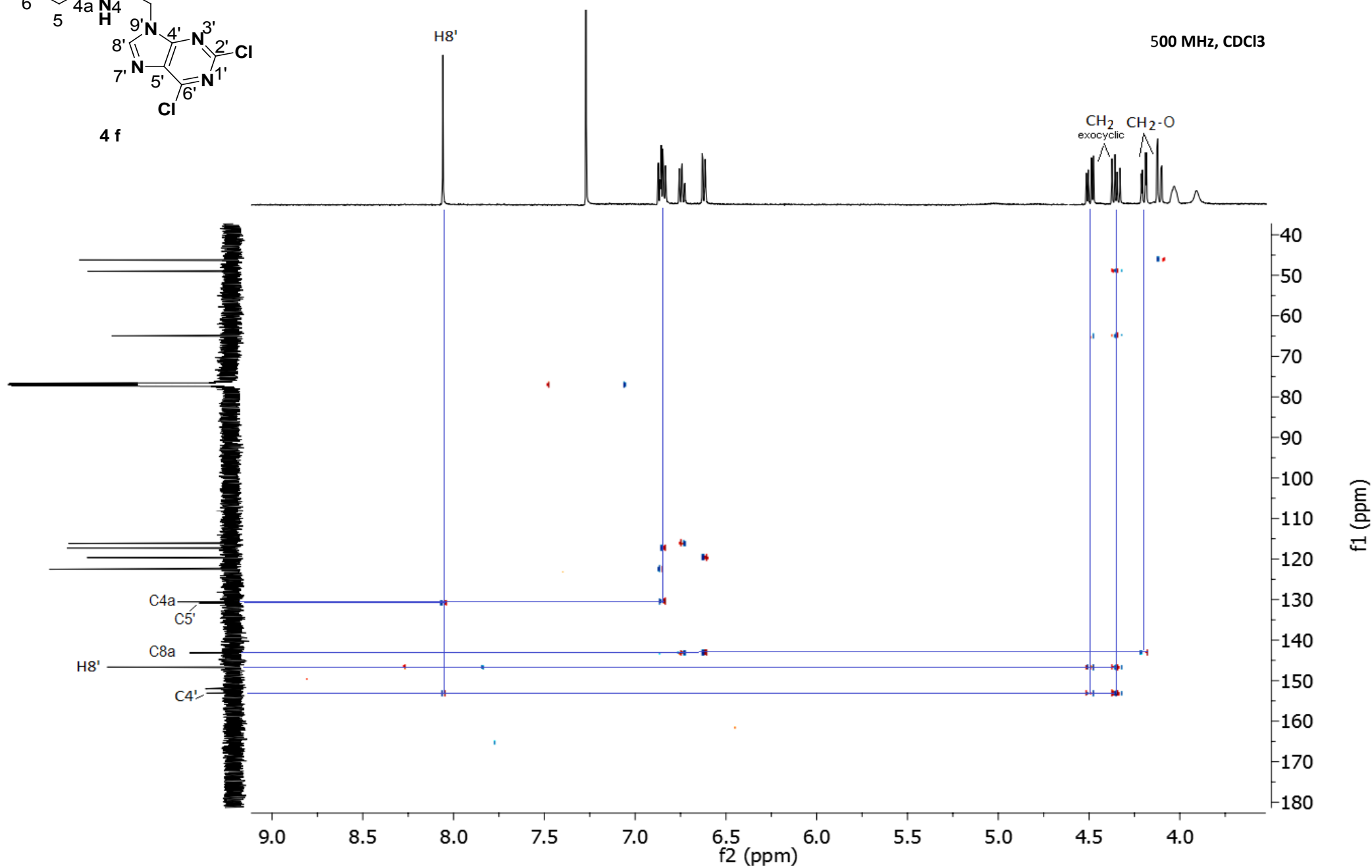
500 MHz, CDCl₃





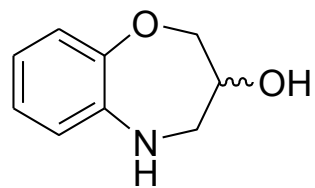
S 21

500 MHz, CDCl₃

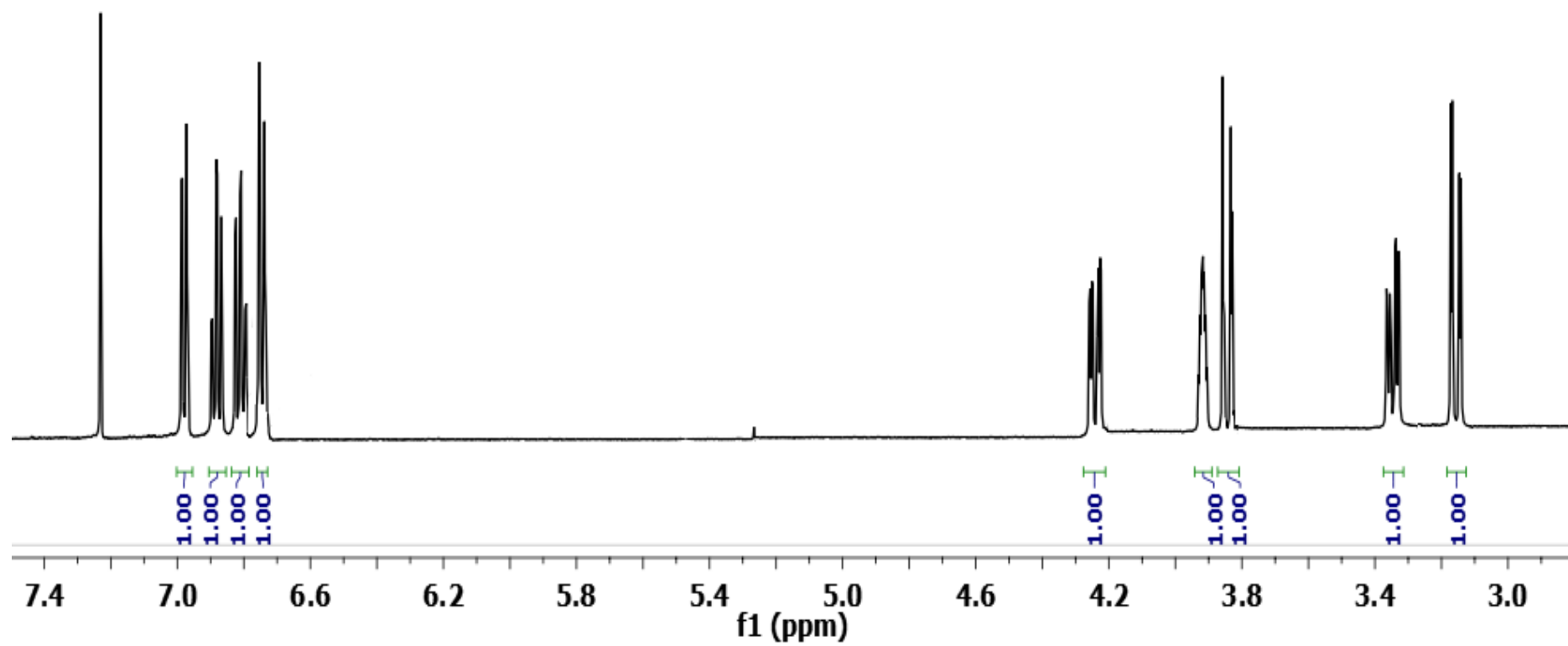


S 22

500 MHz, CDCl₃

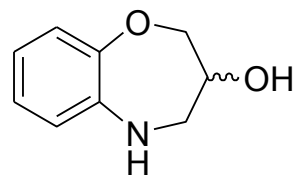


5a

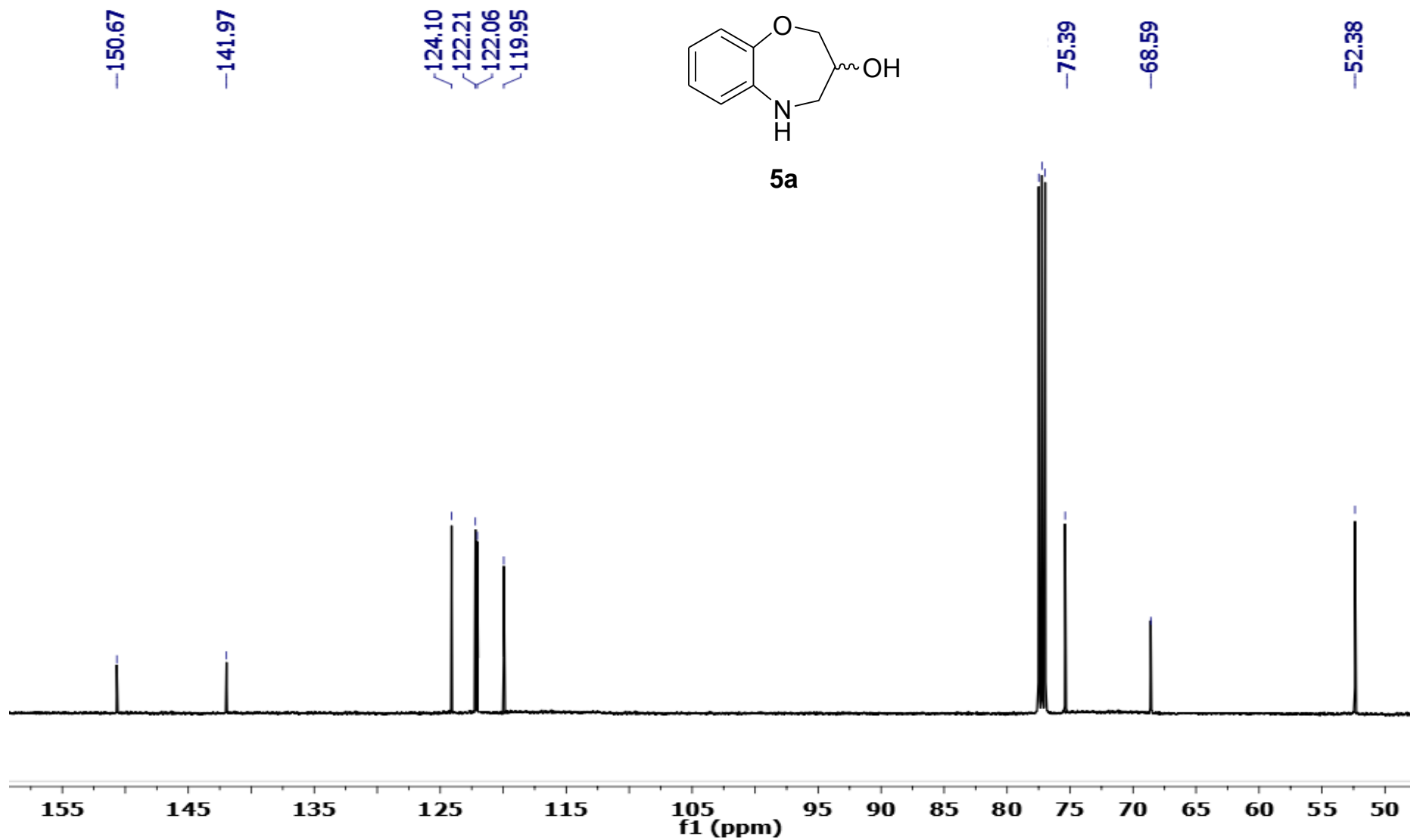


S 23

500 MHz, CDCl₃

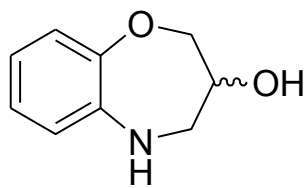


5a

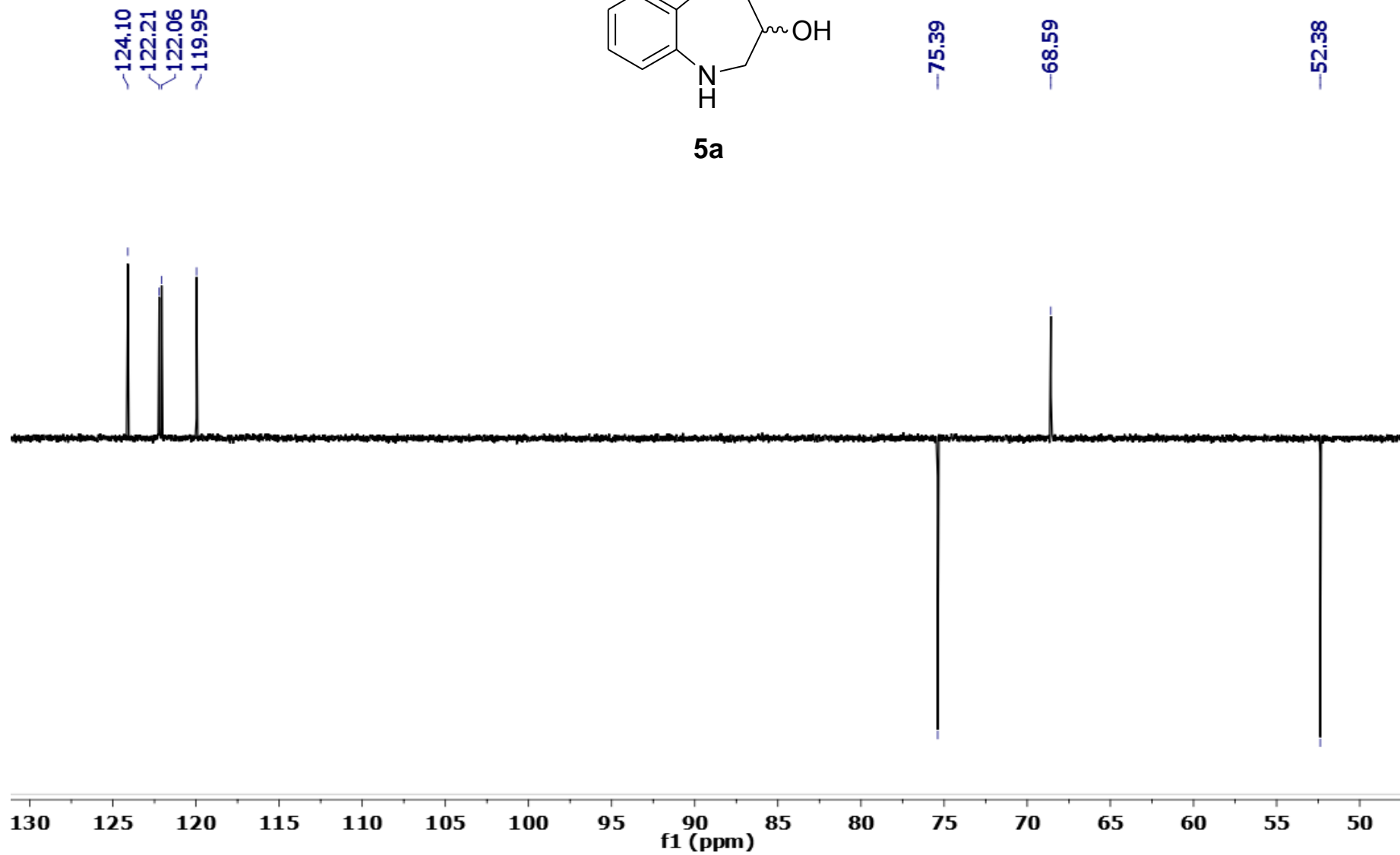


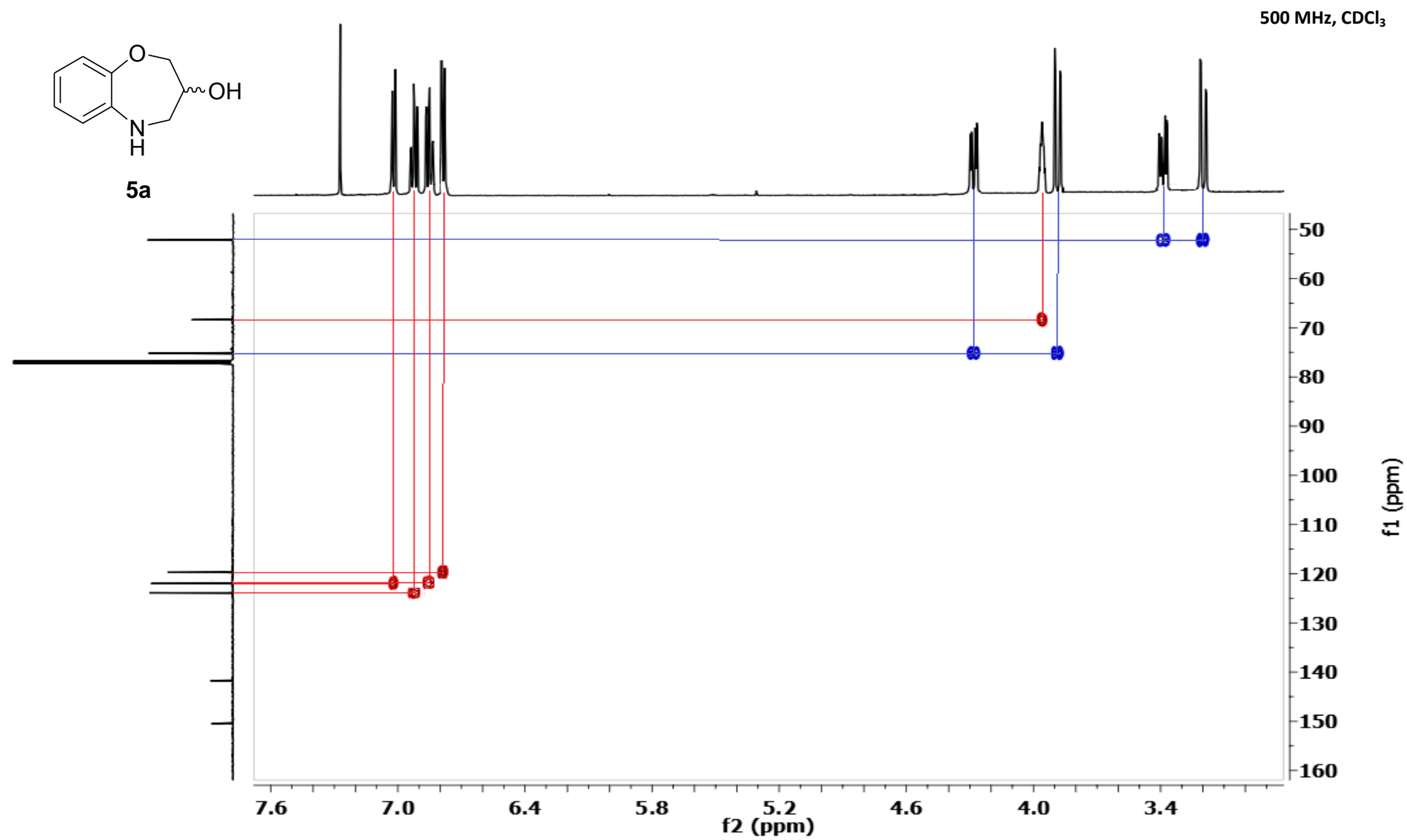
S 24

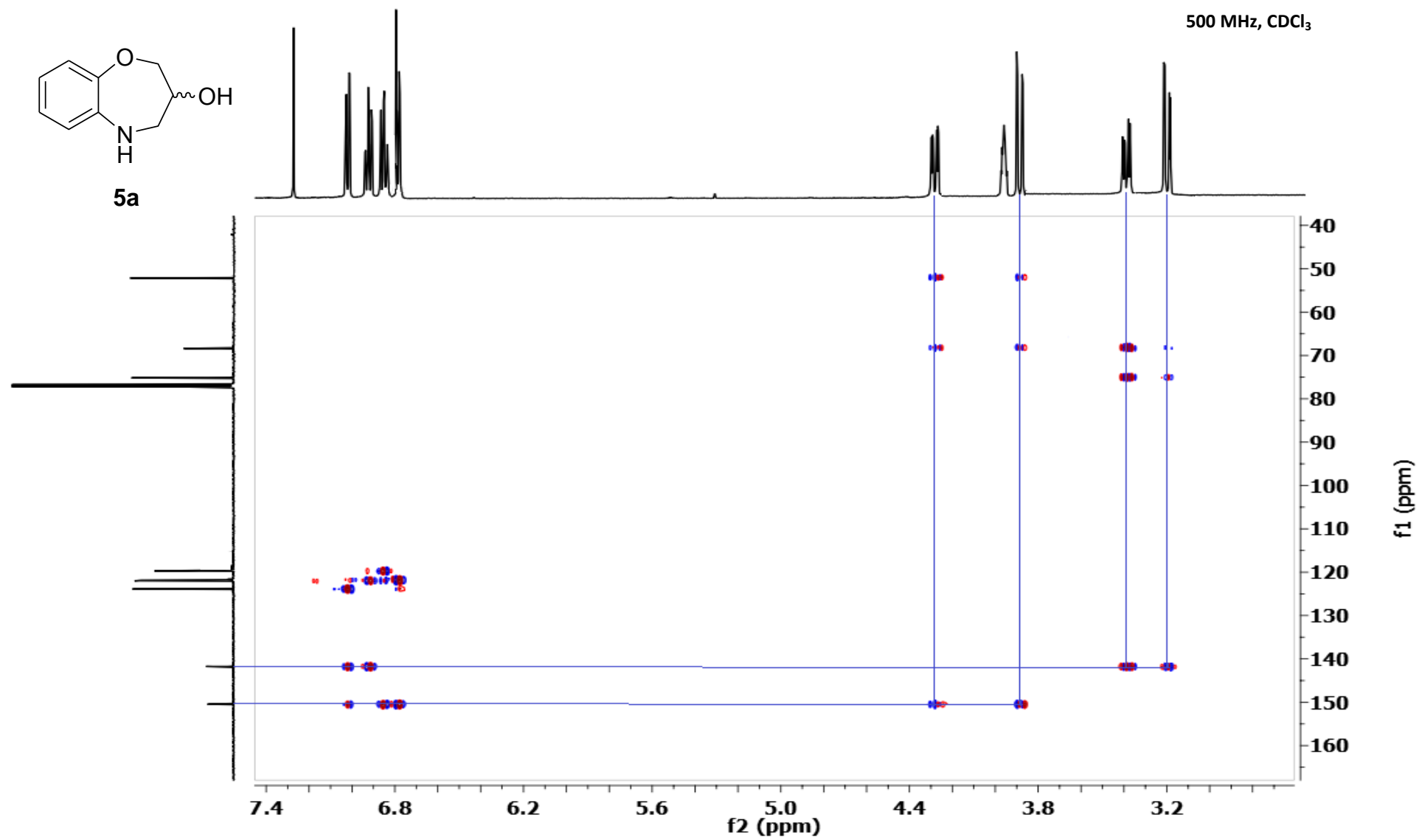
500 MHz, CDCl₃



5a

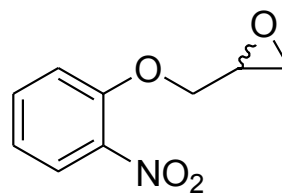




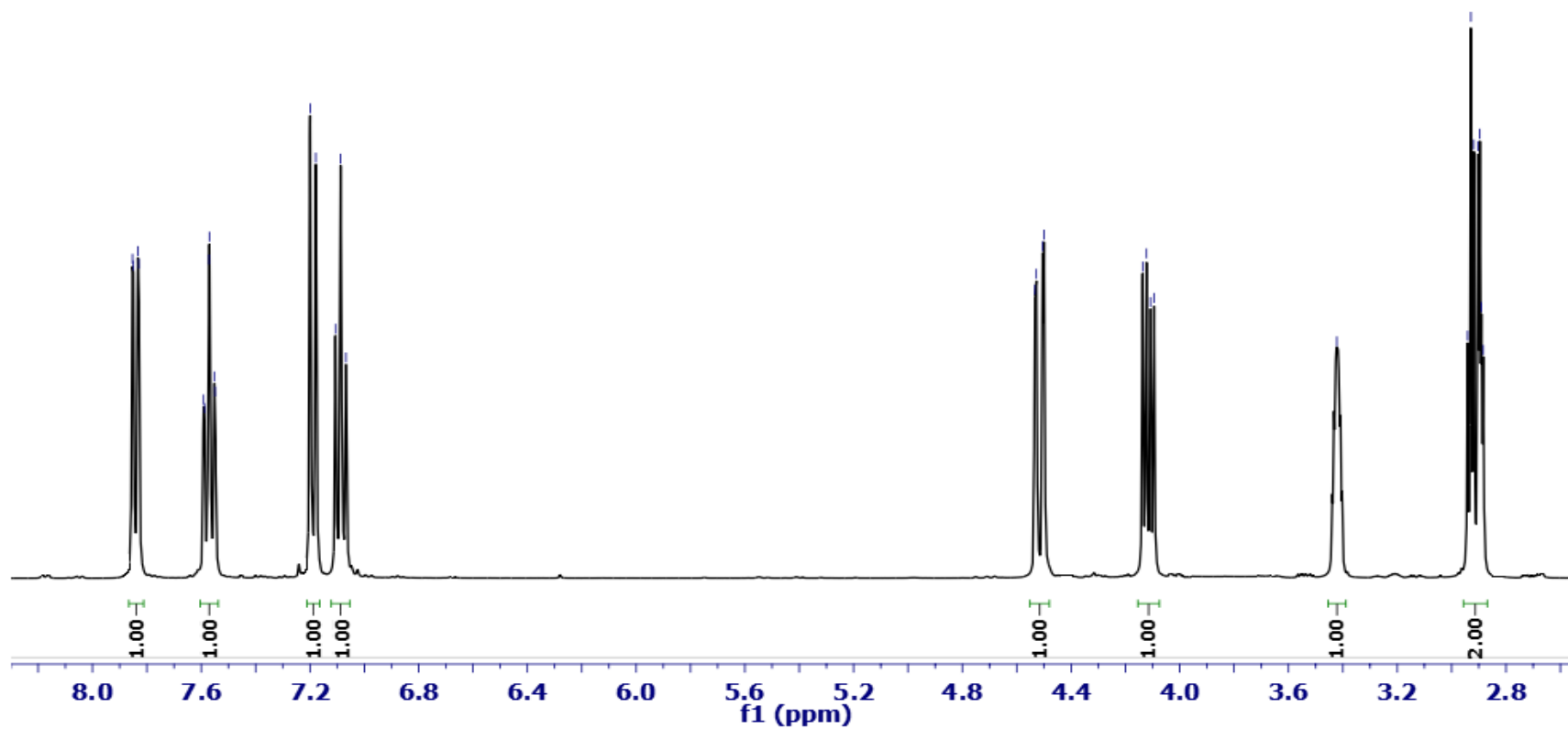


S 27

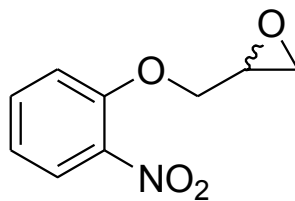
400 MHz, CDCl₃



6

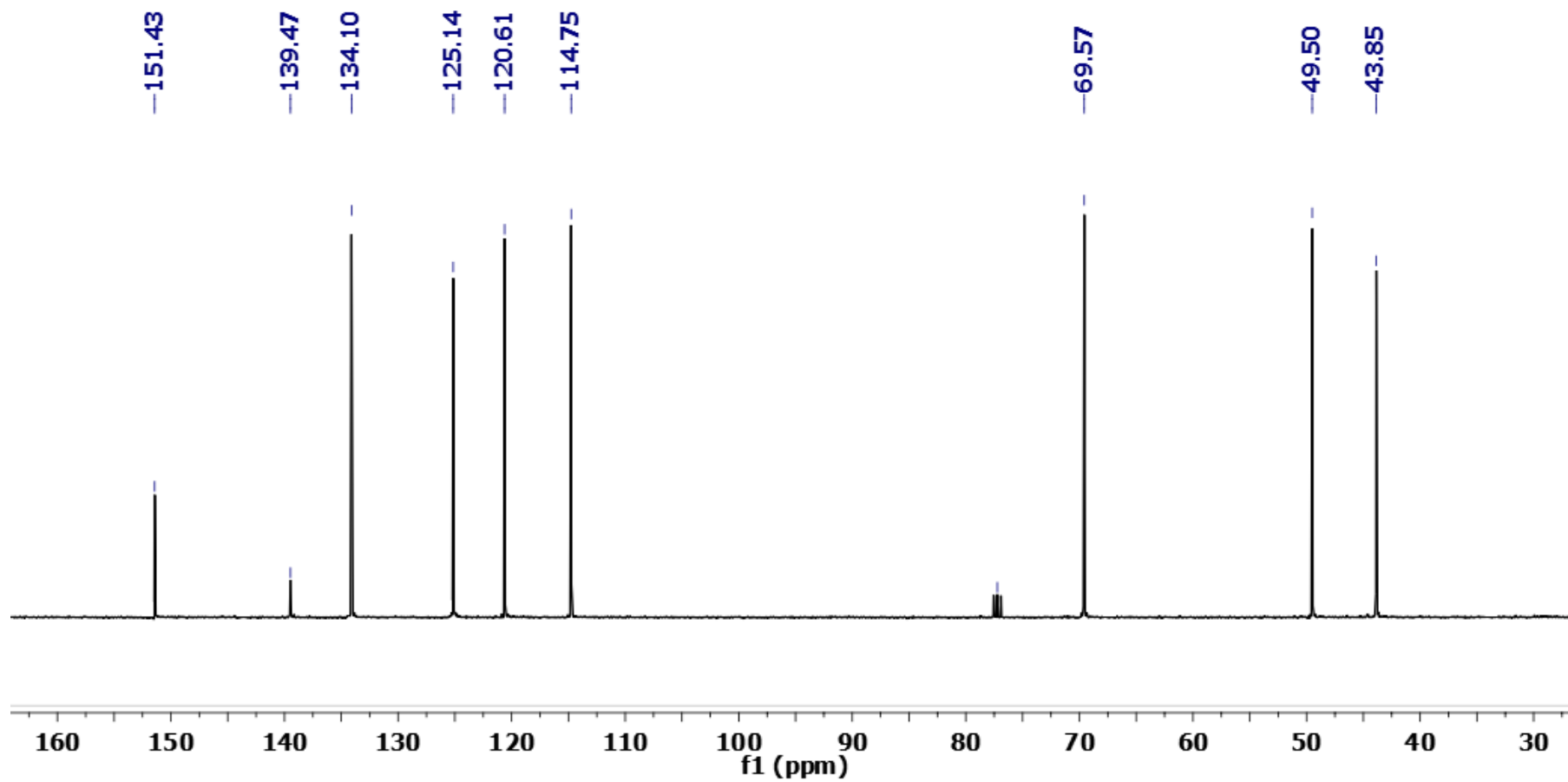


S 28



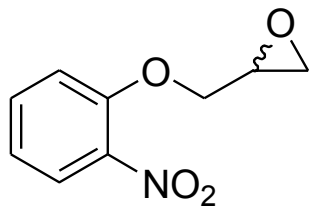
400 MHz, CDCl_3

6

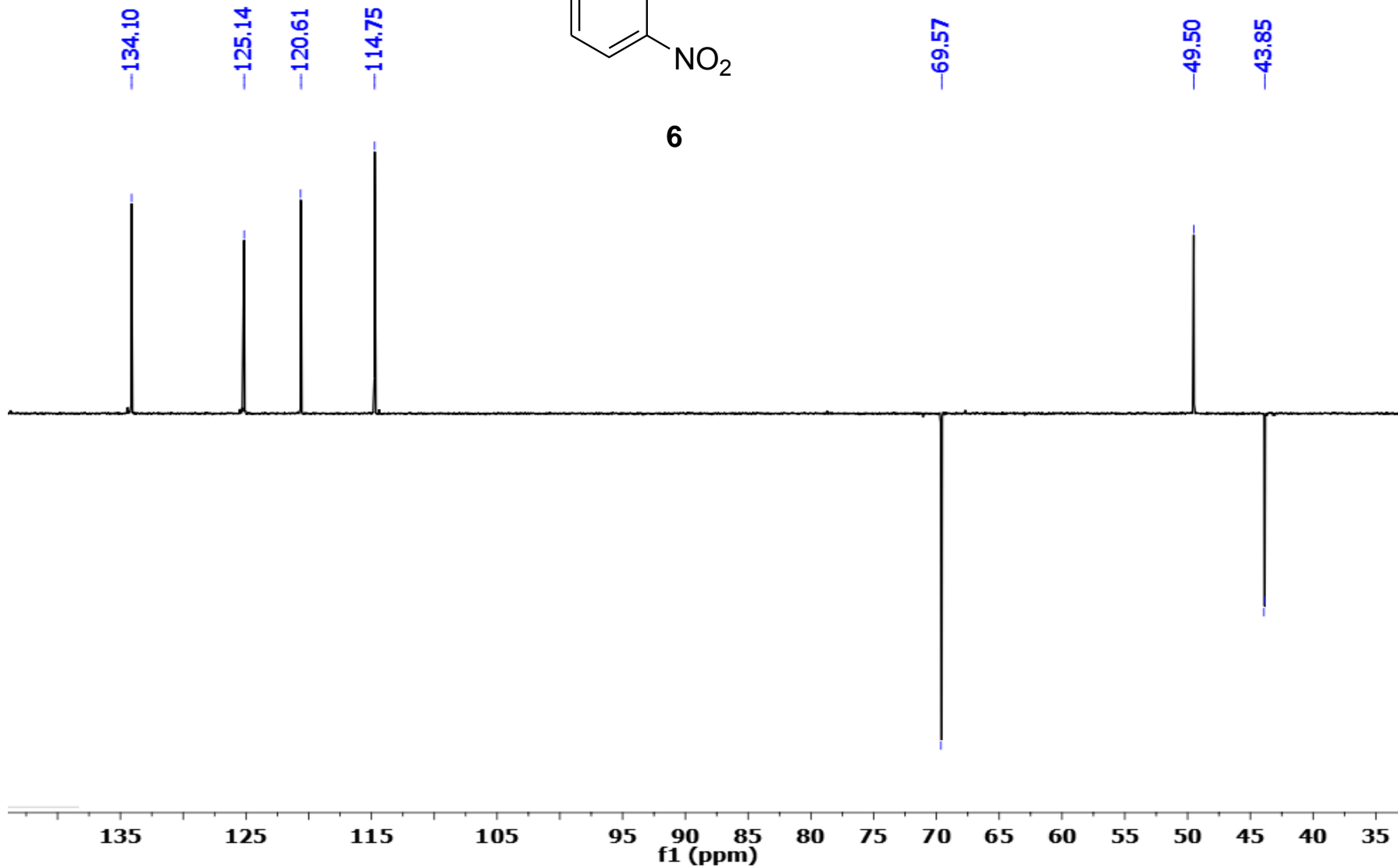


S 29

400 MHz, CDCl₃

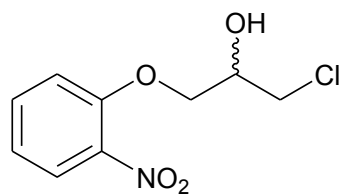


6

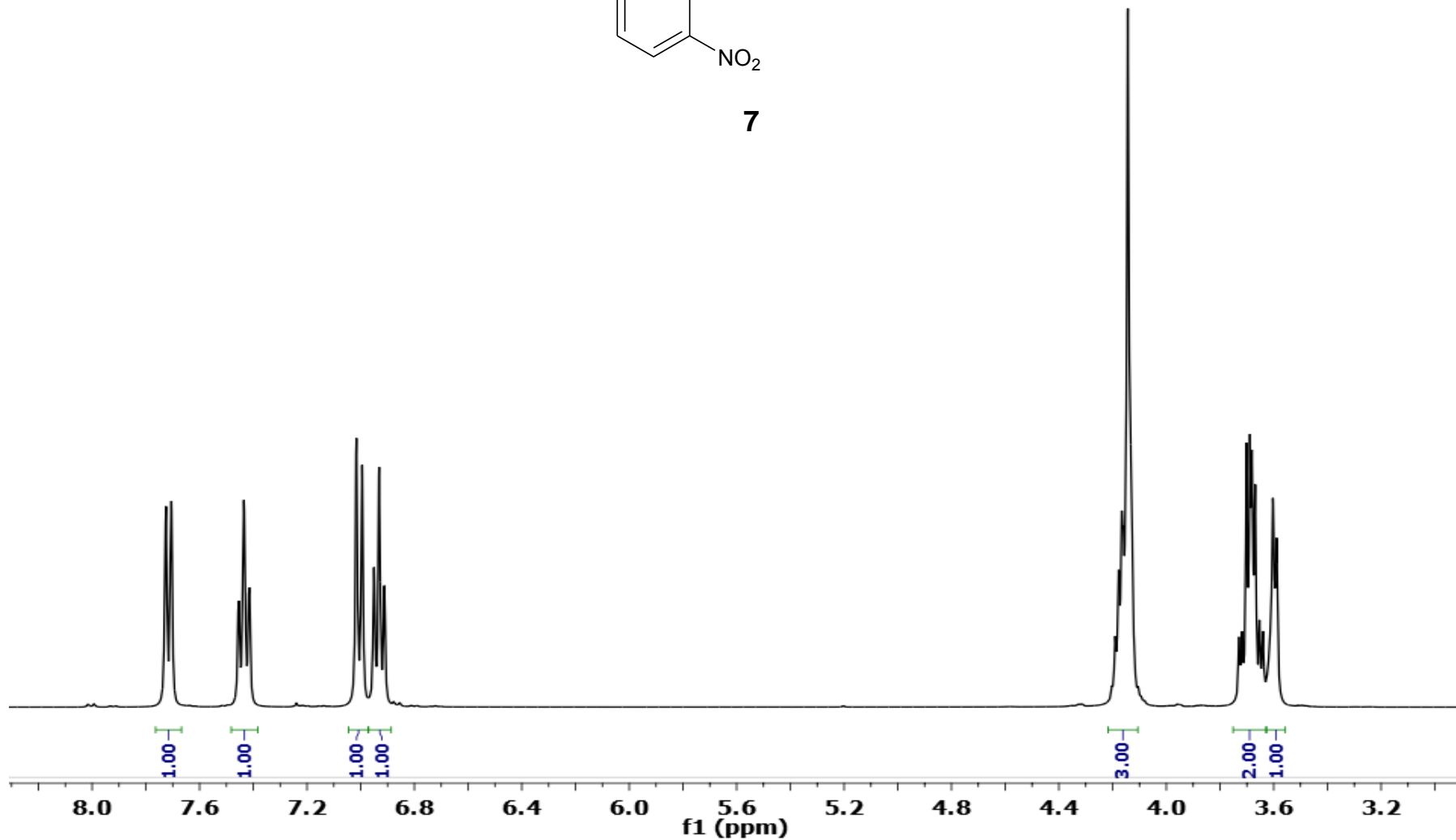


S 30

400 MHz, CDCl₃

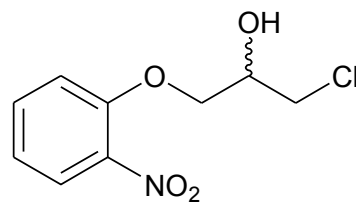


7

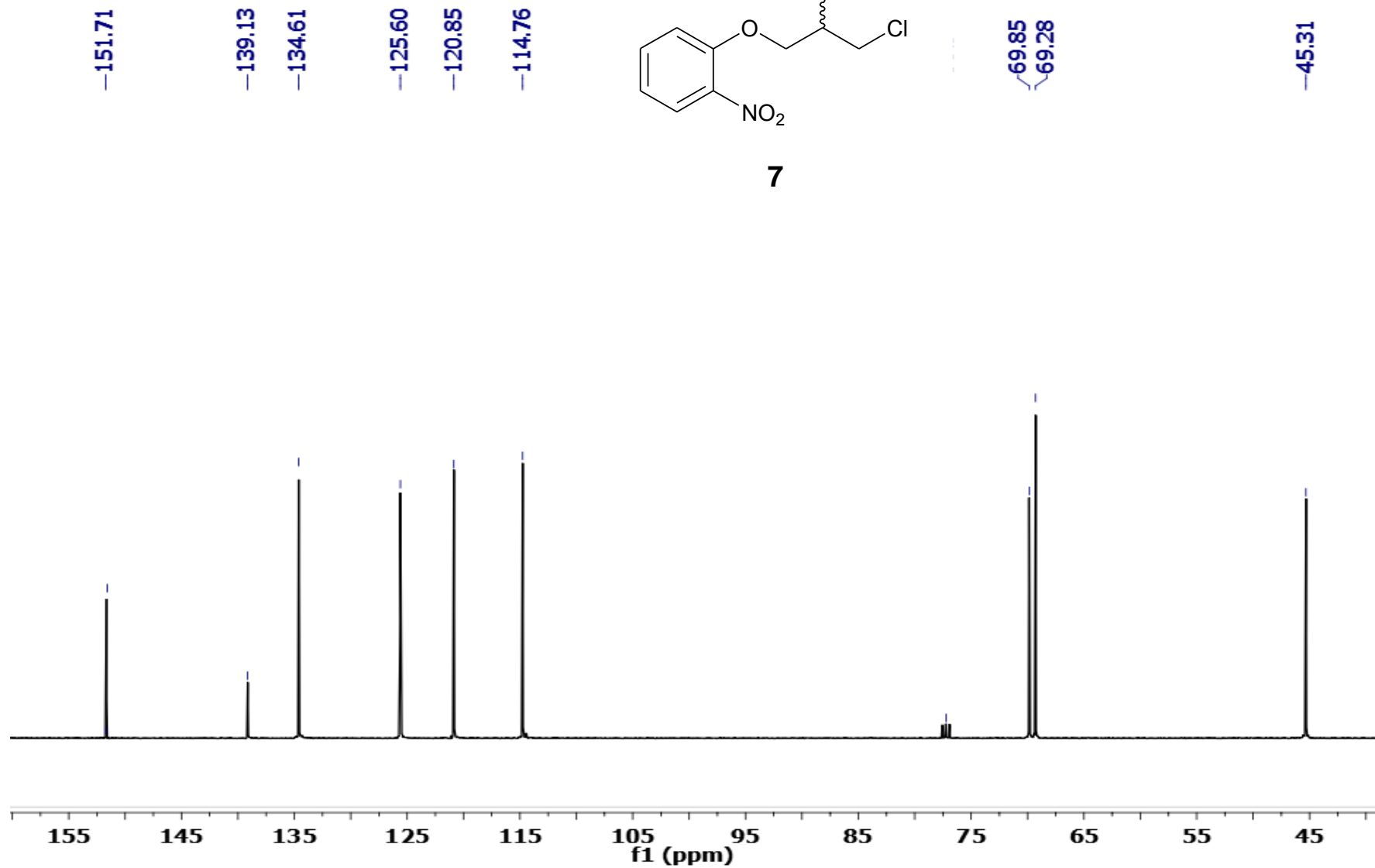


S 31

400 MHz, CDCl₃

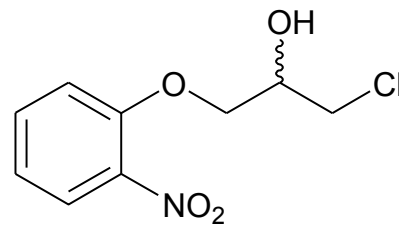


7

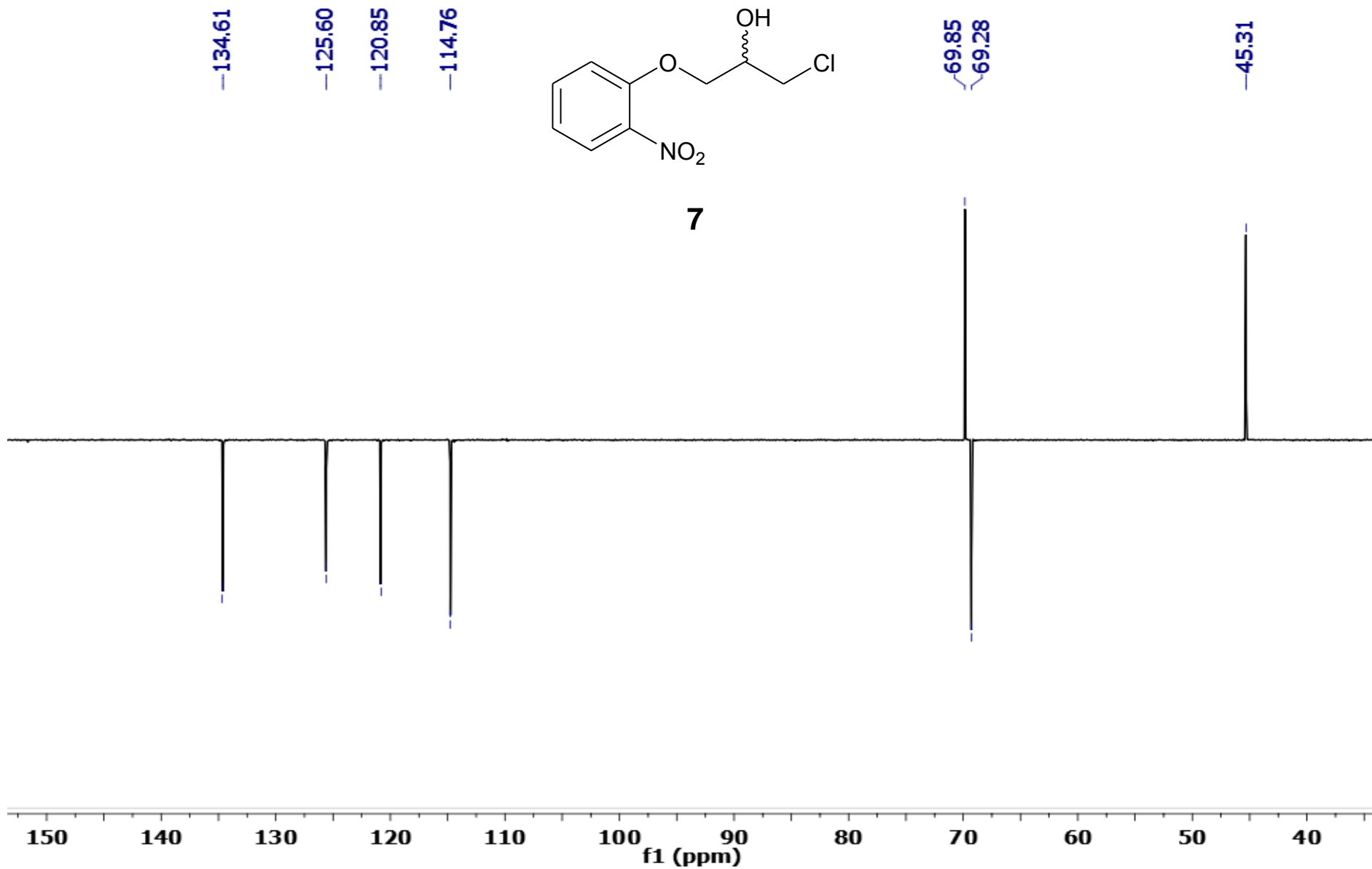


S 32

400 MHz, CDCl₃

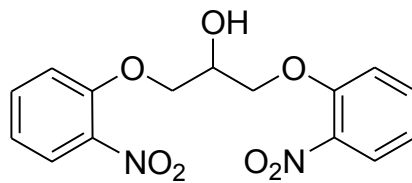


7

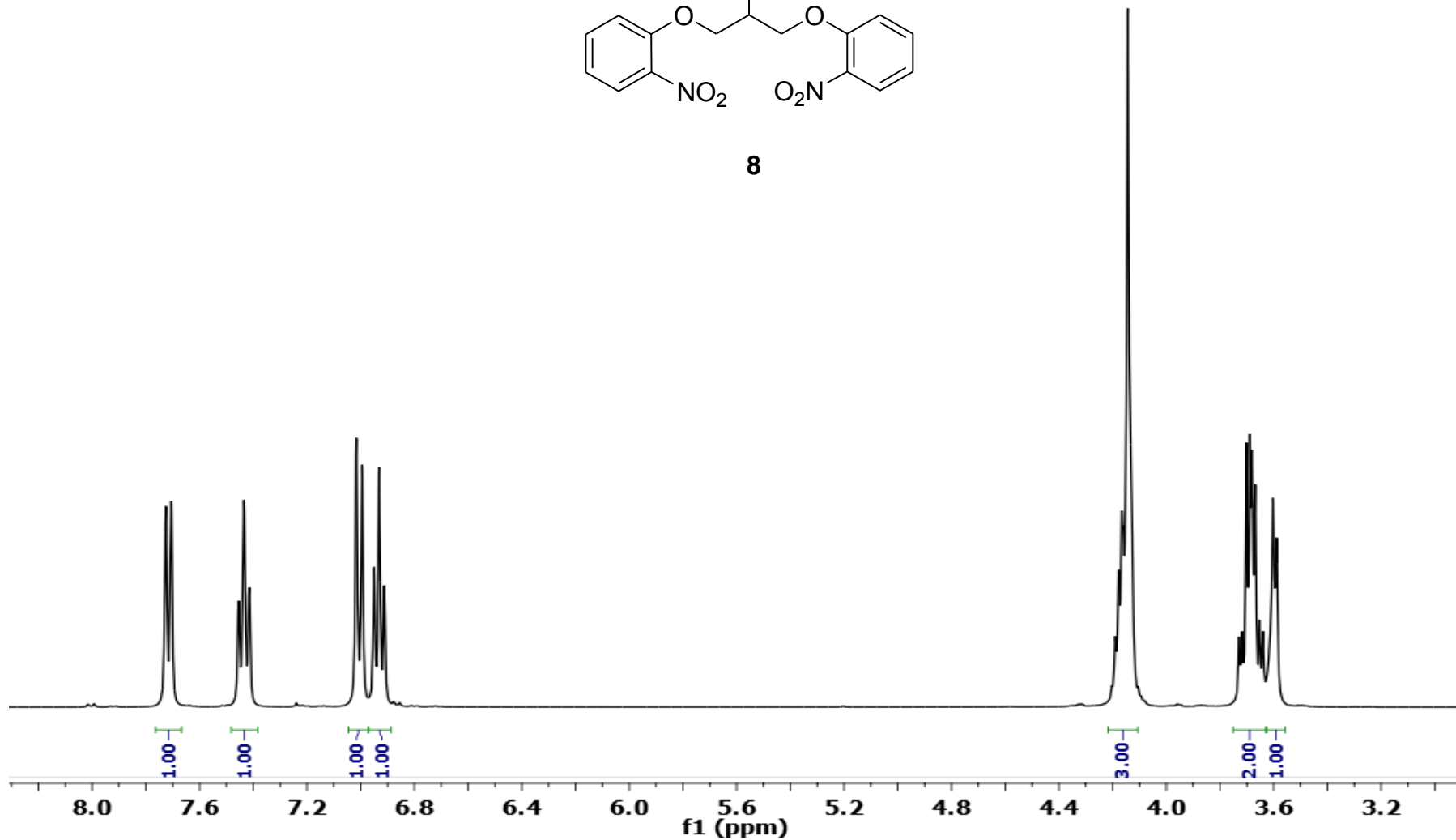


S 33

400 MHz, CDCl₃



8



S 34

400 MHz, CDCl₃

—152.34

—139.62

—134.85

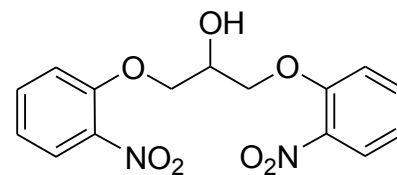
—126.09

—121.07

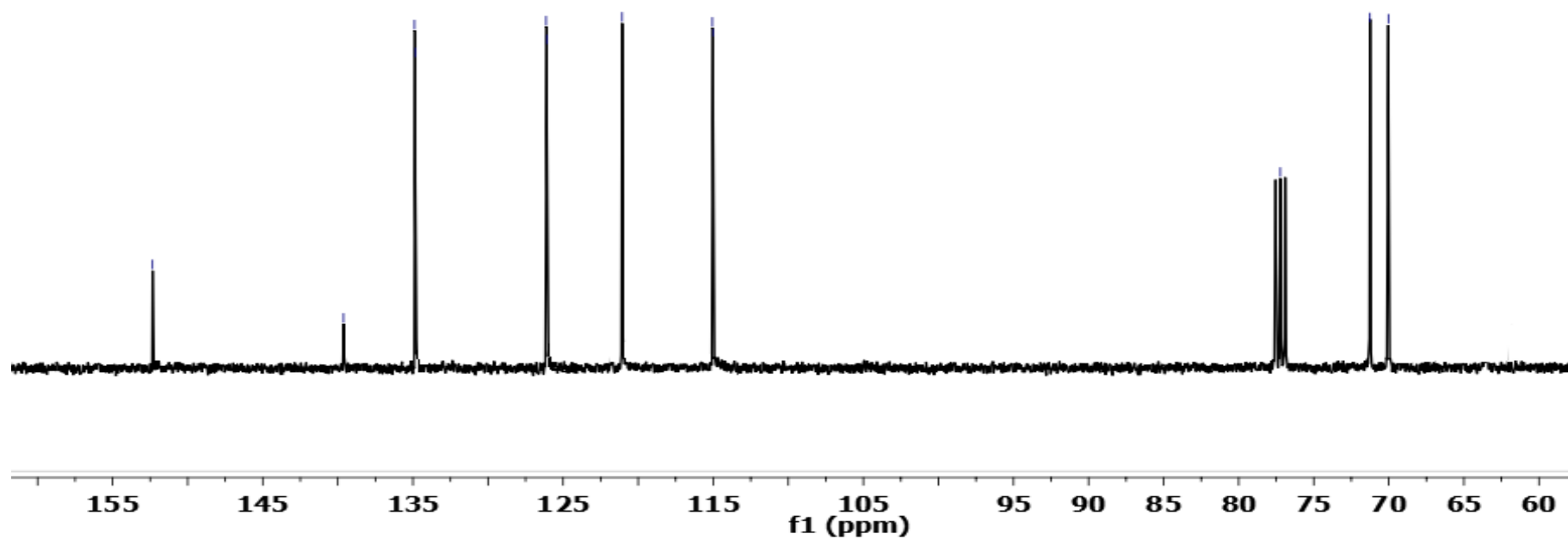
—115.01

~71.26

~70.03



8



S 35

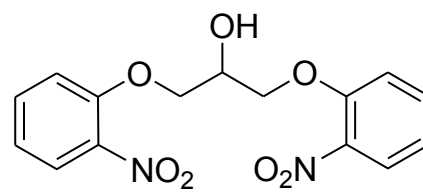
400 MHz, CDCl₃

-134.85

-126.09

-121.07

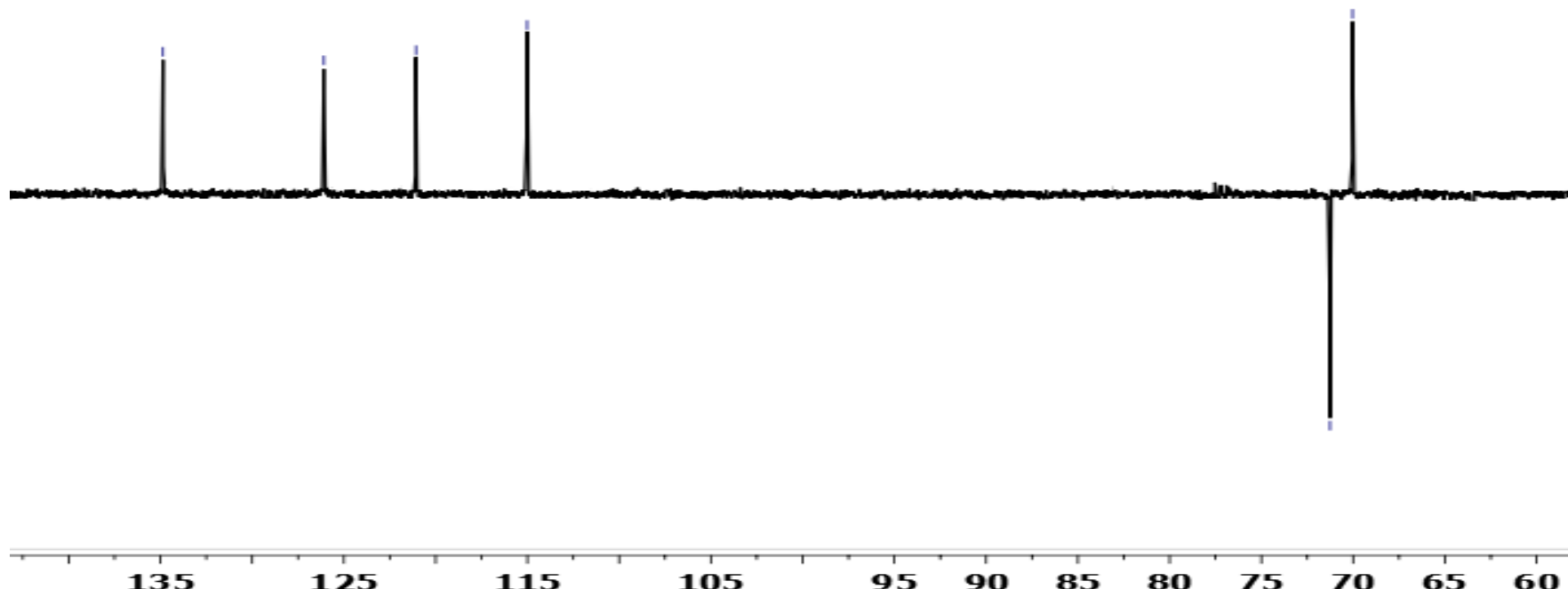
-115.01



8

~71.26

~70.03



PAPER 6

Two tautomeric polymorphs of 2,6-dichloropurine

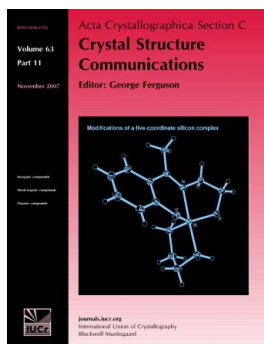
M. Eugenia García-Rubiño, Duane Choquesillo-Lazarte, M. C. Núñez and Joaquín M. Campos

Acta Cryst. (2011). **C67**, o484–o486

Copyright © International Union of Crystallography

Author(s) of this paper may load this reprint on their own web site or institutional repository provided that this cover page is retained. Reproduction of this article or its storage in electronic databases other than as specified above is not permitted without prior permission in writing from the IUCr.

For further information see <http://journals.iucr.org/services/authorrights.html>



Acta Crystallographica Section C: Crystal Structure Communications specializes in the rapid dissemination of high-quality studies of crystal and molecular structures of interest in fields such as chemistry, biochemistry, mineralogy, pharmacology, physics and materials science. The numerical and text descriptions of each structure are submitted to the journal electronically as a Crystallographic Information File (CIF) and are checked and typeset automatically prior to peer review. The journal is well known for its high standards of structural reliability and presentation. *Section C* publishes approximately 1000 structures per year; readers have access to an archive that includes high-quality structural data for over 10000 compounds.

Crystallography Journals **Online** is available from journals.iucr.org

Two tautomeric polymorphs of
2,6-dichloropurineM. Eugenia García-Rubiño,^a Duane Choquesillo-Lazarte,^b
M. C. Núñez^a and Joaquín M. Campos^{a*}^aDepartamento de Química Farmacéutica y Orgánica, Facultad de Farmacia,
Universidad de Granada, Campus de Cartuja s/n, 18071 Granada, Spain, and^bLaboratorio de Estudios Cristalográficos, IACT, CSIC-Universidad de Granada,
Avenida de las Palmeras 4, 18100 Armilla, Granada, Spain

Correspondence e-mail: jmcampos@ugr.es

Received 19 September 2011

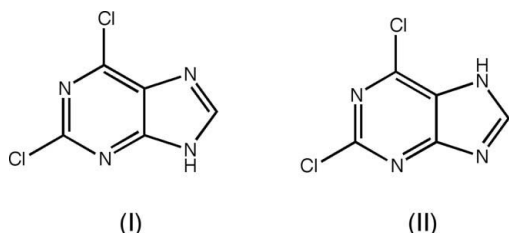
Accepted 20 October 2011

Online 5 November 2011

Two polymorphs of 2,6-dichloropurine, C₅H₂Cl₂N₄, have been crystallized and identified as the 9*H*- and 7*H*-tautomers. Despite differences in the space group and number of symmetry-independent molecules, they exhibit similar hydrogen-bonding motifs. Both crystal structures are stabilized by intermolecular N—H···N interactions that link adjacent molecules into linear chains, and by some nonbonding contacts of the C—Cl···π type and by π–π stacking interactions, giving rise to a crossed two-dimensional herringbone packing motif. The main structural difference between the two polymorphs is the different role of the molecules in the π–π stacking interactions.

Comment

2,6-Dichloropurine is an important pharmaceutical intermediate (Schaefer *et al.*, 1978) used in the preparation of purine nucleosides and nucleotides, and other purine derivatives of great importance owing to their biological properties (Nair & Pal, 1998; Rao Kode & Phadtare, 2011).



Polymorphism, the ability of a given molecule to crystallize in different crystal structures, is a phenomenon often observed for organics (Bernstein, 2011; Brittain, 2011). The term 'tautomeric polymorphs' refers to those tautomers of a given compound that crystallize in different crystal structures and they are very rarely observed (Cruz Cabeza *et al.*, 2011). We present here the crystal structure of the 9*H*-, (I), and 7*H*-, (II), tautomers of 2,6-dichloropurine.

The molecular geometric parameters in the two presented polymorphs are similar, but the structures differ in the finer details of their crystal packing. As shown in Fig. 1, polymorph (I) crystallizes with two independent molecules in the asymmetric unit (*A* and *B*, top and middle) as the 9*H*-tautomer, while polymorph (II) crystallizes with one symmetry-independent molecule (bottom) as the 7*H*-tautomer.

The effect of the different –N(H) position in the tautomeric forms (N9 or N7) gives rise to subtle differences between the relevant bond lengths and angles in both structures in the imidazole ring. In (I), the N=Csp² bond corresponds to N7–C8 [1.310 (5) Å] and N17–C18 [1.307 (5) Å] for molecules *A* and *B*, respectively, while in (II) it is N9–C8 [1.327 (3) Å]. These N=Csp² bond lengths are comparable with those in related structures with 9*H*- (Mahapatra *et al.*, 2008; Trávníček & Rosenker, 2006; Soriano-García & Parthasarathy, 1977) and 7*H*-tautomers (Bo *et al.*, 2006; Ikonen *et al.*, 2009; Watson *et al.*, 1965). The –N(H) tautomeric position is also evident from the greater ring angle at the site where the H atom is attached, namely N9 [C4–N9–C8 = 105.9 (3)°] and N19 [C14–N19–C18 = 105.6 (3)°] for (I), and N7 [C5–N7–C8 = 105.9 (2)°] for (II), compared with the ring angle involving the –N=C– bond [for (I), C5–N7–C8 = 103.6 (3)° and C15–N17–C18 = 103.8 (3)°; for (II), C4–N9–C8 = 103.6 (2)°]. In both polymorphs, the 2,6-dichloropurine molecules form linear chains along the *b* axis through

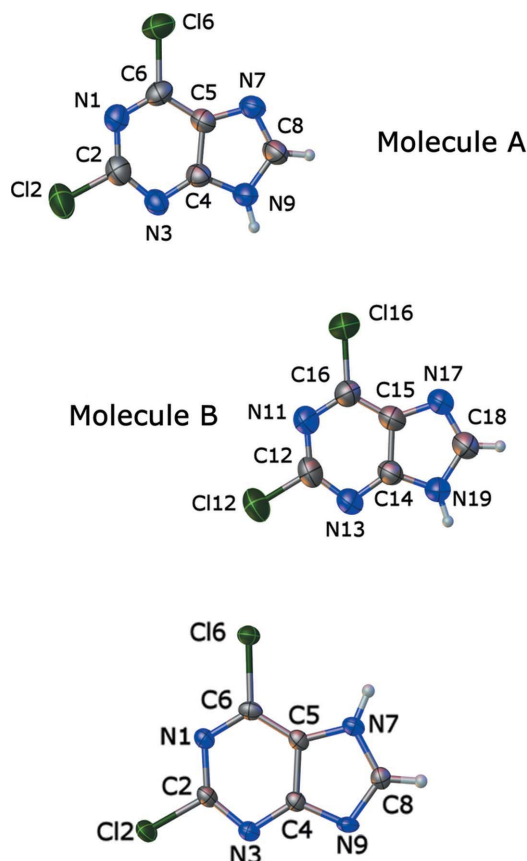


Figure 1

The contents of the asymmetric units of polymorph (I) (top and middle) and polymorph (II) (bottom), showing the atom-numbering schemes. Displacement ellipsoids are drawn at the 50% probability level.

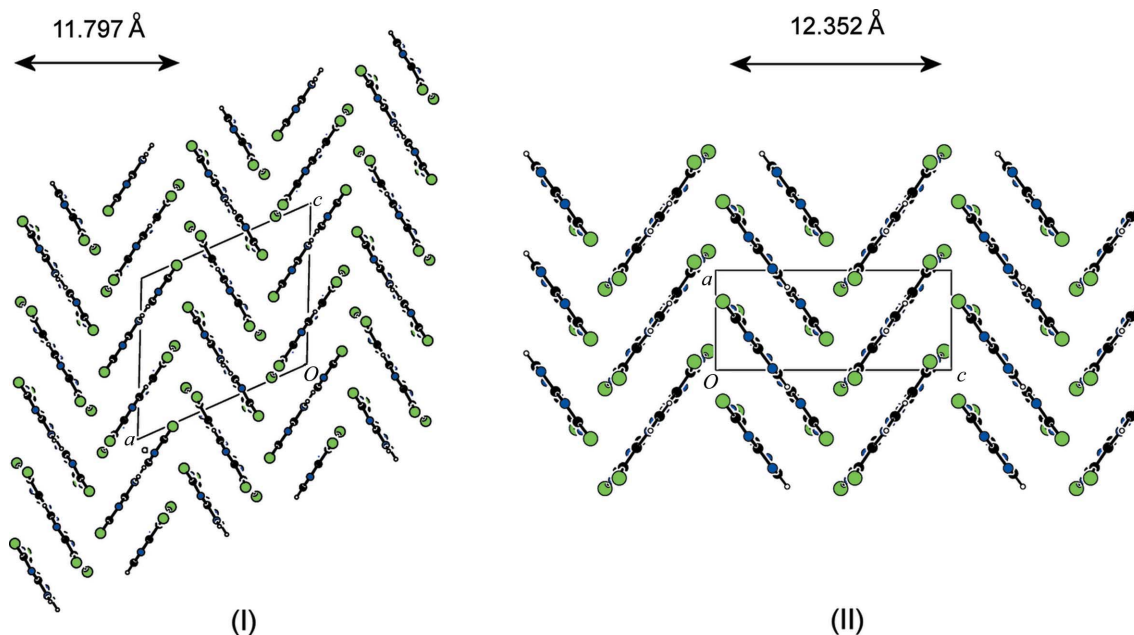


Figure 2
A view of the crystal packing, showing the herringbone arrangement of 2,6-dichloropurine molecules in polymorph (I) (left) and polymorph (II) (right).

intermolecular N—H \cdots N interactions forming C(4) motifs (Bernstein *et al.*, 1995).

In polymorph (I), chains built by molecules of type *A* are linked by intermolecular face-to-face π – π stacking interactions involving the N1/C2/N3/C4–C6 ring and a symmetry-related counterpart at $(-x + 1, -y + 1, -z + 1)$, with a centroid–centroid distance of 3.493 (3) Å. Molecules of type *B* are not involved in π – π stacking interactions. There are also C—Cl \cdots π interactions involving atom Cl16 and ring N1/C2/N3/C4–C6 (*Cg*1_I), with a Cl \cdots centroid distance of 3.468 (2) Å and a C16—Cl16 \cdots *Cg*1_Iⁱ angle of 113.46 (17)° [symmetry code: (i) $x, -y + \frac{1}{2}, z + \frac{1}{2}$], and atom Cl6 and ring N11/C12/N13/C14–C16 (*Cg*2_I), with a Cl \cdots centroid distance of 3.664 (2) Å and a C6—Cl6 \cdots *Cg*2_I angle of 94.54 (13)°, resulting in a structure containing a two-dimensional herringbone-like motif of constituent molecules.

The crystal structure of polymorph (II) is similar to that of polymorph (I). Despite the fact that π – π stacking interactions are not observed in (II), the supramolecular structure features a similar herringbone motif to that in (I), due to the presence of C—Cl \cdots π interactions between atom Cl6 and ring N1/C2/N3/C4–C6 (*Cg*1_{II}), with a Cl \cdots centroid distance of 3.3471 (15) Å and a C6—Cl6 \cdots *Cg*1_{II}ⁱⁱ angle of 108.45 (10)° [symmetry code: (ii) $x - \frac{1}{2}, -y + \frac{3}{2}, -z + 1$]. As a consequence of the absence of stacking interactions in (II), the width of the herringbone motif (12.352 Å) is greater than that of (I) (11.797 Å) (Fig. 2) [the width of the motifs was calculated as the distance between the two planes containing the furthest atoms in the herringbone motif, corresponding to the Cl atoms of 2,6-dichloropurine; Mercury (Macrae *et al.*, 2008)].

Experimental

Polymorph (I) (m.p. 466.05–466.75 K) was obtained unintentionally in an attempted synthesis of (*RS*)-2,6-dichloro-9-(2,3-dihydro-1,4-

benzoxathiin-3-ylmethyl)-9*H*-purine (Díaz-Gavilán *et al.*, 2008). Unreacted 2,6-dichloropurine was recovered using ethyl acetate as eluent. After concentrating the solvent under reduced pressure, suitable crystals of 2,6-dichloropurine were obtained after dissolving the compound in CH₂Cl₂. A vial with a screw top allowed slow evaporation of the solvent at room temperature to produce colourless crystals. Crystals of polymorph (II) (m.p. 467.95–468.85 K) were obtained by solvent evaporation with commercially available 2,6-dichloropurine using ethanol as solvent. The remarkable similarity of the crystal structures of the reported polymorphs yields minimal differences in the shape and position of the peaks in the FT–IR spectra (polycrystalline samples in KBr disks). Hence, the stretching mode ν (N–H) (a weak peak at 3210 cm⁻¹) and the in-plane deformation mode δ (N–H) (1513 cm⁻¹) appear at the same site in (I) and (II).

Polymorph (I)

Crystal data

C₅H₂Cl₂N₄
*M*_r = 189.01
 Monoclinic, *P*2₁/*c*
a = 14.0867 (12) Å
b = 9.4898 (7) Å
c = 12.2656 (9) Å
 β = 115.381 (4)°

V = 1481.4 (2) Å³
Z = 8
 Cu *K*α radiation
 μ = 7.36 mm⁻¹
T = 296 K
 0.12 × 0.10 × 0.06 mm

Data collection

Bruker X8 Proteum diffractometer
 Absorption correction: multi-scan
 (*SADABS*; Bruker, 2001)
*T*_{min} = 0.377, *T*_{max} = 0.753

18199 measured reflections
 2547 independent reflections
 1713 reflections with *I* > 2σ(*I*)
*R*_{int} = 0.085

Refinement

R[*F*² > 2σ(*F*²)] = 0.051
wR(*F*²) = 0.154
S = 1.10
 2547 reflections

199 parameters
 H-atom parameters constrained
 $\Delta\rho_{\max}$ = 0.27 e Å⁻³
 $\Delta\rho_{\min}$ = -0.29 e Å⁻³

Table 1
Hydrogen-bond geometry (Å, °) for polymorph (I).

<i>D</i> —H... <i>A</i>	<i>D</i> —H	H... <i>A</i>	<i>D</i> ... <i>A</i>	<i>D</i> —H... <i>A</i>
N9—H9...N7 ⁱ	0.86	1.96	2.785 (4)	161
N19—H19...N17 ⁱⁱ	0.86	1.94	2.768 (5)	160

Symmetry codes: (i) $-x + 1, y + \frac{1}{2}, -z + \frac{1}{2}$; (ii) $-x + 2, y + \frac{1}{2}, -z + \frac{3}{2}$.

Polymorph (II)

Crystal data

$C_5H_2Cl_2N_4$	$V = 702.5 (2) \text{ \AA}^3$
$M_r = 189.01$	$Z = 4$
Orthorhombic, $P2_12_12_1$	Mo $K\alpha$ radiation
$a = 5.5716 (9) \text{ \AA}$	$\mu = 0.85 \text{ mm}^{-1}$
$b = 9.5820 (16) \text{ \AA}$	$T = 120 \text{ K}$
$c = 13.159 (2) \text{ \AA}$	$0.12 \times 0.10 \times 0.08 \text{ mm}$

Data collection

Bruker SMART APEX diffractometer	6847 measured reflections
Absorption correction: multi-scan (SADABS; Bruker, 2001)	1243 independent reflections
$T_{\min} = 0.905, T_{\max} = 0.935$	1156 reflections with $I > 2\sigma(I)$
	$R_{\text{int}} = 0.041$

Refinement

$R[F^2 > 2\sigma(F^2)] = 0.033$	$\Delta\rho_{\text{max}} = 0.33 \text{ e \AA}^{-3}$
$wR(F^2) = 0.071$	$\Delta\rho_{\text{min}} = -0.22 \text{ e \AA}^{-3}$
$S = 1.38$	Absolute structure: Flack (1983),
1243 reflections	with 489 Friedel pairs
100 parameters	Flack parameter: 0.03 (10)
H-atom parameters constrained	

H atoms on N atoms were located in difference maps and refined as riding, with N—H = 0.86 [in (I)] and 0.94 Å [in (II)], and $U_{\text{iso}}(\text{H}) = 1.2U_{\text{eq}}(\text{N})$. Other H atoms were positioned geometrically and treated as riding, with C—H = 0.93–0.95 Å and $U_{\text{iso}}(\text{H}) = 1.2U_{\text{eq}}(\text{C})$.

For both compounds, data collection: APEX2 (Bruker, 2010); cell refinement: SAINT (Bruker, 2010); data reduction: SAINT; program(s) used to solve structure: SHELXS97 (Sheldrick, 2008); program(s) used to refine structure: SHELXL97 (Sheldrick, 2008); molecular graphics: PLATON (Spek, 2009); software used to prepare material for publication: publCIF (Westrip, 2010).

Table 2
Hydrogen-bond geometry (Å, °) for polymorph (II).

<i>D</i> —H... <i>A</i>	<i>D</i> —H	H... <i>A</i>	<i>D</i> ... <i>A</i>	<i>D</i> —H... <i>A</i>
N7—H7...N9 ⁱ	0.94	1.88	2.774 (3)	158

Symmetry code: (i) $-x + 1, y + \frac{1}{2}, -z + \frac{3}{2}$.

The project 'Factoría de Cristalización, CONSOLIDER INGENIO-2010' provided X-ray structural facilities for this work.

Supplementary data for this paper are available from the IUCr electronic archives (Reference: GG3264). Services for accessing these data are described at the back of the journal.

References

- Bernstein, J. (2011). *Cryst. Growth Des.* **11**, 632–650.
- Bernstein, J., Davis, R. E., Shimoni, L. & Chang, N.-L. (1995). *Angew. Chem. Int. Ed. Engl.* **34**, 1555–1573.
- Bo, Y., Cheng, K., Bi, S. & Zhang, S.-S. (2006). *Acta Cryst.* **E62**, o4174–o4175.
- Brittain, H. G. (2011). *J. Pharm. Sci.* **100**, 1260–1279.
- Bruker (2001). SADABS. Bruker AXS Inc., Madison, Wisconsin, USA.
- Bruker (2010). APEX2 and SAINT. Bruker AXS Inc., Madison, Wisconsin, USA.
- Cruz Cabeza, A. J. & Groom, C. (2011). *CrystEngComm*, **13**, 93–98.
- Díaz-Gavilán, M., Conejo-García, A., Cruz-López, O., Núñez, M. C., Choquesillo-Lazarte, D., González-Pérez, J. M., Rodríguez-Serrano, F., Marchal, J. A., Aránega, A., Gallo, M. A., Espinosa, A. & Campos, J. M. (2008). *ChemMedChem*, **3**, 127–135.
- Flack, H. D. (1983). *Acta Cryst.* **A39**, 876–881.
- Ikonen, S., Valkonen, A. & Kolehmainen, E. (2009). *J. Mol. Struct.* **930**, 147–156.
- Mahapatra, S., Nayak, S. K., Prathapa, S. J. & Guru Row, T. N. (2008). *Cryst. Growth Des.* **8**, 1223–1225.
- Macrae, C. F., Bruno, I. J., Chisholm, J. A., Edgington, P. R., McCabe, P., Pidcock, E., Rodríguez-Monge, L., Taylor, R., van de Streek, J. & Wood, P. A. (2008). *J. Appl. Cryst.* **41**, 466–470.
- Nair, V. & Pal, S. (1998). Int. Patent WO 9817781.
- Rao Kode, N. & Phadtare, S. (2011). *Molecules*, **16**, 5840–5860.
- Schaefer, H. J., Beauchamp, L., de Miranda, P., Elion, G. B., Bauer, D. J. & Collins, P. (1978). *Nature (London)*, **272**, 583–585.
- Sheldrick, G. M. (2008). *Acta Cryst.* **A64**, 112–122.
- Soriano-García, M. & Parthasarathy, R. (1977). *Acta Cryst.* **B33**, 2674–2677.
- Spek, A. L. (2009). *Acta Cryst.* **D65**, 148–155.
- Trávníček, Z. & Rosenker, C. J. (2006). *Acta Cryst.* **E62**, o3393–o3395.
- Watson, D. G., Sweet, R. M. & Marsh, R. E. (1965). *Acta Cryst.* **19**, 573–580.
- Westrip, S. P. (2010). *J. Appl. Cryst.* **43**, 920–925.

7. FUTURE PERSPECTIVES

Cancer stem cells (CSCs) are a small subpopulation of cells within tumours with capabilities of self-renewal, differentiation, and tumourigenicity when transplanted into an animal host. CSCs are resistant to conventional treatment including chemo- and radiation-therapies. CSCs play important roles in cancer relapse and metastasis.²⁰⁰⁻²⁰⁶

Large experimental and clinical data indicate that conventional anti-cancer therapies cannot eradicate CSCs, and moreover, they usually increase their number leading to cancer recurrence and further drug resistance.

If CSCs are responsible for tumour development and metastasis, and are highly resistant to standard anti-cancer therapies, they are likely to be the most crucial target in the treatment of cancer. A better understanding of the relationships between CSCs and tumour angiogenesis is necessary to discover novel opportunities for targeted drug development.

Mechanisms of the CSC resistance to chemo- and radiation-therapies and potential targets for CSC-focused drug development are intensively studied, which is reflected in numerous comprehensive reviews. Failure of conventional treatment options to eliminate the CSC compartment might result in tumour relapse and, more importantly, in the proliferation of therapy-resistant and more aggressive tumour cells, which ultimately reduce patient survival. CSC resistance to conventional therapies may explain why it is difficult to completely eradicate cancer and why recurrence is often inevitable

The following newsworthy article appeared in Drug Discovery Opinion (DDO Limited-Consultancy for Biotech and Pharma), August 20th 2009.

Salinomycin 'attacks cancer stem cells'

A compound that appears to target the master cells which help breast cancers grow and spread has been discovered by US scientists.

In tests in mice, salinomycin killed breast cancer stem cells far more effectively than some existing drugs, and slowed tumour growth.

The drug, a farm antibiotic, has yet to be tested in humans, the journal *Cell* reports.

But UK experts warned a human version could be some years away.

The reasons why, even following powerful chemotherapy, some cancers can grow back, are not fully understood.

Many scientists believe a key role lies with stem cells, which can be resistant to conventional chemotherapy, remaining to 'seed' new tumours and drive their growth.

The drug's potential was identified by researchers at the Massachusetts Institute of Technology, who tested 16,000 existing chemical compounds against breast cancer stem cells in the laboratory.

Those which performed the best were then tried in mice, and compared to existing drugs such as paclitaxel.

Salinomycin appeared to be 100 times better at killing the cells in a test tube, and treated cells were much less likely to start new tumours when injected into mice.

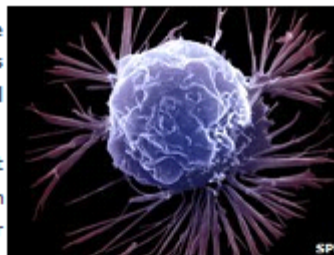
When given to mice with tumours, the growth of the cancer slowed.

However, the researchers stressed that it was too early to know if similar successes could be achieved in human cancer patients.

"Many therapies kill the bulk of a tumour only to see it regrow," said Professor Eric Lander, from MIT. "This raises the prospect of new kinds of anti-cancer therapies."

'Very early research'

Dr John Stingl, group leader in mammary stem cell biology at Cancer Research UK's Cambridge Research Institute, said: "This is one of the biggest advances we have seen this year in this area of research. These scientists have demonstrated that it's possible to selectively target the rare cancer stem cells that drive tumour growth."



Some 16,000 chemicals were tested by researchers

"This is one of the biggest advances we have seen this year in this area of research"

Dr John Stingl
Cancer Research UK Cambridge
Research Institute

The study was also published in the August 13th advance online issue of *Cell*:
'Identification of Selective Inhibitors of Cancer Stem Cells by High-Throughput Screening'. Piyush B. Gupta, Tamer T. Onder, Guozhi Jiang, Kai Tao, Charlotte Kuperwasser, Robert A. Weinberg and Eric S. Lander. *Cell*, Volume 138, Issue 4, 645-659, 13 August 2009

Four of our compounds (**MEGR 294**, **MEGR 447D**, **MEGR 451D**, and **MEGR 453D**; for reasons of patentability can not be shown structural information) present anti-proliferative activity *in vitro* against breast and colon cancer stem cells, equivalent to salinomycin, which removes stem cell cancers much more effectively than the existing drugs such as paclitaxel (Taxol[®]). The *in vivo* activity of these compounds will be tested by implanting cancer stem cells into immunocompromised nude mice, after treatment with these compounds.

8. CONCLUSIONES

Las conclusiones se expondrán de acuerdo con el orden de los artículos publicados en esta tesis. Además, tras las conclusiones químicas se describen (si fuera el caso) los resultados biológicos para facilitar la comprensión de este apartado.

1.- Durante la preparación de varios derivados de (*RS*), (*R*), (*S*)-9-(2,3-dihidro-1,4-benzoxatiin-2-ilmetil)purinas a partir de (*RS*), (*R*), (*S*)-2,3-dihidro-1,4-benzoxatiin-3-metanol y de las bases heterocíclicas 6-cloro-, 6-bromo-, y 2,6-dicloro-purinas bajo condiciones asistidas por microondas se aíslan, también, los productos de isomerización en la posición 3 del anillo de seis miembros dihidroxatiino. Formalmente, tiene lugar una migración 1,4-tio (desde el resto de 2,3-dihidro-1,4-benzoxatiin-2-ilmetilo para producir el fragmento 2,3-dihidro-1,4-benzoxatiin-3-ilmetilo) a través de dos participaciones de grupo vecino O-3 y S-3 (o S-4 más improbable) en el anillo de seis miembros, esto puede explicar, sin embargo, la complejidad de los productos de la reacción de Mitsunobu.

2.- La (*RS*)-2,6-dicloro-9-(2,3-dihidro-1,4-benzoxatiin-2-ilmetil)purina es 3,3 veces más activa como agente antiproliferativo frente a la línea celular de cáncer de mama humana MCF-7 que su correspondiente isómero en posición 3 del anillo de oxatiino, previamente publicado por nosotros. La inducción de apoptosis tras tratamiento durante 48 horas con ambos compuestos está en el mismo rango, hecho destacable porque el compuesto (*RS*)-2,6-dicloro-9-(2,3-dihidro-1,4-benzoxatiin-3-ilmetil)purina es el mayor inductor de apoptosis publicado por nuestro grupo de investigación frente a la línea de cáncer MCF-7.

3.- Los compuestos más activos tienen como objetivo molecular la inhibición de la traducción mediante fosforilación del factor eIF-2 α , e inducción de apoptosis de una manera independiente de p53.

4.- La cuestión de la quiralidad de los fármacos es actualmente un tema de investigación prioritario en el diseño y desarrollo de nuevos fármacos, estando respaldado este hecho por el papel que juega el reconocimiento molecular en muchos procesos farmacológicos importantes. Una ventaja adicional al estudiar la

química del *m*-nitrofenilsulfonato de glicidilo y de la epiclorhidrina homoquirales es que es posible manipular la estereoquímica mediante la acertada elección, tanto del nucleófilo como del sustrato. El desplazamiento nucleófilo del *m*-nitrofenilsulfonato de glicidilo tiene lugar mediante desplazamiento directo del átomo de carbono unido al grupo *m*-nitrofenilsulfonato, con lo que el estereocentro no se afecta. Sin embargo, esto no ocurre con la epiclorhidrina, en la que el resto de epóxido da lugar a un alcóxido que lleva a cabo un segundo desplazamiento sobre el átomo de carbono unido al cloro para reproducir de nuevo el anillo de tres miembros, pero con completa inversión de su configuración.

5.- Cuando se lleva a cabo la reacción de Mitsunobu entre las formas (*RS*), (*R*)- y la (*S*)-3,4-dihidro-2*H*-1,5-benzoxatiepina-3-ol y varias purinas con irradiación en microondas, se reproduce la regioselectividad observada cuando se parte del alcohol secundario (*RS*), (*R*)- y (*S*)- 3,4-dihidro-2*H*-1,5-benzoxatiepina-3-ol y además, los productos de contracción de anillo se obtienen con excelentes enantioespecificidades.

6.- Todos los compuestos homoquirales de este estudio muestran un efecto apoptótico diferente entre enantiómeros de, al menos, un 30%. En bibliografía científica están muy poco referenciadas las publicaciones de distintos porcentajes de apoptosis producidos por enantiómeros. Un caso publicado es el enantiómero D-(-)-lentiginosina, que es el enantiómero no natural del alcaloide polihidroxiado indolizidina y que actúa como inductor de apoptosis en diferentes células tumorales en contraste con su enantiómero natural.

7.- Se han establecido de manera inequívoca mediante el uso de las técnicas DEPT, HSQC y HMBC, los derivados de anillos de siete miembros 2,3,4,5-tetrahidro-1,5-benzoxazepina-3-ol, 7-metil-, y 7-*terc*-butil-2,3,4,5-tetrahidro-1,5-benzoxazepinas-3-ol, cuando en la bibliografía científica se encuentran referenciados, de forma errónea, como las estructuras isómeras de seis miembros, 3,4-dihidro-2*H*-3-hidroximetil-1,4-benzoxazina, 6-metil-, y 6- *terc*-butil-3,4-dihidro-2*H*-3-hidroximetil-1,4-benzoxazinas.

8.- Se ha mejorado el método sintético de 2,3,4,5-tetrahidro-1,5-benzoxazepina-3-ol y de 3,4-dihidro-2*H*-3-hidroxiometil-1,4-benzoxazina, en una reacción de un solo paso entre el *o*-aminofenol y la epíclorohidrina, bajo irradiación en microondas, cuando el método publicado anteriormente implicaba tres pasos de reacción.

9.- Cuando la 2,3,4,5-tetrahidro-1,5-benzoxazepina-3-ol se hace reaccionar bajo las condiciones de Mitsunobu con diversas purinas sustituidas, los productos de reacción son los anillos de seis miembros, 3,4-dihidro-2*H*-3-hidroxiometil-1,4-benzoxazinas unidas al átomo de nitrógeno 9 de la purina, a través de un grupo metilénico, tal como se demuestra mediante la interpretación de los datos de RMN bidimensionales. La contracción del anillo de siete al de seis miembros se puede justificar a través de la formación de un ión aziridinio.

10.- Se han preparado quince nuevos compuestos por reacción de Mitsunobu entre la (*R*)-, (*S*), y la (*RS*)-3,4-dihidro-2*H*-1,5-benzoxatíepinas-3-ol y varias adeninas sustituidas por irradiación en microondas. Los lugares de alquilación se han determinado mediante técnicas de RMN bidimensionales y en tres compuestos, se han confirmado mediante cristalografía de rayos X. La regioselectividad *N*'-9/*N*'-3 se puede justificar fundamentalmente por medio de los efectos electrónicos de los sustituyentes en posiciones 2 y 6 del anillo de purina.

11.- Cuatro de nuestros compuestos (MEGR 294, MEGR 447D, MEGR 451D, MEGR 453D) presentan una actividad antiproliferativa *in vitro* frente a células madre cancerosas de colon y mama equivalente a la de la salinomicina, que elimina las células madre de ambos tipos de cáncer de manera mucho más eficaz que algunos fármacos ya existentes y además, desacelera el crecimiento del tumor. La actividad *in vivo* de los compuestos será ensayada frente a ratones desnudos inmuno-deprimidos, a los que se les implantará células madre cancerosas.

9. REFERENCES

1. 'The global burden of disease: 2004 update'; World Health Organization: **2008**. 144(5):646-674.
2. Hanahan, D.; Weinberg, R. A., 'Hallmarks of cancer: the next generation'. *Cell*, **2011**;
3. Abegunde, D. O.; Mathers, C. D.; Adam, T.; Ortegon, M., et al., 'The burden and costs of chronic diseases in low-income and middle-income countries'. *Lancet*, **2007**; 370(9603):1929-1938.
4. 'World Health Statistics 2010'; World Health Organization: **2010**.
5. 'GLOBOCAN 2008. Cancer Incidence and Mortality Worldwide.'. IARC, **2010**, Available from: <http://globocan.iarc.fr>.
6. Ferlay, J.; Parkin, D. M.; Steliarova-Foucher, E., 'Estimates of cancer incidence and mortality in Europe in 2008'. *Eur J Cancer*, **2010**; 46(4):765-781.
7. Mackay, J. J.; Lee, N. C.; Parkin, D. M., 'The Cancer Atlas'. 1st ed.; American Cancer Society, **2006**.
8. Giancotti, F. G.; Ruoslahti, E., 'Integrin signaling'. *Science*, **1999**; 285(5430):1028-1032.
9. Available at: <http://www.dkfz.de/>. German Cancer Research Center. (Access: 2009).
10. Lodish, H., Berk, A., Zipursky, S. L., Matsudaira, P., Baltimore, D., Darnell, J., 'Overview of the Cell Cycle and Its Control'. In: *Molecular Cell Biology*, 4th ed.; Freeman, W. H., Ed. W. H. Freeman and Company, New York, **2000**.
11. Malumbres, M.; Barbacid, M., 'Mammalian cyclin-dependent kinases'. *Trends Biochem Sci*, **2005**; 30(11):630-641.
12. Sherr, C. J.; Roberts, J. M., 'CDK inhibitors: positive and negative regulators of G1-phase progression'. *Genes Dev*, **1999**; 13(12):1501-1512.
13. Senderowicz, A. M., 'Small-molecule cyclin-dependent kinase modulators'. *Oncogene*, **2003**; 22(42):6609-6620.
14. Singhal, S.; Vachani, A.; Antin-Ozerkis, D.; Kaiser, L. R., 'Prognostic implications of cell cycle, apoptosis, and angiogenesis biomarkers in non-small cell lung cancer: a review'. *Clin Cancer Res*, **2005**; 11(11):3974-3986.
15. Vidal, A.; Koff, A., 'Cell-cycle inhibitors: three families united by a common cause'. *Gene*, **2000**; 247(1-2):1-15.
16. Eymin, B., Gazzeri, S., 'Role of cell cycle regulators in lung carcinogenesis'. *Cell Adh Migr*, **2010**; 4(1):114-123.

REFERENCES

17. Burkhardt, D. L.; Sage, J., 'Cellular mechanisms of tumour suppression by the retinoblastoma gene'. *Nat Rev Cancer*, **2008**; 8(9):671-682.
18. Weinberg, R. A., 'The retinoblastoma protein and cell cycle control'. *Cell*, **1995**; 81(3):323- 330.
19. Malumbres, M.; Barbacid, M., 'To cycle or not to cycle: a critical decision in cancer'. *Nat Rev Cancer*, **2001**; 1(3):222-231.
20. Smith, E. J.; Leone, G.; DeGregori, J.; Jakoi, L., 'The accumulation of an E2F-p130 transcriptional repressor distinguishes a G0 cell state from a G1 cell state'. *Mol Cell Biol*, **1996**; 16(12):6965-6976.
21. Balciunaite, E.; Spektor, A.; Lents, N. H.; Cam, H., 'Pocket protein complexes are recruited to distinct targets in quiescent and proliferating cells'. *Mol Cell Biol*, **2005**; 25(18):8166- 8178.
22. Riley, D. J.; Lee, E. Y.; Lee, W. H., 'The retinoblastoma protein: more than a tumor suppressor'. *Annu Rev Cell Biol*, **1994**; 10:1-29.
23. Harbour, J. W.; Luo, R. X.; Dei Santi, A.; Postigo, A. A., 'Cdk phosphorylation triggers sequential intramolecular interactions that progressively block Rb functions as cells move through G1'. *Cell*, **1999**; 98(6):859-869.
24. Zhang, H. S.; Postigo, A. A.; Dean, D. C., 'Active transcriptional repression by the Rb-E2F complex mediates G1 arrest triggered by p16INK4a, TGFbeta, and contact inhibition'. *Cell*, **1999**; 97(1):53-61.
25. Lundberg, A. S.; Weinberg, R. A., 'Functional inactivation of the retinoblastoma protein requires sequential modification by at least two distinct cyclin-cdk complexes'. *Mol Cell Biol*, **1998**; 18(2):753-761.
26. Blain, S. W.; Montalvo, E.; Massague, J., 'Differential interaction of the cyclin-dependent kinase (Cdk) inhibitor p27Kip1 with cyclin A-Cdk2 and cyclin D2-Cdk4'. *J Biol Chem*, **1997**; 272(41):25863-25872.
27. Cheng, M.; Olivier, P.; Diehl, J. A.; Fero, M., 'The p21(Cip1) and p27(Kip1) CDK 'inhibitors' are essential activators of cyclin D-dependent kinases in murine fibroblasts'. *EMBO J*, **1999**; 18(6):1571-1583.
28. Malumbres, M.; Barbacid, M., 'Cell cycle, CDKs and cancer: a changing paradigm'. *Nat Rev Cancer*, **2009**; 9(3):153-166.
29. Sherr, C. J., 'G1 phase progression: cycling on cue'. *Cell*, **1994**; 79(4):551-555.
30. McDonald, E. R.; El-Deiry, W. S., 'Cell cycle control as a basis for cancer drug development'. *Int J Oncol*, **2000**; 16(5):871-886.
31. Vermeulen, K.; Van Bockstaele, D. R.; Berneman, Z. N., 'The cell cycle: a review of

- regulation, deregulation and therapeutic targets in cancer'. *Cell Prolif*, **2003**; 36(3):131-149.
32. Shapiro, G. I., 'Cyclin-Dependent Kinase Pathways As Targets for Cancer Treatment'. *J Clin Oncol*, **2006**; 24(11):1770-1783.
33. Senderowicz, A. M.; Sausville, E. A., 'Preclinical and clinical development of cyclindependent kinase modulators'. *J Natl Cancer Inst*, **2000**; 92(5):376-387.
34. Abend, M., 'Reasons to reconsider the significance of apoptosis for cancer therapy'. *Int J Radiat Biol*, **2003**; 79(12):927-941.
35. Okada, H.; Mak, T. W., 'Pathways of apoptotic and non-apoptotic death in tumour cells'. *Nat Rev Cancer*, **2004**; 4(8):592-603.
36. Zong, W. X.; Ditsworth, D.; Bauer, D. E.; Wang, Z. Q., 'Alkylating DNA damage stimulates a regulated form of necrotic cell death'. *Genes Dev.*, **2004**; 18:1272-1282.
37. Chan, T. A.; Hermeking, H.; Lengauer, C.; Kinzler, K. W., '14-3-3 σ is required to prevent mitotic catastrophe after DNA damage'. *Nature*, **1999**; 401(6753):616-620.
38. Chu, K.; Teele, N.; Dewey, M. W.; Albright, N., 'Computerized video time lapse study of cell cycle delay and arrest, mitotic catastrophe, apoptosis and clonogenic survival in irradiated 14-3-3[σ] and CDKN1A (p21) knockout cell lines'. *Radiat Res*, **2004**; 162:270-286.
39. Brown, J. M.; Attardi, L. D., 'The role of apoptosis in cancer development and treatment response'. *Nat Rev Cancer*, **2005**; 5(3):231-237.
40. Vitale, I.; Galluzzi, L.; Castedo, M.; Kroemer, G., 'Mitotic catastrophe: a mechanism for avoiding genomic instability'. *Nat Rev Mol Cell Biol*, **2011**; 12(6):385-392.
41. Rikiishi, H., 'Autophagic and apoptotic effects of HDAC inhibitors on cancer cells'. *J Biomed Biotechnol*, **2011**; 2011:830260.
42. Thompson, C. B., 'Apoptosis in the pathogenesis and treatment of disease'. *Science*, **1995**; 267:1456-1462.
43. Danial, N. N.; Korsmeyer, S. J., 'Cell death: critical control points'. *Cell*, **2004**; 116:205-219.
44. Fesik, S. W., 'Promoting apoptosis as a strategy for cancer drug discovery'. *Nat Rev Cancer*, **2005**; 5(11):876-885.
45. Nicholson, D. W., 'From bench to clinic with apoptosis-based therapeutic agents'. *Nature*, **2000**; 407:810-816.
46. Deveraux, Q. L.; Takahashi, R.; Salvesen, G. S.; Reed, J. C., 'X-linked IAP is a direct inhibitor of cell-death proteases'. *Nature*, **1997**; 388:300-304.

REFERENCES

47. Budihardjo, I.; Oliver, H.; Lutter, M.; Luo, X., 'Biochemical pathways of caspase activation during apoptosis'. *Annu Rev Cell Dev Biol*, **1999**; 15:269-290.
48. Baell, J. B.; Huang, D. C. S., 'Prospects for targeting the Bcl-2 family of proteins to develop novel cytotoxic drugs'. *Biochem. Pharmacol.*, **2002**; 64:851-863.
49. Du, C.; Fang, M.; Li, Y.; Li, L., 'Smac, a mitochondrial protein that promotes cytochrome c-dependent caspase activation by eliminating IAP inhibition'. *Cell*, **2000**; 102:33-42.
50. Verhagen, A. M., 'Identification of DIABLO, a mammalian protein that promotes apoptosis by binding to and antagonizing IAP proteins'. *Cell*, **2000**; 102:43-53.
51. Chene, P., 'Inhibiting the p53-MDM2 interaction: an important target for cancer therapy'. *Nature Rev Cancer*, **2003**; 3:102-109.
52. Pain, V. M., Initiation of protein synthesis in eukaryotic cells. *Eur. J. Biochem*, **1996**, 236:747-771.
53. Welsh, G. I.; Price, N. T.; Bladergroen, B. A.; Bloomberg, G.; Proud, C. G., Identification of novel phosphorylation sites in the β -subunit of translation initiation factor eIF-2. *Biochem. Biophys. Res. Commun.*, **1994**, 201:1279-1288.
54. Chakrabarti, A.; Maitra, U., Function of eukaryotic initiation factor 5 in the formation of an 80 S ribosomal polypeptide chain initiation complex. *J. Biol. Chem.*, **1991**, 266:14036-14045.
55. Webb, B. L. J.; Proud, C. G., 'Eukaryotic initiation factor 2B (eIF2B)'. *Int. J. Biochem. Cell Biol.*, **1997**, 29:1127-1131.
56. Hershey, J. W. B.; Merrick, W. C., 'Translational Control of Gene Expression' (Sonenberg, N.; Hershey, J. W. B.; Mathews, M.; eds), **2000**, 33-88.
57. Kimball, S. R.; Heinzinger, N. K.; Horetsky, R. L.; Jefferson, L. S., 'Identification of interprotein interactions between the subunits of eukaryotic initiation factors eIF2 and eIF2B'. *J. Biol. Chem.*, **1998**, 273:3039-3044.
58. Clemens V.; Elia, A., 'The double-stranded RNA-dependent protein kinase PKR: structure and function'. *J. Interf. Cytokine Res.*, **1997**, 17:503-524.
59. Siemann, D. W., 'Vascular targeting agents'. In: *Horizons in Cancer Therapeutics: From Bench to Bedside*, Meniscus, **2002**; vol. 3(2):4-15.
60. Cox, G.; Jones, J. L.; Walker, R. A.; Steward, W. P., 'Angiogenesis and non-small cell lung cancer'. *Lung Cancer*, **2000**; 27(2):81-100.
61. Folkman, J., 'Role of angiogenesis in tumor growth and metastasis'. *Semin Oncol*, **2002**; 29(6 Suppl 16):15-18.

62. Folkman, J., 'Angiogenesis: an organizing principle for drug discovery?'. *Nat Rev Drug Discov*, **2007**; 6(4):273-286.
63. Nguyen, D. X.; Bos, P. D.; Massague, J., 'Metastasis: from dissemination to organ-specific colonization'. *Nat Rev Cancer*, **2009**; 9(4):274-284.
64. Chambers, A. F.; Groom, A. C.; MacDonald, I. C., 'Dissemination and growth of cancer cells in metastatic sites'. *Nature Rev. Cancer*, **2002**; 2:563-572.
65. Mehlen, P.; Puisieux, A., 'Metastasis: a question of life or death'. *Nature Rev. Cancer*, **2006**; 6:449-458.
66. Kim, J. W., 'Rapid apoptosis in the pulmonary vasculature distinguishes non-metastatic from metastatic melanoma cells'. *Cancer Lett.*, **2004**; 213:203-212.
67. MacDonald, I. C.; Groom, A. C.; Chambers, A. F., 'Cancer spread and micrometastasis development: quantitative approaches for in vivo models'. *Bioessays*, **2002**; 24:885-893.
68. Husemann, Y., 'Systemic spread is an early step in breast cancer'. *Cancer Cell*, **2008**; 13:58-68.
69. Joyce, J. A.; Pollard, J. W., 'Microenvironmental regulation of metastasis'. *Nat Rev Cancer*, **2009**; 9(4):239-252.
70. Cameron, M. D., 'Temporal progression of metastasis in lung: cell survival, dormancy, and location dependence of metastatic inefficiency'. *Cancer Res.*, **2000**; 60:2541-2546.
71. Engel, J., 'The process of metastatisation for breast cancer'. *Eur. J. Cancer*, **2003**; 39:1794- 1806.
72. Goodison, S., 'Prolonged dormancy and site-specific growth potential of cancer cells spontaneously disseminated from nonmetastatic breast tumors as revealed by labeling with green fluorescent protein'. *Clin. Cancer Res.*, **2003**; 9:3808-3814.
73. Brackstone, M.; Townson, J. L.; Chambers, A. F., 'Tumour dormancy in breast cancer: an update'. *Breast Cancer Res.*, **2007**; 9:208.
74. Suzuki, M.; Mose, E. S.; Montel, V.; Tarin, D., 'Dormant cancer cells retrieved from metastasis-free organs regain tumorigenic and metastatic potency'. *Am. J. Pathol.*, **2006**; 169:673- 681.
75. Aguirre-Ghiso, J. A., 'Models, mechanisms and clinical evidence for cancer dormancy'. *Nature Rev. Cancer*, **2007**; 7:834-846.
76. Holmgren, L.; O'Reilly, M. S.; Folkman, J., 'Dormancy of micrometastases: balanced proliferation and apoptosis in the presence of angiogenesis suppression'. *Nature Med.*, **1995**; 1:149-153.

REFERENCES

77. Sebolt-Leopold, J. S.; English, J. M., 'Mechanisms of drug inhibition of signalling molecules'. *Nature*, **2006**; 441(7092):457-462.
78. Lewis, T. S.; Shapiro, P. S.; Ahn, N. G., 'Signal Transduction through MAP Kinase Cascades'. In: *Advances in Cancer Research*, George, F. V. W.; George, K., Eds. Academic Press, **1998**; vol. 74:49-139.
79. Meloche, S.; Pouyssegur, J., 'The ERK1/2 mitogen-activated protein kinase pathway as a master regulator of the G1- to S-phase transition'. *Oncogene*, **2007**; 26(22):3227-3239.
80. Neidle, S., 'Cancer Drug Design and Discovery'. Elsevier, **2007**.
81. Cantley, L. C., 'The phosphoinositide 3-kinase pathway'. *Science*, **2002**; 296(5573):1655-1657.
82. Vivanco, I.; Sawyers, C. L., 'The phosphatidylinositol 3-Kinase AKT pathway in human cancer'. *Nat Rev Cancer*, **2002**; 2(7):489-501.
83. Sabatini, D. M., 'mTOR and cancer: insights into a complex relationship'. *Nat Rev Cancer*, **2006**; 6(9):729-734.
84. Keniry, M.; Parsons, R., 'The role of PTEN signaling perturbations in cancer and in targeted therapy'. *Oncogene*, **2008**; 27(41):5477-5485.
85. Duronio, V., 'The life of a cell: apoptosis regulation by the PI3K/PKB pathway'. *Biochem J*, **2008**; 415(3):333-344.
86. Heinrich, M. C.; Corless, C. L.; Duensing, A.; McGreevey, L., 'PDGFRA activating mutations in gastrointestinal stromal tumors'. *Science*, **2003**; 299(5607):708-710.
87. Rubin, B. P.; Singer, S.; Tsao, C.; Duensing, A., 'KIT activation is a ubiquitous feature of gastrointestinal stromal tumors'. *Cancer Res*, **2001**; 61(22):8118-8121.
88. Sordella, R.; Bell, D. W.; Haber, D. A.; Settleman, J., 'Gefitinib-sensitizing EGFR mutations in lung cancer activate anti-apoptotic pathways'. *Science*, **2004**; 305(5687):1163-1167.
89. Schreck, R.; Rapp, U. R., 'Raf kinases: oncogenesis and drug discovery'. *Int J Cancer*, **2006**; 119(10):2261-2271.
90. Schubbert, S.; Shannon, K.; Bollag, G., 'Hyperactive Ras in developmental disorders and cancer'. *Nat Rev Cancer*, **2007**; 7(4):295-308.
91. Vakiani, E.; Solit, D. B., 'KRAS and BRAF: drug targets and predictive biomarkers'. *J Pathol*, **2011**; 223(2):220-230.
92. Cully, M.; You, H.; Levine, A. J.; Mak, T. W., 'Beyond PTEN mutations: the PI3K pathway as an integrator of multiple inputs during tumorigenesis'. *Nat Rev Cancer*, **2006**; 6(3):184-192.

93. Roberts, P. J.; Der, C. J., 'Targeting the Raf-MEK-ERK mitogen-activated protein kinase cascade for the treatment of cancer'. *Oncogene*, **2007**; 26(22):3291-3310.
94. Porta, C.; Figlin, R. A., 'Phosphatidylinositol-3-Kinase/Akt Signaling Pathway and Kidney Cancer, and the Therapeutic Potential of Phosphatidylinositol-3-Kinase/Akt Inhibitors'. *J Urology*, **2009**; 182(6):2569-2577.
95. Arslan, M. A.; Kutuk, O.; Basaga, H., 'Protein kinases as drug targets in cancer'. *Curr Cancer Drug Targets*, **2006**; 6(7):623-634.
96. Fabbro, D.; Ruetz, S.; Buchdunger, E.; Cowan-Jacob, S. W., 'Protein kinases as targets for anticancer agents: from inhibitors to useful drugs'. *Pharmacol Ther*, **2002**; 93(2-3):79-98.
97. Fabbro, D.; Parkinson, D.; Matter, A., 'Protein tyrosine kinase inhibitors: new treatment modalities?'. *Curr Opin Pharmacol*, **2002**; 2(4):374-381.
98. Hunter, T., 'Tyrosine phosphorylation: thirty years and counting'. *Curr Opin Cell Biol*, **2009**; 21(2):140-146.
99. Blume-Jensen, P.; Hunter, T., 'Oncogenic kinase signalling'. *Nature*, **2001**; 411(6835):355-365.
100. Grant, S. K., 'Therapeutic protein kinase inhibitors'. *Cell Mol Life Sci*, **2009**; 66(7):1163-1177.
101. Etzioni, R.; Urban, N.; Ramsey, S.; McIntosh, M., 'The case for early detection'. *Nat Rev Cancer*, **2003**; 3(4):243-252.
102. Veenstra, T. D.; Prieto, D. A.; Conrads, T. P., 'Proteomic patterns for early cancer detection'. *Drug Discov Today*, **2004**; 9(20):889-897.
103. Frank, R.; Hargreaves, R., 'Clinical biomarkers in drug discovery and development'. *Nat Rev Drug Discov*, **2003**; 2(7):566-580.
104. Montagut, C.; Sharma, S. V.; Shioda, T.; McDermott, U., 'Elevated CRAF as a Potential Mechanism of Acquired Resistance to BRAF Inhibition in Melanoma'. *Cancer Res*, **2008**; 68(12):4853-4861.
105. McCormick, F., 'Cancer therapy based on oncogene addiction'. *J Surg Oncol*, **2011**; 103(6):464-467.
106. Klein, S.; McCormick, F.; Levitzki, A., 'Killing time for cancer cells'. *Nat Rev Cancer*, **2005**; 5(7):573-580.
107. Mahdavi, A.; Davey, R. E.; Bhola, P.; Yin, T., 'Sensitivity Analysis of Intracellular Signaling Pathway Kinetics Predicts Targets for Stem Cell Fate Control'. *PLoS Comput Biol*, **2007**; 3(7):e130.

REFERENCES

108. Eyles, J.; Puaux, A. L.; Wang, X.; Toh, B., 'Tumor cells disseminate early, but immunosurveillance limits metastatic outgrowth, in a mouse model of melanoma'. *J Clin Invest*, **2010**; 120(6):2030-2039.
109. Chaffer, C. L.; Weinberg, R. A., 'A Perspective on Cancer Cell Metastasis'. *Science*, **2011**; 331(6024):1559-1564.
110. Higashi, T.; Tsukada, J.; Kato, C.; Iwashige, A., 'Imatinib mesylate-sensitive blast crisis immediately after discontinuation of imatinib mesylate therapy in chronic myelogenous leukemia: report of two cases'. *Am J Hematol*, **2004**; 76(3):275-278.
111. Cortés, J.; O'Brien, S.; Kantarjian, H., 'Discontinuation of imatinib therapy after achieving a molecular response'. *Blood*, **2004**; 104(7):2204-2205.
112. Bonnet, D.; Dick, J. E., 'Human acute myeloid leukemia is organized as a hierarchy that originates from a primitive hematopoietic cell'. *Nat Med*, **1997**; 3(7):730-737.
113. Reya, T.; Morrison, S. J.; Clarke, M. F.; Weissman, I. L., 'Stem cells, cancer, and cancer stem cells'. *Nature*, **2001**; 414(6859):105-111.
114. Clarke, M. F.; Dick, J. E.; Dirks, P. B.; Eaves, C. J., 'Cancer stem cells—perspectives on current status and future directions: AACR Workshop on cancer stem cells'. *Cancer Res*, **2006**; 66(19):9339-9344.
115. Warner, J. K.; Wang, J. C.; Hope, K. J.; Jin, L., 'Concepts of human leukemic development'. *Oncogene*, **2004**; 23(43):7164-7177.
116. Miyamoto, T.; Weissman, I. L.; Akashi, K., 'AML1/ETO-expressing nonleukemic stem cells in acute myelogenous leukemia with 8;21 chromosomal translocation'. *Proc Natl Acad Sci USA*, **2000**; 97(13):7521-7526.
117. Al-Hajj, M.; Wicha, M. S.; Benito-Hernandez, A.; Morrison, S. J., 'Prospective identification of tumorigenic breast cancer cells'. *Proc Natl Acad Sci USA*, **2003**; 100(7):3983-3988.
118. Singh, S. K.; Hawkins, C.; Clarke, I. D.; Squire, J. A., 'Identification of human brain tumour initiating cells'. *Nature*, **2004**; 432(7015):396-401.
119. Bao, S.; Wu, Q.; Sathornsumetee, S.; Hao, Y., 'Stem cell-like glioma cells promote tumor angiogenesis through vascular endothelial growth factor'. *Cancer Res*, **2006**; 66(16):7843-7848.
120. Beier, D.; Hau, P.; Proescholdt, M.; Lohmeier, A., 'CD133(+) and CD133(-) glioblastoma-derived cancer stem cells show differential growth characteristics and molecular profiles'. *Cancer Res*, **2007**; 67(9):4010-4015.
121. Taylor, M. D.; Poppleton, H.; Fuller, C.; Su, X., 'Radial glia cells are candidate stem cells of ependymoma'. *Cancer Cell*, **2005**; 8(4):323-335.
122. Bao, S.; Wu, Q.; McLendon, R. E.; Hao, Y., 'Glioma stem cells promote

- radioresistance by preferential activation of the DNA damage response'. *Nature*, **2006**; 444(7120):756-760.
123. Piccirillo, S. G.; Reynolds, B. A.; Zanetti, N.; Lamorte, G., 'Bone morphogenetic proteins inhibit the tumorigenic potential of human brain tumour-initiating cells'. *Nature*, **2006**; 444(7120):761-765.
124. O'Brien, C. A.; Pollett, A.; Gallinger, S.; Dick, J. E., 'A human colon cancer cell capable of initiating tumour growth in immunodeficient mice'. *Nature*, **2007**; 445(7123):106-110.
125. Ricci-Vitiani, L.; Lombardi, D. G.; Pilozzi, E.; Biffoni, M., 'Identification and expansion of human colon-cancer-initiating cells'. *Nature*, **2007**; 445(7123):111-115.
126. Hermann, P. C.; Huber, S. L.; Herrler, T.; Aicher, A., 'Distinct populations of cancer stem cells determine tumor growth and metastatic activity in human pancreatic cancer'. *Cell Stem Cell*, **2007**; 1(3):313-323.
127. Barabe, F.; Kennedy, J. A.; Hope, K. J.; Dick, J. E., 'Modeling the initiation and progression of human acute leukemia in mice'. *Science*, **2007**; 316(5824):600-604.
128. Visvader, J. E.; Lindeman, G. J., 'Cancer stem cells in solid tumours: accumulating evidence and unresolved questions'. *Nat Rev Cancer*, **2008**; 8(10):755-768.
129. Hope, K. J.; Jin, L.; Dick, J. E., 'Acute myeloid leukemia originates from a hierarchy of leukemic stem cell classes that differ in self-renewal capacity'. *Nat Immunol*, **2004**; 5(7):738-743.
130. Lipinski, C. A.; Lombardo, F.; Dominy, B. W.; Feeney, P. J., 'Experimental and computational approaches to estimate solubility and permeability in drug discovery and development settings'. *Adv Drug Deliv Rev*, **2001**; 46(1-3):3-26.
131. Lipinski, C.; Hopkins, A., 'Navigating chemical space for biology and medicine'. *Nature*, **2004**; 432(7019):855-861.
132. Sausville, E. A.; Burger, A. M., 'Contributions of human tumor xenografts to anticancer drug development'. *Cancer Res*, **2006**; 66(7):3351-3354.
133. Cahn, R. S.; Ingold, C. K.; Prelog, V., 'Specification of Molecular Chirality'. *Angewandte Chemie International Edition*. **1966**; 5 (4):385-415.
134. Mc Creary, M. D.; Lewis, D.W.; Wernick, D. L.; Whitesides, G. M., 'Determination of Enantiomeric Purity Using Chiral Lanthanide Shift Reagents'. *J. Am. Chem. Soc.* **1974**; 96, 1038.
135. Buchwald, S. L.; Anslyn, E. V.; Grubbs, R. H., 'Reaction of Dicyclopentadienylmethylenetitanium with Organic Halides: Evidence for a Radical Mechanism'. *J. Am. Chem. Soc.* **1985**; 107, 1766.

REFERENCES

136. Easson, L. H.; Stedman, E., 'Studies on the relationship between chemical constitution and physiological action. V. Molecular dissymmetry and physiological activity'. *Biochem. J.* **1933**, 27, 1257-1266.
137. Harris, J. R.; Lippman, M. E.; Morrow, M.; Hellman, S., 'Diseases of the Breast' (first edition). **1996**, New York: Lippincott-Raven.
138. Hickman, J. A., 'Apoptosis induced by anticancer drugs'. *Cancer Metastasis Rev*, **1992**; 11(2):121-139.
139. Rasbridge, S. A.; Seymour, A. M.; Patel, K.; Richards, M. A.; Rubens, R. D.; Mills, R. R., 'The effects of chemotherapy on morphology, cellular proliferation, apoptosis and oncoprotein expression in primary breast carcinoma'. *Br J Cancer*, **1994**; 70(2):335-341.
140. Lundberg, A. S.; Weinberg, R. A., 'Control of the cell cycle and apoptosis'. *European Journal of Cancer*, **1998**; 35(4):531.
141. Qin, L. F.; Ng, I. O., 'Induction of apoptosis by cisplatin and its effect on cell cycle-related proteins and cell cycle changes in hepatoma cells'. *Cancer Lett*, **2002**; 175(1):27-38.
142. Matsuo, S.; Tanako, S.; Yamashita, J.; Ogawa, M., 'Synergistic cytotoxic effects of tumor necrosis factor, interferon- γ and tamoxifen on breast cancer cell lines'. *Anticancer Research*, **2000**; 12(5):1575-1579.
143. Trouet, A.; Passioukov, A.; Derpooten, K. V.; Fernández, A. M.; Abarca-Quiñones, J.; Baurain, R.; Lobl, T. J.; Olilla, C.; Dubois, V., 'Extracellularly tumor-activated prodrugs for the selective chemotherapy of cancer: application to doxorubicin and preliminary in vitro and in vivo studies'. *Cancer Res*, **2001**; 61(7):2843-2846.
144. Campos, J.; Pineda, M. J.; Gómez, J. A.; Entrena, A.; Trujillo, M. A.; Gallo, M. A.; Espinosa, A., '5-Fluorouracil Derivatives. 1. Acyclonucleosides through a Tin (IV) Chloride-Mediated Regiospecific Ring Opening of Alkoxy-1,4-Diheteroepanes'. *Tetrahedron*, **1996**; 52(26):8907-8924.
145. Campos, J.; Gómez, J. A.; Trujillo, M. A.; Gallo, M. A.; Espinosa, A., 'Diheterocyclanes as Synthons for the Preparation of Novel Series of Nucleoside and Acyclonucleoside Analogues'. *Il Farmaco*, **1997**; 52(5):263-269.
146. Saniger, E.; Campos, J. M.; Entrena, A.; Marchal, J. A.; Boulaiz, H.; Aranega, A.; Gallo, M. A.; Espinosa, A., 'Medium Benzene-fused Oxacycles with the 5-Fluorouracil Moiety: Synthesis, Antiproliferative Activities and Apoptosis Induction in Breast Cancer Cells'. *Tetrahedron*, **2003**; 59(29):5457-5467.
147. Marchal, J. A.; Marchal, J. A.; Nuñez, M. C.; Suarez, I.; Diaz-Gavilan, M.; Gomez-Vidal, J. A.; Boulaiz, H.; Rodriguez-Serrano, F.; Gallo, M. A.; Espinosa, A.; Aranega, A.; Campos, J. M., 'A synthetic uracil derivative with antitumor activity through decreasing cyclin D1 and Cdk1, and increasing p21 and p27 in MCF-7 cells'. *Breast Cancer Res Treat.*, **2007**; 105(3): p. 237-246.

148. Saniger, E.; Campos, J. M.; Entrena, A.; Marchal, J. A.; Boulaiz, H.; Aránega, A.; Gallo, M. A.; Espinosa, A., 'Neighbouring Group Participation as the Key Step in the Reactivity of Acyclic and Cyclic Salicyl-Derived O,O-Acetals with 5-Fluorouracil. Antiproliferative Activity, Cell Cycle Dysregulation and Apoptotic Induction of New O,N-Acetals against Breast Cancer Cells'. *Tetrahedron*, **2003**; 59(40):8017-8026.
149. Rekker, R. F.; Kort, H. M., 'The hydrophobic fragmental constant; an extension to a 1000 data point set'. **1979**; 14(6):479-488.
150. Campos, J.; Núñez, M. C.; Rodríguez, V.; Gallo, M. A.; Espinosa, A., 'QSAR of 1,1'-(1,2-Ethylenebisbenzyl)bis(4-substitutedpyridinium) Dibromides as Choline Kinase Inhibitors: a Different Approach for Antiproliferative Drug Design'. *Bioorganic & Medicinal Chemistry Letters*, **2000**; 10(8):767-770.
151. Chadderton, A.; Villeneuve, D. J.; Gluck, S.; Kirwan-Rhude, A. F.; Gannon, B. R.; Blais, D. E.; Parissenti, A. M., 'Role of specific apoptotic pathways in the restoration of paclitaxel-induced apoptosis by valspodar in doxorubicin-resistant MCF-7 breast cancer cells'. *Breast Cancer Res Treat*, **2000**; 59(3):231-244.
152. Buur, A.; Bundgaard, H.; Falch, E., 'Prodrugs as drug delivery systems. Part 37. Prodrugs of 5-fluorouracil. Hydrolysis kinetics, bioactivation and physicochemical properties of various N-acyloxymethyl derivatives of 5- fluorouracil'. *International Journal of Pharmaceutics*, **1985**; 24(1):43-60.
153. Gulyaeva, N.; Zaslavsky, A.; Lechner, P.; Chlenov, M.; McConnell, O.; Chait, A.; Kipnis, V.; Zaslavsky, B., 'Relative hydrophobicity and lipophilicity of drugs measured by aqueous two-phase partitioning, octanol-buffer partitioning and HPLC. A simple model for predicting blood-brain distribution'. *European Journal of Medicinal Chemistry*, **2003**; 38(4):391-396.
154. Meyn, R. E.; Stephens, L. C.; Hunter, N. R.; Milas, L., 'Kinetics of cisplatin-induced apoptosis in murine mammary and ovarian adenocarcinomas'. *International Journal of Cancer*, **1995**; 60(5):725-729.
155. Milas, L.; Hunter, N. R.; Kurdoglu, B.; Mason, K. A.; Meyn, R. E.; Stephens, L. C.; Peters, L., 'Kinetics of mitotic arrest and apoptosis in murine mammary and ovarian tumors treated with taxol'. *Cancer Chemother Pharmacol*, **1995**; 35(4):297-303.
156. Saunders, D. E.; Lawrence, W. D.; Christensen, C.; Wappler, N. L.; Ruan, H.; Deppe, G., 'Paclitaxel-induced apoptosis in MCF-7 breast-cancer cells'. *International Journal of Cancer*, **1997**; 70,(2):214-220.
157. Sampath, D.; W. Plunkett., 'Design of new anticancer therapies targeting cell cycle checkpoint pathways'. *Curr Opin Oncol*, **2001**; 13(6):484-490.
158. Gali-Muhtasib, H.B.; Bakkar, N., 'Modulating cell cycle: current applications and prospects for future drug development'. 'Current Cancer Drug Targets', **2002**; 2(4):309-336.

REFERENCES

159. Stacey, D.W., 'Cyclin D1 serves as a cell cycle regulatory switch in actively proliferating cells'. *Curr Opin Cell Biol*, **2003**; 15(2):158-163.
160. Sherr, C.J., 'The Pezcoller lecture: cancer cell cycles revisited'. *Cancer Res*, **2000**; 60(14):3689-3695.
161. Sherr, C.J., 'Mammalian G1 cyclins. *Cell*', **1993**; 73(6):1059-1065.
162. Lees, E. M.; Harlow, E., 'Sequences within the conserved cyclin box of human cyclin A are sufficient for binding to and activation of cdc2 kinase. *Molecular and Cellular Biology*', **1993**; 13(2):1194-1201.
163. Shi, L; Nishioka, W. K.; Th'ng, J.; Bradbury, E. M.; Litchfield, D. W.; Greenberg, A. H., 'Premature p34cdc2 activation required for apoptosis'. *Science*, **1994**; 263(5150):1143-1145.
164. Agarwal, M. L.; Agarwal, A.; Taylor, W. R.; Stark, G. R., 'p53 controls both the G2/M and the G1 cell cycle checkpoints and mediates reversible growth arrest in human fibroblasts'. *Proc Natl Acad Sci U S A*, **1995**; 92(18):8493-8497.
165. Reed, J.C., 'Double identity for proteins of the Bcl-2 family'. *Nature*, **1997**; 387(6635):773-776.
166. Conejo-García, A.; Núñez, M. C.; Marchal, J. A.; Rodríguez-Serrano, F.; Aránega, A.; Gallo, M. A.; Espinosa, A.; Campos, J. M., 'Regiospecific microwave-assisted synthesis and cytotoxic activity against human breast cancer cells of (RS)-6-substituted-7- or 9-(2,3-dihydro-5H-1,4-benzodioxepin-3-yl)-7H- or -9H-purines'. *Eur J Med Chem*, **2008**; 43(8):1742-1748.
167. Núñez, M. C.; Rodríguez-Serrano, F.; Marchal, J. A.; Caba, O.; Aránega, A.; Gallo, M. A.; Espinosa, A.; Campos, J. M., '6'-Chloro-7- or 9-(2,3-dihydro-5H-4,1-benzoxathiepin-3-yl)-7H- or 9H-purines and their corresponding sulfones as a new family of cytotoxic drugs'. *Tetrahedron*, **2007**; 63(1):183-190.
168. Boulaiz, H.; Prados, J.; Melguizo, C.; García, A. M.; Marchal, J. A.; Ramos, J. L.; Carrillo, E.; Aránega, A., 'Inhibition of growth and induction of apoptosis in human breast cancer by transfection of gef gene'. *Br J Cancer*, **2003**; 89(1):192-198.
169. Díaz-Gavilán, M.; Gómez-Vidal, J. A.; Entrena, A.; Gallo, M. A.; Espinosa, A.; Campos, J. M., 'Study of the factors that control the ratio of the products between 5-fluorouracil, uracil, and tetrahydrobenzoxazepine O,O-acetals bearing electron-withdrawing groups on the nitrogen atom'. *J Org Chem*, **2006**; 71(3):1043-1054.
170. Díaz-Gavilán, M.; Choquesillo-Lazarte, D.; González-Pérez, J. M.; Gallo, M. A.; Espinosa, A.; Campos, J. M., 'Synthesis and Reactivity of (RS)-6-Chloro-7- or 9-(1,2,3,5-Tetrahydro-4,1-Benzoxazepin-3-yl)-7H- or 9H-Purines Bearing a Nitrobenzene- sulfonyl Group on the Nitrogen Atom'. *Tetrahedron*, **2007**; 63(24):5274-5286.

171. Díaz-Gavilán, M.; Gómez-Vidal, J. A.; Rodríguez-Serrano, F.; Marchal, J. A.; Caba, O.; Aránega, A.; Gallo, M. A.; Espinosa, A.; Campos, J. M. 'Anticancer activity of (1,2,3,5-tetrahydro-4,1-benzoxazepine-3-yl)-pyrimidines and -purines against the MCF-7 cell line: Preliminary cDNA microarray studies'. *Bioorg Med Chem Lett*, **2008**; 18(4):1457-1460.
172. Díaz-Gavilán, M.; Rodríguez-Serrano, F.; Gómez-Vidal, J. A.; Marchal, J. A.; Aránega, A.; Gallo, M. A.; Espinosa, A.; Campos, J. M., 'Synthesis of Tetrahydrobenzoxazepine Acetals with Electron-Withdrawing Groups on the Nitrogen Atom. Novel Scaffolds Endowed with Anticancer Activity against Breast Cancer Cells'. *Tetrahedron*, **2004**; 60(50):11547-11557.
173. Lin, P.; Ye, R. D., 'The Lysophospholipid Receptor G2A Activates a Specific Combination of G Proteins and Promotes Apoptosis'. *Journal of Biological Chemistry*, **2003**; 278(16):14379-14386.
174. Yoneda T.; Imaizumi, K.; Oono, K.; Yui, D.; Gomi, F.; Katayama, T.; Tohyama, M., 'Activation of caspase-12, an endoplasmic reticulum (ER) resident caspase, through tumor necrosis factor receptor-associated factor 2-dependent mechanism in response to the ER stress'. *J Biol Chem*, **2001**. 276(17):13935-13940.
175. Baugher, P. J.; Krishnamoorthy, L.; Price, J. E.; Dharmawardhane, S. F., 'Rac1 and Rac3 isoform activation is involved in the invasive and metastatic phenotype of human breast cancer cells'. *Breast Cancer Res*, **2005**. 7(6):965-974.
176. Guillaumet, G.; Katritzky, A. R.; Rees, C. W.; Scriven, E. F. V., '1,4-Dioxins, oxathiins, dithiins and their benzo derivatives., in Comprehensive Heterocyclic Chemistry II', **1996**;447-481.
177. Quaglia, W.; Pignini, M.; Piergentili, A.; Giannella, M.; Marucci, G.; Poggesi, E.; Leonardi, A.; Melchiorre, C., 'Structure-activity relationships in 1,4-benzodioxan-related compounds. 6. Role of the dioxane unit on selectivity for alpha(1)-adrenoreceptor subtypes'. *J Med Chem*, **1999**; 42(15): 6359-6370.
178. Pallavicini, M.; Fumagalli, L.; Gobbi, M.; Bolchi, C.; Colleoni, S.; Moroni, B.; Pedretti, A.; Rusconi, C.; Vistoli, G.; Valotti, E., 'QSAR study for a novel series of ortho disubstituted phenoxy analogues of alpha1-adrenoceptor antagonist WB4101'. *Eur J Med Chem*, **2006**; 41(9):1025-1040.
179. Birch, A. M.; Bradley. P. A.; Gill, J. C.; Kerrigan, F.; Needham, P. L., 'N-Substituted (2,3-dihydro-1,4-benzodioxin-2-yl)methylamine derivatives as D(2) antagonists/5-HT(1A) partial agonists with potential as atypical antipsychotic agents'. *Journal of Medicinal Chemistry*, **1999**; 42(17):3342-3355.
180. Satoh, Y.; Powers, C.; Toledo, L. M.; Kowalski, T. J.; Peters, P. A.; Kimble, E. F., 'Derivatives of 2-[[N-(Aminocarbonyl)-N-hydroxyamino]methyl]-1,4-benzodioxan as Orally Active 5-Lipoxygenase Inhibitors' *Journal of Medicinal Chemistry*, **1994**; 38(1):68-75.

REFERENCES

181. Fukuyama, Y.; Hasegawa, T.; Toda, M.; Kodama, M.; Okazaki, H., 'Structures of americanol A and isoamericanol A having a neurotrophic property from the seeds of *Phytolacca americana*'. *Chem Pharm Bull* **1992**; 40(1):252-254.
182. Malet-Martino, M.; Jolimaitre, P.; Martino, R., 'The prodrugs of 5-fluorouracil'. *Curr Med Chem Anticancer Agents*, **2002**; 2(2):267-310.
183. Ozaki, S., 'Synthesis and antitumor activity of 5-fluorouracil derivatives'. *Med Res Rev*, **1996**; 16(1):51-86.
184. Díaz-Gavilán, M.; Conejo-García, A.; Cruz-López, O.; Núñez, M. C.; Choquesillo-Lazarte, D.; González-Pérez, J. M.; Rodríguez-Serrano, F.; Marchal, J. A.; Aránega, A.; Gallo, M. A.; Espinosa, A.; Campos, J. M., 'Synthesis and anticancer activity of (*R,S*)-9-(2,3-dihydro-1,4-benzoxathiin-3-ylmethyl)-9*H*-purines'. *ChemMedChem*, **2008**; 3(1):127-135.
185. Villalobos, M.; Olea, N.; Brotons, J. A.; Olea-Serrano, M. F.; Ruiz de Almodovar, J. M.; Pedraza, V., 'The E-screen assay: a comparison of different MCF7 cell stocks'. *Environ Health Perspect*, **1995**; 103(9):844-850.
186. Marchal, J. A.; Boulaiz, H.; Suárez, I.; Saniger, E.; Campos, J.; Carrillo, E.; Prados, J.; Gallo, M. A.; Espinosa, A.; Aránega, A., 'Growth inhibition, G1-arrest, and apoptosis in MCF-7 human breast cancer cells by novel highly lipophilic 5-fluorouracil derivatives'. *Investigational New Drugs*, **2004**; 22(4):379-389.
187. Campos, J.; Saniger, E.; Marchal, J. A.; Aiello, S.; Suárez, I.; Boulaiz, H.; Aránega, A.; Gallo, M. A.; Espinosa, A., 'New Medium Oxacyclic O,N-Acetals and Related Open Analogues: Biological Activities'. *Current Medicinal Chemistry*, **2005**; 12(12):1423-1438.
188. Núñez, M. C.; Entrena, A.; Rodríguez-Serrano, F.; Marchal, J. A.; Aránega, A.; Gallo, M. A.; Espinosa, A.; Campos, J. M., 'Synthesis of novel 1-(2,3-dihydro-5*H*-4,1-benzoxathiepin-3-yl)-uracil and -thymine, and their corresponding S-oxidized derivatives'. *Tetrahedron*, **2005**, 61, 10363-10369.
189. Núñez, M. C.; Díaz-Gavilán, M.; Conejo-García, A.; Cruz-López, O.; Gallo, M. A.; Espinosa, A.; Campos, J. M., 'Design, Synthesis and Anticancer Activity against the MCF-7 Cell Line of Benzo-Fused 1,4-Dihetero Seven- and Six-Membered Tethered Pyrimidines and Purines'. *Curr. Med. Chem.*, **2008**, 15, 2614-2631.
190. López-Cara, L. C.; Conejo-García, A.; Marchal, J. A.; Macchione, G.; Cruz-López, O.; Boulaiz, H.; García, M. A.; Rodríguez-Serrano, F.; Ramírez, A.; Cativiela, C.; Jiménez, A. I.; García-Ruiz, J. M.; Choquesillo-Lasarte, D.; Aránega, A.; Campos, J. M., 'New (*RS*)-Benzoxazepin-Purines with Antitumor Activity: The Chiral Switch from (*RS*)-2,6-Dichloro-9-[1-(*p*-Nitrobenzenesulfonyl)-1,2,3,5-Tetrahydro-4,1-Benzoxazepin-3-yl]-9*H*-Purine'. *Eur. J. Med. Chem.*, **2011**, 46, 249-258.
191. Naumov, G. N.; Nilsson, M. B.; Cascone, T.; Briggs, A.; Oddbjorn, A.; Akslen, L. A.; Lifshits, E.; Byers, L. A.; Xu, L.; Wu, H.-K.; Jaenne, P.; Kobayashi, S.; Susumu, H.; Halmos, B.; Tenen, D.; Tang, X. M.; Engelman, J.; Yeap, B.; Folkman, J.; Johnson,

- B. E. ; Heymach. J. V., 'Combined Vascular Endothelial Growth Factor Receptor and Epidermal Growth Factor Receptor (EGFR) Blockade Inhibits Tumor Growth in Xenograft Models of EGFR Inhibitor Resistance'. *Clin. Cancer Res.*, **2009**, 15, 3484-3494.
192. Mohammad, R. M.; Wang, S.; Banerjee, S.; Sanjeev, W.; Xihan, Ch.; Jianyong, S.; Fazlul, H., 'Nonpeptidic small-molecule inhibitor of Bcl-2 and Bcl-XL, (-)-gossypol, enhances biological effect of genistein against BxPC-3 human pancreatic cancer cell line'. *Pancreas*, **2005**, 31, 317-324.
193. Sasaki, T.; Kitadai, Y.; Nakamura, T.; Kim, J.-S.; Tsan, R. Z.; Kuwai, T.; Langley, R. R.; Fan, D.; Kim, S.-J.; Fidler, I. J., 'Inhibition of epidermal growth factor receptor and vascular endothelial growth factor receptor phosphorylation on tumor-associated endothelial cells leads to treatment of orthotopic human colon cancer in nude mice'. *Neoplasia*, **2007**, 9, 1066-1077.
194. Marchal, J.A.; Aránega, A.; Conejo, A.; Chaves, M.A.; Cruz, O.; Boulaiz, H.; Rodríguez, F.; Cativiela, C.; Perán, M.; Jiménez, A. I.; García, J.M.; Choquesillo, D.; Campos, J.M., 'Enantiómeros de derivados benzoheteroepínicos y su uso como agentes anticancerígenos'. P201030415, 22 de marzo de 2010. Universidad de Granada y Servicio Andaluz de Salud.
195. Díaz-Gavilán, M.; Conejo-García, A.; Cruz-López, O.; Núñez, M. C.; Choquesillo-Lazarte, D.; González-Pérez, J. M.; Rodríguez-Serrano, F.; Marchal, J. A.; Aránega, A.; Gallo, M. A.; Espinosa, A.; Campos, J. M., 'Synthesis and Anticancer Activity of (RS)-9-(2,3-Dihydro-1,4-Benzoxathiin-3-ylmethyl)-9H-Purines'. *ChemMedChem*, **2008**, 3, 127-135.
196. Gupta, S.; Hussain, T.; Mukhtar, H., *Arch. Biochem. Biophys.* **2003**, 410, 177 - 185
197. Núñez, M. C.; García-Rubiño, M. E.; Conejo-García, A.; Cruz-López, O.; Kimatrai, M.; Gallo, M. A.; Espinosa, A.; Campos, J. M., 'Homochiral Drugs: a Demanding Tendency of the Pharmaceutical Industry'. *Curr. Med. Chem.* **2009**, 16, 2064-2074.
198. Woodgett, J., 'We must be open about our mistakes'. *Nature*, **2012**, 489, 7.
199. Huczynski. A., 'Salinomycin – A New Cancer Drug Candidate'. *Chem. Biol. Drug. Des.* **2012**, 79, 235-238.
200. Liu, G.; Yuan, X.; Zeng, Z.; Tunici, P.; Ng, H.; Abdulkadir, I. R.; Lu, L.; Irvin, D.; Black, K. L.; Yu, J. S., 'Analysis of gene expression and chemoresistance of CD133+ cancer stem cells in glioblastoma'. *Mol. Cancer*, **2006**; 5 (67).
201. Zeppernick, F.; Ahmadi, R.; Campos, B.; Dictus, C.; Helmke, B. M.; Becker, N.; Lichter, P.; Unterberg, A.; Radlwimmer, B.; Herold-Mend, C. C., 'Stem cell marker CD133 affects clinical outcome in glioma patients'. *Clin. Cancer Res.* **2008**, 14: 123-129.

REFERENCES

202. Maeda, S.; Shinci, H. H.; Kurahara, H. Y.; Mataka, Y.; Maemura, K.; Sato, M.; Natsugoe, S.; Aikou, T.; Takao, S. S., 'CD133 expression is correlated with lymph node metastasis and vascular endothelial growth factor-C expression in pancreatic cancer'. *Brit. J. Cancer.* **2008**, 98:1389-1397.
203. Wang, L. M.; Kevans, D.; Mulcahy, H.; O'Sullivan, J.; Fennelly, D.; Hyland, J.; O'Donoghue, D.; Sheahan, K., 'Tumor budding is a strong and reproducible prognostic marker in T3N0 colorectal cancer', *Am. J. Surg. Pathol.* **2009**, 33:134-141.
204. Mehra, N.; Penning, M.; Maas, J.; Beerepoot, L. V.; van Daal, N.; van Gils, C. H.; Giles, R. H.; Voest, E. E., 'Progenitor marker CD133 mRNA is elevated in peripheral blood of cancer patients with bone metastases', *Clin. Cancer Res.* **2006**, 12:4859-4866.
205. Lin, E.H.; Hassan, M.; Li, Y.; Zhao, H.; Nooka, A.; Sorenson, E.; Xie, K.; Champlin, R.; Wu, X.; Li, D., 'Elevated circulating endothelial progenitor marker CD133 messenger RNA levels predict colon cancer recurrence'. *Cancer* **110**, **2007** 534-542.

